

Durham E-Theses

Early-life stress in Transylvania: the use of macroscopic and isotopic analyses to examine how early life stress affected survival during periods of political transition.

KAYLA DIANE CROWDER

How to cite:

CROWDER, KAYLA DIANE (2019) Early-life stress in Transylvania: the use of macroscopic and isotopic analyses to examine how early life stress affected survival during periods of political transition. Doctoral thesis, Durham University.

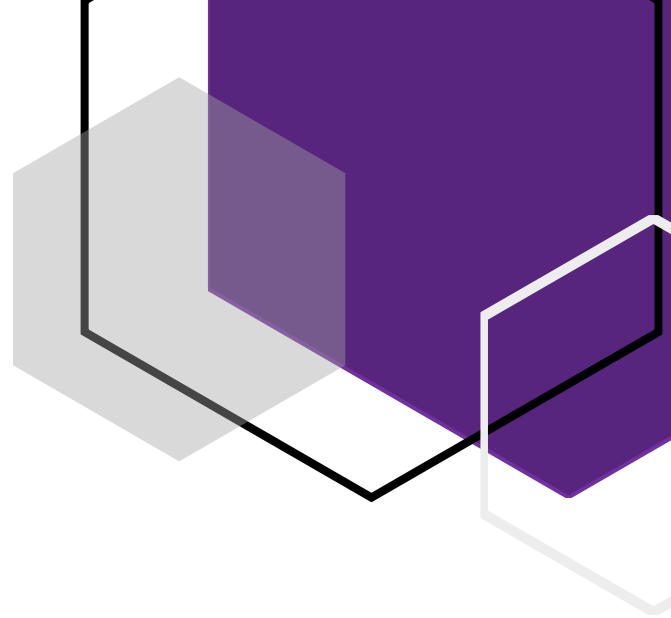
Use policy

The full-text may be used and/or reproduced, and given to third parties in any format or medium, without prior permission or charge, for personal research or study, educational, or not-for-profit purposes provided that:

- a full bibliographic reference is made to the original source
- a <https://etheses.durham.ac.uk/id/eprint/13405/> is made to the metadata record in Durham E-Theses
- the full-text is not changed in any way

The full-text must not be sold in any format or medium without the formal permission of the copyright holders.

Please consult the [full Durham E-Theses policy](#) for further details.



Early-life stress in Transylvania:

the use of macroscopic and isotopic analyses to examine how early life stress affected survival during periods of political transition.

Kayla Diane Crowder

A thesis submitted in fulfilment of the requirements for the degree of Doctor of Philosophy

Department of Archaeology

Durham University

2019

Abstract

As we see today, and throughout history, continued unrest in a region can have a dramatic impact on the health of the conquered and conquering populations, and the subsequent generations. The aims of this study were to integrate isotopic data (showing diet and mobility) and palaeopathological (disease) analyses to understand the impact of aspects of life such as living conditions, economy and diet, and migration, in locals and non-locals, had on morbidity and mortality. The Iclod Necropolis has been associated with the Kingdom of the Gepids, one of many tribes vying for power in Transylvania during this post-Roman transition of the Migration Period. The Bögöz Church and Fenyéd cemetery were occupied during the Arpadian expansion of the Hungarian Kingdom into Transylvania during the Middle Ages.

Macroscopic skeletal analyses confirmed both populations had substantial evidence (>50%) of physiological and metabolic stress. Strontium and oxygen isotope data established biosphere isotope ranges for the Transylvania Basin and were used to identify seven possible non-local individuals between the two populations. Carbon and nitrogen isotope analysis revealed both populations consumed a diet of terrestrial C₃/C₄ resources, with the Migration Period population consuming significantly more millet (C₄) than the Middle Ages population. Significant differences were also found between the diet of males and females, with males consuming higher portions of meat, and females consuming more millet. Isotope life-history profiles revealed early-life stress during critical growth periods, as well as increased frailty and/or early death associated with limited consumption of breastmilk during childhood.

These data, and the substantial evidence of physiological/metabolic stress, support research linking early-life stress with increased frailty and early death. The outcomes of this project offer original contextually driven insights regarding morbidity and mortality of Medieval Transylvanian populations and help increase knowledge about these people who lived in this region of Eastern Europe.

Declaration and Statement of Copyright

The material contained in this research has not previously been submitted for a degree in this or any other institution and is not part of any joint research projects.

The copyright of this thesis rests with the author. No quotation from it should be published without the author's prior written consent and information derived from it should be acknowledged.

A handwritten signature in black ink, appearing to read "Kayla Crowder". The signature is fluid and cursive, with a long horizontal stroke at the end.

Kayla Diane Crowder

Acknowledgements

I would like to thank Dr. Mihai Gligor at 1 Decembrie 1918 University in Alba Iulia and Dr Zsolt Nyaradi Haáz Rezső Museum in Odorhei Secuiesc for granted me access to the skeletal collections and allowing me to work at their facilities for data collection. Thank you to IsoAnalytics for providing laboratory assistance for oxygen isotope analysis. To Joanne Peterkin and Dr Geoff Nowell, thank you for the technical support, always answering my questions and helping me expand my knowledge and lab skills.

Thank you to University College (Durham), the Rosemary Cramp Fund and the Institute of Medieval and Early Modern Studies for helping to funding this research. I am indebted to Dr Darren Gröcke (Stable Isotope and Biogeochemical Laboratory, Durham University) for funding the carbon and nitrogen isotope analyses and for always providing new learning opportunities.

I am extremely grateful to the faculty and staff in the Department of Archaeology at Durham University for the continued training and support throughout my degree. I would also like to thank Dr Steve Robertson, Dr Beth Upex, Dr Vicky Garlick and Dr Kurt Gron for their guidance and assistance in the isotope laboratory. Thanks are due to Professor Charlotte Roberts, Dr Claire Hodson, Dr Anwen Caffell, Dr Tina Jacob and Professor Rebecca Gowland for teaching me how to analyse and record human remains. To Professor Janet Montgomery, thank you for always encouraging me to learn new methods and continually providing me with new learning opportunities.

I will be forever inspired and humbled by the generosity and kindness shown to me by my supervisors, Professor Charlotte Roberts and Professor Janet Montgomery. The unwavering guidance and support mean more to me than I can express.

Dr Jason Nadell, you have been the best partner-in-crime a person could wish for and I am honoured to share my life with a person as intelligent, compassionate and generous as you.

And finally, thank you to my friends and family for always supporting my dreams, pushing me to be better and making me laugh every day. I get my strength from you and would not have been able to do any of this without you.

This thesis is dedicated to my family, past and present.

<u>Darrell Doney</u>	<u>Jody Doney</u>	<u>Wayne Crowder</u>	<u>Joan Crowder</u>	<u>Dave Crowder</u>
11.27.1930	11.3.1931	2.4.1935	9.1.1935	5.25.1953
–	–	–	–	–
8.18.1977	11.24.2010	4.4.2002	1.31.2019	9.7.2018

Table of contents

Table of contents	a
List of figures and tables	d
Chapter 1: Exploring early-life stress in Transylvania	1
1.1. Research questions, aims and hypotheses.....	4
1.2. Thesis structure.....	5
Chapter 2: Introduction to the history of Transylvania and bioarchaeological methods for examining early-life stress.....	7
2.1. Transylvania, Romania.....	7
2.1.1. A brief history of Transylvania	9
2.2. Bioarchaeology.....	16
2.2.1. Bioarchaeology in and around Transylvania.....	18
2.2.2. Demography and its relationship to “stress”	23
2.2.3. Palaeopathological methods used to assess “stress” in the past.....	30
2.3. Summary.....	51
Chapter 3: An introduction to isotope analyses and their applications in the field of bioarchaeology.....	53
3.1. Introduction to isotope analysis.....	54
3.1.1. Isotopes in body tissues	56
3.2. Carbon and nitrogen stable isotope analyses.....	60
3.2.1. Carbon and nitrogen isotopes	60
3.2.2. Applications of carbon and nitrogen isotope analysis.....	64
3.3. Strontium and oxygen isotope analyses.....	72
3.3.1. Strontium isotopes.....	73
3.3.2. Oxygen Isotopes.....	75
3.3.3. Applications of strontium and oxygen isotope analysis	78
3.4. Summary.....	81
Chapter 4: Material and Methods	83
4.1. Introduction.....	83
4.2. Materials (skeletal remains).....	83
4.2.1. Migration Period	83
4.2.2. Middle Ages	86
4.3. Materials (samples for isotope analyses).....	88
4.3.1. Sampling protocol: life-history profiles	88

4.3.2. Sampling protocol – local biosphere	91
4.3.3. Isotope samples: strontium, oxygen, carbon and nitrogen.....	92
4.4. Methods.....	93
4.4.1. Macroscopic skeletal analysis	93
4.4.2. Carbon and nitrogen stable isotope analysis.....	96
4.4.3. Mobility isotope analysis	103
4.5. Statistical analyses.....	112
4.6. Summary.....	112
Chapter 5: Results	114
5.1. Macroscopic skeletal analyses.....	114
5.1.1. Demography.....	114
5.1.2. Palaeopathology	121
5.2. Carbon and nitrogen stable isotopic analyses.....	127
5.2.1. Biosphere data	127
5.2.2. Bone collagen data.....	128
5.2.3. Incremental dentine data	131
5.3. Mobility isotope analyses.....	136
5.3.1. Biosphere data	136
5.3.2. Strontium isotope data	137
5.3.3. Oxygen (carbonate) isotope data	140
5.4. Summary.....	142
Chapter 6: Discussion.....	143
6.1. Demography and health profiles.....	143
6.1.1. Arrested skeletal growth and attained stature	144
6.1.2. Stress-related skeletal lesions	147
6.1.3. Summary	152
6.2. Biosphere and mobility status.....	153
6.2.1. Local biosphere ranges	153
6.2.2. Assessing residential origins and mobility	157
6.3. Diet, breastfeeding/weaning practices, and early-life stress isotopic profiles	162
6.3.1. Overall dietary pattern	163
6.3.2. Breastfeeding and weaning practices.....	170
6.3.3. Perceived formation offset: An examination of a possible offset between tooth formation stages and between EH and changes in early-life isotope profiles.	180

6.3.4. Early-life stress	189
6.4. Summary.....	203
Chapter 7: Key findings, future research prospects and concluding remarks.....	204
7.1. Summary of key findings.....	204
7.2. Considerations for future research.....	209
7.3. Concluding remarks.....	210
References	213
Appendices.....	i
Appendix 4.1. Isotope sample inventory.....	i
Appendix 4.2. Adult recording forms.....	v
Appendix 4.3. IsoAnalytics report.....	xix
Appendix 5.1. Results: statistical analysis.....	xxi
Appendix 5.2. Inventory of macroscopic skeletal analysis (digital Access database)	
Appendix 5.3. Results: palaeopathology.....	xxv
Appendix 5.4. Results: incremental dentine (C, N).....	xxxv
Appendix 6.1 Differential diagnoses.....	liii
Appendix 6.2 Early life-history profiles.....	lxii

List of Figures

Figure 2.1. A map of the barbarian kingdoms of Europe after the withdrawal of Roman troops south of the Danube River	11
Figure 2.2. Map of most of Europe inset with Romania.	16
Figure 2.3. Simplified diagram of a human tooth (molar) and enamel formation. ...	35
Figure 2.4. Example of enamel hypoplasia (pitting).	37
Figure 2.5. Example of porotic lesion (CO) along the left orbital roof.	38
Figure 3.1. Diagram of the structure and direction (arrows) of dentine formation..	58
Figure 3.2. Graph representing the range of $\delta^{13}\text{C}$ and $\delta^{15}\text{N}$ values of different dietary resources..	65
Figure 3.3. A model of an incremental dentine early life-history profile.....	70
Figure 3.4. Example of a map of regional modern precipitation oxygen isotope values used to examine human mobility in the past	77
Figure 3.5. Lithology of the Transylvanian Basin and geological maps demonstrating the diverse bedrock of the archaeological sites in the study.....	78
Figure 3.6. Summary of the strontium isotope ratios reported near the Transylvanian Basin.	79
Figure 4.1. Site map from the the Iclod Necropolis.	85
Figure 4.2. Site maps of the Bögöz and Fenyéd sites	87
Figure 4.3. The equipment setup used to photograph dentition samples to be processed for 3-D photogrammetry models.....	93
Figure 4.4. Examples of new woven bone, mixed woven and lamellar bone, and lamellar bone.....	96
Figure 4.5. Photographs of tooth and bone samples in 0.5M HCl during the demineralisation process.	98
Figure 4.6. Example of the column setup for collecting strontium samples.	107
Figure 5.1. The percentage of individuals in each age category according to skeletal assemblage.	120
Figure 5.2. Percentage of individuals in each sex estimation category by skeletal assemblage.	121

Figure 5.3. Percentage of individuals with lesions by skeletal assemblage.....	121
Figure 5.4. Cuspal enamel defects (Skeleton FEN52).....	123
Figure 5.5. Possible abnormal porosity on the right parietal bone (BOG66).....	124
Figure 5.6. Porous new bone formation across the left orbital roof (ICL131).....	125
Figure 5.7. Probable haemorrhagic staining on the left os coxa and femur (BOG240)	126
Figure 5.8. Porosity on the anterior mandible (ICL129).....	127
Figure 5.9. The results of the bone collagen carbon and nitrogen stable isotope analyses plotted with the animal and plant data.....	130
Figure 5.10. The results of the mean incremental dentine carbon and nitrogen stable isotope analyses plotted with the animal and plant data (a) and by skeletal assemblage (b).....	133
Figure 5.11. The results of the water sample analyses for oxygen isotope analyses plotted with the Global Meteoric Water Line.....	137
Figure 5.12. The results of the strontium concentration and isotope analyses plotted by site and sample type.....	139
Figure 5.13. The results of the enamel oxygen and carbon isotope analysis plotted by site.....	140
Figure 6.1. Strontium and oxygen isotope data from the ancient human, and modern animal, plant and soil samples in this study plotted with the biosphere and human data from the regions outside Transylvania.....	155
Figure 6.2. Precipitation data ($\delta^{18}\text{O}$) collected by International Atomic Energy Agency compared to the rain and river water samples collected in this study.....	156
Figure 6.3. $^{87}\text{Sr}/^{86}\text{Sr}$ and $\delta^{18}\text{O}_{\text{VSMOW}}$ data from the human samples organised by archaeological site.....	158
Figure 6.4. The $\delta^{18}\text{O}_{\text{VSMOW}}$ and $\delta^{13}\text{C}_{\text{VPDB-CARB}}$ data from human enamel samples at each archaeological site plotted with comparative human data from Hungarian Plain during the Roman Period.....	159
Figure 6.5. Oxygen isotope values ($\delta^{18}\text{O}_{\text{VSMOW}}$) of human enamel from sites in the Carpathian Basin and Transylvanian Basin organised from lowest to highest altitude (meters).....	161

Figure 6.6. Carbon and nitrogen stable isotope data of samples from modern plants, ancient animal, and ancient humans to establish the overall dietary patterns for each population..	164
Figure 6.7. $\delta^{13}\text{C}$ values from dentine collagen (mean) and enamel apatite plotted with C_3/C_4 regression data from Kellner and Schoeninger (2007) and Froehle et al. (2010).	165
Figure 6.8. Carbon and nitrogen stable isotope data demonstrating the difference in means for males and females, within and between periods.....	167
Figure 6.9. Carbon and nitrogen isotope data of the human dentine (mean) and bone isotope values for each population to examine changes in diet throughout life. ...	168
Figure 6.10. Examples of the Pattern A carbon and nitrogen isotopic profiles for breastfeeding and weaning for two individuals.....	172
Figure 6.11. Examples of the Pattern B carbon and nitrogen isotopic profiles for breastfeeding and weaning for two individuals.....	175
Figure 6.12. Two examples of the profiles for Pattern C breastfeeding and weaning..	177
Figure 6.13. Examples of life-history profiles for individuals who may not have been breastfed.	180
Figure 6.14. Examples of early-life profiles of four individuals plotted with a possible offset between the isotope ratio changes and the timing of the EH.....	183
Figure 6.15. Simplified theoretical model of a first molar to show the different $\delta^{15}\text{N}$ isotope profiles between dentitions still forming at death and the complete permanent dentition	186
Figure 6.16. Examples of early-life profiles of four individuals with incomplete (still forming at death) and complete teeth.....	188
Figure 6.17. Examples of two early-life isotope profiles of non-local individuals. ..	190
Figure 6.18. Early-life isotope profiles of two individuals with stress related lesions.	192
Figure 6.19. Two examples of older adults with evidence of early-life stress profiles..	195
Figure 6.20. Examples of the two types of profiles containing data for prenatal increments.....	197

Figure 6.21. Examples of elevated $\delta^{15}\text{N}$ values and “stress” during infancy in two individuals.....	198
Figure 6.22. Examples of stress signals during mid-childhood in two individuals. ...	200
Figure 6.23. Examples of the profiles of two individuals with adolescent stress signals	201

List of Tables

Table 2.1. Examples of palaeopathological studies conducted on skeletal assemblages from Romania.....	33
Table 2.2. Summary of the non-specific indicators of stress studied and the differential diagnoses for each lesion.	41
Table 2.3. The macroscopic skeletal lesions commonly associated with scurvy and the possible differential diagnoses	45
Table 2.4. The macroscopic skeletal lesions commonly associated with rickets and the possible differential diagnoses.....	49
Table 3.1. The range of isotope values of associated with different plant types.	62
Table 4.1. Summary of individuals selected for isotopic analyses	90
Table 4.2. The preferred sampling protocol for teeth and bones for isotopic analyses.	91
Table 4.3. A summary of samples collected for strontium and oxygen isotope analyses to establish a baseline biosphere range for each population.	92
Table 4.4. Summary of the defined age and sex categories used in this study.	94
Table 4.5. List of methods used for the macroscopic analyses.....	95
Table 4.6. The process for cleaning the strontium chemistry columns	106
Table 4.7. The elution procedure to collect the strontium samples from the columns.	107
Table 4.8. The equations used to convert the oxygen isotope values.....	111
Table 4.9. Statistical tests used to determine significantly different relationships in the data.	112

Table 5.1. Results of the macroscopic skeletal analysis of individuals from the Iclod Necropolis	115
Table 5.2. Results of the macroscopic skeletal analysis of individuals from the Bögöz and Fenyéd cemeteries	119
Table 5.3. Crude prevalence rates for individuals with EH by age category and biological sex.	122
Table 5.4. Crude prevalence rates for individuals with CO by age category and biological sex.	125
Table 5.5. The results of the stable carbon and nitrogen isotope analyses of plant and animal remains from the regions of both skeletal populations.....	128
Table 5.6. The results of the carbon and nitrogen stable isotope analysis of bone collagen for each skeletal assemblage.	129
Table 5.7. The statistically significant differences in the bone collagen data.....	131
Table 5.8. The results for all individuals selected for incremental dentine stable isotope analyses.	132
Table 5.9. The statistically significant different results for the incremental dentine stable isotope analyses.....	135
Table 5.10. The results of the strontium and oxygen isotope analyses to establish baseline biosphere from each assemblage	136
Table 5.11. The results of the oxygen isotope analyses on water samples from each region.....	137
Table 5.12. The results of the strontium isotopes and concentrations from human enamel.....	138
Table 5.13. The statistically significant different results for the strontium isotope analyses.	139
Table 5.14. The results of the enamel carbonate oxygen and carbon isotope analyses.	141
Table 5.15. Summary of the results for each method of isotope analyses by population.....	138
Table 6.1. Individuals with arrested skeletal growth: skeletal and dental ages compared.....	146

Table 6.2 Summary of individuals with metabolic disorders as a differential diagnosis.	151
Table 6.3. Summary of individuals found to be non-locals to the burial region.....	162
Table 6.4. Summary of the individuals with Pattern A breastfeeding and weaning profiles.....	173
Table 6.5. Summary of the individuals with Pattern B breastfeeding and weaning profiles.....	176
Table 6.6. Summary of the individuals with Pattern C breastfeeding and weaning profiles.....	178
Table 6.7. Summary of the individuals without breastfeeding signals in the early-life profiles.....	179
Table 6.8. Summary of the AFM and PFM isotope data used for examining intrauterine stress.....	196

Chapter 1: Exploring early-life stress in Transylvania

As we see throughout history, continued unrest in a region can have a dramatic impact on the health of the conquered and conquering populations, as well as the subsequent generations (Pedersen, 2002; Thomas and Thomas, 2004; Benson *et al.*, 2011). The region of Transylvania, Romania has experienced periods of unrest for centuries, from the Roman invasion, barbarian raids, migration of the Slavs, and the expansion of the Kingdom of Hungary (Giuresci, 2002). Situated along key trade and migration routes between the Mediterranean and Balkans, and between the Black Sea and Europe, abundant natural resources such as gold and salt, and fortification provided by the surrounding Carpathian Mountains, make Transylvania a highly coveted territory (Sherratt, 1993; Quinn and Ciugudean, 2018). Whether the exchange of power is civil or violent, changes in a person's social, political and economic standing can increase psychosocial stress, as well as affect the production and access to adequate food, leading to increased physiological and metabolic stress and poor health (Miller and Rasmussen, 2010; Benson *et al.*, 2011).

The Developmental Origins of Health and Disease theory, otherwise known as 'Barker's Hypothesis' (Barker *et al.*, 1989) has shown that health insults to the foetus *in utero* and during early childhood development, particularly undernutrition, can significantly affect the health and survivorship of an individual later in life, as well as impact the health of future generations (Hales and Barker, 2001; de Boo and Harding, 2006; Barker, 2012). If populations in Transylvania experienced early-life stress, it is possible the immediate and long-term negative effects could be seen in skeletal remains of past populations. This can be examined through an array of bioarcheological methods.

In bioarchaeology, historical and archaeological data are used to establish the structure of a site and provide clues as to cultural identity, settlement size and economy (e.g. rural or urban). Historical documents tend to be written by the victors, which can provide a biased history focusing on the noble and elite members of society. Likewise, the history of Transylvania has been found to change depending on the political affiliation of the historian (Dobos, 2009) and can be exaggerated to

support the chosen narrative of the political system in power at the time (Dreisziger, 2009). For this reason, reliable historical information about medieval Transylvania is limited, requiring additional methods of research to be conducted.

Macroscopic skeletal analysis of human remains provides information about a person's biological sex, age at death, growth, and health during life (Larsen, 2002; Chamberlain, 2006; Murphy and Chamberlain, 2017). Demography and health profiles can be created from archaeological context, artefact materials and skeletal remains to help establish morbidity and mortality patterns within and between populations (Larsen, 2002; Chamberlain, 2006; Murphy and Chamberlain, 2017; Steckel and Kjellström, 2018). A person's socio-economic standing, migratory status (local or non-local to their burial region), and access to adequate nutrition are all very important when attempting to understand how a population lived and died. Biomolecular analysis of skeletal remains is used to establish dietary pattern, breastfeeding and weaning practices, mobility status and health insults during development. This research employs these methods to help fill the gap in research regarding medieval Transylvania, as well as to better understand the interrelated risk factors relevant to critical periods of development, which have been found to contribute to poor health and early death.

"Stress", its meaning, and how it may be measured

The term "stress" can be used to discuss a myriad of factors in bioarchaeology (Temple and Goodman, 2014). Research focusing on stress can range from clinical medical studies to bone changes from mechanical loading (Mekota *et al.*, 2006; Ruff, 2008). For the purpose of this research, the word "stress" is used to discuss skeletal lesions and biomolecular changes commonly associated with physiological and psychosocial duress and metabolic/nutritional inadequacy. When a person experiences a stressor, such as psychosocial stress, physiological stress, metabolic/nutritional stress, the body's "fight or flight" mode activates the sympathetic nervous system and releases hormones to deal with the stress event (Selye, 1956; Brown, 1981). The effects of stressors have been found to manifest in

the body as early as six to 12 days after the stress event (Beisel, 1975, 1977; D'Ortenzio *et al.*, 2015). This stress reaction causes macroscopic and isotopic changes to the skeleton which are used to assess health in past populations.

The skeleton reacts to stress in one of two ways: bone forming or bone resorbing (Ortner and Turner-Walker, 2003, pg. 14; Roberts and Manchester, 2005a, pg. 7). Palaeopathological research is limited to the information obtained from skeletal and dental remains. Therefore, methods and disease characteristics have been established based on the types and locations of lesions present. This provides researchers clues as to the morbidities in past populations.

Examination of macroscopic changes to bone and teeth provide information about the types of diseases prevalent within a population and are used to create individual and population level health profiles (Roberts and Connell, 2004; Waldron, 2009; Reitsema and McIlvaine, 2014). When the body is forming new tissues (bone, skin, teeth) elements from the environment and diet are incorporated into the tissues. These elements can then be analysed through isotope analysis to create childhood life-history profiles. Isotope analyses are used to establish an array of details about past populations.

Strontium and oxygen isotope analysis provides information about the geology and climate of the region a person inhabited during childhood (Ericson, 1985; Montgomery, 2010; Evans *et al.*, 2012) and can be used to establish if a person was local to their burial regions (Montgomery *et al.*, 2000; Price *et al.*, 2004; Evans *et al.*, 2012). Carbon and nitrogen stable isotope analysis are used to establish dietary patterns of populations (DeNiro and Epstein, 1978; Schoeninger and DeNiro, 1984), how long a person was breastfed and how long it took to wean them onto solid foods (Fuller *et al.*, 2006; Bourbou *et al.*, 2013; Beaumont *et al.*, 2015; Craig-Atkins *et al.*, 2018), and if they underwent metabolic/nutritional stress during development (Beaumont *et al.*, 2016, 2018; King, *et al.*, 2018; Siebke *et al.*, 2019). Combined with macroscopic skeletal data, these methods help to better understand the interrelated factors of early-life stress.

Macroscopic and isotopic analytical methods provide information about the health and well-being, diet and mobility histories to assess the negative impacts of early-life stress on health. To date, there is a dearth of comparable skeletal and isotopic data from Transylvania. Two archaeological sites form the basis of this study to help fill the gap in bioarchaeological research of Medieval Transylvania. The Iclod Necropolis has been associated with the Kingdom of the Gepids, one of many barbarian tribes vying for power in Transylvania during the post-Roman transition of the Migration Period (Maxim *et al.*, 2002). The large-scale population movements during this time are believed to be associated with changes in climate, disease and famine which have been documented in Eastern Europe (Thompson, 1982; Büntgen *et al.*, 2016). During the Middle Ages, the Hungarian Kingdom expanded into the Transylvania Basin and established military and judicial centers (Dreiszigler, 2009; Popa-Gorjanu, 2012; Pop, 2013). The Bögöz Church and Fenyéd cemetery were occupied during the Arpadian expansion of the Hungarian Kingdom and are believed to have been inhabited by the first wave of Hungarian settlers during the time (Gáll, 2013; Zsolt, 2015). Both populations lived during times of political transition.

This study employs bioarchaeological methods to examine metabolic/nutritional inadequacies, dietary patterns, cultural practices, residential origins and mobility, and the impact these factors had on childhood health in during periods of political transitions in Transylvania.

1.1. Research questions, aims and hypotheses

This project utilizes macroscopic and isotopic methods to reveal health and well-being, diet, and mobility histories of two populations from Medieval Transylvania, Romania. As mentioned in the previous section, there is a lack of skeletal and isotopic data originating from Transylvania. This research sets out to broaden knowledge about the people from this region of Eastern Europe, by answer the following research questions.

- I. Is there evidence of stress (skeletal manifestations and/or isotopic changes) present in the two Transylvanian populations?
- II. Can the timing of onset of evident skeletal disease (metabolic disorders) be established through increases in nitrogen isotope profiles using incremental dentine stable isotopic analysis?

The aims of this study are to integrate isotopic data (showing diet and mobility during life) and palaeopathological (disease) analyses to understand the impact of aspects of life such as living conditions, economy and diet, and migration, in locals and non-locals, on morbidity and mortality. As a result of the regions instability due to war and invasions, which could impact the production and availability of food and potentially lead to increased psychosocial, physiological and metabolic stress, it is hypothesised that:

- There will be substantial evidence (>50%) of physiological stress and/or metabolic conditions (including dietary deficiencies) in excavated human skeletal remains representing people who lived in Transylvania during the Migration Period and the Middle Ages.
- Individuals who migrated to the region later in life will display changes in their overall dietary profile and breastfeeding patterns.
- Stress-related lesions (skeletal and biomolecular) will be present in local and non-local individuals.
- Early-life stress will negatively impact frailty, resulting in increased morbidity and early death.

1.2. Thesis structure

This thesis is divided into seven chapters. The present chapter has introduced the overall aims of the project, research hypotheses and thesis structure. Chapter 2 introduces the geopolitical history of Transylvania to better understand the continued unrest in the region and transitions of political powers. The second chapter also introduces the methods and applications of macroscopic skeletal analysis implemented in this research to explore demographic profiles, morbidity (disease) and mortality (death) of the two Transylvanian populations. Chapter 3 introduces the

field of isotope analysis, the application of isotope analysis in bioarchaeology and how these methods were used in this study to reveal more information about mobility, diet and early-life stress of 39 individuals selected from the two Transylvanian populations. Historical and archaeological information from each population and detailed information regarding the specific processes employed using each method of analysis are provided in Chapter 4. The results generated using each method are presented in Chapter 5. The interpretations of the data, how the data from the two transitional periods studied compare to one another, and how these data compare to the wider research context of Eastern Europe are presented in Chapter 6. The sixth chapter also combines historical, archaeological, palaeopathological and biomolecular data to gain a deeper understanding of the interrelated risk factors of early-life stress, and how these factors led to frailty within and between these two Transylvanian populations. The seventh and final chapter provides a complete summary of the key finds, potential future research and concluding remarks.

Chapter 2: Introduction to the history of Transylvania and bioarchaeological methods for examining early-life stress

As outlined in Chapter 1, this research considered two populations from Transylvania to explore whether two populations, who lived during periods of political transition, had evidence of “stress.” Before we can begin to understand how these people lived and died, it is important to understand the wider historical and archaeological context surrounding both the Migration Period and the Middle Ages. This chapter provides: a brief historical summary of the geopolitical landscape of Transylvania (Section 2.1.); an introduction to the methodology utilized in this study to gain more information about these burial populations (Section 2.2); and the palaeopathological methods used to examine early–life stress (Section 2.2.3).

2.1. Transylvania, Romania

The region of Transylvania has been inhabited by several political, cultural, and religious powers throughout its history. Territorial claims to Transylvania have been fought for centuries because of its geographic location and valuable natural resources. Romania has the advantage of being geographically located to connect long-distance trade routes from Western Europe to the Black Sea, and the Mediterranean with Scandinavia (Sherratt, 1993; Quinn and Ciugudean, 2018). The unique landscape of the Transylvanian Basin (plateau) in Romania provides a natural fortification, with the Apuseni Mountains to the west, the Eastern Carpathian Mountains to the north and east, and the Transylvania Alps (Southern Carpathian Mountains) to the south. The natural seclusion of Transylvania led to differences in religious and cultural practices between Transylvania and the surrounding regions. For example, ancient Dacian (modern day Romania) religious practices in the Black Sea and Getae regions had Greek influence but there is no evidence of this reaching Transylvania (Grumeza, 2009). Likewise, the exchange of ideas for weaponry design has been linked to military raids by Germanic societies in the region, but there is also no evidence of this in Transylvania (Kontny, 2017). The political, cultural, and physical

landscape of Transylvania made the inhabitants uniquely placed compared to the surrounding regions.

The history of Transylvania can vary depending on which political system was in power and what was written (Dobos, 2009). Some historical documents produced by the Hungarian historian Anonymus, centuries after the Hungarian conquests, have been found to exaggerate the truth to support the political views of the time (Dreisziger, 2009). The territorial claim to Transylvania has centered around the inhabitants of the region throughout history. The Austro-Hungarians laid claim to Transylvania as uninhabited settled territory, the *terra deserta* theory, which posits that all Dacians left the region after the withdrawal of the Roman troops south of the Danube River (Ellis, 1998). Some Hungarian books promoted this theory until the late 19th century, attempting to discredit the idea that Romanians continuously inhabited Transylvania and claiming that they left following the Roman withdrawal and returned in the 13th century (Bucur and Costea, 2009). This research was funded by the Hungarian Habsburg Empire and is not supported by historical or archaeological data. The argument is further complicated by the lack of credible historical documentation. During the Reformation, many manuscripts and historical documents were destroyed by the conquerors (i.e. Tartar invasion), leaving the majority of documents on medieval history being imported from France and Italy, rather than having been produced locally (Papahagi, 2015). Strict ethnic and cultural divides established by early researchers, such as Márton Roska, still persist in some aspects of Romanian archaeology (Gáll, 2012). After World War II, the Soviets and the Romanian Communist Party supported historical and archaeological research focused on emphasizing Slavic influences and diminishing the Roman influence in the region (Gabinschi, 1997; Ellis, 1998). This is not to say that all research regarding the colonization of Transylvania is inaccurate, but it is very important to be aware of these challenges when reading about the history of Transylvania.

2.1.1. A brief history of Transylvania

(i) Prehistory

The Transylvanian Basin has been inhabited by humans since the Palaeolithic (Musat and Ardeleanu, 1985). The Someşul Mic and Mare rivers provide connections to the Pannonian Plain which were used to trade salt from the Neolithic to the Middle Ages (Lazarovici and Lazarovici, 2015). Rich soils, coveted natural resources (gold, salt, copper, timber), and a temperate climate made Transylvania crucial to economies in Bronze Age communities (Coles and Harding, 2015; Quinn and Ciugudean, 2018). Copper resources and gold were exported from Transylvania to Central Europe during the Bronze Age (Bogucki and Crabtree, 2004). During the Middle Bronze Age (between 1900 C. BC and 1450 C. BC) settlements were usually small farmsteads but the emergence of large population settlements like Otomani were starting to emerge in the region (Bogucki and Crabtree, 2004). Funerary practices from this period were of the Wietenberg Culture, mostly revealing cremation burials (90%) with a few inhumations in cemeteries or in group graves (10%) (Palincaş, 2014). In terms of chronology, much of the relatively dated ceramics used to date archaeological sites during this period are being redefined as new information arises with radiocarbon dating (Ciugudean and Quinn, 2014).

In the 1st C. BC, the Dacians in Transylvania were believed to be transhumant pastoralists, with both temporary (seasonal) summer houses and permanent valley-side settlements (Taylor, 2011). The natural fortification of the Transylvanian Basin provided some reprieve for the Transylvania Dacians, while those south of the Danube had continuous encounters with the Romans (Bogucki and Crabtree, 2004). The Dacians had monotheist beliefs with strong astronomical ties and divine sites, and the main religious sites were located in Transylvania (Grumeza, 2009). At this time, Dacia had a homogenous society with a thriving military, economy, trade and culture, all of which were supported by the local gold and salt trade (Grumeza, 2009).

(ii) Roman period

The Roman Emperor Trajan saw Dacia's growing power as a threat and offered diplomatic terms to the Dacian leader, Decebal. Having confidence in the stability of Dacia, Decebal led two major wars against the Roman Empire (101 and 106 AD), eventually requesting an armistice which resulted in him becoming a client king for the Empire (Grumeza, 2009). The Romanization of Dacia began during the second half of the 3rd C. AD (Ellis, 1998). The Romans saw those who spoke pure Latin and believed in Roman gods as *civilis* (modern), while those who didn't were considered *barbarous* (savage) (Grumeza, 2009). Roman political and cultural influence was strong in Transylvania (Dobson, 1936). During the Aurelian withdrawal (270–275 AD) the Romans still had power over central and southern Dacia (Transylvania and Wallachia), while the north, east and west territories remained as "free Dacia" to act as a buffer for the Empire against the rising barbarian populations (Ellis, 1998; Grumeza, 2009).

(iii) Migration or post-Roman period (4th-9th C. AD)

In the first half of the 4th C. AD, the Romans withdrew from the trans-Danubian Dacia region (now Transylvania), and set their northern border at the Danube River (Figure 2.1) (Ellis, 1998; Grumeza, 2009). This resulted in the numerous barbarian tribes in the surrounding regions competing for power (Migration Period). The Daco-Romans (Romanised Dacians, including *Carpi* and free Dacians) strengthened the Dacian presence in the post-Roman province after the withdrawal of the Romans, and were considered separate (archaeologically) from the influence of the "migrants" which was evident in artefact remains and burial practices (Previt -Orton, 1975; Madgearu, 2012). The "migrant" influence referred to the large-scale migration of nomadic Germanic tribes [i.e. Gothic, Visigoths (west Germanic), Gepids (east Germanic), Langobards (southern Scandinavia)] during the Migration Period.

The migrants settled in open spaces while the Daco-Romans inhabited existing cities (Niculescu, 2005). There was an increase in the number of Christian artefacts in the post-Roman Dacia region and it is believed this was a way of self-identifying as Roman Christian to the "heathen Slavs" (Madgearu, 2012). During the Late Antique Little Ice

Age (536 to 660 AD), the northern hemisphere experience long-lasting cooling which are believed to have contributed to the Justinian plague, movements of populations and transformation of the eastern Roman Empire (Büntgen *et al.*, 2016). The deteriorating climate in Scandinavia is believed to have led to Gothic and Gepidic populations fleeing to more fertile lands closer to large Roman settlements to gain access to their markets (Bogucki and Crabtree, 2004). Early Gepid communities were documented as having lived as allies of the Roman Empire (Previt -Orton, 1975). The Huns, allied with Gepid and Ostrogoths armies, attacked the western reaches of the Roman Empire at the end of the 5th C. AD taking control over most of the post-Roman Dacia province (Bogucki and Crabtree, 2004). After the death of the Hunnic leader, Attila, forces led by the Gepid king, Adarich, defeated Attila’s sons and took control of Transylvania (Dobos, 2014).



Figure 2.1. A map of the barbarian kingdoms of Europe after the withdrawal of Roman troops south of the Danube River (Gepid territory indicated in red). Map created by Marzolino/Shutterstock.com

The Gepidic Period in Transylvania lasted from 454 to 568 AD. Historical and archaeological data from this period can be contradictory. For this reason, the

archaeological finds after the Hunnic Period in the region of the Gepid Kingdom are typically assigned to the Middle-Danubian material culture (Tejral, 2012) which is based on geographical location rather than ethnic group (Dobos, 2014). During the 5th and 6th Centuries (AD), Gepid cemeteries contained high numbers of burials, some numbering in the hundreds (Bogucki and Crabtree, 2004). A change in burial practices to row-grave cemeteries (*Reihengräberfelder* culture) is associated with Merovingian burial rites, providing evidence of western and central European influences during this period (Dobos, 2009). The Langobards expanded into the Carpathian Basin (526 AD) and are believed to have co-existed with the Gepids until 535 AD (Bogucki and Crabtree, 2003). Unrest grew as the Gepid and Byzantine militaries fought the Langobards and Avars (ethnic group originating from Northeast Caucasian region), until the Gepids were defeated by the Avars in 567–568 AD (Bogucki and Crabtree, 2004).

The Avar conquest of the Transylvanian Basin took place during the first campaign, towards the end of the 6th C. AD, with the Gepid elites either being eliminated or integrated into the Avar hierarchy in rural micro-communities (Gáll, 2014). Some believed the Avar campaign was a chance to unify military alliances between Transdanubia, Transylvania, and the Hungarian Plain (Holló *et al.*, 2008). The *Reihengräberfelder* burial practice continued into the Early Avar period, but there are conflicting theories as to whether the Avars in the region adopted the practice, or that the row-graves during the Early Avar period belonged to the remaining Gepid populations (Dobos, 2014). One way of distinguishing between the two cultures is exemplified by the Avar society, which held horses in high esteem and would sometimes bury warriors and the elite with their horses (Bogucki and Crabtree, 2003). During the 8th C. AD, there were low numbers of Avar artefacts from Transylvania, a change to bi-ritual funerary practices (cremation and inhumation burials), as well as Christian evidence associated with Byzantine contact (Țiplic and Țiplic, 2014). The Avar Empire was defeated by Bulgar, Lombardy, and Saxony military campaigns (774–804 AD) at the order of the Frankish king, Charlemagne (Bogucki and Crabtree, 2003).

(iv) Middle Ages

In the second half of the 9th C. AD, Árpád, the head of the Hungarian tribal confederation, led the expansion of the Hungarian Empire (Dreisziger, 2009). Árpád's citizens in the Carpathian Basin (Hungary and western Romania) were Turkic-speaking, agriculturally based nomads known as the Magyars (Dreisziger, 2009; Popa-Gorjanu, 2012). The Székely were also Hungarian citizens, but this population was culturally distinct from the Magyar and aided in settling the eastern border counties in Transylvania (Dreisziger, 2013; Brie and Mészáros, 2014). The Magyar cavalry conducted raids for decades in the early 10th C. AD and conquered Byzantium in 972 AD (Bogucki and Crabtree, 2003).

Transylvania experienced high levels of colonization and was home to many ethnically distinct populations (Slavs, Magyars, Szeklers, Pechengues, Saxons, Italians, etc.) from the 11th C. AD onwards (Popa-Gorjanu, 2012). The Saxons were known to remain in urban settings while the Székely were rurally based agriculturalists (Dreisziger, 2009). Archaeological finds in eastern Transylvania support the theory that “westernization” of the region took place in the 12th C. AD with the expansion of Christianity and the Hungarian Kingdom (Zsolt and Gáll, 2015). Transylvania was seen as the eastern border of the Hungarian Kingdom, and the borders of Transylvania were redefined in 1200 AD as the region surrounded by the Carpathian Mountains; seven counties were given to the Saxons and Székely (Pop, 2013). The Székely and Saxons were tasked with protecting the southern and eastern borders of the Transylvanian province (12th and 13th C. AD) while the ruling nobility spent much of the 14th C. AD establishing religious, judicial and legislative organizations under the Hungarian central authority (Popa-Gorjanu, 2012; Pop, 2013).

The Hungarian Empire began to unravel in the 15th C. AD. The Orthodox Romanians in Transylvania were ostracized and not allowed government representatives, despite their continued military support against the Ottomans (Pop, 2013). Romanian and Hungarian citizens of the lower classes (tenant-peasants) rebelled against the noble elite, eventually forcing them to re-organise themselves and form the “three nations” of Transylvania: Romanians; Saxons; and Szeklers (Popa-Gorjanu, 2012; Pop,

2013). The mid-sixteenth century saw the rise of the Protestant Reformation, and Transylvania adopted this as one of their four accepted religions, the other three being Calvinism, Lutheranism, and Unitarianism (Pop, 2013). Between 1540–1690 AD, Transylvania became a semi-independent principality under the Ottomans and Habsburgs (Popa-Gorjanu, 2012; Pop, 2013) and in 1691 AD Transylvania was annexed to the Habsburgs and the Ottoman Empire (Papp, 2013). Romanians in Transylvania created a national emancipation document in 1791 AD, claiming ancient Roman heritage and non-nomadic lineages (Bucur and Costea, 2009). In 1867 AD, Transylvania once again became part of Hungary (Papp, 2013) until the Treaty of Trianon (1920) following World War I when it finally became part of the country of Romania (Papp, 2013; Admiraal, 2015).

(v) Skeletal assemblages

This study examined the skeletons of two burial populations from Transylvania that lived during periods of political transition (Figure 2.2.). The first group, from the Iclod Necropolis, has been associated with a small population associated with the Gepid Kingdom dating to the Migration Period. The second group, from the Bögöz and Fenyéd archaeological sites, lived during the time of the Hungarian expansion into Transylvania in the Middle Ages. Additional information about each site can be found in Section 4.2. These assemblages were selected because the cemeteries were in-use through the transitions of political powers. Because of this, it was hypothesized that both the local inhabitants, and incomers, would have stress-related lesions evident in their skeletons.

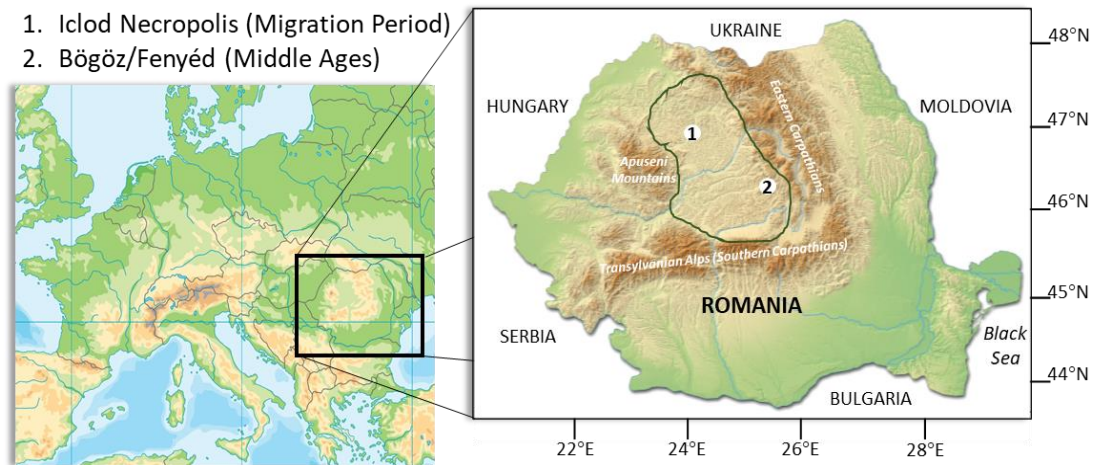
(a) Migration Period - Iclod Necropolis

The Iclod Necropolis, Cluj County, Romania was selected to represent the Migration Period. The site is located in the north-west Transylvania Mountain Basin (Figure 2.2) and is a multi-phased settlement with burials both within and outside of the settlement grounds (Gáll, 2014). Artefacts buried with the skeletons from the Migration Period context associate these individuals with a population from Kingdom

of the Gepids in the Transylvanian Basin. This skeletal assemblage was selected because this site was in use when the Roman Empire withdrew south of the Danube River, leaving multiple barbarian tribes competing for power in northern Romania (Dobos, 2013). There were also documented periods of unrest and famine during this time (Todd, 1995). If the inhabitants of the Iclod Necropolis experienced chronic “stress” it was expected that the skeletons would display related skeletal lesions.

(b) Middle Ages – Bögöz and Fenyéd cemeteries

Two populations were combined to form the medieval (Middle Ages) assemblage. Both the Bögöz Church and Fenyéd Cemeteries have been radiocarbon dated to the 11th-12th C. AD, are in the same county, and have a similar geology and climate (see Figure 2.2). Both sites were in use during the Hungarian expansion into Transylvania (Gáll, 2013; Zsolt, 2013). The Bögöz Church is a rural church located in the south-east Transylvanian Basin (Mugeni, Romania). Artefacts buried with the skeletons, such as hair pins, link this population with the Székley, Hungarian Kingdoms (Gáll, 2013). The Fenyéd Cemetery is in south-east Transylvania (Brădești, Romania) and has been associated with the Székley, Hungarian Kingdoms (Gáll, 2013). Hairpins with Western European characteristics found in the burial context provide evidence of the westernization of Hungarian Kingdom at this time (12th C. AD) (Gáll, 2013).



Site	County	Latitude	Longitude	Elevation
Iclod	Cluj	46.978° N	23.816° E	265m
Bögöz	Odorhei	46.260° N	25.223° E	444m
Fenyéd	Odorhei	46.341° N	25.340° E	496m

Figure 2.2. Map of most of Europe inset with Romania. The Transylvanian Basin is outlined in green and the two regions of the sites studied are marked. Image adapted from Cartarium and Schwabenblitz/Shutterstock.com

2.2. Bioarchaeology

This section provides a brief introduction to the field of bioarchaeology and the amount of information that can be obtained from analyzing human remains. Macroscopic examination of skeletons remains, or macroscopic skeletal analysis, can reveal a great deal about past populations, for example biological sex; age-at-death; morbidity (illness) and mortality (death) profiles; migration patterns; cultural practices; and subsistence. There are many terms used to describe research based on past skeletal remains, for example biological/physical anthropology; osteoarchaeology; bioarchaeology (Goldstein, 2006; Roberts, 2018). The term “bioarchaeology” first appeared in the 1950’s and has been applied to a wide array of research topics (see Buikstra and Beck, 2006). The term bioarchaeology is used in this study to encompass research dealing with “human remains from archaeological sites, from a multidisciplinary perspective, and integrating the biological data from the human remains with archaeological and other data in order to understand our ancestors’ lives” (Roberts, 2018, pg. 6).

Following the mid-20th C. AD, theoretical and technological advances in population genetics and statistical analyses moved the field towards a wider concept of human variation (Cook, 2006). The field of bioarchaeology began to improve its methodology and re-examine ethical practices and pedagogical theory (Baker and Agarwal, 2017; Roberts, 2018, pg. 17-18). Some ageing techniques were found to mimic the structure of the documented population on which the method was developed (Bocquet-Appel and Masset, 1982), which is known to bias the resulting mortality profiles of the buried populations being analysed (Chamberlain, 2000, pg. 105). This realization was met with new methods of estimating age-at-death based on varying skeletal elements such as the sternal rib ends (İşcan *et al.*, 1984), the auricular surface (Lovejoy *et al.*, 1985; Buckberry and Chamberlain, 2002), and the os pubis (Brooks and Suchey, 1990).

Shifts in the theoretical underpinning of studying demography and illness in the past were also happening during the second half of the 20th century and the beginning of the 21st century. The “Osteological Paradox” questioned assumptions regarding studying health and well-being using skeletal remains and emphasized the importance of factors such as selective mortality (differential risk factors), demographic non-stationarity (migration) and hidden heterogeneity (i.e. genetic predisposition) (Wood *et al.*, 1992; Wright and Yoder, 2003; Marklein *et al.*, 2016). Wood and colleagues (1992) also questioned ideas surrounding active versus inactive pathological lesion interpretations, stating that individuals with healed/inactive skeletal lesions were strong enough to live through the stress event they had experienced and were actually the “survivors” (Fried *et al.*, 2001; Yaussy *et al.*, 2016). Waldron (1994: Fig. 2.1) emphasized the importance of how to think about the burial population (all individuals buried), the excavated population (those individuals excavated from the site), and the analysed population (those individuals analysed from the excavated population), and how each might have only have been a small portion of the original living population, and therefore may not be a realistic representation of the once living population who were buried at a site. Both Wood and colleagues (1992) and Waldron (1994, pg. 11) remind us that the dead are

inherently biased samples of the living population (they are dead), and this must be taken into consideration when interpreting data from skeletal remains.

The progress made towards understanding the many factors and processes leading to death pushed the field towards a multidisciplinary approach, utilizing specialist analytical techniques from other scientific fields. Bioarchaeologists are encouraged to collaborate with clinicians to broaden the understanding of skeletal data as a means of interpreting morbidity in the past (Jurmain, 1999, pg. 264-5) For example, ancient DNA (aDNA) can be used track population flow and migration (Hervella *et al.*, 2015), and show the presence of certain diseases, particularly infectious, within a population (Masson *et al.*, 2015; Köhler *et al.*, 2017). Imaging (radiography, computed tomography) and have been successful applied within bioarchaeology to investigate factors like: taphonomy (Booth *et al.*, 2016); histological changes associated with disease (Zuckerman *et al.*, 2014); and cross-sectional geometry of long bones (Larsen, 2015, pg. 255). Microscopy can be used to reveal microscopic osteological changes or inclusions in tissue such as dental calculus (Blatt *et al.*, 2011); changes due to disease (Bell and Jones, 1991; Hassett, 2014); and tissue formation processes (Reid and Dean, 2000; Ivancik *et al.*, 2014). Stable isotope analysis is used to examine diet patterns (DeNiro and Epstein, 1981; Schoeninger *et al.*, 1983), cultural practices (Fuller *et al.*, 2006; Brettell *et al.*, 2012; King *et al.*, 2018), and health status (Fuller *et al.*, 2004; Mekota *et al.*, 2006; Beaumont and Montgomery, 2016). These technological advances can expand our knowledge about the past, but they are not without limitations. These limitations are discussed further in subsequent sections.

2.2.1. Bioarchaeology in and around Transylvania

Bioarchaeology began to grow as a field in Transylvania in the second half of the 19th C. AD with the work of anthropological scientist, Aurel Török, a Professor in histology and pathology (Gál, 2011). In 1926, Francisc Rainer, a Professor in histology and embryology, founded the School of Anthropology in Bucharest and began accumulating skulls to study (Gál, 2011). As previously mentioned, there are many

terms used for the study of human remains. Within Romania, the name of the field changed as it developed. For example, skeletal analysis of human remains from an archaeological site was classified under “paleoanthropology” from 1946–1969, “historical anthropology” from 1970–1978, and then returned to “paleoanthropology” in 1999 and continues today (Ion, 2014). After the Second World War, a clear distinction between archaeological excavation and crime scene recovery of human remains was established in response to investigations of human rights violations by the communist parties of the time (Gál, 2011). Since the fall of communism in Romania, the country has prioritized cultural heritage, which has led to developing archaeological resources and legal frameworks (Musteață, 2015). Due to producing regulations on the excavation of human remains from archaeological sites in Romania there has been progress towards protecting skeletal remains, but there are limited standards available for recording or guidance for storing those remains (see Gál, 2011 for methodology being used). The absence of unified standards (methods) for skeletal analysis thus makes it difficult to find comparable skeletal datasets from this region.

The historic claims of Romanians and Hungarian to the Transylvania region rested on the continued occupation of the region, therefore, past research focused on the structures and artefactual remains from archaeological sites with limited research being conducted on human remains. This resulted in scant research being produced on human skeletal remains dated between the Roman occupation and the Hungarian occupation within Transylvania. Early research was typically published in local journals, and did not reach the wider academic community; this has started to change in the last two decades (Gál, 2011). This added to the difficulty in synthesizing the skeletal data in this research. Because of the limited data available on skeletal remains from the Transylvanian Basin, data from the surrounding regions (Bulgaria, Hungary, Moldavia, Romania, Ukraine) from all archaeological time periods were utilized to contextualise the data within this study.

The need to fill the gap in research regarding medieval archaeology in general and human skeletal analyses in particular in Transylvania has sparked a growing body of work in this region. Some studies have focused on the burial context including the

position of burials, and inclusions (e.g. artefacts, animal remains) and how they relate to the human remains (Cosma, 2015; Gáll, 2015; Zsolt and Gáll, 2015). Morphological studies have been conducted on crania to explore cultural deformation (de Cupere *et al.*, 2000; Molnár *et al.*, 2014; Mayall, 2018), on cranial sexual dimorphism (Soficaru *et al.*, 2014), and animal domestication (Evin *et al.*, 2017). There are also a growing number of palaeopathological studies (see Section 2.2.3).

(i) Studying “stress” in bioarchaeology

Early work examining biological factors and cultural determinants of disease (‘biocultural phenomenon’) began to reconsider the concept of stress and expanded the definition to include the perception of stress and psychosocial related stressors (subjective stressors such as anxiety and fear, which can vary from person to person – Selye, 1974; Brown, 1981). The Selyean concept of stress is related to when the body is in “fight or flight” mode. An overall general stress response occurs, which activates the sympathetic nervous system and the hypothalamus to release stress hormones (adrenaline and cortisol - Selye, 1936, 1956: pg. 133; for a comprehensive review of the physiological stress response see Brown, 1981). Anthropologists began to examine these stress responses in living populations using behavior, physiological measurements and psychological tests (Pichot and Hassan, 1973). Without documented collections and written accounts of a person’s lived experience, it is impossible to apply psychological tests, measure physiology in the modern sense (adrenaline, cortisol, heart rate, blood pressure – Bassett *et al.*, 1987), or use behavioral scales when working with skeletons. However, recent progress has been made to examine cortisol levels from human remains (e.g. hair) using an ELISA enzyme immunoassay kit to assess stress level in the past (Webb *et al.*, 2015). Compared to medical anthropologists working with living populations, bioarchaeologists are constrained with the amount of information potentially available from skeletal remains. However, the presence of “stress” in an ancient population can start to be examined based on (macroscopic) skeletal changes, alongside biomolecular analyses (discussed further in Section 3.2.2).

Within bioarchaeology, the term “stress” is used to describe a myriad of stressors (causes) and manifestations of stress, as observed in the skeleton (Temple and Goodman, 2014). The definition of “stress” can also vary depending on the aims and scope of the research. For example, the term stress in bone morphology studies refers to the relationship between bone changes and mechanical loading (Ruff, 2008; Nadell and Shaw, 2016). Although each definition might slightly differs, the general definition of “stress” within the field of anthropology is “the disruption of the body’s homeostasis as a result of environmental constraints, cultural systems and/or host resistance” (Larsen, 2015, pg. 9). For the purposes of this research, evidence of “stress” was used in discussing poor health as a result of nutritional and metabolic disorders, and physiological and/or psychosocial stress, bearing in mind the discussion above about the difficulties of measuring physiological and/or psychosocial stress. The terminology used to talk about different types of stressors and their manifestations varies depending on the type of stressor being discussed (Reitsema and McIlvaine, 2014; Temple and Goodman, 2014). Nutritional stress was used to refer to an inadequate amount of food consumed, its poor quality, or the poor uptake/absorption of key nutrients in the food eaten (Sisodia and Singh, 2012). The term physiological stress was used in this study to describe stressors of a physical nature, both internal/innate (e.g. pregnancy in women, weaning in children, and growth spurts) and external (e.g. low socioeconomic status, high workload, and low levels of sanitation – Temple and Goodman, 2014). Stress can occur as early as the prenatal environment and can continue throughout life (Barker, 1998).

A growing field of bioarchaeological research has applied clinical stress pedagogies to expand our understanding about stress in the past. For example, the Developmental Origins of Health and Disease, also referred to as the “Barker Hypothesis” or DOHAD, has linked early-life “stress” (e.g. under- or malnutrition) *in utero* and/or during the critical growth period to higher rates of heart disease, high blood pressure, diabetes, and “strokes” with earlier death in adulthood (Barker, 1998; Wadhwa *et al.*, 2010). A healthy environment in which the foetus develops is critical when the body is programming molecular markers for metabolism, which can impact health later in life (Hales and Barker, 2001). If a foetus experiences stress *in*

utero, they survive on nutrients by processing fat and protein stored in the mother's body tissues (James, 1997). This can result in increased nutritional and physical demands for both the mother and foetus. Poor uterine health has been found to cause changes in the developmental programming of a foetus. For example, the "thrifty phenotype" hypothesis proposed by Hales and Barker (2001) can be explained through poor foetal and infant growth, leading to an increased risk of developing insulin-resistant type 2 diabetes later in life. Given that the majority of human development is achieved in the first 1000 days following conception (Barker, 2012; Said-Mohamed *et al.*, 2017), insults during this period can increase a person's frailty later in life, leading to increased susceptibility to disease and a decrease in immune response (Marklein *et al.*, 2016).

Early-life stress can be evaluated in several ways in bioarchaeology. Demographic and palaeopathological analysis of skeletons from an archaeological site can provide insight into morbidity and mortality (Sections 2.2.2 and 2.2.3). Metrical analysis of the bones of the skeleton can reveal individuals who had arrested skeletal growth compared to their age, estimated from the dentition; this is commonly attributed to poor health. For example, diminished stature (height) and vertebral neural canal size have been linked to health insults in childhood and early adulthood (Steckel, 2005; Watts, 2011; Newman and Gowland, 2015; Roberts *et al.*, 2016). Skeletal measurements and stress-related lesions (chronic and acute) can also be quantified to create a skeletal frailty index (SFI) for individuals, providing a way of evaluating life-long effects of stress on health (Marklein *et al.*, 2016)¹. Biomolecular analysis in the form of stable isotope analysis of micro sections of incremental dentine can reveal the approximate onset and duration of stress events during the time the tooth was growing (Section 3.1.2). The DOHAD theoretical framework has also been successfully applied in bioarchaeology. For example, the presence of enamel hypoplasia, an early-life stress indicator, has been linked to an earlier than expected death in adulthood (Armelagos *et al.*, 2009; Amoroso *et al.*, 2014). The DOHAD framework has also been applied to mortality profiles based on skeletal remains to

¹ This method was attempted on the two populations in the study but, due to the poor preservation and fragmentation of the skeletal remains, this method could not be implemented.

further explore interrelated risks throughout life and during the four critical growth periods - intrauterine, infancy, mid-childhood, and adolescence (see Cameron and Demerath, 2002). As previously stated, increased stress in early life can increase a person's frailty later in life.

2.2.2. Demography and its relationship to "stress"

Data on age-at-death and biological sex are used to build a demographic profile for a skeletal population (Larsen, 2002; Chamberlain, 2006; Murphy and Chamberlain, 2017). These data can provide information related to the funerary context for the populations being analysed. Catastrophic cemeteries contain burials associated with a mortality crisis (such as the bubonic plague) resulting in a high mortality risk for all age categories and it is believed to mimic the structure of the living population (Gowland and Chamberlain, 2005; Dewitte, 2012). Attritional cemeteries reflect gradual accumulation of the dead over a long period of time and therefore these contexts are expected to have both male and female individuals dying within all age categories, with higher percentages of non-adults and a gradual increase in mortality with age (Chamberlain, 2000; Margerison and Knüsel, 2002; Gowland and Chamberlain, 2005). The mortality pattern of an attritional cemetery reflect children and elderly members of a population who had a greater risk of death (Chamberlain, 2000). Care must be taken when working with possible attritional cemeteries because this type of mortality pattern can also be found for populations where famine affected the most vulnerable members, such as children and elderly (Margerison and Knüsel, 2002; Gowland and Chamberlain, 2005; Yaussy *et al.*, 2016). Both skeletal populations in this study were excavated from attritional cemeteries.

Macroscopic skeletal analysis of the skeletal remains was conducted to establish the demographic profile for each population assessing age-at-death and biological sex. The analysis also considered stature and the prevalence of paleopathological lesions. This study followed the standardised methods of examining human remains based on guidelines published by BBAO for studying skeletons (Brickley and McKinley, 2004) to ensure the data gathered in this research is comparable with other European

studies. The subsequent sections discuss the techniques and limitations for the methods employed.

(i) Estimating age-at-death

Age-at-death estimation is a key component in building a demographic profile for a population. Having an approximate age-at-death provides clues as to the risk factors and frailties each person experienced and helps to compare age-at-death related patterns within and between populations. Age estimation methods have often been developed on entire skeletal assemblages with documented/known age-at-death. This can introduce inherent error when these methods are applied to individual skeletons from other population and have been found to increase inaccuracy with increasing age of the skeleton (Saunders *et al.*, 1992; Wittwer-Backofen *et al.*, 2008; Cheverko and Hubbe, 2017). This is why it is important to implement a multifactorial approach using different age estimation methods to reach a more accurate age range (Saunders *et al.*, 1992; O'Connell, 2004; Cunha *et al.*, 2009; Brickley *et al.*, 2016).

The development and subsequent degeneration of the human skeleton follows general age-related patterns, although there are factors that can accelerate ageing (e.g. specific work patterns). Age estimation of non-adult individuals tends to be more precise compared to adult age-at-death estimation because the skeleton and dentition were still in the process of developing at the time of death. Estimating age-at-death for non-adult skeletal remains relies on the formation and eruption of the dentition, long bone length, and epiphyseal fusion rates. The formation and eruption of the dentition has been researched extensively and is the most reliable way to estimate age-at death in non-adults (Hillson, 1996; Brickley, 2004b; AlQahtani *et al.*, 2010). Advances are being made to understand pulp/tooth ratios in older adults to estimate age-at-death (D'Ortenzio *et al.*, 2018). Bone formation of primary (initially a cartilaginous template) and secondary (epiphyses, growth plate) ossification centers are well documented and a full review can be found in Cunningham *et al.* (2016). The mean age at which specific epiphyses fuse to primary ossification sites and long bone length can be used to estimate age-at-death in non-adult skeletons (Brickley, 2004b;

Cunningham *et al.*, 2016). However, the rate of growth and remodeling of bone can decrease or completely stop during periods of stress, which can result in skeletal age estimations younger than the actual age. This can introduce error for estimating age-at-death but can of course also be used to show stress. Normal dental formation and eruption rates can vary slightly, but the rates do not significantly decrease during periods of stress (AlQahtani *et al.*, 2010; Hillson, 2014). Therefore, if an individual's skeletal age was estimated to be younger than the estimated age of dental formation/eruption, that individual can be considered to have experienced arrested skeletal growth. As a person ages, their skeleton begins to degenerate, and the methods used to estimate age-at-death shift focus to degenerative age-related changes.

The age of young adults with a fully erupted dentition can be refined by using late-fusing skeletal elements such as the medial clavicle, the vertebral epiphyseal plates and the sacral segments (Cunningham *et al.*, 2016). Once the skeleton reaches full maturity (complete skeletal fusion), age estimation methods focus on degeneration of parts of the skeleton to estimate age-at-death, such as the joints. For example, Todd (1920) developed age-at-death assessments based on skeletal remains from individuals with documented age and biological sex, finding age-related changes in the appearance of the pubic symphysis (Brooks and Suchey, 1990). The age related characteristics of the auricular surface (on the os coxa) can also be used to estimate age-at-death but the complex scoring system has been found to introduce some error (Lovejoy *et al.*, 1985; Buckberry and Chamberlain, 2002). Tests of this method and a revised scoring component have decreased its subjectivity and broadened the age categories, lowering the amount of error for this method (Buckberry and Chamberlain, 2002). The ossification of cartilage and deterioration of bone at the sternal end of the ribs (2nd to 9th) can also be used for adult age estimation (İşcan *et al.*, 1984; İşcan *et al.*, 1985; Yoder *et al.*, 2001). Because these three aforementioned methods rely on the appearance of the bone surface of a joint, which can be affected by taphonomic and post-mortem damage, they can be difficult to apply to poorly preserved skeletons. Another method of estimating adult age-at-death involves the attrition (wear) of teeth. The occlusal surface (chewing surface) of the molar teeth

wears down as people use their teeth. If the diet and rate of attrition is believed to have been steady (not unusual or uneven wear patterns), patterns of attrition may be considered to estimate age-at-death (Brothwell, 1981; Solheim, 1993). However, if there was a substantial change in a person's diet, such as the introduction of cereals and sugars in post-medieval English diets (Hillson, 2001; Ball, 2002), the rate of attrition can change, making this an unsuitable method for adult age estimation.

There are limitations to be aware of when estimated age-at-death in adult skeletons. The subjective nature of features in the skeleton recorded using macroscopic methods can introduce varying inter- and intra-observer errors (Beck, 2006). For instance, cranial suture closure, arachnoid granulations and degenerative joint disease have also been used to assess age-at-death but were not used in this study due to their inaccuracy and unreliability (O'Connell, 2004). Bone-loss due to old age and taphonomic destruction can result in poor preservation and a high degree of fragmentation, making it difficult to assess the different age-related stages for the methods used to estimate age-at-death in older individuals. Recently, the validity of many of the standardised methods have been called into question (Cunha *et al.*, 2009; Agarwal, 2012; Appleby, 2017). It is believed that most methods can be biased towards the profile of the skeletal assemblage on which the methods were developed (e.g. the Hamman-Todd collection and the pubic symphysis method in the 1920s). For this reason, and the other limitations listed, estimated adult age-at-death was assigned using the methods described and each skeleton was then assigned a general age category (see Section 4.4.1).

(ii) Estimating biological sex

When the human body undergoes changes associated with increased hormones levels during puberty, male and female skeletons develop sexually dimorphic features (Acsádi *et al.*, 1970; Shapland and Lewis, 2013). Sexual dimorphism can be used to estimate the biological sex of a person based on their skeletal remains. Like age-at-death, biological sex estimation can provide information about differential risk factors (when analysed with morbidity and mortality data) and cultural practices (e.g.

possible differences in gender roles) within and between populations (Ortner, 1999; Agarwal, 2012; Gowland, 2017). Male and female children who have not reached pubertal age tend to have very similar skeletal morphology until puberty (Marshall and Tanner, 1969; Shapland and Lewis, 2013). Attempts have been made to assess non-adult biological sex estimation from skeletal traits, but the accuracy level for the proposed traits is low (Brickley and Buckberry, 2017). Ancient DNA (aDNA) analysis has been effective in estimating non-adult biological sex but this method can be expensive and requires well preserved skeletal material (Skoglund *et al.*, 2013). For these reasons, non-adult biological sex was not estimated in this study. However, a new method of analysing sex-dependent amelogenin peptide from tooth enamel has proven successful on archaeological skeletal remains for individuals from all age categories, and on skeletons with varied preservation (Stewart *et al.*, 2016, 2017). This method could be applied to the individuals in the study in the future. The maturation (shape) of the cervical vertebral bodies has also been successful in assessing the stages of puberty from skeletal remains (Shapland and Lewis, 2013), but the initiation and duration of puberty is highly susceptible to changes in stress and/or the environment (Marshall, 1978; Watts, 2011; Newman and Gowland, 2015). Therefore, individuals in this study who were estimated to be between 12-20 years old at the time of death were assigned a tentative biological sex-estimation if the skeletal traits appeared to show sexual dimorphism.

Sexual dimorphism is most pronounced in the cranial and pelvic bones of the skeleton. Biological sex estimation of adult skeletons (≥ 20 years old) in this study followed the UK guidelines (Brickley, 2004a). It is recommended that analysis should use material temporally and geographically comparable to the population being analysed to minimize the variation associated with evolutionary trends and population genetics associated with particular climates (Brickley and Buckberry, 2017). This proved difficult in this study due to limited macroscopic skeletal data from Romania during the Migration Period and Middle Ages. The reader is referred to the cited publications for descriptions and illustrations of the skeletal traits used for biological sex-estimation.

The shape of the pelvis in adult females tends to be wider, has a ventral arc on the pubic bone, a subpubic concavity, and wider sciatic notch compared to adult males (Phenice, 1967; Buikstra and Ubelaker, 1994; Brickley, 2004a). There are some researchers that evaluate the possible pelvic changes associated with childbirth (parturition scars), but this method has been criticized and was not used in this study (Ubelaker and De La Paz, 2012). Adult male skulls are usually more robust, with a pronounced external occipital bone protuberance, supra-orbital ridge/ glabella, mastoid process, and mental eminence of the mandible, when compared to adult females from the same population (Buikstra and Ubelaker, 1994; Brickley, 2004a). The general evolutionary trend for human sexual dimorphism shows male skeletons to be generally more robust and taller than female skeletons (Koepke and Baten, 2005b, 2005a). Metrical analysis of long bone dimensions also helps to quantify sexual dimorphism of a population and aid biological sex estimation.

Estimating biological sex from skeletal remains is not without limitations. Climate, genetics, disease and normal variation can all impact a person's growth, altering the degree of sexual dimorphism within a population. Oestrogen levels naturally decrease in women after the menopause which has been found to make women prone to age-related osteoporosis, as well as skeletal changes resulting in ambiguous or masculine features, which can result in inaccurate biological sex estimation (Raisz, 2005). Age-related osteoporosis can also make the structure of bones weaker, and more susceptible to degradation in the burial environment, and obscuring characteristic features required for biological sex estimation. Like age-at-death estimation, it is important to use a multifactorial approach to assess biological sex.

(iii) Stature

A person's attained stature can provide information about factors that can influence height, such as their genetic makeup, the climate, and their standards of living (Robb *et al.*, 2001; Koepke and Baten, 2005a; Dewitte and Hughes-Morey, 2012; Azcorra *et al.*, 2016). Children living in developing nations or impoverished environments are generally small in size for their age (Larsen, 2015, pg. 9; Armas, 2018). A study by

Macintosh and colleagues (2016) examined how body size was affected by living conditions and stress in central and southeastern Europe after the transition to farming. Although a gradual increase in body size over thousands of years was noted, particularly in women, the authors concluded that, despite technological advances, more efficient agricultural productivity, and improvements in sanitation and infrastructure, no rapid or population-wide increases were evident. The authors posit the lack of rapid growth to increased population density, high disease load, urbanization and socioeconomic complexity as the likely causes. However, men and women from Europe in the early Medieval period did display a marked increase in body size with the introduction of farming. Climate can also affect stature. Koepke and Baten (2005) examined the impact climate had on living standards throughout Europe over the past 2000 years. They found that if population density was controlled for, urbanization had a positive impact, with a negative correlation between temperature and height (decreased temperature/decreased height) from the 9th C. AD onwards. Height increased slightly in Northern and Eastern Europe from the 1st–3rd C. AD, decreased during the 4th C. AD (possibly linked to the onset of large-scale population migrations), and increased again in the 5th–6th C. AD after the fall of the Roman Empire and outbreak of the bubonic plague (Koepke and Baten, 2005b). These factors were considered when assessing the stature of the two populations from Transylvania in this study.

In terms of methods of estimating stature, physical anthropological research on the long bones of skeletons of military casualties (American WWII and Korean War) generated regression equations for estimating the stature of a person from their skeletal measurements (Trotter and Gleser, 1944, 1952; Trotter, 1970). As previously mentioned, the skeletal assemblage used to establish a new method can bias the results when the method is applied to other populations. Mays (2016) examined stature estimation equations established on archaeological human remains from similar ecogeographical zones and found that they were not any more accurate than those based on recent populations. In more recent work, new methods using measurements of all the bones of the skeleton, with soft-tissue corrections, were established and have been found to decrease the error of stature calculations from

dry bone(s) (Raxter *et al.*, 2007, 2008). Stature estimation using these new methods requires well preserved skeletal remains. The fragmentary state of the skeletal remains in this study limited the use of the newer methods. However, it is very important to make sure the method used is appropriate for the population being analysed. The white male and female equations from Trotter (1952) were found to best match the populations living in Transylvania during the Migration Period and Middle Ages.

2.2.3. Palaeopathological methods used to assess “stress” in the past

It is believed that the first use of the term “palaeopathology” was in 1892 by Dr Robert Wilson Shufeldt (Buikstra and Roberts, 2012, pg. xii; Cook, 2012). Later in the early 20th C. AD, Sir Marc Armand Ruffer (French/German physician) defined palaeopathology as, “diseases which can be demonstrated on the basis of human and animal remains” (Ruffer, 1913, pg. 149; Roberts, 2018, pg. 7). Palaeopathology is the study (*logos*) of suffering (*pathos*) and takes a multidisciplinary approach examining primary (e.g. skeletons from archaeological sites) and secondary (e.g. historical data) sources of evidence to explore the origin, evolution and history of diseases (Aufderheide *et al.*, 1998, pg. 9; Roberts and Manchester, 2005a, pg. 1). When a person experiences a bodily ‘insult’ or ‘stressor’, bone responds in one of two ways. As a result of osteoblast activity (bone forming cells), new bone is deposited as a response (Ortner and Turner-Walker, 2003, pg. 11; Roberts and Manchester, 2005a, pg. 7), and destruction of bone occurs when the stressor triggers osteoclast activity (bone-resorbing cells). Prolonged exposure to a stressor such as a pathogen (chronic illness) can result in healing, where the body may remodel the destructive lesions (Ortner and Turner-Walker, 2003, pg. 14; Roberts and Manchester, 2005a, pg. 7). Bone formation (woven and lamellar bone) provides researchers with information regarding the state of an illness at the time of death.

The “Osteological Paradox” was a milestone in how bioarchaeologists interpreted data for disease from bone changes in the skeleton (Wood *et al.*, 1992). As previously mentioned, individuals with skeletal lesions indicate those who survived the illness

long enough for bone changes to manifest themselves (Wood *et al.*, 1992; Wright and Yoder, 2003). Individuals without skeletal lesions may not have been ill, or they could have succumbed to their illness before skeletal changes could occur (*ibid*). Disorganised new woven bone formation as a result of disease (i.e. not associated with normal skeletal growth) indicates the illness was active at the time of death, while healed lesions (organized lamellar bone) indicate the person overcame the illness prior to death (Wood *et al.*, 1992; Ortner, 2003). A mixed appearance (woven and lamellar bone) could suggest chronic illness and/or the person was in the process of recovery when they died, or that they incurred several 'bouts' of the disease (Wood *et al.*, 1992; Roberts and Manchester, 2005b, pg. 8). The different appearances of pathological lesions thus help to assess a person's frailty. The type and location of the lesions can also assist researchers in assigning possible aetiologies for the bone changes.

Descriptions of the bone changes and patterning observed throughout the skeleton can help to reach a diagnosis although differential diagnostic options have to be considered. Some diseases affect the skeleton in a distinct way and patterns (pathognomonic) allowing palaeopathologists to assign a diagnosis with some degree of confidence, such as destruction of the maxillary alveolar bone and pressure erosion of the phalanges in the hands and feet associated with leprosy (Ortner, 2003, pg. 268). However, diseases with systemic disruptive bone formation, such as those associated with poor nutrition, can result in lesions indicative of numerous aetiologies. People can also suffer from more than one disease/condition at the same time (co-morbidity) making a precise diagnosis even more difficult (Brickley and Ives, 2008). Therefore, it is very important to take a multifactorial and multidisciplinary approach when examining health in the past (Grauer, 2018). As a field within bioarchaeology, palaeopathology is also rooted in anthropology (physical, medical, social) and archaeology, and the technical fields employed to generate environmental, biological, and cultural data (e.g. clinical medicine, biomolecular analysis - Larsen, 2002, 2015, pg. 301). The interaction between human biology, culture and environment can be evaluated to create a skeletal biology or life-history profile for specific individuals or entire populations (Larsen, 1997; Wright and Yoder,

2003). This biocultural approach has been employed to examine themes such as prehistoric population movement (Larsen and Milner, 1994) and the transition to agriculture (Cohen and Armelagos, 1984). This latter research examined political, environmental, cultural and socio-economic factors to see how they may have impacted early-life stress in the past.

Socioeconomic standing, quality of the diet, the environment and a genetic predisposition are just a few of the factors that can impact a person's health (Wadhwa *et al.*, 2010; Yaussy *et al.*, 2016; Baker and Agarwal, 2017; Mopin *et al.*, 2018). Skeletal evidence of "stress" has been found in Romania dating back to the Neolithic (Lundberg, 2015) and Bronze Age (Agurajua, 2017). The growing number of studies examining the mortality and morbidity of burial populations within Romania help to provide insight about the quality of life in past populations. A person's socioeconomic status can greatly impact their ability to survive (Barker, 1998; Thayer and Kuzawa, 2014; Floyd, 2016). For example, the analysis of the skeletons representing a Magyar peasant population in north-west Transylvania (14th–17th C. AD) found evidence of infection, nutritional deficiency, joint disease, trauma and high child mortality rate in line with low socioeconomic standing (Eng and Szocs, 2003). Spina bifida occulta has been identified in medieval and post-medieval skeletons at Lasi in north-eastern Romania, possibly related to deficiencies in the maternal nutritional environment (Groza *et al.*, 2013).

Period	Location	Evidence of “stress”	Source
<i>Neolithic</i>	Alba Iulia, RO	17% - evidence of non-specific stress	(Lundberg, 2015)
<i>Bronze Age</i>	Carpathian Bend, RO	12% - evidence of non-specific stress	(Agurauja, 2017)
		35% - evidence of metabolic disease	
<i>Early Medieval</i>	Jucu, RO	12% - evidence of non-specific/metabolic stress	(Dianna and Meşter, 2013)
	Braşov, RO	10% - evidence of physiological stress	(Istrate and Diana, 2017)
		11% - evidence of metabolic disease	
<i>Late Medieval</i>	Telekfalva, RO	98% - infantile metabolic stress	(Osterholtz et al., 2014)
	Transylvania, RO	24% - evidence of non-specific stress	(Eng and Szocs, 2003)
<i>Post-medieval</i>	Iasi City, RO	4% - spina bifida associate with poor maternal health	(Groza et al., 2013)

Table 2.1. Examples of palaeopathological studies conducted on skeletal assemblages from Romania and the percentage of individuals with evidence non-specific, physiological and/or metabolic disease.

A change in climate, which occurred in Europe towards the end of the Middle Ages (14th–19th C. AD) is also believed to have negatively impacted the health of populations in the affected region (Lafferty, 2009; McMichael, 2012). Diana (2014) examined the skeletons from two urban contexts from southern Romania and found a decrease in stature and increases in violence related trauma, infection, and nutritional deficiency which the author attribute to the change in climate. Environmental changes from anthropogenic impacts such as water management and salt mining in Medieval Transylvania (AD 1000) are thought to have resulted in a decrease in forest density and increased salt concentration in the surrounding environment such as halophytic species (salt marsh plants) in nearby areas (Tóth *et al.*, 2018). The application of stable isotope analyses to skeletons from sites in the region are also beginning to expand our knowledge of: dietary patterns (Bréhard *et al.*, 2014; Noche-Dowdy, 2015; Voas *et al.*, 2018); cultural practices of animal husbandry (Gillis *et al.*, 2013); population migration (Price *et al.*, 1994; Gerling, Heyd, *et al.*, 2012; Allen, 2017; Hakenbeck *et al.*, 2017). More information about these isotopic studies and others can be found in Chapter 3.

Morbidity and mortality profiles of groups within and between populations (high vs. low socioeconomic standing, local vs. non-local, non-adult vs. adult) can further

suggest differential levels of stress during life (Ubelaker *et al.*, 2006; Ubelaker and Pap, 2008, 2009). Initial finds from the Early Medieval phase of the Jucu cemetery (Cluj county, Romania) found that juveniles had a higher mortality rate compared to adults, and males had higher morbidity than females (Dianna and Meşter, 2013). Skeletal data from a medieval population in Braşov, a centre for travellers, political power and trade in south-east Transylvania, revealed a high mortality and low life-expectancy (Istrate and Diana, 2017), correlating with the expected quality of life for medieval populations (Chamberlain, 2006, pg 54). Osterholtz and colleagues (2014) found evidence of perinatal scurvy in a medieval Romanian population which the authors attributed to poor maternal health and/or dietary practices (Osterholtz *et al.*, 2014). Although skeletal data from Transylvania are limited, these studies helped to contextualise the data collected on the indicators of “stress” for this study.

Chronic stress can weaken the immune system leading to disease, and chronic disease can cause a stress response (Selye, 1956; Dodge and Martin, 1970). Stress and disease should be thought of as a continuum and not simply be considered in terms of presence or absence (Larsen, 2015, Chp. 2). This study employed a biocultural approach, combining biological and cultural data with historical records and environmental factors (Brothwell, 1967; Roberts, 2006; Baker and Agarwal, 2017), to build a more complete picture of how early-life stress impacted people residing in Transylvania. As previously mentioned, insults during critical periods of development can have lasting negative effects on a person’s health (Lucas, 1991, 1994).

Palaeopathological analyses in this study focused on skeletal and dental changes associated with nutritional deficiencies, metabolic disorders, and non-specific indicators of stress [porotic hyperostosis (PH), cribra orbitalia (CO), and enamel hypoplasia (EH)]. The identification of specific aetiologies for the non-specific stress lesions observed was not attempted. Instead, the prevalence of the non-specific stress lesions acted as an indicator for poor health and early-life stress at the individual and population levels.

(i) Non-specific indicators of stress

(a) Enamel hypoplasia

A record of a person's health and diet is captured in their bones and teeth as they grow (Goodman *et al.*, 1980; Hillson, 1996; Beaumont and Montgomery, 2016). Unlike bone, the layered structures of teeth undergo little to no turnover (continuous, slow replacement of tissue) after their initial development (Hillson, 2014). Primary dentine, beneath the enamel, remains relatively consistent throughout life. Secondary and tertiary dentine can be secreted within the pulp cavity to prevent breakthrough to the nerve by crown attrition or damage (discussed further in Section 3.1) (Hillson, 1996). Enamel, the hard outer layer of tooth crown does not remodel once it is mineralized (Figure 2.3) and remains effectively unchanged by the burial environment (Hillson, 1996). Mature enamel is acellular and made up of 96% hydroxyapatite, an inorganic material (Hillson, 2005). Because of their inorganic crystalline structure, teeth tend to survive the burial environment well, often better than bone, and have been successfully used to assess health and diet in the past (Armelagos *et al.*, 2009; AlQahtani *et al.*, 2010; Hillson, 2014).

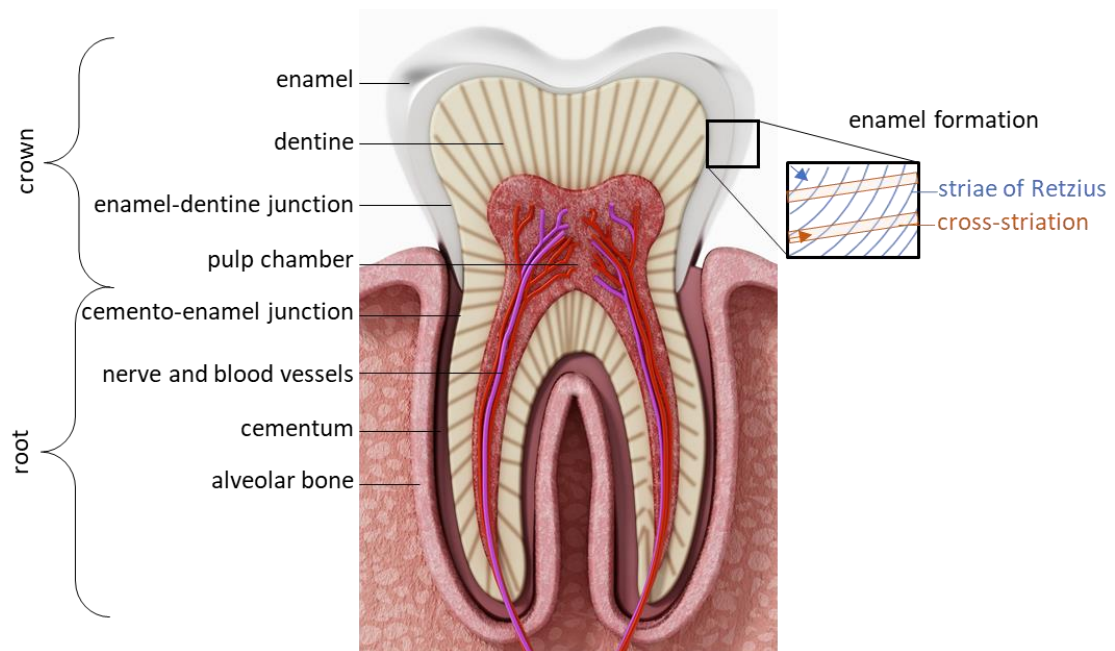


Figure 2.3. Simplified diagram of a human tooth (molar) and enamel formation. Image modified from Cigdem/Shutterstock.com

Human teeth begin forming *in utero* at 14 weeks and the layered structures are secreted at consistent rates throughout development (Hillson, 1996, 2014). The enamel matrix is formed by amelogenesis, the secretion and maturation of the enamel matrix by ameloblast cells (Hillson, 2005). Striae of Retzius, or Retzius lines, are incremental bands of enamel matrix, and are also referred to as perikymata when they appear on the outer surface of enamel (Retzius, 1837; Goodman and Rose, 1990; Hillson, 2005; Mahoney *et al.*, 2017). Cross-striations of enamel are approximately 2–6µm apart and are believed to represent a 24 hour growth cycle (Bromage and Dean, 1985; Beynon and Wood, 1987). Additional information regarding the histology of enamel can be found in (Hillson, 2005, 2014).

Disruptions in the secretion of the enamel matrix can result in hypoplasia or hypocalcifications (opaque areas, lines pits or grooves in enamel – Goodman and Rose 1990; Hillson, 2014, and Figure 2.4). When the body experiences stress, whether that is nutritionally driven, psychosocially related, or connected to physiological disruption or disease (or a combination of these drivers), ameloblast activity declines, resulting in diminished enamel thickness during the stress event (Goodman *et al.*, 1980, 1984; Duray, 1996; Hillson, 2005; Grauer, 2012). While there is much debate about the specific aetiology of EH, its presence has been linked to physiological stress, nutritional deficiency, poor uterine environment, infection and low socio-economic status (Goodman *et al.*, 1980; Goodman and Rose, 1990; Armelagos *et al.*, 2009; Radu and Soficaru, 2016; Yaussy *et al.*, 2016). Because EH can be attributed to multiple aetiologies, EH is thus classed as a non-specific indicator of stress. EH is a “nearly indelible record of evidence of physiological disruption” (Armelagos *et al.*, 2009: 265). Extensive research on the matrix deposition of enamel provide a chronological map of teeth which can be used to assign the occurrence of EH to an approximate age during life (Moorrees *et al.*, 1963; Reid and Dean, 2000; AlQahtani *et al.*, 2010). Enamel formation and maturation begins in-utero and continues until approximately 15 years, when the enamel of the latest forming teeth is completely mineralized (AlQahtani *et al.*, 2010; Beaumont and Montgomery, 2015). This enables researchers

to use the prevalence and timing of EH to assess the negative impacts of early-life stress (Armélagos *et al.*, 2009; AlQahtani *et al.*, 2010; Bereczki *et al.*, 2018).

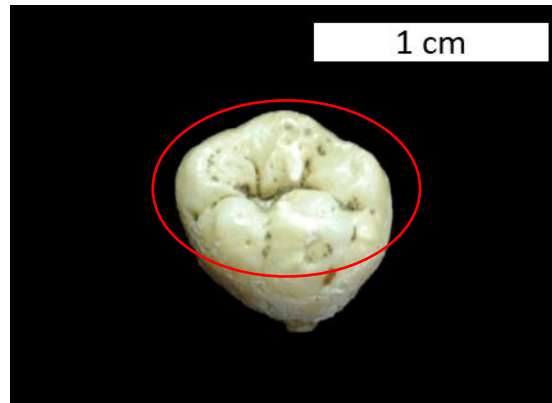


Figure 2.4. Example of EH (pitting).

The method for recording the timing of enamel defects published by Reid and Dean (2000, 2006) separate the enamel surface into deciles to assign an approximate age to the EH. This allows for natural variation in the size of the dentition but can also introduce a degree of intra- and interobserver error (Roberts and Connell, 2004; Henriquez and Oxenham, 2019). A recent study by Henriquez and Oxenham (2019) using exponential regression methods found that the relationship between crown height and that time (chronology) was curvilinear rather than linear. This could implicate additional errors in the decile method, but more research is required to confirm these finds. For the purpose of this research, and keeping with the recommendations of the UK standards, the timing and prevalence of EH was assessed using the Reid and Dean method (2000, 2006) to examine early-life stress in the two populations from Transylvania. The approximate age of the EH was also used in conjunction with isotope life-history profiles to examine possible correlations between EH and changes in isotope values (see Section 3.2.2).

(b) Cribra orbitalia (CO) and porotic hyperostosis (PH)

The phrase porotic hyperostosis is descriptive and can be applied to “any porous enlargement of bone tissues” from marrow hypertrophy (Ortner, 2003:55). However, the phrase cribra orbitalia is often used to refer to porotic lesions on the orbital roof (Figure 2.5) and PH is generally used to describe porotic lesions on the cranium (Brickley and Ives, 2008). Like EH, PH and CO are classified as non-specific indicators of stress because both have been associated with multiple aetiologies (Ribot and Roberts, 1996; Brickley, 2018). CO and PH have both been attributed to various types of anaemia (acquired iron deficiency, megaloblastic, thalassaemia, sickle cell, and parasite-induced hemoblastic) and nutritional deficiencies (e.g. scurvy, rickets) (Stuart-Macadam, 1991; Ortner and Ericksen, 1997; Walker *et al.*, 2009; Grauer, 2012). CO and PH common in female skeletons is believed to be linked to the females’ physiological requirements for iron during lactation, pregnancy and menstruation (Buikstra, 2019, pg. 22).

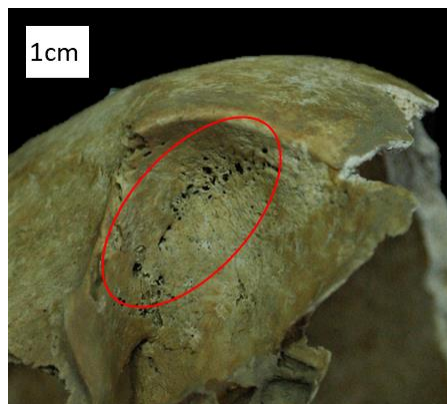


Figure 2.5. Example of porotic lesion (CO) along the left orbital roof.

Although it is difficult to determine the specific aetiology CO and PH, advances are being made in macroscopic recording and more sophisticated techniques for distinguishing between the subtle differences in the types of porotic lesions (Stuart-Macadam, 1991; Walker *et al.*, 2009; Zariņa *et al.*, 2016; Brickley, 2018; Gardner *et al.*, 2019). For example, computed tomography (CT) has been used to measure cranial vault thickness (CVT) to distinguish between scurvy (thicker cranial vaults) and

anaemia (Zuckerman *et al.*, 2007, 2014). Research is also being done to re-classify the diagnostic criteria to improve observer error for CO (Gardner *et al.*, 2019). A combined palaeopathological and biomolecular study (trace element concentrations) has also found a significant correlation between the presence of CO and decreased levels of iron which the authors posit is indicating megaloblastic anaemia as the aetiology (Zariņa *et al.*, 2016). Although these methods are proving to be useful in deciphering the possible aetiology of the lesion, they require advanced tools and infrastructure that may not be widely available to the general research community. Due to equipment, time and budget constraints, imaging techniques were not available for this study. For this reason, the methodology applied followed the UK guidelines for macroscopic identification of CO (Stuart-Macadam, 1991), and the identification of PH was documented as tentative pending radiograph confirmation, which is essential to confirm whether the key characteristics of PH are present – thinning of the outer cranial cortical layer and diploic expansion, and hair on end appearance (Roberts and Connell, 2004; Garcia *et al.*, 2018).

As with most macroscopically based recording methods for observed features, grading systems for severity can introduce error. Because of this, the prevalence of CO and PH were simply recorded as present or absent and acted as a general indicator of stress (specific aetiologies were not assigned). The data were analysed to determine if the prevalence of CO and/or PH negatively affected a person's ability to survive in the past.

(c) Arrested growth

When the body undergoes stress, whether that be from inadequate nutrition or other extrinsic factors, the formation/turnover of bone can slow down or completely arrest (Brickley and Ives, 2008, pg. 33). Arrested growth can manifest in the skeleton as opaque horizontal lines near metaphyses on radiographs of long bones (Harris lines) and/or diminished stature (Martin *et al.*, 1985; Ribot and Roberts, 1996; Watts, 2011; Said-Mohamed *et al.*, 2017). However, the natural remodeling of bone throughout life can resorb the lesions making it difficult to assess (Lewis, 2006). When it is not possible to use radiography, arrested growth can be established in non-adult skeletal

remains by comparing the estimated age of dental formation (AlQahtani *et al.*, 2010) and skeletal growth and epiphyseal fusion stages (Cunningham *et al.*, 2016). As previously mentioned, even in times of nutritional and physiological stress, the dentition continues to form at almost constant rates, providing a more accurate age-at-death. If the estimated age-at-death from long bone length and epiphyseal fusion was younger than that based on dental formation and eruption, that individual likely experienced arrested skeletal growth. Arrested growth can be difficult to assess in adult skeletal remains. If a person survived the stress event during their childhood, the body will attempt to adapt through catch-up growth. This could make it appear as though the person (as reflected in their adult skeleton) never experienced arrested growth. Lower than expected stature in adulthood, i.e. below the mean stature for their population, could be the result of early-life stress from many potential causes (Larsen, 2015 pg. 19).

Arrested growth and diminished stature are often linked with other indicators of early-life stress such as CO, PH and EH (e.g. Steckel, 2005; Buchhorn *et al.*, 2016; Roberts and Steckel, 2019). Undernutrition in infancy can cause an adaptive physiological response where the energy load is directed to the brain and other vital organs, limiting other functions like bone formation/repair (Fogel *et al.*, 1983; Said-Mohamed *et al.*, 2017). The growth of the vertebral neural canal (VNC) diameters can slow during early-life stress, which has been found to have negatively impacted adult health (Watts, 2011; Newman and Gowland, 2015). Application of this method was attempted on the two populations in this study, but due to the poor preservation and fragmentation of the skeletal remains, it could not be used. As previously mentioned, Harris lines signify arrested skeletal growth and are associated with physiological stress, although their precise aetiology is debated (Ribot and Roberts, 1996). The prevalence of Harris lines was not included in this study due to time, financial and equipment constraints. Environmental and psychosocial stressors can also lead to arrested skeletal growth (Kelly *et al.*, 2012; Clark *et al.*, 2014; Wells, 2014). The prevalence of arrested skeletal growth was assessed for the populations in this study to examine the possible negative impacts arrested growth had on frailty and

mortality. Table 2.2 lists the non-specific stress lesions examined and the possible aetiologies associated with each lesion.

Lesion	Differential Diagnosis	Sources
<i>Enamel hypoplasia</i>	- Under- and/or malnutrition - Infection - Metabolic disorders (scurvy, rickets) - Physiological stress	(Goodman <i>et al.</i> , 1984; Ortner, 2003; King <i>et al.</i> , 2005)
<i>Cribriform orbitalia</i>	- Anaemia (iron, megaloblastic, hemolytic) - Under- and/or malnutrition - Infection - Metabolic disorders - Physiological stress	(Stuart-Macadam P, 1985; Walker <i>et al.</i> , 2009; Zuckerman <i>et al.</i> , 2014)
<i>Porotic hyperostosis</i>	- Anaemia - Under- and/or malnutrition - Infection - Metabolic disorders - Physiological stress	(Stuart-Macadam P, 1985; Walker <i>et al.</i> , 2009)
<i>Arrested skeletal growth</i>	- Under- and/or malnutrition - Infection - Metabolic disorders - Physiological stress - Anaemia	(Steckel, 2005; Watts, 2011; Said-Mohamed, Pettifor and Norris, 2017)

Table 2.2. Summary of the non-specific indicators of stress studied, the differential diagnoses for each lesion.

(ii) Metabolic disorders

In 1948 Albright and Reifenstein defined metabolic bone disease (MBD) as conditions which affected bone formation and remodeling processes involving the entire skeleton. Like “stress,” MBD has been adapted and expanded over many years of research. For the purpose of this study, MBD refers to conditions affecting the formation and remodeling of the bones of the skeleton due to inadequate intake or absorption of nutrients (Brickley and Ives, 2008, pg. 2). While MBD can be acute, it is often a chronic process that an individual might have lived with for many years. Because the skeletal manifestations of malnutrition are systemic, the general patterns/distribution of lesions on the skeleton often indicate multiple aetiologies. Co-morbidities can also occur (e.g. iron deficiency anaemia and scurvy). Subtle differences in the location of skeletal lesions can help to decide which MBD(s) were most likely and prevalent at the time of death of the person (discussed further in subsequent sections). As for other morbidities, intrinsic factors (age, sex, ethnicity,

immune system strength) and extrinsic factors (e.g. the lived environment, cultural practices, socio-economic status) can greatly impact the development of MBD. For example, attritional cemeteries are often associated with a particular cultural group, which can help to interpret various aspects of the lives of the burial population (e.g. Robb *et al.*, 2001). While historical documentation of food available during the Middle Ages often reflects the diets of the noble and elite families, it usually neglects to mention what the common citizen ate, thus skewing information about the quality and quantity of food available (Brickley and Ives, 2008, pg. 12).

It is clear that historical sources for diet can be limited, but stable isotope analysis can also help to establish dietary and nutritional stress patterns at the individual and population levels (e.g. Schoeninger *et al.*, 1999; Balasse *et al.*, 2001; Beaumont and Montgomery, 2016 and see Section 3.2.2). Another challenge related to the skeletons that are studied is that MBD can weaken the structure of bones making them more susceptible to taphonomic damage. This adds to the difficulty of assigning a specific aetiology to the bone changes and leads to classifying individuals into a general MBD category. This problem can also be conflated by age-related bone loss (osteoporosis) which is/was common in older women (Black and Rosen, 2016). Problems with older-adult age estimation methods, the lack of an acceptable standardised biological sex estimation methods for non-adult skeletons, and age-related bone loss in older women can all impact the demographic profile of a population. The importance of the “Osteological Paradox” cannot be understated in these situations, and care must be taken when establishing the prevalence of MBD across age-at-death and biological sex categories (Wright and Yoder, 2003; Brickley and Ives, 2008).

Scurvy and rickets/osteomalacia have become some of the most studied MBDs in bioarchaeology following the advances by Ortner (2003) (discussed further in subsequent sections). Scurvy has been linked with long voyages, famine and long-term military campaigns due to the inadequate access to proper foods (Stone, 1966; Wells, 1975, pg. 756; Ortner, 2003, pg. 384; Brickley and Ives, 2008, pg. 44). Rickets and osteomalacia are commonly associated with cultural and religious practices, socio-economic status, the environment and poor living conditions, each potentially leading to lack of UV light exposure, the main factor causing vitamin D deficiency

(Ortner, 2003; Holick, 2003; Mays *et al.*, 2006; Snoddy *et al.*, 2016). Both populations in this study lived during times of political transition, periods of starvation and famine and were possibly from mixed socio-economic backgrounds. These factors could have increased their frailty and affected their ability to survive. Scurvy, rickets, and osteomalacia were assessed to examine levels of metabolic stress within and between the two populations from Transylvania. Histological and radiographic analyses were not used and therefore the prevalence data only reflect macroscopic assessments of the skeletons. The prevalence of MBD within this study followed the lesion description and distribution patterns recommended in the UK guidelines for palaeopathological data collection (Roberts *et al.*, 2004) and information from Ortner (2003) and Brickley *et al.* (2008).

(a) Scurvy

Scurvy (also known as Moller-Barlow's disease) is the result of vitamin C deficiency (Ortner, 2003, pg. 384; Meyer, 2016). Vitamin C (ascorbic acid) is involved in the formation and maintenance of collagen, the metabolism of iron and folate, and maintaining immune function (Brickley and Ives, 2008, pg. 47). Although most mammals can produce their own ascorbic acid, humans cannot and need to obtain vitamin C from dietary resources (Stone, 1966). Vitamin C is a water-soluble molecule that is most commonly found in fresh fruits (high in citrus) and vegetables (green peppers, potatoes, cabbage, tomatoes), with small amounts available in fish, meat and milk (García-Closas *et al.*, 2004; Brickley and Ives, 2008, pg. 42-44). Details regarding the evolutionary mechanisms and the process of synthesizing vitamin C can be found in Stone (1966). While scurvy was commonly associated with long sea voyages during the Age of Discovery (15th–17th C. AD- Wells, 1975), the earliest possible description of the signs and symptoms of scurvy date back to Hippocrates in the 5th to 4th C. BCE (Stone, 1966). This vitamin is also found in human breastmilk, which normally contains adequate levels of vitamin C required for infant development (Grewar, 1965). However, if a mother is vitamin C deficient or alternative milk sources were used (e.g. cow's milk) the infant may not receive adequate levels of vitamin C (Grewar, 1965; Fain, 2005). A healthy human body can

last for 29 to 90 days completely deprived of ascorbic acid before symptoms develop (Pimentel, 2003). The modern recommendation of vitamin C is 30mg/day, but research has found that just 6.5-10mg/day is sufficient to prevent scurvy (Cheung *et al.*, 2003; Brickley and Ives, 2008, pg. 47-48). Pregnancy and lactation can also increase the required daily intake of vitamin C to 70mg/day and 95mg/day respectively (Pimentel, 2003).

Vitamin C is an enzyme involved in numerous physiological processes, and is required for ATP generation (adenosine triphosphate; carries energy in cells) and stabilization of the collagen triple helix (Padayatty and Levine, 2001; Snoddy *et al.*, 2017). Collagen works as a building-block for connective tissues (tendons, ligaments, skin, blood vessels, cartilage, cornea, bone, intestines, intervertebral discs), including being inherent in new bone formation (Armelagos *et al.*, 2014). Inadequate levels of vitamin C can result in soft tissue and bodily changes such as fatigue (Hodges *et al.*, 1971), emotional changes (*ibdi*), swollen gums (*ibdi*), hypertrophy of the gingiva (Fain, 2005), periodontal bleeding (Hirschman and Raugi, 1999), bleeding of the skin (Hirschman and Raugi, 1999; Fain, 2005), and bleeding into joints and muscles (Maat, 2004; Fain, 2005). Insufficient vitamin C can also lead to a compromised immune system making the individual more susceptible to other factors like infection (Follis *et al.*, 1950; Ortner, 2003). The main signs and symptoms of scurvy are haemorrhagic in nature and are due to weakened soft tissue and bone as the result of poor collagen synthesis (Ortner, 2003, pg. 383; Brickley and Ives, 2008, pg. 48; Armelagos *et al.*, 2014). Skeletal manifestations of scurvy include antemortem tooth loss, slower bone turnover rates, irregular dentine production, subperiosteal new bone formation and haemorrhagic staining (Ortner, 2003; Maat, 2004; Brickley *et al.*, 2008). As previously stated, this study followed the UK guidelines for recording scorbutic skeletal lesions (Brickley and Ives, 2008, pg. 57-61; Brickley and Mays, 2019, pg 351-537). Table 2.3 lists the diagnostic skeletal lesions associated with scurvy, as well as the other possible causes for those lesions (differential diagnoses).

Scurvy						
Element	Lesion(s)	Differential Diagnosis	Non-adults	Adults	Diagnostic	Sources
<i>Skull</i>	abnormal porosity/new bone formation (beyond normal variation) on the:	rickets	Y		D	(Ortner and Ericksen, 1997; Sloan <i>et al.</i> , 1999; Ortner, 2003; Brickley and Ives, 2006)
	cranial vault	anaemia				
	sphenoid bone	infection				
	orbits	trauma				
	maxilla	normal growth				
	mandible					
	new woven bone on:		Y		D	
	cranial vault					
<i>Dentition</i>		non-specific stress				(Wolbach and Howe, 1926; Jaffe, 1972; Hillson, 1996; Pangan and Robinson, 2001; Ortner, 2003)
	hypoplastic defects	congenital syphilis	Y		G	
	antemortem tooth loss		Y	Y	G	
	caries	periodontal disease		Y	G	
	periapical lesions					
<i>Ribs</i>	transverse fractures at costochondral sites	trauma		Y	D	(Ortner, 2003:386)
	fracture near costochondral junction	trauma	Y		D	
	scorbutic rosary (enlargement of bone near costochondral junction)	rickets	Y		D	
<i>Vertebrae</i>	osteopenia	trauma		Y	G	(Joffe, 1961)
	bi-concave compression	osteoporosis ,tuberculosis		Y	G	
<i>Pelvis</i>	porosity	infection	Y		G	(Ortner, 2003)
	new woven bone	normal growth				
	sub-periosteal haemorrhage causing staining of the bone (rare)	postmortem changes				
<i>Long Bones</i>		infection	Y	Y	D	(Wolbach and Howe, 1926; Ratanachu-Ek <i>et al.</i> , 2003; Fain, 2005)
	new woven bone (near metaphyses)	trauma				
		normal growth				

Table 2.3. The macroscopic skeletal lesions commonly associated with scurvy and the possible differential diagnoses (after Brickley and Ives (2010, pg 57,61). Key: D – skeletal lesion is diagnostic of scurvy: multiple D changes are required for diagnosis; G – general lesion associated with many metabolic disorders and not diagnostic alone (i.e. not pathognomonic; combine with D lesions).

The most common factors associated with scurvy in the past were severely restricted diets, food storage and preparation practices (Brickley and Ives, 2008, pg. 57-58; Snoddy *et al.*, 2017; Brickley and Mays, 2019, pg. 532). Fresh foods are difficult to obtain during extended travel (Tickner and Medvei, 1958; Pendery and Koon, 2013), famine (Crawford, 1988), and during war and/or captivity (Prinze, 1999; Hampl *et al.*, 2004). Prolonged storage and cooking practices also reduce the amount of vitamin C in foods making people using these practices more susceptible to scurvy (Grewar, 1965; Fain, 2005). For example, wealthy families in 19th C. AD London were able to afford heat-treated milk and manufactured infant foods, but these foods were low in vitamin C due to the heating processes, resulting in infantile and non-adult scurvy (Pimentel, 2003). Recovery from scurvy can be relatively rapid. Once vitamin C is incorporated into the diet, improvements can be seen within 48 hours (Greenfield, 1986) with most of the physical signs and symptoms resolving within two weeks (Pimentel, 2003). Rapid bone turnover in non-adults can mean histological manifestations of scurvy could be eradicated as soon as three months after receiving adequate levels of vitamin C (Follis *et al.*, 1950). Therefore, individuals with skeletal lesions indicative of scurvy either experienced chronic vitamin C deficiency or died before the lesions could full heal.

Skeletal evidence of scurvy has been identified in Romania during the Middle Ages (Osterholtz *et al.*, 2014). Local resources and agricultural practices in Transylvania could have provided adequate sources of vitamin C in the past (Boner, 1865), but both populations investigated in this study lived during times of political transition, famine and/or climate change. These factors may have restricted the access these groups had to adequate resources. Skeletal lesions were recorded that could be used to assess the prevalence of scurvy as an indicator of nutritional and/or socio-economic stress within and between the two populations from Transylvania.

(b) Vitamin D deficiency

Vitamin D is a pro-hormone which requires synthesis/transformation by the human body (Holick, 2003). The different terminology used to describe this process refers to the metabolic status of vitamin D at difference stages. More information regarding

the terminology and the synthesis of vitamin D in the human body can be found in Brickley and Ives (2008), Snoddy *et al.*, (2016), and Holick (2007). Rickets (vitamin D deficiency in non-adults) and osteomalacia (vitamin D deficiency in adolescents and adults) are the result of inadequate amounts of vitamin D either due to low UVB exposure or insufficient intake/access to proper foods, causing pathological changes to occur (Brickley and Ives, 2008, pg. 77). Because pathological manifestation is the final stage of vitamin D deficiency, its skeletal manifestations are thought of as the end of the spectrum of morbidity (Holick, 2006; Snoddy *et al.*, 2016).

Vitamin D is required for the proper mineralization of the organic bone matrix osteoids (Mays *et al.*, 2006; Holick 2007; Brickley and Ives, 2008, pg. 75). The primary source of vitamin D is cutaneous exposure to sunlight (5-15 minutes/day) and subsequent production, but dietary vitamin D can also be found in resources such as oily fish and eggs (Holick, 2003). Insufficient levels of vitamin D in the blood serum (<75 nmol/l) can affect the absorption of calcium and phosphorus in the intestine (Holick and Adams, 1998; Pearce and Cheetham, 2010). This prompts the body to increase bone resorption in order to release calcium into the blood serum. Skeletal manifestations occur when vitamin D levels in blood serum drop below 25 nmol/l (Pearce and Cheetham, 2010). The time it takes for bone changes to manifest varies depending on the age-related rate of cell turnover for each individual (Pearce and Cheetham, 2010). This is due to the slower rate of turnover in adults, and has also been associated with decreased kidney function (reduced vitamin D synthesis) and age-related osteoporosis during late adulthood (Holick and Adams, 1998; Brickley and Ives, 2008, pg. 79).

The terms rickets and osteomalacia describe different processes of vitamin D deficiency. Rickets affects the endochondral (cartilaginous) bone growth in non-adults (Holick, 2006; Lewis *et al.*, 2007; Snoddy *et al.*, 2016). Osteomalacia affects the regions of trabecular bone in the axial skeleton, and individuals with prolonged osteomalacia can experience bending of bones due to unmineralized osteoids (Ortner, 2003, pg. 393; Whyte *et al.*, 2009). Therefore, non-adults can have both osteomalacia and rickets, but adolescents and adults whose bones are fully formed can only be classified as having osteomalacia (Snoddy *et al.*, 2016). Rickets is common

during periods of rapid growth, such as 8 to 24 months old and during adolescence, and presents with abnormally thin cortical bone due to decreased mineralization of osteoid (Oppenheimer and Snodgrass, 1980; Whyte and Thakker, 2009). Columnar cartilage accumulates below the growth plates, which can cause swelling in the sternal region of the chest and a flared appearance near the metaphyses of long bones (Holick, 2006; Mays *et al.*, 2006). Bowing deformities are the result of mechanical loading (crawling or walking) on bones with poor mineralisation (Ives and Brickley, 2014). The bending deformities may correct themselves through remodeling over time once adequate vitamin D levels are restored (Ortner and Mays, 1998; Holick, 2003). Extreme bending deformities from severe rickets can last into adulthood, well after the individual's vitamin D levels returned to normal, and this is considered an indicator of healing or healed rickets and residual rickets (Mays *et al.*, 2006; Snoddy *et al.*, 2016). Like scurvy, vitamin D deficiency can affect the structural integrity of bones making them more susceptible to taphonomic damage. This study followed the UK guidelines for recording lesions associated with vitamin D deficiency (Roberts and Connell 2004) alongside Brickley and Ives (2008, pg. 103-108) and Brickley and Mays (2019, pg. 540-547). Table 2.4 lists the diagnostic skeletal lesions associated with rickets and the differential diagnoses for each lesion.

Rickets				
Element	Lesion(s)	Differential Diagnosis	Diagnostic	Sources
<i>Skull</i>	irregular porous new bone formation	normal growth, scurvy, anaemia	D	(Hess, 1930; Pettifor and Daniels, 1997; Ortner and Mays, 1998; Pettifor, 2003; Mays <i>et al.</i> , 2006)
	frontal and parietal bossing	anaemia, scurvy	G	
	cranial bone thinning	osteopenia	G	
	craniotabes	normal variation, premature birth, osteogenesis imperfecta, congenital syphilis	G	
	delayed fontanelle closure	congenital/developmental condition, hydrocephaly	G	
	formation of large square-shaped head	swaddling, normal variation	G	
<i>Dentition/ Mandible</i>	medial angulation of mandibular ramus		D	(Hess, 1930; Hillson, 1996; Berry <i>et al.</i> , 2002)
	hypoplastic defects	influence of sex, scurvy, childhood stress,	G	
	delayed eruption of dentition	nutritional problems, disease	G	
	dental caries		G	
<i>Ribs/ Sternum</i>	straightening of lateral rib shaft	age-related deterioration	D	(Pettifor and Daniels, 1997; J. Scheuer and Black, 2000; Pettifor, 2003)
	Rib/neck/angle changes	age-related deterioration	D	
	"pigeon-chested" related rib angulation and sternal protrusions	Scurvy	D	
	"rachitic rosary" flaring and swelling of costochondral joints	Scurvy	D	
<i>Vertebrae</i>	scoliosis or kyphosis	developmental or congenital conditions underlying vertebral fractures due to infection osteoporosis	D	(Hess, 1930; Pettifor and Daniels, 1997; Pettifor, 2003)
<i>Pelvis/ Sacrum</i>	"protrusio acetabulae"; acetabulae pushed dorsally and angled anteriorly		D	(Hess, 1930; Ortner and Mays, 1998)
	ilium curved medio-laterally	developmental conditions	D	
	uneven growth of pelvis		G	
<i>Long Bones</i>	flaring of distal metaphyses	scurvy	D	
	growth plate porosity	PMD	D	

Rickets (continued)				
Element	Lesion(s)	Differential Diagnosis	Diagnostic	Sources
	fraying of growth plate margins	PMD	D	
<i>Long Bones (cont.)</i>	"cupping" deformities (growth plates and metaphyses)	severe trauma	D	(Hess, 1930; Pettifor and Daniels, 1997; Mays, 1998; Ortner and Mays, 1998; Pettifor, 2003)
	genu varum/varus (bending of forearm (crawling) and leg bones (walking))	scurvy PMD	D	
	bone thickening from healed rickets	trauma, non-specific infections, scurvy, congenital syphilis	D	
	coxa-vara: angulation of femoral neck	osteopenia, developmental conditions	D	
	"knock-knee" angulation of knee joint	Blount's disease	G	
	bending/compensatory remodeling	trauma, non-specific infections, scurvy, congenital syphilis	G	
	arrested growth, shortening of limbs, gross deformity	trauma, childhood illnesses	G	
	fractures	scurvy, congenital syphilis, osteogenesis imperfecta, variant form of rickets	G	

Table 2.4. The macroscopic skeletal lesions commonly associated with rickets and the possible differential diagnoses (after Brickley and Ives 2010: 103-105). Key: D – skeletal lesion is diagnostic of scurvy: multiple D changes are required for diagnosis; G – general lesion associated with many metabolic disorders and not diagnostic alone (i.e. not pathognomonic: combine with D lesions; PMD – post-mortem damage.

There are numerous factors that can affect a person's access to adequate vitamin D. Genetic adaptations of melanin and skin pigmentation (cutaneous absorption of UV light) can alter dermal production of vitamin D (Holick, 2003). Cultural practices, socio-economic status, living conditions and environment can also impact the amount of sun exposure and resources a person received. Limited sun exposure and clothes which fully cover the body during pregnancy can increase the risk of mother and infant vitamin D deficiency (Serenius *et al.*, 1984; Kazemi *et al.*, 2009). For example, Turkish women who wear clothing covering their entire body for cultural and religious reason were found to have increased risk of osteomalacia between the ages of 21 and 50 (Güllü *et al.*, 1998). A person's socio-economic status can affect their access to proper foods and living conditions, such as the amount of open outside space, air pollution. Living in urban environments with dense air pollution and tall buildings has also been found to limit a person's sun exposure (Sachan *et al.*, 2005). Populations living at greater latitudes experience drastic changes in seasonal sunlight exposure and can even stop producing vitamin D during winter months (Holick and Adams, 1998). Vitamin D deficiency can increase a person's frailty and has been linked to increased risk of infection, cardiovascular disease, autoimmune diseases and certain types of cancers (Snoddy *et al.*, 2016). All these factors can greatly impact a person's ability to survive. The two Transylvanian populations in this study were examined to assess the prevalence of vitamin D deficiency in the past.

2.3. Summary

The region of Transylvania has been highly coveted by many political powers for the last millennium. The rich natural resources, natural fortification provided by the Carpathian Mountains, and geographical location between the Mediterranean and the Balkans resulted in continued population movement due to military campaigns and trade routes. This study utilized macroscopic skeletal analysis to establish demographic, morbidity and mortality profiles of two populations who lived in Transylvania during the Migration Period and Middle Ages. As previously mentioned, some pathological conditions can weaken bone structures resulting in greater taphonomic damage in the burial environment. The varied preservation and high

level of fragmented skeletal remains of the two populations analysed in the study limited the amount of information that could be obtained from macroscopic skeletal analyses alone. Isotopic analysis can help to reveal the diet, nutritional status, and mobility of past populations (Chapter 3). By combining the macroscopic and palaeopathological data with isotope analysis, it was possible to generate a greater breadth of knowledge about the interrelated factors of early-life stress and how it affected survival in these populations in Romania.

Chapter 3: An introduction to isotope analyses and their applications in the field of bioarchaeology

Macroscopic skeletal analysis provides researchers with a glimpse into the morbidity and mortality of past peoples. However, this type of analysis is limited to those trauma and diseases that result in macroscopically visible changes in the bones and teeth. However, this does not account for those individuals who died before changes could manifest in the skeleton or for diseases that only affect the soft tissues of the body. There are also intrinsic (e.g. psychosocial stress) and extrinsic (e.g. migration) risk factors that might have impacted a person's frailty, making them more susceptible to developing poor health. As discussed in the previous chapter, a multitude of factors can exacerbate and result in early-life stress. The application of isotope analysis within the field of bioarchaeology has afforded researchers the opportunity to expand on what we can learn from macroscopic analysis of past populations, as well as enhancing a multifactorial approach to understanding the interrelated risk factors for early-life stress.

Isotopes are incorporated into the body via ingested food and water and are stored in the developing bodily tissues, allowing researchers to examine snapshots of that person's life during development. For example, stable carbon (C) and nitrogen (N) isotope analysis can reveal how long a person was breastfed and the length of the weaning process (Balasse *et al.*, 1999b; Fuller *et al.*, 2006; Beaumont *et al.*, 2015; Burt, 2015), dietary patterns (DeNiro and Epstein, 1978, 1981; Schoeninger *et al.*, 1983; Agurauja *et al.*, 2018; Gamarra *et al.*, 2018), and periods of physiological/nutritional related stress (Fuller *et al.*, 2005; Mekota *et al.*, 2006; Wadhwa *et al.*, 2010; Hatch, 2012; King, Halcrow, *et al.*, 2018). Strontium (Sr) and oxygen (O) isotope analyses are also commonly used together to determine if a person's childhood isotopes match the region in which they were buried (Ericson, 1985; Montgomery, 2010; Evans *et al.*, 2012; Neil *et al.*, 2017; Vaiglova *et al.*, 2018). Having a deeper and more nuanced knowledge about how past people lived and died provides a greater understanding of the demographic, palaeopathological and historical significance of each populations studied.

Isotope research in bioarchaeology has been validated in a wide variety of successful studies (see subsequent sections). Interpreting isotope data can be challenging. However, historical documents, archaeological data and isotope biosphere mapping are all very useful resources for interpreting isotope data. As mentioned in Section 2.1, the historical data from Transylvania during the Migration Period and Middle Ages is scant and can vary depending on the perspective of the historian. Compared to other European regions, there remains very little isotopic data from human skeletal remains recovered within the Transylvanian Basin. Because of this, historical, archaeological, osteological and biomolecular data from nearby regions such as Hungary were compiled to help contextualise the data from this study in order to begin to fill the bioarchaeological gaps in the history of Transylvania. Section 3.1. introduces early isotope research, how isotopes are incorporated into the human body, and how the resulting isotope ratios can be utilized within bioarchaeology. Section 3.2 provides information about carbon and nitrogen stable isotope analysis and how it can be used to examine diet, cultural practices (breastfeeding and weaning) and periods of “stress” for the two populations from Transylvania. Section 3.3 introduces strontium and oxygen isotopes and how childhood isotope ratios can be used to establish the local isotope biosphere range, as well as explore individual mobility status (local or non-local when compared to their burial location).

3.1. Introduction to isotope analysis

The field of isotope analysis was founded in geochemistry. In 1913, Margaret Todd and Frederick Soddy coined the term “isotope” to discuss variations of an element with physically identical properties which had different atomic masses (Soddy, 1913). Over the next few decades researchers such as J.J. Thomson, F. Soddy, J. Chadwick, G. Gamow, E. Rutherford and F.W. Aston continued to expand the understanding of the structure of atoms. Thomson and colleagues (1921) identified that the element chlorine had two isotopes with different masses and the same atomic charge which led to Chadwick (1932) to propose the existence of a subatomic particle called a neutron (subatomic particle with a neutral charge). The most accepted definition of an isotope is “a particular form of an element defined by a specific number of

neutrons” (Sharp, 2017, pp. 21). For example, the element carbon has two stable isotopes and one radioactive isotope (^{14}C): ^{12}C (6 proton, 6 neutrons); ^{13}C (6 protons, 7 neutrons); ^{14}C (6 protons, 8 neutrons) (Sharp, 2017). Early work focused on radioactivity (i.e. spontaneous disintegration of large atoms to smaller fragments) and interest in stable isotopes (i.e. those which do not undergo spontaneous disintegration) would follow (Sharp, 2017, pp. 11). Over the next two decades research found that processes such as melting, crystallization, and volatilization could cause variations in the abundance of isotopes (fractionation) in nature and that this fractionation of light elements should also theoretically occur in living matter (Gilfillan, 1934; Urey and Greiff, 1935; Wickman, 1941). An instrument was being created and refined and in 1940 the theory could finally be tested when a mass spectrometer was built to measure the isotope abundance of a sample (Nier, 1940). Urey (1947) published calculations for the isotope fractionation of stable isotopes of light elements, launching the field of light stable isotope geochemistry.

As the field of isotope analysis progressed, the application of these methods began to be implemented in many other disciplines such as climatology, plant physiology, ecology, archaeology, meteorology. The reader is referred to Sharp (2017) and Roberts *et al.* (2017) for terminology and guidelines for isotope analysis. Archaeologists and ecologists began using the systematic difference between the isotopic composition of the diet and the isotope ratios of the consumer’s tissues to infer dietary patterns in past populations. The environmental sciences began to map geographical movements of species via strontium and oxygen isotope ratios, allowing researchers to explore migration patterns (Harman *et al.*, 1981; Price *et al.*, 1994). Researchers also examined the influence different dietary resources had on light isotope ratios of carbon and nitrogen in animal tissues (DeNiro and Epstein, 1978, 1981; Schoeninger *et al.*, 1983; Schoeninger and DeNiro, 1984). Within the field of bioarchaeology, the use of isotope analysis has provided researchers with a means of expanding our knowledge at an individual and population level (discussed further in subsequent sections).

It is important to remember that isotope data cannot be analysed in a vacuum. There are some key points to be aware of when undertaking isotope analysis.

- A single isotope ratio can represent several possibilities. For example, elevated nitrogen ($\delta^{15}\text{N}$ values) can signify the ingestion of breastmilk, physiological stress, and/or a change in the protein component of a person's diet (Section 3.2).
- A single strontium isotope ratio ($^{87}\text{Sr}/^{86}\text{Sr}$) indicates the age and lithology of the bedrock where a person's food was grown during childhood which could match the geology of the region in which they were buried; however, it can also indicate other regions with similar bedrock.
- It is also important to understanding the composition of the body's tissues, and the possible postmortem alteration to those tissues (e.g. bone) that can occur in the burial environment (diagenesis).

These factors make certain tissues better for specific isotope analyses, such as the use of enamel for strontium isotope analysis. When preparing for isotope analyses, it is critical to account for as many variables as possible in order to better understand the life-history profiles for each individual.

3.1.1. Isotopes in body tissues

As the body grows and maintains its tissues (e.g. dentine, enamel, bone), elements from the diet and environment are incorporated into the developing tissues (Ambrose, 1990; Balasse *et al.*, 1999a; D'Ortenzio *et al.*, 2015; Reynard and Tuross, 2015). Systematic isotope fractionations and the resulting isotope ratios of these elements can reveal information about certain periods of life of people who lived in the past (Schoeninger *et al.*, 1983). This section introduces the processes behind the formation of dentition and bone, and how those processes are used to assign isotope ratios to specific periods of life.

As previously stated, the structure of teeth makes them less susceptible to taphonomic and diagenetic alteration in the burial environment compared to bone.

The maxillary and mandibular deciduous dentition begins forming *in utero* encapsulating the isotope ratios from the mother's diet in the earliest forming tissues (AlQahtani *et al.*, 2010; Hillson, 2014). The permanent teeth begin to form as early as 0.3 years after birth and continue to form until adolescence/early adulthood (AlQahtani *et al.*, 2010; Beaumont and Montgomery, 2015). Therefore, isotope data from enamel and dentine reflect childhood and adolescent isotope ratios. Both enamel and dentine are secreted and mineralized at known rates. The reader is referred to Section 2.2.3 for information regarding secretion and mineralization rates of enamel. The stages of formation of specific sections of tooth enamel correlate to an approximate age during life. For example enamel from the crown of a permanent first molar reflects the period between ~0.3 to ~3.5 years of age (AlQahtani *et al.*, 2010; Beaumont and Montgomery, 2015). The permanent third molar is typically the last tooth to form, with the crown being completed around 14.5 years of age. (AlQahtani *et al.*, 2010; Beaumont and Montgomery, 2015). As enamel is mostly inorganic and has minimal diagenetic interaction with the burial environment, this makes enamel a suitable body tissue for strontium and oxygen isotope analysis (Bentley, 2006).

Dentine, the dense tissue beneath enamel, is secreted and mineralised at a rate of 3–5 μm per day and is fully mineralized within 5–8 days after secretion (Schour and Poncher, 1937; Kawasaki *et al.*, 1980; Dean and Scandrett, 1995). The initial matrix of dentine is almost entirely organic (fibrous collagen protein), with mineral apatite crystallites then being “seeded” into the matrix, resulting in tissue approximately 60% mineral by weight (Hillson, 2014). Figure 3.1 is a simplified diagram of the structure and the direction of dentine formation. Isotope analysis of bulk dentine (i.e. the entire tooth) would reflect the average isotope ratios for the entire period of formation. Incrementally sampled dentine provides isotope ratio snapshots from defined periods of life and enables changes to be seen throughout development. As demonstrated in Figure 3.1, the formation and mineralization of dentine is complex. While micro-sampling techniques are continually improving, the most common methodology involves straight horizontal sections to be taken from the earliest forming dentine (cuspal dentine) to the root apex. For example, Method 2 outlined

by Beaumont and colleagues (2013) suggests 1mm increments which correspond to ~100–150 days of formation, depending on the dentine thickness between the pulp chamber and the EDJ/CDJ. Secondary and tertiary dentine may also be secreted to repair damaged primary dentine (e.g. due to trauma, caries or wear). Current methodology and guidelines suggest sampling from areas without damage/lesions and to abrade the surface of the pulp chamber prior to sampling to be sure only primary dentine is sampled (Beaumont et al., 2013a; Roberts et al., 2017).

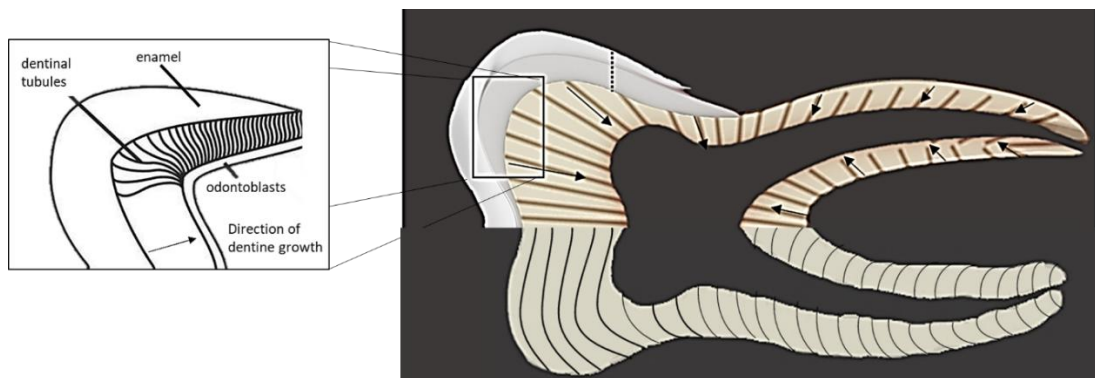


Figure 3.1. Diagram of the structure and direction (arrows) of dentine formation. Modified from Beaumont et al. (2013).

The rate of dentine secretion and mineralization can vary between tooth types (i.e. deciduous vs permanent) and along the length of a tooth. The deciduous dentition forms at a faster rate compared to the permanent dentition. Dentine secretion rates for deciduous teeth can vary between 3.2 and 4.4 μm per day. The permanent teeth that have tall crowns have been found to secrete dentine at rates of approximately 5 to 6 μm per day, while the cervical region of the permanent teeth, close to the EDJ and the CDJ, can slow to rates around 1.3 and 2.0 μm per day (Dean and Scandrett, 1995). When sampling for incremental analysis, the horizontal sections bisect a varying number of depositional layers of dentine depending of the stage of formation and the region of the tooth being sectioned. This means that the isotope values (e.g. $\delta^{15}\text{N}$) obtained from a single increment reflects an average of the isotope ratio from each depositional layer, which corresponds to an approximate age during development. Therefore, sectioning along the curve of dentinal tubules might not

actually increase the resolution of the isotope signal. This is because the value would still represent the average of the isotope ratios for each tubule, due to the direction of mineralization (Beaumont et al., 2013a, 2013b). Incremental dentine isotope profiles provide age-related changes for isotope ratios throughout development, allowing researchers to examine whether a person's diet and breastfeeding and weaning strategies led to early-life stress.

Adult carbon and nitrogen isotope ratios from bone can be examined to establish the accumulated isotope ratios of the years prior to death. As bone grows and maintains its structure, tissue turnover accumulates isotope values over many years. For example, human femoral cortical bone can provide values from 10–20 years prior to death and has been found to have substantial collagen that has been synthesized from the adolescent years (Ambrose, 1993; Hedges et al., 2007). Bone turnover in adolescent males and females is approximately 10–30% per year from 20 to 80 years of age, female turnover rates decrease from 4% to 3% per year while males decrease from 3% to 1.5% per year (Hedges et al., 2007). Bone collagen, the organic component of bone, has been successfully used to establish *in vivo* carbon and nitrogen isotope ratios, while the inorganic component has been found to be problematic for dietary studies due to postmortem alteration in the burial environment (Nelson et al., 1986). Collagen is the most abundant organic fraction of bone and makes up 20–22% of fresh bone weight (Ambrose, 1993). Fresh bone collagen is approximately 40–47% (wt) carbon and 15–17% (wt) nitrogen, making bone collagen a suitable body tissue for dietary and environmental isotope analysis (Ambrose, 1990, 1993).

The small crystalline structure of bone is also susceptible to diagenetic alteration of trace elements from the burial environment (e.g. Sr, Pb). However, the biogenic carbon and nitrogen are major elements in collagen and biogenic carbon and nitrogen isotope ratios from bone and/or dentine collagen, have been found to have little to no alteration from the burial environment. This makes collagen a suitable tissue to establish *in vivo* carbon and nitrogen isotope ratios. However, taphonomic damage can greatly impact the quality of collagen in archaeological bone (Hedges et al., 1995; High et al., 2015). Overall, bone composition and histological features can

also be affected by acidic burial soils which can accelerate the loss of bone mineral components in the burial environment (High *et al.*, 2015). Protein content, porosity, crystallinity and histological preservation are all used as parameters to assess diagenesis (Hedges *et al.*, 1995). Imaging and histological analyses were not performed in this study and therefore quality control parameters were used to assess the preservation of the analysed bone collagen (see Section 4.4.2). Criteria have been established to assess the quality of collagen in order to ensure the isotope ratios obtained are accurate (Schoeninger and DeNiro, 1984; Van Klinken, 1999); these were used in the study. The processes for enamel and collagen sample preparation can be found in Sections 4.4.2. and 4.4.3.

3.2. Carbon and nitrogen stable isotope analyses

The use of carbon and nitrogen stable isotope analysis both in clinical and bioarchaeological research, has been successful, in revealing information about diet, cultural practices (e.g. breastfeeding and weaning), and physiological/nutritional stress in populations and individuals alike. This section introduces carbon and nitrogen isotopes and how the isotope ratios obtained from human tissues can be used to gain information about how past people lived and died.

3.2.1. Carbon and nitrogen isotopes

(i) Carbon isotopes

Carbon has three naturally occurring isotopes, two stable isotopes and one radiogenic isotope (^{14}C). The two stable isotopes of carbon are ^{12}C and ^{13}C and the natural abundance are 98.89% and 1.11%, respectively. Early work on the incorporation of carbon into bodily tissues suggested the majority of carbon in collagen is from dietary protein and to a lesser extent from dietary carbohydrates and lipids (Krueger and Sullivan, 1984; Lee-Thorp *et al.*, 1989; France and Owsley, 2015). The fractionation effects of light isotopes (C, N, H, O, S) are small and therefore the isotope ratio of the sample is presented relative to a reference standard to magnify the slight changes. Carbon isotope ratios are thus reported as δ values (Equation 3.1),

i.e. as the difference between the sample and an accepted reference standard. Because the equation is multiplied by a factor of 1000, the units are ‘per mil’ (‰). If the isotope ratio of the sample is greater than the standard, the δ value will be positive, and vice-versa. Because plant values are more depleted in ^{13}C compared to the international standard (e.g. VPDB), $\delta^{13}\text{C}$ values of human tissues are typically negative (Pollard *et al.*, 2017).

$$\delta^{13}\text{C} = \left[\frac{^{13}\text{C}/^{12}\text{C sample}}{^{13}\text{C}/^{12}\text{C standard}} - 1 \right] \times 1000 \text{ ‰}$$

Equation 3.1. Carbon isotope ratio equation for calculating the delta value (Schoeninger et al., 1983).

Recent studies suggest carbon isotopes of consumer collagen are related to routing of particular amino acids from the consumed collagen (Howland *et al.*, 2003; Froehle *et al.*, 2010), resulting in a diet:collagen fractionation of $\sim 1\text{--}2\text{‰}$ in herbivores (Froehle *et al.*, 2010) and $\sim 2\text{--}5\text{‰}$ in carnivores and omnivores (Balasse *et al.*, 1999b). Isotope fractionation can also help to reveal the type of plant being consumed. Certain types of plants use different photosynthetic pathways. The type of photosynthetic pathway results in different carbon isotope fractionation, making it possible to distinguish between plant types. C_3 plants use the Calvin-Benson cycle to fix reduced carbon and convert it into carbohydrates (Sharp, 2017, Section 7-5). During this process carboxylation occurs (carbon dioxide is condensed with an existing molecule) and the partial removal of CO_2 results in carbon isotope fractionation (Sharp, 2017, Section 7-5). C_3 plants (fruits, vegetables, grasses, herbs, shrubs, aquatic plants) thrive in cooler, temperature climates and at high altitudes. Plants such as millet, maize, sugarcane, tropical grasses and sorghum use C_4 photosynthetic pathways. The C_4 dicarboxylic acid pathway uses the Hatch-Slack cycle which limits C_3 photorespiration and concentrates CO_2 at the site of carboxylation in the plant epidermal layer (Sharp, 2017, Section 7-5). This is beneficial in arid environments and warm temperatures when it is critical to minimize water

loss (Sharp, 2017, Section 7-5). The range of $\delta^{13}\text{C}$ values associated with C_3 , C_4 and marine plant types are listed in Table 3.1.

plants	$\delta^{13}\text{C}$ (range)	source
C_3	-33 to -23‰ (mean: -27‰)	(Schoeninger et al., 1984; Mekota et al., 2006; Sharp, 2017, Section 7-6)
C_4	-16 to -9‰ (mean: -12‰)	(Schoeninger et al., 1984; Sharp, 2017, Section 7-6)
marine	-22 to -16‰ (mean: -19‰)	(Schwarcz et al., 1991; Sharp, 2017, Section 7-6)

Table 3.1. The range of isotope values of associated with different plant types.

Social and environmental factors can also affect $\delta^{13}\text{C}$ values in human tissues. In regions of dense forestation, plants close to the ground incorporate ^{12}C preferentially (canopy effect), resulting in $\delta^{13}\text{C}$ values approximately 5‰ lower than the vegetation at the top of the canopy (Cerling *et al.*, 2004). Dietary shifts due to environmental and socio-economic standing can also be identified through changes in $\delta^{13}\text{C}$ values. For example, during the Great Irish famine, maize (a C_4 plant) was imported to help supplement the diet of starving populations (Beaumont and Montgomery, 2016). The drastic increase in C_4 consumption, compared to the previous C_3 potato dominated diet, led to substantial increases in human $\delta^{13}\text{C}$ values. The application of $\delta^{13}\text{C}$ values within bioarchaeology are discussed further in Section 3.2.2.

(ii) Nitrogen isotopes

Nitrogen is the major element component of air (Sharp, 2017, Section 9-1). The two stable isotopes of nitrogen are ^{14}N and ^{15}N and their natural abundances are 99.6% and 0.4%, respectively. Diatomic nitrogen (N_2) from air is used by organisms in the energy consumption process known as nitrogen fixation (Sharp, 2017, Section 9-2). Nitrogen isotope fractionation is almost all achieved through metabolic-related processes and is dependent on the amount of nutrients and reaction rates (Sharp, 2017, Section 9-3). The difference in nitrogen isotopes ratios of the sample and standard are reported as $\delta^{15}\text{N}$ values (Equation 3.2).

$$\delta^{15}\text{N} = \left[\frac{{}^{15}\text{N}/{}^{14}\text{N sample}}{{}^{15}\text{N}/{}^{14}\text{N standard}} - 1 \right] \times 1000 \text{ ‰}$$

Equation 3.2. Nitrogen isotope ratio equation for calculating the delta value (Schoeninger et al., 1983).

Nitrogen isotope ratios in human tissue primarily reflect the protein content of the diet if sufficient protein is being consumed (DeNiro and Epstein, 1981) which can be used to help explore the palaeoeconomy of a population, such as hunting, pastoralism or agriculture (O’Connell and Hedges, 1999). The tissue of the consumer is generally heavier, enriched in ^{15}N , than the food being consumed (Schoeninger and DeNiro, 1984; Sealy *et al.*, 1987). Approximately 40% of dietary nitrogen is excreted in the urine and is believed to be the reason why animals have elevated values relative to their diet (Schoenheimer, 1964; Sharp, 2017, Section 9-11). The $\delta^{15}\text{N}$ values of the consumer indicate their position in the food chain; carnivores have elevated $\delta^{15}\text{N}$ values compared to the herbivores they consume (Schoeninger and DeNiro, 1984; O’Connell and Hedges, 1999). This fluctuation in values from one type of consumer to another (e.g. herbivore and carnivore) is known as the trophic level effect. Generally, the trophic level shift between dietary sources and consumer collagen is approximately $\delta^{15}\text{N} + 2\text{--}6\text{‰}$ (DeNiro and Epstein, 1981; Schoeninger *et al.*, 1983; Ambrose, 1993).

The $\delta^{15}\text{N}$ value of plants from terrestrial, freshwater and marine ecosystems can vary between -2‰ to 10‰ (Schoeninger and DeNiro, 1984; Katzenberg and Krouse, 1989). For example, Schoeninger and DeNiro (1984) analysed the carbon and nitrogen composition of bone collagen from marine and terrestrial animals and found that those feeding on terrestrial foods exclusively had $\delta^{15}\text{N}$ values of $\leq 9\text{‰}$, and those feeding on marine foods had values of $\geq 15\text{‰}$. Other factors can affect $\delta^{15}\text{N}$ values. When infants consume breastmilk, they are consuming the mother’s secondary protein (milk), resulting in the infant’s values increasing a trophic level above the mother. Similar patterns occur during period of “stress.” The human body responds to stress - nutritional, physiological, psychosocial - by processing stored biomolecules (nitrogen) in the bodily tissues (catabolism) and effectively consuming itself, which

leads to an increase in $\delta^{15}\text{N}$ values (discussed further in Section 3.2.2 - Katzenberg and Lovell, 1999; Hatch, 2012; Beaumont *et al.*, 2015). The climate, precipitation and animal physiology can also affect the baseline variation of isotope ratios documented in a region (Sealy *et al.*, 1987; Gröcke *et al.*, 1997; O'Connell and Hedges, 1999). In arid regions or during period of drought, a physiological response occurs in humans (concentrating urine and excreting isotopically depleted urea) in an attempt to conserve water (Ambrose, 1991; Johnson *et al.*, 1997). Combining carbon and nitrogen isotope data can help to differentiate the possible sources of variation in isotope ratios and the $\delta^{15}\text{N}$ and $\delta^{13}\text{C}$ values can be used to examine dietary patterns, cultural practices and health status within and between archaeological populations (see Section 3.2.2).

3.2.2. Applications of carbon and nitrogen isotope analysis

Isotope values ($\delta^{13}\text{C}$, $\delta^{15}\text{N}$) from human collagen can be used to establish subsistence strategies and dietary practices. Fluctuation in isotope life-history profiles through the analysis of incremental dentine can further reveal changes in the consumption of C and N during development, including those associated with breastfeeding and weaning. The processes and developments regarding the use of stable isotope analyses for dietary and environmental reconstruction can be found in Ambrose (1993) Koch (1994) and Katzenberg (2007). As previously mentioned, baseline variation in isotope ratios can be impacted by a number of factors (Sealy *et al.*, 1987; Gröcke *et al.*, 1997; O'Connell and Hedges, 1999). The lack of isotope data from Transylvania makes establishing baseline ranges difficult, but ecological and environmental data from studies in the surrounding regions were compiled to extrapolate probable isotope ranges and dietary patterns in the Transylvanian Basin.

(i) Dietary patterns

The systematic offset between the isotope ratios of dietary resources and human skeletal tissues has successfully been used to examine dietary patterns (DeNiro and Epstein, 1978; Van Der Merwe and Vogel, 1978; Schoeninger *et al.*, 1983;

Schoeninger and DeNiro, 1984; Murray and Schoeninger, 1988; O’Connell *et al.*, 2012). Figure 3.2 demonstrates the range of values associated with various resources, as outlined in Section 3.2.1. It is important to remember that a single isotope value can reflect several possibilities. For example, the $\delta^{13}\text{C}$ and $\delta^{15}\text{N}$ values of primary (meat) and secondary (milk and eggs) animal protein from the same animal will have the same isotope values because the proteins are derived from one source (Webb *et al.*, 1980; O’Connell and Hedges, 1999). Combining carbon and nitrogen isotope data can also help to establish if marine and freshwater resources were consumed (Schoeninger and DeNiro, 1984; Webb *et al.*, 2015). Examining isotope data in conjunction with historical and archaeological data can help to confirm or establish dietary patterns between groups (e.g. age, sex, religion, socio-economic status).

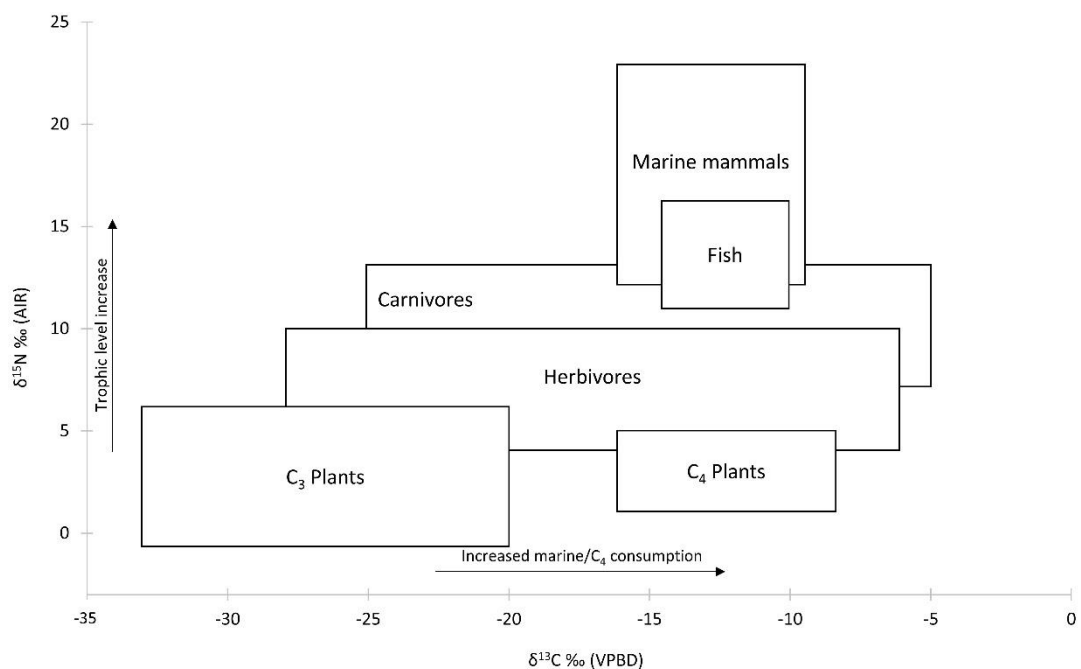


Figure 3.2. Graph representing the range of $\delta^{13}\text{C}$ and $\delta^{15}\text{N}$ values of different dietary resources. Note: boxes reflect the range (endmembers) for each category. Modified from Schoeninger *et al.*, (1983; Schulting, 1998; Pollard *et al.*, 2017).

Of course, differential access to resources can be examined between males and females, age groups and socio-economic groups. In previous work in Romania and other nearby modern day countries, stable isotope life-history profiles of six non-adult individuals from a small population associated with Gepid Kingdom (Archiud,

RO) revealed a mixed C₃/C₄ terrestrial diet, with increased C₄ consumption during adolescence for two individuals (Crowder *et al.*, 2019). Nearby in Hungary, Noche-Dowdy (2015) examined human bone collagen from a socially stratified Avar site during the late Migration Period and found evidence of C₄ consumption across the population, and although there were no statistically significant differences, slight dietary variation was found between social groups, and slightly higher variation between $\delta^{13}\text{C}$ and $\delta^{15}\text{N}$ values in males and females (males > females). This possibly indicates more meat consumption by males compared to females. Murray and Schoeninger (1988) examined diet, status and social structure in Iron Age Central Europe and posit millet cultivation in spring could have produced enough crop to last year-round with young-middle adult males having slightly elevated $\delta^{13}\text{C}$ values compared to females. Childhood and adult dietary patterns were analysed for 24 skeletons from the 13th century AD site of Solt-Tételhegy, Hungary also finding varying quantities of C₄ resources ($\delta^{13}\text{C}_{\text{COL-BONE}}$ -17.1‰, $\delta^{13}\text{C}_{\text{COL-DENTINE}}$ -17.4‰, $\delta^{13}\text{C}_{\text{ENAMEL}}$ -11.1‰). A relatively egalitarian animal protein consumption was also found between individuals whose burial practice suggested different social status ($\delta^{15}\text{N}_{\text{BONE}}$ 10.6‰, $\delta^{15}\text{N}_{\text{DENTINE}}$ 9.8‰ – Gugora *et al.*, 2018). Variations in dietary patterns between different religious groups can also be examined. A comparative isotope study of two groups, one associated with a Christian population and the other a Muslim population, found that the Muslim individuals consumed significantly more fish and C₄ foods compared to the Christian individuals from the same living environment (Alexander *et al.*, 2015). The authors posit the difference in diet was due to inequality of access to foods and/or cultural preferences associated with each religious practice.

Ecology and subsistence strategies can be established by examining human and faunal remains from different time periods. Analysis of human and faunal remains from two Bronze Age sites in Romania found a mostly terrestrial diet with an increase of animal protein during the later phase associated with deliberate movement of livestock through herding or trade (Aguraiuja, 2017; Aguraiuja *et al.*, 2018). Gillis and colleagues (2013) conducted isotope analysis to examine cattle husbandry in south-east Romania (Bordușani- Popină) during the 5th C. BC and found: bone collagen

values of $\delta^{13}\text{C}$ from -11.4 to -7.3‰ and $\delta^{15}\text{N}$ values from 6.3 to 9.7‰, that there was seasonal and age group variation in the types of plants used for animal fodder, that slaughter took place once lactation ended and the primary use of the animals was for meat and dairy. Balasse and colleagues (2013) examined seasonality and animal husbandry of domesticated faunal remains from a 6th C. BC site in southern Romania (Măgura-Boldul lui Moș Ivănuș). They found evidence for extensive herding practices for cattle and pigs, with some sheep having ^{13}C -enriched resources in late winter possibly coinciding with lactation. Comprehensive analysis of all possible factors provides researchers with a greater understanding of past populations. During the Migration Period and Middle Ages, Transylvanian populations were mostly farmers (Giurescu, 1969; Madgearu, 2001; Pop and Nagler, 2010). Milling and processing cereal grains into flour or meal has been practiced in Dacia since the time of the Roman Empire (Bogucki and Crabtree, 2004). Animal domestication, such as pigs, has been documented in Romania since the Neolithic (Evin *et al.*, 2017). These data help to establish subsistence practices and dietary isotope baseline for this region of Eastern Europe. Based on extant stable isotope data, the two populations in this study are expected to have had a mixed C_3/C_4 diet consisting of terrestrial plant and animal resources.

(ii) Breastfeeding and weaning practices

During gestation, the isotope ratios of foetal tissues are expected to reflect the mother's diet assuming the foetus does not have a metabolic disorder or nutritional deficiency (Fuller *et al.*, 2006; Bourbou *et al.*, 2013; Beaumont *et al.*, 2013). After birth, if an infant is breast fed, they are effectively consuming the mother's tissues, elevating their isotope values a trophic level above the mother. This results in characteristic increases in the $\delta^{15}\text{N}$ (+ 2–3‰) and $\delta^{13}\text{C}$ (+ ~1‰) values (see Figure 3.3) which can be used to explore breastfeeding and weaning patterns (Fuller *et al.*, 2006; Beaumont *et al.*, 2015; Reynard and Tuross, 2015; King *et al.*, 2018). The mean of the isotope ratios obtained from adult female bone collagen (AFM), within an analysed population can act as a proxy for overall dietary practice (Beaumont *et al.*, 2015b; D'Ortenzio *et al.*, 2015; Fuller *et al.*, 2006). This provides a way of quantifying the

changes in the isotope profile due to breastfeeding, weaning and stress. Weaning can be examined using infant/childhood bone collagen, but the nature of bone turnover and the accumulated isotope ratios can mask the changes from prenatal values as well as possible periods of physiological/nutritional stress (Beaumont *et al.*, 2018). The deciduous teeth begin forming *in utero* and permanent dentition (e.g. first permanent molar) forms during the first year of life. These teeth capture the changes caused by umbilical nutrients, breastfeeding and weaning foods. Incrementally sampling dentine that formed during these dental development stages provides researchers with a method of examining age-related changes.

Medieval medical texts suggested exclusive breastfeeding continued until around six months when weaning foods, such as starch-based soft foods often mixed with animal milk and honey were introduced, and the weaning process was completed between three and four years of age (Orme, 2003; Newman, 2007). Incremental dentine stable isotope analysis (C, N) of six non-adult individuals from Archiud (northern Transylvania) revealed breastfeeding and weaning patterns following the medieval medical suggestion (Crowder *et al.*, 2019). Voas and colleagues (2018) conducted nitrogen isotope analysis on root dentine from 16 non-adult individuals from the Bögöz populations to examine weaning patterns. They found that the majority of individuals (14 of 15) consumed at least some breastmilk and weaning was completed between three to four years of age ($\delta^{15}\text{N}$ from 10.2 to 15.2‰, mean $12.4 \pm 1.3\text{‰}$), also keeping with historical recommendations. Variations in the breastfeeding and weaning curves can indicate different breastfeeding/weaning practices, change in dietary resources and/or periods of increased stress. Substantial changes between the prenatal values and infant values (i.e. $\delta^{15}\text{N} \geq 4\text{‰}$) indicate a difference between the mother's diet during pregnancy and the diet of the individual during breastfeeding. The practice of wet nursing was employed by the Romans (Bradley, 1986) and could also account for substantial differences between prenatal values and breastfeeding signals. The breastmilk produced in the first few days after birth provides vital nutrients and immunological protection for the infant (Stuart-Macadam and Dettwyler, 1995). Maternal malnutrition can adversely affect the

quality of breastmilk, which can lead to anaemia and arrested growth in infants (Miranda *et al.*, 1983; Sandberg *et al.*, 2014).

Variation in isotope life-history profiles can also provide details about an individual's early-life history. Fluctuations in the $\delta^{15}\text{N}$ profile can indicate periods of nutritional/physiological stress (see Section 3.2.2.iii). Individuals who only received breastmilk for a short period and/or were not breastfed would not display the characteristic increase in isotope values after birth (Balasse *et al.*, 1999a; Fuller *et al.*, 2006; Craig-Atkins *et al.*, 2018). Individuals who were not breastfed have a higher risk of infection as well as mal- and undernutrition (WHO, 2009; Craig-Atkins *et al.*, 2018). Examining breastfeeding and weaning practices using osteological data can reveal possible differences between cultural practices for males and females, or between "survivors" (survived into adulthood) and "non-survivors" (died as non-adults). Non-adult bone collagen was compared to adult incremental-dentine collagen to examine the possible differences between "non-survivors" and "survivors" from Bronze Age Romania in the south-east Carpathian Mountains but no significant difference in weaning patterns was found (Agurajua, 2017). However, the process of weaning can negatively impact the well-being of non-adults. The loss of passive immunity from the mother's breastmilk, less nutritious and/or digestible foods and a less stable food resource can result in physiological stress (Katzenberg *et al.*, 1996; Larsen, 2015). These factors are compounded for those individuals of lower socio-economic status, who were not able to overcome the stress-event (Katzenberg *et al.*, 1996; King *et al.*, 2005).

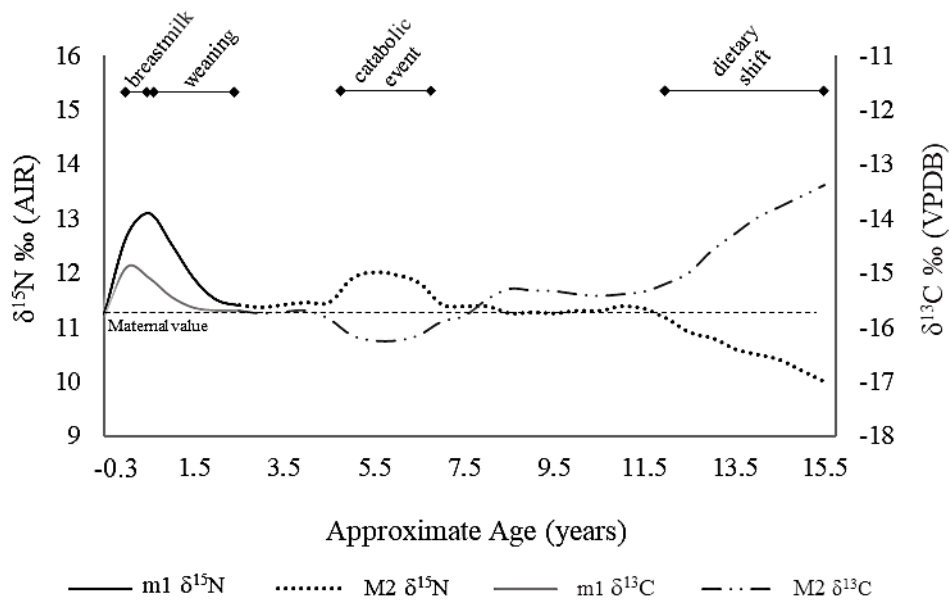


Figure 3.3. A model of an incremental dentine early life-history profile demonstrating the duration of breastfeeding and weaning (birth to 2.5–3 years), a catabolic event (4.5 to 7 years) and a dietary shift to increased protein and/or C_4 resources (11.5 to 15.5 years) (Crowder *et al.*, 2019).

(iii) Examine “stress” using nitrogen isotope ratios

A person is considered to be in a state of metabolic equilibrium when there is a balance between anabolic (tissue building) and catabolic (tissue breakdown) processes (Fuller *et al.*, 2005; Hatch *et al.*, 2006; Mekota *et al.*, 2006; D’Ortenzio *et al.*, 2015). During growth, or recovery from stress, the body is in an anabolic state and builds biomolecules via metabolic pathways (Fuller *et al.*, 2005; Mekota *et al.*, 2006; Little *et al.*, 2007). In an anabolic state, like pregnancy, the body increases protein synthesis and decreases nitrogen excretion, entering a state of positive nitrogen balance, which has been shown to decrease $\delta^{15}\text{N}$ values (Fuller *et al.*, 2004). During a catabolic state, when a person is experiencing stress (e.g. starvation, fasting, malnutrition, metabolic disease, physiological stress), the body breaks down biomolecules, such as muscle proteins, in an attempt to maintain energy (Hatch *et al.*, 2006; Mekota *et al.*, 2006; Little *et al.*, 2007). Negative nitrogen balance, lean muscle catabolism and increased nitrogen excretion, has been found to increase $\delta^{15}\text{N}$ values (Fuller *et al.*, 2004). The breakdown and metabolization of muscle protein

in the body result in the remaining tissues being enriched in ^{15}N (increased $\delta^{15}\text{N}$ values) (Fuller *et al.*, 2005; Reitsema and McIlvaine, 2014; D'Ortenzio *et al.*, 2015).

Isotope ratios have been found to have intraskeletal variation between normal bone (no pathological lesion) and pathological bone (Katzenberg and Lovell, 1999; Olsen *et al.*, 2014). A catabolic state can also be seen in isotope life-histories based on profiles of incremental dentine (see Figure 3.3). Isotope ratios obtained from the earliest forming dentine in the deciduous dentition are incorporated during gestation and can be used as a proxy for the mother's isotope ratios during pregnancy. Isotope life-history profiles which capture this stage of development can track changes from gestation through early childhood (Beaumont *et al.*, 2013). Infant-mother stress can be seen if an individual has elevated prenatal $\delta^{15}\text{N}$ values compared to the adult female mean value (AFM) for the population.

Stress events in the isotope life-history profiles can be used in conjunction with osteological and historical data to examine possible aetiologies. As previously mentioned, increased physiological stress, such as that which occurs during the weaning process, can result in pathological changes (e.g. EH) (Henderson *et al.*, 2014; Sandberg *et al.*, 2014). This enables a comparison to be made between the duration of the stress event and the approximate age at which the EH occurred (Franz-Odenaal *et al.*, 2003; Sandberg *et al.*, 2014; Crowder *et al.*, 2019). Likewise, if an individual died with active skeletal lesions, identified by the presence of new woven bone, and while dentition was still forming, it is possible the stress-event could be seen in the isotope life-history profile. This would enable researchers to assign an approximate age of onset and duration of the stress event, assuming the cause of the catabolic state and bone changes were the same (Geber and Murphy, 2012; Beaumont and Montgomery, 2016; Crowder *et al.*, 2019). Armit and colleagues (2015) used a multi-isotope approach (Sr, O, C, N) to explore evidence of rickets in a Neolithic individual from the Inner Hebrides (UK) and found that stress (catabolism) was also evident in the isotope ratios. The authors posit that this could have been the result of low marine food consumption, lack of access to milk, and/or confinement. Changes in the climate have also been linked to human survival in the past. A poor climate can affect crop yields (Beaumont and Montgomery, 2016) and access to fresh

water, which can increase population displacement, infectious disease loads and conflict. For example, famine resulting from a lack precipitation, starvation and pestilence has been related to cold episodes during the 8th–9th C. AD in Europe (McMichael, 2012).

As discussed in Section 2.2.2, there are many interrelated factors which can impact health during childhood. Childhood can be thought of as both a social construct with cultural differences seen between populations, and a biological process of growth (Panter-Brick, 1998). Thus, the occurrence of stress events identified in isotope life-history profiles can provide evidence as to the possible factors contributing to early-life stress, and how it affected the two Transylvanian populations in this study.

3.3. Strontium and oxygen isotope analyses

Isotope ratios of food and water can reveal a great deal about the region where those resources originated and have successfully been used to examine the mobility of past populations (Ericson, 1985; Montgomery, 2010; Evans *et al.*, 2012). The high organic content of bone and recrystallization which can occur in the burial environment make bone highly susceptible to diagenetic alteration, particularly of trace elements (Tuross *et al.*, 1989; Ayliffe *et al.*, 1994; France and Owsley, 2015). The enamel matrix is approximately $\frac{1}{3}$ mineral, $\frac{1}{3}$ water and $\frac{1}{3}$ protein until the entire matrix is mineralised. Ameloblasts complete the maturation process by removing the protein and water portion of the matrix, producing enamel which is 99% mineral (Hillson, 2014). The rigid crystalline structure makes enamel ideal for archaeological analysis because it survives the burial environment with minimal diagenetic alteration (Nelson *et al.*, 1986). As previously mentioned in Section 2.2.3, the layered secretion and mineralization of enamel captures childhood and adolescence isotope ratios enabling examination of isotope ratios from discrete periods of a person's life (Montgomery, 2010). Strontium isotope ratios ($^{87}\text{Sr}/^{86}\text{Sr}$) of human enamel reflect the bedrock where a person sourced their food when their dentition was forming (Evans *et al.*, 2010; Montgomery, 2010; Emery *et al.*, 2018). Oxygen isotope values ($\delta^{18}\text{O}$) of human enamel reflect the climate within which a person lived, and the water

source a person accessed during tissue formation (Pellegrini *et al.*, 2011; Evans *et al.*, 2012; Chiocchini *et al.*, 2016).

Strontium and oxygen isotope ratios found in human tissues have been successfully used to assess mobility in the past (Bentley, 2006; Montgomery, 2010). However, Romania, and most of Eastern Europe, has yet to be mapped for biosphere isotopes (specifically Sr and O), which can make it difficult to establish local isotope ranges for specific archaeological sites. Isotope ratios of plant, animal, water and soil samples from modern and archaeological sites help to establish the local biosphere isotope ranges (Evans *et al.*, 2006; Montgomery, 2010). This section introduces strontium and oxygen isotopes and how the isotope ratios can be used to establish local biosphere ranges and examine residential origins of past populations.

3.3.1. Strontium isotopes

Jonathon Ericson (1985) proposed examining geographic origins of past peoples by analysing strontium isotope ratios of human skeletal tissue. Since then archaeologists have utilized strontium isotope analysis to investigate mobility and transhumance (Sealy *et al.*, 1987, 1991; Price *et al.*, 1994; Montgomery *et al.*, 2000; Gibling, 2009; Neil *et al.*, 2017; Emery *et al.*, 2018) (discussed further in Section 3.3.3). Strontium is an alkaline earth metal and has four naturally occurring isotopes. The natural abundance of the three stable isotopes and one radiogenic isotope (^{87}Sr) are: ^{86}Sr (~9.87%); ^{87}Sr (~7.04%); ^{88}Sr (~82.53%) (Price *et al.*, 1994). The abundance of the stable strontium isotopes are constant through time while the amount of ^{87}Sr continually increases over time due to the slow radioactive decay of rubidium (^{87}Rb) (Faure, 1986, pg. 119). Because the two isotopes are similar in abundance, measuring the relative abundance of ^{87}Sr to ^{86}Sr ($^{87}\text{Sr}/^{86}\text{Sr}$ ratio) reduces the measurement error (Equation 3.3 – Faure, 1986, pg. 119). Unlike light isotopes (C, N, O), the mass-dependent fractionation of strontium isotopes is negligible with comparatively small differences between the masses of heavy isotopes (for example $^{87}\text{Sr}/^{86}\text{Sr}$ compared to $^{16}\text{O}/^{18}\text{O}$) (Faure, 1986, pg. 186; Graustein, 1989; Montgomery, 2002). The $^{87}\text{Sr}/^{86}\text{Sr}$

ratio from a rock mineral depends on: the time since formation (t); and the $^{87}\text{Sr}/^{86}\text{Sr}$ when the rock crystallized; and the $^{87}\text{Rb}/^{86}\text{Sr}$ ratio (Faure, 2013, pg. 4-6).

$$\frac{^{87}\text{Sr}}{^{86}\text{Sr}} \cong \left(\frac{^{87}\text{Sr}}{^{86}\text{Sr}} \right)_0 + \frac{^{87}\text{Rb}}{^{86}\text{Sr}} \lambda t.$$

Equation 3.3. Equation for strontium isotope ratio (λ the decay constant, N_0 the initial ratio, and t is time) (Faure et al., 2009, pg. 77).

The Rb-Sr decay and resulting ^{87}Sr content of rocks can produce a wide array of values and the decay is used in geochronology to determine the age of rocks (Bentley, 2006; Faure and Mensing, 2009, pg. 77-78; Dickin, 2018, pg. 42). Rock over 100 million years ago (mya) has a high original Rb/Sr and generally produces values above 0.710, while rocks less than 10 mya have a low Rb/Sr producing $^{87}\text{Sr}/^{86}\text{Sr}$ ratios below 0.704 (Bentley, 2006). Strontium is released from rocks as a result of chemical weathering (Graustein, 1989; Miller et al., 1993; Montgomery, 2002). The large atomic mass and the negligible fractionation (mass-dependent, kinetic, equilibrium) means strontium isotopes remain virtually unaltered after being released from rocks into the soil, plants, animals and water reservoirs (Graustein, 1989; Montgomery, 2002; Bentley, 2006). However, this does not mean that the $^{87}\text{Sr}/^{86}\text{Sr}$ ratio of the bedrock will directly match soil, plant, animal and human $^{87}\text{Sr}/^{86}\text{Sr}$ ratios.

Weathering of rocks releases strontium into dust, precipitation and river water (Blum et al., 1993; Montgomery, 2002; Price et al., 2002; Bentley, 2006). Thus, mixing of different sources of strontium isotopes can impact the resulting $^{87}\text{Sr}/^{86}\text{Sr}$ ratio obtained from teeth. For example, humans who consume resources from a region with diverse bedrock geology are expected to have a $^{87}\text{Sr}/^{86}\text{Sr}$ ratio which reflects the isotopic composition of the local geology (Price et al., 2002; Montgomery, 2010). Some argue that in areas of diverse geology, whole rock and soil analyses do not reflect the bioavailable strontium taken up by plants and humans, and therefore should not be used to examine human diet (Price et al., 2002; Montgomery, 2010). Labile strontium acid leached from soil and from animal tissues have been found to

be adequate proxies for human dietary ratios (Price *et al.*, 2002). The $^{87}\text{Sr}/^{86}\text{Sr}$ ratio of soil can also increase or decrease depending on the source of strontium in the local meteoric water (Sharp, 2017, Section 6-17). The concentration of strontium in samples (ppm) can vary geographically due to variation in food and water consumed, subsistence and dietary patterns and the bedrock (Turekian and Kulp, 1956; Montgomery, 2010). Mobile and labile strontium can be examined by comparing concentrations in samples, i.e. concentrations above the expected range may indicate diagenetic alteration (Montgomery, 2010). Comprehensive reviews of strontium isotopes in skeletal tissues can be found in Price *et al.* (2002); Bentley (2006); and Montgomery (2010).

3.3.2. Oxygen Isotopes

Oxygen has three naturally occurring isotopes: ^{16}O (99.76%); ^{17}O (0.04%); ^{18}O (0.2%) (Coplen *et al.*, 2002; Sharp, 2017, Section 4-2). Like carbon and nitrogen, oxygen isotope ratios are converted to δ values to better examine the fractionation effect (Equation 3.4). Oxygen isotope analysis measures the difference in proportion of ^{18}O relative to the international standard (Vienna Standard Mean Ocean Water, VSMOW – Sharp, 2017, Section 4-1). Isotopic composition of natural water can be modified by physical chemical properties: exchange reaction; evaporation; condensation; mixing (Epstein and Mayeda, 1953; Friedman, 1953). Large bodies of water such as large lakes and oceans have a relatively well-mixed stable isotope composition while smaller bodies of water are more susceptible to phase changes (i.e. evaporation) and can vary widely (Gat, 1996; Sharp, 2017, Section 4-1). Ocean water ($\delta^{18}\text{O} = 0\text{‰}$) evaporates into vapor ($\delta^{18}\text{O} = -13\text{‰}$) which condenses into clouds; as the clouds move away from the water source the heavier isotopes drop out via rain, resulting in an isotopic gradient as clouds moves across land (i.e. $\delta^{18}\text{O}$ from -3 to -17‰) (Dansgaard, 1964; Sharp, 2017, Section 4-19). Isotopic gradients have also been found in relation to the isotope composition of precipitation at different latitudes ($\delta^{18}\text{O}$ values change by 0.5‰ per degree of latitude) and altitudes (Dansgaard, 1964; Sharp, 2017, Section 4-21). Additional information regarding the meteoric water cycle can be found in Sharp (2017, Chapter 4).

$$\delta^{18}\text{O} = \left[\frac{^{18}\text{O}/^{16}\text{O} \text{ sample}}{^{18}\text{O}/^{16}\text{O} \text{ standard}} - 1 \right]$$

Equation 3.4. Oxygen isotope ratio equation to calculate the delta value (Sharp, 2017, Section 2-5).

In 1973 Longinelli proposed using oxygen isotope data obtained from bone and teeth to determine terrestrial endotherms and ancient continental environments (Longinelli, 1973; Sharp, 2017, Section 8-4). Koch and colleagues (1989) examined mammalian apatite and found seasonal variation in $\delta^{18}\text{O}$ values with lower values correlating to cold seasons and determined oxygen isotopes in dentinal hydroxyapatite retain the initial values from the time the tissue was forming. The $\delta^{18}\text{O}$ values of mammalian tissues reflect the oxygen isotope ratio of body water and are a function of drinking water (i.e. ingested meteoric water) and metabolism (Sharp, 2017, Section 8-4). As previously mentioned, oxygen isotope values ($\delta^{18}\text{O}$) of meteoric water are a function of altitude, latitude and temperature (Sharp, 2017, Section 8-4). A positive correlation was found between an increase in atmospheric temperature and increasing $\delta^{18}\text{O}$ values (i.e. elevated $\delta^{18}\text{O}$ values with higher temperatures - Kotov *et al.*, 1997). Because oxygen isotope fractionation is affected by temperature, the constant mammalian body temperature means that $\delta^{18}\text{O}$ (phosphate) values of apatite (bone or teeth) can be used as an indirect proxy for ancient meteoric water values (Longinelli, 1984; Sharp, 2017, Section 8-4). Carbonate of enamel hydroxylapatite is resilient to recrystallization and has been found to retain original isotopic signatures (Schoeninger and DeNiro, 1982; Lee-Thorp and Van Der Merwe, 1987; Koch *et al.*, 1997; Chenery *et al.*, 2012). Oxygen isotopes in human tissues come from: drinking water (related to local water sources); food oxygen (related to local water source); and atmospheric oxygen (metabolic water, constant value $\delta^{18}\text{O}$ 23.8‰ - Luz *et al.*, 1984). Luz and colleagues (1984) also found that the rapid equilibration between the environment and body water can be used to track seasonal isotopic variation.

The systematic fractionation of oxygen isotopes in relation to geographic location provides a way to compare oxygen isotope ratios of human enamel to a geographic location (see Figure 3.4). Tooth enamel from permanent teeth captures isotope ratios from childhood (three months after birth to approximately 12 years - AlQahtani *et al.*, 2010) which can be used to examine mobility in the past (Chenery *et al.*, 2011; Montgomery *et al.*, 2011; Neil *et al.*, 2016). It is important to be aware of the physical and chemical processes that can affect oxygen isotope ratios. For example, heating treatment such as boiling water ($\delta^{18}\text{O} + \sim 0.4\text{‰}$), brewing beer ($\delta^{18}\text{O} + 1.3\text{‰}$) and/or stewing foods ($\delta^{18}\text{O} + 10.2\text{‰}$) can all affect *in vivo* isotope ratios ($\delta^{18}\text{O}$) (Brettell *et al.*, 2012). Brettell and colleagues (2012) determined that if the population/person had diets consisting of approximately 10-20% of food/drink treated with these heating processes, a correction of $+2.3\text{‰}$ ($\delta^{18}\text{O}$) should be added to the calculated drinking water values obtained from tooth enamel. A single $\delta^{18}\text{O}$ value can reflect multiple regions and/or a large region, and can be affected by several factors, which is why it is important to account for as many variables as possible before interpreting the data (cultural practices, altitude, latitude, precipitation, temperature).

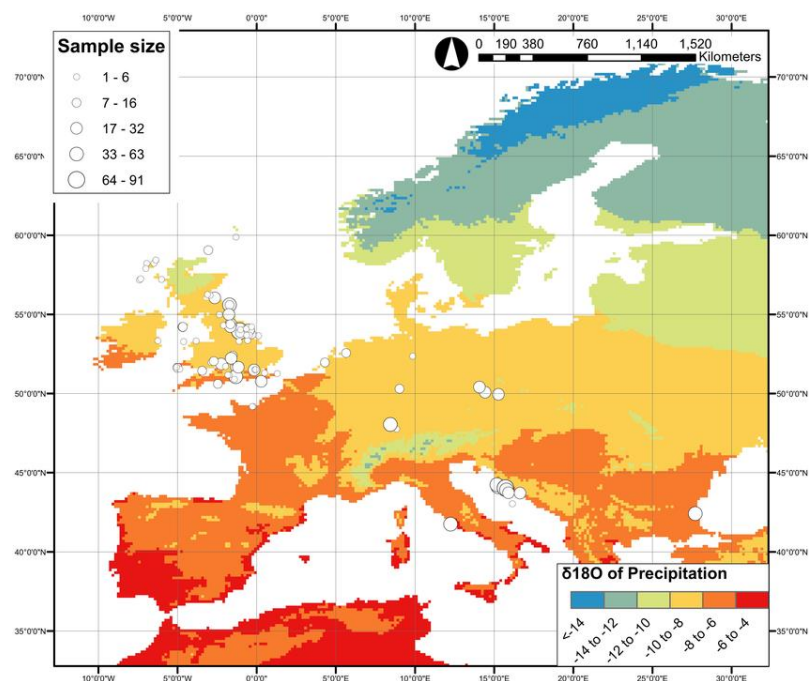


Figure 3.4. Example of a map of regional modern precipitation oxygen isotope values used to examine human mobility in the past (Lightfoot and O'Connell, 2016).

3.3.3. Applications of strontium and oxygen isotope analysis

(i) Establishing baseline local biosphere isotope ranges

Transylvania is made up of a Paleogene geology in the north-west, south-west and southern basin, Lower Miocene arc in the north-west of the basin from the Maramureş river to the front of the Pienides, Middle to Upper Miocene geology extending between the Someş and Olt rivers, and a volcanic back-arc along the eastern margin of the basin (Filipescu, 2011; Krézsek, 2011). The Transylvanian Basin is mostly Neogene-Quaternary sediment deposits (Seghedi *et al.*, 2004) and also contains deep-marine middle Miocene shales (Krézsek, 2011) (Figure 3.5). Central and Eastern European lowlands are covered in loess and marine carbonate deposits and the main source along the Danubian corridor are Alpine carbonates with $^{87}\text{Sr}/^{86}\text{Sr}$ ratios between 0.7085 and 0.7104 (Grupe *et al.*, 1997; Bentley and Knipper, 2005; Bentley *et al.*, 2012). Given the lack of biosphere isotope mapping for Romania, it is not possible to assign isotope ranges specific to each burial site studied, but it is possible to propose biosphere isotope ranges for the Transylvanian Basin. Figure 3.6 is a summary of the strontium isotope ratios reported in the regions near the Transylvanian Basin with similar geology. These data were used to extrapolate a proposed strontium isotope ratio range for the Transylvanian Basin.

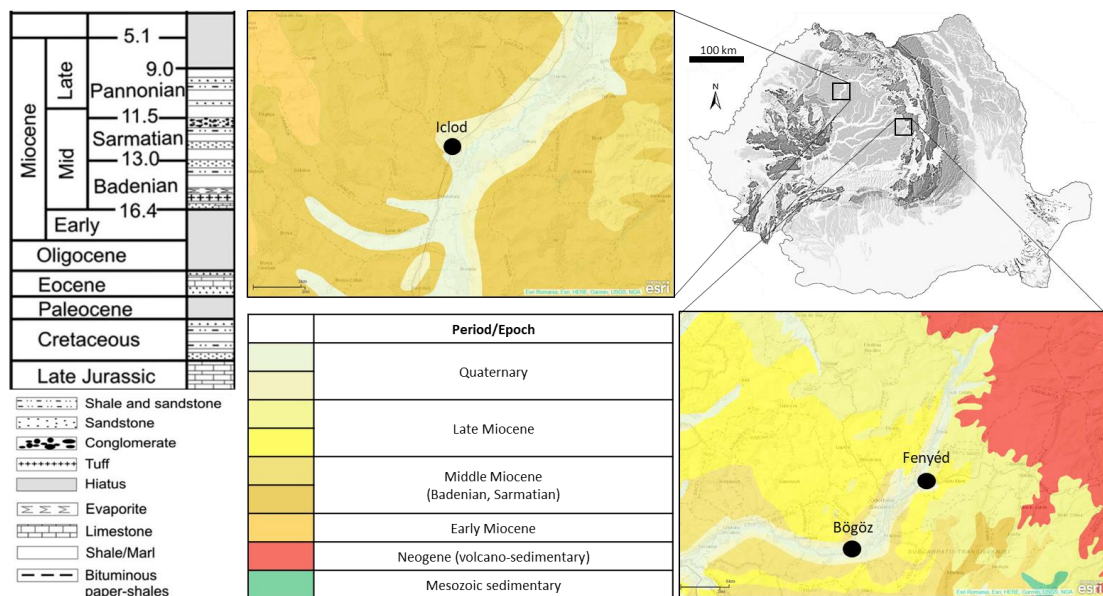
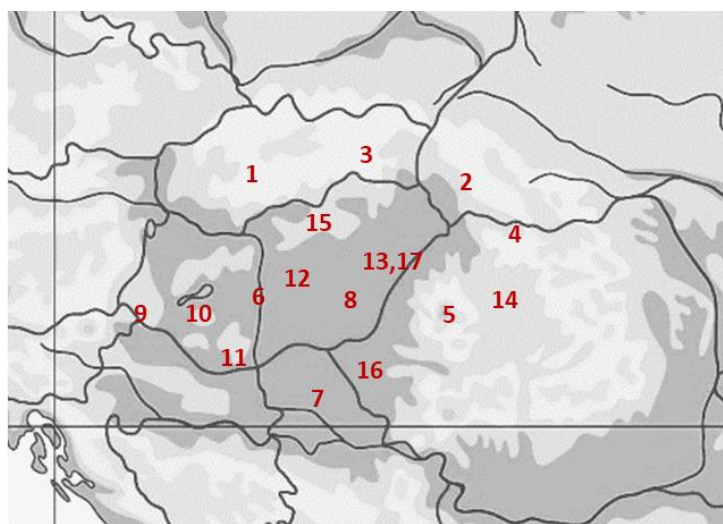


Figure 3.5. Lithology of the Transylvanian Basin (left) (adapted from Krézsek *et al.*, 2010) and geological maps (right) demonstrating the diverse bedrock of the archaeological sites in the study. Map created using ArcGIS 10.4 with Esri data and maps.



Location	Age	$^{87}\text{Sr}/^{86}\text{Sr}$	Source	Reference
1 Bukk Mountains	15-18 mya	0.71002 ± 0.00121 (1sd)	whole rock	(Seghedi et al., 2004)
2 N. Transcarpathian Basin	15 mya	0.70892 ± 0.00011 (1sd)	whole rock	(Seghedi et al., 2004)
3 Tokaj Mountains	12 mya	0.70742	whole rock	(Seghedi et al., 2004)
4 Gutai Mountains	1-11 mya	0.70901 ± 0.00073 (1sd)	whole rock	(Seghedi et al., 2004)
5 Apuseni Mountains	1-13 mya	0.70513 ± 0.00116 (1sd)	whole rock	(Seghedi et al., 2004)
6 Danube River	modern	0.70955 ± 0.00005 (1sd)	water	(Price et al., 2004)
7 Tisza River	modern	0.70960	water	(Palmer and Edmond, 1989)
8 Körös region	Neolithic	0.70965 ± 0.00014 (1sd)	human enamel	(Giblin, 2009)
	Copper Age	0.70955 ± 0.00024 (1sd)	human enamel	(Giblin, 2009)
		0.70977 ± 0.00030 (1sd)	faunal enamel	(Giblin, 2009)
9 Keszthely-Fenékpuszta	4 th -9 th C. AD	0.70969 ± 0.00102 (1sd)	human enamel	
		0.70924 ± 0.00107 (1sd)	environmental samples	
10 Hács-Béndekpuszta	3 rd -5 th C. AD	0.71027 ± 0.00099 (1sd)	human enamel	
		0.70848 ± 0.00037 (1sd)	environmental samples	(Alt et al., 2014; Hakenbeck et al., 2017)
11 Mözs	3 rd -5 th C. AD	0.70981 ± 0.00064 (1sd)	human enamel	
		0.71002 ± 0.00126 (1sd)	environmental samples	
12 Szolnok-Szanda	5 th -6 th C. AD	0.70985 ± 0.00048 (1sd)	human enamel	
		0.70978 ± 0.00032 (1sd)	environmental samples	
13 Hungary	modern	0.70901 - 0.71100	water	(Voerkelius et al., 2010)
14 Archiud	4 th -7 th C. AD	0.70984 ± 0.00021 (1sd)	human enamel	(Crowder, 2015)
15 Sajópetri	6 th -9 th C. AD	0.71034 ± 0.00027 (1sd)	human enamel	(Noche-Dowdy, 2015)
16 Timișoara	16 th -17 th C. AD	0.71058 ± 0.00058 (1sd)	faunal enamel	(Allen, 2017)
		0.70955 ± 0.00096 (1sd)	human enamel	(Allen, 2017)
17 Sárrétudvari-Órhalom	4 th C. BC	0.70979 ± 0.00041 (1sd)	human enamel	(Gerling et al., 2012)

Figure 3.6. Summary of the strontium isotope ratios reported near the Transylvanian Basin.

The Online Isotope in Precipitation Calculator (OIPC) predicts a $\delta^{18}\text{O}$ value of -9.2 to -9.0‰ (V-SMOW, 95% CI \pm 0.2‰), based on the longitude, latitude and altitude of the Bögöz and Fenyéd sites, and a $\delta^{18}\text{O}$ value of -8.4‰ (V-SMOW, 95% CI \pm 0.1‰) for Iclod (Bowen et al., 2018). Paleoclimate research on land snail shells predicted drinking water values for Pannonia to be approximately $\delta^{18}\text{O}_{\text{DW}} = -9.0\text{‰}$, with mountainous regions even more depleted (lower $\delta^{18}\text{O}$ values) compared to the surrounding lowlands (Lécolle, 1985; Evans *et al.*, 2006). As previously stated, varying temperature can result in seasonal changes in oxygen isotope values (Kotov *et al.*,

1997; Bowen *et al.*, 2005). The temperate climate of Romania has been found to result in a wide variation in $\delta^{18}\text{O}$ values (from $\sim 1\text{--}14\text{‰}$) in rain and river water samples due to seasonal temperature fluctuations (IAEA/WMO, 2019). Isotope analysis of human enamel carbonate from the population at Archiud (associated with the Gepid Kingdom) in norther Transylvania found $\delta^{18}\text{O}_{\text{VSMOW}}$ values ranging from 23.9 to 25.5‰ (Crowder *et al.*, 2019). Research on skeletons from five sites within Pannonia (5th C. AD), with similar altitudes and latitudes as those in the Transylvanian Basin were reported to have human enamel values ($\delta^{18}\text{O}_{\text{VSMOW}}$) of 21.6 to 26.1‰.

Based on the available comparative archaeological data, biosphere isotope data and the basin bedrock, the extrapolated proposed local ranges for the Transylvanian Basin are $^{87}\text{Sr}/^{86}\text{Sr}$ values between 0.7078 and 0.7120 and $\delta^{18}\text{O}_{\text{VSMOW}}$ values between 21.9 and 26.1‰ (Crowder *et al.*, 2019). The differences in altitude, latitude and geology of the burial locations are expected to result in slight differences in the biosphere isotope ranges specific to each site.

(ii) Assessing mobility and residential origins

Strontium and oxygen isotopes can only be used to identify probable local and non-local individuals buried at a particular site and cannot be used to assign a specific place of origin for non-local individuals. This is because numerous regions can have similar biosphere isotope ranges (similar geology, latitude and climate). For example, most of the Eastern European lowlands consist of sedimentary rock of a Tertiary age, and they experience similar climates. This results in strontium and oxygen biosphere isotope ranges that reflect multiple regions and/or a large region in Eastern Europe. As previously mentioned, strontium and oxygen isotope ratios have been successful used to explore mobility in past population (Sealy *et al.*, 1991; Nglan *et al.*, 2000; Montgomery *et al.*, 2003; Price *et al.*, 2004; Neil *et al.*, 2016). Archaeological data (e.g. burial context) and isotope life-history profiles (C, N) can be used to support the identification of non-local individuals. For example, burials from multiple Romano-British burial sites have revealed individuals with childhood isotopes inconsistent with British origins; Burial rites and artefact data were used to support continental

and/or Eastern Europe as a possible place of origin (Chenery *et al.*, 2011; Müldner *et al.*, 2011; Eckardt *et al.*, 2015). Non-local individuals have also been identified by examining dietary practices which deviate from the pattern of the local population (e.g. C₄ consumption in Roman Britain - Chenery *et al.*, 2010). By analyzing the demographic profile of local and non-local individuals in relation to isotope data, patterns can be revealed between age categories, biological sex, socio-economic status and morbidity (Montgomery *et al.*, 2007; Leach *et al.*, 2010; Müldner *et al.*, 2011).

3.4. Summary

The application of isotope analysis within bioarchaeology has proved successful in gaining a deeper understanding of how past populations lived and died. Analysing isotope data in conjunction with demographic data discussed in Chapter 2 can provide a better understanding of the morbidity and mortality profiles for populations. Carbon and nitrogen isotope analysis of collagen from bone and dentine provides information about diet, breastfeeding and weaning practices, and metabolic stress at individual and population levels. Comparing diet and breastfeeding/weaning practices between populations can also reveal differences in cultural or religious practices, and/or differential access to resources associated with socio-economic status. Elevated $\delta^{15}\text{N}$ values associated with catabolic “stress events” can be further used to examine the possible age at onset of stress events and be compared with the presence of skeletal lesions purportedly related to stress. Strontium and oxygen isotope analysis of modern and ancient biological and environmental samples can help to fill gaps in biosphere data for regions with no such data, for example Eastern Europe. Strontium and oxygen isotope ratios from human enamel reveal information about the region a person inhabited during childhood (bedrock and climate which are related to the food and water sources) and can be used to examine residential origins and mobility within and between populations. The prevalence of “stress” (metabolic and/or physiological) can also be examined in local and non-locals to explore the impact migration had on health. In this study the results of the macroscopic skeletal analysis and isotope analyses were combined to gain a deeper understanding of how

early-life stress impacted the two population from Transylvania. The results for each method of analysis can be found in Chapter 5, following the next chapter that describes the sites studied and the methods used (Chapter 4).

Chapter 4: Material and Methods

4.1. Introduction

To answer the research questions outlined in Chapter 1, two populations from different time periods and regions within the Transylvanian territory of Romania were analysed to explore similarities and differences. By analyzing these individuals, it was hypothesized that it may be possible to determine if specific ecological niches and socio-culturally related aspects of life, such as economy and diet, including breastfeeding and related weaning patterns, were similar. If the palaeopathological and isotopic profiles were different, it was hypothesized that this may be the result of changing socio-cultural practices with the introduction of a different religion and/or political powers. It is known that from the Migration Period to the Middle Ages, the Transylvanian Basin was subject to Christian, Catholic, and Muslim rulers (Power, 2006).

Both skeletal assemblages were analyzed to explore demographic parameters, the prevalence or absence of metabolic stress, overall dietary patterns and related breastfeeding and weaning practices, alongside migratory status. The data from both groups were analyzed to determine if there were differences between biological sex and age-at-death categories, within and between the two populations. Section 4.2 provides information regarding the archaeological context for each skeletal assemblage, the sampling protocol and a complete list of isotopic samples can be found in section 4.3. Section 4.4 provides information for each method applied in this study.

4.2. Materials (skeletal remains)

4.2.1. Migration Period

The Iclod Necropolis was a multi-phased settlement, with a strong fortification system and located in the north-west of the Transylvanian Basin on a low terrace of the Someșul Mic River. Iclod was active in the salt trade in Transylvania dating back to the Middle Neolithic (Maxim *et al.*, 2002). It utilized the Someșul Mic and Someșul

Mare rivers, which provided access to the Pannonian Plain (Lazarovici and Lazarovici, 2015). The continuous occupation at the site revealed evidence for cultural, religious and economic changes (Maxim *et al.*, 2002). Survey and initial excavation started in the 1970s and continued until 2010. Geomagnetic test surveys were conducted from 2008 to 2010 which found a minimum of 33 structures organized in three concentric rings (Alrichs, 2015). Two overlapping burial phases have been associated with the Neolithic and Migration Periods. The Neolithic burial phase (dated around 4200 BC based on stratigraphy and artefacts) was close to the settlement, just outside the inhabited area (Gligor and Crişan, 2014); 24 inhumations with burial rites linked to astronomical directions were found (Maxim *et al.*, 2002). The site of the graveyard, Iclod C, has been associated with the Zau culture. The burials inside the settlement were inhumations, mostly in a crouched position, lying on their left or right sides, with various grave goods (pottery, stone tools, bones, horns, shell artefacts – Gáll, 2014). The Zau culture is used to establish a regional chronology between settlements from the Middle Neolithic to the Early Eneolithic (Harper, 2016). The later phase and graveyard of Iclod C (Figure 4.1) spans the slope of the settlement down to the river (Alrichs, 2015). Erosion of the slope face prompted rescue excavations which revealed burials from the Migration Period (6th–7th C. AD – Gáll, 2014).

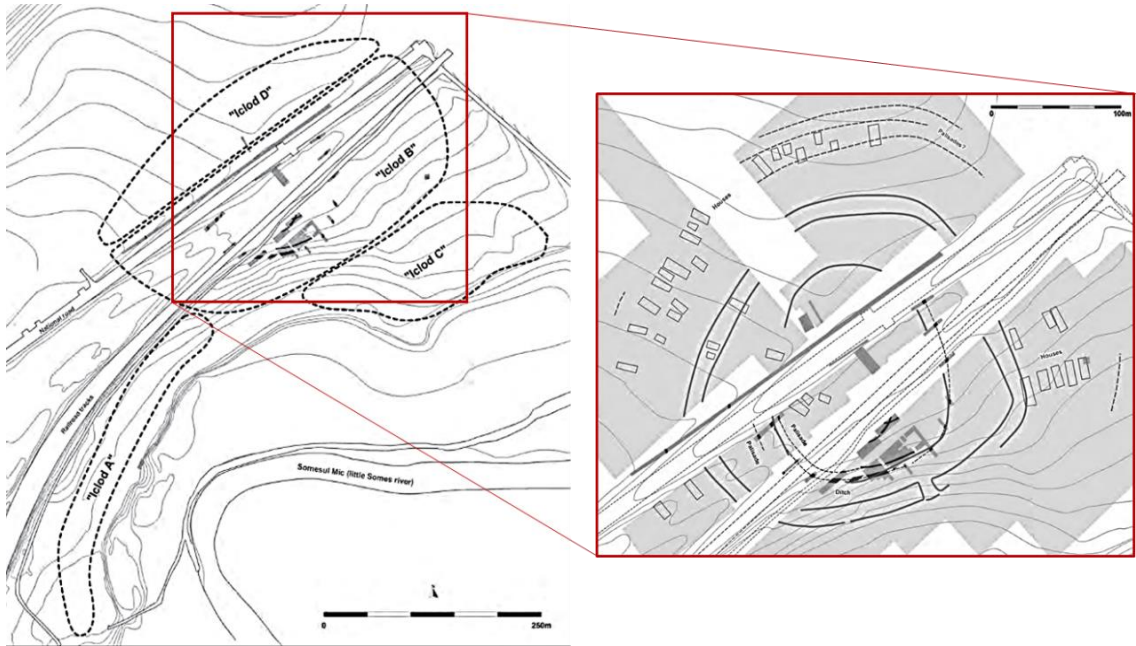


Figure 4.1. Site map from the geomagnetic survey and excavations (left) and the concentric structure (right) of the main settlement at the Iclod Necropolis. The Migration Period skeletons were excavated from "Iclod C." Images modified from Mischka (2012).

The row-graves and burial goods from the Migration Period link these individuals to a population belonging to the Kingdom of the Gepids in the Transylvanian Basin (Dobos, 2014). Some see the Gepids as one of the “neglected barbarian” populations that were subsumed into the histories of other empires (Kharalambieva, 2010). As previously mentioned, historical documentation regarding this period can be skewed towards the victors. One source reported that the Gepids “disappeared from history and the Avars took possession of the Danube plain and of the serf inhabitants” (Previt -Orton, 1975, pg. 202). Although the Gepids were ultimately defeated, sporadic populations of Gepids are described in historical records until AD 600 (Todd, 1995). During the Migration Period, the general climate in Europe and the Carpathian Basin in particular became cooler and drier. One theory even attributes the downfall of the Avar Empire to loss of livestock due to a drier climate, causing widespread starvation in their military (Vadas and Racz, 2011). Periods of starvation, famine and plague also occurred in Eastern Europe during the Migration Period (Thompson, 1982; Todd, 1995; Brandes, 1999). The continued unrest, disease and famine would have negatively impacted the health of those living in Transylvania during this time.

This study focuses on the individuals (6th-7th c. AD) excavated before 2016 from outside of the settlement in the “Iclod C” location, which have been associated with the Gepid Kingdom (25 of the 53) (Gáll, 2014). The skeletal assemblage is curated at 1 Decembrie 1918 University (Alba Iulia University) in Alba Iulia, Romania. Permission to conduct macroscopic and isotopic analyses was granted by Dr. Mihai Gligor. Macroscopic skeletal analyses were conducted by the researcher in August 2016 at Alba Iulia University, under the supervision of Dr Gligor.

4.2.2. Middle Ages

At the beginning of the 12th C. AD, the Hungarian Kingdom mounted a strong campaign to organize central-eastern Transylvania (Harhoiu and Gáll, 2014). The Fenyéd (*Brădești*) and Bögöz (Mugeni) sites were 15km apart and located in the south-east Transylvanian Basin near the Târnava Mare River (Zsolt, 2015). Radiocarbon dating sets both sites between the 11th-12th C. AD (Gáll, 2013). Both have a church structure and graveyard associated with these local rural communities (see Figure 4.2) (Harhoiu and Gáll, 2014). The skeletal remains from these sites were highly fragmented and had taphonomic damage, which limited the amount information to be learned. Because both sites were very similar in terms of geography, culture, and archaeological context, the information obtained from the two sites were combined to represent those living in this region at the time.

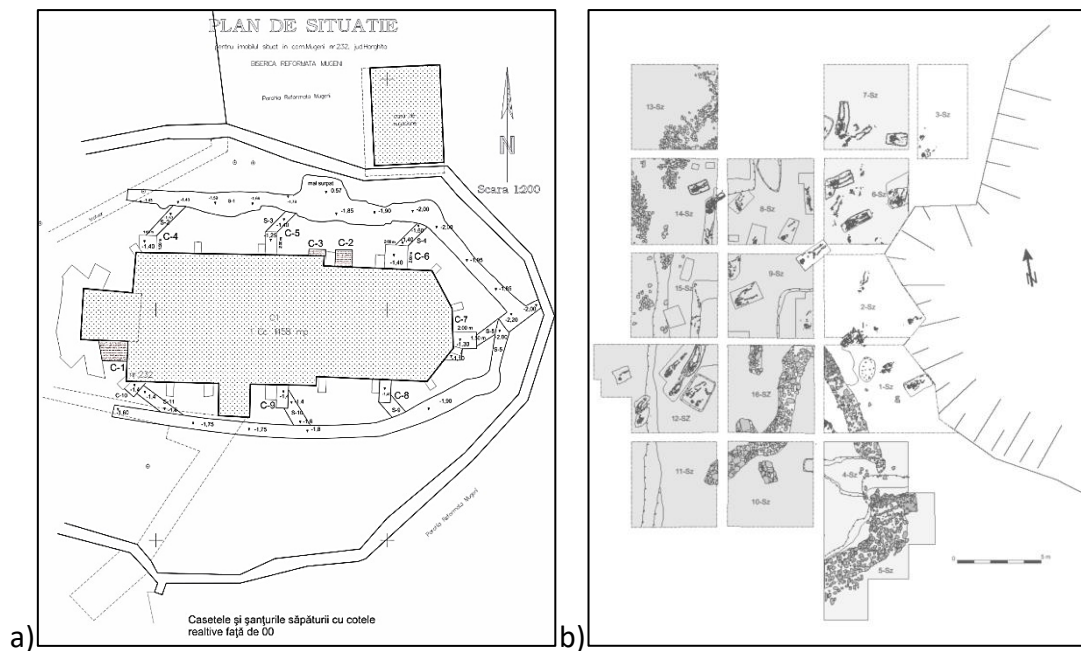


Figure 4.2. Site maps from the excavations showing the walls of the churches and associated human burials at Bögöz (a) and Fenyéd (b). Images and permissions provided by Nyaradi Zsolt at the Haáz Rezső Museum in Odorhei Secuiesc, Romania.

The Bögöz church was built in multiple phases starting in the 11th C. AD (Zsolt, 2015). Restoration and excavation took place between 2009–2013, uncovered 300 skeletons from inside and outside the church walls (Zsolt, 2015). Artefacts found with the skeletons (hair pins) have linked the earlier burial phase of burials with the Székley ruling class of the Hungarian Empire (Gáll, 2013). The Hungarian Kingdom divided Transylvania into autonomous regions to be ruled by Hungarian nobility from the Székley, Saxon and Teutonic Knights (Brie and Mészáros, 2014). The Székley were typically employed to guard the borders (Dreisziger, 2013). Burials from inside the church are believed to be among the first Árpáadian Age (11th C. AD) settlers in the region (Burial ID 226–290), and individuals buried outside the church walls are associated with the subsequent populations. In 2010, construction near the Târnava River caused soil slippage which revealed human remains. A rescue excavation was conducted and mortar and brick remains from the Fenyéd Pinewood church were found with 52 associated human burials (Nyárádi, 2017). Artefacts with western influences from the 12th C. AD Hungarian Empire (hair pins and hair rings) were associated with these burials (Gáll, 2013). Radiocarbon dating also found this site to have been in use in during 11th to 12th C. AD (Nyárádi, 2017).

Both the Bögöz and Fenyéd sites were in use during the time the Hungarian Empire expanded into the Transylvanian Basin and have artefact evidence linked to the Árpáadian culture. The Bud Fortress was a settlement on the bank of the Târnava Mare River near the Bögöz and Fenyéd sites and was a main military and juridical center for the Székley (Niță and Roșian, 2012), further supporting the link between these sites and incoming Hungarian populations. The climate began to warm again after the 9th C. AD and resulted in documented periods of droughts in Eastern Europe during the Árpáadian Period (11th to 13th C. AD – Vadas and Racz, 2011). The droughts and incursion of the Hungarian Empire were likely to have resulted in increased stress for both the conquering and conquered populations.

Both skeletal collections are curated at the Haáz Rezső Museum in Odorhei Secuiesc, Romania. Permission to conduct macroscopic and isotopic analyses was granted by Dr Zsolt Nyaradi. Macroscopic skeletal analyses and isotopic sampling was conducted by the researcher in August 2016 under the supervision of Dr Nyaradi.

4.3. Materials (samples for isotope analyses)

4.3.1. Sampling protocol: life-history profiles

Importantly, this research included destructive analysis of samples from the human remains studied. Analyses were conducted according to the Durham Ethics Policy (Chapman & Gowland, 2015), as well as the British Association of Biological Anthropology and Osteoarchaeology (BABAO) Codes of Ethics and Practices for the Curation, Sample Collection, and Analysis (BABAO, 2010a; 2010b). Proper training was received in appropriate sampling and analysis techniques prior to any sample collection and/or analysis, and destructive sampling were conducted in accordance with The Advisory Panel on Archaeology of Burials in England (Mays *et al.*, 2013). The destructive analyses within this research were not taken lightly. Due to the limited nature of the information that could be obtained from macroscopic analysis alone, the additional use of isotopic analyses provided more nuanced data about how these two populations lived and died. Previous work in the region has demonstrated that adequate collagen yields can be achieved for isotopic analyses, in spite of the poor

skeletal preservation (Crowder, 2015). Stable isotope analysis was employed to gain further knowledge and were only conducted following the completion of macroscopic analysis, this being essential prior to destructive sampling.

Thirty-nine adult and non-adult individuals from the skeletal assemblages were selected for isotopic analyses. The number of individuals selected was restricted by financial and time constraints imposed by these analyses. It is acknowledged that this modest sample size will not be representative of the picture of the entire population (Wood *et al.*, 1992; Waldron, 1994, Chapter 2). The data from both groups were analysed to examine any possible patterns across the landscape. The non-adults were selected to act as a proxy for the non-survivors of the two populations, and the adults, who survived the stress of childhood, would act as a proxy for the survivors of the two populations. By examining both adult and non-adult early life-history profiles through incremental dentine analysis, it was hypothesized that it might be possible to detect whether insults experienced during critical growth periods affected the survival of these individuals. The 39 individuals were further categorized into those with “no lesions” (those who died without or before lesions manifested in bones/teeth), and as “stressed” (those who died with skeletal changes associated with active, healing or healed stress-related lesions). Table 4.1 is a summary of the individuals who were selected for isotopic analysis. Non-adults with “stress” lesions were preferentially selected so that, where possible, active lesions might be correlated with changes in isotopic life-history profiles. Although it would have been more ideal to select an even number of individuals from each category, the actual number of individuals for each category depended on the sex, age and preservation of the skeletal assemblages. For example, there were no non-adults, without skeletal stress lesions in the 30 individuals analysed from the Iclod Necropolis.

Migration Period	No lesions	'Stressed'
<i>Non-adults</i>	N = 0	N = 3
<i>Adults</i>	N = 5	N = 11
Middle Ages	No lesions	'Stressed'
<i>Non-adults</i>	N = 2	N = 10
<i>Adults</i>	N = 3	N = 5

Table 4.1. Summary of individuals selected for isotopic analyses from the two Transylvanian sites.

Table 4.2 was the preferred sampling strategy for each age category. Sample selection was assessed after macroscopic analysis of the skeletons and was adjusted according to the teeth and bones available. Loose teeth were selected preferentially to minimize tissue damage that can occur during tooth extraction from dry bone. Bone samples were taken from disarticulated rib fragments. If a fragment of rib was not available, then a fragment of femur was taken instead. To minimize the bone or dental sample required for destructive analyses within this project, the sampling protocol called for a certain amount of fluidity. Two teeth were selected from individuals that were estimated to be approximately 16 years or younger at the time of death (AlQahtani *et al.*, 2010). This was so that the entire life-history was captured in the overlap between the earliest and latest forming dentition. Bone samples (rib or femur) were only taken from the adult skeletons estimated to be older than 25 years of age at the time of death. This was so that the average dietary intake of the person for the years leading up to death could be examined (Hedges and Reynard, 2007). Ribs can reflect the diet from a few years before death and a femur can reflect the diet all the way from the last growth spurt during adolescence up to death (DeNiro and Epstein, 1981; Sealy *et al.*, 1995; Hedges *et al.*, 2007). Enamel was sampled for strontium and oxygen isotopic analysis, and dentine was utilized for incremental carbon and nitrogen stable isotope analysis.

	Preferred tooth	Option 2	Bone sample
Non-Adult (<i>deciduous dentition</i>)	m1, m2	m1, i1	---
Adolescent (<i>mixed dentition</i>)	m1, M1	m2, C	---
Adult (<i>permanent dentition</i>)	C, M3	M1, M3	rib or femur

Table 4.2. The preferred sampling protocol for teeth and bones for isotopic analyses.

4.3.2. Sampling protocol – local biosphere

Before the migratory history of these two groups could be assessed, environmental samples from the locality of the cemeteries needed to be collected to establish comparative baseline strontium and oxygen isotope values. Soil, water, plant and animal (enamel) samples were collected to determine the local values specific to each region. Water samples were taken from flowing rivers closest to each archaeological site (August 2016) and analysed for oxygen isotopes. As previously stated, the temperature and climate can impact oxygen isotope ratios and will be considered when interpreting these data. Strontium isotope analysis were not conducted on water samples due to budget constraints. Soil samples were taken from inhumations at each site and analysed for strontium isotopes. Two archaeological animals were found at the Iclod Necropolis and were analysed for carbon and nitrogen stable isotope analysis. No animal remains were recovered at the Bögöz or Fenyéd sites. A single plant sample was taken from farmland nearest to each site. Corn husk was chosen to assess the strontium isotope ratios as well as carbon and nitrogen isotope ratios. The fact that this is a new world plant sourced from farmland most likely using agricultural fertilizer may impact the results and will be taking into consideration when interpreting these data (Maurer *et al.*, 2012). The number of samples was limited by funding and time constraints. Due to the expensive nature of biosphere mapping, only one sample of each sample type was collected from each region. A complete list of samples collected to establish the local baseline biosphere range specific to each population can be found in Table 4.3.

Sample	Migration Period	Middle Ages
<i>Human enamel</i>	16	16
<i>Soil</i>	1	1
<i>Plant</i>	1	1
<i>Animal (enamel)</i>	2	0
<i>Water</i>	1	2
TOTAL	21	20

Table 4.3. A summary of samples collected for strontium and oxygen isotope analyses to establish a baseline biosphere range for each population.

4.3.3. Isotope samples: strontium, oxygen, carbon and nitrogen

A complete list of isotopic samples taken organized by period, site and the type of analysis that was conducted on each sample can be found in Appendix 4.1. Adults, non-adults and males and females were analyzed. Permission to perform destructive analyses and to take the samples out of Romania was granted by the curators of the skeletal remains. All bones and teeth were photographed prior to destructive analyses. The dentition was also imaged using photogrammetry techniques to create a 3-dimensional image. This was done so that any features or pathology could still be seen after destructive sampling. A tooth was placed on a stage in the center of a rotating platform. Photographs were taken of the top half of the tooth at a 45° angle from 32 points around the circumference of the tooth (see Figure 4.3). The tooth was then flipped, and the process was repeated on the lower half. Next, the images were combined and processed using Agisoft PhotoScan Professional software to create the 3-dimensional images. Images were also given to the curators for archival purposes and remnant samples were sent back to the curating institution.



Figure 4.3. The equipment setup used to photograph tooth samples to be processed for 3-D photogrammetry models.

4.4. Methods

Both skeletal assemblages were analyzed to establish demographic characteristics (age and sex), the presence/absence of metabolic stress, mobility history, and dietary patterns and related breastfeeding and weaning practices. The data were analyzed to determine any differences between sex, age and health, within and between both populations. Statistical analyses were performed to determine if any observable differences were significant (see Section 4.5). As previously mentioned in Chapter 1, one objective of this research was to create early life-history profiles to explore breastfeeding and weaning practices, as well as consider the possibility of delineating the onset of evident metabolic stress during the person's life. Data from the carbon and nitrogen stable isotope analyses were utilized to create an overall dietary profile for each population. The use of strontium and oxygen isotope analyses were utilised to help reconstruct the migration status of each individual (local vs. non-local), as well as establish baseline biosphere data specific to each region.

4.4.1. Macroscopic skeletal analysis

All analyses and sampling were conducted according to the BABA Code of Ethics and Practice (BABA Working Group for Ethics and Practice, 2010b, 2010a) and

destructive analyses according to APABE (2013). Sample collection for isotopic analyses was only conducted once all macroscopic skeletal analyses were complete. The forms used for recording macroscopic skeletal data can be found in Appendix 4.2. A summary of the age-at-death and biological sex estimation categories used for this study can be found in Table 4.4. The age-at-death, biological sex, and stature estimation data obtained from this analysis was entered into an Access database (see Appendix 5.2). A complete list of standards and references employed to conduct the macroscopic skeletal analyses can be found in Table 4.5. The skeletal remains were examined macroscopically to estimate age-at-death (Brickley, 2004b; O’Connell, 2004), sex (Brickley, 2004a), stature (Brothwell and Zakrzewski, 2004), and assess palaeopathological evidence (Roberts and Connell, 2004) – see below for specific references (Table 4.5).

Age Estimation Categories			Sex Estimation Categories		
<i>Non-adult</i>	infant	birth – 1 year	<i>Male</i>	male	M
	child	1 year – 12 years		probable male	M?
	adolescent	12 – 20 years	<i>Female</i>	female	F
<i>Adult</i>	young adult	20 – 35 years		probable female	F?
	middle adult	35 – 45 years		<i>Indeterminate</i>	Ambiguous
	older adult	+45 years			

Table 4.4. Summary of the defined age and sex categories used in this study.

Method	Standard
<i>Stature estimation</i>	(Trotter and Gleser, 1958)
Age estimation	
<i>Bone growth/epiphyseal fusion</i>	(Scheuer and Black, 2000)
<i>Dental formation/eruption</i>	(AlQahtani, Hector and Liversidge, 2010)
<i>Pubic symphysis</i>	(Brooks and Suchey, 1990)
<i>Auricular surface</i>	(Lovejoy <i>et al.</i> , 1985; Buckberry and Chamberlain, 2002)
<i>Sternal rib ends</i>	(Iscan <i>et al.</i> , 1985)
<i>Dental attrition</i>	(Brothwell, 1981)
Sex estimation	
<i>Os coxae morphology</i>	(Phenice, 1967; Buikstra and Ubelaker, 1994)
<i>Cranial morphology</i>	(Buikstra and Ubelaker, 1994; Brickley, 2004a)
Pathology	
<i>Enamel hypoplasia</i>	(Reid and Dean, 2000; Ortner, 2003: 589-606)
<i>Cribra orbitalia</i>	(Ortner, 2003: pg. 102-104; Brickley and Ives, 2010)
<i>Porotic hyperostosis</i>	(Ortner, 2003: pg. 102-104; Brickley and Ives, 2010)
<i>Scurvy</i>	(Ortner, 2003: pg. 383-393; Brickley and Ives, 2010, pg. 56-69)
<i>Rickets</i>	(Ortner, 2003: pg. 393-404; Brickley and Ives, 2010, pg. 97-112)

Table 4.5. List of methods used for the macroscopic analyses.

An osteometric measuring board and sliding metal callipers were used for measurements. Non-adult age measurements and adult stature measurements were taken from long bones placed on the osteometric board. Stature measurements were taken from complete long bones and followed Trotter and Gleser (1958). The calculation for 'white' male and white female were used as to best fit the Eastern European features expected in this region. Metal callipers were used to measure dental features and lesion diameters. Chapter 2 provides the justification for the specific pathological lesions selected for this study. Evident skeletal pathologies associated with metabolic stress (CO, PH, EH, scurvy, rickets) were analysed to create prevalence rates and patterns. These traits were recorded as present, absent or unobservable (broken or missing skeletal element). If a bone forming lesion was present on a bone, the lesion was further classified as active (woven bone), healing (mixed woven and lamellar bone), or healed (lamellar bone – see Figure 4.4). Severity and grading systems were not used due to the added intra- and interobserver error

that these systems introduce. The neural arch diameters were not recorded because the highly fragmented nature of the remains made this impossible.

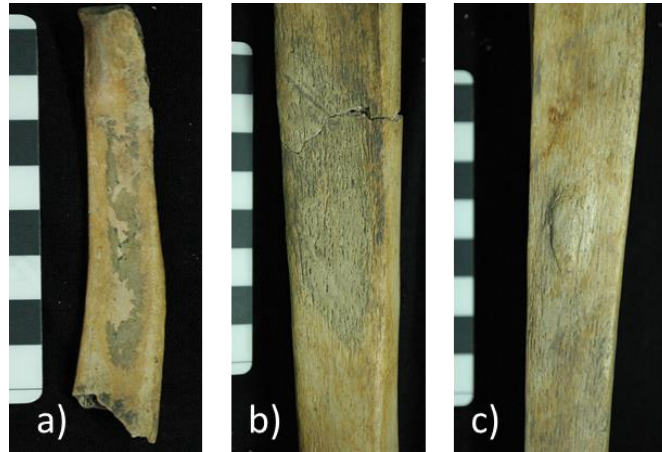


Figure 4.4. Examples of new woven bone (a), mixed woven and lamellar bone (b), and lamellar bone (c). Scale in centimeters.

a) Woven bone present on the visceral surface of the rib (Sk. B255). b) Mixed woven and lamellar bone present on the midshaft of the left tibia (Sk. B135). c) A “button” of lamellar bone present on the midshaft of the right tibia (Sk. B135).

Macroscopic skeletal analyses were conducted on the 25 individuals (25/53, 47%)² from the Iclod Necropolis. The number of skeletons analysed was limited. Each skeleton required extensive cleaning which accounted for half of the time spent working on this collection. Macroscopic skeletal analyses were performed on 97 individuals (97/300, 33%) from the Bögöz Church and 49 individuals (49/52, 94%) from the Fenyéd Cemetery. The high number of individuals analysed from the medieval skeletal assemblage (Bögöz and Fenyéd) was possible due to a high number of burials with poor preservation, highly fragmented remains and less than 25% completeness.

4.4.2. Carbon and nitrogen stable isotope analysis

This section provides the detailed procedures used to prepare the samples for isotope analysis as well as the process of analysing the samples using mass spectrometry.

² At the time of analysis, only 25 individuals associated with the Migration Period had been excavated from the Iclod Necropolis.

(i) Sample preparation

The sample preparation was conducted in the Department of Archaeology at Durham University under the supervision of Prof Janet Montgomery. Protective eyewear, a laboratory coat, and gloves, were worn at all times to ensure safety and to minimize contamination.

(a) Bone

Bone samples were cut using a crushed diamond blade with a hand-held dental drill. Approximately 0.5g of bone was sampled for carbon and nitrogen stable isotope analysis (Mays *et al.*, 2013). All samples were weighed prior to demineralization so collagen yield could be calculated. Bone samples were then put individually in ultrapure water and placed in an Ultrawave (model U50) ultrasonic bath for five minutes to removed large amounts of debris that may have infiltrated them in the burial environment. The bone samples were then placed in individual glass test tubes and filled with approximately 10ml of 0.5M hydrochloric acid (HCl) and stored at 4°C to demineralise (see Figure 4.5b). The 0.5M HCl was created by diluting concentrated HCl with ultrapure water (18.2 MilliQ). The demineralisation process creates a gaseous biproduct, and therefore a marble was placed over the opening of the test tube to allow the gas to escape, while preventing contaminants from falling in. The HCl solution was changed every 3-4 days until the bone was pliable and the mineral component of the bone had been removed. If the samples no longer produced bubbles or floated to the top, they were accepted as completely demineralised. The bone samples were decanted using an EZ-filter and rinsed three times with ultrapure water to eliminate any remaining debris and bring to neutral pH.

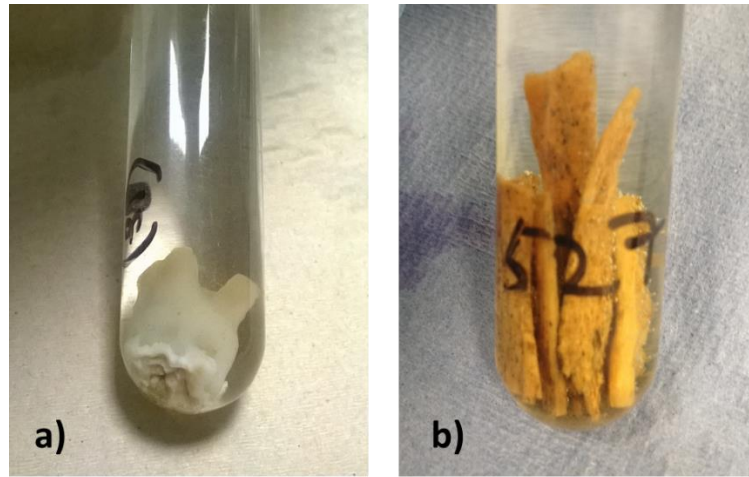


Figure 4.5. Photographs of tooth (a) and bone (b) samples in 0.5M HCl during the demineralisation process.

(b) Incremental dentine

The protocol outlined below follows Method 2 from Beaumont et al (2013). Each tooth was examined. The total length, presence of pathology, wear, and any other anomalies were noted. If EH was present, measurements were taken from the cervical line to the middle of the enamel defect. This enabled an estimation of the timing of the stress event to be plotted onto the isotopic life-history profiles (Reid and Dean, 2000, 2006).

A Seayang Microtech Marathon-3 hand drill with a metal dental burr was used to remove $\sim 100 \mu\text{m}$ from the surface of each tooth to clear away burial environment contamination. Deciduous teeth were left whole to ensure adequate collagen yield was achieved after sectioning. Permanent teeth were sectioned mesio-distally with a drill and a diamond blade attachment. The pulp cavity, dental caries, and cracks in the tooth were reamed with a dental burr to remove the possibility of secondary dentine inclusions. One half of the tooth was stored, and the other half was used for incremental analysis. The enamel was removed from all samples using a diamond dental burr and diamond cutting blade. A small amount of enamel was left on the surface of the tooth so that the enamel-dentine junction remained intact. The enamel removed was then collected for strontium and oxygen isotope analysis. The prepared

dentine sample was then weighed so the collagen yield could be calculated after the dry collagen was produced.

Once the dentine samples were measured and weighed, they were placed in individually labelled 15ml glass test tube and filled with approximately 10ml of 0.5M HCl and stored at 4°C to demineralise (see Figure 4.5a). Like the bone samples, the 0.5M HCl solution was changed every 3-4 days until the samples were demineralised and were malleable enough for sectioning. Each sample was rinsed three times with ultra-pure water to remove any remaining acid and bring to a neutral pH. The samples were stored in ultrapure water at 4°C until all samples were ready to be sectioned.

Latex gloves were worn when handling demineralised dentine samples to prevent contamination during the sectioning process. Sectioning took place when each tooth was pliable and could easily be cut with a metal surgical scalpel. All tools and surfaces were cleaned with Fisher Scientific laboratory grade acetone before and after each sample. A metal surgical scalpel and metal ruler were used to make 1mm sections. Consecutive 1mm sections were cut starting from the dentine crown and continuing towards the root apex, which follows the depositional pattern during formation (Hillson, 2014). It should be noted that the first section of first permanent molars can be less than 1mm in an attempt to only sample the dentine horns, which are formed *in utero* and act as a proxy for the prenatal environment (Beaumont *et al.*, 2015). Sections may be greater than 1mm if the tooth root is too thin (i.e. root apex), to ensure adequate collagen yield. Each section was stored in sequentially labelled microtubes with ultrapure water and stored at 4°C.

(ii) Sample processing

The following procedure was conducted on both bone and dentine samples. A pH3 solution was made using 0.5M HCl and ultrapure water, and the pH was determined using coloured litmus paper. All samples were drained of the ultrapure water and the pH3 solution was added to each storage container. Spot tests were performed throughout this process to confirm a uniform pH. All samples were then transferred to a Techne Dri-block DB200/3 heating block set to 71°C, covered with aluminium foil

to ensure uniform heat, and left for 24-48 hours to denature the samples. Samples were removed from the heating block when the collagen pseudomorph had dissipated into the solution. Once this was achieved, all samples were centrifuged to ensure any debris was separated to the bottom of the tube conical. Bone samples were centrifuged in a Boeco C-28 set to 3500rpm for five minutes. Dentine microtubes were centrifuged on a Sigma 1-14 set to 3500rpm for five minutes. The samples were then stored at -35°C to freeze. Next, each sample was covered with perforated parafilm, to allow adequate airflow while preventing cross contamination during the drying process. The samples were transferred to a Lablyo (Frozen in Time Ltd.) freeze dryer (24-48 hours) to remove all liquid from the collagen samples. Once dry, the samples were weighed to determine the dry collagen yield achieved for each sample.

Next, approximately 0.3mg of dry collagen was transferred into pressed tin capsules (OEA, 5.0x3.5mm) in preparation for mass spectrometer analysis. A Sartorius MSE3.6P-000-DM microbalance was used to weigh the collagen samples. All tools and surfaces were cleaned with acetone before and after each sample. The collagen sample was taken from the top of the tube to avoid the possibility of including the centrifuged debris at the bottom of the conical. Metal tweezers and a spatula were used to transfer the collagen samples from the storage tubes into the tin capsule. The tin capsule containing the collagen sample was then folded and pressed to limit the amount of air in the capsule, and all edges were smoothed to prevent the sample from getting stuck in the mass-spectrometer autosampler.

The collagen samples in the tin capsules are then placed into the CF/EA-IRMS auto-sampler and dropped into the oxidation chamber where the samples undergo flash combustion with helium gas. After combustion, the collagen samples are converted to CO₂ and N₂ gas which is processed by gas chromatography. Conventional gas chromatography (GC) IRMS use the masses of isotopologues of reference gases of N₂ (44, 45, 46) and CO₂ (28, 29, 30) to measure the relative abundance of isotope ratios in the sample (Sharp, 2017, Section 2-1). Because carbon and nitrogen have differential atomic weight, the ratios of each element can be measured independent of each other. C:N atomic values outside 3.1-3.6 were deemed inadequate and not

used when interpreting the resulting data (Schoeninger and DeNiro, 1984). Any samples with less than 1% collagen yield were also classified as insufficient (Van Klinken, 1999). The results of the carbon and nitrogen stable isotope analysis can be found in Chapter 5 (Section 5.2) and were analyzed to determine overall dietary patterns for the individuals selected, explore breastfeeding and weaning practices, and to create incremental dentine early-life history profiles to examine possible periods of stress.

Carbon and nitrogen isotope ratios of collagen can be measured using an IRMS with a high degree of accuracy and precision (Carter *et al.*, 2011; Sharp, 2017, Section 2-26). Carbon and nitrogen stable isotope analysis were conducted at Durham University. Analysis took place in the Stable Isotope Biogeochemistry Laboratory (SIBL), under the supervision of Dr Darren R. Gröcke, in the Department of Archaeology. A Thermo Delta V Continuous Flow Isotope Ratio Mass Spectrometer (CF-IRMS) with an elemental analyser was used to determine the isotopic ratios of the bone and dentine samples. By using a mass spectrometer coupled with an elemental analyser (EA), the analytical problem of nitrogen transfer in vacuum lines is eliminated (Sharp, 2017, Section 9-1). A CF-IRMS instrument measures carbon and nitrogen isotope ratios within a 0.2% uncertainty (Meier-Augenstein, 2010). The reader is referred to (Sharp, 2017, Chp. 2) for additional information regarding IRMS. To assure proper calibration integrity of the mass spectrometer, each batch of samples was run with international standards. Within this study, carbon isotope data were calibrated with international standards: Vienna PDB (VPDB); ANU sucrose (IAEA-C6); graphite (USGS²⁴); and L-glutamic acid (USGS⁴⁰ – Sharp, 2017; IAEA, 2018). Nitrogen isotope data were calibrated using international standards: atmospheric nitrogen (AIR); L-glutamic acid (USGS⁴⁰); and caffeine (IAEA-600 – Pollard *et al.*, 2017; Sharp, 2017; IAEA, 2018).

(iii) Isotope profiles

(a) Overall dietary pattern

To explore overall dietary patterns of the selected individuals from each population, the results of the incremental dentine analysis were combined with bone collagen data and analyzed by site, age-at-death, biological sex estimation, and presences of stress-related lesions rather than on an individual basis. By assigning an approximate age to each incremental dentine data point, it is possible to track changes (dietary and/or stress) through childhood at an individual and population level.

(b) Individual early-life history profiles

The results of the incremental dentine stable isotope analysis enabled sub-annual profiles to be created. As noted in Section 3.1, dentine begins forming in the womb and continues through adolescence (AlQahtani *et al.*, 2010; Hillson, 2014). High-resolution sampling techniques can show changes in the $\delta^{15}\text{N}$ and $\delta^{13}\text{C}$ values at specific ages, which can reveal stress episodes which may relate to the timing of breastfeeding and weaning, and changes in the diet (Beaumont *et al.*, 2013; Beaumont and Montgomery, 2016; King *et al.*, 2018). The age categories for each increment were assigned using the method designed by Beaumont and Montgomery (2015). The isotopic life-history profiles are analysed in Chapter 6 (Section 6.2).

(c) Breastfeeding and weaning practices

As demonstrated in previous studies (see Section 3.2.2.), the impact of breastfeeding and weaning practices on diet/stress can also be revealed through incremental dentine stable carbon and nitrogen analysis (Fuller *et al.*, 2006; Pearson *et al.*, 2010; Beaumont *et al.*, 2015; Reynard and Tuross, 2015). At birth, $\delta^{15}\text{N}$ values are typically representative of the mother's values. After birth, with the introduction of breastmilk, the $\delta^{15}\text{N}$ values increase by one trophic level (2-5‰) (Fuller *et al.*, 2006). As the infant is weaned onto solid foods, the $\delta^{15}\text{N}$ values will then gradually decline to the values seen before breastfeeding, assuming the child is being weaned onto a similar diet as the mother. By tracking this process through incremental dentine sampling, it is possible to approximate the duration of breastfeeding and weaning. The individual profiles were analysed by population, biological sex estimation

category, age-at-death, and the presence of pathological lesions to explore if practices differed across time and space. One challenge for incremental dentine research is the variations that can occur in life-history profiles. Characteristic changes can be identified but the co-occurrence of dietary changes and stress has proven to be harder to interpret. One explanation offered is the effect metabolic stress can have on isotope values.

(d) Metabolic stress profiles

Modern clinical research has found that periods of stress correlate with increased $\delta^{15}\text{N}$ values in high resolution profiles (Hatch *et al.*, 2006; Mekota *et al.*, 2006; D'Ortenzio *et al.*, 2015; King, Halcrow, *et al.*, 2018). Chapter 3 (Section 3.2.2.) further details the possible changes that may be observed. As previously mentioned, dentine forms at a fairly consistent rate and sectioned increments correlate to discrete periods of life and growth. This allows for stress events to be assigned to an approximate age during life. High resolution incremental sampling provides insight into changes between $\delta^{15}\text{N}$ and $\delta^{13}\text{C}$ values, which also helps to differentiate dietary changes and periods of stress.

4.4.3. Mobility isotope analysis

The preparation of samples for mobility isotope analyses follows Evans *et al.* (2010) and Montgomery (2010). In order to determine local biosphere ranges of strontium and oxygen specific to each site, modern and archaeological samples were collected. As stated in Chapter 3 (Section 3.3.3.), plant, soil, and animal enamel samples help to establish the local strontium isotope range ($^{87}\text{Sr}/^{86}\text{Sr}$). Isotope ratios from skeletal remains reflect the bioavailable strontium from the area where a person's food was sourced. River and rain water provides the oxygen isotope ($\delta^{18}\text{O}$) range, which also reflects the effect of latitude and elevation on rainfall, and is captured isotopically in developing skeletal tissue (teeth) of people living in the region (section 3.3.2).

The sample preparation was conducted in the Department of Archaeology at Durham University under the supervision of Prof Janet Montgomery. All tools were cleaned

between each sample with a 2% Decon solution in an ultrasonic bath for five minutes and rinsed three times with ultrapure water. The surface of each tooth was cleaned using a hand-held drill with a crushed diamond dental burr to remove ~100 µm from all surfaces to clear away any contaminants from the burial environment. A diamond blade was used to remove the enamel samples. Approximately 30mg of human enamel was sampled. The enamel samples were examined under a microscope and light source to ensure no dentine was present. Approximately 7-10mg of enamel was stored in a labeled microtube for strontium isotope analysis. The remaining 15-20mg of enamel was powdered and stored in a labeled microtube for oxygen isotope analysis. The dry plant and soil samples were ground by hand with an agate mortar and pestle to maximize the surface area during the chemical dissolution process.

(i) Strontium isotope analysis

All samples were stored in sealed containers and transferred to the analytical facilities. Strontium isotope analyses were conducted at Durham University's Arthur Holmes Laboratory (Department of Earth Sciences) under the supervision of Dr Geoff Nowell. The methodology followed the laboratory protocols and health and safety procedures.

(a) Enamel samples

A Milty Zerostat 3 (anti-static remover) was used to eliminate static charge from each sample before weighing. Approximately 7-10mg of enamel was weighed into a labeled Teflon beaker using a Mettler Toledo AX105 Delta Range microbalance. Next, 500µl of 3M nitric acid (HNO₃) was added to the enamel samples and placed on a hot block (100°C) overnight to dissolve the sample. A 100µl aliquot of the sample was taken prior to column chemistry to measure strontium concentrations. Although steps are taken to minimize strontium contamination during column chemistry, small amounts of contamination can result in different concentrations before and after column chemistry.

(b) Plant samples

The following procedure was used to prepare the plant samples for strontium isotope analysis. Approximately 0.5-1.0mg of ground plant sample was weighed using the microbalance and transferred to a labelled Teflon beaker. Next, 4ml of concentrated HNO₃ was added to each sample to remove the organic components. The samples were placed on a hot plate (100°C) overnight. The reaction of the nitric acid produced a red/brown nitrogen gas. The lids of the Teflon beakers were left loose so that the gas could be extracted through the fume hood while still leaving the samples covered to prevent contamination. Next, 500µl of hydrogen peroxide (30% H₂O₂) was added to each beaker. The reaction causes the sample to effervesce. Once the reaction calmed, the lids were replaced, and the samples were returned to the hotplate for approximately 30 minutes. The hydrogen peroxide step was then repeated. Once the reaction was completed for all the samples, the lids were removed, and the samples were left open on a hotplate (120°C) to allow them to evaporate. The lids were cleaned with ultrapure water to remove any contaminants. Once the samples were dry, 2ml of conc. HNO₃ was added to continue removing any organic material still present in the sample, and the beakers were then returned to the hotplate. After 1-2 hours, 1ml of hydrogen peroxide was added and the beakers were left on the hotplate overnight with loose lids. Once the samples were completely dried, 0.5ml of 3M HNO₃ was added. All samples were centrifuged in a Heraeus Labofuge 300 centrifuge (10,000rpm/5minutes) to ensure any remaining debris was separated to the bottom of the tube conical. The remaining sample was decanted into clean Teflon beakers with a pipette, being careful not to incorporate any debris from the conical. The treated samples were then processed using the strontium column chemistry outlined in Table 4.6 and 4.7.

(c) Soil samples

The following procedure was used to prepare the soil samples for strontium isotope analysis. Approximately 1.5-2.0mg was weighed into a labeled Teflon beaker using a microbalance. As for the plant samples, 4ml of concentrated HNO₃ was added and the samples were placed on a hot plate (100°C) overnight with loose lids. Next, 500µl hydrogen peroxide (30% H₂O₂) was added. Once the reaction calmed, this step was

repeated and then the samples were placed back on the hot plate for 30 minutes with their lids on. Once the reaction was complete, the lids were removed and cleaned, and the samples were left open to dry down. With the samples completely dry, 1ml of conc. HNO₃ and 3ml of hydrofluoric acid (HF) were added to each sample, the lids were fastened, and were then returned to the hotplate overnight. The next day 1ml conc. HNO₃ was added and the samples were left open on the hotplate to dry. Next, 1ml conc. HNO₃ was added, the lids were fastened, and all samples were left on the hotplate overnight. Next, the lids were removed, and the samples were left on the hotplate again to allow the samples to dry. One milliliter of conc. HNO₃ was added and they were left to dry on the hotplate once more. Finally, 1ml of 3M HNO₃ was added, the samples were centrifuged, and then transferred to clean analysis beakers using a pipette.

Once all enamel, plant and soil samples were dissolved, the following column chemistry process was employed (see Figure 4.6). Sample blanks were added to each run to test for any contamination during the preparation and column chemistry processes. Table 4.6 is a step-wise process for cleaning the strontium columns. Once the columns were cleaned, the sample solutions were loaded into the columns (Table 4.7). This was achieved using a pipette and slow dripping the sample onto the resin while taking care not to disrupt the resin. The elution procedure outlined below was conducted to collect the strontium samples for analysis.

<u>Step</u>	<u>Reagent</u>	<u>Volume</u>
<i>Cleaning</i>	MQ H ₂ O	1CV
<i>Cleaning</i>	TD 6N HCl	1CV
<i>Cleaning</i>	MQ H ₂ O	1CV
<i>Loading resin</i>	Sr-Spec Resin	2 drops (~100µl)
<i>Resin cleaning</i>	TD 6N HCl	1CV
<i>Resin cleaning</i>	MQ H ₂ O	2CV
<i>Precondition</i>	3N HNO ₃	200µl

Table 4.6. The process for cleaning the strontium chemistry columns (TD – Teflon distilled, CV – column volume).

Step	Reagent	Volume	Collect
Sample Loading	TD 3N HNO ₃	100-1000µl	NO
Waste Elution	TD 3N HNO ₃	2 x 250µl	NO
Switch out waste beakers for sample collection microtubes			
Sr Collection	MQ H ₂ O	2 x 250µl	YES

Table 4.7. The elution procedure to collect the strontium samples from the columns.

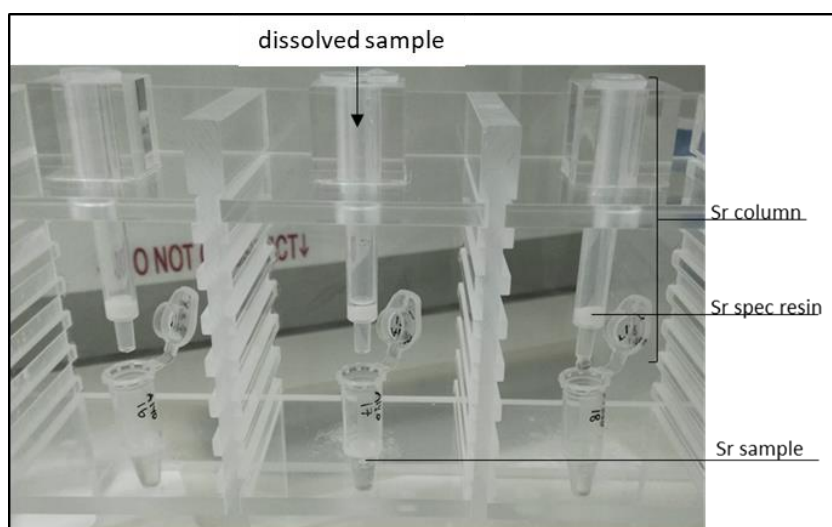


Figure 4.6. Example of the column setup for collecting strontium samples.

After the 500ml of strontium sample had been collected, 22µl of concentrated HNO₃ was added to each microtube to acidify the sample and create a 3% HNO₃ solution for analysis. Each sample was placed on a vortex for 5 seconds to ensure the sample was homogeneous. Next, test concentrations were performed. The nebuliser was placed into the sample and was taken out as soon as the ⁸⁶Sr peak began to level out on the analysis screen. The voltage of the ⁸⁸Sr was used to determine the amount of dilution that would need to take place so that the sample would be approximately 20 volts (⁸⁸Sr) during analysis. In the example below, the sample was diluted so that of the 500µl HNO₃, 398µl comprised the strontium sample collected from the column chemistry.

⁸⁶ Sr (V)	⁸⁸ Sr (V)	For 20V of 88Sr (from Test solution)
3.0	3.0*8.375 = 25.1	20 / 25.1*500 = 398

Analysis was conducted on a Thermo Fisher Neptune Plus plasma sources multi-collector mass spectrometer (MC-ICP-MS). Multi-collector systems allow static simultaneous detection of the desired isotopes which limits the instabilities of the plasma and drift of signal intensity (Jakubowski *et al.*, 2011). A nebuliser (PFA-50) was used with a Cinnabar spray chamber and an uptake set to 90 μ l/minute. The results of the strontium isotope analyses can be found in Chapter 5 (Section. 5.3). The reader is referred to Jakubowski *et al.* (2011) for additional instrument information.

(ii) Oxygen isotope analysis

(a) Carbonate isotope analysis - enamel

The prepared enamel samples were individually ground into powder using an agate mortar and pestle. All surfaces were cleaned with laboratory grade acetone prior to and between each sample to prevent sample contamination. Carbonate oxygen isotope analyses were conducted at two laboratories. The equipment at Durham University (Department of Earth Science) was undergoing maintenance when the first round of samples was ready for analysis. Therefore, the first round (n=20) was sent to IsoAnalytics (<https://www.isoanalytics.com>) for carbonate oxygen analysis. The second round of samples (n=20) were analyzed at Durham University's Arthur Holmes Laboratory (Department of Earth Sciences) when their equipment was running. To assure the accuracy and reproducibility of the results from both laboratories, an enamel sample from the Iclod pig tooth was analysed in both laboratories to determine if there was an offset between the two instruments used.

The first round of carbonate isotope analysis ($\delta^{13}\text{C}$ and $\delta^{18}\text{O}$) was conducted by Steve Brookes at IsoAnalytics Laboratory. The following information regarding the analysis was taken from his report. The full report can be found in Appendix 4.3.

'Samples were weighed into clean Exetainer™ tubes and then flushed with 99.995 % helium. After flushing, phosphoric acid was added to the samples and they could react in the acid overnight to allow complete conversion of carbonate to CO₂. Reference and control materials were prepared the same way. The CO₂ gas liberated from samples was then analysed by Europa

Scientific 20-20 Continuous Flow-Isotope Ratio Mass Spectrometry (CF-IRMS). Carbon dioxide was sampled from the Exetainer™ tubes into a continuously flowing He stream using a double holed needle. Gas species of different mass are separated in a magnetic field then simultaneously measured using a Faraday cup collector array to measure the isotopomers of CO₂ at m/z 44, 45, and 46.

The phosphoric acid used for digestion had been prepared for isotopic analysis in accordance with Coplen *et al.* (1983) was injected through the septum into the vials. The reference material used during analysis was IA-R022 (Iso-Analytical working standard calcium carbonate). IA-R022, NBS-18 and IA-R066 were run as quality control check samples during analysis. The results obtained for the NBS18 and IA-R066 controls are used to check and correct the data as required. The equivalent calcium carbonate content values (%) were derived by comparing the total ion beam data for the samples against the pure calcium carbonate references.

The second round of carbonate isotope analysis was conducted at the Arthur Holmes Laboratory (Durham University) under the supervision of Dr Geoff Nowell and Ms Joanne Peterkin. The powdered enamels were weighed on a microbalance by placing a small square of foil on the balance pan, taring the balance to zero, and transferring approximately 2mg of sample onto the foil using a metal spatula. The weight was recorded, and the samples were transferred into Exetainer™ vials. After the vials were sealed, each was tapped with metal tweezers to ensure the entire sample was collected in the bottom. Once all samples were weighed, the glass vials were placed in the sampling rack. Reference standards (DCS01, NBS18, IAEACOI, LSVEC, DOBBINS) were placed at the beginning, middle, and end of the rack to ensure calibration and drift throughout the entire run. Before the analysis could begin, needle alignment had to be calibrated to avoid any misalignment problems during analysis. Alignment was confirmed across the entire sampling rack. The vials were flushed with 99.9% helium gas. This was achieved by piercing the airtight septum of the vial with a double-holed needle, injecting helium gas, and releasing the air. Once the samples reached 70°C, phosphoric acid was injected into the vials to convert the carbonate

sample into CO₂. Analysis was conducted on a Finnigan Gasbench II CF-IRMS with a CTC analytics PAL system with a precision of less than 0.08‰ for δ¹⁸O and less than 0.06‰ for δ¹³C (Thermo Electron Corporation, 2004).

(b) Oxygen isotope analysis – water samples

Water samples were collected to establish a local δ¹⁸O baseline for each site. River water was collected from the nearest river to each archaeological site. Samples were collected from running water at a location away from local roads and cities to minimise pollution. Rainwater was collected (Odorheiu Secuiesc, August 2016) using a clean container and funnel placed in the middle of an open field to prevent runoff contamination. All samples were stored in air-tight containers at 4°C until analysis. Analysis and sample preparation took place at the SIBL facilities (Durham University) under the supervision of Dr Darren R. Gröcke. A 5ml syringe (no needle) was attached to a Millex 0.45µm syringe filter. The filter was flushed through one time with the sample to saturate the filter pad. Next, 1.5mL of sample was transferred to the analysis vials. Liquid water samples can be analysed using a needle-injector system (Figure 3.8). The needle-injection system takes 20 consecutive analyses from each sample to ensure calibration. Oxygen isotopes from liquid water were measured via laser absorption with high-reflectivity mirrors which quantifies the amount of absorbance at specific wavelength needed to determine the absolute abundance of individual molecules. International reference standards ensure adequate calibration of the instrument. The water samples were analysed on a Los Gatos DLT-100 liquid-water stable isotope instrument which measures hydrogen and oxygen via laser absorption with a precision of 0.2‰ for δ¹⁸O (IAEA, 2009).

The equations in Table 4.8 were used to convert the oxygen isotope data. The results of these analyses can be found in Chapter 5 (Section 5.3) and helped to establish a local biosphere range for each site and explore the migratory status of the individuals sampled.

Conversion	Equation
$\delta^{18}\text{O}_{\text{VPDB}}$ to $\delta^{18}\text{O}_{\text{VSMOW}}$	$\delta^{18}\text{O}_{\text{VSMOW}} (\text{‰}) = (1.03091 * \delta^{18}\text{O}_{\text{VPDB}}) + 30.91$
$\delta^{18}\text{O}_{\text{C}}$ to $\delta^{18}\text{O}_{\text{p}}$	$\delta^{18}\text{O}_{\text{p}} (\text{‰}) = (1.0322 * \delta^{18}\text{O}_{\text{VSMOW}}) - 9.6894$
$\delta^{18}\text{O}_{\text{VSMOW}}$ to $\delta^{18}\text{O}_{\text{DW}}$ (equation 6)	$\delta^{18}\text{O}_{\text{DW}} (\text{‰}) = (1.590 * \delta^{18}\text{O}_{\text{VSMOW}}) - 48.634$

Table 4.8. The equations used to convert the oxygen isotope values (Chenery *et al.*, 2012).

(iii) Local biosphere range and migratory status

To examine the migratory history of the individuals within this study, it was first necessary to establish a local biosphere range for each region studied. As previously mentioned, there are very little comparable data from the Transylvanian Basin that can be used to contextualise the archaeological strontium and oxygen isotope data from this region. As outlined in Chapter 3 (Section 3.3.3), data from other studies in regions with similar geology and climate to Transylvania were compiled to create an extrapolated range for the Transylvanian Basin (Seghedi *et al.*, 2004; Voerkelius *et al.*, 2010; Giblin *et al.*, 2013; Alt *et al.*, 2014; Hakenbeck *et al.*, 2017). The proposed local ranges for the Transylvanian Basin are $^{87}\text{Sr}/^{86}\text{Sr}$ values between 0.7078 and 0.7120 and $\delta^{18}\text{O}_{\text{CARB-VSMOW}}$ values between 21.9 and 26.1‰. To establish ranges specific to each region, samples from archaeological animal enamel, and modern soil, plant, and water samples, were compiled to narrow the biosphere isotope ranges.

Human enamel data were used in this study to see if the individuals fell within the local range. If an individual's values fell outside the established local range or was a clear outlier from the rest of the cluster, that individual was classified as non-local. As the values obtained from human enamel represent the childhood values of that person, it is therefore only possible to determine if a person was non-local if they moved after the enamel was completely developed and were from a region with differential local values to that of the Transylvanian Basin. For this reason, small-scale migrants, or people from a place with a similar geology and climate are difficult to identify. It is acknowledged that strontium and oxygen isotope data can be represented in a large region and/or many regions, and therefore each outlier ('non-local') is examined further in Chapter 6 (Section 6.2.2).

4.5. Statistical analyses

Statistical analyses were conducted to determine if there were significant differences between the two groups of people, and to help identify the outliers. The data were analysed using IBM SPSS software platform. First, each variable was tested for normality to determine if parametric (normally distributed data) or non-parametric (abnormally distributed data) tests should be used. Statistical tests were chosen based on the distribution of the data and number and type of variables being compared. Table 4.9 lists the statistical tests used for these data. The confidence interval is 95% [significance (p) < 0.05]. The significant results of the statistical tests for each method of analysis are reported in the corresponding sections of Chapter 5 and a complete list of tests can be found in Appendix 5.1.

	Variables	Test	Significance
Parametric Tests	Compare 2 variables	Independent T-test	(p) \leq 0.05
	Compare >2 variables	One-way Anova	(p) \leq 0.05
Non-parametric Tests	Compare 2 variables	Independent-sample	(p) \leq 0.05
		Kolmogorov-Smirnov	
	Compare >2 variables	Independent-sample Kruskal-Wallis	(p) \leq 0.05

Table 4.9. Statistical tests used to determine significantly different relationships in the data.

4.6. Summary

The morbidity and mortality patterns of the selected burial populations were assessed through palaeopathological analysis of their skeletal remains. Macroscopic skeletal analysis was performed in order to establish disease patterns within groups (e.g. biological sex, age at death), as well as to compare the prevalence of stress-related osteological and dental lesions between the two populations from Transylvania. The information to be obtained from macroscopic skeletal analysis alone was limited due to the poor condition and fragmentary state of the human

remains studied. Isotopic analyses were thus utilized to gain a deeper understanding of the lives of the people from each population.

When new body tissues are forming (bone, skin, teeth), elements of the environment and diet, such as carbon, nitrogen, strontium and oxygen, are incorporated into the tissues. These elements can then be detected and analysed through isotope analysis to indicate 1. If that person was local to the region of burial (Montgomery *et al.*, 2000; Price *et al.*, 2004; Evans *et al.*, 2012), 2. How long a person was breastfed and the length of time it took to wean them onto solid foods (Fuller *et al.*, 2006; Bourbou *et al.*, 2013; Beaumont *et al.*, 2015; Craig-Atkins *et al.*, 2018), and 3. If they underwent metabolic/nutritional stress during their early life (Beaumont *et al.*, 2016, 2018; King, *et al.*, 2018; Siebke *et al.*, 2019). Combined with macroscopic skeletal data, these methods help to better understand the many and interrelated factors causing early-life stress.

Strontium and oxygen isotope analysis provides information about the geology and climate of the region a person inhabited during childhood (Ericson, 1985; Montgomery, 2010; Evans *et al.*, 2012). A person's mobility status (local or non-local) can be examined by comparing the childhood isotopes encapsulated in forming tooth enamel with the isotope biosphere of their burial environment (Montgomery *et al.*, 2000; Leach *et al.*, 2009; Kendall *et al.*, 2013). One limitation for this project was the dearth of comparable strontium and oxygen isotope data specific to the Transylvania Basin, thus far. To help fill this gap, plant, water, and soil samples were also analysed to establish local baseline biosphere ranges for each archaeological site. Mobility and biosphere data from the surrounding regions, with a similar climate, geology, latitude and altitude, were compiled to extrapolate a proposed local isotope biosphere range for the Transylvanian basin.

The results of each method employed in this study are reported in Chapter 5.

Chapter 5: Results

This chapter provides the results for each method of analysis used. Demographic and palaeopathological profiles can be found in Section 5.1. The results of the carbon and nitrogen stable isotope analyses are reported in Section 5.2 and the results of the strontium and oxygen isotope analyses in Section 5.3. All data were analyzed by period, site, age-at-death, biological sex, and pathological conditions, to explore patterns within and between populations. Statistical analyses were conducted to determine whether the differences observed were significant. The significant results can be found in the corresponding section and a complete inventory of statistical tests performed can be found in Appendix 5.1.

5.1. Macroscopic skeletal analyses

This section reports the results of the macroscopic skeletal analyses. The following information summarizes the results of the demographic and palaeopathological analyses. Details pertaining to how age-at-death, biological sex estimation, and stature calculations were assessed can be found in Appendix 5.2 (digital).

5.1.1. Demography

(i) Migration Period

Macroscopic skeletal analyses were performed on 25 individuals from the Iclod Necropolis (Table 5.1). As previously mentioned, these burials have been associated with the Migration Period and burial artefacts have linked them with the Kingdom of the Gepids. Skeletal preservation ranged from poor to good with the level of fragmentation from severe to good. As mentioned in Section 4.2.1, the Iclod Necropolis was a rescue excavation. Some burials were exposed to the elements in the topsoil, resulting in those individuals having greater taphonomic damage. Most skeletons were 50-100% complete.

Of the 25 individuals analysed, four were non-adults (16%) and 21 were categorised as adults (84%). There were nine male/probable males (43%), 11 female/probable females (52%) and one individual with ambiguous biological sex. Stature calculations could be performed on 16 individuals (64%) and ranged from 161cm to 168cm (\pm 4.7cm 1sd). Mean stature was significantly different between males/M? (170 ± 3.1 cm 1sd) and females/F? (162 ± 3.3 cm 1sd), $t(13) = 4.7050$, $p = 0.0004$.

ID	COMPLETENESS	FRAGMENTATION	PRESERVATION	AGE	SEX	STATURE (CM)
				CATEGORY	ESTIMATION	
ICL111	<25%	severe	poor	young adult	N/A	N/A
ICL120	50-75%	poor	fair	young adult	male?	162-169
ICL122	<25%	poor	fair	adult	male?	N/A
ICL123	50-75%	poor	fair	young adult	male?	172-175
ICL124	<25%	fair	fair	adult	male?	N/A
ICL125	<25%	poor	fair	young adult	male?	N/A
ICL127	50%	fair	fair	child	N/A	
ICL129	75-100%	good	good	child	N/A	
ICL130	75%	fair	fair	middle adult	female?	161-169
ICL131	75-100%	fair	good	child	N/A	
ICL134	50%	fair	fair	adult	female	157-164
ICL135	75-100%	good	good	young adult	female?	158-165
ICL136	75-100%	fair	good	middle adult	female?	158-166
ICL137	50-75%	fair	good	young adult	female?	155-163
ICL138	25%	poor	fair	young adult	male?	N/A
ICL139	50-75%	fair	good	middle adult	female?	161-168
ICL140	75-100%	good	good	middle adult	male	165-172
ICL141	75-100%	fair	good	young adult	male	168-175
ICL142	>25%	poor	good	adolescent	?/male?	N/A
ICL149	75-100%	good	good	middle adult	female	155-163
ICL151	25-50%	poor	fair	adult	ambiguous	163-170
ICL153	25%	poor	fair	middle adult	?/female?	N/A
ICL154	50%	good	good	young adult	female?	163-172
ICL155	50-75%	fair	fair	middle adult	female?	158-165
ICL156	75-100%	good	good	middle adult	female	152-160

Table 5.1. Results of the macroscopic skeletal analysis of individuals from the Iclod Necropolis (Migration Period). Key: N/A - trait could not be assessed due to missing element (s) or lack of diagnostic features; ? – ambiguous biological sex; female? – probable female; male? – probable male. See Section 4.4.1 for defined age categories.

(ii) Middle Ages

Two skeletal populations, Fenyéd and Bögöz, comprise the assemblage for the Middle Ages (n = 144). The data from the two populations are combined (Table 5.2). Most skeletons were 0-75% complete, preservation varying from poor to good, and fragmentation from poor to fair. It was estimated that there were 62 non-adults (43%), 79 adults (55%), and three individuals whose age-at-death could not be estimated (indeterminate). Many individuals (Fenyéd n = 26, Bögöz n = 66) were represented by less than 25% of the skeleton which resulted in a high percentage of individuals where biological sex could not be assessed (57%). Age-at-death estimation was attempted for these individuals (<25% complete) only if the recovered skeletal element(s) had diagnostic features (e.g. fused epiphyses). Sixty-two individuals were complete enough to be analysed for biological sex, and there were 36 male/probable males (25%), 24 female/probable females (17%) and two ambiguous skeletons (1%). The remaining 57% of the population could not be assessed for biological sex. Stature calculations were possible for 35 individuals (24%) and the range was from 160cm to 168cm ($\pm 8.8\text{cm}$ 1sd). Mean stature was significantly different between males/M? ($170 \pm 5.8\text{cm}$ 1sd) and females/F? ($156 \pm 6.1\text{cm}$ 1sd), $t(29) = 6.281406$, $p = 0.000001$.

ID	Complete	Fragmentation	Preservation	Age Category	Sex Estimation	Stature (cm)
<i>FEN1</i>	50%	fair	Poor	adolescent	N/A	N/A
<i>FEN2</i>	50-75%	fair	Poor	adolescent	N/A	N/A
<i>FEN3</i>	<25%	poor	Poor	middle adult	female	N/A
<i>FEN5</i>	<25%	severe	Poor	middle adult	female?	N/A
<i>FEN6</i>	50-75%	fair	Fair	young adult	male	163-170
<i>FEN7</i>	<25%	poor	Fair	child	N/A	
<i>FEN9</i>	25%	poor	Poor	older adult	female?	N/A
<i>FEN10</i>	50%	fair	Poor	adolescent	N/A	N/A
<i>FEN11</i>	<25%	poor	Poor	N/A	N/A	N/A
<i>FEN12</i>	<25%	poor	Fair	young adult	ambiguous	N/A
<i>FEN13</i>	<25%	poor	Poor	N/A	N/A	N/A
<i>FEN14</i>	25-50%	poor	Poor	middle adult	female?	N/A
<i>FEN15</i>	25%	poor	Poor	child	N/A	
<i>FEN16</i>	<25%	poor	Poor	middle adult	N/A	N/A
<i>FEN17</i>	75-100%	good	Good	older adult	male	164-170
<i>FEN17A</i>	<25%	fair	Good	middle adult	female	N/A
<i>FEN18</i>	<25%	poor	Fair	middle adult	male	N/A

FEN19	50-75%	good	Fair	middle adult	female?	152-159
FEN20	50-75%	fair	Poor	middle adult	?/female?	160-169
FEN21	<25%	poor	Poor	child	N/A	
FEN22	<25%	poor	Fair	child	N/A	
FEN23	50%	fair	poor	young adult	male?	169-175
FEN24	<25%	poor	poor	adult	N/A	N/A
FEN25	25-50%	poor	poor	child	N/A	
FEN26	<25%	poor	poor	N/A	N/A	N/A
FEN27	50-75%	poor	fair	child	N/A	
FEN28	<25%	poor	fair	child	N/A	
FEN29	75-100%	good	fair	young adult	female	149-156
FEN30	25-50%	poor	fair	child	N/A	
FEN32	50%	poor	poor	young adult	male?	N/A
FEN34	<25%	poor	poor	middle adult	male?	N/A
FEN35	<25%	poor	poor	young adult	male?	N/A
FEN36	<25%	fair	good	child	N/A	
FEN37	25-50%	poor	poor	young adult	male?	N/A
FEN38	25%	poor	poor	child	N/A	
FEN39	<25%	poor	poor	older adult	female	N/A
FEN40	<25%	severe	poor	middle adult	male?	N/A
FEN41	75-100%	fair	fair	young adult	male?	174-180
FEN42	25%	poor	good	infant	N/A	
FEN43	25%	fair	good	adolescent	N/A	N/A
FEN44	<25%	poor	poor	middle adult	male?	N/A
FEN45	50-75%	poor	poor	child	N/A	
FEN46	<25%	poor	poor	child	N/A	
FEN48	75-100%	good	good	young adult	male?	177-183
FEN49	50%	fair	poor	child	N/A	
FEN50	50-75%	fair	fair	adolescent	N/A	N/A
FEN52	25-50%	poor	poor	adolescent	N/A	N/A
BOG1	25%	fair	good	older adult	female?	161-169
BOG3	50-75%	fair	fair	child	N/A	
BOG6	<25%	fair	fair	N/A	N/A	N/A
BOG10	75-100%	good	good	young adult	?/m?	162-170
BOG13	50-75%	fair	fair	young adult	male	171-179
BOG14	75-100%	good	good	middle adult	?/m?	162-170
BOG16	<25%	poor	poor	child	N/A	
BOG18	75-100%	good	good	middle adult	female	140-147
BOG19	50-75%	good	good	older adult	male	167-175
BOG33	<25%	fair	fair	infant	N/A	
BOG35	75-100%	good	good	older adult	female?	153-161
BOG40	<25%	fair	fair	child	N/A	
BOG52	<25%	fair	fair	adult	N/A	N/A
BOG54	75-100%	good	good	older adult	female?	144-151
BOG55	<25%	good	good	young adult	male	N/A
BOG57	<25%	poor	poor	adult	female?	158-166
BOG59	50-75%	good	good	adolescent	?/male?	
BOG63	<25%	fair	fair	adult	N/A	N/A

BOG66	50%	fair	good	middle adult	female?	N/A
BOG67	<25%	fair	fair	adult	N/A	N/A
BOG77	<25%	fair	poor	child	N/A	
BOG78	<25%	good	good	child	N/A	
BOG79A	<25%	Poor	poor	adult	male	N/A
BOG79B	<25%	fair	fair	child	N/A	
BOG85	<25%	fair	good	child	N/A	
BOG89	<25%	fair	fair	adult	N/A	N/A
BOG93	<25%	poor	poor	adult	N/A	N/A
BOG95	<25%	fair	fair	adolescent	N/A	N/A
BOG102	50%	fair	good	adolescent	N/A	N/A
BOG103	<25%	fair	fair	child	N/A	
BOG107	25-50%	poor	poor	child	N/A	
BOG108	25-50%	fair	poor	child	N/A	
BOG109	75-100%	good	good	child	N/A	
BOG112	50%	good	good	older adult	female?	152-161
BOG123	<25%	fair	fair	adult	N/A	153-160
BOG125	<25%	poor	poor	adult	N/A	N/A
BOG127	<25%	fair	good	child	N/A	
BOG128	<25%	fair	good	child	N/A	
BOG129	<25%	poor	fair	adolescent	N/A	N/A
BOG130	<25%	poor	fair	adolescent	N/A	N/A
BOG131	<25%	fair	poor	child	N/A	
BOG132	<25%	poor	poor	adolescent	N/A	N/A
BOG134	<25%	fair	fair	adult	N/A	N/A
BOG135	<25%	good	good	middle adult	ambiguous	174-181
BOG137	75-100%	good	good	young adult	male?	160-168
BOG138	<25%	fair	fair	young adult	male?	N/A
BOG144	50-75%	fair	good	adolescent	N/A	149-158
BOG146	<25%	fair	fair	adult	N/A	N/A
BOG149	75-100%	fair	fair	middle adult	male	161-168
BOG152	<25%	fair	fair	middle adult	male	N/A
BOG153	<25%	good	good	adolescent	N/A	N/A
BOG161	<25%	good	good	young adult	male?	N/A
BOG169	<25%	fair	fair	adult	N/A	N/A
BOG172	<25%	poor	poor	young adult	female?	N/A
BOG174	<25%	fair	fair	adult	female?	154-162
BOG176	<25%	fair	good	middle adult	male	N/A
BOG177	50-75%	fair	fair	adolescent	male?	168-175
BOG179	<25%	fair	fair	adolescent	N/A	N/A
BOG182	<25%	fair	fair	adult	N/A	N/A
BOG194	75-100%	good	good	adolescent	N/A	N/A
BOG196	25%	fair	fair	middle adult	?/female?	N/A
BOG197	75-100%	good	good	middle adult	male	160-166
BOG200	50%	fair	good	older adult	male	167-175
BOG210	<25%	fair	fair	child	N/A	
BOG211	<25%	fair	fair	child	N/A	
BOG212	<25%	fair	fair	adult	N/A	N/A

BOG231	<25%	poor	poor	adult	N/A	N/A
BOG240	25-50%	poor	poor	adolescent	?/male?	N/A
BOG243	<25%	poor	poor	infant	N/A	
BOG246A	<25%	poor	poor	infant	N/A	
BOG246B	<25%	poor	poor	child	N/A	
BOG247	50-75%	fair	good	child	N/A	
BOG248	<25%	fair	good	young adult	male	170-178
BOG249	25-50%	good	good	young adult	female?	150-159
BOG250	75-100%	good	good	child	N/A	
BOG251	25%	fair	good	young adult	female?	153-162
BOG252	50-75%	good	good	middle adult	male?	153-161
BOG253	<25%	poor	poor	infant	N/A	
BOG254	<25%	fair	good	non-adult	N/A	
BOG255	25%	good	good	young adult	female	152-161
BOG260	<25%	poor	poor	young adult	N/A	N/A
BOG262	<25%	fair	fair	adult	male?	N/A
BOG264	<25%	good	good	infant	N/A	
BOG265	75-100%	good	good	infant	N/A	
BOG270	<25%	fair	fair	adult	N/A	N/A
BOG272	50%	fair	good	middle adult	female?	N/A
BOG273	<25%	poor	poor	adult	female?	N/A
BOG275	<25%	good	good	child	N/A	
BOG276	<25%	poor	poor	infant	N/A	
BOG281	50-75%	good	good	child	N/A	
BOG282	25%	good	good	adult	male	170-179
BOG283	<25%	fair	fair	adult	N/A	161-169
BOG284	25%	good	fair	infant	N/A	
BOG286	50%	fair	good	middle adult	male?	171-178
BOG287	<25%	fair	fair	adult	N/A	N/A
BOG289	<25%	fair	good	middle adult	male?	N/A
BOG290	<25%	fair	good	middle adult	male	N/A

Table 5.2. Results of the macroscopic skeletal analysis of individuals from the Bögöz and Fenyéd cemeteries (Middle Ages). Key: N/A - trait could not be assessed due to missing bones or parts of bone(s) or lack of diagnostic features; ? – ambiguous biological sex; female? – probable female; male? – probable male. See Section 4.4.1 for defined age categories.

When the Migration Period and medieval assemblages were combined, the mean statures were significantly different between males/M? ($169.8 \pm 5.4\text{cm}$ 1sd) and females/F? ($158.6 \pm 5.7\text{cm}$ 1sd), as determined by one-way ANOVA ($F(3,44) = 17.40493$, $p = 0.00000$). The percentages of adult, non-adult and indeterminate individuals for both skeletal assemblages are compared in Figure 5.1. The individuals from the medieval assemblage were nearly even across non-adult and adult age

categories, and age-at-death could not be assessed for 2% (3/144) of individuals due to a lack of identifiable skeletal features. The Migration Period assemblage comprised mostly adults with only 16% (4/25) of the population assessed as non-adult.

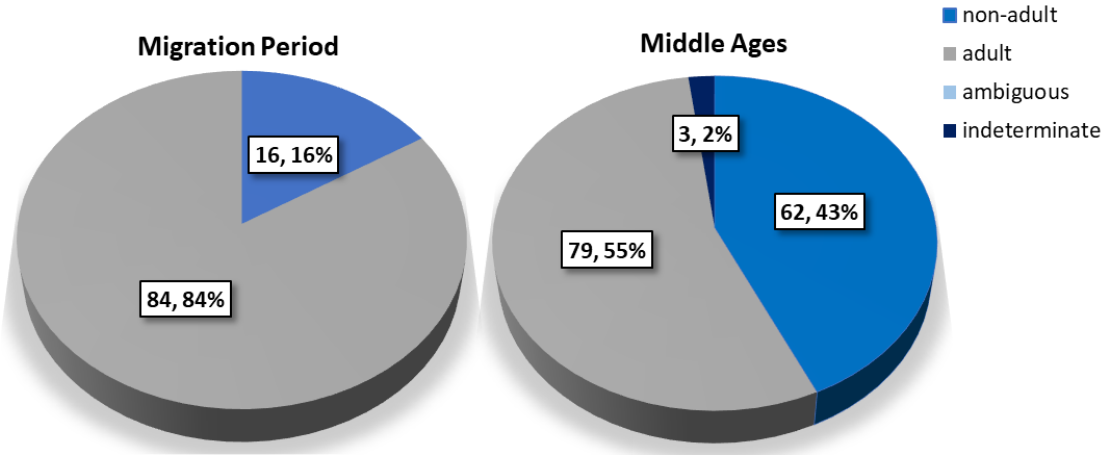


Figure 5.1. The percentage of individuals in each age category according to skeletal assemblage.

The percentage of individuals in each sex category are compared in Figure 5.2. The individuals from the Migration Period were nearly even across male and female categories, the biological sex of one individual (4%) was found to be ambiguous, and four individuals could not be assessed (indeterminate, 16%). The medieval assemblage had two individuals (1%) whose sex related skeletal traits were found to be ambiguous. The high number of individuals with less than 25% completeness resulted in 57% (82/144) of the medieval assemblage whose biological sex could not be assessed.

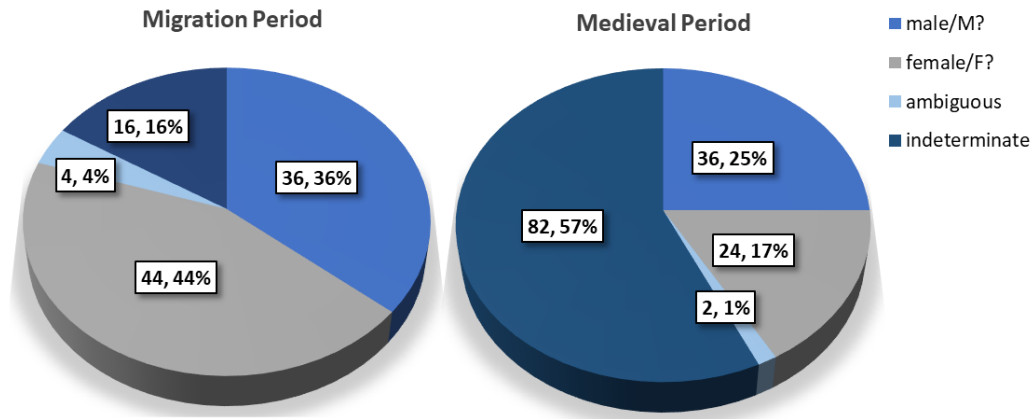


Figure 5.2. Percentage of individuals in each sex estimation category by skeletal assemblage.

5.1.2. Palaeopathology

The following section summarizes the results of the palaeopathological analysis. Detailed information for each individual and descriptions of skeletal lesions can be found in Appendix 5.3. The percentage of individuals from each skeletal assemblage that had one or more of the stress-related lesions is shown in Figure 5.3. Overall 64% (16/25) of individuals from the Migration Period and 32% (46/144) of individuals from the medieval assemblage had one or more skeletal lesions consistent with metabolic disorders and/or physiological stress.

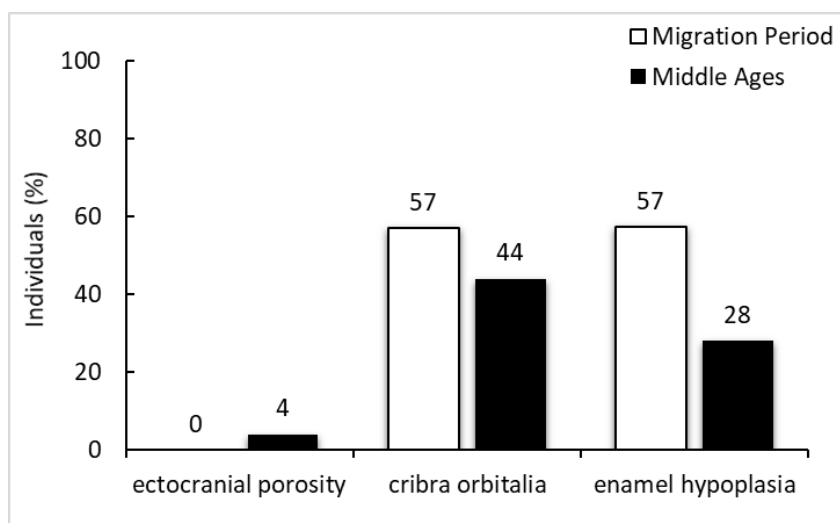


Figure 5.3. Percentage of individuals with lesions by skeletal assemblage. The percentage of individuals represents the crude prevalence rate for each lesion (number of individuals with the lesion ÷ number of individuals who had the skeletal element*100).

(i) Enamel hypoplasia

An EH lesion was marked as being present if the enamel defect was visible without the use of magnification under a light source or was palpable by gliding a fingernail over the surface of the tooth to feel the deformity that results from the hypoplasia. The prevalence of EH by age-at-death category and biological sex estimation can be found in Table 5.3. Overall, when the presence of EH was analysed by age category, young adults had the highest prevalence of individuals with one or more hypoplastic events (8/25, 32%). Eleven males/m? and 11 females/f? had EH, and female/f? had the highest prevalence (11/32, 34%).

Age category	Migration Period		Middle Ages		Combined total		
	present	total	present	total	present	total	%
infant	2	4	0	5	2	9	22
child		0	3	27	3	27	11
non-adult		0	0	1	0	1	0
adolescent	0	1	5	15	5	16	31
young adult	2	8	6	17	8	25	32
middle adult	6	8	4	26	10	34	29
adult	1	4	1	3	2	7	29
older adult			1	8	1	8	13
	11/25, 44%		20/102, 20%		31/127, 24%		
Biological Sex	Migration Period		Middle Ages		Combined total		
	present	total	present	total	present	total	%
male/M?	2	9	9	34	11	43	26
female/F?	7	11	4	21	11	32	34
ambiguous		0	0	2	0	2	0
	9/20, 45%		13/57, 23%		22/77, 29%		

Table 5.3. Crude prevalence rate for individuals with EH by age category and biological sex. The highest prevalence/percentage are indicated with bold font. Key: present - individual had at least one tooth with EH; total - the total number of individuals with dentitions present.

Examination of individuals from the Migration Period revealed 57% had enamel defects. Forty-three teeth of the 395 preserved had one or more enamel defects (11%). When the presence of enamel defects was analysed by age category, middle adults had the highest prevalence (6/8, 75%), and female/probable female category had the highest prevalence (7/11, 64%). Examination of individuals from the Middle

Ages found 28% of individuals had at least one enamel defect (see Figure 5.4). Sixty-five teeth of the 1089 preserved in the medieval assemblage had enamel defects (5.9%). When the presence of enamel defects was analysed by age category, young adults had the highest prevalence (6/17, 35%), with the highest prevalence in male/m? category (9/34, 26%).

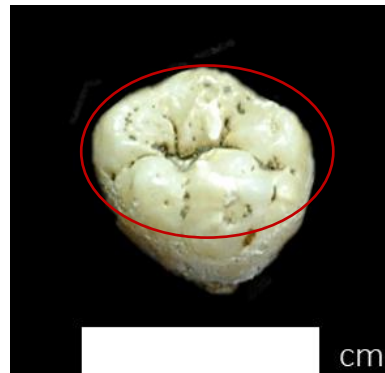


Figure 5.4. Cuspal enamel defects (Skeleton FEN52).

(ii) Porotic hyperostosis

Fourteen individuals of twenty-five analysed from the Migration Period had cranial fragments preserved well enough to record PH, none of which had evidence of PH. Two individuals analysed from the medieval assemblage had evidence of porosity present on the ectocranial surface of the cranium (see Figure 5.5). As mentioned in Section 2.2.3, a radiograph is required to confirm PH, but radiography was not used in this study (Roberts and Connell, 2004; Garcia *et al.*, 2018). The tentative prevalence of PH within the medieval assemblage was 3.7% (2/54 individuals).



Figure 5.5. Abnormal porosity (compared to the rest of the population) on the right parietal bone (Skeleton BOG66).

(iii) Cribra orbitalia

When the presence of CO was analysed by age category overall, the child (1-12 years) and middle adult age categories (35-50 years) had the highest occurrence (10/16 and 10/29 respectively), and 100% of infants had lesions in their orbits (4/4 – Table 5.4). Males and females had equal prevalence rates (38%) for orbital lesions (8/21 and 9/24 respectively). Fourteen of the 25 individuals from the Migration Period had orbital elements preserved well enough for analysis, and eight individuals had lesions on one or both orbits (57%) (see Figure 5.6). Lesions were present in seven of the right and seven of the left orbits (true prevalence = 14/28, 48%) and six individuals had lesions present in both orbits. When the presence of CO was analysed by age category, infants (3/3, 100%) and young adults (3/4, 75%) had the highest prevalence rates. Fifty-five individuals from the medieval assemblage had at least one orbital roof preserved, and 24 had lesions present in one or both orbits (44%). The lesion was present in 15 of the right orbits and 18 of the left orbits (true prevalence = 33/99, 34%) and six individuals had lesions present in both orbits. When the presence of CO was analysed by age category, the infant (1/1, 100%) and child categories showed the highest prevalence rates (10/16, 63%), and females/probable females had the highest prevalence (6/14, 43%) when compared to males/probable males.

Age category	Migration Period		Middle Ages		Combined total		
	present	total	present	total	present	total	%
infant	2	2	1	1	3	3	100
child		0	10	16	10	16	63
adolescent	0	0	3	6	3	6	50
young adult	3	4	4	9	7	13	54
middle adult	3	8	7	19	10	27	37
adult	0	1	0	2	0	3	0
older adult			0	3	0	3	0
	8/15, 53%		25/56, 45%		33/71, 46%		
Biological Sex	Migration Period		Middle Ages		Combined total		
	present	total	present	total	present	total	%
male/M?	3	3	5	18	8	21	38
female/F?	3	10	6	14	9	24	38
	6/13, 46%		11/32, 34%		17/45, 38%		

Table 5.4. Crude prevalence rates for individuals with CO by age category and biological sex. The highest prevalence rates/percentages are indicated with bold font. Key: present - individual with evidence of CO in one or both orbits; total - the total number of individuals with orbits present.



Figure 5.6. Porosity and new bone formation across the left orbital roof (Skeleton ICL131).

(iv) Arrested growth

The skeleton has been found to slow down or cease the process of growth when a person is under- or malnourished. However, the teeth maintain a steady growth and development rate during stress events. This can result in the dentition estimating an older age than the bones of the skeleton. This can be seen in the archaeological record by comparing the estimated skeletal age against the dental formation and eruption age estimation. If the skeletal age was estimated to be younger than the dental age, individuals were considered to have arrested growth (see Section 2.2.3).

Three individuals from the Migration Period had enough teeth and skeletal elements preserved to compare dental formation age estimation against skeletal growth and epiphyseal fusion rates. All three had skeletal age estimations younger than the dental formation age, indicating growth arrest. Thirteen non-adult individuals from the medieval assemblage could be assessed for growth arrest and 10 individuals had skeletal age estimates younger than dental formation age estimation (77%).

(v) Metabolic disorders

Metabolic disorders, like scurvy and rickets, can manifest in the skeleton in numerous ways. The location and types of lesions utilised within this study can be found in Section 2.2.3. Figures 5.7 and 5.8 are two examples of probable metabolic disease related skeletal changes found in the skeletal assemblages studied. Seventeen individuals from the Migration Period (68%, 17/25) were found to have one or more lesions associated with metabolic/nutritional deficiency and five of those individuals (20%, 5/25) had multiple lesions consistent with the presence of scurvy and/or rickets. Fifty-nine individuals from the medieval assemblage (41%, 59/144) had one or more skeletal lesions and 12 of those (8%) had multiple skeletal lesions consistent with scurvy and/or rickets.

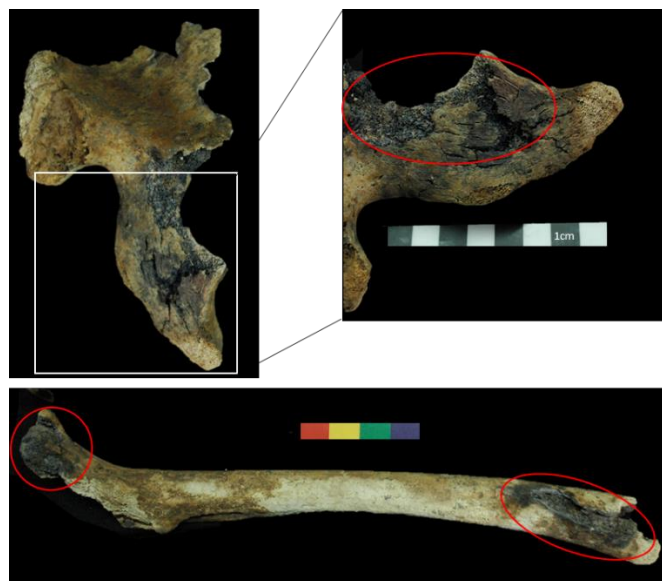


Figure 5.7. Probable haemorrhagic staining on the left os coxa and femur of Skeleton BOG240.



Figure 5.8. Abnormal porosity (compared to the rest of the population) on the anterior part of the mandible of Skeleton ICL129.

5.2. Carbon and nitrogen stable isotopic analyses

Carbon and nitrogen stable isotope analyses were performed on human, plant and animal samples. The results of these analyses provide information regarding the ecology and subsistence pattern for each population.

5.2.1. Biosphere data

Samples of modern plant and ancient animal remains were analysed to produce an approximate local baseline for each skeletal assemblage. The results of these analyses can be found in Table 5.5. Archaeological remains of one pig and one cow were excavated from the Iclod Necropolis and they were sampled for bulk dentine carbon and nitrogen stable isotope analysis. Both animal samples were analysed twice to confirm the results. The animal remains from the Iclod Necropolis had $\delta^{15}\text{N}$ values from 7.2 to 9.5‰ (n = 4, mean: $8.4 \pm 1.1\%$ 1sd) and $\delta^{13}\text{C}$ values from -21.5 to -20.6‰ (n = 4, mean: $-21.1 \pm 0.4\%$ 1sd). There were no archaeological plant remains available at either site therefore a modern corn husk was sampled from each region. The plant material was analysed three times to confirm the results. Modern samples were adjusted ($\delta^{13}\text{C}$ -1.5‰) to account for the Suess Effects (Suess, 1958; Friedli *et al.*, 1986). The two modern plant samples had $\delta^{15}\text{N}$ values from -0.3 to 3.1‰ (mean: $1.2 \pm 1.4\%$ 1sd) and $\delta^{13}\text{C}$ values from -13.9 to -13.6‰ (mean: $-13.8 \pm 0.1\%$ 1sd). The small sample size is acknowledged and was taken into consideration when interpreting these data.

ID	$\delta^{15}\text{N}_{\text{AIR}}$ (‰)				$\delta^{13}\text{C}_{\text{V-PBD}}$ (‰)			
	Max	Min	Mean	1sd	Max	Min	Mean	1sd
ICL_PLANT*	0.1	-0.3	-0.2	0.17	-13.9	-13.9	-13.9	0.03
ICL_PIG	9.5	9.4	9.4	0.06	-20.6	-20.7	-20.7	0.07
ICL_COW	7.4	7.2	7.3	0.06	-21.4	-21.5	-21.5	0.04
BF_PLANT*	3.1	2.3	2.7	0.30	-13.6	-13.9	-13.7	0.14

KEY ICL Iclod (Migration Period)
 BF Bögöz/Fenyéd (Middle Ages)
 * Modern sample

Table 5.5. The results of the stable carbon and nitrogen isotope analyses of plant and animal remains from the regions of both skeletal populations.

5.2.2. Bone collagen data

As mentioned in Section 4.3, bone samples were taken from adults estimated to be older than 25 years at the time of death. The bone collagen values help to reveal the average adult diet consumed during the years leading up to death. All bone samples had well-preserved collagen with yields great than 1% (Van Klinken, 1999) and C:N atomic values between 2.9-3.6 (Schoeninger and DeNiro, 1984). The $\delta^{15}\text{N}_{\text{BONE}}$ of samples analysed from the Migration Period skeletons (n=15) range from 9.7 to 11.0‰ (mean: $10.5 \pm 0.4\%$ 1sd) and $\delta^{13}\text{C}_{\text{BONE}}$ range from -18.5 to -17.3‰ (mean: $-18.0 \pm 0.3\%$ 1sd). The bone collagen for samples from the medieval skeletons (n=8) have $\delta^{15}\text{N}_{\text{BONE}}$ values ranging from 9.1 to 11.8‰ (mean: $10.2 \pm 0.9\%$ 1sd) and $\delta^{13}\text{C}_{\text{BONE}}$ from -19.8 to -17.4‰ (mean: $-18.9 \pm 0.8\%$ 1sd). A complete list of the bone collagen data can be found in Table 5.6 and are plotted by population in Figure 5.9.

Period	I.D.	%N	$\delta^{15}\text{N}_{\text{AIR}} \text{‰}$	%C	$\delta^{13}\text{C}_{\text{VPDB}} \text{‰}$	Yield (%)	C:N atomic
<i>Migration</i>	<i>ICL120</i>	15.7	10.1	43.3	-18.1	5.1	3.2
	<i>ICL123</i>	15.9	10.9	42.8	-18.2	5.7	3.1
	<i>ICL130</i>	15.9	9.7	43.7	-17.9	6.8	3.2
	<i>ICL134</i>	15.7	10.1	43.7	-17.3	8.0	3.2
	<i>ICL135</i>	15.2	10.4	42.2	-17.8	10.9	3.2
	<i>ICL136</i>	16.0	10.9	44.0	-17.9	18.0	3.2
	<i>ICL137</i>	15.8	10.8	43.6	-18.2	11.7	3.2
	<i>ICL138</i>	15.2	10.0	42.5	-17.4	5.0	3.3
	<i>ICL139</i>	15.6	10.5	42.8	-18.1	12.3	3.2
	<i>ICL140</i>	15.1	10.2	41.8	-17.8	4.6	3.2
	<i>ICL141</i>	15.3	11.0	44.0	-18.1	4.8	3.4
	<i>ICL149</i>	15.2	10.5	41.7	-18.1	12.7	3.2
	<i>ICL154</i>	14.9	11.0	42.4	-18.5	3.1	3.3
	<i>ICL155</i>	15.4	10.4	42.8	-18.4	8.2	3.2
	<i>ICL156</i>	14.8	10.6	40.2	-18.1	11.4	3.2
	<i>Middle Ages</i>	<i>FEN6</i>	15.2	9.4	40.7	-18.6	7.9
<i>FEN9</i>		15.6	10.7	43.4	-19.8	5.2	3.2
<i>FEN14</i>		15.5	9.1	42.0	-17.4	8.2	3.1
<i>FEN17</i>		16.0	11.0	43.8	-19.6	10.1	3.2
<i>BOG10</i>		15.1	9.8	42.2	-18.1	5.7	3.3
<i>BOG66</i>		15.9	11.8	43.8	-19.2	9.0	3.2
<i>BOG252</i>		14.7	9.7	40.4	-18.7	3.3	3.2
<i>BOG255</i>		14.4	10.4	39.9	-19.4	3.6	3.2

Table 5.6. The results of the carbon and nitrogen stable isotope analysis of bone collagen for each skeletal assemblage.

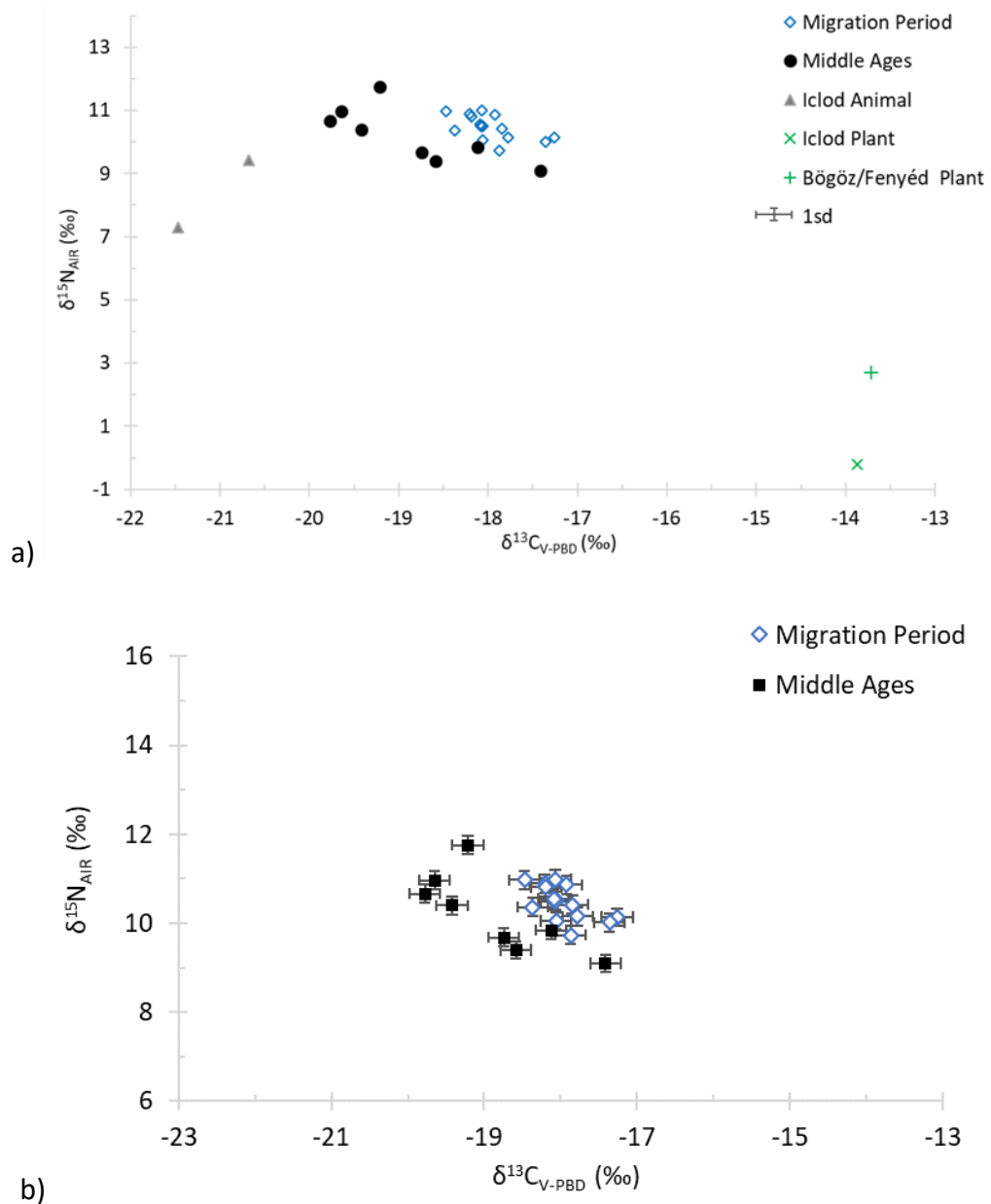


Figure 5.9. The results of the bone collagen carbon and nitrogen stable isotope analyses plotted with the animal and plant data (a) and by skeletal assemblage (b). Analytical error = $\pm 0.2\text{‰}$.

Statistical analyses were performed on the bone collagen carbon and nitrogen stable isotope data. The significant relationships can be found in Table 5.7. There were no significant differences in the $\delta^{13}\text{C}_{\text{BONE}}$ values when compared by site, biological sex, and the presence of arrested growth lesions. There was a significant difference between the $\delta^{13}\text{C}_{\text{bone}}$ values for individuals from the Migration and medieval assemblages. There were no significant differences when the $\delta^{15}\text{N}_{\text{bone}}$ results were

compared by site, period, age-at-death, or the presence of lesions. There was a significant difference in $\delta^{15}\text{N}_{\text{bone}}$ values when males and females from both skeletal assemblages were combined and compared.

<i>Test Variable</i>	<i>Grouping Variable</i>	<i>Statistical Test</i>	<i>P (0.05)</i>	<i>Significant relationships</i>
Combined				
$\delta^{13}\text{C}_{\text{BONE}}$	Period	Independent-sample Kolmogorov-Smirnov	0.006	Migration Period - Middle Ages
	Site	Independent-sample Kruskal-Wallis	0.020	Migration Period - Middle Ages
$\delta^{15}\text{N}_{\text{BONE}}$	Sex Estimation	Independent-sample Kolmogorov-Smirnov	0.049	male/M? - female/F?

Table 5.7. The statistically significant differences in the bone collagen data.

5.2.3. Incremental dentine data

Stable carbon and nitrogen analyses were performed on the teeth of 39 individuals (Migration Period – 19, medieval – 20). All dentine samples had C:N values between 2.9-3.6 and yields greater than 1%, both indicating well-preserved collagen. The incremental dentine $\delta^{15}\text{N}_{\text{INCR}}$ results for individuals from the Migration Period ranged from 8.4 to 16.0‰ (mean: $10.8 \pm 1.3\%$ 1sd) and for $\delta^{13}\text{C}_{\text{INCR}}$ ranging from -20.9 to -11.6‰ (mean: $-17.4 \pm 1.1\%$ 1sd). The incremental dentine data for the medieval assemblage had $\delta^{15}\text{N}_{\text{INCR}}$ values ranging from 8.8 to 15.4‰ (mean: $11.2 \pm 1.3\%$ 1sd) and $\delta^{13}\text{C}_{\text{INCR}}$ from -23.5 to -16.1‰ (mean: $-19.1 \pm 1.0\%$ 1sd). The complete data set with results for each increment for each tooth sampled from each individual can be found in Appendix 5.4. The summary values for all individuals sampled for incremental dentine can be found in Table 5.8 and are plotted by population in Figure 5.10. Life-history profiles for each individual can be found in Appendix 6.2.

Period	Skeleton	$\delta^{13}\text{C}_{\text{V-PBD}}$ (‰)			$\delta^{15}\text{N}_{\text{AIR}}$ (‰)			Yield (%)	C:N
		Mean	Max	Min	Mean	Max	Min	Mean	Mean
Migration	<i>ICL111</i>	-17.6	-16.1	-19.2	10.2	10.9	9.6	9.8	3.2
	<i>ICL120</i>	-18.1	-17.0	-20.9	10.3	11.5	9.3	14.1	3.2
	<i>ICL123</i>	-18.0	-16.4	-19.6	11.0	13.0	9.0	13.3	3.1
	<i>ICL127</i>	-18.1	-16.1	-19.9	12.5	14.7	10.3	11.6	3.3
	<i>ICL129</i>	-17.5	-15.6	-20.3	12.4	13.9	9.8	2.5	3.3
	<i>ICL130</i>	-16.3	-14.0	-18.2	9.8	12.3	8.9	15.6	3.2
	<i>ICL131</i>	-18.1	-16.9	-18.8	12.9	14.8	10.8	4.5	3.3
	<i>ICL134</i>	-17.0	-15.8	-18.2	10.9	14.0	10.1	12.0	3.2
	<i>ICL135</i>	-17.6	-16.5	-18.4	10.7	11.8	9.4	17.9	3.2
	<i>ICL136</i>	-16.9	-14.8	-18.4	11.6	13.1	10.5	16.9	3.3
	<i>ICL137</i>	-18.0	-15.9	-19.2	11.3	12.6	9.3	12.1	3.2
	<i>ICL138</i>	-17.3	-15.5	-19.4	10.6	14.9	9.7	11.6	3.2
	<i>ICL139</i>	-16.6	-13.8	-18.4	10.1	13.3	9.2	13.7	3.2
	<i>ICL140</i>	-17.2	-13.7	-19.2	9.6	12.0	8.7	14.9	3.3
	<i>ICL141</i>	-17.8	-16.9	-18.5	11.7	16.0	10.5	15.2	3.2
	<i>ICL149</i>	-16.7	-14.5	-18.3	10.1	13.3	8.7	13.8	3.2
	<i>ICL154</i>	-17.3	-15.0	-19.7	10.7	15.2	9.2	12.8	3.3
<i>ICL155</i>	-18.5	-17.1	-19.8	11.7	15.5	10.2	10.5	3.3	
<i>ICL156</i>	-16.7	-11.6	-18.9	10.1	15.2	8.4	16.4	3.3	
Middle Ages	<i>FEN6</i>	-18.5	-16.9	-19.5	9.8	14.0	8.8	14.7	3.1
	<i>FEN9</i>	-18.0	-16.1	-19.6	10.6	14.6	9.6	15.9	3.2
	<i>FEN10</i>	-19.7	-18.8	-20.4	10.8	14.2	10.1	13.5	3.1
	<i>FEN14</i>	-18.0	-17.2	-18.9	9.7	10.9	9.3	15.7	3.2
	<i>FEN15</i>	-19.2	-18.8	-19.5	13.0	14.4	11.1	11.9	3.3
	<i>FEN17</i>	-19.8	-19.1	-20.3	12.5	14.3	11.6	18.4	3.3
	<i>FEN42</i>	-19.6	-19.3	-20.1	13.0	13.7	12.6	5.1	3.3
	<i>FEN43</i>	-21.0	-18.9	-23.5	11.3	11.8	11.0	13.3	3.2
	<i>FEN50</i>	-20.5	-19.6	-21.4	11.1	14.4	10.1	12.0	3.2
	<i>FEN52</i>	-17.7	-16.6	-19.2	10.4	13.4	9.3	13.3	3.3
	<i>BOG10</i>	-18.5	-16.6	-21.4	10.6	13.3	9.1	14.2	3.3
	<i>BOG59</i>	-19.4	-19.0	-19.9	11.0	13.8	9.9	13.1	3.1
	<i>BOG66</i>	-19.4	-19.1	-19.9	11.4	12.2	10.8	17.0	3.1
	<i>BOG109</i>	-18.8	-18.2	-19.9	13.5	15.4	11.8	10.4	3.1
	<i>BOG161</i>	-18.3	-16.1	-19.3	11.1	12.7	9.9	17.9	3.2
	<i>BOG240</i>	-19.2	-18.7	-20.1	11.5	12.7	10.7	16.6	3.2
	<i>BOG250</i>	-19.3	-18.7	-19.9	12.3	14.1	10.5	9.2	3.2
<i>BOG252</i>	-19.0	-17.6	-21.2	10.4	11.5	9.4	13.9	3.2	
<i>BOG255</i>	-19.3	-18.7	-19.7	10.9	13.3	9.9	13.8	3.1	
<i>BOG265</i>	-17.3	-16.6	-17.7	13.5	14.5	13.0	10.9	3.2	

Table 5.8. Incremental dentine stable isotope analysis results (maximum, minimum, and mean).

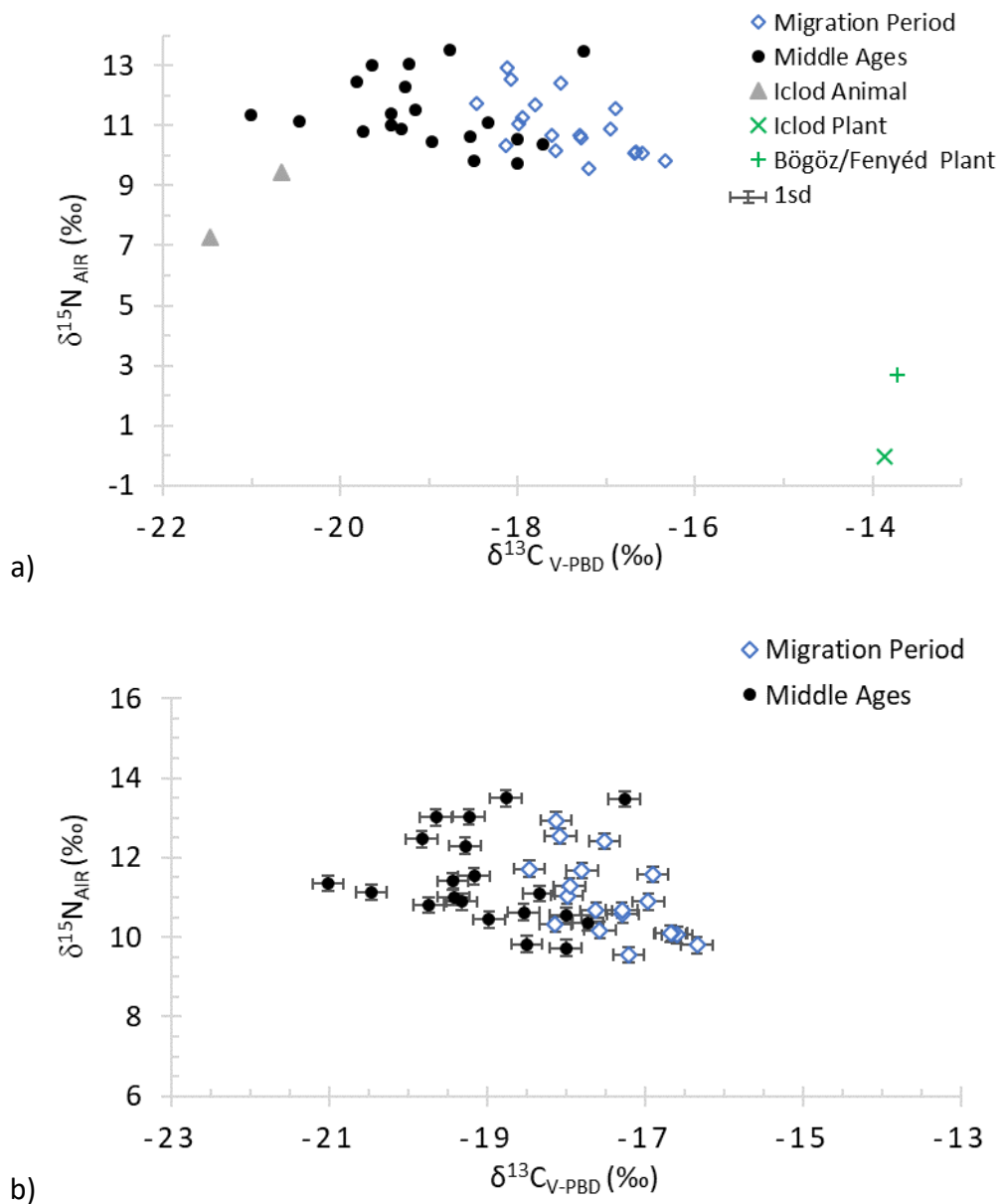


Figure 5.10. The results of the mean incremental dentine carbon and nitrogen stable isotope analyses plotted with the animal and plant data (a) and by skeletal assemblage (b). Analytical error = $\pm 0.2\text{‰}$.

Statistical analyses were performed on the data. The results from each increment were combined to create a mean dentine value for each individual and this was used to test for significant differences. There were no significant differences between both populations when the $\delta^{13}\text{C}_{\text{INCR}}$ results were compared by age-at-death category or by the presence of skeletal “stress” lesions. There were significant differences between the mean $\delta^{13}\text{C}_{\text{INCR}}$ values between individuals from the Migration Period and the medieval period, according to biological sex, age-at-death, and the presence of

“stress” lesions within and between the assemblages. There were no significant differences in $\delta^{15}\text{N}_{\text{INCR}}$ values according to time period, biological sex or presence of “stress” lesions when the data from both assemblages were combined. However, there were significant differences between age categories between and within the skeletal assemblages. All statistically significant relationships can be found in Table 5.9. The implications and interpretations of these data are discussed in detail in Section 6.2

<i>Test Variable</i>	<i>Grouping Variable</i>	<i>Statistical Test</i>	<i>P (0.05)</i>	<i>Significantly different relationships</i>
$\delta^{13}\text{C}_{\text{INCR}}$ (mean)	Combined			
	Period	Independent-sample Kolmogorov-Smirnov	0.000	Migration Period - Middle Ages
	Site	Independent-sample Kruskal-Wallis	0.015	Fenyed - Iclod (Adj. Sig. 0.028)
	Sex Estimation	Independent-sample Kolmogorov-Smirnov	0.028	male/M? - female/F?
	Assemblage Comparison			
	Period/Sex Estimation	Independent-sample Kruskal-Wallis	0.003	MP female - MA males (Adj Sig. 0.003) MP female - MA female (Sig. 0.020) MP male - MP female (Sig. 0.009)
	Period/Age Category	Independent-sample Kruskal-Wallis	0.013	MP adults - MA non-adults (Adj, Sig. 0.048) MP adults - MA adults (Adj Sig. 0.002)
	Lesions/Sex Estimation	Independent-sample Kruskal-Wallis	0.018	MA Male without lesions - MP female without lesions (Sig. 0.040) MA male without lesions - MP female with lesions (Sig. 0.012) MP male without lesions - MP female without lesions (Sig. 0.032) MP male without lesions - MP female with lesions (Sig. 0.004) MA male with lesions - MP female without lesions (Sig. 0.037) MA male with lesions - MP female with lesions (Sig. 0.005)
	Lesions/Age Category	Independent-sample Kruskal-Wallis	0.015	MA non-adults with lesions - MP adults with lesions (Adj. Sig. 0.022) MP non-adults without lesions - MP adults with lesions (Sig. 0.026) MA adults with lesions - MP adults with lesions (Sig 0.015) MP adults without lesions - MP adults with lesions (Sig. 0.043)
	$\delta^{15}\text{N}_{\text{INCR}}$ (mean)	Combined		
Age Category		Independent-sample Kruskal-Wallis	0.001	middle adult - child (Adj. Sig. 0.001) middle adult - infant (Sig. 0.004) young adult - child (Adj. Sig. 0.025) young adult - infant (Sig. 0.018) adolescent - child (Sig. 0.009) adolescent - infant (Sig. 0.044)
Assemblage Comparison				
Period/Age Category		Independent-sample Kruskal-Wallis	0.004	MP adults - MP non-adult (Sig. 0.036) MP adults - MA non-adults (Adj. Sig. 0.008) MA adults - MA non-adults (Sig. 0.016)
Lesions/Age Category		Independent-sample Kruskal-Wallis	0.002	MP non-adults without lesions - MA non-adults with lesions (Sig. 0.016) MP non-adults without lesions - MP non-adults with lesions (Sig. 0.011) MA adults with lesions - MA non-adults with lesions (Sig. 0.004) MA adults with lesions - MP non-adults with lesions (Sig. 0.005) MP adults with lesions - MA non-adults with lesions (Adj. Sig. 0.048) MP adults with lesions - MP non-adults with lesions (Sig. 0.003) MP adult without lesions - MA non-adults with lesions (Sig. 0.015) MP adults without lesions - MP non-adults with lesions (Sig. 0.015)

Table 5.9. The statistically significant different results for the incremental dentine stable isotope analyses. Key: MP – Migration Period, MA – Middle Ages.

5.3. Mobility isotope analyses

The results of the strontium and oxygen isotope analyses provided baseline biosphere data for each assemblage, these data helping to contextualise values obtained from the human enamel samples. Each individual sampled was analysed to explore whether the childhood values matched those of the burial environment or not.

5.3.1. Biosphere data

To begin to establish baseline values for the two periods strontium and oxygen isotope analyses were performed on soil, plant and faunal samples from the two regions (Table 5.10). The archaeological faunal samples (n=2) from the Iclod Necropolis had $\delta^{18}\text{O}_{\text{V-PDB}}$ values ranging from -6.8 to -5.2‰ (mean: $-6.0 \pm 0.03\text{‰}$ 1sd), $\delta^{13}\text{C}_{\text{V-PDB}}$ values from -14.0 to -12.2‰ (mean: $-13.1 \pm 0.04\text{‰}$ 1sd), and $^{87}\text{Sr}/^{86}\text{Sr}$ values ranging from 0.7093 to 0.7097 (mean: 0.7094 ± 0.00001 2sd). The strontium isotope data for sediment and plant samples can be found in Table 5.10. These data were used to help differentiate possible non-local individuals buried during the two periods.

ID	Sample	$^{87}\text{Sr}/^{86}\text{Sr}$	2 σ	Sr ppm	$\delta^{18}\text{O}_{\text{V-PDB}}$ (‰)	1 σ	$\delta^{18}\text{O}_{\text{V-SMOW}}$ (‰)	$\delta^{18}\text{O}_{\text{P}}$ (‰)	$\delta^{18}\text{O}_{\text{DW}}$ (‰)
ICL_PLANT	corn husk*	0.70908	0.00000						
ICL_SOIL	grave soil	0.71496	0.00001						
ICL_PIG	enamel	0.70927	0.00001	232	-5.2	0.1	25.6	16.7	-8.0
ICL_PIG	dentine	0.70933	0.00001	488					
ICL_COW	enamel	0.70970	0.00001	306	-6.8	0.0	23.9	15.0	-10.7
ICL_COW	dentine	0.70933	0.00001	496					
BF_PLANT	corn husk*	0.71026	0.00000						
BF_SOIL	grave soil	0.71692	0.00001						

Table 5.10. The results of the strontium and oxygen isotope analyses used to establish a baseline biosphere for each assemblage. Key: * - modern samples. The oxygen isotope conversion equations and sources can be found in Section 4.4.3.

Three water samples were collected for oxygen isotope analysis. One river sample was taken from the closest water source to each archaeological site and one rain sample was collected in Odorhei County, Romania (August 2016). All samples were

analysed twice to confirm the results (Table 5.11). The results of the oxygen isotope analysis are plotted alongside the Global Meteoric Water Line (GMWL) in Figure 5.11.

ID	Sample	$\delta^2\text{H}$	$\delta^2\text{H } 1\sigma$	$\delta^{18}\text{O}$	$\delta^{18}\text{O } 1\sigma$
ICL_RIVER	Someşul Mic	-62.9	0.5	-8.8	0.1
		-64.6	0.3	-8.6	0.1
BF_RIVER	Târnava Mare	-68.0	0.6	-9.0	0.1
		-69.1	0.6	-9.6	0.2
BF_RAIN	rain water	-39.4	0.2	-6.1	0.1
		-39.2	0.5	-5.7	0.1

Table 5.11. The results of the oxygen isotope analyses on water samples from each region.

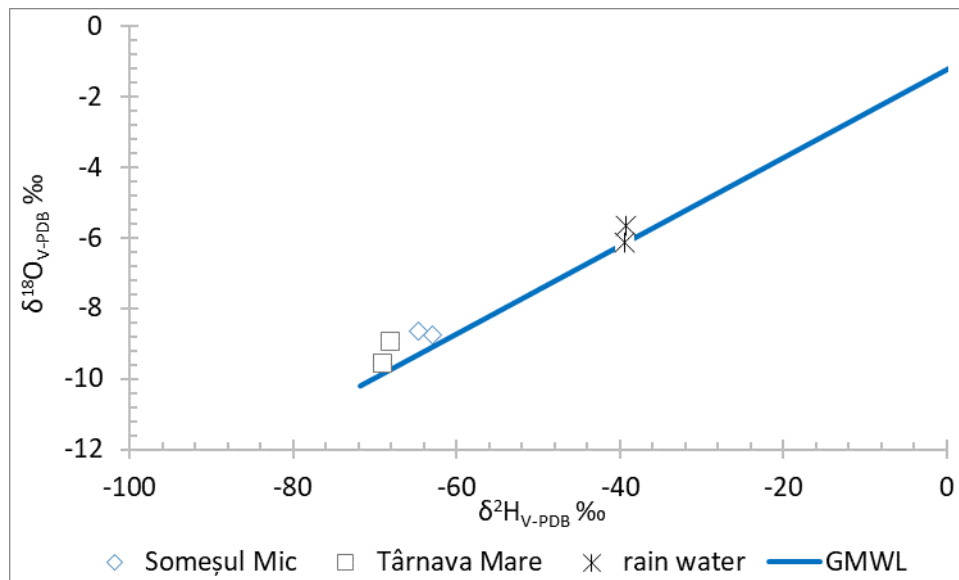


Figure 5.11. The results of the water sample oxygen isotope analyses plotted with the Global Meteoric Water Line (GMWL) to demonstrate the relationship between δ values and vapor pressure.

5.3.2. Strontium isotope data

Strontium isotope analysis was performed on dental enamel from 30 individuals (Migration Period - 14, medieval - 16) and the data can be found in Table 5.12. Strontium concentrations analyses were only performed on half of the samples to ensure time and budget restrictions were not exceeded. The individuals from the

Migration Period (n=14) had $^{87}\text{Sr}/^{86}\text{Sr}$ values ranging from 0.7093 to 0.7101 (mean: 0.7096 ± 0.0003 1sd), with strontium concentrations from 68 to 138ppm (mean: 99 ± 23 ppm 1sd). The individuals from the medieval assemblage (n=16) had $^{87}\text{Sr}/^{86}\text{Sr}$ values ranging from 0.7088 to 0.7104 (mean: 0.7093 ± 0.0005 1sd), with strontium concentrations from 50 to 134ppm (mean: 86 ± 24 ppm 1sd). The strontium isotope and concentration data can be seen in Figure 5.12, plotted by site and sample type. The data are separated by site (not period) to examine possible differences between the Bögöz and Fenyéd data.

Period	ID	Sample Type	$^{87}\text{Sr}/^{86}\text{Sr}$	2σ $^{87}\text{Sr}/^{86}\text{Sr}$	Sr ppm
Migration	ICL111	enamel	0.70923	0.00001	
	ICL120	enamel	0.70942	0.00001	84
	ICL130	enamel	0.70925	0.00001	
	ICL134	enamel	0.70932	0.00001	
	ICL135	enamel	0.70952	0.00001	
	ICL136	enamel	0.71002	0.00001	80
	ICL137	enamel	0.70944	0.00001	103
	ICL138	enamel	0.71007	0.00001	94
	ICL139	enamel	0.70989	0.00001	
	ICL140	enamel	0.70936	0.00001	138
	ICL149	enamel	0.70928	0.00001	
	ICL154	enamel	0.70962	0.00001	68
	ICL155	enamel	0.70953	0.00001	123
	ICL156	enamel	0.70932	0.00001	
Middle Ages	FEN6	enamel	0.70904	0.00001	74
	FEN9	enamel	0.70897	0.00001	50
	FEN10	enamel	0.70872	0.00001	
	FEN14	enamel	0.71037	0.00001	65
	FEN17	enamel	0.70893	0.00001	
	FEN43	enamel	0.70877	0.00001	82
	FEN50	enamel	0.70908	0.00001	
	FEN52	enamel	0.70933	0.00001	
	BOG10	enamel	0.70990	0.00002	
	BOG59	enamel	0.70981	0.00001	134
	BOG66	enamel	0.70920	0.00001	86
	BOG109	enamel	0.70921	0.00001	
	BOG161	enamel	0.70906	0.00001	114
	BOG240	enamel	0.70916	0.00001	79
	BOG252	enamel	0.70995	0.00001	
	BOG255	enamel	0.70928	0.00001	90

Table 5.12. The results of the strontium isotopes and concentrations from human enamel.

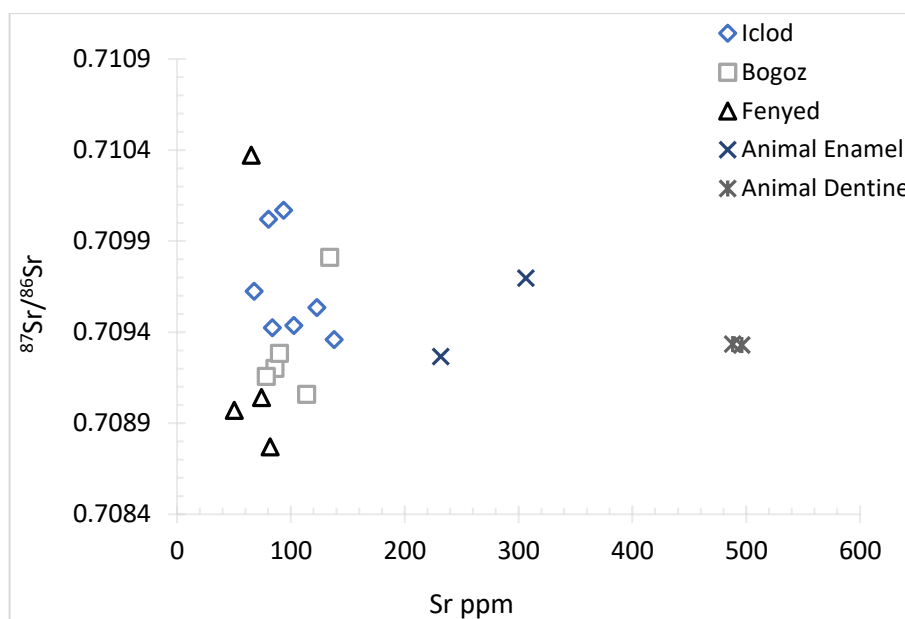


Figure 5.12. The results of the strontium concentration and isotope analyses plotted by site and sample type. Non-animal data are from human enamel. Analytical error for $^{87}\text{Sr}/^{86}\text{Sr}$ was 0.002 (2sd within the symbol).

Non-parametric statistical analyses were performed on the strontium data and no significant differences were found between biological sex estimation or the presence of arrested growth and/or physiological stress-related lesions. However, there was a significant difference in the strontium isotope values between the Migration Period and medieval individuals. The significant difference between the strontium isotope values between sites is discussed further in Section 6.2. Further tests revealed the significant difference was between the Iclod Necropolis and the Fenyéd Cemetery (see Table 5.13). These data are combined with the oxygen isotope and biosphere data in Section 6.2.2 to examine possible non-locals within each assemblage.

Test Variable	Grouping Variable	Statistical Test	P (0.05)	Significant Relationships
$^{87}\text{Sr}/^{86}\text{Sr}$	Combined			
	Period	Independent-sample Kolmogorov-Smirnov	0.006	Migration Period - Middle Ages
	Site	Independent-sample Kruskal-Wallis	0.027	Fenyed - Iclod (Adj. Sig. 0.021)

Table 5.13. The statistically significant different results for the strontium isotope analysis.

5.3.3. Oxygen (carbonate) isotope data

The oxygen isotope analyses were performed at two laboratories (see Section 4.4.3). Batch 1 was conducted at IsoAnalytics (UK) and batch 2 at Durham University in the Department of Earth Sciences. The analytical offset between the two laboratories were within the standard error, allowing the data from both laboratories to be validly compared. This is also supported when the oxygen and carbon isotope data are plotted (see Figure 5.13). The $\delta^{18}\text{O}_{\text{V-PDB}}$ results from human enamel samples of individuals from the Migration Period (n=14) ranged from -6.4 to -4.4‰ (mean: $-5.5 \pm 0.15\text{‰}$ 1sd) and $\delta^{13}\text{C}_{\text{V-PDB}}$ ranged from -11.7 to -6.3‰ (mean: $-9.8 \pm 0.06\text{‰}$ 1sd). The medieval skeletal assemblage (n=16) had $\delta^{18}\text{O}_{\text{V-PDB}}$ values from -6.5 to -4.3‰ (mean: $-5.4 \pm 0.11\text{‰}$ 1sd) and $\delta^{13}\text{C}_{\text{V-PDB}}$ values ranged from -13.5 to -9.5‰ (mean: $-12.1 \pm 0.06\text{‰}$ 1sd). Statistical analyses were performed on the $\delta^{18}\text{O}$ data and no significant differences were found when compared within or between periods and sites according to age-at-death, biological sex, or the presence/absence of stress-related lesions. These data were then analysed with the biosphere and strontium data to estimate local ranges for each region and to identify possible non-locals buried at each site (see Figure 5.13 and Table 5.14).

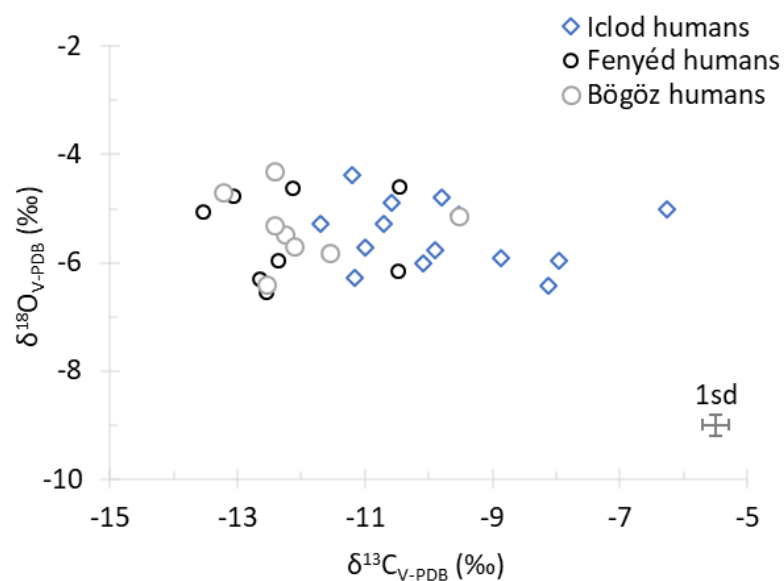


Figure 5.13. The results of the enamel oxygen and carbon isotope analysis plotted by site. Analytical error for $\delta^{13}\text{C}$ and $\delta^{18}\text{O}$ were $\pm 0.1\text{‰}$.

Period	I.D.	$\delta^{13}\text{C}_{\text{V-PDB}}$ (‰)	$\delta^{18}\text{O}_{\text{V-PDB}}$ (‰)	$1\sigma \delta^{18}\text{O}_{\text{V-PDB}}$ (‰)	$\delta^{18}\text{O}_{\text{V-SMOW}}$ (‰)	$\delta^{18}\text{O}_{\text{P}}$ (‰)	$\delta^{18}\text{O}_{\text{DW}}$ (‰)
Batch 1							
Migration	<i>ICL120</i>	-10.7	-5.3	0.3	25.0	16.1	-8.9
	<i>ICL135</i>	-11.7	-5.3	0.1	25.5	16.6	-8.1
	<i>ICL136</i>	-10.6	-4.9	0.0	25.9	17.0	-7.5
	<i>ICL137</i>	-10.1	-6.0	0.2	24.7	15.8	-9.3
	<i>ICL138</i>	-9.5	-5.1	0.4	25.7	16.8	-7.8
	<i>ICL140</i>	-6.3	-5.0	0.4	25.7	16.9	-7.7
	<i>ICL154</i>	-9.8	-4.8	0.3	26.0	17.1	-7.3
	<i>ICL155</i>	-11.2	-4.4	0.3	26.4	17.6	-6.6
Middle Ages	<i>FEN6</i>	-12.4	-6.0	0.0	24.8	15.9	-9.2
	<i>FEN9</i>	-10.5	-4.6	0.1	26.2	17.4	-7.0
	<i>FEN14</i>	-12.1	-4.6	0.1	26.2	17.3	-7.1
	<i>FEN43</i>	-13.1	-4.8	0.0	26.0	17.2	-7.3
	<i>FEN52</i>	-10.5	-6.2	0.1	24.6	15.7	-9.6
	<i>BOG59</i>	-12.3	-5.5	0.0	25.3	16.4	-8.4
	<i>BOG66</i>	-12.4	-5.3	0.1	25.5	16.6	-8.2
	<i>BOG161</i>	-9.5	-5.1	0.1	25.6	16.8	-7.9
	<i>BOG240</i>	-13.2	-4.7	0.2	26.1	17.2	-7.2
	<i>BOG255</i>	-12.1	-5.7	0.1	25.1	16.2	-8.8
Batch 2							
Migration	<i>ICL111</i>	-11.2	-6.3	0.0	24.4	15.5	-9.8
	<i>ICL130</i>	-9.9	-5.8	0.1	25.0	16.1	-8.9
	<i>ICL134</i>	-11.0	-5.7	0.1	25.0	16.1	-8.9
	<i>ICL139</i>	-8.1	-6.4	0.0	24.3	15.4	-10.0
	<i>ICL149</i>	-8.9	-5.9	0.0	24.8	15.9	-9.2
	<i>ICL156</i>	-8.0	-6.0	0.0	24.8	15.9	-9.3
Middle Ages	<i>FEN10</i>	-12.7	-6.3	0.1	24.4	15.5	-9.8
	<i>FEN17</i>	-13.5	-5.0	0.3	25.7	16.8	-7.8
	<i>FEN50</i>	-12.6	-6.5	0.0	24.2	15.3	-10.2
	<i>BOG10</i>	-11.6	-5.8	0.1	24.9	16.0	-9.0
	<i>BOG109</i>	-12.4	-4.3	0.0	26.5	17.7	-6.5
	<i>BOG252</i>	-12.6	-6.4	0.4	24.3	15.4	-10.0

Table 5.14. The results of the enamel carbonate oxygen and carbon isotope analyses. Batch 1 was analysed at IsoAnalytics and batch 2 at Durham University.

5.4. Summary

The demographic profile of both populations revealed similar numbers of males and females, as well as individuals from all age-at-death categories, for both populations in this study. Within the medieval population, a high number of individuals, 57% of the analysed population, had less than 25% of their skeleton recovered during excavation which hindered biological sex and age-at-death estimations. Palaeopathological analyses revealed 64% (16/25) of individuals from the Migration Period and 32% (46/144) of medieval individuals had one or more stress-related skeletal lesions. Table 5.15 summarizes the results for each method of isotope analyses organised by population. The interpretations of the results of this research can be found in Chapter 6.

	Migration Period	Middle Ages
$\delta^{13}C$ – bone collagen	-18.5 to -17.3‰ (mean: $-18.0 \pm 0.3\%$ 1sd)	-19.8 to -17.4‰ (mean: $-18.9 \pm 0.8\%$ 1sd)
$\delta^{15}N$ – bone collagen	9.7 to 11.0‰ (mean: $10.5 \pm 0.4\%$ 1sd)	9.1 to 11.8‰ (mean: $10.2 \pm 0.9\%$ 1sd)
$\delta^{13}C$ – incremental dentine	-20.9 to -11.6‰ (mean: $-17.4 \pm 1.1\%$ 1sd)	-23.5 to 16.1‰ (mean: $-19.1 \pm 1.0\%$ 1sd)
$\delta^{15}N$ – incremental dentine	8.4 to 16.0‰ (mean: $10.8 \pm 1.3\%$ 1sd)	8.8 to 15.4‰ (mean: $11.2 \pm 1.3\%$ 1sd)
$^{87}Sr/^{86}Sr$ – tooth enamel	0.7093 to 0.7101 (mean: 0.7096 ± 0.0003 1sd)	0.7088 to 0.7104 (mean: 0.7093 ± 0.0005 1sd)
$\delta^{18}O$ – tooth enamel carbonate	-6.4 to -4.4‰ (mean: $-5.5 \pm 0.15\%$ 1sd)	-6.5 to -4.3‰ (mean: $-5.4 \pm 0.11\%$ 1sd)
$\delta^{13}C$ – tooth enamel carbonate	-11.7 to -6.3‰ (mean: $-9.8 \pm 0.06\%$ 1sd)	-13.5 to -9.5‰ (mean: $-12.1 \pm 0.06\%$ 1sd)

Table 5.15. Summary of the results for each method of isotope analyses by population.

Chapter 6: Discussion

This study aimed to integrate palaeopathological data with isotope data to gain a better understanding of how aspects of life such as living conditions, economy and diet and migration had on morbidity and mortality, impacted early-life stress and a person's ability to survive. The resulting data and demographic and health profiles are now used to explore how these populations fit into the wider picture of Eastern Europe during this period (Section 6.1), and in relation to the known archaeological and historical context. The mobility status of the individuals buried in each cemetery are also considered to establish which people were non-local to their burial place, and the possible impact migration had on their health (Section 6.2.). Section 6.3 explores the stable carbon and nitrogen isotope data to establish: the overall dietary patterns for each population (Section 6.3.1); the different practices identified for breastfeeding and weaning (Section 6.3.2); the perceived offset between the approximate age of formation of enamel hypoplastic defects linked to changes in the isotope profiles; and between different types of dentition (i.e. still forming at death vs complete development – Section 6.3.3). Age-at-death, biological sex, the duration of breastfeeding and weaning and if a person's is local or non-local, are all important factors when attempting to understanding the interrelated risks associated with early-life stress. All data and interpretations were compiled to examine early-life stress identified within the incremental dentine isotope profiles, and how it might have affected individual frailty and age at death (Section 6.3.4).

6.1. Demography and health profiles

This section explores the skeletal data to establish demographic profiles for each population. Macroscopic skeletal analyses of the 25 individuals from the Migration Period phase of the Iclod Necropolis found mostly adults (21/25, 84%), with a similar number of males (9/25, 43%) and females (11/25, 52%). The lower percentage of non-adult individuals compared to adults could indicate a low mortality rate among children but it is crucial to remember that the excavated population will likely not be representative of the living population and the sample sizes were relatively small

(Waldron, 1994, pg. 11). It could be that a separate burial site was used for the other deceased children (Brothwell, 1972), or the children were not excavated either due to, as yet, non-discovery of an unknown burial location or that taphonomic destruction led to non-survival of the remains to be excavated (Scheuer and Black, 2000; Lewis and Gowland, 2007; Murphy and Chamberlain, 2017). However, the excavation of the Migration Period phase of this site is ongoing and may reveal a very different demographic profile after excavation has been completed. To date, there are only 25 individuals excavated from the Migration Period phase of the Iclod Necropolis. Therefore, the profiles for the Migration Period individuals from this site are preliminary and will have to be reassessed in the future as more data is available. The medieval population had similar numbers of adults (79/144, 55%) and non-adults (62/144, 43%), and a slightly higher percentage of males (36/62, 25%) than females (24/62, 17%). The high number of burials with less than 25% of the skeleton recovered/preserved resulted in 57% of the analysed individuals whose biological sex could not be assessed; this of course severely alters the demographic profile of this population, but the profiles of both populations from this site follow what is expected from attritional burial sites (Chamberlain, 2000; Margerison and Knüsel, 2002).

6.1.1. Arrested skeletal growth and attained stature

As outlined in Section 2.2.2 and 2.2.3, arrested skeletal growth and diminished attained stature are often linked to stress-related skeletal lesions such as EH, PH and CO (Steckel, 2005; Buchhorn *et al.*, 2016; Roberts and Steckel, 2019). When a person is undernourished, the body concentrates the energy load for the brain and vital organs, limiting other functions such as bone formation and repair (Fogel *et al.*, 1983; Said-Mohamed *et al.*, 2017). A person was considered to have had arrested growth when their skeletal age (long bone length and epiphyseal fusion rates - Cunningham *et al.*, 2016) is younger than their dental age (dental formation/eruption age estimation - AlQahtani *et al.*, 2010). All three individuals from the Migration Period, who had sufficient skeletal and dental elements preserved for assessment, had arrested skeletal growth. Thirteen individuals from the Middles Ages could be assessed and ten had evidence of arrested growth. The method of determining

arrested skeletal growth in non-adult skeletons was applied to individuals whose dentitions were still forming at the time of death and, for adults, diminished attained stature was used to track arrested growth (see Section 2.2.3). This was established by comparing attained stature to mean stature for males and females in each population. Because the bones of the skeleton are continually remodelling, recovery from arrested growth during childhood can occur when the cause of the stress is addressed, for example, when a person gains access to a more well-balanced diet. There was no evidence of diminished stature between those adults with or without stress-related lesions in the study. This would indicate that people who survived into adulthood never experienced arrested skeletal growth or had the means to overcome it. Individuals ICL127, FEN1, and BOG194 had skeletal development at least three years behind their dental development, indicating severe arrested growth (>3 years difference between skeletal age and dental age). The 13 non-adults (Table 6.1) with arrested growth died before recovery occurred, which may indicate these individuals did not have access to adequate resources (e.g. food) to overcome the stress that resulted in higher frailty. These findings support DOHAD research (see Section 2.2.2), connecting arrested skeletal growth to increased frailty and/or early death (Watts, 2011; Dewitte and Hughes-Morey, 2012; Newman and Gowland, 2015).

Skeleton	Skeletal Age (years)	Dental Age (years)	Degree
<i>ICL127</i>	6.5-7.5	10.5-11.5	severe
<i>ICL129</i>	1.5-3.5	4.5-5.5	moderate
<i>ICL131</i>	2.5-3.5	4.5-5.5	moderate
<i>FEN1</i>	7.5-8.5	11.5-12.5	severe
<i>FEN45</i>	6.5-7.5	7.5-8.5	slight
<i>BOG3</i>	2.5-3.5	5.5-6.5	moderate
<i>BOG109</i>	2.5-3.5	3.5-4.5	slight
<i>BOG144</i>	12-15	15.5-16.5	slight
<i>BOG194</i>	9.5-10.5	14.5-15.5	severe
<i>BOG240</i>	14-16	15.5-16.5	slight
<i>BOG247</i>	0.5-1.5	2.5-3.5	moderate
<i>BOG250</i>	1.5-3.5	4.5-5.5	moderate
<i>BOG281</i>	3.5-4.5	4.5-5.5	slight

Table 6.1. Individuals with arrested skeletal growth: skeletal and dental ages compared. Degree: slight = 0 – 1 year; moderate = 2 – 3 years; severe = >4 years.

Stature comparisons within each population helped to reveal those individuals with possible diminished achieved stature due to problems with growth during childhood. There was a significant difference [$t(13) = 4.7050, p=0.0004$] between the mean statures of males (M/M? = $170 \pm 3.1\text{cm}$) and females (F/F? = $162 \pm 3.3\text{cm}$) from the Migration Period. Copper Age populations in Hungary had similar stature trends as the individuals from the Migration Period individuals in this study (mean female stature – 157cm, mean male stature – 168cm) (Ubelaker and Pap, 2009). There was also a significant difference [$t(29) = 6.281406, p=0.000001$] in the medieval population between the mean statures of males (M/M? = $170 \pm 5.8\text{cm}$) and females (F/F? = $156 \pm 6.1\text{cm}$). Ubelaker and Pap (2008) report similar stature estimates to the medieval population in this study for individuals from north-east Hungary during the Arpadian Age (mean female stature 156cm, mean male stature 168cm). These trends follow the general historic and evolutionary trends of sexual dimorphism in the past (Koepeke and Baten, 2005b, 2005a).

Mean stature data from both populations was analysed in conjunction with the palaeopathological data to examine possible correlations between diminished

stature and the prevalence of lesions related to physiological distress or metabolic disorders. There were no statistical differences in mean stature when individuals with lesions are compared to those without lesions. Final attained stature is the combined result of genetic and environmental factors that may indicate that the individuals in this study were more adapted to survive early-life stress and/or had access to adequate resources to fully recover from adverse stress. For example, Meinzer and colleagues (2018) analysed anthropometric values to assess the interrelated factors of agriculture, urbanization, workload and stature in Europeans over time and found that the Middle Ages was a period characterized by high income and robust health. If the evidence for stress was the precursor for the stress-related lesions observed, this suggests that the presence of childhood stress did not directly, or adversely, affect stature for either population. However, this does not agree with research linking arrested skeletal growth and diminished achieved stature (compared to the rest of the population) with insults during critical growth periods (Steckel, 2005; Watts, 2011; Dewitte and Hughes-Morey, 2012). These data suggest that the attained stature of individuals with evidence of early-life stress (stress-related lesions and/or changes in the isotope profiles), who survived into adulthood, had low frailty or had the means to overcome the stress during development (e.g. higher socio-economic standing).

6.1.2. Stress-related skeletal lesions

This section explores the skeletal lesions commonly associated with physiological/metabolic stress to answer research question I (see Chapter 1). As explained in Section 2.2.3, this study did not aim to link lesions to specific aetiologies (which would be challenging because the health indicators can be caused by many risk factors), but rather to use the presence of lesions to assess the degree of physiological and metabolic stress within and between the two populations. The non-specific skeletal lesions commonly associated with physiological and metabolic stress are discussed separately to examine the impact each type of lesions had on morbidity and mortality within each population, as well as comparing the prevalence between both populations.

(i) Enamel hypoplasia (EH)

When analysed by age category, the highest prevalence of EH from the Iclod Necropolis occurred in the middle adult age-at-death category (6/8, 75%) and in females (7/11, 64%) when analysed according to biological sex estimation (see Table 5.3). These data support the finding that childhood related stress lesions (EH) prevalent in adults reflects lower, rather than higher individual frailty because they survived the stress event (Dewitte and Yaussy, 2016). There were more females than males within the analysed population, which could suggest that the data reflects an inherent sampling bias. Ubelaker and Pap (2009) assessed the prevalence of EH in a population from Hungary who lived in the Copper Age and also found that the condition was higher in females compared to males (1.7% and 0.3% respectively). This pattern supports research finding that women have a stronger immune response than men (Ortner, 1999; Janele, 2006; Roberts and Steckel, 2018). Historically, in rural communities, males were preferentially given higher quality and quantity foodstuffs (Carloni, 1981; Ortner, 1999). These data could reflect a higher level of nutritional stress for women due to possible sex/gender-based differences if men were given preferential access to high quality foods such as meat and fish (Carloni, 1981; Ortner, 1999; Craig *et al.*, 2009). These patterns are discussed further in Section 6.3. these

Within the medieval population, the young adult groups (6/17, 35%) and males (9/34, 26%) rather than females had the highest prevalence of EH. The percentage of individuals where biological sex estimation was possible to estimate, was slightly more for males than females and this may be biasing the results. The higher prevalence of EH in the males could again be attributed to the difference in male and female immune responses, where oestrogen enhances immunocompetence in females and androgens reduce it in males (Grossman, 1985; Ortner, 1998; Janele, 2006; Dewitte, 2010; Roberts and Steckel, 2018).

When the prevalence of EH from both populations were combined and analysed by age at death, young adults had the highest prevalence (32%). These individuals were able to survive the initial stress event during childhood that resulted in EH (Dewitte and Yaussy, 2016). However, as DOHAD related research has found, stress during critical growth periods can lead to compromised health later in life. The immune

systems of those with EH may have made them more susceptible to health problems and early death (Steckel, 2005; Armelagos *et al.*, 2009; Yaussy *et al.*, 2016). The prevalence of EH appears to increase over time, with 1–5% of individuals from Neolithic and Copper Age populations in Hungary having EH (Ubelaker, 2006; Ubelaker and Pap, 2009), to 40% of individuals from Medieval populations in Romania (Istrate and Diana, 2017) and Hungary with EH (Ubelaker and Pap, 2008).

(ii) Cribra orbitalia (CO) and porotic hyperostosis (PH)

Orbital lesions were present in 100% (3/3) of males and 30% (3/10) of females from the Migration Period, but the high numbers of males studied from the Migration Period reflects a sampling bias. Within the Migration Period population, both infants (2/2, 100%) and three of the four young adults (75%) had CO. Due to the small sample size, additional skeletal data would be required to confirm these trends are realistic. The highest prevalence of CO in the medieval population was in the childhood category (63%, 10/16 individuals). Twenty-eight percent of the males (5/18) and 43% of females (6/14) from the medieval population had CO. When the populations are combined, the prevalence of CO in males and females are equal (38%, 8/21 and 9/24 respectively), with the highest prevalence occurring in the infant (100%, 4/4) and child (63%, 10/16) age-at-death categories. These data suggest equal susceptibility to a stressor resulting in CO among males and females between the two periods and that CO during development may negatively affect frailty (Marklein *et al.*, 2016; Roberts and Steckel, 2018).

Abnormal porosity on the ectocranial surface of the skull (PH) is commonly associated with non-specific stress and metabolic bone disease (Stuart-Macadam, 1991; Ortner and Ericksen, 1997; Walker *et al.*, 2009; Grauer, 2012). There was no evidence of PH in the Migration Period individuals but two individuals from the medieval population had some evidence of ectocranial porosity. The lack of PH in both populations may suggest deficiencies of dietary elements (e.g. iron) and/or metabolic diseases, and inherited anaemias such as thalassaemia may have been low. European skeletons have generally been found to have low prevalence rates of PH compared to other

parts of the world like North America (Roberts and Steckel, 2018, pg. 344). As mentioned in Section 2.2.3, a lateral cranial radiograph is necessary to confirm the presence of porotic hyperostosis, but because the skeletal remains could not be removed from their curating facilities, no radiographic equipment could be used to explore such a diagnosis. As such, the medieval two individuals were categorized as possibly having porotic hyperostosis.

Roberts and Steckel (2018) examined European skeletal data to examine the negative effects of early-life conditions and adult age-at-death and found that CO and PH had a statistically significant impact on a person having an early death. Whether the porotic lesions in the orbits or cranium were the result of iron deficiency anaemia, infection or nutritional stress, the presence of the lesions supports the link between CO and early death. However, it doesn't necessarily mean the cause of death was the same as that which caused the CO, only that having CO may have increased their frailty.

(iii) Metabolic bone disease (MBD)

As outlined in Section 2.2.3, this study considered skeletal lesions commonly associated with MBD, such as scurvy and rickets. The state of the skeletal remains studied (completeness, preservation, fragmentation) impacted the ability to firstly assess the distribution pattern of abnormal (pathological) lesions and, secondly, to consider possible differential diagnoses. The more well preserved and complete skeletons allowed for a more comprehensive analysis of lesion distribution. Those with poor preservation and high level of bone fragmentation could only be categorised as possibly having MBD. A complete inventory of the skeletal lesions identified, and the corresponding differential diagnoses can be found in Appendix 6.1.

Seventeen of the 25 individuals from the Migration period (68%) had at least one skeletal lesion that, variously, could have been associated with physiological stress, nutritional deficiency and/or a metabolic disorder. Of those individuals, five (5/25, 20%) had multiple lesions indicative of scurvy and/or rickets (see Table 6.2). Within

the medieval population, there were 59 individuals (59/144, 41%) with at least one stress lesion, 12 of which (8%) had multiple lesions indicating scurvy and/or rickets. The Migration Period individuals had a higher prevalence than those who were living in the Middle Ages. This could mean the individuals living during the Migration Period experienced greater metabolic strain compared to the medieval population, but additional bioarchaeological data would be required to confirm this pattern. The higher prevalence of MBD in the Migration Period population compared to the medieval population may also reflect the differences between the preservation of the analysed populations. The majority of the skeletal remains from the medieval assemblage were highly fragmented, or less than 25% of the skeleton excavated, which could be biasing the data to make it appear as though the bones were not affected.

ID	Age	Sex	Metabolic disorder(s)	
			scurvy	rickets
ICL120	young adult	male?		P
ICI129	child		L	
ICI131	child		L	
ICL137	young adult	female?		P
ICL141	young adult	male	P	
FEN1	adolescent		P	
FEN10	adolescent		L	
BOG3	child		P	
BOG10	young adult	male?/?	L	
BOG54	older adult	female?	P	P
BOG109	child		P	
BOG194	adolescent		P	
BOG240	adolescent		L	P
BOG247	child		L	
BOG250	child		L	
BOG264	infant		P	
BOG265	infant		L	

Table 6.2. Summary of individuals with metabolic disorders as a likely (L) and/or possible (P) differential diagnosis.

Of the 17 individuals with possible scurvy/rickets, 12 were non-adults and four were young adults when they died, further supporting the link between childhood stress with increased frailty and/or early death. Biological sex estimation could not be conducted on non-adults and therefore differences in frequency rates between male and female non-adults could not be assessed. Among the adults, there were three males and two females with possible metabolic disorders. If it is assumed that possible lower limb bending and rotation (*gena valgus/varus/varum*) was the result of vitamin D deficiency, four individuals (ICL120, ICL137, BOG54, BOG240) had skeletal changes that may indicate rickets, residual rickets, or osteomalacia. However, the skeletal lesions of the four individuals concerned are not pathognomonic for any of these conditions, and therefore a differential diagnosis of possible rickets can only be tentative. Lesions indicating an individual was recovering from a metabolic disorder (mixed woven and lamellar bone) or died while suffering from a metabolic disorder (new woven bone) are further examined in the incremental dentine life-history profiles.

6.1.3. Summary

Palaeopathological studies of populations from Romania and surrounding regions have found varying evidence of physiological and/or metabolic stress (see Table 2.1 - Eng and Szocs, 2003; Ubelaker *et al.*, 2006; Ubelaker and Pap, 2008; Osterholtz *et al.*, 2014; Lundberg, 2015; Radu *et al.*, 2015). For example, Istrate and Diana (2017) report 10% of a Medieval population from Brasov, Romania with skeletal evidence of physiological stress, with an additional 11% having skeletal lesions indicating metabolic disease. Sixty-four percent (16/25) of the Migration Period and 32% (46/144) of the medieval population had one or more skeletal lesion associated with physiological stress and/or metabolic disorder. There were several individuals that were recovered without preserved dentition and without the necessary skeletal elements or parts of elements (e.g. the orbital roof) to assess whether a person had experienced stress or not. If these individuals are excluded, and only those with teeth and/or skeletal elements preserved that could be analysed are considered, 76% (16/21) of the people analysed from the Migration Period and 56% (46/82) of the

medieval population had one or more stress lesions. This is not to say that the excluded individuals did not have stress-related lesions, only that the skeletons were not complete enough to estimate prevalence. Although the sample size is small and will likely not reflect the overall health pattern of the living populations, these data suggest the two populations in this study had a higher prevalence of physiological and metabolic stress compared to other populations in the region. This confirms the hypothesis that both populations would have had substantial evidence of physiological/metabolic stress ($\geq 50\%$ of the analysed population).

6.2. Biosphere and mobility status

Isotopic analyses were performed on 14 individuals from the Migration Period and 16 medieval individuals, across all age, sex, and health status categories. In interpreting the isotope data appropriate historical, archaeological, demographic and palaeopathological data were integrated to assess the variables relevant to each person's early-life history. Strontium and oxygen isotope data from the animal, plant, soil and water samples were examined to narrow the proposed local isotope ranges specific to each site (Section 6.2.1). The isotope data from each skeletal assemblage were compared to the available biosphere data from studies at a similar altitude and latitude, and the same underlying geology as the sites under study. This was undertaken to determine if the childhood isotope values were the same or differed from those representing that person's burial environment (Section 6.2.2)

6.2.1. Local biosphere ranges

Within this study, the proposed local isotope ranges for humans with origins in the Transylvanian Basin were established as $\delta^{18}\text{O}_{\text{VSMOW}}$ between 21.9 and 26.1‰, and $^{87}\text{Sr}/^{86}\text{Sr}$ values between 0.7078 and 0.7120 (Section 3.3.3). The data from the modern plant and archaeological animal samples fell within the proposed local $^{87}\text{Sr}/^{86}\text{Sr}$ range. As mentioned in Section 3.3.1., strontium isotope ratios from whole rock and soil samples from areas with diverse geology might not reflect the bioavailable strontium taken up by humans and plants (Price *et al.*, 2002). Although

the soils in this study were acid leached prior to analysis, the $^{87}\text{Sr}/^{86}\text{Sr}$ values of the leached soil are more radiogenic (+ ~0.004 $^{87}\text{Sr}/^{86}\text{Sr}$) compared to the human samples from the same region. This could indicate possible strontium isotope contamination via airborne sources and/or fertilizer having been used on the land (Bentley, 2006; Gerling *et al.*, 2012). Acid leaching soil and rock samples prior to analysis has also been found to give different isotope ratios due to the acid dissolving minerals which are not normally accessed by rainwater/soil water through natural conditions (Montgomery *et al.*, 2000). The $^{87}\text{Sr}/^{86}\text{Sr}$ values of human enamel represent an average value of dietary inputs during childhood, and thus may reflect and record a mix of the different types of geology in the region where they sources their food (Montgomery *et al.*, 2007). Because the Transylvanian Basin consists of various Tertiary/Quaternary sediments, it is plausible that the humans who lived in this region would have had isotope values reflecting a region of diverse bedrock (Figure 6.1).

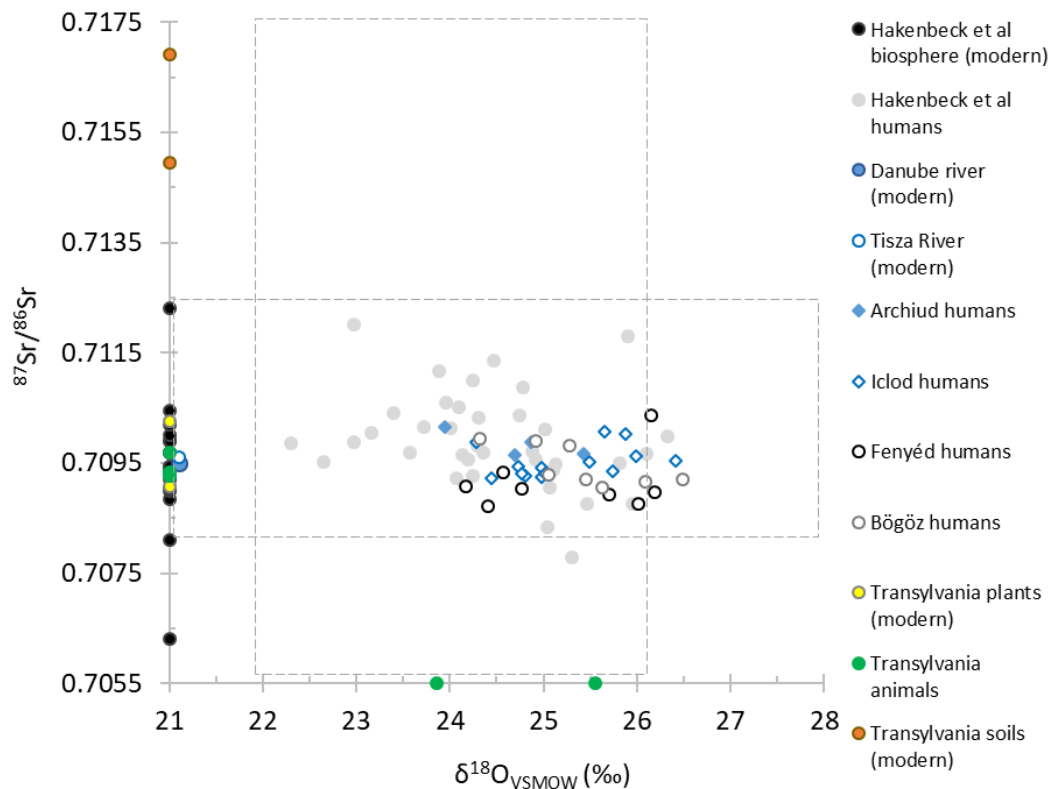


Figure 6.1. Strontium and oxygen isotope data from the ancient human, and modern animal, plant and soil samples in this study plotted with the biosphere and human data from the regions outside Transylvania (Alt et al., 2014; Hakenbeck et al., 2017). The dashed-line boxes indicate the proposed local range for Transylvania (Section 3.3.3). Analytical error: $\delta^{18}O_{VSMOW} = \pm 0.2\text{‰}$ (1sd); $^{87}Sr/^{86}Sr = \pm 0.002$ (2sd).

Figure 6.2 illustrates the fluctuation in monthly rainwater ($\delta^{18}O$) collected from two locations in Transylvania throughout 2016 (IAEA/WMO, 2019). As the graph indicates, the $\delta^{18}O$ values are highly susceptible to temperature, with the values decreasing in the colder months (January, mean: 1.4°C) and increasing in the warmer months (July, mean: 21.4°C), with a mean annual value of -9.8‰ (IAEA/WMO, 2019). These data vary from the Online Isotopes in Precipitation Calculator (OIPC) which predict $\delta^{18}O$ values for the Transylvania region to be between -9.2 and -8.4‰ (Bowen, 2018). The two river water samples from Târnava Mare and Someșul Mic had values of approximately 3‰ ($\delta^{18}O$) lower than the rainwater sample. As marine air (water vapour) moves from the coast onto the continent, the air mass is cooled and causes moisture dropout, resulting in the $\delta^{18}O$ values decreasing the further inland the marine air travels (Dansgaard, 1964; Gat, 1996). The difference in $\delta^{18}O$ values between the river and rain water samples in this study (see Figure 5.11) may reflect

water depleted in ^{18}O (river) due to distance from the water vapour source, but also temperature, altitude and/or latitude (Gat, 1996). The hydro-climate of Romania is under the influence of pressure centres which transports humid oceanic air from the north-west and west of the country all year, with cold continental systems during January (Gastescu *et al.*, 1975).

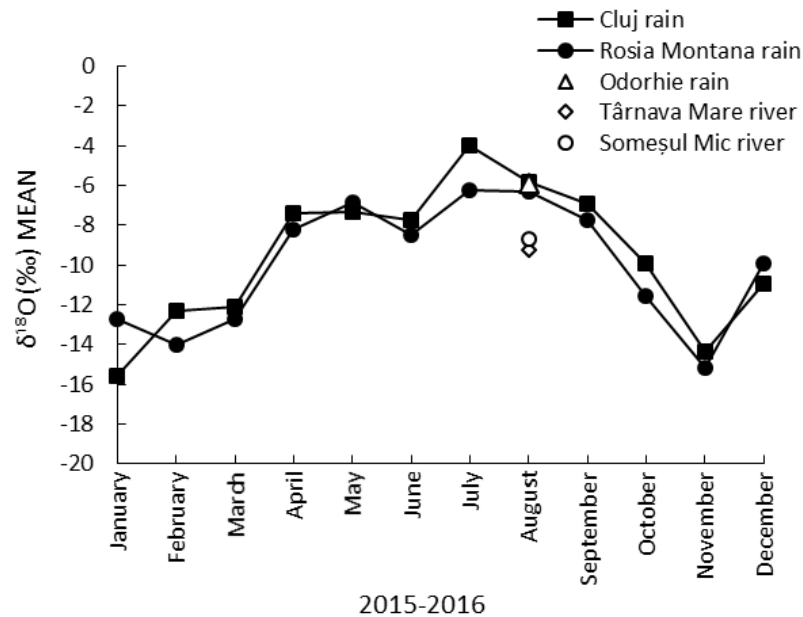


Figure 6.2. Precipitation data ($\delta^{18}\text{O}$) collected by IAEA compared to the rain and river water samples collected in this study (IAEA/WMO, 2019).

Although the sample size was small, differences could be seen isotopically between the two populations in this study. The $^{87}\text{Sr}/^{86}\text{Sr}$ and $\delta^{18}\text{O}_{\text{VSMOW}}$ data from each archaeological site are plotted in Figure 6.3. All individuals fall within the proposed local range for the Transylvanian Basin. As discussed in Section 3.3.3, most of the lowlands in Eastern Europe consist of sedimentary rock of Quaternary and Tertiary age. Because of this, the $^{87}\text{Sr}/^{86}\text{Sr}$ isotope range associated with this geological period can represent multiple and/or very large regions of land in Eastern Europe. Therefore, the geology around each site was examined to help further differentiate the possible local $^{87}\text{Sr}/^{86}\text{Sr}$ isotope ranges specific to each site (see Figure 3.5). The Iclod Necropolis is located in a region with Middle Miocene geological formations overlain by later Quaternary sediments. The Bögöz and Fenyéd sites are in a region of more

diverse geology compared to Iclod, consisting of Middle and Late Miocene geology with Neogene (volcanic) formations to the east and Mesozoic sediments to the south-east. There was a statistically significant difference ($p = 0.006$) between the mean $^{87}\text{Sr}/^{86}\text{Sr}$ values for each population, further highlighting the diverse bedrock of each site (see Figure 3.5). The isotope ratios for the humans studied from these regions are expected to have $^{87}\text{Sr}/^{86}\text{Sr}$ values that reflect a mix of the diverse bedrock. The refined proposed local isotope biosphere rangers are $^{87}\text{Sr}/^{86}\text{Sr}$ between 0.7085 and 0.7097, and $\delta^{18}\text{O}_{\text{VSMOW}}$ between 21.9 and 26.1‰. The sample size was limited by time and budget constraints, but these data begin to fill the gap in the biosphere data for Romania and Eastern Europe

6.2.2. Assessing residential origins and mobility

The results and interpretations of the strontium and oxygen (carbonate) isotope data are explored in this section to assess residential origins and mobility. When the strontium and oxygen isotope data from the human samples were analysed, three individuals from the Migration Period (ICL136, 138, 139) and four medieval individuals (BOG10, BOG59, BOG252, FEN14) had childhood isotope values that suggest a region of origin different to their burial environment (Figure 6.3). The cluster of individuals from the Migration Period had slightly more radiogenic $^{87}\text{Sr}/^{86}\text{Sr}$ ($\sim + 0.0001$ to 0.0009) values compared to the medieval individuals, reflecting the possible difference between the diverse bedrock at each site. All individuals from the Iclod Necropolis fall above the $^{87}\text{Sr}/^{86}\text{Sr}$ value for seawater and three individuals (ICL136, 138, 139) had $^{87}\text{Sr}/^{86}\text{Sr}$ values above 0.7097. Most of the individuals from Bögöz and Fenyéd fall around or below the $^{87}\text{Sr}/^{86}\text{Sr}$ value for seawater and four people (BOG10, BOG59, BOG252, FEN14) had values above 0.7097, similar to the three individuals from the Migration Period.

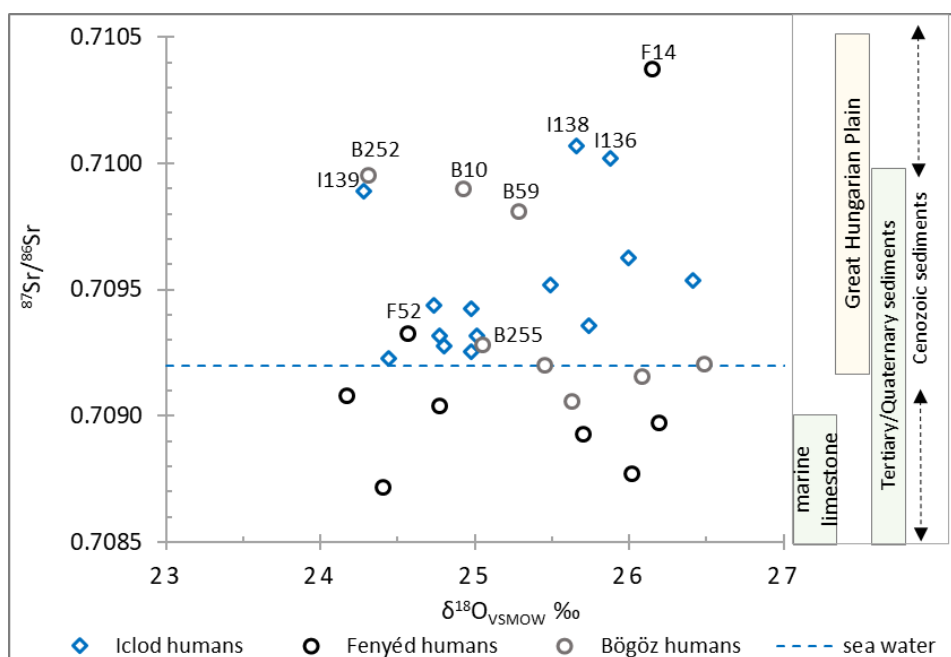


Figure 6.3. $^{87}Sr/^{86}Sr$ and $\delta^{18}O_{VSMOW}$ data from the human samples organised by archaeological site. Geological $^{87}Sr/^{86}Sr$ ratios from: Montgomery *et al.*, 2003; Bentley, 2006; Gerling *et al.*, 2012; Hakenbeck *et al.*, 2017. Analytical error: $\delta^{18}O_{VSMOW} = \pm 0.4\text{‰}$ 1sd; $^{87}Sr/^{86}Sr = \pm 0.002$ 2sd.

As mentioned in Section 4.2.2, the individuals excavated from inside the Church at Bögöz (skeletons BOG226-290) were believed to be among the earliest Arpadian settlers in this region which would support BOG252 being incomers to the region. The burial practice/rituals of all seven possible non-local individuals did not indicate these individuals were culturally different from the rest of the burials at the site. As discussed in Section 3.3.1, the Central and Eastern European lowlands are covered in loess and marine carbonate deposits with $^{87}Sr/^{86}Sr$ ratios between 0.7085 and 0.7104 (Grup/e *et al.*, 1997; Bentley and Knipper, 2005; Bentley *et al.*, 2012). Price and colleagues (2004) found that soil samples from Bell Beaker cemeteries in Eastern Europe had strontium isotope ratios between 0.70897 and 0.70989; fluvial deposits of the Danube system reflect a mixture of central European geologies with $^{87}Sr/^{86}Sr$ ratio of approximately 0.709. Most medieval individuals had strontium isotope ratios around 0.709 which may indicate the Fenyéd and Bögöz region has a strontium isotope biosphere similar to the Danube fluvial deposits, but due to the small sample size, additional analysis would be required to confirm this. The possible non-local people to the regions ($^{87}Sr/^{86}Sr$ above 0.7097) had values indicative of Lower

Mesozoic/Palaeozoic sediments (Evans *et al.*, 2010) which could indicate regions of the Carpathian Mountains surrounding the Transylvanian Basin. Sorocovschi and Pandi (2002) conducted a study of the river flow characteristics of the Transylvanian Basin found that 72.8% of water there had originated from the mountains. Water runoff from mountain regions of older bedrock, with more radiogenic strontium isotope ratios, would impact the strontium isotope ratios downstream, i.e. the Transylvanian Basin. However, further biosphere mapping is required to examine the isotopic differences between the different regions within the Transylvanian Basin and the surrounding Eastern European lowlands, such as the Hungarian Plain.

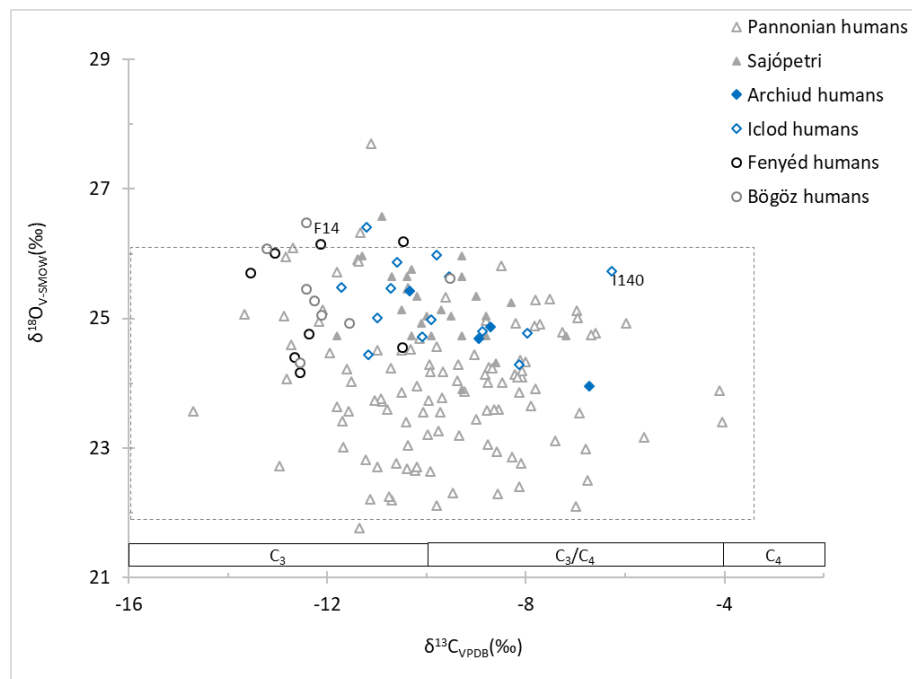


Figure 6.4. The $\delta^{18}O_{VSMOW}$ and $\delta^{13}C_{VPDB-CARB}$ data from human enamel samples at each archaeological site plotted with comparative human data from the Hungarian Plain during the Roman Period (Alt *et al.*, 2014; Hakenbeck *et al.*, 2017) and the Avar Period (Nochedowdy, 2015). The grey-dashed box indicates the proposed local $\delta^{18}O_{VSMOW}$ range for the Transylvanian Basin. Analytical error: $\delta^{18}O_{VSMOW} = \pm 0.4\text{‰}$ 1sd; $\delta^{13}C_{VPDB} = \pm 0.2\text{‰}$ 1sd.

The $\delta^{18}O$ and $\delta^{13}C$ data from the human enamel samples are plotted in Figure 6.4. The $\delta^{13}C$ values from enamel (apatite) carbonate reflect a person's diet during their childhood. A different diet, or a change in diet over time, could signify immigration and support the argument for possible non-locals buried at a site. Carbonate ions in

enamel apatite are more enriched in ^{13}C than bone collagen and a diet:apatite fractionation has been reported as $\delta^{13}\text{C} +\sim 12\text{‰}$ (Krueger and Sullivan, 1984; Lee-Thorp *et al.*, 1989; Cerling *et al.*, 1993). Although individual ICL140 had elevated $\delta^{13}\text{C}$ value compared to the other individuals from Iclod, indicating increased consumption of C_4 foods, their childhood strontium and oxygen isotope ratios indicate they were local to their burial environment. These dietary differences are examined further in Section 6.3.1. The $\delta^{18}\text{O}$ values allude to the climate, latitude and altitude where a person lived during childhood. Four individuals, ICL155, FEN9, FEN14 and BOG109, had $\delta^{18}\text{O}$ values that fell just outside the upper range of the proposed local range for the Transylvanian Basin. Of the four individuals, FEN14 was the only person with a strontium isotope ratio that also suggests a region different to their burial location. It is possible these individuals were from a region of higher altitude or latitude than the burial region (Dansgaard, 1964; Sharp, 2017, Section 4-21), or had a diet treated with a heating process such as boiling or brewing (Brettell *et al.*, 2012). However, if the analytical error is considered ($\delta^{18}\text{O} \pm 0.4\text{‰}$ 1sd), these individuals could have originated from elsewhere in the Transylvanian Basin or Carpathian Basin.

The individuals from the Transylvanian Basin have $\delta^{18}\text{O}$ values at or above those from the Carpathian Basin. When the sites were analysed by latitude and altitude, sites at higher altitudes had higher $\delta^{18}\text{O}_{\text{VSMOW}}$ values compared to sites at lower altitudes (Figure 6.5). Precipitation becomes depleted in heavy isotopes of oxygen with increased elevation, possessing a gradient of $\delta^{18}\text{O}$ values between -0.15‰ and -0.5‰ per 100 meters (Clark and Fritz, 1997; Cozma *et al.*, 2017). These data may offer a way of differentiating between those from the Transylvanian Basin and those from the Carpathian Basin in Hungary, but additional biosphere mapping is required to confirm the difference between the oxygen isotope biosphere of Transylvanian Basin and the Carpathian Basin.

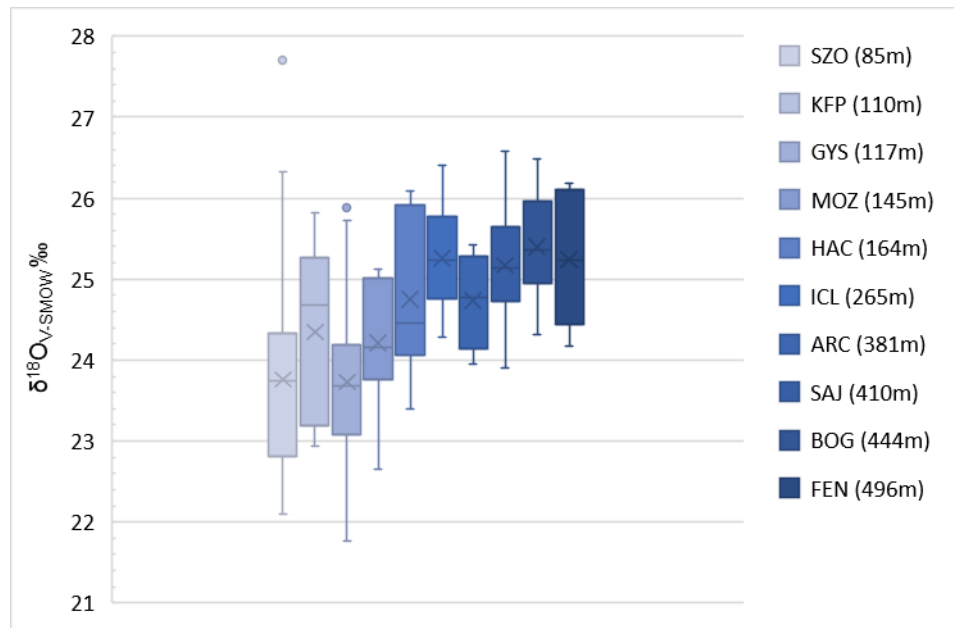


Figure 6.5. Oxygen isotope values ($\delta^{18}O_{VSMOW}$) of human enamel from sites in the Carpathian Basin and Transylvanian Basin organised from lowest to highest altitude (meters). The boxes represent the inner quartile range (Q1-Q3) and the whiskers show the smallest and largest values in each category. Within each box, the x indicates the mean values and the line (–) indicates the median values. The single outlier was 1.5 times greater than the upper quartile.

Key: SZO - Szolnok-Szanda; KFP - Keszthely-Fenekpuszta ; GYS - Győr-Széchenyi; MOZ - Mözs; HAC - Hács-Béndekpuszta; ICL – Iclod; ARC – Archiud; SAJ – Sajópetri ; BOG – Bögöz; FEN – Fenyéd. Comparative data from (Alt et al., 2014; Noche-Dowdy, 2015; Hakenbeck et al., 2017)

The combined strontium, oxygen and carbon isotope data helped to identify the possible non-local individuals in each population. The strongest argument for differences between the biosphere isotopes of the two analysed populations was found in the strontium isotope data. Table 6.3. lists the individuals with childhood isotopes which suggest a region of origin different to their burial location. A person can be identified as non-local if one the isotope ratios from childhood, such as their $^{87}Sr/^{86}Sr$, differs from their burial environment. However, the lack of isotope biosphere mapping in the region of Transylvania make it difficult to clearly identify non-locals therefore both strontium and oxygen isotope ratios were used together to assess mobility status. If an individual had a single childhood isotope ratio (e.g. only $^{87}Sr/^{86}Sr$) outside the local range, they were classified as “possible” non-locals. If an individual had both strontium and oxygen childhood isotopes outside the updated

local range, they were classified as a “probable non-local” (see Table 6.3). The seven probable/possible non-local individuals had childhood isotopes which may suggest origins in the nearby mountain regions, or the Carpathian Basin in the Hungarian lowlands. Although the sample size is small, the data suggest both men and women migrated during or after adolescence. Six of the seven individuals found to be possible/probable non-locals to their burial location had skeletal evidence of stress. The possible relationship between mobility and the prevalence of skeletal stress lesions is discussed further in Section 6.3.4.

Skeleton	Age category	Biological sex	Stress lesions	$^{87}\text{Sr}/^{86}\text{Sr}$	$\delta^{18}\text{O}_{\text{VSMOW}}$	Mobility status
ICL136	middle adult	F?	N	possible	local	possible
ICL138	young adult	M?	Y	possible	local	possible
ICL139	middle adult	F?	Y	possible	local	possible
FEN14	middle adult	F?	y	possible	possible	probable
BOG10	young adult	M?/?	y	possible	local	possible
BOG59	adolescent	M?/?*	y	possible	local	possible
BOG252	middle adult	M?	y	possible	local	possible

Table 6.3. Summary of individuals found to be non-locals to the burial region.

*Tentative biological sex estimation, assuming the individual was post-pubescent.

6.3. Diet, breastfeeding/weaning practices, and early-life stress isotopic profiles

This section provides the interpretation of the isotope data to establish overall dietary patterns, breastfeeding/weaning practices, and to generate profiles to identify early-life stress from incremental dentine analysis. Before the early-life profiles could be examined, dietary patterns and breastfeeding/weaning practices were assessed to establish patterns for each population. Understanding a person’s mobility history (Sr and O isotopes), their health (skeletal lesions) and overall diet helped to interpret the early-life profiles in order to explore possible changes in diet, such as a change due to migration. The early-life isotope profiles for the 39 individuals in this study can be found in Appendix 6.2.

6.3.1. Overall dietary pattern

Data from ancient animal and modern plant samples within this study, as well as faunal data from archaeological research in the surrounding regions, helped to establish dietary isotope ratios and begin to build dietary baselines that could be used, to contextualise the human data (Figure 6.6) (Makarewicz and Sealy, 2015). As discussed in Section 3.2.1, C₃ plants have $\delta^{13}\text{C}$ values between -35 and -20‰ and C₄ plants have $\delta^{13}\text{C}$ values between -16 and -9‰ (van der Merwe, 1982). Human bone collagen is increased by ~5‰ ($\delta^{13}\text{C}$) above the dietary resources (van der Merwe, 1982; Tykot, 2006). The values of two modern C₄ plant samples (corn husks) were adjusted for the Suess effect ($\delta^{13}\text{C}$ -1.5‰) and were within the expected range for C₄ plants. As discussed in Section 3.2., Transylvanian populations during the Migration Period and Middle Ages were mostly farmers (Giurescu, 1969; Madgearu, 2001; Pop and Nagler, 2010). While pastoralism was not the main subsistence strategy, animal domestication in Romania has been practised since the Neolithic (Evin *et al.*, 2017). Isotope data from faunal remains at archaeological sites in Hungary during the Roman period (Pannonia) were plotted to begin to establish a possible faunal baseline for Eastern Europe. Schoeninger and DeNiro (1984) found terrestrial carnivores and herbivores had mean $\delta^{15}\text{N}$ bone collagen values of 8.0‰ and 5.3‰ respectively. The single value obtained from the archaeological cow tooth from the Iclod Necropolis (Figure 6.6) indicates an entirely C₃ diet at approximately 2–3‰ ($\delta^{15}\text{N}$) below the human values. An increase in $\delta^{15}\text{N}$ values between 2–6‰ indicates a trophic level shift (DeNiro and Epstein, 1981; Schoeninger *et al.*, 1983; Ambrose, 1993). The 2–3‰ ($\delta^{15}\text{N}$) difference between the cow's values and human values suggests that cow protein was not a major portion of the diet for either population. Gillis and colleagues (2013) report bone collagen values from juvenile and young adult cattle from south-east Romania (5th C. BC) of $\delta^{13}\text{C}$ from -11.4 to -7.3‰ and $\delta^{15}\text{N}$ values from 6.3 to 9.7‰, demonstrating a cattle diet consisting of C₄ plant fodder. The $\delta^{15}\text{N}$ value obtained from the single archaeological pig (Figure 6.6), also from the Iclod Necropolis, fell just below the human values (<1‰) with a $\delta^{13}\text{C}$ value approximate 3‰ lower than the humans from Iclod; this suggests a C₃ diet with no C₄ resources. Balasse and colleagues (2013) examined animal herding practices in the

6th C. BC (south-west Romania), reporting domesticated pig bone collagen $\delta^{13}\text{C}$ values from -21.0 to -20.9‰ and $\delta^{15}\text{N}$ values from 6.7 to 6.9‰. These data indicate the single pig from Iclod ate an omnivorous diet composed of terrestrial C_3 resources. Although the sample size is small, these data help to establish a faunal baseline for eastern European lowlands.

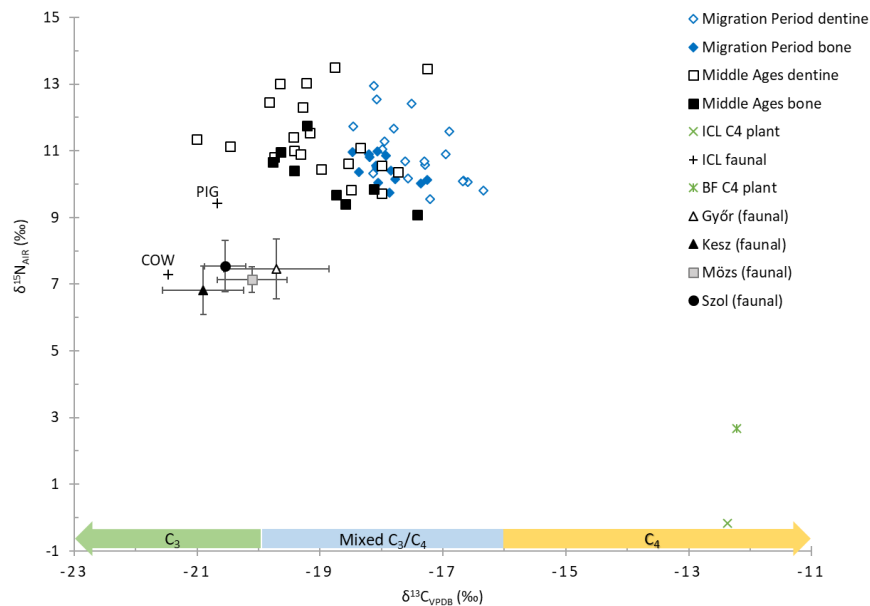


Figure 6.6. Carbon and nitrogen stable isotope data from samples from modern plants, ancient animal, and ancient humans to establish the overall dietary patterns for each population. Comparative data from archaeological faunal remains from Hungary are plotted to help establish a faunal baseline (symbol represents the mean \pm 2sd) (Alt et al., 2014; Hakenbeck et al., 2017).

Marine resources (e.g. marine fish, mammals, and birds) have isotope values of $\delta^{15}\text{N}$ from 10 to 25‰ and $\delta^{13}\text{C}$ from -22 to -16‰ (Schoeninger and DeNiro, 1984; Schwarcz and Schoeninger, 1991; Sharp, 2017, Section 7-6). Although the majority of individuals appeared to fall within the range for marine resources, these values probably represent a mix of C_3 (plant and animal protein) and C_4 foodstuffs, such as millet. It is possible both populations were consuming some protein from marine resources, such as salted fish, but the $\delta^{15}\text{N}$ values would be expected to be higher ($\delta^{15}\text{N}$ 10-25‰ + a 2-6‰ trophic level increase - Schoeninger and DeNiro, 1984).

Figure 6.7 illustrates the $\delta^{13}\text{C}$ values for the dentine collagen (mean) and enamel apatite alongside the linear regression data of Froehle et al. (2010) to help distinguish between terrestrial and marine dietary sources. A positive correlation can be seen, which follows the regression for C_3 protein, as well as increased consumption of carbohydrate C_4 resources within the Iclod Necropolis. Both populations appear to have consumed a terrestrial C_3 diet with the Migration Period people consuming significantly more C_4 foods ($\delta^{13}\text{C}_{\text{INCR}} p = 0.000$, $\delta^{13}\text{C}_{\text{BONE}} p = 0.006$). Broomcorn millet, a C_4 plant, was a favoured cereal crop due to its short growing season and limited agricultural tending required, and (Gyulai, 2006, 2014). Quick moving populations, like nomadic populations in the Carpathian Basin during the Migration Period, regularly used millet both in food and drink (Van Zeist *et al.*, 1991; Gyulai, 2014). Later, during the Hungarian conquest Árpáadian Period, broomcorn was an important crop in the Great Plain, while common bread wheat and rye became more evidence in Hungary and Transdanubia (Gyulai, 2014). This pattern may account for the significant difference in the $\delta^{13}\text{C}$ values between the Migration Period and medieval populations in this study.

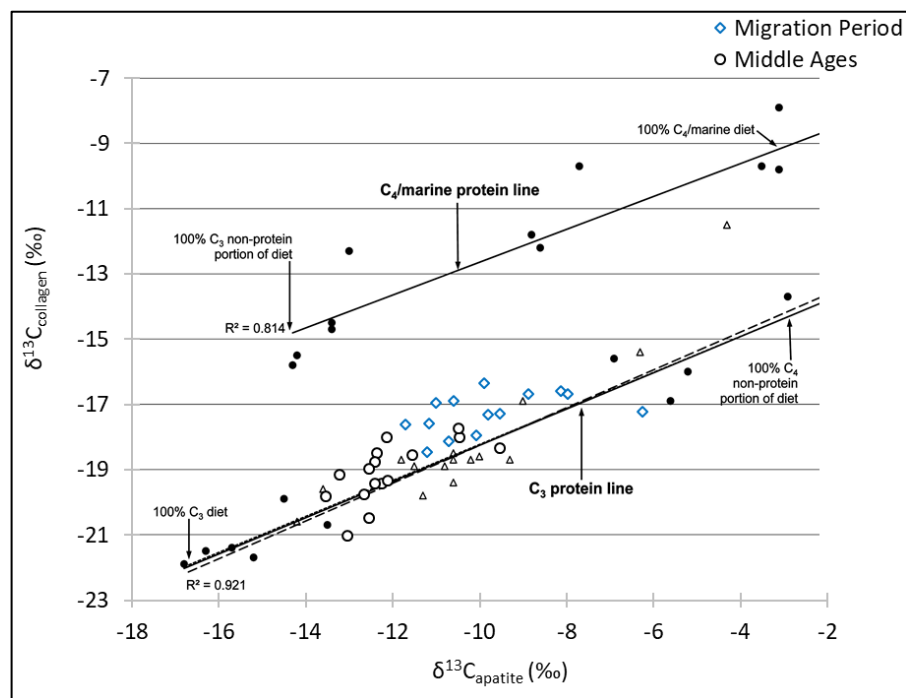


Figure 6.7. $\delta^{13}\text{C}$ values from dentine collagen (mean) and enamel apatite plotted with C_3/C_4 regression data from Kellner and Schoeninger (2007) and Froehle et al. (2010).

Migration Period females had significantly higher $\delta^{13}\text{C}$ values ($p = 0.020$) compared to females from the medieval assemblage. Within the medieval assemblage, women had significantly higher $\delta^{13}\text{C}$ values ($p = 0.009$) compared to the men (see Figure 6.8). When the data from both populations are combined and analysed by biological sex, females had significantly higher $\delta^{13}\text{C}$ values compared to males. These data suggest the consumption of millet was higher for women, indicating a gender/sex-based dietary pattern. Populations in Central Europe in the Iron Age used millet as a regular dietary component and animal protein has been found to be affected by a person's social status (Murray and Schoeninger, 1988; Le Huray and Schutkowski, 2005). When the bone collagen data from both populations were analysed together, males had significantly higher $\delta^{15}\text{N}$ values ($p = 0.049$) compared to females, which could signify differential access to foods like animal protein. Historical documentation also indicate boys were given preferential access to higher quality food, such as meat/fish, compared to girls (Carloni, 1981; Ortner, 1999; Craig *et al.*, 2009).

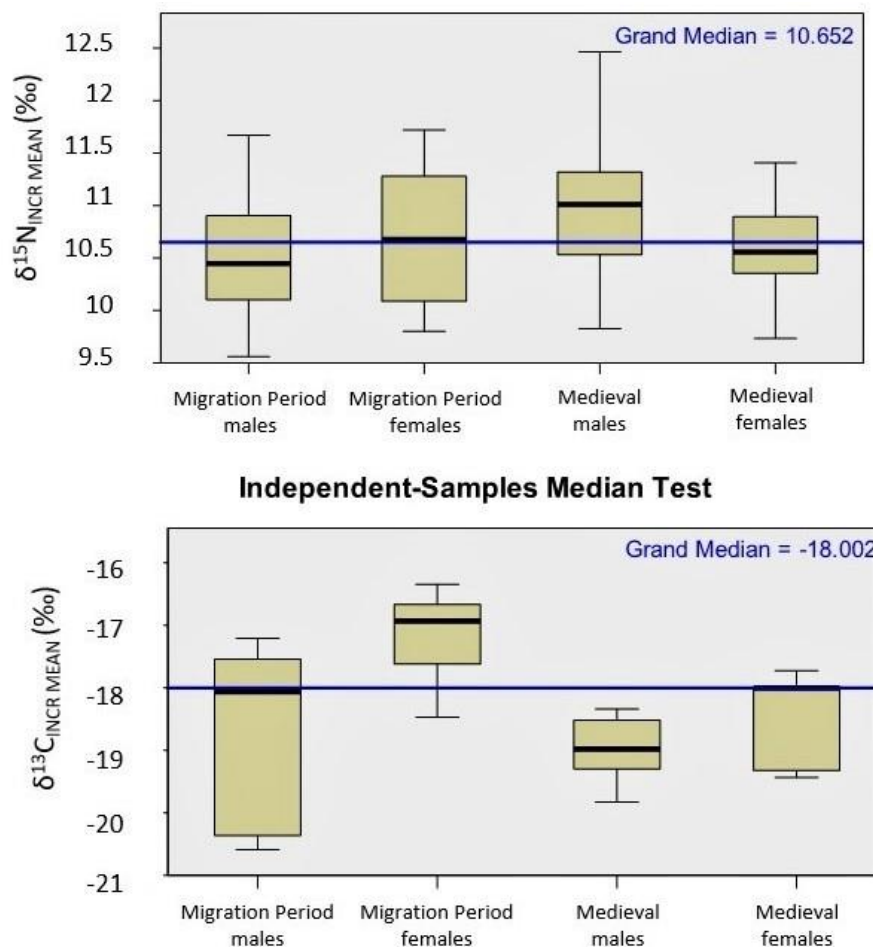


Figure 6.8. Results of carbon and nitrogen stable isotope data (incremental dentine) to demonstrate the difference in means for males and females, within and between periods.

As demonstrated in Figure 6.9, four adult individuals (FEN9, FEN14, FEN17 BOG10) had isotope values that suggest a change in diet from early childhood (mean dentine values) to adulthood (bone values). Individuals FEN14 and BOG10 consumed a diet of mixed C_3/C_4 resources early in their lives with increased millet consumption ($\delta^{13}\text{C}$ decreased $\sim 1\text{‰}$) prior to death. As previously mentioned, FEN14 and BOG10 also had elevated $^{87}\text{Sr}/^{86}\text{Sr}$ values compared to the other individuals in the burial population studied. If BOG10 and FEN14 were in fact incomers to their burial region, the increased C_4 consumption could be the result of a change in diet associated with migrating to the Bögöz/ Fenyéd regions. Individual FEN9 (Figure 6.9), a local older-adult female with EH, had childhood values similar to those of people buried in the Iclod Necropolis (mixed C_3/C_4 diet) and shifted to a diet with less C_4 later in life. FEN9 obviously survived the early-life stress event (EH), which could suggest low frailty

and/or having the means to overcome the stress (e.g. higher socio-economic standing). The incremental dentine isotope profile for individual FEN9 (see Appendix 6.2) shows a 1-3‰ increase in $\delta^{13}\text{C}$ values between the ages of six and 13 years old (maximum $\delta^{13}\text{C}$ values of -16.1‰) which indicates increased millet consumption (van der Merwe, 1982). As previously discussed, C_4 resources such as millet were commonly used to increase caloric intake during periods of physiological stress (e.g. illness, growth spurt) and to supplement inadequate diets during famine, or accessible to those from a lower socio-economic status (Thompson, 1982; Murray and Schoeninger, 1988; Le Huray and Schutkowski, 2005).

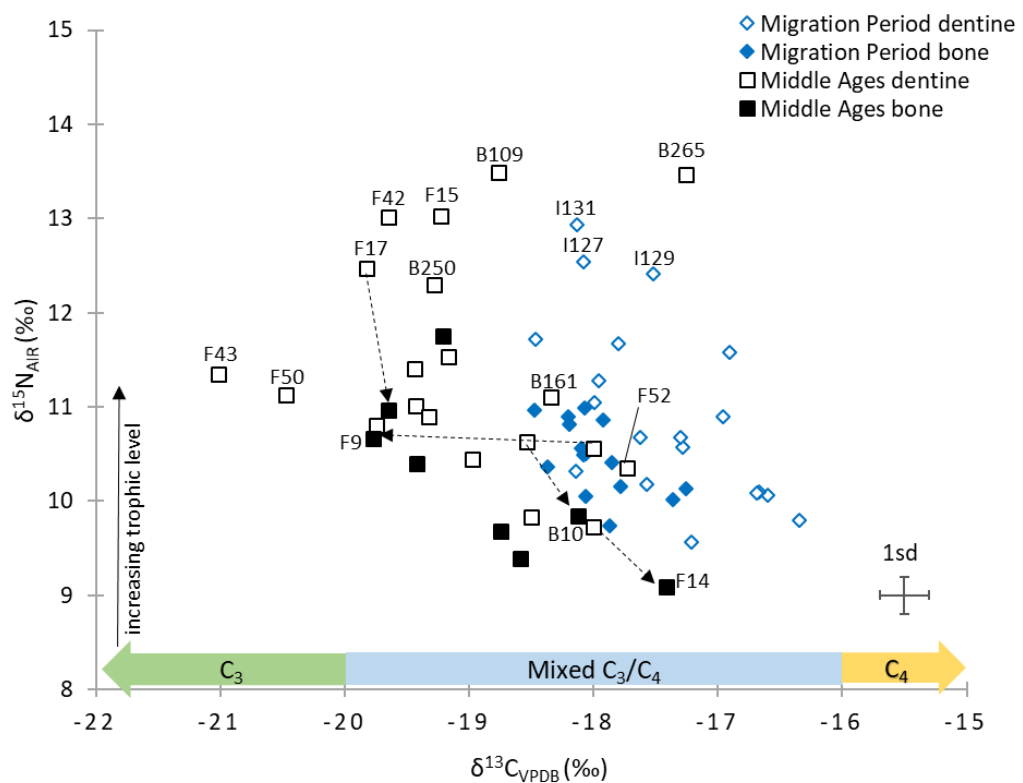


Figure 6.9. Carbon and nitrogen isotope data of the human dentine samples (mean) and bone isotope values for each population used to examine changes in diet throughout life.

Individuals FEN43 and FEN50 (Figure 6.9) were both adolescents when they died and appear to have consumed no C_4 resources. Two individuals, FEN52 a local adolescent and BOG161 a young adult local, appear to have consumed some C_4 foods during their early development. Both FEN52 and BOG161 (Figure 6.9) had skeletal lesions

associated with stress. This might suggest supplemental C₄ foods, such as gruel made from animal milk and millet, which were used to compensate for the metabolic/physiological stress experienced (Thompson, 1982; Voas *et al.*, 2018), or that they were consuming protein from animals that had a diet containing C₄ foods (Gillis *et al.*, 2013). Ten individuals from the Migration Period [female (6), male (3), unknown (1)], and three individuals from the medieval assemblage [female (1), male (1), adolescent (1)] showed periods of elevated $\delta^{13}\text{C}$ in their early-life isotope profiles (Appendix 6.2), which indicate varied consumption of millet. The majority of these people were adult women, which supports both the gender-related use for C₄ as well as C₄ supplementary foods during critical growth periods.

Nine individuals had elevated dentine $\delta^{15}\text{N}$ values (>12‰) compared to their burial population, and eight of them were non-adults. Their elevated $\delta^{15}\text{N}$ values were age-related and this is likely to be the result of breastfeeding and/or stress (see Section 6.3.2). This is supported by the statistically significant difference between age categories and the $\delta^{15}\text{N}$ values (see Table 5.9). As discussed in Section 3.1.1, the layered structure of dentine encapsulates isotope ratios throughout childhood (AlQahtani *et al.*, 2010; Beaumont and Montgomery, 2015), and bone reveals the average of the accumulated isotope ratios in the years leading up to death (Ambrose, 1993; Hedges *et al.*, 2007). Individual FEN17, the only adult with $\delta^{15}\text{N}_{\text{DENTINE}}$ values above 12‰, was classed as an older male local adult, and he had a 1.5‰ decrease of $\delta^{15}\text{N}$ from dentine_{mean} to rib bone collagen (Figure 6.9). The first maxillary permanent incisor was sampled from FEN17 for incremental dentine analysis, which captured his early-life profile from approximately 0.5 to 9.5 years. The mean dentine values from skeleton FEN17 may reflect a breastfeeding signal averaged with values following weaning. However, it may also indicate that he had chronic metabolic/physiological stress during development. The decline in $\delta^{15}\text{N}$ may reflect decreased stress later in life, or a change from their childhood diet. The trends discussed in this section are explored further in Sections 6.3.2 and 6.3.4.

6.3.2. Breastfeeding and weaning practices

Each early-life isotope profile, based on incremental dentine, was analysed to establish the duration and cessation of breastfeeding in the populations considered, and the approximate age the weaning process was completed. As previously discussed, all the early-life profiles produced can be found in Appendix 6.2. These data were analysed in conjunction age-at-death, biological sex and palaeopathological evidence to establish patterns within and between populations. Although each profile is unique to that person's lived experience, general breastfeeding and weaning patterns could be seen. Of the 19 individuals from the Migration Period, 17 had profiles constructed from teeth that began forming before or around the time of birth, thus capturing the period of life during breastfeeding/weaning. The majority of those individuals (14/17) appear to have been breastfed for the first ~6 months of life and ICL156 until ~1 year. Seventeen individuals had completed the weaning process between 2–3.5 years of age. Individual ICL136 (Appendix 6.2) had elevated $\delta^{15}\text{N}$ values until ~4–4.5 years, with $\delta^{13}\text{C}$ values fluctuating around two years and again at four years old, which could indicate a change in weaning foods, possibly incorporating C_4 foods. Overall, the individuals from the Migration period were breastfed for ~1-6 months and completed the weaning process between 2–3.5 years of age. This follows the recommendation of medical and Christian practices during this period (Fulminante, 2015).

All of the medieval individuals had profiles from teeth forming at or around the time of birth. FEN14, BOG66, BOG252, and BOG255 (see Appendix 6.2) had teeth with natural wear extending well into the dentine under the occlusal surface, and thus the earliest forming dentine was not present. Information relating to the weaning process could be seen for all four, but the duration of breastfeeding as the sole foodstuff could not be determined. Fourteen individuals only consumed breastmilk until six months and BOG250 (see Appendix 6.2) is the only individual who appears to have been breastfed until ~1 year of age. The weaning process was completed between 2-3 years for eight individuals and between 3–4 years for 10 individuals. Although the earliest forming dentine was naturally worn away, the profile for FEN14 (see Appendix 6.2) indicates they completed the weaning process around 1.5–2 years

of age. The individuals from the medieval assemblage were breastfed for the first ~6 months and completed weaning between 2–4 years of age. These data support Medieval medical texts which reflect the Soranus and Galen practices (breastmilk until six months and weaned by three years - Fulminante, 2015). However, the slightly older age of some of the individuals (weaned between 3-4 years) suggests practices from Classical, Byzantine and Muslim scholars which were adopted widely in the Middle Ages (Bourbou *et al.*, 2013; Fulminante, 2015). When the patterns were analysed, three general breastfeeding/weaning practices were revealed (A, B and C).

(i) Pattern A

Pattern A included those individuals that closely followed the “expected” breastfeeding and weaning curve, with an increase in values when breastmilk is consumed, and a gradual decline during the weaning process (see Figure 3.3). As outlined in Section 3.2.2, the adult female mean (AFM) for each population reflects the average of all adult female bone collagen values within each population studied. Weaning was considered to be complete when the values reach the AFM for that population and/or when the values flattened, indicating a consistent diet without breastmilk. The profiles for these individuals co-vary, both $\delta^{13}\text{C}$ and $\delta^{15}\text{N}$ values vary together, with the introduction of breastmilk, and gradually decreased until the weaning process was completed. As shown in Figure 6.10, the early-life isotopic profile for ICL127 showed an increase in $\delta^{13}\text{C}$ and $\delta^{15}\text{N}$ after birth with the introduction of breastmilk (0-1 year), and then $\delta^{13}\text{C}$ and $\delta^{15}\text{N}$ gradually decreased during the weaning process (from 1 to 3-3.5 years of age). FEN6 appears to have been consuming breastmilk for approximately four months and was weaned onto a diet of mixed terrestrial C_3 foods from six months to three years. The first permanent molar begins to form at approximately 0.3 years (AlQahtani *et al.*, 2010), which is why the profile starts at an age just after birth, possibly missing the initial increase in values at birth with the introduction of breastmilk.

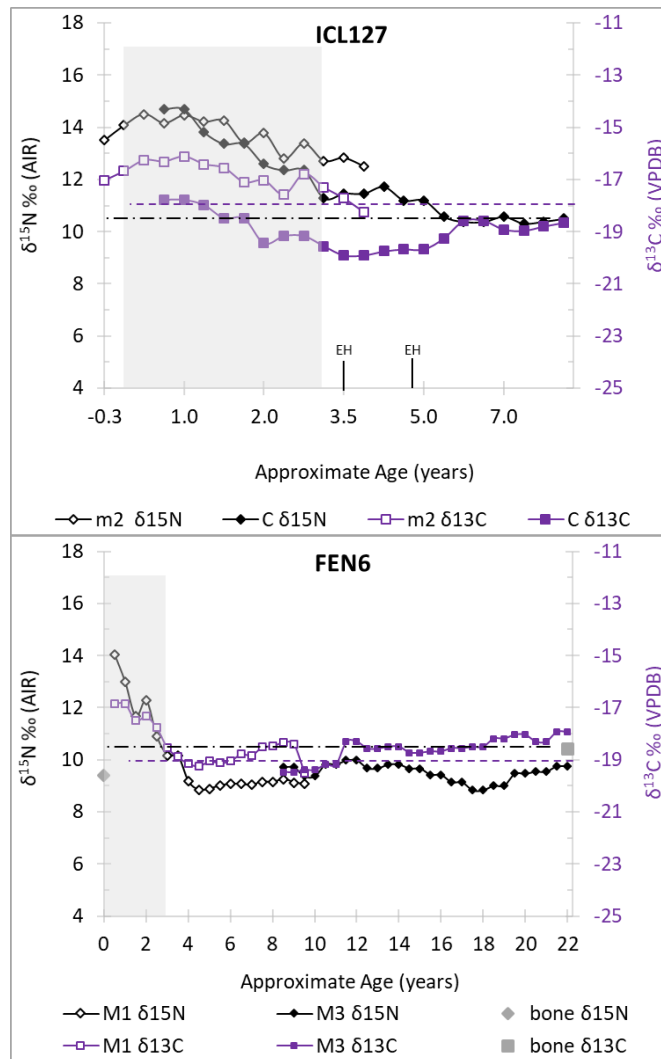


Figure 6.10. Examples of the Pattern A carbon and nitrogen profiles for breastfeeding and weaning for two individuals. The vertical shaded boxes indicate the probable breastfeeding/weaning period. AFM (adult female mean): $\delta^{13}\text{C}$ – dashed purple line; $\delta^{15}\text{N}$ – dot-dash black line. EH signifies the approximate age at which the hypoplastic event occurred.

Of the 14 people with Pattern A profiles, ten were from the Migration Period and four from the medieval assemblage (Table 6.4). The latter were all adults (three males, one female) and all had skeletal evidence of stress. Most of the individuals from the Migration Period assemblage were adults when they died (eight of 10), both male and female, (three males, four females, one unknown) with eight of 10 people had at least one stress-related lesion. This pattern may reflect a possible sampling bias, with 84% of the Migration Period assemblage being adults. However, when the data from both assemblages are combined, most were classified as young or older adults (8/14). As Wood and colleagues (1992) outlined in their Osteological Paradox, a person's socioeconomic status and environment, and temporal trends in health, can all impact

a person's frailty. The health trends identified during the Migration Period and Middle Ages match the recommendations for breastfeeding, the introduction of weaning foods around six months of age, and completion of weaning process (i.e. no breastmilk) between the three to four years old (Orme, 2003; Fulminante, 2015). Breastfeeding has been found to have short and long term benefits including reduced morbidity and mortality (Khan *et al.*, 2015; Sankar *et al.*, 2015; Said-Mohamed *et al.*, 2017). The benefits of breastfeeding during the first 1000 days of life, which has been found to be a critical period of growth and development (Barker, 2012), act as a buffer against insults later in life by helping the infant/child adapt to stress later in life (Black *et al.*, 2013; Said-Mohamed *et al.*, 2017). The data for Pattern A indicate that people with a "typical" or "expected" breastfeeding/weaning profile, with an absence of stress in the isotope profiles (i.e. rising $\delta^{15}\text{N}$ coupled with falling $\delta^{13}\text{C}$) during the first critical growth period; they were able to survive into adulthood despite the presence of stress related skeletal lesions. Despite the small sample size, these data support the long-term benefits of breastfeeding.

Pattern A				
Period	Skeleton	Age at death (years)	Biological sex	Stress related lesions
Migration	<i>ICL111</i>	25-35	n/a	Y
	<i>ICL123</i>	25-35	M?	N
	<i>ICL127</i>	8.5-9.5		Y
	<i>ICL129</i>	3.5-4.5		Y
	<i>ICL135</i>	25-35	F?	Y
	ICL136	35-45	F?	N
	ICL138	25-35	M?	Y
	<i>ICL140</i>	>45	M	Y
	<i>ICL149</i>	>45	F	Y
	<i>ICL156</i>	30-40	F	Y
Middle Ages	<i>FEN6</i>	25-35	M	Y
	<i>FEN9</i>	50-60	F?	Y
	BOG10	25-35	M?	Y
	<i>BOG161</i>	17-25	M?	Y

Table 6.4. Summary of the individuals with Pattern A breastfeeding and weaning profiles. Bold skeleton IDs signify non-locals to the population.

(ii) Pattern B

The individuals with Pattern B profiles varied slightly from the “expected” breastfeeding/weaning curve. While the $\delta^{15}\text{N}$ values followed the trophic level increase of breastmilk and gradually decrease during weaning, the $\delta^{13}\text{C}$ values remained relatively flat throughout the first few years of life. Figure 6.11 shows two examples of this pattern, with both FEN10 and ICL155 having $\delta^{15}\text{N}$ values decreasing while the $\delta^{13}\text{C}$ profile remains relatively consistent. The gradual decrease in the $\delta^{15}\text{N}$ profiles supports the consumption of protein but the low $\delta^{13}\text{C}$ profile could indicate that breastmilk was limited (Craig-Atkins et al., 2018), or that milk from animals rather than human breastmilk was consumed (Metges et al., 1990). As the individual is weaned, the $\delta^{15}\text{N}$ values drop as expected in traditional weaning, while the $\delta^{13}\text{C}$ profile remains consistent with the introduction of mixed C_3 terrestrial foods. Fourteen individuals had breastfeeding and weaning profiles that follow Pattern B. Four were from the Migration Period and ten were medieval (see Table 6.5). Pattern B is the exact inverse of Pattern A. The Migration Period individuals with this pattern comprised one non-adult, two young adults (one female, one male), and one middle adult (F?), all of whom had at least one skeletal stress lesion. Of the 10 medieval individuals, nine had “stress” related lesions, and most were non-adults (7 of 10). Weaning practice similar to Pattern B was used more by the medieval assemblage, but it is important to remember that the analysed assemblage is may not be representative of the living population, especially as the sample sizes here are small (Wood *et al.*, 1992; Waldron, 1994, Chapter 2).

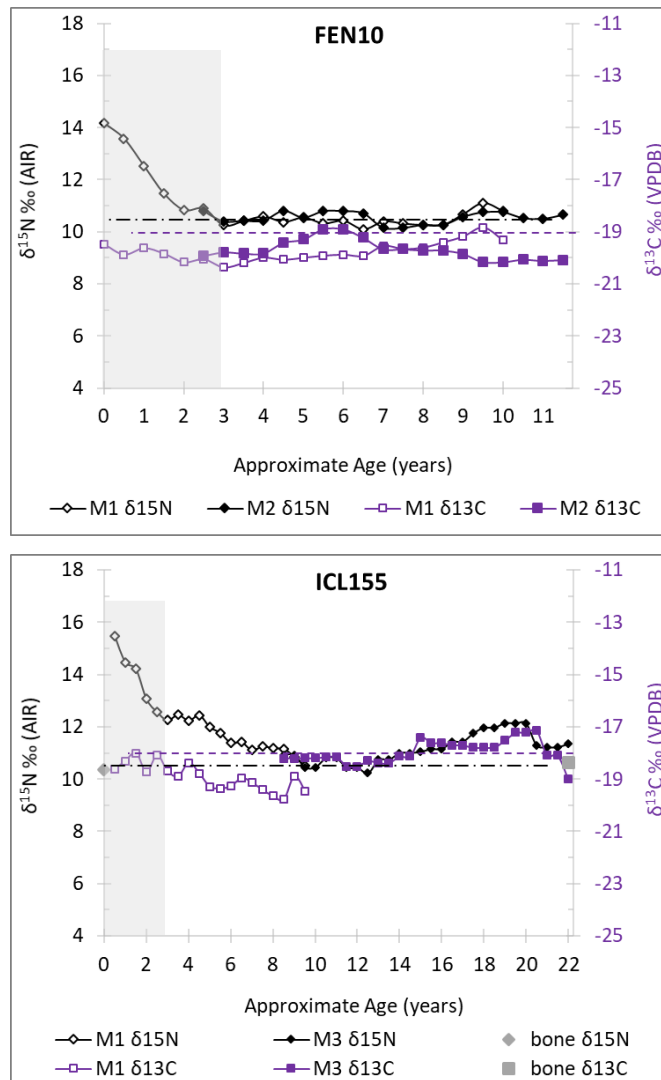


Figure 6.11. Examples of the carbon and nitrogen isotopic profiles of two individuals for Pattern B breastfeeding and weaning. The vertical shaded boxes indicate the probable breastfeeding/weaning period. AFM (adult female mean): $\delta^{13}\text{C}$ – dashed purple line; $\delta^{15}\text{N}$ – dot-dash black line.

Human and animal milk differ both in quality and quantity of nutrients. The high protein content of animal milk compared to human milk has been found to overload an infant's kidneys with waste nitrogen products (WHO, 2009). Animal milk also lacks the passive immunity and anti-infective properties of breastmilk (Katzenberg *et al.*, 1996; WHO, 2009). The World Health Organisation (2009) examined infant and child feeding practices in developing countries. They found limited breastmilk and solid weaning foods before six months of age resulted in 10% of the disease burden in children under five years old and resulted in 1.4 million deaths. If it is assumed Pattern B does indeed reflect individuals being weaned with animal milk rather than

human breastmilk, their younger ages at death could indicate this weaning practice was not as efficient during critical growth periods, resulting in high frailty. The older adults (ICL155, FEN17, BOG252; see Appendix 6.2) clearly overcame whatever “stress” they experienced, and survived well into adulthood, which could indicate access to a higher quantity and increased quality nutrients in their diet. (Fuller *et al.*, 2006; Craig-Atkins *et al.*, 2018).

Pattern B				
Period	Skeleton	Age at death (years)	Biological sex	Stress related lesions
Migration	<i>ICL131</i>	4.5-5.5		Y
	<i>ICL134</i>	>18	F	Y
	<i>ICL141</i>	18-20	M	Y
	<i>ICL155</i>	40-50	F?	Y
Middle Ages	<i>FEN10</i>	11.5-12.5		Y
	<i>FEN15</i>	5.5-6.5		Y
	<i>FEN17</i>	50-60	M	N
	<i>FEN50</i>	13.5-14.5		Y
	<i>BOG59</i>	16.5-17.5	*M?	Y
	<i>BOG109</i>	3.5-4.5		Y
	<i>BOG240</i>	15.5-16.5	*M?	Y
	<i>BOG250</i>	4.5-5.5		Y
	<i>BOG252</i>	40-50	M?	Y
	<i>BOG255</i>	25-35	F?	Y

Table 6.5. Summary of the individuals with Pattern B breastfeeding and weaning profiles.

*Tentative biological sex estimation assuming the individual was post-pubescent. Bold skeleton IDs signify non-locals in the population.

(iii) Pattern C

Seven individuals had early-life profiles that suggest limited breastfeeding, with weaning onto a diet different from their mothers and/or rest of the population studied (see two examples in Figure 6.12). The $\delta^{15}\text{N}$ values follow the expected decline during weaning, but the $\delta^{13}\text{C}$ values remain relatively consistent and/or increase during the weaning period. This would occur if the weaning foods contained

greater proportions of animal protein/C₄ resources compared to the mother's diet, or AFM. Individual ICL130 (Figure 6.12) has three periods of elevated $\delta^{13}\text{C}$ values with the $\delta^{15}\text{N}$ values remaining consistent, indicating no trophic level shift. FEN52 (Figure 6.12) had elevated $\delta^{13}\text{C}$ values (compared to the AFM) with opposing co-variance in the $\delta^{15}\text{N}$ values (i.e. increase in $\delta^{13}\text{C}$ values and a decrease in $\delta^{15}\text{N}$ values), which has been found during the period of growth (Mays et al., 2002; Pearson *et al.*, 2015) or increased protein consumption (Waters-Rist and Katzenberg, 2009).

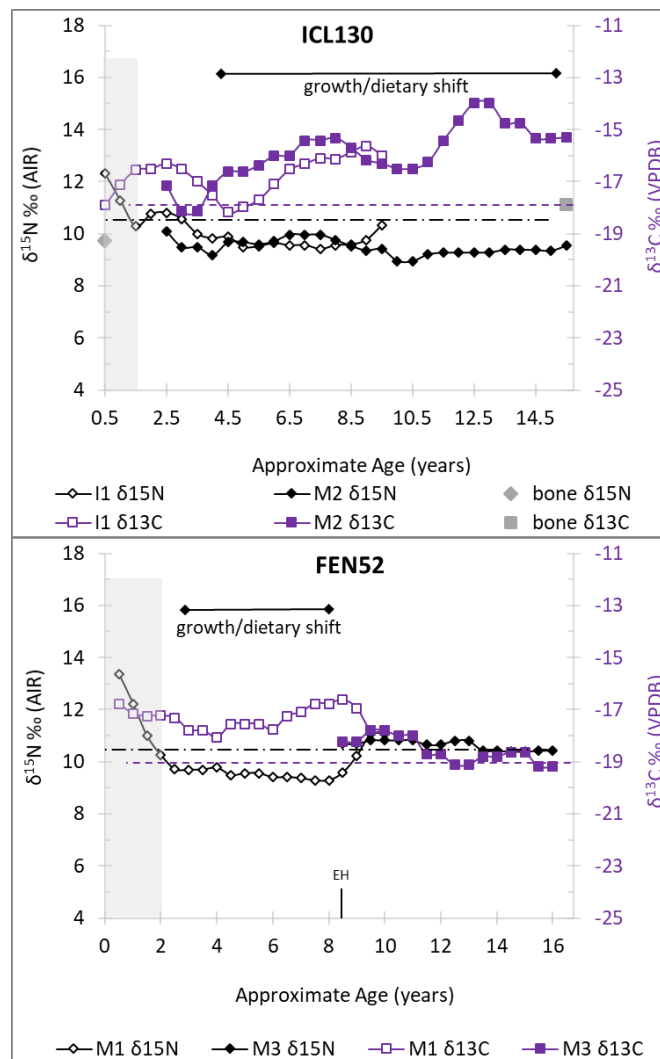


Figure 6.12. Two examples of the profiles for Pattern C breastfeeding and weaning. The vertical shaded boxes indicate the probable breastfeeding/weaning period. AFM (adult female mean): $\delta^{13}\text{C}$ – dashed purple line; $\delta^{15}\text{N}$ – dot-dash black line. EH signifies the approximate age at which hypoplastic event occurred.

Five individuals from the Migration Period had breastfeeding/weaning profiles similar to Pattern C. All five were adults (three females, two males) and all but one person had skeletal evidence of stress (Table 6.6). The profile for ICL120 (see Appendix 6.2) begins at age three (formation of the tooth sampled). If it is assumed ICL120 was breastfed, the $\delta^{13}\text{C}$ increased once weaning was completed. One adult and one non-adult from the medieval assemblage had weaning profiles similar to Pattern C, and both were females with skeletal evidence of physiological stress. When the data from both populations are analysed together, most of the individuals with a Pattern C weaning practice were young adults with stress lesions. As previously mentioned, C_4 food such as millet was a component of the normal diet and was also documented to be used to supplement poor diets when an adequate diet was hard to access (e.g. famine, war, low socio-economic status – Thompson, 1982). Ambrose and colleagues (2003) examined the diet of a Native American population and found higher status individuals ate more meat and 10% less maize (C_4 plants) compared to the lower status individuals, supporting the increased use of C_4 foods for those with poor access to adequate foods. The addition of millet during the critical growth period, increasing caloric intake for energy/growth, could help support survival through childhood. However, if a person's diet is not properly balanced with other nutrients (e.g. fruits, vegetables, animal protein), millet may only delay the inevitable physiological effects of malnutrition.

Pattern C				
Period	Skeleton	Age at death (years)	Biological sex	Stress related lesions
Migration	<i>ICL130</i>	35-45	F?	Y
	<i>ICL137</i>	25-35	F?	Y
	<i>ICL139</i>	>45	M	Y
	<i>ICL154</i>	25-35	F?	N
	<i>ICL120**</i>	25-35	M?	Y
Middle Ages	<i>FEN14</i>	35-45	F?	Y
	<i>FEN52</i>	15.5-16.5	*F?	Y

Table 6.6. Summary of the individuals with Pattern C breastfeeding and weaning profiles. Key: * biological sex assuming FEN52 was post-pubescent; ** assumes ICL120 was breastfed. Bold skeleton IDs signify non-locals to the population.

(iii) Pattern D: lack of breastfeeding

Four individuals from the medieval assemblage had early-life isotope profiles showing little to no breastfeeding/weaning signal (Table 6.7). As shown in Figure 6.13, the $\delta^{13}\text{C}$ profile of FEN43 varied, while the $\delta^{15}\text{N}$ profile remained relatively consistent throughout development. The profiles of BOG66 co-vary and are also relatively consistent throughout development. These profiles could indicate that these people were not breastfed, and therefore do not exhibit the expected trophic level increase after birth (Fuller *et al.*, 2006; Craig-Atkins *et al.*, 2018). However, the slight variations in values for the earliest dentine sections may signify a faint weaning signal (Figure 6.13: FEN43 0-1.5 years; BOG66 1-2 years). The fluctuating $\delta^{13}\text{C}$ values seen in FEN43 indicate a change in terrestrial C_3 resources without a trophic level shift in the $\delta^{15}\text{N}$ profile, indicating no change in meat or dairy consumption.

As previously stated, clinical research has found that children who were not breastfed, or breastfed for a short amount of time <6 months, had higher risks of infection and a higher mortality rate compared to children who were exclusively breastfed for at least six months (WHO, 2009; Sankar *et al.*, 2015). Three of the four individuals with Pattern D profiles died during childhood, and FEN43, BOG66 and BOG265 died with stress related skeletal lesions. It is possible that BOG66 was completing the weaning process when the profile started, around 1.5–2 years of age, and survived into adulthood. This could also indicate BOG66 had access to high quality and/or quantity foods compared to the other individuals who were not breastfed. FEN42 died in infancy. If Pattern D profiles do reflect a lack of breastfeeding during life, these data support an increased risk of disease and mortality for children who do not consume breastmilk for at least the first six months of life (WHO, 2009; Sankar *et al.*, 2015).

Period	Skeleton	Age at death (years)	Biological sex	Stress related lesions
Middle Ages	FEN42	10.5m-1.5		N
	FEN43	14.5-15.5		Y
	BOG66	>45	F?	Y
	BOG265	4.5m-8m		Y

Table 6.7. Summary of the individuals without breastfeeding signals in the early-life profiles.

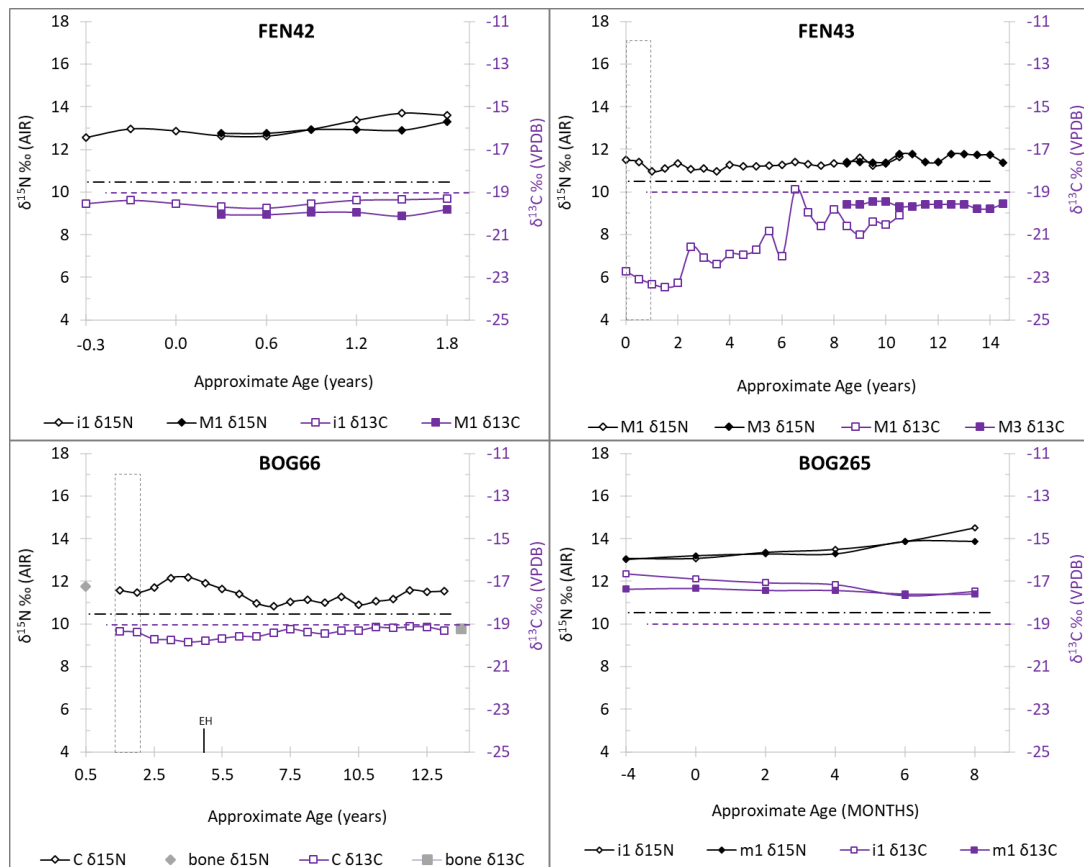


Figure 6.13. Examples of the individuals with profiles that were not breastfed. Vertical dashed boxes represent the possible breastfeeding/weaning signal. AFM (adult female mean): $\delta^{13}\text{C}$ – dashed purple line; $\delta^{15}\text{N}$ – dot-dash black line. EH signifies the approximate age at which the hypoplastic event occurred.

6.3.3. Perceived formation offset: An examination of a possible offset between tooth formation stages and between EH and changes in early-life isotope profiles.

When the early-life isotope profiles were examined, two perceived offsets were observed. The first was a possible delay between the estimated age EH occurred in an individual's enamel compared to changes in the dentine isotope profile. The second was an offset in the isotope values from teeth at different stages of formation from a single individual. This section explores the possible explanations for these perceived offsets.

(i) Enamel hypoplasia

Clinical research has found that catabolic events can manifest in a person's body as early as 6–12 days after the metabolic imbalance occurred (Beisel, 1975, 1977; D'Ortenzio *et al.*, 2015). As discussed in Section 2.2.3, EH represents physiological disruption in the formation of the enamel striae and has been linked to metabolic bone disease, infection, physiological stress, and mal/undernutrition (Armelagos *et al.*, 2009). If the stress event that caused the EH also resulted in a catabolic state, the EH would be expected to correspond to changes in the isotope profile (increased $\delta^{15}\text{N}$ values, decreased $\delta^{13}\text{C}$ values). When the teeth sampled for incremental dentine analysis had EH present, the age of the stress event was estimated (Reid and Dean, 2000) and plotted on the early-life isotope profile. Of the 39 individuals with early-life isotope profiles, 18 had teeth with at least one EH (Migration Period – 10, Middle Ages – 8).

Examination of the age at which EH occurred revealed that 67% of individuals (12/18) had EH around the time weaning was completed (after the $\delta^{15}\text{N}$ values declined back to the AFM). No clear patterns were found between the two populations, or between the age-at-death categories, biological sexes or weaning patterns (type or rate of weaning). As outlined in Section 3.2.2, the weaning process can impact morbidity, mortality and the immune system strength of an infant (Katzenberg *et al.*, 1996). Evidence of the cessation of breastmilk being made available to infants and the introduction of weaning, along with supplementary foods has been found to coincide with the presence of EH (Katzenberg *et al.*, 1996; Reitsema *et al.*, 2016). Nava and colleagues (2019) examined EH (via microscopic accentuated lines of Retzius) and report that the highest occurrence of EH coincided with the beginning of weaning in isotope profiles. Reitsema and McIlvaine (2014) and Sandberg and colleagues (2014) reported EH during the weaning process but not before or after the weaning period. The data in this study support the findings of Reitsema and McIlvaine (2014) and Sandberg and colleagues (2014) in that there is a correlation between the occurrence of EH and weaning. However, the data in this study found that the highest prevalence of EH occurred at the end of the weaning process. The timing of stress events within this study also coincided with period of life when teething is occurring (eruption of

the dentition through the gums) and the mid-childhood critical growth period, both of which can cause physiological stress during development (Cameron and Demerath, 2002; Khalifa, 2014). Further research would be required to examine the possible aetiologies for this pattern.

Five of the 12 individuals who had EH coinciding with weaning also had slight fluctuations in their $\delta^{15}\text{N}$ profiles (ICL127, ICL141, FEN9, BOG59, BOG161). The brief increase in $\delta^{15}\text{N}$ values suggests added physiological/metabolic stress during the weaning process (Figure 6.14, ICL141). This could reflect attempts to change the weaning foods provided or a new stressor occurring during weaning. The initial change in the course of the $\delta^{15}\text{N}$ weaning curve occurred approximately one year before the estimated age of the hypoplastic event for all five individuals. It could be that the EH was not directly related to the fluctuations seen during the weaning process, or that the added stress that occurred during weaning was chronic, and took approximately one year to reach the point at which the body was under a level of stress that disrupted the secretion of the enamel matrix (Hillson, 1996). The approximate age of EH and the age assigned to the incremental sections of dentine have a margin of uncertainty, which may also account for the perceived offset. Dental formation rates can vary normally by ± 0.5 –6 months (AlQahtani *et al.*, 2010), and uncertainty for the approximate age of EH is between 1–12 months (Reid and Dean, 2006; Hassett, 2014). Additional work, including histological examination of the periodicity of striae of Retzius would aid in establishing the onset and duration of the disruption in enamel formation and to confirm the approximate age of the stress event (Hillson, 1996; Mahoney *et al.*, 2017).

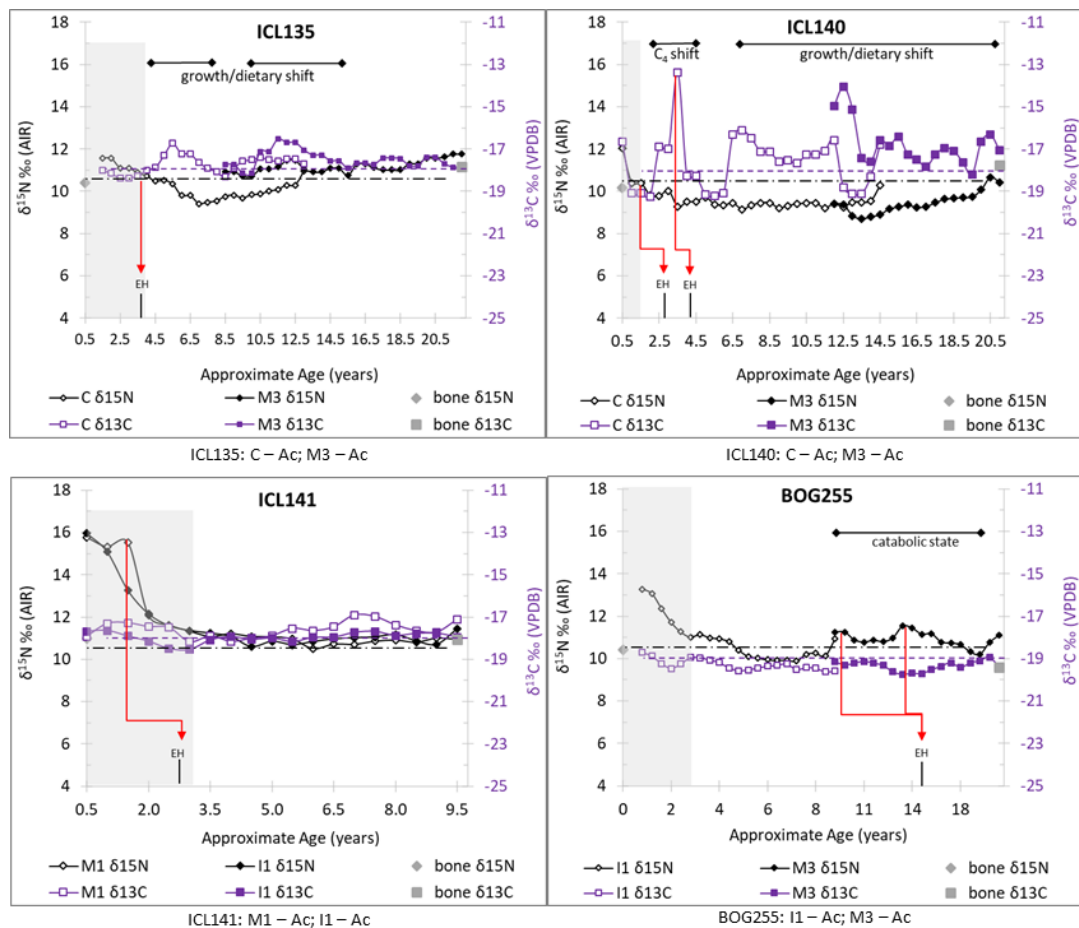


Figure 6.14. Examples of early-life profiles of four individuals plotted with a possible offset between the isotope ratio changes and the timing of the EH. The vertical shaded boxes indicate the probable breastfeeding/weaning period. AFM (adult female mean): $\delta^{13}\text{C}$ – dashed purple line; $\delta^{15}\text{N}$ – dot-dash black line. EH signifies the approximate age at which the hypoplastic event occurred. Red arrows demonstrate the perceived offset between changes in the isotope profile and timing of EH (assuming the two events resulted from the same stressor/stress event).

Seven individuals had EH that coincided with increased $\delta^{13}\text{C}$ values, rather than $\delta^{15}\text{N}$ values (ICL137, ICL139, ICL140, ICL149, ICL156, FEN52, BOG161; see Appendix 6.2). Four of the seven individuals with EH had increased $\delta^{13}\text{C}$ values and a Pattern C breastfeeding/weaning practice (see Figure 6.11). Elevated $\delta^{13}\text{C}$ values can occur during periods of increased consumption of C₄ and/or animal protein when the body is forming new tissues for normal or catch-up growth (anabolic state). Five of the seven individuals had EH during or just after weaning (with the obvious dietary shift, see Appendix 6.2). Two individuals, ICL149 and FEN52 (Appendix 6.2), displayed hypoplastic events during the mid-childhood growth period, which occurred well after (+2 years) the initial increase in $\delta^{13}\text{C}$ values (Figure 6.14 – ICL140). Opposing

covariance between the $\delta^{13}\text{C}$ (increase) and $\delta^{15}\text{N}$ (decrease) values has been found to occur during increased animal protein consumption when skeletal growth is occurring (Hatch *et al.*, 2006; Mekota *et al.*, 2006). FEN52 and ICL139 (Appendix 6.2) were also found to be non-local to their burial location, which could account for the added stress and dietary changes. Although the sample size is small, these data suggest changes in diet can cause physiological stress. However, not all individuals with substantial dietary shifts had resulting EH, which could indicate a relative difference in frailty.

Six individuals had EH associated with elevated $\delta^{15}\text{N}$ profiles, which were not associated with weaning signals (ICL127, ICL134, BOG59, BOG66, BOG252, BOG255; see Appendix 6.2). When the changes in the isotope profile are compared to the approximate age of the hypoplastic event, there was a substantial offset in 4–5 individuals. However, if the stress event (EH) did not result in a catabolic state, corresponding changes in the isotope profile would not be expected. Therefore, it is possible that the perceived offset between EH and increased $\delta^{15}\text{N}$ values was not correlated because the aetiology of EH was not metabolic in nature (e.g. infection). However, most causes of EH result in systemic physiological stress, which would be reflected in the isotope profile. If it is assumed the EH was the result of a stressor that resulted in a catabolic event, then the earliest increase in $\delta^{15}\text{N}$ values would theoretically represent the onset of the stress event. The peak would reflect the point at which recovery began, and full recovery would be achieved when the values reached the AFM. This pattern can be seen in the early-life profile of BOG252 with the hypoplastic event corresponding to the peak $\delta^{15}\text{N}$ values. The other five individuals had a one to two-year offset between the earliest increase in $\delta^{15}\text{N}$ values and the estimated age of formation of EH. As stated previously, the uncertainty for estimating the approximate chronological age of EH is between 1–12 months (Reid and Dean, 2006; Hassett, 2014). The uncertainty could account for the offset between the estimated age of EH and changes in the isotope profile, assuming both were caused by the same stressor. BOG255 (Figure 6.14) had evidence of a catabolic event with two distinct peaks in $\delta^{15}\text{N}$ values between 8-9 years and 13-14 years. A stress event causing EH occurred around 15 years of age. The perceived offset

between peak $\delta^{15}\text{N}$ values and EH varied between one and five years. This pattern could reflect an offset between the stress event being recorded in the forming dentine compared to the enamel (see Section 3.1). These data may also reflect a delay between the onset of the stress event (initial changes in the isotope profile) and the point at which enamel striae disruption occurs. Due to the small sample size, further research would be required to confirm these finds.

(ii) Type of tooth: still forming or complete

AlQahtani and colleagues (2010) compiled extensive research on the formation and eruption of human dentition. The age range data for dental formation and eruption used in this study reflect the midpoint ages outlined by AlQahtani and colleagues (2010), and therefore some variation in the exact timing of formation assigned may be present. Dentine formation rates for the deciduous dentition, and regions of the permanent teeth (coronal and apical regions), can vary (Dean and Cole, 2013; Beaumont and Montgomery, 2015), with an average dentine formation rate of 4–6 $\mu\text{m}/\text{day}$ (Dean and Scandrett, 1995). Beaumont and Montgomery (2015) proposed a method based on the average dentine formation rate (4–6 $\mu\text{m}/\text{day}$) for assigning a corresponding estimated age to sequentially samples dentine (1mm).

Human dentine was sequentially sectioned along the direction of formation (crown to root tip). Figure 6.15 is a simplified theoretical model of the formation of a permanent first molar tooth, along with an illustration of the 14 sections and their ages at formation (1mm increments) along with $\delta^{15}\text{N}$ early-life isotope profiles. As discussed in Section 3.1, dentinal tubules form S-shaped bands towards the pulp chamber (see Figure 3.1) and tooth formation proceeds along the length of the tooth from the crown to the tip of the roots. Crown formation follows the shape of the enamel cap; therefore, dentine is secreted in curving horizontal layers. Because dentine is not secreted in straight lines, one incremental section (1mm) can reflect multiple phases of dentine secretion and an average of the isotope values during those periods of formation (see Figure 6.15). Therefore, each incremental section is seen as an average of values and the resulting early-life isotope profile thus reflects

a running average over the entire formation period for each tooth (Beaumont and Montgomery, 2015). If a person died while their dentition was still forming (e.g. increment nine, between 5.5–6.0 years of age) the increments before death will reflect a shorter average period of formation. If the person lived past six years of age and dentine continued to be secreted, the values would reflect a longer period of formation. The difference in the number of dentine layers and formation stages could result in differing values between the incomplete tooth compared to a complete tooth from the same period of life (see Figure 6.15 theoretical graph). It is therefore very important to note the formation stage of the tooth sampled to account for possible fluctuations conflated by formation stages, rather than changes in diet, growth or levels of stress.

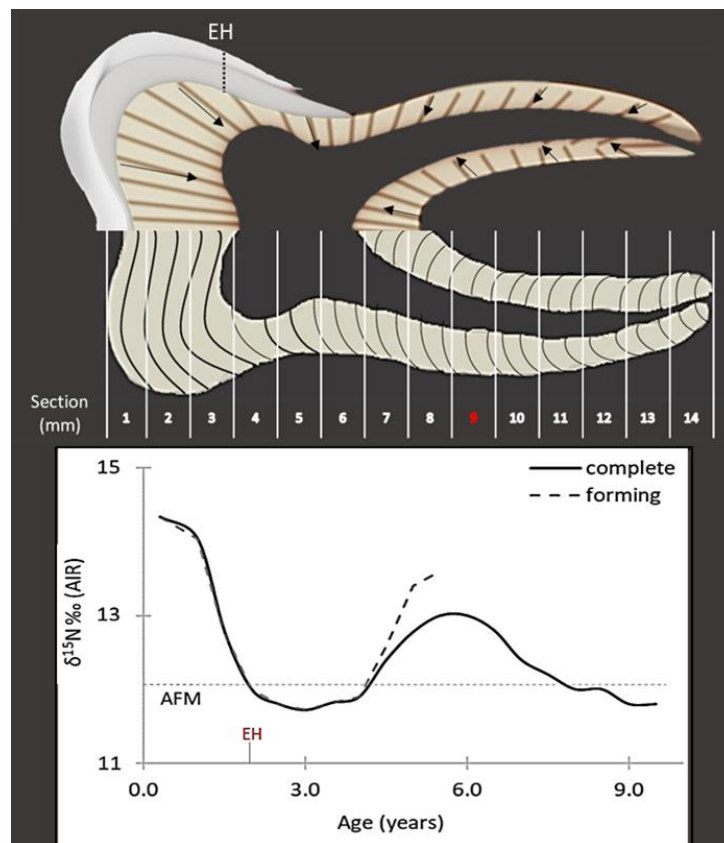


Figure 6.15. Simplified theoretical model of a first molar to show the different $\delta^{15}\text{N}$ isotope profiles between dentitions still forming at death and the complete permanent dentition (AlQahtani et al., 2010; Hillson, 2014; Beaumont and Montgomery, 2015). The top image shows the depositional layers of dentine and the direction of secretion and mineralisation. The bottom is a theoretical diagram of an isotope profile from that tooth.

Examples of early-life isotope profiles from individuals with a range of different teeth at different stages of formation (incomplete versus complete) can be seen in Figure 6.16. BOG265 died in infancy with both the deciduous first incisor and deciduous first molar still forming. Because both deciduous teeth were in the early stages of formation, only slight variations between the teeth were documented in the early-life isotope profiles. ICL129 (Figure 6.16) died between 3.5–4.5 years of age with their deciduous second incisor complete and their first permanent molar still forming (crown complete, no root). There was substantial variation in the isotope values between the complete tooth and the incomplete tooth (still forming at death). The fluctuations are the result of changes in the isotope values during life, but this isotope profile would be different if the tooth had completed formation. The exaggerated fluctuations are presumably the result of the increments recording a different stage of formation between the tooth types, with the incomplete molar reflecting a shorter period of averaged values, and thus making the shifts in isotope ratios seem considerable (e.g. the forming model in Figure 6.15). BOG109 (Figure 6.16) died between 3.5–4.5 years of age with their deciduous first molar complete and their first permanent incisor still forming (initial root formation – Ri). Because the crown of the permanent incisor was complete and root formation had begun, the values from the later forming increments were not as varied compared to the complete deciduous first molar. This can also be seen in the profile for FEN15 (Figure 6.16) whose canine crown was completely formed with the root $\frac{1}{4}$ complete.

Values from a tooth that was still forming at the time of death can make it appear as though higher levels of stress or dietary changes occurred when compared to a completely developed tooth. Isotope values from incomplete teeth are true reflections of input values recorded in dentine during that person's development. The values of the final increment(s) leading up to death in an incomplete tooth reflect a shorter period of formation, with fewer depositional layers of dentine. If formation continued, the isotope values from that increment would reflect the average from a longer period of formation. The perceived offset almost certainly reflects the difference between the averages from varying numbers of depositional layers of dentine and appears less varied compared to the increment of the incomplete tooth.

Although the sample size was small, the perceived offset between the different formation stages is extremely important when interpreting early-life isotope profiles and requires further research to confirm these trends.

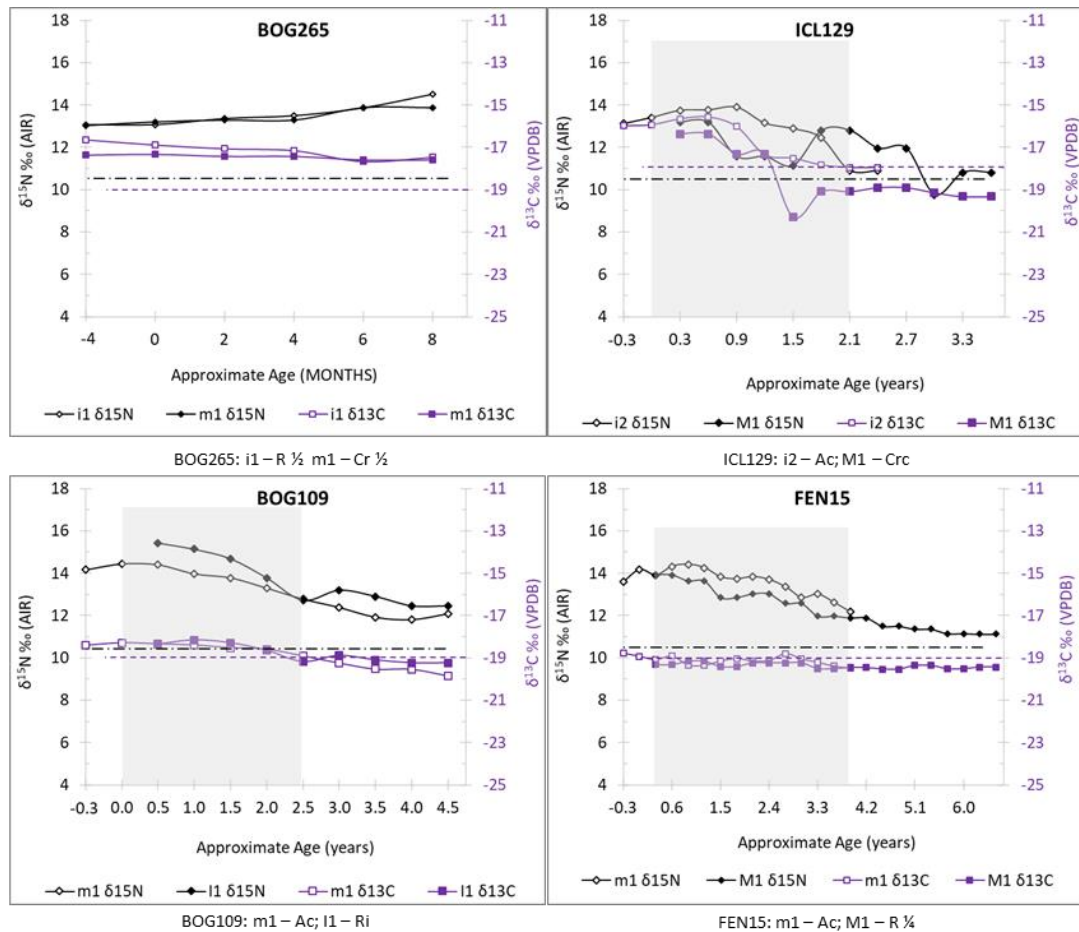


Figure 6.16. Examples of early-life profiles of four individuals with incomplete (still forming at death) and complete teeth. The vertical shaded boxes indicate the probable breastfeeding/weaning period. AFM (adult female mean): $\delta^{13}\text{C}$ – dashed purple line; $\delta^{15}\text{N}$ – dot-dash black line. Tooth formation stages from (AlQahtani et al., 2010).

6.3.4. Early-life stress

Early-life isotope profiles were created from the stable carbon and nitrogen isotope data (bone and incremental dentine) for each person analysed. Each profile was analysed alongside mobility, demographic and palaeopathological data to establish possible patterns between them and early-life stress signals in the isotope profiles. This section discusses the patterns within and between both populations based on: (i) mobility; (ii) active and healed skeletal lesions; (iii) critical growth periods; and (iv) frailty

(i) Early-life stress and mobility

Strontium and oxygen isotope analysis of human enamel reflects an average of a person's childhood isotope values (Montgomery *et al.*, 2000, 2007; Redfern *et al.*, 2016). If the childhood values of a tooth are different from those of the burial environment, that person was considered to have moved to the burial region while that tooth was forming, or after formation was complete. If a person migrated while the dentition was forming, a change in diet or a stress event, perhaps from the process of migration, could be captured in the early-life isotope profile (see Figure 6.17). Migration, whether it be large or small distances, or due to relocation or conflict, can have short- and long-term health consequences (Pedersen, 2002; Amuna and Zotor, 2008; Miller and Rasmussen, 2010). Cameron (2003) examined physical growth of children (n = 4,000) in transitioning economies after the South African apartheid and found: all children had low birth weights compared to other developed countries; white children recovered to their normal body mass index (BMI) within one year; and non-white children continued to have a low BMI throughout childhood and adolescence. Clinical research has also found that scurvy was common among refugee populations in Afghanistan due to limited dietary diversity, isolation, droughts and loss of livelihood due to being displaced (Cheung *et al.*, 2003). As discussed in Section 6.2.2, the majority of non-locals identified were adults with stress related lesions, supporting the hypothesis that both local and non-local people will have evidence of physiological/metabolic stress.

Wheaton (1994) refers to all the elements that contribute to stress as the “stress universe” and states that status differences in stress exposure can lead to systematic underestimation of stress. The psychosocial effects of changes in social, economic and political circumstances can increase daily exposure to stressors (Miller and Rasmussen, 2010). Benson and colleagues (2011) examined coping mechanisms of 665 people between the ages of 15 and 20 years after the Bosnian war and found that psychosocial stressors were still prevalent five years after the war ended. Analysing historical, archaeological, palaeopathological and biomolecular data together can help to create a more complete picture of a person’s early-life experience in relation to stress events. Of the seven individuals found to be non-locals when compared to the rest of the burial population, five had substantial changes in their early-life isotope profiles that could have been the result of dietary changes due to migration. Six of the seven individuals had one or more skeletal lesions associated with stress. ICL136 (see Appendix 6.2), a middle adult female (F?), was the only individual without stress related lesions, but their early-life isotope profile suggests two catabolic events during development (15–18 years and 20–23 years), further supporting the evidence for stress in the non-locals.

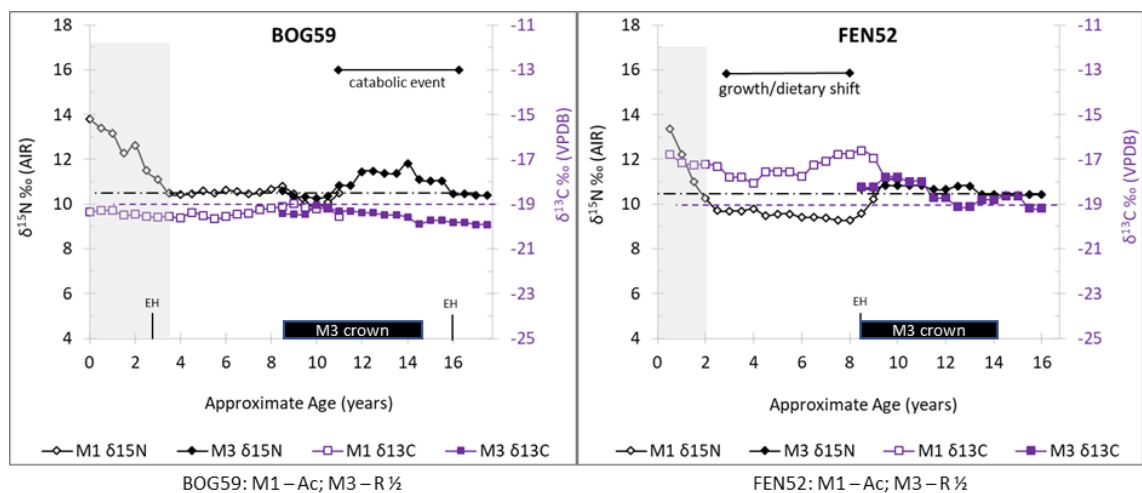


Figure 6.17. Examples of two early-life isotope profiles of non-local individuals. BOG59 (male??) and FEN52 (F??) were adolescents with stress related lesions. Enamel from the crown of the third molars was used for strontium and oxygen isotope analysis to assess mobility. The vertical shaded boxes indicate the probable breastfeeding/weaning period. AFM (adult female mean): $\delta^{13}\text{C}$ – dashed purple line; $\delta^{15}\text{N}$ – dot-dash black line. EH signifies the approximate age at which the hypoplastic event occurred.

It is impossible to know when each person moved to the region without detailed historical documentation. If the non-local adults migrated after their dentition had completely developed, changes in their early-life profiles would not reflect their mobility patterns. FEN52 and BOG59 died while their dentition was still forming. Therefore, if migration resulted in a change in diet and/or led to stress, it would have been captured in their isotope profiles. The elevated $\delta^{15}\text{N}$ values during the adolescent critical growth period could be linked to the physiological stress of migration (see Figure 6.17 – BOG59: 11-16 years). Individual BOG255 is believed to be a possible non-local and had an early-life profile very similar to that of BOG59, which could further support both these individuals being non-local to the region. Both BOG59 and BOG255 had an elevated $\delta^{15}\text{N}$ value and EH during adolescence, which may suggest migration occurred during adolescence. FEN52 was also found to be a possible non-local. If the dietary change between two and eight years was the result of a change in diet due to migration, it would follow that the strontium and oxygen isotope values should reflect an average of both the region of origin and the burial region. Although the sample size is small, these data could offer new insight into the timing of migration at an individual level.

(ii) Early-life stress and skeletal lesions

As previously mentioned, EH is the only stress lesion in this study that can be associated with an approximate age (macroscopically). If a person died while the dentition was still forming and had active stress-related skeletal lesions at the time of their death, it might be possible to correlate changes in the early-life isotope profiles with those lesions to assign an approximate age of onset and duration for the stress event. Individual BOG240 was local to their burial environment, buried with their skull between their lower limbs and died during adolescence with evidence of haemorrhagic staining of the bones that could be linked to scurvy (Maat, 2004; Brickley and Ives, 2008). Dental formation indicated that this individual died between 15.5 and 16.5 years of age (AlQahtani et al., 2010) while epiphyseal fusion rates indicated they were approximately 14 years or younger (unfused femoral head and distal fibula - Cunningham *et al.*, 2016). These data indicated slight arrested skeletal

growth. The early-life isotope profile for BOG240 (Figure 6.18) shows elevated $\delta^{15}\text{N}$ values, compared to the AFM, throughout their development, but the $\delta^{15}\text{N}$ values were only elevated 0–3‰ above the AFM with minimal opposing covariance (0.5–1 year, 8–10 years of age) (Fuller *et al.*, 2004; Mekota *et al.*, 2006; Beaumont, *et al.*, 2013). The profile for BOG240 could reflect a diet with higher animal protein consumption compared to the AFM, or periods of metabolic stress throughout childhood. If the elevated $\delta^{15}\text{N}$ profile is the result of metabolic stress and not dietary changes, it is plausible that the stressor causing the stress-related skeletal lesions and the catabolic state increased their frailty and led to early death.

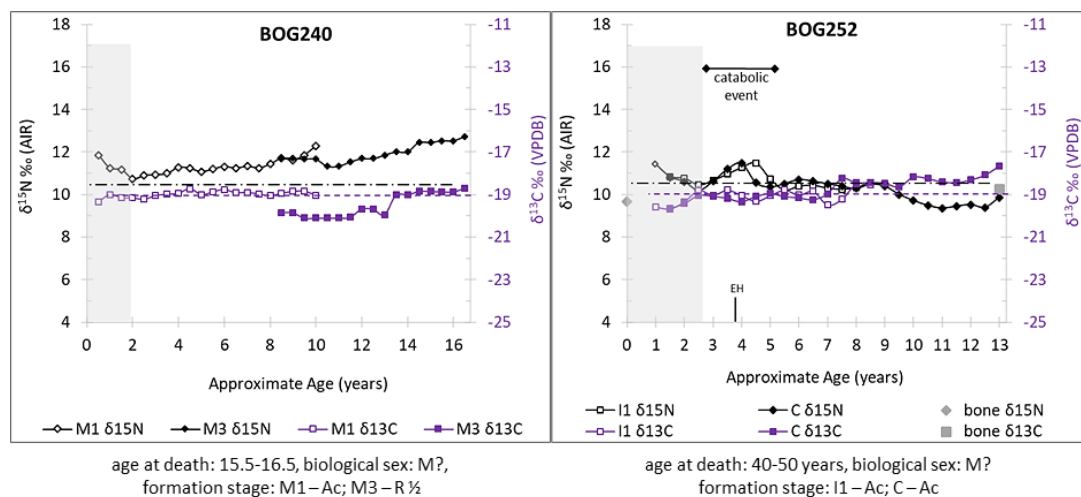


Figure 6.18. Early-life isotope profiles of two individuals with stress related lesions. The vertical shaded boxes indicate the probable breastfeeding/weaning period. AFM (adult female mean): $\delta^{13}\text{C}$ – dashed purple line; $\delta^{15}\text{N}$ – dot-dash black line. EH signifies the approximate age at which the hypoplastic event occurred.

A stress event that resulted in EH would have occurred during childhood, and therefore EH could be seen as a “healed stress lesion.” Thus, an adult with EH could be considered to have survived the childhood stress event. Of the 39 early-life isotope profiles, 18 individuals had EH and increases in $\delta^{15}\text{N}$ values: four non-adults (Migration Period = 1; Middle Ages = 3), seven young adults (Migration Period = three females, two males; Middle Ages = one female, one male), one middle adult (Migration Period female) and six older adults (Migration Period = one female, two males; Middle Ages = two females, one male). The age-at-death categories of young

and older adults contained the highest prevalence of EH alongside elevated $\delta^{15}\text{N}$ values. These data could be reflecting differences in frailty and/or socio-economic standing. Those who died as a non-adult or a young adult could have had higher frailty and/or lower socio-economic standing than those who survived into older adulthood.

Individual BOG252 was an older adult non-local man who died without active skeletal stress lesions, but he did have EH (Figure 6.18). When the approximate age of the hypoplastic event was plotted on the early-life isotope profile, it matched with an elevated $\delta^{15}\text{N}$, which correlated with the occurrence of a stress event. The $\delta^{15}\text{N}$ profile begins to increase between two and a half and three years (onset of stress event), reaches its highest point at the approximate age of formation of the EH, and decreases to normal around five years of age (end of stress event). It does not appear that the childhood stress event negatively affected their frailty enough to cause early death, but BOG252 had a shorter attained stature when compared to the rest of the analysed population (mean population stature = $170 \pm 5.8\text{cm}$; BOG252 stature = 153-161cm). Shorter stature and periods of arrested skeletal growth have been linked to childhood stress and increased frailty (Cameron, 2003; Watts, 2011; Dewitte and Hughes-Morey, 2012; Newman *et al.*, 2019). Incremental dentine stable isotope analysis was applied to twenty-six of the individuals who could be assessed for arrested skeletal growth (i.e. had preserved long bones), and eight had evidence of arrested growth (44%). All eight individuals had isotopic stress signals and/or EH during childhood. These data support the link between early-life stress and arrested skeletal growth.

(iii) Chronic early-life stress

As mentioned in previous sections, a number of individuals had early-life isotope profiles that showed elevated $\delta^{15}\text{N}$ profiles compared to the AFM throughout development. This section examines the possible differences in frailty among individuals who had more than one indicator of stress during development (e.g. catabolic event, EH, arrested skeletal growth). Chronic metabolic/physiological stress during development can lead to arrested skeletal growth (Newman and Gowland,

2015; Jankauskas and Grupe, 2018). Due to poor preservation and fragmentary skeletal remains, arrested skeletal growth could not be assessed for eight of the individuals with catabolic changes in their early-life profiles (FEN10, FEN15, FEN42, FEN43, FEN50, BOG66, BOG161, BOG240; see Appendix 6.2). Ten individuals with stress events in the isotope profile could be assessed for arrested skeletal growth. Four individuals had no evidence of arrested growth (ICL155, FEN17, BOG59, BOG255) and six had marked arrested skeletal growth compared to their dental development (ICL127, ICL129, ICL131, BOG109, BOG250, BOG265). Although the margin is small, these data support elevated $\delta^{15}\text{N}$ values being due to stress rather than dietary changes alone.

Fluctuations in the $\delta^{15}\text{N}$ values can result from changes in dietary protein ($\delta^{13}\text{C}$ and $\delta^{15}\text{N}$ profiles co-vary) or physiological/metabolic stress ($\delta^{13}\text{C}$ and $\delta^{15}\text{N}$ show opposing co-variance – Beaumont *et al.*, 2018). Four individuals (FEN17, FEN50, BOG109, BOG240; see Appendix 6.2) had Pattern C breastfeeding/weaning profiles, with periods of elevated $\delta^{15}\text{N}$ profiles compared to the AFM (+ 2–4‰) following the perceived completion of weaning; this suggests these individuals were under physiological and/or metabolic distress. To a lesser extent, three additional people with Pattern C breastfeeding/weaning profiles also showed periods of elevated $\delta^{15}\text{N}$ compared to the AFM after weaning had been completed (ICL155, FEN10, BOG59; see Appendix 6.2). Their young ages at-death coupled with stress-related skeletal lesions, supports the likelihood that these profiles reflect physiological and/or metabolic stress.

Despite the correlations between elevated $\delta^{15}\text{N}$ profiles and early death, two individuals (FEN17, BOG66) with consistently elevated $\delta^{15}\text{N}$ values compared to the AFM died as older adults (Figure 6.19). Both FEN17 and BOG66 were found to be local to their burial location. FEN17 was an older adult man found to have skeletal changes indicative of healing/healed stress-related lesions (Figure 6.19). BOG66 was an older adult female with EH during childhood and possible PH. The $\delta^{13}\text{C}$ and $\delta^{15}\text{N}$ profiles show opposing co-variance throughout development, which is expected with catabolism. Although the changes in the isotope profile are subtle, the presence of stress-related skeletal lesions support the changes resulting from catabolism rather

than dietary changes alone. The profiles would be expected to co-vary if these changes were due to an extended weaning period or a different diet when compared to the mother/population's diet. It is possible these individuals experienced metabolic/physiological stress as children and were able to overcome the stress during development. This scenario would suggest that these older adults with early-life stress had lower frailty (hidden heterogeneity) or they had the means to survive due to a higher socio-economic standing (Wood *et al.*, 1992).

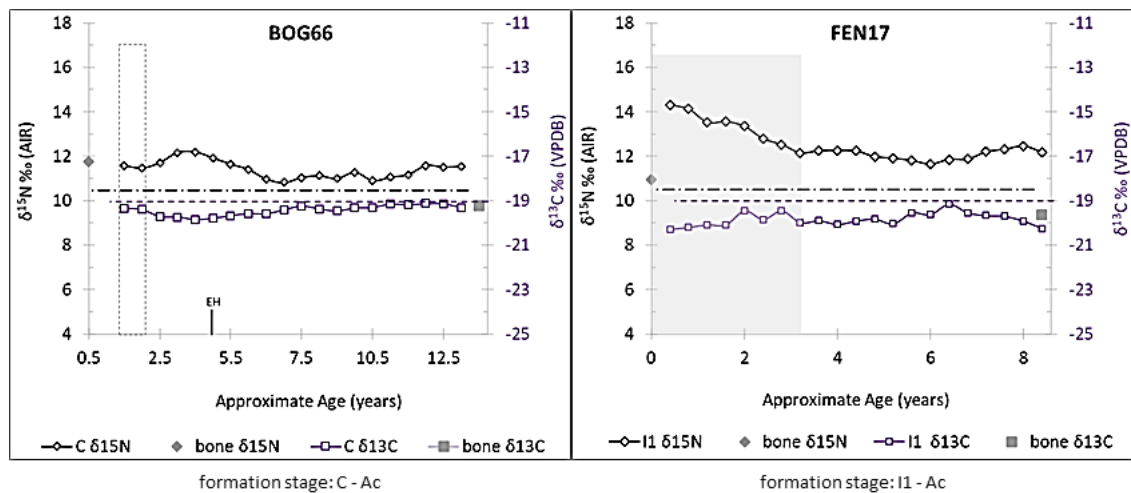


Figure 6.19. Two examples of older adults with evidence of early-life stress profiles. The vertical shaded/dashed boxes indicate the probable breastfeeding/weaning period. AFM (adult female mean): $\delta^{13}\text{C}$ – dashed purple line; $\delta^{15}\text{N}$ – dot-dash black line. EH signifies the approximate age at which the hypoplastic event occurred.

(iv) Stress during critical growth periods

Mammalian programming and development requires specific environmental stimuli in order to achieve normal maturation (Cameron and Demerath, 2002). Detrimental and long-term health effects have been linked to insults which occurred during the critical growth periods (Barker, 1998; Cameron and Demerath, 2002). This section examines early-life stable isotope profiles to examine the effect of insults during the four critical growth periods.

(a) Intrauterine

High-resolution incremental dentine sampling can provide a glimpse into the prenatal environment. Dentine begins forming around 30 weeks *in-utero*, thus capturing the mother's diet and intrauterine nutrition of the foetus (AlQahtani et al., 2010; Beaumont and Montgomery, 2015). The first increment of the deciduous dentition (prenatal increment) was used as a proxy for intrauterine health. As mentioned in Section 3.2.2, the mean isotope values ($\delta^{13}\text{C}$ and $\delta^{15}\text{N}$) of the adult female (AFM) bone collagen within a population were used to quantify breastfeeding and weaning curves (Fuller et al., 2006; Beaumont et al., 2015; Burt, 2015). The AFM assumes all female data are a true representation of the female diet, without changes associated with physiological/metabolic stress (e.g. elevated $\delta^{15}\text{N}$ values). Because the dentine begins to form *in-utero*, values obtained from the prenatal dentine act as a proxy for the health and diet of the mother during gestation (Beaumont, et al., 2013; Craig-Atkins et al., 2018; King, et al., 2018). Like the adult female mean (AFM), the pregnant female mean (PFM) was calculated by finding the mean of the isotope values of dentine increments which formed prior to birth. The prenatal values for each population were analysed to compare the PFM with the AFM to assess intrauterine stress (Table 6.8).

	Pregnant female mean (PFM)		Adult female mean (AFM)	
	$\delta^{13}\text{C}_{\text{VPDB}}$ (‰)	$\delta^{15}\text{N}_{\text{AIR}}$ (‰)	$\delta^{13}\text{C}_{\text{VPDB}}$ (‰)	$\delta^{15}\text{N}_{\text{AIR}}$ (‰)
Migration Period (n=4)	-17.3 ± 1.0	13.2 ± 0.02	(n= 10) -18.0 ± 0.3	10.5 ± 0.3
Middle Ages (n= 5)	-18.4 ± 1.0	13.3 ± 0.6	(n= 5) -19.0 ± 0.9	10.5 ± 0.9

Table 6.8. Summary of the AFM and PFM isotope data used for examining intrauterine stress.

The data from both populations reveal a ~1‰ increase in $\delta^{13}\text{C}$ values from the AFM to PFM and a ~3‰ decrease in $\delta^{15}\text{N}$ values from the PFM to AFM. Four of the individuals with prenatal increments (ICL127, ICL129, ICL131, BOG265) had elevated $\delta^{15}\text{N}$ and $\delta^{13}\text{C}$ prenatal values compared to the AFM (Figure 6.20). This may indicate the mother's diet varied from the overall dietary pattern of the AFM and/or that

other milk sources were used (e.g. wet nurse – Schmidt et al. 2016, Craig-Atkins et al., 2018). Four individuals had profiles which suggest elevated $\delta^{15}\text{N}$ prenatal values compared to the AFM, with $\delta^{13}\text{C}$ prenatal values at or around the AFM (FEN15, FEN42, BOG109, BOG250). Elevated *in utero* $\delta^{15}\text{N}$ values (PFM), with little to no change in $\delta^{13}\text{C}$ PFM values, may reflect physiological stress rather than a change in diet (Craig-Atkins et al., 2018; King et al., 2018). Pregnancy, even without added nutritional stress, takes a significant physiological toll on the body (Fuller et al., 2006), therefore it is possible that the elevated $\delta^{15}\text{N}$ values of the PFM are the result of normal physiological stress during pregnancy. All individuals with prenatal increments died during childhood, which supports this pattern reflecting intrauterine stress leading to higher frailty during development. However, this trend might also be the result of an inherent sampling bias. Prenatal increments from the deciduous dentition are typically only available when individuals died during childhood. With the exception of the first permanent molar, and unless the deciduous dentition was retained after the permanent dentition erupted, the *in-utero* increments of the deciduous teeth are lost by those who survive into adulthood. Therefore it is only possible to examine the non-survivors (Wood et al., 1992; Waldron, 1994, Chapter. 4).

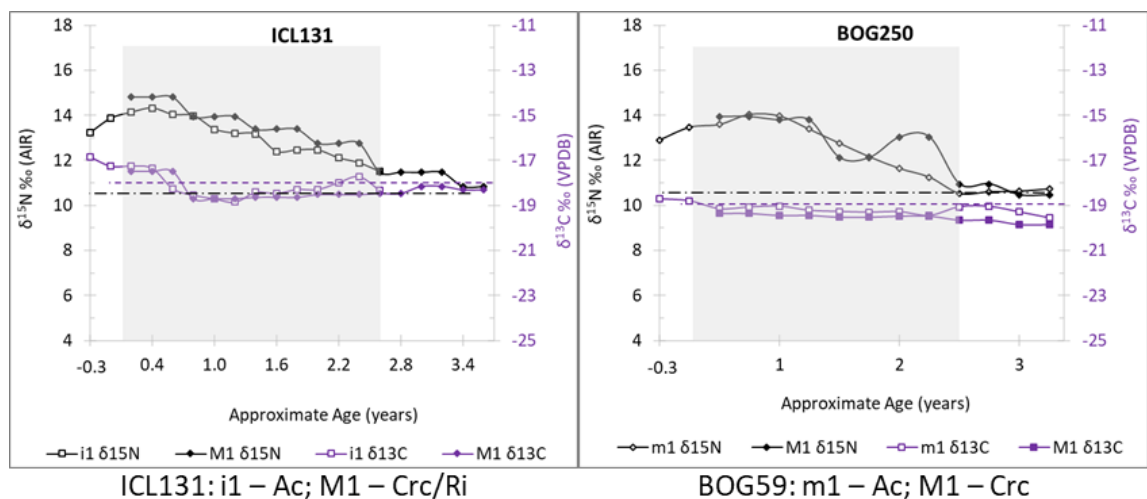


Figure 6.20. Examples of the two types of profiles containing data for prenatal increments. The vertical shaded boxes indicate the probable breastfeeding/weaning period. AFM (adult female mean); $\delta^{13}\text{C}$ – dashed purple line; $\delta^{15}\text{N}$ – dot-dash black line. EH signifies the approximate age at which the hypoplastic event occurred.

(b) Infancy (birth to one year)

The offset in $\delta^{15}\text{N}$ values between a mother and an infant consuming breastmilk can be 2-3‰ (Fogel et al., 1989). Elevated $\delta^{15}\text{N}$ values during infancy (>4‰ above the AFM) could indicate a change in the mother's diet during breastfeeding or be a result of physiological stress during infant development (Figure 6.21). Six individuals from the Migration Period and six medieval individuals had elevated $\delta^{15}\text{N}$ values during infancy. Of the twelve individuals, there were five non-adults, five female adults and two male adults. Although the sample size is small, this pattern supports the historical and archaeological data from Medieval Eastern Europe which suggest children and females had different access to certain foods (e.g. less meat consumption compared) compared to males (Murray and Schoeninger, 1988; Le Huray and Schutkowski, 2005; Noche-Dowdy, 2015). Identifying non-adult biological sex via amelogenin peptide or aDNA analysis would be required to confirm this trend. Non-adults and adults were almost equally affected, which suggests individuals with $\delta^{15}\text{N}$ values >4‰ above the AFM did not have a significant impact on frailty within the current study. Individual FEN50 was the only person in this study with EH in the first year of their life (age-at-death 13.5 to 14.5 years); the co-occurrence of elevated $\delta^{15}\text{N}$ values and EH could have negatively affected their frailty.

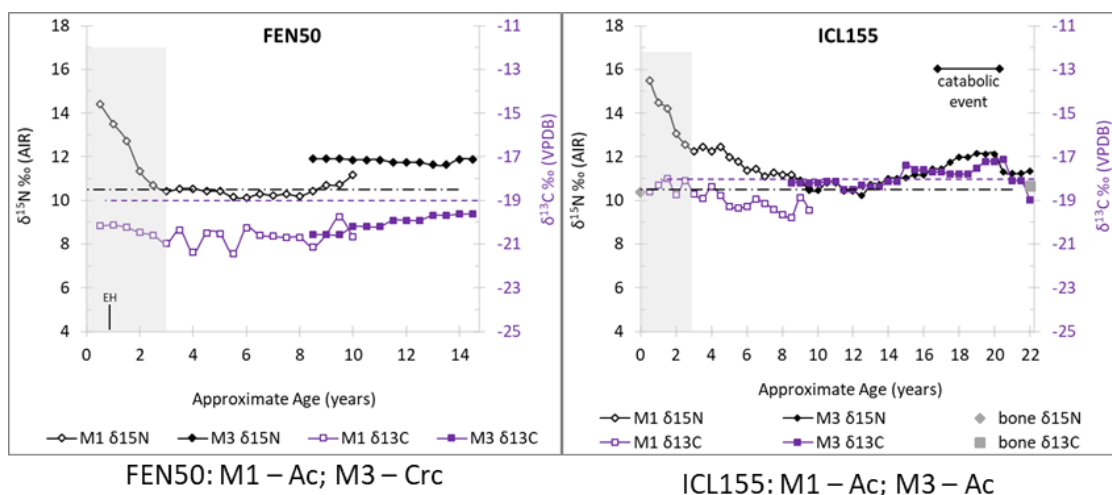


Figure 6.21. Examples of elevated $\delta^{15}\text{N}$ values and “stress” during infancy in two individuals. FEN50 died as an adolescent and ICL155 died as an older adult. The vertical shaded boxes indicate the probable breastfeeding/weaning period. AFM (adult female mean): $\delta^{13}\text{C}$ – dashed purple line; $\delta^{15}\text{N}$ – dot-dash black line. EH signifies the approximate age at which the hypoplastic event occurred.

(c) Mid-childhood

The third critical growth period is between one and six years old. During this period, the growth rate of the body slowly declines, the child (if breastfed) will be weaned onto solid foods, and the body begins to develop buffering systems to deal with stressors (Wells, 2014). Research has found that health insults and the age at which adiposity rebound (lean mass or fat mass) occurs can lead to poor health later in life such as obesity (Cameron and Demerath, 2002; Wells, 2014; Said-Mohamed et al., 2017). Elevated $\delta^{15}\text{N}$ values within the mid-childhood profile signify catabolic stress, and an elevated $\delta^{13}\text{C}$ reflects increased animal protein/ C_4 consumption and/or periods of skeletal growth.

Within this study, 31 individuals appear to have been stressed, exhibiting EH and/or elevated $\delta^{15}\text{N}$ during the mid-childhood critical growth period (Migration Period = 15, Middle Ages = 16). These data indicate similar levels of mid-childhood stress between the two populations (Figure 6.22). Within the Migration Period assemblage, three non-adults, six young adults (three males, three females), two middle adults (two females) and four older adults (two males, two females) had evidence of early-life stress. In the medieval assemblage there were nine non-adults (one infant, three children, five adolescents), three young adults (two males, one female) and four older adults (two males, two females) with evidence of stress during the mid-childhood growth period. Three individuals (3/7, 49%) had skeletal evidence of arrested growth (only seven could be assessed). Non-adults and young adults make up 68% (21/31) of the individuals with mid-childhood stress when the data from both populations were combined. The higher number of non-adult and young adult individuals could reflect increased frailty as a result of mid-childhood stress events. The nearly equal number of males and females affected (M/M? = 9, F/F? = 10) reveal that mid-childhood stress was prevalent in both biological sex categories.

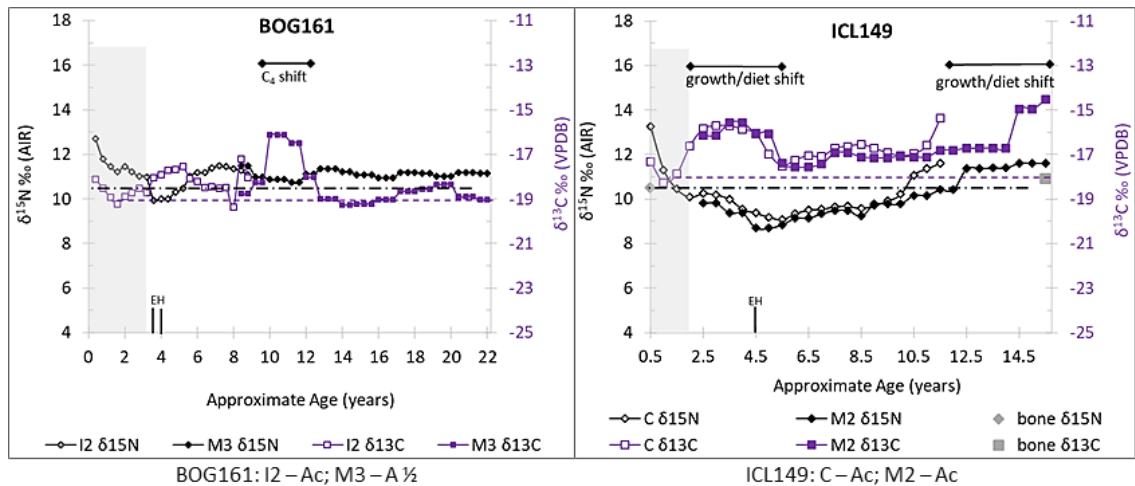


Figure 6.22. Examples of stress signals during mid-childhood in two individuals. BOG161 died as a young adult and ICL149 died as an older adult. The vertical shaded boxes indicate the probable breastfeeding/weaning period. AFM (adult female mean): $\delta^{13}\text{C}$ – dashed purple line; $\delta^{15}\text{N}$ – dot-dash black line. EH signifies the approximate age at which the hypoplastic event occurred.

As previously mentioned, elevated $\delta^{13}\text{C}$ profiles, compared to the AFM, can occur with increased millet and/or animal protein consumption, or when the body is building tissue in an anabolic state. Twelve adult individuals from the Migration period had elevated $\delta^{13}\text{C}$ values during the mid-childhood growth period and eight also had EH, indicating early-life stress. Five medieval individuals had elevated mid-childhood $\delta^{13}\text{C}$ values (one non-adult, four adults), two of whom had EH. As previously mentioned, the use of millet was regularly used throughout the Migration Period, and to a slightly lesser extent during the medieval period, and would likely be a normal part of the every-day diet (Gyulai, 2006, 2014). There is also evidence of increased consumption of high-calorie C_4 resources during period of famine and for those with limited access to high quality foods for those from a lower socio-economic status (Thompson, 1982; Murray and Schoeninger, 1988; Le Huray and Schutkowski, 2005). If it is assumed that the periods of elevated $\delta^{13}\text{C}$ values (e.g. Figure 6.22, ICL149) are associated with increased millet (C_4) consumption, these data support the use of millet during critical growth periods and/or periods of metabolic/nutritional stress. Overall, despite the prevalence of stress lesions (EH), elevated $\delta^{13}\text{C}$ values during periods of growth or recovery, when adequate nutrients are consumed, appear to support decreased frailty during development.

(d) Adolescence

The adolescent critical growth period is estimated to begin around 10-11 years old for females and 11-12 years old for males, and continues until the end of the adolescent growth spurt (Marshall and Tanner, 1969, 1970; Cameron and Demerath, 2002). However, the age of initiation and completion of the adolescent growth spurt is dependent on the release of hormones during puberty, the timing of which is highly susceptible to environmental factors and varies widely throughout history (Marshall, 1978; Shapland and Lewis, 2013). This section examines stress signals (elevated $\delta^{15}\text{N}$ values and/or EH) and increases in $\delta^{13}\text{C}$ values in individuals between the ages of 10 and 18 years of age. Five people from the Migration Period (two males, three females) and nine medieval individuals (three non-adults, three males, three females) had signals of stress during adolescence (Figure 6.23, BOG59). The higher prevalence of stress and the younger range of ages at death of the people from the Middle Ages suggest higher levels of adolescent stress compared to the Migration Period. When the data from both populations are combined, the highest prevalence of adolescent stress occurred in individuals who died as adolescents (6/14, 43%) or in young adulthood (5/14, 36%). These data support the link between stress during adolescence and increased frailty/early death.

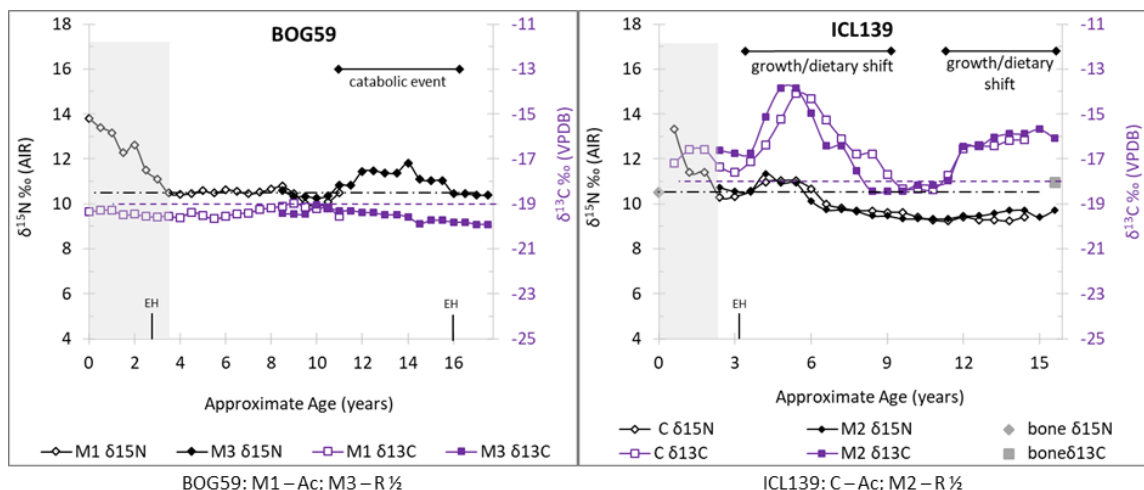


Figure 6.23. Examples of the profiles of two individuals with adolescent stress signals (BOG59 – adolescent, ICL139 – older adult male). The vertical shaded boxes indicate the probable breastfeeding/weaning period. AFM (adult female mean): $\delta^{13}\text{C}$ – dashed purple line; $\delta^{15}\text{N}$ – dot-dash black line. EH signifies the approximate age at which the hypoplastic event occurred.

During the building phases of the body tissues (normal growth or following recovery from arrested growth), $\delta^{15}\text{N}$ values decrease as the BMI increases (Mekota *et al.*, 2006). When stress is attenuated, the growth rate accelerates (catch-up growth) to bring the body back to its normal growth trajectory (Prader *et al.*, 1963). Increased protein consumption during growth/recovery in an anabolic state results in opposing co-varying isotope profiles - $\delta^{15}\text{N}$ decreases and $\delta^{13}\text{C}$ increases (Hatch *et al.*, 2006; Mekota *et al.*, 2006; Beaumont *et al.*, 2018). The early-life isotope profile of ICL139 (Figure 6.23) shows two types of changes in the $\delta^{13}\text{C}$ profile with a stress event (EH) around 3 years of age. Following the approximate timing of the hypoplastic event in the mid-childhood growth period, the profiles co-vary with a substantial $\delta^{13}\text{C}$ peak indicative of C_4 consumption (3–8 years of age). This would support the finding that supplementary foods, such as millet, were accessed to increase caloric intake during periods of metabolic/physiological stress (Thompson, 1982). The isotope profiles have opposing covariance between 12 and 16 years of age. Declines in $\delta^{15}\text{N}$ values during periods of rapid growth, such as during the adolescent growth period, have also been found in isotope studies of bone collagen. Some attribute these patterns to a plant-only diet prior to puberty or a normal physiological effect during growth. This is because this pattern has been found in Neolithic, Medieval, and modern studies from various regions around the world, and in multiple animal species (Waters-Rist and Katzenberg, 2009; Pearson *et al.*, 2015).

Eleven people from the Migration Period (five males, five females, one non-adult) and four people from the medieval assemblage (three males, one female) had increased $\delta^{13}\text{C}$ values during the adolescent growth period. The higher occurrence of elevated $\delta^{13}\text{C}$ profiles in the Migration Period people supports the finding of a significantly higher C_4 consumption compared to people in the Middle Ages. All individuals with elevated $\delta^{13}\text{C}$ during adolescence survived into adulthood with 47% (7/15) dying as middle or older adults. Whether the elevated $\delta^{13}\text{C}$ values were the result of increased C_4 and/or animal protein consumption, or normal growth, these data support decreased frailty during the adolescent growth period.

6.4. Summary

Archaeological data and macroscopic skeletal analysis support both populations being part of attritional burial sites. Palaeopathological analysis established a high prevalence of stress-related skeletal lesions in both populations compared to other studies in the region, supporting the hypothesis that both populations would have substantial evidence (>50% of the population) of physiological and/or metabolic stress.

Both the Migration Period and medieval populations consumed a diet of terrestrial C₃ and C₄ resources, with the Migration Period people consuming significantly more millet compared to the medieval population. Differences in dietary resources were also observed between males and females, with females consuming significantly more millet compared to males. Additionally, five of the seven possible non-local individuals had changes in their isotope profiles, possibly associated with a change in diet associated with migration, supporting the hypothesis that non-local individuals would display dietary shifts in the early-life profiles.

Early-life isotope profiles revealed three distinct patterns of breastfeeding and weaning practices which supported research linking limited and/or no breastmilk to increased frailty and early death. Additionally, all seven individuals believed to be non-local to their burial environment had skeletal and/or isotopic evidence of childhood stress, supporting the hypothesis that both locals and non-locals had similar levels of stress.

The outcomes of this research provided answers for both of the research questions outlined in Chapter 1. The key findings of this research, the limitations and future research prospects are discussed further in Chapter 7.

Chapter 7: Key findings, future research prospects and concluding remarks

The outcomes of this research offer promising insights into the demography, morbidity and mortality of two population from Transylvania. However, due to time and budgetary constraints, the small sample size studied limited the full interpretation of these data to the *analysed* portion of each burial population (Wood *et al.*, 1992). Additional research is required to confirm whether the findings of this study reflect the entire population, or only those analysed. This section first provides a summary of the key findings (Section 7.1) of this research, the limitations of the study and it further explores future research prospects (Section 7.2) and concluding remarks (Section 7.3).

7.1. Summary of key findings

Both the Migration Period and medieval populations had demographic profiles supporting archaeological data indicating both populations were part of attritional cemeteries (Chamberlain, 2000; Maxim *et al.*, 2002; Zsolt, 2015). The data in this study suggest the local biosphere isotope range for the Transylvanian Basin is $^{87}\text{Sr}/^{86}\text{Sr}$ between 0.7085 and 0.7097 and $\delta^{18}\text{O}_{\text{VSMOW}}$ between 21.9 and 26.1‰. Although all the individuals in this study fell within the original proposed local biosphere range for the Transylvanian Basin, strontium and oxygen isotope analysis revealed seven individuals with childhood isotopes suggesting origins from a region with more radiogenic bedrock, possibly in the nearby Carpathian Mountains (ICL136, ICL138, ICL139, BOG10, BOG59, BOG252, FEN14, see Section 6.2.2). The oxygen isotope values ($\delta^{18}\text{O}$) of human enamel supported the link between altitude/elevation and increased $\delta^{18}\text{O}$ values (Clark and Fritz, 1997; Cozma *et al.*, 2017). The Transylvania Basin is at a slightly higher elevation compared to the Carpathian Basin which could provide a way of differentiating between individuals who originated in the Transylvanian Basin compared to the Hungarian lowlands. Further analysis of environmental samples would be required to establish local biosphere isotope ranges specific to each archaeological site.

Stature estimation from long bone length revealed that the mean stature of adult males was significantly greater than the mean for adult females (Section 6.1.1). This pattern was present within each population and remained so when the data from both populations were analysed together; this follows evolutionary trends of human sexual dimorphism (Koepke and Baten, 2005b, 2005a). Thirteen individuals who died as non-adults showed evidence of arrested skeletal growth supporting the DOHAD research linking arrested skeletal growth to increased frailty and/or early death (Steckel, 2005; Buchhorn *et al.*, 2016; Roberts and Steckel, 2019). Eight of the 13 people with arrested skeletal growth were also assessed using incremental dentine analysis. All eight individuals had isotope stress signals further supporting the link between early-life stress and arrested growth. There was no significant difference in attained stature between adult individuals with and without stress-related lesions, suggesting childhood stress did not directly, or adversely affect stature for either population. This does not agree with researched linking arrested skeletal growth with insult during critical growth periods (Steckel, 2005; Watts, 2011; Dewitte and Hughes-Morey, 2012). These data indicate those who survived childhood stress and reached adulthood either never experience arrested skeletal growth, had the means to overcome the stressor (higher socio-economic status) and/or had low frailty.

Early-life conditions linked to physiological/metabolic stress have been found to negatively impact health, resulting in early death (Roberts and Steckel, 2018). Within this study the prevalence of EH was highest in individuals who died as young adults, supporting research which suggest that this trend represents lower rather than higher frailty because they were able to survive childhood stress (Dewitte and Yaussy, 2016). Within the Migration Period, more females had EH compared to males, which supports historical documentation which states that males were preferentially given higher quality foods, resulting in higher nutritional stress for females (Carloni, 1981; Ortner, 1999; Craig *et al.*, 2009). Conversely, males from the medieval population had a higher prevalence of EH compared to females, which could be attributed to the difference in male and female immune responses, supporting males having weaker immune systems compared to females (Grossman, 1985; Ortner, 1998; Janele, 2006; Dewitte, 2010; Roberts and Steckel, 2018). The prevalence of CO was the same

between males and females suggesting equal susceptibility to stressors which resulted in CO. The highest prevalence of CO occurred in non-adults which supports DOHAD research linking CO with increased frailty and early death (Marklein *et al.*, 2016; Roberts and Steckel, 2018). Skeletal evidence of metabolic bone disease (MBD) was higher in the Migration Period population which could indicate greater metabolic strain compared to the medieval population. Twelve of the 17 people believed to have had MBD died as children, suggesting MBD during childhood resulted in increased frailty and early death. Although the sample size was limited, these data suggest that the two populations in this study had higher physiological/metabolic stress compared to other populations in the region and supported the hypothesis that more than 50% of both populations would have evidence of physiological and/or metabolic stress. Additionally, all seven individuals believed to be non-local to their burial location had skeletal and/or isotopic evidence of stress, supporting the hypothesis that both local and non-locals would have stress-related lesions.

Carbon and nitrogen stable isotope analysis revealed that both populations consumed a diet of terrestrial C₃ and C₄ resources, with the Migration Period population consuming significantly more millet (C₄) compared to the medieval population. Females had significantly higher $\delta^{13}\text{C}$ values compared to males, both within each population and when the populations were analysed together, suggesting a higher consumption of millet for females. Males from both populations had significantly higher $\delta^{15}\text{N}$ values than females, indicating increased meat/fish consumption. These data support historical documentation of males given preferential access to higher quality foods (meat/fish) compared to females. (Carloni, 1981; Ortner, 1999; Craig *et al.*, 2009). Elevated $\delta^{13}\text{C}$ values associated with increased millet or animal protein consumption during adolescence was observed in 15 people, all of whom survived into adulthood. These data indicate that increased protein during the adolescent critical growth period decreased frailty. Five of the seven possible non-local individuals showed changes in their early-life history isotope profiles, possibly resulting from a change in diet associated with migration; this supports the hypothesis that non-local individuals would display a shift in overall dietary patterns.

Overall, individuals from the Migration Period were breastfed for ~1-6 months and completed the weaning process between 2–3.5 years of age, which follows medical recommendations during that period (Fulminante, 2015). The majority of individuals from the medieval population were also breastfed for ~1-6 months with weaning typically being completed between 2–4 years of age. This suggests practices from Classical, Byzantine and Muslim scholars were widely adopted in the Middle Ages (Bourbou *et al.*, 2013; Fulminante, 2015). Early-life history isotope profiles of 39 individuals revealed three distinct variations regarding the durations of breastfeeding and weaning.

Pattern A follows the Medieval medical recommendations of exclusive breastmilk for the first six months with weaning completed between 3–4 years of age and was the dominant pattern for the population from the Migration Period (10/14). The older age-at-death combined with limited stress-related skeletal lesions, support research linking breastfeeding with decreased frailty due to passive immunity transfer from mothers to infants, and buffering against insults later in life (Barker, 2012; Black *et al.*, 2013; Said-Mohamed *et al.*, 2017). Twelve of 18 people had evidence of EH around the time weaning was complete, supporting the link between increased metabolic/physiological stress associated with weaning, teething and the childhood critical growth period (Reitsema and McIlvaine, 2014; Sandberg *et al.*, 2014).

Pattern B breastfeeding/weaning practice suggests limited breastmilk consumption and possible animal milk supplementation. The majority of people with a Pattern B breastfeeding/weaning pattern were from the medieval population (10/14). Overall, the age-at-death of individuals with Pattern B were younger than Pattern A, supporting clinical research which reports that a lack of passive immunity and anti-infective properties of breastmilk can lead to increased frailty and early death (Katzenberg *et al.*, 1996; WHO, 2009).

Pattern C breastfeeding/weaning indicated an increased consumption of protein (C₄ and/or animal protein) during weaning and the childhood growth spurt. Individuals with Pattern C early-life profiles were young adults with stress-related skeletal lesions which may indicate that the increased caloric intake during development helped them survive into adulthood. However, the limited consumption of breastmilk could

have led to increased frailty later in life. Four individuals had early-life history profiles with little to no evidence of breastmilk consumption. Three of the four individuals died before the age of five supporting an increased risk of disease and mortality for children who do not consume breastmilk for at least the first six months of life (WHO, 2009; Sankar *et al.*, 2015).

Two offsets were observed in the early-life history isotope profiles from incremental dentine. The first was noted between changes in isotope early-life history profiles, compared to the approximate age of EH. The variation between the approximate age at which EH occurred compared to changes seen in the isotope profile were between one and five years. The apparent offset could be the result of a delay between stress being recorded in dentine, compared to the enamel or could be due to the natural variation in the formation rates of dental tissues. A second offset was observed between teeth at different stages of formation. Within this study, isotope profiles of incomplete teeth (still forming at the time of death) showed more variation in the individual incremental isotope values compared to the range of values from a complete tooth, which formed during the same period of life. The perceived offset is believed to reflect the varying number of depositional layers of dentine within each incrementally sectioned sample of dentine, with values from incomplete teeth reflecting fewer depositional layers and a shorter amount of time compared to complete teeth. However, due to the small sample size, additional isotope research of paired teeth (incomplete and complete) would be required to confirm this offset.

The prevalence of stress-related skeletal lesions was assessed alongside the stress signals (elevated $\delta^{15}\text{N}$ values) in the isotope profiles to examine the impact early-life stress had on frailty. The co-occurrence of EH and elevated $\delta^{15}\text{N}$ values was found in individuals who died before reaching middle adulthood. Insults during critical growth periods have been found to increase frailty and can result in early death (Cameron and Demerath, 2002; Barker, 2012). Twelve people, five non-adults, five adult females, and two adult males, had stress signals in their isotope profiles during infancy. These data indicate metabolic stress during the infant critical growth period led to increased frailty for women and children. Thirty-one people (of 39) exhibited EH and/or elevated $\delta^{15}\text{N}$ values during the mid-childhood critical growth period.

Similar levels of stress during mid-childhood were seen between the two populations, and between males and females. The higher number of non-adults and young adults could reflect increased frailty as a result of stress during mid-childhood. The medieval assemblage had a higher prevalence of stress (EH and/or elevated $\delta^{15}\text{N}$ values) during adolescence, as well as a younger age range, suggesting higher levels of adolescent stress compared to the Migration Period.

7.2. Considerations for future research

As discussed in Section 4.2, macroscopic and isotopic analyses were conducted on the available skeletal remains from two archaeological populations. The Migration Period phase of the burial site at the Iclod Necropolis has yet to be completely excavated. A complete analysis of all the skeletal remains associated with the Migration Period population is required in order to provide a complete demographic and palaeopathological profile of the population. Likewise, macroscopic skeletal analysis of the remaining individuals from the Fenyéd and Bögöz cemeteries would be required to confirm the macroscopic findings for the medieval population.

Due to the time consuming and costly nature of isotope analysis, in particular high-resolution incremental dentin analysis, the sample size within this study was limited. Sampling strategies were designed to analyse individuals from all age-at-death categories, and from both males and females, with and without stress-related skeletal lesions, to capture the possible variations in isotope data for each population. Additional carbon and nitrogen stable isotope analysis of archaeological floral and faunal samples from archaeological sites within Transylvania would help establish baseline dietary values specific to the climate and environment of this region. Having a better understanding of the baseline isotope values of dietary resources for the people studied would help to identify subtle differences in the dietary practices within each population, as well as dietary changes over time. Analysing the remaining individuals from each site for carbon and nitrogen isotope ratios may confirm breastfeeding and weaning practices, dietary patterns and periods of early-life stress already established in the current study. Romania, and most of Eastern Europe has yet to be mapped for strontium and oxygen isotope

ratios. The results of this research begin to fill the gap in the biosphere data within the Transylvanian Basin, but additional analysis of environmental samples such as from plants, animals, soil, water and rock samples is required to establish biosphere ranges for the region, as well as contextualize data on human mobility research in Eastern Europe.

Two offsets were observed in the isotope life-history profiles. The first was between the approximate age at which EH occurred compared to changes in the isotope profile. The second was an offset between the isotope values from the same period of life obtained from incomplete and complete teeth. Additional research is required to examine whether these patterns are the result of normal variation between the secretion and mineralisation of the enamel and dentine matrices. Microscopic and histological analysis of enamel and dentine offer more precise estimations of the period of life associated with the disruption in tooth formation due to poor health (Mahoney, 2012; Mahoney *et al.*, 2017; Lorentz *et al.*, 2019). The precise timing of onset and duration of stress could help to clarify the possible offset between EH and changes in the isotope profile.

Lastly, the ability to assess the biological sex of people whose biological sex could not be ascertained and the non-adults from each population would help to determine if the differences between diet, morbidity and mortality profiles for the adult males and females also applied to children. Biomolecular analysis of sexual dimorphic amelogenin peptides from tooth enamel has been successfully applied to archaeological populations to assess non-adult biological sex (Stewart *et al.*, 2016, 2017). The application of peptide analysis to the non-adults within this study would enable further examination of possible sex-based differences of these populations.

7.3. Concluding remarks

The aim of this study was to integrate isotopic data and palaeopathological analyses to better understand how early-life stress impacted morbidity and mortality of individuals from two Transylvania populations who lived during periods of political transition. This was successfully achieved. Macroscopic skeletal analysis of the two

populations generate new data which helps to fill the gap in research of skeletal remains from Transylvania. Despite the small sample size and poor preservation of the skeletal remains, both of the research questions outlined in Chapter 1 were answered. Both the Migration Period and medieval skeletal assemblages had substantial evidence of stress (>50%) supporting the hypothesis that individuals living during periods of political transition would be negatively impacted by the unrest. Evidence of stress was found across all age categories, in both males and females, and was seen in locals and non-locals.

Macroscopic, palaeopathological and mobility isotope data were combined with Incremental dentine early-life profiles to provide a unique glimpse into the interrelated risk factors of those who lived in Transylvania during the Migration Period and Middle Ages. Novel isotopic data generated by this research help to establish mobility status, cultural practices, subsistence patterns and periods of early-life stress for these Transylvanian individuals. The new strontium and oxygen isotope data begins to establish isotope biosphere values for the Transylvania Basin. Carbon and nitrogen isotope data established both populations subsisted on a mixed diet of terrestrial C₃ and C₄ resources, with the Migration Period population consuming significantly more millet than the medieval population. Significant differences in millet consumption were also seen between males and females, suggesting a possible gender/sex bias in the consumption of millet. Incremental dentine early-life isotope profiles found most of the individuals from both populations were breastfed for approximately the first six months of life and completed the weaning process inline with contemporary medical recommendations of that time. Increased frailty and early death were found in those individuals whose profile suggest limited to no consumption of breastmilk, as well as those who had evidence of catabolic stress events during the critical growth periods of childhood. These data support the hypothesis that early-life stress negatively impacted health and led to increased frailty and/or early death.

Carbon and nitrogen incremental dentine early-life isotope profiles in this study were used in conjunction with skeletal evidence of stress. Correlation between skeletal stress indicators and changes in isotope profiles were able to be seen, providing

information about the possible time of onset and duration for stress events. Analysis of the early-life isotope profiles also found offsets between the timing of EH and changes in the isotope profiles, and between isotope values of forming teeth when compared to values obtained from completed teeth from the same individual. These data impact interpretations of incremental isotope profiles in this study, as well as the wider research community.

The outcomes of this research provide novel insight into the morbidity and mortality of two population who lived in the Transylvanian Basin during periods of changing political powers and unrest. This research not only expands the understanding of how these populations lived and died in Transylvania but also helps to fill the gaps in research for medieval Transylvania.

References

- Acsádi, G., Nemeskéri, J. and Balás, K. (1970) *History of human life span and mortality*. Akademiai kiado Budapest.
- Admiraal, B. (2015) 'Religion and National Identity in Borderlands : Greek Catholics and Hungarian Reformed in Transylvania', *Occasional Papers on Religion in Eastern Europe*, 35(3), pp. 17–42.
- Agarwal, S. C. (2012) 'The Past of Sex, Gender, and Health: Bioarchaeology of the Aging Skeleton', 114(2), pp. 322–335. doi: 10.1111/j.1548-1433.2012.01428.x.
- Aguraiuja, Ü. (2017) *Isotopic evidence of Bronze Age diet and subsistence practices in the southeastern Carpathian Bend area , Romania*. University of Edinburgh.
- Aguraiuja, Ü. *et al.* (2018) 'Bronze Age subsistence strategies in the southeastern Carpathian Bend area, Romania: Results from stable isotope analyses', *Journal of Archaeological Science: Reports*. Elsevier, 17(October 2017), pp. 510–519. doi: 10.1016/j.jasrep.2017.12.013.
- Albright, F. and Reifenstein, E. C. (1948) 'The Parathyroid Glands and Metabolic Bone Disease.', *The Parathyroid Glands and Metabolic Bone Disease*. Baltimore: Waverley Press, Inc.
- Alexander, M. M. *et al.* (2015) 'Diet, society, and economy in late medieval Spain: Stable isotope evidence from muslims and christians from Gandía, Valencia', *American Journal of Physical Anthropology*, 156(2), pp. 263–273. doi: 10.1002/ajpa.22647.
- Allen, K. G. (2017) *Migration, Conversion and the Creation of an Identity in Southeast Europe: A Biological Distance and Strontium Isotope Analysis of Ottoman Communities in Romania, Hungary and Croatia*. University of Buffalo, State University of New York.
- AlQahtani, S. J., Hector, M. P. and Liversidge, H. M. (2010) 'Brief communication: The London atlas of human tooth development and eruption', *American Journal of Physical Anthropology*, 142(3), pp. 481–490. doi: 10.1002/ajpa.21258.
- Alrichs, J. (2015) *Universitätsforschungen zur prähistorischen Archäologie, Universtätsforschungen zur prähistorischen Archäologie*.
- Alt, K. W. *et al.* (2014) 'Lombards on the Move - An integrative study of the migration period cemetery at szó lá d,Hungary', *PLoS ONE*, 9(11). doi: 10.1371/journal.pone.0110793.
- Ambrose, S. H. (1990) 'Preparation and characterization of bone and tooth collagen for isotopic analysis', *Journal of Archaeological Science*, 17(4), pp. 431–451. doi: 10.1016/0305-4403(90)90007-R.
- Ambrose, S. H. (1991) 'Effects of diet, climate and physiology on nitrogen isotope abundances in terrestrial foodwebs', *Journal of Archaeological Science*, 18(3), pp. 293–317. doi: 10.1016/0305-4403(91)90067-Y.

- Ambrose, S. H. (1993) 'Isotopic Analysis of Paleodiets: Methodological and Interpretive Considerations', in Sandford, M. K. (ed.) *Investigations of Ancient Human Tissue: Chemical analyses in Anthropology*. Amsterdam: Gordon and Breach Science Publishers, pp. 59–130.
- Ambrose, S. H., Buikstra, J. and Krueger, H. W. (2003) 'Status and gender differences in diet at Mound 72, Cahokia, revealed by isotopic analysis of bone', *Journal of Anthropological Archaeology*, 22(3), pp. 217–226. doi: 10.1016/S0278-4165(03)00036-9.
- Amoroso, A., Garcia, S. J. and Cardoso, H. F. V. (2014) 'Age at death and linear enamel hypoplasias: Testing the effects of childhood stress and adult socioeconomic circumstances in premature mortality', *American Journal of Human Biology*, 26(4), pp. 461–468. doi: 10.1002/ajhb.22547.
- Amuna, P. and Zotor, F. B. (2008) 'Epidemiological and nutrition transition in developing countries: impact on human health and development', *Proceedings of the Nutrition Society*, 67(1), pp. 82–90. doi: 10.1017/s0029665108006058.
- Appleby, J. (2017) 'Ageing and the Body in Archaeology', pp. 1–49.
- Armas, Y. C. De (2018) 'Assessing the association between subsistence strategies and the timing of weaning among indigenous archaeological populations of the Caribbean', (June), pp. 492–509. doi: 10.1002/oa.2695.
- Armelagos, G. J. *et al.* (2009) 'Enamel hypoplasia and early mortality: Bioarcheological support for the Barker hypothesis', *Evolutionary Anthropology*, 18(6), pp. 261–271. doi: 10.1002/evan.20239.
- Armelagos, G. J. *et al.* (2014) 'Analysis of nutritional disease in prehistory: The search for scurvy in antiquity and today', *International Journal of Paleopathology*. Elsevier Inc., 5, pp. 9–17. doi: 10.1016/j.ijpp.2013.09.007.
- Armelagos, G. J. and Cohen, M. N. (1984) *Paleopathology at the Origins of Agriculture*. Academic Press Orlando (FL).
- Armit, I. *et al.* (2015) 'Difference in Death? A Lost Neolithic Inhumation Cemetery with Britain's Earliest Case of Rickets, at Balevullin, Western Scotland', *Proceedings of the Prehistoric Society*, 2(May), pp. 1–16. doi: 10.1017/ppr.2015.7.
- Aufderheide, A. C., Rodríguez-Martín, C. and Langsjoen, O. (1998) *The Cambridge encyclopedia of human paleopathology*. Cambridge: Cambridge University Press.
- Ayliffe, L. K., Chivas, A. R. and Leakey, M. G. (1994) 'The retention of primary oxygen isotope compositions of fossil elephant skeletal phosphate', *Geochimica et Cosmochimica Acta*. Elsevier, 58(23), pp. 5291–5298.
- Azcorra, H., Dickinson, F. and Datta Banik, S. (2016) 'Maternal height and its relationship to offspring birth weight and adiposity in 6- to 10-year-old Maya children from poor neighborhoods in Merida, Yucatan', *American Journal of Physical Anthropology*, 161(4), pp. 571–579. doi: 10.1002/ajpa.23057.

- BABAO Working Group for Ethics and Practice (2010a) *Code of Ethics*. doi: 10.1210/jcem.2015.100.issue-12.toc.
- BABAO Working Group for Ethics and Practice (2010b) *Code of Practice*. doi: 10.1210/jcem.2015.100.issue-12.toc.
- Baker, B. J. and Agarwal, S. C. (2017) 'Stronger Together: Advancing a Global Bioarchaeology', *Bioarchaeology International*, 1(1–2), pp. 1–18. doi: 10.5744/bi.2017.1005.
- Balasse, M. *et al.* (2001) 'Detection of Dietary Changes by Intra-tooth Carbon and Nitrogen Isotopic Analysis: An Experimental Study of Dentine Collagen of Cattle (*Bos taurus*)', *Journal of Archaeological Science*, 28(3), pp. 235–245. doi: 10.1006/jasc.1999.0535.
- Balasse, M. *et al.* (2013) 'Early herding at Măgura-Boldul lui Moș Ivănuș (early sixth millennium BC, Romania): environments and seasonality from stable isotope analysis', *European Journal of Archaeology*, 16(2), pp. 221–246. doi: 10.1179/1461957112y.0000000028.
- Balasse, M., Bocherens, H. and Mariotti, A. (1999a) 'Composition Used as Evidence of a Change of Diet', *Journal of Archaeological Science*, 26, pp. 593–598. doi: 10.1006/jasc.1998.0376.
- Balasse, M., Bocherens, H. and Mariotti, A. (1999b) 'Intra-bone variability of collagen and apatite isotopic composition used as evidence of a change of diet', *Journal of Archaeological Science*, 26(6), pp. 593–598. doi: 10.1006/jasc.1998.0376.
- Ball, J. (2002) 'A critique of age estimation using attrition as the sole indicator.', *The Journal of forensic odonto-stomatology*, 20(2), pp. 38–42.
- Barker, D. J. P. *et al.* (1989) 'Growth in utero, blood pressure in childhood and adult life, and mortality from cardiovascular disease.', *BMJ (Clinical research ed.)*, 298(6673), pp. 564–7. doi: 10.1136/bmj.298.6673.564.
- Barker, D. J. P. (1998) 'In utero programming of chronic disease', *Clinical Science*, 95(2), pp. 115–128. doi: 10.1042/cs0950115.
- Barker, D. J. P. (2012) 'Developmental origins of chronic disease', *Public Health*. Elsevier Ltd, 126(3), pp. 185–189. doi: 10.1016/j.puhe.2011.11.014.
- Bassett, J. R., Marshall, P. M. and Spillane, R. (1987) 'The physiological measurement of acute stress (public speaking) in bank employees.', *International journal of psychophysiology: official journal of the International Organization of Psychophysiology*. Netherlands, 5(4), pp. 265–273.
- Beaumont, J., Gledhill, A., Lee-Thorp, J., *et al.* (2013) 'Childhood diet: A closer examination of the evidence from dental tissues using stable isotope analysis of incremental human dentine*', *Archaeometry*, 55(2), pp. 277–295. doi: 10.1111/j.1475-4754.2012.00682.x.

- Beaumont, J., Geber, J., Powers, N., *et al.* (2013) 'Victims and survivors: Stable isotopes used to identify migrants from the Great Irish Famine to 19th century London', *American Journal of Physical Anthropology*, 150(1), pp. 87–98. doi: 10.1002/ajpa.22179.
- Beaumont, J. *et al.* (2015) 'Infant mortality and isotopic complexity: New approaches to stress, maternal health, and weaning', *American Journal of Physical Anthropology*, 157(3), pp. 441–457. doi: 10.1002/ajpa.22736.
- Beaumont, J. *et al.* (2018) 'Comparing apples and oranges: Why infant bone collagen may not reflect dietary intake in the same way as dentine collagen', *American Journal of Physical Anthropology*, (June), pp. 524–540. doi: 10.1002/ajpa.23682.
- Beaumont, J., Gledhill, A. and Montgomery, J. (2013) 'Isotope analysis of incremental human dentine: towards higher temporal resolution.', *Archaeometry*, 55(2), pp. 277–295.
- Beaumont, J. and Montgomery, J. (2015) 'Oral histories: a simple method of assigning chronological age to isotopic values from human dentine collagen', *Annals of Human Biology*, 4460(August), pp. 1–8. doi: 10.3109/03014460.2015.1045027.
- Beaumont, J. and Montgomery, J. (2016) 'The great irish famine: Identifying starvation in the tissues of victims using stable isotope analysis of bone and incremental dentine collagen', *PLoS ONE*, 11(8), pp. 1–21. doi: 10.1371/journal.pone.0160065.
- Beck, L. A. (2006) 'Kidder, Hooton, Pecos, and the Birth of Bioarchaeology', in Buikstra, J. E. and Beck, L. A. (eds) *Bioarchaeology: the contextual analysis of human remains*. London: Academic Press, pp. 83–94.
- Beisel, W. R. (1975) 'Metabolic Response to Infection', *Annual Review of Medicine*, 26(1), pp. 9–20. doi: 10.1146/annurev.me.26.020175.000301.
- Beisel, W. R. (1977) 'Magnitude of the host nutritional responses to infection', *The American Journal of Clinical Nutrition*, 30(8), pp. 1236–1247. doi: 10.1093/ajcn/30.8.1236.
- Bell, L. S. and Jones, S. J. (1991) 'Macroscopic and microscopic evaluation of archaeological pathological bone: Backscattered electron imaging of putative pagetic bone', *International Journal of Osteoarchaeology*, 1(3–4), pp. 179–184. doi: 10.1002/oa.1390010307.
- Benson, M. A. *et al.* (2011) 'Measurement of post-war coping and stress responses: A study of Bosnian adolescents', *Journal of Applied Developmental Psychology*, 32(6), pp. 323–335. doi: 10.1016/j.appdev.2011.07.001.
- Bentley, R. A. (2006) 'Strontium isotopes from the earth to the archaeological skeleton: A review', *Journal of Archaeological Method and Theory*, 13(3), pp. 135–187. doi: 10.1007/s10816-006-9009-x.
- Bentley, R. A. *et al.* (2012) 'Community differentiation and kinship among Europe's first farmers', *Pnas*, 109(24), pp. 9326–9330. doi: 10.1073/pnas.1113710109/-/DCSupplemental.www.pnas.org/cgi/doi/10.1073/pnas.1113710109.

- Bentley, R. A. and Knipper, C. (2005) 'Geographical patterns in biologically available strontium, carbon and oxygen isotope signatures in prehistoric SW Germany', *Archaeometry*. Wiley Online Library, 47(3), pp. 629–644.
- Bereczki, Z. *et al.* (2018) 'Growth Disruption in Children: Linear Enamel Hypoplasia', *The Backbone of Europe: Health, Diet, Work and Violence over Two Millennia*. Edited by R. Steckel *et al.* Cambridge: Cambridge University Press, (1960), pp. 175–197. doi: 10.1017/9781108379830.008.
- Berry, J. L., Davies, M. and Mee, A. P. (2002) 'Vitamin D metabolism, rickets, and osteomalacia', in *Seminars in musculoskeletal radiology*. Copyright© 2002 by Thieme Medical Publishers, Inc., 333 Seventh Avenue, New ..., pp. 173–182.
- Beynon, A. D. and Wood, B. A. (1987) 'Patterns and rates of enamel growth in the molar teeth of early hominids', *Nature*, 326(6112), pp. 493–496. doi: 10.1038/326493a0.
- Black, D. M. and Rosen, C. J. (2016) 'Postmenopausal osteoporosis', *New England Journal of Medicine*. Mass Medical Soc, 374(3), pp. 254–262.
- Black, R. E. *et al.* (2013) 'Maternal and child undernutrition and overweight in low-income and middle-income countries', *The Lancet*, 382(9890), pp. 427–451. doi: 10.1016/S0140-6736(13)60937-X.
- Blatt, S. H. *et al.* (2011) 'Dirty teeth and ancient trade: Evidence of cotton fibres in human dental calculus from Late Woodland, Ohio', *International Journal of Osteoarchaeology*, 21(6), pp. 669–678. doi: 10.1002/oa.1173.
- Blum, J. D., Erel, Y. and Brown, K. (1993) '⁸⁷Sr/⁸⁶Sr ratios of Sierra Nevada stream waters: Implications for relative mineral weathering rates', *Geochimica et Cosmochimica Acta*. Elsevier, 57(21–22), pp. 5019–5025.
- Bocquet-Appel, J.-P. and Masset, C. (1982) 'Farewell to paleodemography', *Journal of Human Evolution*. Elsevier, 11(4), pp. 321–333.
- Bogucki, P. and Crabtree, P. J. (2004) *Ancient Europe: Encyclopedia of the barbarian world (8000CB-AD1000) Vol 2*. Edited by P. Bogucki and P. J. Crabtree. New York: Charles Scribner's Sons.
- Bogucki, P. I. and Crabtree, P. J. (2003) *Ancient Europe 8000BC to AD 1000: encyclopedia of the barbarian world*. Edited by P. I. Bogucki and P. J. Crabtree. New York: Charles Scribner's Sons Publishing.
- Boner, C. (1865) *Trasylvania; Its products and its people*. Available at: <https://books.google.co.uk/books?id=47Ja6HeVU38C>.
- de Boo, H. and Harding, J. (2006) 'The developmental origins of adult disease (Barker) hypothesis', *The Australian and New Zealand Journal of Obstetrics and Gynaecology*, 46(1), pp. 4–14. doi: 10.1111/j.1479-828X.2006.00506.x.
- Booth, T. J., Redfern, R. C. and Gowland, R. L. (2016) 'Immaculate conceptions: Micro-CT analysis of diagenesis in Romano-British infant skeletons', *Journal of Archaeological Science*. Elsevier, 74, pp. 124–134.

- Bourbou, C. *et al.* (2013) 'Nursing mothers and feeding bottles: Reconstructing breastfeeding and weaning patterns in Greek Byzantine populations (6th-15th centuries AD) using carbon and nitrogen stable isotope ratios', *Journal of Archaeological Science*. Elsevier Ltd, 40(11), pp. 3903–3913. doi: 10.1016/j.jas.2013.04.020.
- Bowen, G J; West, J.B.; Miller, C.C; Zhao, L; Zhang, T. (2018) *IsoMAP: Isoscapes Modeling, Analysis and Prediction (version 1.0)*, *The IsoMAP Project*. Available at: <http://isomap.org>.
- Bowen, G. J. (2018) *The Online Isotopes in Percipitation Calculator*. Available at: <http://www.waterisotopes.org> (Accessed: 1 March 2018).
- Bowen, G. J., Wassenaar, L. I. and Hobson, K. A. (2005) 'Global application of stable hydrogen and oxygen isotopes to wildlife forensics', *Oecologia*, 143(3), pp. 337–348. doi: 10.1007/s00442-004-1813-y.
- Bradley, K. R. (1986) 'Wet-nursing at Rome: a study in social relations', *The family in ancient Rome: new perspectives*. Cornell University Press, Ithaca, pp. 201–229.
- Brandes, W. (1999) 'Byzantine Cities in the 7th and 8th Centuries: different sources, different histories?', in Brogiolo, G. Pietro and Ward-Perkins, B. (eds) *The idea and ideal of the town between Late Antiquity and the Early Middle Ages*. Leiden: Koninklijke Brill NV, pp. 25–57.
- Bréhard, S. *et al.* (2014) 'Food Supply Strategies in the Romanian Eneolithic: Sheep/Goat Husbandry and Fishing Activities from Hârşova Tell and Borduşani-Popină (5th Millennium BC)', *European Journal of Archaeology*, 17(3), pp. 407–433. doi: 10.1179/1461957113Y.0000000051.
- Brettell, R., Montgomery, J. and Evans, J. (2012) 'Brewing and stewing: the effect of culturally mediated behaviour on the oxygen isotope composition of ingested fluids and the implications for human provenance studies', *Journal of Analytical Atomic Spectrometry*, 27(5), pp. 778–785. doi: 10.1039/c2ja10335d.
- Brickley, M. (2004a) 'Determination of sex from archaeological skeletal material and assessment of parturition', in Brickley, M. and McKinley, J. I. (eds) *Guidelines to the standards for recording human remains*. Southampton: British Association for Biological Anthropology and Osteoarchaeology, pp. 23–26.
- Brickley, M. (2004b) 'Guidance on recording age at death in juvenile skeletons', in Brickley, M. and McKinley, J. I. (eds) *Guidelines to the standards for recording human remains*. Southampton: British Association for Biological Anthropology and Osteoarchaeology, pp. 21–23.
- Brickley, M. B. (2018) 'Cribra orbitalia and porotic hyperostosis: A biological approach to diagnosis', *American Journal of Physical Anthropology*, 167(4), pp. 896–902. doi: 10.1002/ajpa.23701.
- Brickley, M. B. and Mays, S. A. (2019) 'Metabolic Disease', in Buikstra, J. E. (ed.) *Ortner's Identification of Pathological Conditions in Human Skeletal Remains*. London, UK: Academic Press, pp. 531–584.

- Brickley, M. and Buckberry, J. (2017) 'Undertaking sex assessment', in Mitchell, P. D. and Brickley, M. (eds) *Updated Guidelines to the Standards for Recording Human Remains*, pp. 33–35.
- Brickley, M., Dragomir, A. M. and Lockau, L. (2016) 'Age-at-Death Estimates from a Disarticulated, Fragmented and Commingled Archaeological Battlefield Assemblage', *International Journal of Osteoarchaeology*, 26(3), pp. 408–419. doi: 10.1002/oa.2430.
- Brickley, M. and Ives, R. (2008) *The Bioarchaeology of Metabolic Bone Disease*. Edited by M. Brickley and R. Ives. Oxford: Academic Press is an imprint of Elsevier Lt.
- Brickley, M. and McKinley, J. I. (eds) (2004) *Guidelines to the Standards for Recording Human Remains*. Reading: Institute of Field Archaeologists and British Association of Biological Anthropology and Osteoarchaeology, University of Reading.
- Brie, M. and Mészáros, E. L. (2014) 'Regionalization and historical – cultural dimension of Northwest Romania', *Transylvanian Review*, XIX(1).
- Bromage, T. G. and Dean, M. C. (1985) 'Re-evaluation of the age at death of immature fossil hominids', *Nature*, 317(6037), pp. 525–527. doi: 10.1038/317525a0.
- Brooks, S. and Suchey, J. M. (1990) 'Skeletal age determination based on the os pubis: A comparison of the Acsádi-Nemeskéri and Suchey-Brooks methods', *Human Evolution*, 5(3), pp. 227–238. doi: 10.1007/BF02437238.
- Brothwell, D. (1967) 'The bio-cultural background to disease', *Diseases in antiquity*. Springfield: Charles C. Thomas, pp. 45–68.
- Brothwell, D. (1972) 'Palaeodemography and earlier British populations', *World Archaeology*, 4(1), pp. 75–87. Available at: <https://about.jstor.org/terms> (Accessed: 14 December 2018).
- Brothwell, D. (1981) *Digging up bones: the excavation, treatment, and study of human skeletal remains*. Edited by C. U. Press.
- Brothwell, D. and Zakrzewski, S. R. (2004) 'Metric and non-metric studies of archaeological human bone', in Brickley, M. and McKinley, J. I. (eds) *Guidelines to the standards for recording human remains*. Southampton: British Association for Biological Anthropology and Osteoarchaeology, pp. 27–34.
- Brown, D. E. (1981) 'General Stress in Anthropological Fieldwork', *American Anthropologist*, 83(1), pp. 74–92. doi: 10.1525/aa.1981.83.1.02a00050.
- Buckberry, J. L. and Chamberlain, A. T. (2002) 'Age estimation from the auricular surface of the ilium: A revised method', *American Journal of Physical Anthropology*, 119(3), pp. 231–239. doi: 10.1002/ajpa.10130.
- Bucur, I.-M. and Costea, I. (2009) 'Transylvania between Two National Historiographies. Historical Consciousness and Political Identity', *Frontiers, Regions and Identities in Europe*, 940, pp. 271–285.

- Buikstra, J. E. and Beck, L. A. (eds) (2006) *Bioarchaeology: the contextual analysis of human remains*. London: Academic Press.
- Buikstra, J. E. and Ubelaker, D. H. (eds) (1994) *Standards for Data Collection from Human Skeletal Remains*. Fayetteville, Ark: Arkansas Archeological Survey.
- Buikstra, J. and Roberts, C. (2012) *The global history of paleopathology: Pioneers and prospects*. Oxford University Press on Demand.
- Büntgen, U. *et al.* (2016) 'Cooling and societal change during the Late Antique Little Ice Age from 536 to around 660 AD', *Nature Geoscience*, 9(3), pp. 231–236. doi: 10.1038/ngeo2652.
- Burt, N. M. (2015) 'Individual dietary patterns during childhood: An archaeological application of a stable isotope microsampling method for tooth dentin', *Journal of Archaeological Science*. Elsevier Ltd, 53, pp. 277–290. doi: 10.1016/j.jas.2014.10.019.
- Cameron, N. (2003) 'Physical growth in a transitional economy: The aftermath of South African apartheid', *Economics and Human Biology*, 1(1), pp. 29–42. doi: 10.1016/S1570-677X(02)00008-4.
- Cameron, N. and Demerath, E. W. (2002) 'Critical periods in human growth and their relationship to diseases of aging', *Yearbook of Physical Anthropology*, 45, pp. 159–184. doi: 10.1002/ajpa.10183.
- Carloni, A. S. (1981) 'Sex disparities in the distribution of food within rural households.', *Food and Nutrition*, 7(1), pp. 3–12.
- Carter, J. and Barwick, V. (2011) *Good practice guide for isotope ratio Mass Spectrometry*, Firms. Available at: http://www.forensic-isotopes.org/assets/IRMS Guide Finalv3.1_Web.pdf.
- Cerling, T. E., Hart, J. A. and Hart, T. B. (2004) 'Stable isotope ecology in the Ituri Forest', *Oecologia*. Springer, 138(1), pp. 5–12.
- Cerling, T. E., Wang, Y. and Quadet, J. (1993) 'Expansion of C4 ecosystems as an indicator of global ecological change in the late Miocene', *Nature*, 361(January), pp. 9–10.
- Chadwick, J. (1932) 'The existence of a neutron', *Proceedings of the Royal Society of London. Series A, Containing Papers of a Mathematical and Physical Character*. The Royal Society London, 136(830), pp. 692–708.
- Chamberlain, A. (2000) 'Problems and prospects in palaeodemography', in Cox, M. and Mays, S. (eds) *Human osteology in archaeology and forensic science*. Cambridge: Cambridge University Press, pp. 101–115.
- Chamberlain, A. T. (2006) *Demography in archaeology*. Cambridge University Press.
- Chenery, C. *et al.* (2010) 'Strontium and stable isotope evidence for diet and mobility in Roman Gloucester, UK', *Journal of Archaeological Science*, 37(1), pp. 150–163. doi: 10.1016/j.jas.2009.09.025.

- Chenery, C. A. *et al.* (2012) 'The oxygen isotope relationship between the phosphate and structural carbonate fractions of human bioapatite', *Rapid Communications in Mass Spectrometry*, 26(3), pp. 309–319. doi: 10.1002/rcm.5331.
- Chenery, C., Eckardt, H. and Müldner, G. (2011) 'Cosmopolitan Catterick? Isotopic evidence for population mobility on Rome's Northern frontier', *Journal of Archaeological Science*. Elsevier Ltd, 38(7), pp. 1525–1536. doi: 10.1016/j.jas.2011.02.018.
- Cheung, E. *et al.* (2003) 'An epidemic of scurvy in Afghanistan: Assessment and response', *Food and Nutrition Bulletin*, 24(3), pp. 247–255. Available at: <http://ovidsp.ovid.com/ovidweb.cgi?T=JS&PAGE=reference&D=emed6&NEWS=N&AN=14564929>.
- Cheverko, C. M. and Hubbe, M. (2017) 'Comparisons of statistical techniques to assess age-related skeletal markers in bioarchaeology', *American Journal of Physical Anthropology*, 163(2), pp. 407–416. doi: 10.1002/ajpa.23206.
- Chiocchini, F. *et al.* (2016) 'Isoscapes of carbon and oxygen stable isotope compositions in tracing authenticity and geographical origin of Italian extra-virgin olive oils', *Food Chemistry*. Elsevier Ltd, 202, pp. 291–301. doi: 10.1016/j.foodchem.2016.01.146.
- Ciugudean, H. and Quinn, C. P. (2014) 'The end of the Wietenberg Culture in the Light of new 14 C dates and its Chronological relation Towards the noua Culture Horia', in Nemeth, R. E. and Rezi, B. (eds) *Bronze Age chronology in the Carpathian Basin*. Târgu Mureş: Editura Mega, pp. 147–178.
- Clark, A. L., Tayles, N. and Halcrow, S. E. (2014) 'Aspects of health in prehistoric mainland Southeast Asia: Indicators of stress in response to the intensification of rice agriculture', *American Journal of Physical Anthropology*. Wiley Online Library, 153(3), pp. 484–495.
- Clark, I. and Fritz, P. (1997) *Environmental isotopes in hydrogeology*, Lewis Publ., New York. New York, USA: Lewis Publishers.
- Coles, M. and Harding, A. F. (2015) *The Bronze Age in Europe: An introduction to the prehistory of Europe c.2000-700 BC*. Volume 18. New York: Routledge of Taylor and Francis Group.
- Cook, D. C. (2006) 'The Old Physical Anthropology and the New World: A Look at the Accomplishments of an Antiquated Paradigm', in Buikstra, J. E. and Beck, L. (eds) *Bioarchaeology: the contextual analysis of human remains*. London: Academic Press, pp. 22–71.
- Cook, D. C. (2012) 'Neglected Ancestors: Robert Wilson Shufeldt, MD (1850–1934)', in Buikstra, J. E. and Roberts, C. A. (eds) *The Global History of Paleopathology: Pioneers and Prospects*. London: Oxford University Press on Demand, pp. 192–196.
- Coplen, T. B. *et al.* (2002) 'Isotope-abundance variations of selected elements (IUPAC Technical Report)', *Pure and Applied Chemistry*. De Gruyter, 74(10), pp. 1987–2017.

- Coplen, T. B., Kendall, C. and Hopple, J. (1983) 'Comparison of stable isotope reference samples', *Nature*, 302(5905), pp. 236–238. doi: 10.1038/302236a0.
- Cosma, C. (2015) 'Notes on the presence of Avar warriors in the Transylvanian Plateau during the 7th-8th Centuries', *Transylvanian Review*, XXIV(2), pp. 228–246.
- Cozma, A. I. *et al.* (2017) 'Isotopic composition of precipitation in western Transylvania (Romania) reflected by two local meteoric water lines', *Carpathian Journal of Earth and Environmental Sciences*, 12(2), pp. 357–364.
- Craig-Atkins, E., Towers, J. and Beaumont, J. (2018) 'The role of infant life histories in the construction of identities in death: An incremental isotope study of dietary and physiological status among children afforded differential burial', *American Journal of Physical Anthropology*, 167(3), pp. 644–655. doi: 10.1002/ajpa.23691.
- Craig, O. E. *et al.* (2009) 'Stable isotopic evidence for diet at the imperial roman coastal site of Velia (1st and 2nd centuries AD) in Southern Italy', *American Journal of Physical Anthropology*, 139(4), pp. 572–583. doi: 10.1002/ajpa.21021.
- Crawford, E. (1988) 'Scurvy in Ireland during the Great Famine', *Social History of Medicine*, 1(3), pp. 281–300. doi: 10.1093/shm/1.3.281.
- Crowder, K. *et al.* (2019) 'Romans, barbarians and foederati: a possible region of origin for the "Headless Romans" and other burials from Britain', *forthcoming*.
- Crowder, K. D. (2015) *Isotopic profiling of diet, health, and mobility amongst the non-adult Gepid population buried at the Archiud Cemetery in Transylvania, Romania (4th – 7th centuries AD)*. (unpublished master thesis, Durham University).
- Crowder, K. D. *et al.* (2019) 'Childhood "stress" and stable isotope life histories in Transylvania', *International Journal of Osteoarchaeology*, 29(4), pp. 644–653. doi: 10.1002/oa.2760.
- Cunha, E. *et al.* (2009) 'The problem of aging human remains and living individuals : A review', 193, pp. 1–13. doi: 10.1016/j.forsciint.2009.09.008.
- Cunningham, C., Scheuer, L. and Black, S. (2016) *Developmental juvenile osteology*. Academic Press.
- de Cupere, B. *et al.* (2000) 'Osteological Evidence for the Draught Exploitation of Cattle: First Applications of a New Methodology', *International Journal of Osteoarchaeology*, 10(February), pp. 254–267. doi: 10.1002/1099-1212(200007/08)10:4<254::AID-OA528>3.0.CO;2-
- D'Ortenzio, L. *et al.* (2015) 'You are not what you eat during physiological stress: Isotopic evaluation of human hair', *American Journal of Physical Anthropology*, 157(3), pp. 374–388. doi: 10.1002/ajpa.22722.
- D'Ortenzio, L. *et al.* (2018) 'Age estimation in older adults: Use of pulp/tooth ratios calculated from tooth sections', *American Journal of Physical Anthropology*, 165(3), pp. 594–603. doi: 10.1002/ajpa.23371.

- Dansgaard, W. (1964) 'Stable isotopes in precipitation', *Tellus*. Taylor & Francis, 16(4), pp. 436–468.
- Dean, M. C. and Cole, T. J. (2013) 'Human Life History Evolution Explains Dissociation between the Timing of Tooth Eruption and Peak Rates of Root Growth', *PLoS ONE*, 8(1). doi: 10.1371/journal.pone.0054534.
- Dean, M. C. and Scandrett, A. E. (1995) 'Rates of dentin mineralization in permanent human teeth', *International Journal of Osteoarchaeology*, 5(4), pp. 349–358.
- DeNiro, M. J. and Epstein, S. (1981) 'Influence of diet on the distribution of nitrogen isotopes in animals*', *Geochemica et Cosmochemica Acta*, 45, pp. 341–351. doi: 10.1016/0016-7037(81)90244-1.
- DeNiro, M. J. M. J. and Epstein, S. (1978) 'Influence of diet on the distribution of carbon isotopes in animals', *Geochimica et Cosmochimica Acta*, 42(5), pp. 495–506. doi: 10.1016/0016-7037(78)90199-0.
- Dewitte, S. N. (2010) 'Sex differentials in frailty in Medieval England', *Am J Phys Anthropol*, 143(2), pp. 285–297. doi: 10.1002/ajpa.21316.Sex.
- Dewitte, S. N. (2012) 'Sex differences in periodontal disease in catastrophic and attritional assemblages from medieval london', *American Journal of Physical Anthropology*, 149(3), pp. 405–416. doi: 10.1002/ajpa.22138.
- Dewitte, S. N. and Hughes-Morey, G. (2012) 'Stature and frailty during the Black Death: the effect of stature on risks of epidemic mortality in London, A.D. 1348e1350', *Journal of Archaeological Science*, 39, pp. 1412–1419. doi: 10.1016/j.jas.2012.01.019.
- Dewitte, S. and Yaussy, S. (2016) 'Skeletal marker of physiological stress might indicate good , rather than poor , health', pp. 3–6.
- Diana, A. (2014) 'Contributions of Human Osteo-archaeology to the reconstruction of climatic shifts in medieval Romania', in Gradinaru, I. (ed.) *Late Pleistocene and Holocene climate variability in the Carpathian-Balkan region*. Ștefan cel Mare University Press, pp. 29–31.
- Dianna, A. and Meșter, M. (2013) 'Meeting an Early Medieval Community: A Preliminary Analysis of the Human Skeletal Remains from the Jucu Cemetery (Cluj-Napoca, Romania)', *Materiale și Cercetări Arheologice*, IX, pp. 199–218.
- Dickin, A. P. (2018) *Radiogenic isotope geology*, *Geological Magazine*. Cambridge university press. doi: 10.1017/S0016756800008852.
- Dobos, A. (2009) 'The Reihengräberfelder in Transylvania after 100 years of Archaeological Resarch', *Acta Archaeologica Carpathica*, XLIV.
- Dobos, A. (2013) 'The Gepidic Period in the Carpathian Basin'. Cluj-Napoca: Lecture.
- Dobos, A. (2014) 'Transylvania in the Gepidic Period; Results and Perspectives', *Hungarian Archaeology*, 264, pp. 1–6.

Dodge, D. L. and Martin, W. T. (1970) 'Social stress and chronic illness: Mortality patterns in industrial society.' U. Notre Dame Press.

Dreiszigler, N. (2009) 'The Székelys: Ancestors of Today's Hungarians? A New Twist to Magyar Prehistory.', *Hungarian Studies Review*, 36, pp. 153–169. Available at: <http://search.ebscohost.com/login.aspx?direct=true&db=hia&AN=44894970&site=ehost-live>.

Dreiszigler, N. (2013) 'Ármin Vámbéry (1832-1913) as a Historian of Early Hungarian Settlement in the Carpathian Basin', *Hungarian Cultural Studies*, 6, pp. 18–39. doi: 10.5195/ahca.2013.110.

Duray, S. M. (1996) 'Dental indicators of stress and reduced age at death in prehistoric native Americans', *American Journal of Physical Anthropology*, 99(2), pp. 275–286. doi: 10.1002/(SICI)1096-8644(199602)99:2<275::AID-AJPA5>3.0.CO;2-Y.

Eckardt, H., Müldner, G. and Speed, G. (2015) 'The Late Roman Field Army in Northern Britain? Mobility, Material Culture and Multi-Isotope Analysis at Scorton (N Yorks.)', *Britannia*, 46, pp. 191–223. doi: 10.1017/S0068113X1500015X.

Ellis, L. (1998) "'terra deserta": Population, politics, and the [de]colonization of dacia', *World Archaeology*, 30(2), pp. 220–237. doi: 10.1080/00438243.1998.9980408.

Emery, M. V. *et al.* (2018) 'Mapping the origins of Imperial Roman workers (1st-4th century CE) at Vagnari, Southern Italy, using $^{87}\text{Sr}/^{86}\text{Sr}$ and $\delta^{18}\text{O}$ variability', *American Journal of Physical Anthropology*, 166(4), pp. 837–850. doi: 10.1002/ajpa.23473.

Eng, J. T. and Szocs, P. L. (2003) 'Bioarchaeological analysis of an agricultural population from Late Medieval Transylvania', *American Journal of Physical Anthropology*, 120(S36), p. 93.

Epstein, S. and Mayeda, T. (1953) 'Variation of O^{18} content of waters from natural sources', *Geochimica et Cosmochimica Acta*, 4(5), pp. 213–224. doi: 10.1016/0016-7037(53)90051-9.

Ericson, J. E. (1985) 'Strontium isotope characterization in the study of prehistoric human ecology', *Journal of Human Evolution*. Academic Press, 14(5), pp. 503–514. doi: 10.1016/S0047-2484(85)80029-4.

Evans, J. A. *et al.* (2010) 'Spatial variations in biosphere $^{87}\text{Sr}/^{86}\text{Sr}$ in Britain', *Journal of the Geological Society, London*, 167(January), pp. 1–4. doi: 10.1144/0016-76492009-090.

Evans, J. A., Chenery, C. A. and Montgomery, J. (2012) 'A summary of strontium and oxygen isotope variation in archaeological human tooth enamel excavated from Britain', *Journal of Analytical Atomic Spectrometry*, 27, pp. 754–764. doi: 10.1039/c2ja10362a.

Evans, J., Stoodley, N. and Chenery, C. (2006) 'A strontium and oxygen isotope assessment of a possible fourth century immigrant population in a Hampshire cemetery, southern England', *Journal of Archaeological Science*, 33(2), pp. 265–272. doi: 10.1016/j.jas.2005.07.011.

- Evin, A., Dobney, K. and Cucchi, T. (2017) 'A history of pig domestication: New ways of exploring a complex process', in Melletti, M. and Meijaard, E. (eds) *Ecology, conservation and management of wild pigs and peccaries*. Cambridge: Cambridge University Press, pp. 39–48.
- Fain, O. (2005) 'Musculoskeletal manifestations of scurvy', *Joint Bone Spine*, 72(2), pp. 124–128. doi: 10.1016/j.jbspin.2004.01.007.
- Faure, G. (1986) 'Isotope systematics in two-component mixtures', *Principles of isotope geology*. Jhon Wiley and Sons, pp. 141–153.
- Faure, G. (2013) *Origin of igneous rocks: the isotopic evidence*. Springer Science & Business Media.
- Faure, G. and Mensing, T. M. (2009) *Isotopes: Principles and Applications*. Wiley India. Available at: <https://books.google.co.uk/books?id=HC10CgAAQBAJ>.
- Filipescu, S. (2011) 'Cenozoic lithostratigraphic units in Transylvania. In: Bucur I & Săsăran E (eds.) – Calcareous algae from Romanian Carpathians', in Bucur, I. and Săsăran, E. (eds) *Calcareous algae from Romanian Carpathians*. Cluj: Cluj University press, pp. 37–48.
- Floyd, B. (2016) 'The magnitude of changes in linear growth within Taiwanese families: intrinsic sex-associated biology, socially mediated behaviors, or both?', *American Journal of Physical Anthropology*, 161(3), pp. 456–466. doi: 10.1002/ajpa.23048.
- Fogel, M. L., Tuross, N. and Owsley, D. W. (1989) 'Nitrogen isotope tracers of human lactation in modern and archaeological populations', *Carnegie Institution of Washington Yearbook*. Geophysical Laboratory Washington, 88, pp. 111–117.
- Fogel, R. W. *et al.* (1983) *Secular Changes in American and British Stature and Nutrition, The Journal of Interdisciplinary History*. Available at: <https://www.jstor.org/stable/203716> (Accessed: 29 November 2018).
- Follis, R., Park, E. and Jackson, D. (1950) 'The prevalence of scurvy at autopsy during the first two years of age.', *Bulletin of the Johns Hopkins Hospital*, 87, pp. 569–592.
- France, C. A. M. and Owsley, D. W. (2015) 'Stable Carbon and Oxygen Isotope Spacing Between Bone and Tooth Collagen and Hydroxyapatite in Human Archaeological Remains', *International Journal of Osteoarchaeology*, 25(3), pp. 299–312. doi: 10.1002/oa.2300.
- Franz-Odendaal, T. A., Lee-Thorp, J. A. and Chinsamy-Turan, A. (2003) 'Insights from stable light isotopes on enamel defects and weaning in Pliocene herbivores', *Journal of Biosciences*, 28(6), pp. 765–773. doi: 10.1007/BF02708437.
- Fried, L. P. *et al.* (2001) 'Frailty in Older Adults: Evidence for a Phenotype', *The Journals of Gerontology Series A: Biological Sciences and Medical Sciences*, 56(3), pp. M146–M157. doi: 10.1093/gerona/56.3.M146.
- Friedli, H. *et al.* (1986) 'Ice core record of the $^{13}\text{C}/^{12}\text{C}$ ration of atmospheric CO_2 in the past two centuries', *Nature*, 324(6094), pp. 237–238.

- Friedman, I. (1953) 'Deuterium content of natural waters and other substances', *Geochimica et Cosmochimica Acta*. Elsevier, 4(1–2), pp. 89–103.
- Froehle, A. W., Kellner, C. M. and Schoeninger, M. J. (2010) 'FOCUS: effect of diet and protein source on carbon stable isotope ratios in collagen: follow up to Warinner and Tuross (2009)'. doi: 10.1016/j.jas.2010.06.003.
- Fuller, B. T. *et al.* (2004) 'Nitrogen balance and $\delta^{15}\text{N}$: Why you're not what you eat during pregnancy', *Rapid Communications in Mass Spectrometry*, 18(23), pp. 2889–2896. doi: 10.1002/rcm.1708.
- Fuller, B. T. *et al.* (2005) 'Nitrogen balance and $\delta^{15}\text{N}$: why you're not what you eat during nutritional stress', *Rapid Communications in Mass Spectrometry*, 19(18), pp. 2497–2506. doi: 10.1002/rcm.2090.
- Fuller, B.T. *et al.* (2006) 'Detection of breastfeeding and weaning in modern human infants with carbon and nitrogen stable isotope ratios', *American Journal of Physical Anthropology*, 129(2), pp. 279–293. doi: 10.1002/ajpa.20249.
- Fuller, B. T. *et al.* (2006) 'Isotopic evidence for breastfeeding and possible adult dietary differences from Late/Sub-Roman Britain', *American Journal of Physical Anthropology*, 129(1), pp. 45–54. doi: 10.1002/ajpa.20244.
- Fulminante, F. (2015) 'Infant Feeding Practices in Europe and the Mediterranean from Prehistory to the Middle Ages: A Comparison between the Historical Sources and Bioarchaeology', *Childhood in the Past*, 8(1), pp. 24–47. doi: 10.1179/1758571615Z.00000000026.
- Gabinschi, M. (1997) 'Reconvergence of Moldavian towards Romanian', *CONTRIBUTIONS TO THE SOCIOLOGY OF LANGUAGE*. MOULTON DE GRUYTER, 78, pp. 193–214.
- Gál, S. (2011) 'Romania/România: a brief history and current state of physical anthropology in Romania', in Marquez-Grant, N. and Fibiger, L. (eds) *The Routledge Handbook of Archaeological Human Remains and Legislation: An International Guide to Laws and Practice in the Excavation and Treatment of Archaeological Human Remains*. New York: Taylor & Francis (Routledge handbooks), pp. 355–362. Available at: <https://books.google.co.uk/books?id=Lzi4N-74QmAC>.
- Gáll, E. (2012) 'Márton Roska and archaeology in Transylvania: from early 20th to 21st Century. Some critical notes to the Hungarian-Armenian scholars early medieval studies and recent evolution of archaeology in transylvania', *Acta Archaeologica Carpathica*, XLVII, pp. 127–165.
- Gáll, E. (2013) 'Churchyard Cemeteries in Transylvania Basin from the 11th–first half of the 13th Centuries. On the beginning of institutionalised Christianity', *MARISIA Studii și materiale Arheologie*, 33, pp. 135–250.
- Gáll, E. (2014) 'THE AVAR CONQUEST AND WHAT FOLLOWED. SOME IDEAS ON THE PROCESS OF "AVARISATION" OF TRANSYLVANIAN BASIN (6TH– 7TH CENTURIES)', in Cociș, S. (ed.) *Gedenkschrift zum hundertsten Geburtstag von Kurt Horedt*. Cluj-Napoca: Editura Mega, pp. 295–324.

- Gáll, E. (2015) 'An attempt to classify the stirrups dating from the 10th century and the first quarter of the 11th century in the Transylvanian Basin, the Crişana/Partium and the Banat with an outlook to the Carpathian Basin', in Cosma, C. (ed.) *Warriors, weapons, and harness from the 5th - 10th Centuries in the Carpathian Basin*. Cluj-Napoca: Mega Publishing House, pp. 355–406.
- Gamarra, B. *et al.* (2018) '5000 Years of Dietary Variations of Prehistoric Farmers in the Great Hungarian Plain', *PLoS ONE*, 13(5), pp. 1–20. doi: 10.1371/journal.pone.0197214.
- García-Closas, R. *et al.* (2004) 'Dietary sources of vitamin C, vitamin E and specific carotenoids in Spain', *British Journal of Nutrition*. 2007/03/09. Cambridge University Press, 91(6), pp. 1005–1011. doi: DOI: 10.1079/BJN20041130.
- Garcia, K. E., Kroenke, C. D. and Bayly, P. V (2018) 'Mechanics of cortical folding : stress , growth and stability'.
- Gardner, B., Jakob, T. and Jørkov, M. (2019) 'Improving observer error in orbital roof lesion analysis: A new classification system', in *46th Annual Meeting of the Palaeopathology Association*. Cleveland, USA.
- Gastescu, P. *et al.* (1975) 'The Hydro-Climatic Particularities of Romania', *Geoforum*, 6, pp. 29–37.
- Gat, J. R. (1996) 'Oxygen and Hydrogen Isotopes in the Hydrologic Cycle', *Annual Review of Earth and Planetary Sciences*, 24(1), pp. 225–262. doi: 10.1159/000088336.
- Geber, J. and Murphy, E. (2012) 'Scurvy in the great irish famine: Evidence of vitamin C deficiency from a mid-19th century skeletal population', *American Journal of Physical Anthropology*, 148(4), pp. 512–524. doi: 10.1002/ajpa.22066.
- Gerling, C., Heyd, V., *et al.* (2012) 'Identifying kurgan graves in Eastern Hungary: A burial mound in the light of strontium and oxygen isotope analysis', in *Population Dynamics in Prehistory and Early History*. Berlin, Boston: DE GRUYTER, pp. 165–176. doi: 10.1515/9783110266306.165.
- Gerling, C., Bánffy, E., *et al.* (2012) 'Immigration and transhumance in the Early Bronze Age Carpathian Basin: the occupants of a kurgan', *Antiquity*, 86, pp. 1097–1111. Available at: <http://antiquity.ac.uk/ant/086/ant0861097.htm> (Accessed: 27 November 2018).
- Giblin, J. I. (2009) 'Strontium isotope analysis of Neolithic and Copper Age populations on the Great Hungarian Plain', *Journal of Archaeological Science*. Elsevier Ltd, 36(2), pp. 491–497. doi: 10.1016/j.jas.2008.09.034.
- Giblin, J. I. *et al.* (2013) 'Strontium isotope analysis and human mobility during the Neolithic and Copper Age: A case study from the Great Hungarian Plain', *Journal of Archaeological Science*, 40(1), pp. 227–239. doi: 10.1016/j.jas.2012.08.024.
- Gilfillan, J. J. (1934) 'The isotopic composition of sea water', *Journal of the American Chemical Society*. ACS Publications, 56(2), pp. 406–408.

- Gillis, R. *et al.* (2013) 'Sophisticated cattle dairy husbandry at Borduşani-Popină (Romania, fifth millennium BC): the evidence from complementary analysis of mortality profiles and stable isotopes', *World Archaeology*, 45(3), pp. 447–472. doi: 10.1080/00438243.2013.820652.
- Giuresci, C. (2002) *Transylvania in the History of Romania*. London: The Garnstone Press Ltd.
- Giurescu, C. C. (1969) *Transylvania in the History of Romania*. London: The Garnstone Press Ltd.
- Gligor, M. and Crişan, S. (2014) 'Inhumation versus cremation in Transylvanian Neolithic and Eneolithic', *Studia Antiqua et Archaeologica*, XX, pp. 37–67.
- Goldstein, L. (2006) 'Mortuary Analysis and Bioarchaeology', in Buikstra, J. E. and Beck, L. A. (eds) *Bioarchaeology: the contextual analysis of human remains* 2. London, UK: Academic Press.
- Goodman, A. H., Armelagos, G. J. and Rose, J. C. (1980) 'Enamel Hypoplasias as Indicators of Stress in Three Prehistoric Populations from Illinois', *Human Biology*, 52(3), pp. 515–528.
- Goodman, A. H., Armelagos, G. J. and Rose, J. C. (1984) 'The chronological distribution of enamel hypoplasias from prehistoric dickson mounds populations', *American Journal of Physical Anthropology*, 65(3), pp. 259–266. doi: 10.1002/ajpa.1330650305.
- Goodman, A. H. and Rose, J. C. (1990) 'Assessment of systematic physiological perturbations from dental enamel hypoplasias and associated histological structures', *American Journal of Physical Anthropology*, 33(S11), pp. 59–110.
- Gowland, R. (2017) 'Embodied Identities in Roman Britain: A Bioarchaeological Approach', *Britannia*, 48, pp. 177–194. doi: 10.1017/s0068113x17000125.
- Gowland, R. L. and Chamberlain, A. T. (2005) 'Detecting plague: palaeodemographic characterisation of a catastrophic death assemblage', *Antiquity*, 79(303), pp. 146–157. doi: 10.1017/s0003598x00113766.
- Grauer, A. L. (2012) *A Companion to Paleopathology, A Companion to Paleopathology*. doi: 10.1002/9781444345940.
- Grauer, A. L. (2018) 'A century of paleopathology', *American Journal of Physical Anthropology*, 165(4), pp. 904–914. doi: 10.1002/ajpa.23366.
- Graustein, W. C. (1989) '87Sr/86Sr Ratios Measure the Sources and Flow of Strontium in Terrestrial Ecosystems', in Rundel, P. W., Ehleringer, J. R., and Nagy, K. A. (eds) *Stable Isotopes in Ecological Research*. New York, NY: Springer New York, pp. 491–512. doi: 10.1007/978-1-4612-3498-2_28.
- Greenfield, G. B. (1986) *Radiology of bone disease, 4th edition*. United States: R Health Professions. Available at: http://inis.iaea.org/search/search.aspx?orig_q=RN:18060927.

- Grewar, D. (1965) 'Infantile Scurvy', *Clinical Pediatrics*, 4(2), pp. 82–89. doi: 10.1097/00007611-191705000-00009.
- Gröcke, D. R., Bocherens, H.-V. and Mariotti, A. (1997) 'Collagen: Application As a Palaeoprecipitation Indicator', *Earth and Planetary Science Letters*, 153, pp. 279–285.
- Grossman, C. (1985) 'Interactions between the gonadal steroids and the immune system', *Science*, 227(4684), pp. 257–261. doi: 10.1126/science.3871252.
- Groza, V., Simalcsik, A. and Bejenaru, L. (2013) 'Spina Bifida Occulta in Medieval and Post-Medieval Skeletons From Iasi City , in North-East Romania', LIX, pp. 101–113.
- Grumeza, I. (2009) *Dacia: Land of Transylvania, Cornerstone of Ancient Eastern Europe*. University Press of America.
- Grupe, G. *et al.* (1997) 'Mobility of Bell Beaker people revealed by strontium isotope ratios of tooth and bone: a study of southern Bavarian skeletal remains', *Applied Geochemistry*. Elsevier, 12(4), pp. 517–525.
- Gugora, A., Dupras, T. L. and Fóthi, E. (2018) 'Pre-dating paprika: Reconstructing childhood and adulthood diet at medieval (13th century CE) Solt-Tételhegy, Hungary from stable carbon and nitrogen isotope analyses', *Journal of Archaeological Science: Reports*. Elsevier, 18(January), pp. 151–160. doi: 10.1016/j.jasrep.2017.12.036.
- Güllü, S. *et al.* (1998) 'A Potential Risk for Osteomalacia due to Sociocultural Lyfestyle in Turkish Women', *Endocrine journal*. The Japan Endocrine Society, 45(5), pp. 675–678.
- Gyulai, F. (2006) 'Historical Plant-Biodiversity in the Carpathian Basin', in Jerem, E., Mester, Z., and Benczes, R. (eds) *Archaeological and Cultural Heritage Preservation*. Budapest, pp. 63–72. Available at: <http://citeseerx.ist.psu.edu/viewdoc/download?doi=10.1.1.620.8238&rep=rep1&type=pdf>.
- Gyulai, F. (2014) 'The history of broomcorn millet (*Panicum miliaceum* L.) In the Carpathian-basin in the mirror of archaeobotanical remains II. From the roman age until the late medieval age', *Columella : Journal of Agricultural and Environmental Sciences*, 1(1), pp. 39–48. doi: 10.18380/szie.colum.2014.1.1.39.
- Hakenbeck, S. E. *et al.* (2017) 'Practising pastoralism in an agricultural environment: An isotopic analysis of the impact of the Hunnic incursions on Pannonian populations', *PLOS ONE*. Edited by D. Caramelli, 12(3), p. e0173079. doi: 10.1371/journal.pone.0173079.
- Hales, C. N. and Barker, D. J. P. (2001) 'The thrifty phenotype hypothesis', *British Medical Bulletin*, 60(5–20).
- Hampl, J. S., Taylor, C. A. and Johnston, C. S. (2004) 'Vitamin C Deficiency and Depletion in the United States: The Third National Health and Nutrition Examination Survey, 1988 to 1994', *American Journal of Public Health*. American Public Health Association, 94(5), pp. 870–875. doi: 10.2105/AJPH.94.5.870.

Harhoiu, R. and Gáll, E. (2014) 'NECROPOLA DIN SECOLUL XII DE LA SIGHIȘOARA-DEALUL VIILOR, PUNCTUL „NECROPOLĂ”. CONTRIBUȚII PRIVIND HABITATUL EPOCII MEDIEVALE TIMPURII ÎN TRANSILVANIA ESTICĂ', *ANALELE BANATULUI ARHEOLOGIE – ISTORIE*, XXII, pp. 195–243.

Harman, M., Molleson, T. and Price, J. (1981) 'Burials, bodies and beheadings in Romano-British and Anglo-Saxon cemeteries', *Bulletin of the British Museum of Natural History (Geology)*, 35(3), pp. 145–188. Available at: https://archive.org/details/cbarchive_109664_burialsbodiesandbeheadingsinro1949/page/n17.

Harper, T. K. (2016) *Climate, migration, and false cities on the Old European periphery: a spatial-demographic approach to understanding the Tripolye giant-settlements* by. University of Buffalo, State University of New York.

Hassett, B. R. (2014) 'Missing defects? A comparison of microscopic and macroscopic approaches to identifying linear enamel hypoplasia', *American Journal of Physical Anthropology*, 153(3), pp. 463–472. doi: 10.1002/ajpa.22445.

Hatch, K. *et al.* (2006) 'An objective means of diagnosing anorexia nervosa and bulimia nervosa using 15N/14N and 13C/12C ratios in hair', *Rapid communications in mass spectrometry: RCM*, 20, pp. 3367–3373. doi: 10.1002/rcm.2740 An.

Hatch, K. A. (2012) 'The Use and Application of Stable Isotope Analysis to the Study of Starvation, Fasting, and Nutritional Stress in Animals', in McCue, M. D. (ed.) *Comparative Physiology of Fasting, Starvation, and Food Limitation*. Berlin, Heidelberg: Springer Berlin Heidelberg, pp. 337–364. doi: 10.1007/978-3-642-29056-5_20.

Hedges, R. E. M. *et al.* (2007) 'Collagen turnover in the adult femoral mid-shaft: Modeled from anthropogenic radiocarbon tracer measurements', *American Journal of Physical Anthropology*. Wiley-Blackwell, 133(2), pp. 808–816. doi: 10.1002/ajpa.20598.

Hedges, R. E. M., Millard, A. R. and Pike, A. W. G. (1995) 'Measurements and Relationships of Diagenetic Alteration of Bone from Three Archaeological Sites', *Journal of Archaeological Science*, 22(2), pp. 201–209. doi: 10.1006/jasc.1995.0022.

Hedges, R. E. M. and Reynard, L. M. (2007) 'Nitrogen isotopes and the trophic level of humans in archaeology', *Journal of Archaeological Science*, 34(8), pp. 1240–1251. doi: 10.1016/j.jas.2006.10.015.

Henderson, R. C., Lee-Thorp, J. and Loe, L. (2014) 'Early life histories of the London poor using $\delta^{13}\text{C}$ and $\delta^{15}\text{N}$ stable isotope incremental dentine sampling', *American Journal of Physical Anthropology*, 154(4), pp. 585–593. doi: 10.1002/ajpa.22554.

Henriquez, A. and Oxenham, M. F. (2019) 'New distance-based exponential regression method and equations for estimating the chronology of linear enamel hypoplasia (LEH) defects on the anterior dentition', *American Journal of Physical Anthropology*, 168(3), pp. 510–520. doi: 10.1002/ajpa.23764.

- Hervella, M. *et al.* (2015) 'Ancient DNA from South-East Europe reveals different events during early and middle neolithic influencing the European genetic heritage', *PLoS ONE*, 10(6), pp. 1–20. doi: 10.1371/journal.pone.0128810.
- Hess, A. F. (1930) *Rickets including osteomalacia and tetany*. Henty Kimpton: London.
- High, K. *et al.* (2015) 'Apatite for destruction: Investigating bone degradation due to high acidity at Star Carr', *Journal of Archaeological Science*. Elsevier Ltd, 59, pp. 159–168. doi: 10.1016/j.jas.2015.04.001.
- Hillson, S. (1996) *Dental Anthropology*. Cambridge: Cambridge University Press.
- Hillson, S. (2001) 'Recording dental caries in archaeological human remains', *International Journal of Osteoarchaeology*, 11(4), pp. 249–289. doi: 10.1002/oa.538.
- Hillson, S. (2005) *Teeth*. 2nd edn. Cambridge: Cambridge University Press.
- Hillson, S. (2014) *Tooth Development in Human Evolution and Bioarchaeology*. 1st edn. Cambridge: Cambridge University Press.
- Hirschman, J. and Raugi, G. (1999) 'Adult scurvy', *Journal of the American Academy of Dermatology*, 41(6), pp. 895–910.
- Hodges, R. E. *et al.* (1971) 'Clinical manifestations of ascorbic acid deficiency in man', *The American Journal of Clinical Nutrition*, 24(4), pp. 432–443. doi: 10.1093/ajcn/24.4.432.
- Holick, M. and Adams, J. (1998) 'Vitamin D metabolism and biological function', in Avioli, L. and Krane, S. (eds) *Metabolic bone disease and clinically related disorders*. Academic Press, pp. 123–164.
- Holick, M. F. (2003) 'Vitamin D: A millenium perspective', *Journal of Cellular Biochemistry*, 88(2), pp. 296–307. doi: 10.1002/jcb.10338.
- Holick, M. F. (2006) 'High Prevalence of Vitamin D Inadequacy and Implications for Health', *Mayo Clinic Proceedings*, 81(3), pp. 353–373. doi: 10.4065/81.3.353.
- Holick, M. F. (2007) 'Vitamin D deficiency', *New England Journal of Medicine*. Mass Medical Soc, 357(3), pp. 266–281.
- Holló, G. *et al.* (2008) 'History of the Peoples of the Great Hungarian Plain in the First Millennium: A Craniometric Point of View', *Human Biology*, 80(6), pp. 655–667. doi: 10.3378/1534-6617-80.6.655.
- Howland, M. R. *et al.* (2003) 'Expression of the dietary isotope signal in the compound-specific $\delta^{13}\text{C}$ values of pig bone lipids and amino acids', *International Journal of Osteoarchaeology*. Wiley Online Library, 13(1-2), pp. 54–65.
- Le Huray, J. D. and Schutkowski, H. (2005) 'Diet and social status during the La Tène period in Bohemia: Carbon and nitrogen stable isotope analysis of bone collagen from Kutná Hora-Karlov and Radovesice', *Journal of Anthropological Archaeology*, 24(2), pp. 135–147. doi: 10.1016/j.jaa.2004.09.002.

IAEA/WMO (2019) *Global Network of Isotopes in Precipitation, The GNIP Database*. Available at: <https://nucleus.iaea.org/wiser/index.aspx>.

IAEA (2009) *Laser Spectroscopic Analysis of Liquid Water Samples for Stable Hydrogen and Oxygen Isotopes*. Vienna: IAEA.

IAEA (2018) *Materials characterized for stable isotopes, Reference Materials*. Available at: https://nucleus.iaea.org/rpst/referenceproducts/referencematerials/Stable_Isotopes/index.htm (Accessed: 18 September 2018).

Ion, A. (2014) 'Osteoarchaeological studies in the history of the Annuaire Roumain D'anthropologie journal', *Annuaire Roumain d'Anthropologie*, 51(1), pp. 7–9.

Işcan, M. Y., Loth, S. R. and Wright, R. K. (1985) 'Age Estimation from the Rib by Phase Analysis: White Females', *Journal of Forensic Sciences, JFSCA*, 30(3), pp. 853–863. doi: 10.1520/JFS11018J.

Işcan, M. Y., Loth, S. R. and Wright, R. K. (1984) 'Metamorphosis at the sternal rib: A new method to estimate age at death in males', *American Journal of Physical Anthropology*, 65, pp. 147–156.

Istrate, D. and Diana, A. (2017) 'The Black Church Cemetery: Interdisciplinary approaches to the study of a medieval urban skeletal assemblage (Braşov, Romania)', *Studies in Digital Heritage*, 1(2), p. 364. doi: 10.14434/sdh.v1i2.23233.

Ivancik, J. *et al.* (2014) 'Differences in the microstructure and fatigue properties of dentine between residents of North and South America', *Archives of Oral Biology*. Elsevier Ltd, 59(10), pp. 1001–1012. doi: 10.1016/j.archoralbio.2014.05.028.

Ives, R. and Brickley, M. (2014) 'New findings in the identification of adult vitamin D deficiency osteomalacia: Results from a large-scale study', *International Journal of Paleopathology*. Elsevier Inc., 7, pp. 45–56. doi: 10.1016/j.ijpp.2014.06.004.

Jakubowski, N. *et al.* (2011) 'Inductively coupled plasma- and glow discharge plasma-sector field mass spectrometry', *Journal of Analytical Atomic Spectrometry*, 26, pp. 693–726.

James, W. (1997) 'Long-term fetal programming of body composition and longevity', *Nutr Rev*, 55, pp. S41–S43.

Janele, D. (2006) 'Effects of Testosterone, 17beta-Estradiol, and Downstream Estrogens on Cytokine Secretion from Human Leukocytes in the Presence and Absence of Cortisol', *Annals of the New York Academy of Sciences*, 1069(1), pp. 168–182. doi: 10.1196/annals.1351.015.

Jankauskas, R. and Grupe, G. (2018) 'Contextual Dimensions of Health and Lifestyle: Isotopes, Diet, Migration, and the Archaeological and Historical Records', in Steckel, R. *et al.* (eds) *The Backbone of Europe: Health, Diet, Work and Violence over Two Millennia*. Cambridge, UK: Cambridge University Press, pp. 11–51.

- Johnson, B. J. *et al.* (1997) 'The determination of late quaternary paleoenvironments at Equus Cave, South Africa, using stable isotopes and amino acid racemization in ostrich eggshell', *Palaeogeography, Palaeoclimatology, Palaeoecology*, 136(1–4), pp. 121–137. doi: 10.1016/S0031-0182(97)00043-6.
- Jurmain, R. (1999) *Stories from the Skeleton: Behavioral Reconstruction in Human Osteology*. Amsterdam: Gordon and Breach Science Publishers.
- Katzenberg, A. M., Herring, A. D. and Saunders, S. R. (1996) 'Weaning and infant mortality: evaluating the skeletal evidence', *American journal of ...*, 39, pp. 177–199. doi: 10.1002/(SICI)1096-8644(1996)23+<177::AID-AJPA7>3.0.CO;2-2.
- Katzenberg, M. A. (2007) 'Stable Isotope Analysis: A Tool for Studying Past Diet, Demography, and Life History', in Katzenberg, M. A. and Saunders, S. R. (eds) *Biological Anthropology of the Human Skeleton*. Hoboken, USA: John Wiley & Sons, Inc., pp. 411–441. doi: 10.1002/9780470245842.ch13.
- Katzenberg, M. A. and Krouse, H. R. (1989) 'Application of stable isotope variation in human tissues to problems in identification', *Canadian Society of Forensic Science Journal*. Taylor & Francis, 22(1), pp. 7–19.
- Katzenberg, M. and Lovell, N. (1999) 'Stable isotope variation in pathological bone', *International Journal of ...*, 9(May), pp. 316–324. doi: 10.1002/(SICI)1099-1212(199909/10)9:5<316::AID-OA500>3.0.CO;2-D.
- Kawasaki, K., Tanaka, S. and Ishikawa, T. (1980) 'On the daily incremental lines in human dentine', *Archives of Oral Biology*, 24, pp. 939–943.
- Kazemi, A. *et al.* (2009) 'High Prevalence of Vitamin D Deficiency among Pregnant Women and their Newborns in an Iranian Population', *Journal of Women's Health*, 18(6), pp. 835–839. doi: 10.1089/jwh.2008.0954.
- Kellner, C. M. and Schoeninger, M. J. (2007) 'A simple carbon isotope model for reconstructing prehistoric human diet', *American Journal of Physical Anthropology*, 133(4), pp. 1112–1127. doi: 10.1002/ajpa.20618.
- Kelly, H. W. *et al.* (2012) 'Effect of inhaled glucocorticoids in childhood on adult height', *New England Journal of Medicine*. Mass Medical Soc, 367(10), pp. 904–912.
- Kendall, E. J. *et al.* (2013) 'Mobility, mortality, and the middle ages: Identification of migrant individuals in a 14th century black death cemetery population', *American Journal of Physical Anthropology*, 150(2), pp. 210–222. doi: 10.1002/ajpa.22194.
- Khalifa, A. M. (2014) 'Relationship between gestational age, birth weight and deciduous tooth eruption', *Egyptian Pediatric Association Gazette*. The Egyptian Paediatric Association, 62(2), pp. 41–45. doi: 10.1016/j.epag.2014.04.001.
- Khan, J. *et al.* (2015) 'Timing of Breastfeeding Initiation and Exclusivity of Breastfeeding During the First Month of Life: Effects on Neonatal Mortality and Morbidity—A Systematic Review and Meta-analysis', *Maternal and Child Health Journal*, 19(3), pp. 468–479. doi: 10.1007/s10995-014-1526-8.

- Kharalambieva, A. (2010) 'Gepids in the Balkans: A survey of the archaeological evidence', in Curta, F. (ed.) *Neglected Barbarians*. Turnhout: Brepols Publishing, pp. 245–261.
- King, C. L., Millard, A. R., *et al.* (2018) 'A comparison of using bulk and incremental isotopic analyses to establish weaning practices in the past', *STAR: Science & Technology of Archaeological Research*. Taylor & Francis, 0(0), pp. 1–9. doi: 10.1080/20548923.2018.1443548.
- King, C. L., Halcrow, S. E., *et al.* (2018) 'Let's talk about stress, baby! Infant-feeding practices and stress in the ancient Atacama desert, Northern Chile', *American Journal of Physical Anthropology*, 166(1), pp. 1–17. doi: 10.1002/ajpa.23411.
- King, T., Humphrey, L. T. and Hillson, S. (2005) 'Linear enamel hypoplasias as indicators of systemic physiological stress: Evidence from two known age-at-death and sex populations from postmedieval London', *American Journal of Physical Anthropology*, 128(3), pp. 547–559. doi: 10.1002/ajpa.20232.
- Van Klinken, G. J. (1999) 'Bone Collagen Quality Indicators for Palaeodietary and Radiocarbon Measurements', *Journal of Archaeological Science*, 26, pp. 687–695.
- Koch, P. L. (1994) 'Tracing the diets of fossil animals using stable isotopes', *Stable isotopes in ecology and environmental science*. Blackwell Scientific Pub., pp. 63–92.
- Koch, P. L., Fisher, D. C. and Dettman, D. (1989) 'Oxygen isotope variation in the tusks of extinct proboscideans - ma measure of season of death and seasonality', *Geology*, 17, pp. 515–519.
- Koch, P. L., Tuross, N. and Fogel, M. L. (1997) 'The effects of sample treatment and diagenesis on the isotopic integrity of carbonate in biogenic hydroxylapatite', *Journal of Archaeological Science*, 24(5), pp. 417–429. doi: 10.1006/jasc.1996.0126.
- Koepke, N. and Baten, J. (2005a) 'Climate and its impact on the biological standard of living in north-east, centre-west and south Europe during the last 2000 years', *History of Meteorology*, 2, pp. 147–159. doi: 10.1061/40906(225)11.
- Koepke, N. and Baten, J. (2005b) 'The biological standard of living in Europe during the last two millennia', *European Review of Economic History*, 9(1), pp. 61–95. doi: 10.1017/S1361491604001388.
- Köhler, K. *et al.* (2017) 'Possible cases of leprosy from the Late Copper Age (3780–3650 cal BC) in Hungary', *PLoS ONE*, 12(10), pp. 1–25. doi: 10.1371/journal.pone.0185966.
- Kontny, B. (2017) 'Brothers-in-Arms . Balt Warriors and Their Interregional Contacts in the Roman and Migration Periods (the Case of the Bogaczewo and Sudovian Cultures)', *LIETUVOS ARCHEOLOGIJA*, 43(February), pp. 11–62.
- Kotov, O. I. *et al.* (1997) 'Conversion of phase modulation of light into intensity modulation by means of an external fiber-optic interferometer', *Technical Physics Letters*, 23(5), pp. 380–382. doi: 10.3402/tellusa.v16i4.8993.

Kr zsek, C. *et al.* (2010) 'Miocene facies associations and sedimentary evolution of the Southern Transylvanian Basin (Romania): Implications for hydrocarbon exploration', *Marine and Petroleum Geology*, 27(1), pp. 191–214. doi: 10.1016/j.marpetgeo.2009.07.009.

Kr zsek, C. (2011) *Petroleum Systems of Romania**. Available at: <http://europe.aapg.org/wp-content/uploads/2011/03/> (Accessed: 27 November 2018).

Krueger, H. W. and Sullivan, C. H. (1984) 'Models for carbon isotope fractionation between diet and bone', *Stable isotopes in nutrition*. American Chemical Society Washington, DC, 258, pp. 205–220.

Lafferty, K. D. (2009) 'Calling for an ecological approach to studying climate change and infectious diseases', *Ecology*, 90(4), pp. 932–933. doi: 10.1890/08-1767.1.

Larsen, C. S. (1997) *Bioarchaeology: Interpreting behavior from the human skeleton*. 1st edn. Cambridge: Cambridge University Press.

Larsen, C. S. (2002) *Bioarchaeology: The Lives and Lifestyles of Past People*, *Journal of Archaeological Research*. Available at: <https://link.springer.com/content/pdf/10.1023%2FA%3A1015267705803.pdf> (Accessed: 2 December 2018).

Larsen, C. S. (2015) *Bioarchaeology: interpreting behavior from the human skeleton*. Cambridge University Press.

Larsen, C. S. and Milner, G. R. (1994) 'In the wake of contact: biological responses to conquest', in *In the wake of contact: biological responses to conquest*. Wiley-Liss, New York.

Lazarovici, G. and Lazarovici, C.-M. (2015) 'New data and observations related with exploitation and transport of salt in Transylvanian prehistory (Romania)', *Archaeology of Salt: Approaching an invisible past*. Sidestone Press, p. 139.

Leach, S. *et al.* (2009) 'Migration and diversity in Roman Britain: A multidisciplinary approach to the identification of immigrants in Roman York, England', *American Journal of Physical Anthropology*, 140(3), pp. 546–561. doi: 10.1002/ajpa.21104.

Leach, S. *et al.* (2010) 'A Lady of York: migration, ethnicity and identity in Roman Britain', *Antiquity*, 84, pp. 131–148. doi: 10.1002/ajpa.21104.

L colle, P. (1985) 'The oxygen isotope composition of landsnail shells as a climatic indicator: Applications to hydrogeology and paleoclimatology', *Chemical Geology: Isotope Geoscience Section*, 58(1–2), pp. 157–181. doi: 10.1016/0168-9622(85)90036-3.

Lee-Thorp, J. A. and Van Der Merwe, N. J. (1987) 'Carbon isotope analysis of fossil bone apatite', *South African Journal of Science*, 83(11), pp. 712–715.

- Lee-Thorp, J. A., Sealy, J. C. and van der Merwe, N. J. (1989) 'Stable carbon isotope ratio differences between bone collagen and bone apatite, and their relationship to diet', *Journal of Archaeological Science*, 16(6), pp. 585–599. doi: 10.1016/0305-4403(89)90024-1.
- Lewis, D. *et al.* (2007) 'Rickets and scurvy presenting in a child as apparent non accidental injury', *Internet J Orthop Surg*, 4(2).
- Lewis, M. E. (2006) *The Bioarchaeology of Children*, *New England Journal of Medicine*. doi: 10.1017/CBO9780511542473.
- Lewis, M. E. and Gowland, R. (2007) 'Brief and Precarious Lives: Infant Mortality in Contrasting Sites from Medieval and Post-Medieval England (AD 850-1859)', *American Journal of Physical Anthropology*, 134, pp. 117–129. doi: 10.1002/ajpa.20643.
- Lightfoot, E. and O'Connell, T. C. (2016) 'On the Use of Biomineral Oxygen Isotope Data to Identify Human Migrants in the Archaeological Record: Intra-Sample Variation, Statistical Methods and Geographical Considerations.', *PloS one*, 11(4), p. e0153850. doi: 10.1371/journal.pone.0153850.
- Little, D. G., Ramachandran, M. and Schindeler, A. (2007) 'The anabolic and catabolic responses in bone repair', *J Bone Joint Surg Br*, 89-B(4), pp. 425–433. doi: 10.1302/0301-620x.89b4.18301.
- Longinelli, A. (1973) 'Preliminary oxygen-isotope measurements of phosphate from mammal teeth and bones', in *Colloq. Int. CNRS*, pp. 267–271.
- Longinelli, A. (1984) 'Oxygen isotopes in mammal bone phosphate: A new tool for paleohydrological and paleoclimatological research?', *Geochimica et Cosmochimica Acta*, 48(2), pp. 385–390. doi: 10.1016/0016-7037(84)90259-X.
- Lorentz, K. O. *et al.* (2019) 'Use of dental microstructure to investigate the role of prenatal and early life physiological stress in age at death', *Journal of Archaeological Science*. Elsevier, 104(January), pp. 85–96. doi: 10.1016/j.jas.2019.01.007.
- Lovejoy, C. O. *et al.* (1985) 'Chronological metamorphosis of the auricular surface of the ilium: A new method for the determination of adult skeletal age at death', *Am J Phys Anthropol*, 68, pp. 15–28.
- Lucas, A. (1991) 'Programming and adult disease', in Bock, G. and Whelen, J. (eds) *The Childhood Environmental and Adult Disease*. Chinchester: Wiley, pp. 38–55.
- Lucas, A. (1994) 'Role of nutritional programming in determining adult morbidity', *Arch Dis Child*, 71, pp. 288–290.
- Lundberg, C. (2015) 'Place of Death and Place of Rest. Commingled Human Remains from Alba Iulia-Lumea Nouă 2015 Early Eneolithic Funerary Discovery', *Annales Universitatis Apulensis Series Historica*, 19(2), pp. 71–103.

- Luz, B., Kolodny, Y. and Horowitz, M. (1984) 'Fractionation of oxygen isotopes between mammalian bone-phosphate and environmental drinking water', *Geochimica et Cosmochimica Acta*, 48(8), pp. 1689–1693. doi: 10.1016/0016-7037(84)90338-7.
- Maat, G. J. R. (2004) 'Scurvy in adults and youngsters: The Dutch experience. A review of the history and pathology of a disregarded disease', *International Journal of Osteoarchaeology*, 14(2), pp. 77–81. doi: 10.1002/oa.708.
- Macintosh, A. A., Pinhasi, R. and Stock, J. T. (2016) 'Early Life Conditions and Physiological Stress following the Transition to Farming in Central/Southeast Europe: Skeletal Growth Impairment and 6000 Years of Gradual Recovery', *PLoS ONE*, 11(2). doi: 10.1371/journal.pone.0148468.
- Madgearu, A. (2001) 'Salt trade and warfare in Early Medieval Transylvania', *Ephemeris Napocensis*, XI, pp. 271–283.
- Madgearu, A. (2012) 'The Significance of the Early Christian Artefacts in Post-Roman Dacia', *Christianisierung Europas: Entstehung, Entwicklung und Konsolidierung im archäologischen Befund*, pp. 1988–1989.
- Mahoney, P. (2012) 'Incremental enamel development in modern human deciduous anterior teeth', *American Journal of Physical Anthropology*, 147(4), pp. 637–651. doi: 10.1002/ajpa.22029.
- Mahoney, P. *et al.* (2017) 'Enamel biorhythms of humans and great apes: the Havers-Halberg Oscillation hypothesis reconsidered', *Journal of Anatomy*, 230(2), pp. 272–281. doi: 10.1111/joa.12551.
- Makarewicz, C. A. and Sealy, J. (2015) 'Dietary reconstruction, mobility, and the analysis of ancient skeletal tissues: Expanding the prospects of stable isotope research in archaeology', *Journal of Archaeological Science*. Elsevier Ltd, 56, pp. 146–158. doi: 10.1016/j.jas.2015.02.035.
- Margerison, B. J. and Knüsel, C. J. (2002) 'Paleodemographic comparison of a catastrophic and an attritional death assemblage', *American Journal of Physical Anthropology*, 119(2), pp. 134–143. doi: 10.1002/ajpa.10082.
- Marklein, K. E., Leahy, R. E. and Crews, D. E. (2016) 'In sickness and in death: Assessing frailty in human skeletal remains', *American Journal of Physical Anthropology*, 161(2), pp. 208–225. doi: 10.1002/ajpa.23019.
- Marshall, W. A. (1978) 'Puberty', in Falkner, F. and JM, T. (eds) *Human Growth*. Vol 2: Pos. New York: Plenum Press, pp. 141–181.
- Marshall, W. A. and Tanner, J. M. (1969) 'Variations in pattern of pubertal changes in girls', *Archives of Disease in Childhood*, 44(235), pp. 291–303. doi: 10.1136/ad.44.235.291.
- Marshall, W. A. and Tanner, J. M. (1970) 'Variations in the pattern of pubertal changes in boys', *Archives of disease in childhood*. BMJ Publishing Group Ltd, 45(239), pp. 13–23.

- Martin, D. L., Goodman, A. H. and Armelagos, G. J. (1985) 'Skeletal pathologies as indicators of quality and quantity of diet. U: The analysis of prehistoric diet (ur. Gilbert R., Mielke J.)'. New York: Academic Press.
- Masson, M. *et al.* (2015) '7000 year-old tuberculosis cases from Hungary e Osteological and biomolecular evidence', *Tuberculosis*, 95, pp. S13–S17. doi: 10.1016/j.tube.2015.02.007.
- Maurer, A. F. *et al.* (2012) 'Bioavailable $^{87}\text{Sr}/^{86}\text{Sr}$ in different environmental samples - Effects of anthropogenic contamination and implications for isoscapes in past migration studies', *Science of the Total Environment*. Elsevier B.V., 433, pp. 216–229. doi: 10.1016/j.scitotenv.2012.06.046.
- Maxim, Z. *et al.* (2002) 'The astronomical aspects of the orientation of the graves in the burial site of Iclod', in Barlai, K. and Bogнар-Kutzian, I. (eds) *'Unwritten Messages' from the Carpathian Basin*. Budapest: Konkoly Observatory Monographs, pp. 19–29.
- Mayall, P. R. (2018) *An investigation of intentionally modified crania in Georgia and Europe in the Migration Period (4th – 7th c AD)*. University of Melbourne.
- Mays, S. *et al.* (eds) (2013) 'Science and the Dead: a guideline for the destructive sampling of archaeological human remains for scientific analysis', in. The Advisory Panel on Archaeology of Burials in England.
- Mays, S. (2016) 'Estimation of stature in archaeological human skeletal remains from Britain', *American Journal of Physical Anthropology*, 161(4), pp. 646–655. doi: 10.1002/ajpa.23068.
- Mays, S. A. (1998) 'Mays - The Archaeology of Human Bones.pdf', *American Antiquity*, p. 582. doi: 10.2307/2694542.
- Mays, S. A., Richards, M. P. and Fuller, B. T. (2002) 'Bone stable isotope evidence for infant feeding in Medieval England', *Antiquity*, 76(June), pp. 654–656.
- Mays, S., Brickley, M. and Ives, R. (2006) 'Skeletal manifestation of rickets in infants and young children in a historic population from England', *American Journal of Physical Anthropology*, 129(3), pp. 362–374. doi: 10.1002/ajpa.20292.
- McMichael, A. J. (2012) 'Insights from past millennia into climatic impacts on human health and survival', *Proceedings of the National Academy of Sciences*, 109(13), pp. 4730–4737. doi: 10.1073/pnas.1120177109.
- Meinzer, N. J., Steckel, R. H. and Baten, J. (2018) 'Agricultural Specialization, Urbanization, Workload, and Stature', in Steckel, R. H. *et al.* (eds) *The Backbone of Europe: Health, Diet, Work and Violence over Two Millennia*. Cambridge, UK: Cambridge University Press, pp. 231–252.
- Mekota, A.-M. *et al.* (2006) 'Serial analysis of stable nitrogen and carbon isotopes in hair: monitoring starvation and recovery phases of patients suffering from anorexia nervosa', *Rapid Communications in Mass Spectrometry*, 20(10), pp. 1604–1610. doi: 10.1002/rcm.2477.

- van der Merwe, N. J. (1982) 'Carbon Isotopes, Photosynthesis, and Archaeology: Different pathways of photosynthesis cause characteristic changes in carbon isotope ratios that make possible the study of prehistoric human diets', *American Scientist*, 70(6), pp. 596–606.
- Van Der Merwe, N. J. and Vogel, J. C. (1978) '¹³C Content of human collagen as a measure of prehistoric diet in woodland North America', *Nature*. Nature Publishing Group, 276, p. 815. Available at: <https://doi.org/10.1038/276815a0>.
- Metges, C., Kempe, K. and Schmidt, H.-L. (1990) 'Dependence of the carbon-isotope contents of breath carbon dioxide, milk, serum and rumen fermentation products on the δ C value of food in dairy cows', *British Journal of Nutrition*, 63(02), p. 187. doi: 10.1079/BJN19900106.
- Meyer, A. (2016) 'Assessment of diet and recognition of nutritional deficiencies in paleopathological studies: A review', *Clinical Anatomy*. Wiley Online Library, 29(7), pp. 862–869.
- Miller, E. K., Blum, J. D. and Friedland, A. J. (1993) 'Determination of soil exchangeable-cation loss and weathering rates using Sr isotopes', *Nature*. Nature Publishing Group, 362(6419), p. 438.
- Miller, K. E. and Rasmussen, A. (2010) 'War exposure, daily stressors, and mental health in conflict and post-conflict settings: Bridging the divide between trauma-focused and psychosocial frameworks', *Social Science and Medicine*. Elsevier, 70(1), pp. 7–16. doi: 10.1016/j.socscimed.2009.09.029.
- Miranda, R. *et al.* (1983) 'Effect of maternal nutritional status on immunological substances in human colostrum and milk', *The American Journal of Clinical Nutrition*, 37(4), pp. 632–640. doi: 10.1093/ajcn/37.4.632.
- Mischka, C. (2012) 'Late Neolithic Multiphased Settlements in Central and Southern Transylvania: A Geophysical Survey and Test Excavation', *Tells: Social and Environmental Space*. Bonn: Habelt, pp. 153–166.
- Molnár, M. *et al.* (2014) 'Artificially deformed crania from the Hun-Germanic Period (5th–6th century ad) in northeastern Hungary: historical and morphological analysis', *Neurosurgical Focus*, 36(April), p. E1. doi: 10.3171/2014.1.focus13466.
- Montgomery, J. (2002) *Lead and Strontium Isotope Compositions of Human Dental Tissues as an Indicator of Ancient Exposure and Population Dynamics: PhD thesis*. York: Archaeology Data Service. doi: <https://doi.org/10.5284/1000249>.
- Montgomery, J. (2010) 'Passports from the past: Investigating human dispersals using strontium isotope analysis of tooth enamel', *Annals of Human Biology*, 37(3), pp. 325–346. doi: 10.3109/03014461003649297.
- Montgomery, J., Budd, P. and Evans, J. (2000) 'Reconstructing the Lifetime Movements of Ancient People: A Neolithic Case Study from Southern England', *European Journal of Archaeology*, 3(3), pp. 370–385. doi: 10.1177/146195710000300304.

Montgomery, J., Evans, J. A. and Cooper, R. E. (2007) 'Resolving archaeological populations with Sr-isotope mixing models', *Applied Geochemistry*, 22(7), pp. 1502–1514. doi: 10.1016/j.apgeochem.2007.02.009.

Montgomery, J., Evans, J. A. and Neighbour, T. (2003) 'Sr isotope evidence for population movement within the Hebridean Norse community of NW Scotland', *Journal of the Geological Society*, 160(5), pp. 649–653. doi: 10.1144/0016-764903-037.

Montgomery, J., Knüsel, C. J. and Tucker, K. (2011) 'Identifying the origins of decapitate male skeletons from 3 Driffield Terrace, York, through isotope analysis: Reflections of the cosmopolitan nature of Roman York in the times of Caracalla', in Bonogofsky, M. (ed.) *The Bioarchaeology of the Human Head: Decapitation, Decoration, and Deformation*. Gainesville: University Press of Florida, pp. 141–178.

Moorrees, C., Fanning, E. and Hunt, E. (1963) 'Age Variation of Formation Stages for Ten Permanent Teeth', *Journal of Dental Research*. SAGE Publications Inc, 42(6), pp. 1490–1502. doi: 10.1177/00220345630420062701.

Mopin, C. *et al.* (2018) 'Developmental stability and environmental stress: A geometric morphometrics analysis of asymmetry in the human femur', *American Journal of Physical Anthropology*, 167(1), pp. 144–160. doi: 10.1002/ajpa.23613.

Müldner, G., Chenery, C. and Eckardt, H. (2011) 'The "Headless Romans": Multi-isotope investigations of an unusual burial ground from Roman Britain', *Journal of Archaeological Science*. Elsevier Ltd, 38(2), pp. 280–290. doi: 10.1016/j.jas.2010.09.003.

Murphy, A. and Chamberlain, A. (2017) 'Looking forward to look back: How investigations of historical burial populations can inform our interpretations of prehistoric burial practice', in Bradburry, J. and Scarre, C. (eds) *Engaging with the dead: exploring changing human beliefs about death, mortality, and the human body*. Havertown: Oxbow Books Limited, pp. 103–116.

Murray, M. L. and Schoeninger, M. J. (1988) 'Diet, Status, and Complex Social Structure in Iron Age Central Europe: Some Contributions of Bone Chemistry', in Gibson, D. B. and Geselowitz, M. N. (eds) *Tribe and Polity in Late Prehistoric Europe: Demography, Production, and Exchange in the Evolution of Complex Social Systems*. Boston, MA: Springer US, pp. 155–176. doi: 10.1007/978-1-4899-0777-6_7.

Musat, M. and Ardeleanu, I. (1985) *From ancient Dacia to modern romania*. Bucharest: Editura Stiintifica si Enciclopedica.

Musteață, S. (2015) 'Preserving archaeological remains in situ: from the legal to the practical issues. The Romanian case', in Musteață, S. and Caliniuc, Ș. (eds) *Current trends in archaeological heritage perservation: national and international perspectives*. Iasi, Romania: BAR. Available at: <http://ir.obihiro.ac.jp/dspace/handle/10322/3933>.

Nadell, J. A. and Shaw, C. N. (2016) 'Phenotypic plasticity and constraint along the upper and lower limb diaphyses of Homo sapiens', *American Journal of Physical Anthropology*, 159(3), pp. 410–422. doi: 10.1002/ajpa.22889.

- Nava, A., Frayer, D. W. and Bondioli, L. (2019) 'Longitudinal analysis of the microscopic dental enamel defects of children in the Imperial Roman community of Portus Romae (necropolis of Isola Sacra, 2nd to 4th century CE, Italy)', *Journal of Archaeological Science: Reports*. Elsevier, 23(September 2018), pp. 406–415. doi: 10.1016/j.jasrep.2018.11.007.
- Neil, S. *et al.* (2016) 'Isotopic evidence for residential mobility of farming communities during the transition to agriculture in Britain', *Royal Society open science*, 3(1), p. 150522. doi: 10.1098/rsos.150522.
- Neil, S. *et al.* (2017) 'Land use and mobility during the Neolithic in Wales explored using isotope analysis of tooth enamel', *American Journal of Physical Anthropology*, 164(2), pp. 371–393. doi: 10.1002/ajpa.23279.
- Nelson, B. K. *et al.* (1986) 'Effects of diagenesis on strontium, carbon, nitrogen and oxygen concentration and isotopic composition of bone', *Geochimica et Cosmochimica Acta*, 50(9), pp. 1941–1949. doi: 10.1016/0016-7037(86)90250-4.
- Newman, P. B. (2007) *Growing up in the Middle Ages*. McFarland.
- Newman, S. L. and Gowland, R. L. (2015) 'The use of non-adult vertebral dimensions as indicators of growth disruption and non-specific health stress in skeletal populations', *American Journal of Physical Anthropology*, 158(1), pp. 155–164. doi: 10.1002/ajpa.22770.
- Newman, S. L., Gowland, R. L. and Caffell, A. C. (2019) 'North and south: A comprehensive analysis of non-adult growth and health in the industrial revolution (AD 18th-19th C), England', *American Journal of Physical Anthropology*, (October 2018), pp. 1–18. doi: 10.1002/ajpa.23817.
- Ngland, S. E. *et al.* (2000) 'Movements of Ancient People', *European Journal of Archaeology*, 3(3), pp. 370–385.
- Niculescu, G. A. (2005) 'ARCHAEOLOGY, NATIONALISM AND "THE HISTORY OF THE ROMANIANS" (2001)', *DACIA, N.S., tomes*, 18(2001), pp. 99–124.
- Nier, A. O. (1940) 'A mass spectrometer for routine isotope abundance measurements', *Review of Scientific Instruments*. AIP, 11(7), pp. 212–216.
- Niță, A. and Roșian, G. (2012) 'Some aspects regarding the territorial evolution of Odoerheiu Secuiesc Town', *Geographia Napocensis*, (1).
- Noche-Dowdy, L. D. (2015) *Multi-Isotope Analysis to Reconstruct Dietary and Migration Patterns of an Avar Population from Sajópetri, Hungary, AD 568-895*. University of South Florida.
- Nyárádi, Z. (2017) *Lessons from an excavation dig: Pinewood devastated Medieval Church*. Odoerheiu Secuiesc.
- O'Connell, L. (2004) 'Guidance on recording age at death in adults', in Brickley, M. and McKinley, J. I. (eds) *Guidelines to the standards for recording human remains*. Southampton: British Association for Biological Anthropology and Osteoarchaeology, pp. 18–21.

- O'Connell, T. C. *et al.* (2012) 'The diet-body offset in human nitrogen isotopic values: A controlled dietary study', *American Journal of Physical Anthropology*, 149(3), pp. 426–434. doi: 10.1002/ajpa.22140.
- O'Connell, T. C. and Hedges, R. E. M. (1999) 'Investigations into the effect of diet on modern human hair isotopic values', *American Journal of Physical Anthropology*, 108(4), pp. 409–425. doi: 10.1002/(SICI)1096-8644(199904)108:4<409::AID-AJPA3>3.0.CO;2-E.
- Olsen, K. C. *et al.* (2014) 'Intraskkeletal isotopic compositions ($\delta^{13}\text{C}$, $\delta^{15}\text{N}$) of bone collagen: Nonpathological and pathological variation', *American Journal of Physical Anthropology*, 153(4), pp. 598–604. doi: 10.1002/ajpa.22459.
- Oppenheimer, S. J. and Snodgrass, G. J. (1980) 'Neonatal rickets. Histopathology and quantitative bone changes.', *Archives of Disease in Childhood*, 55(12), pp. 945–949. doi: 10.1136/adc.55.12.945.
- Orme, N. (2003) *Medieval children*. Yale University Press.
- Ortner, DJ (ed.) (2003) *Identification of pathological conditions in human skeletal remains*. 2nd edn. San Diego: Academic Press is an imprint of Elsevier Lt.
- Ortner, D (2003) 'Metabolic Disorders', in Ortner, D. J. (ed.) *Identification of Pathological Conditions in Human Skeletal Remains*. London: Academic Press, pp. 398–418.
- Ortner, D. J. (1999) 'Male-female immune reactivity and its implications for interpreting evidence in human skeletal paleopathology', in Grauer, A. L. and Stuart-Macadam, P. (eds) *Sex and gender in paleopathological perspective*. Cambridge: Cambridge University Press. p, pp. 79–92.
- Ortner, D. J. and Ericksen, M. F. (1997) 'Bone changes in the human skull probably resulting from scurvy in infancy and childhood', *International Journal of Osteoarchaeology*, 7(3), pp. 212–220. doi: 10.1002/(SICI)1099-1212(199705)7:3<212::AID-OA346>3.0.CO;2-5.
- Ortner, D. J. and Mays, S. (1998) 'Dry-bone Manifestations of Rickets in Infancy and Early Childhood', *International Journal of Osteoarchaeology*, 8(1), pp. 45–55. doi: 10.1002/(SICI)1099-1212(199801/02)8:1<45::AID-OA405>3.0.CO;2-D.
- Ortner, D. J. and Putschar, W. G. J. (1981) *Identification of pathological conditions in human skeletal remains*, *Smithsonian*. Washington: Smithsonian Institution Press. doi: 10.1017/CBO9781107415324.004.
- Ortner, D. and Turner-Walker, G. (2003) 'The Biology of Skeletal Tissues', in Ortner, D. (ed.) *Identification of pathological conditions in human skeletal remains*. San Diego, USA: Elsevier Academic Press, pp. 11–36.
- Osterholtz, A. J. *et al.* (2014) 'Possible prenatal and perinatal scurvy at Telekfalva, Romania', *American Journal of Physical Anthropology*, 153(S53), p. 201.
- Padayatty, S. J. and Levine, M. (2001) 'New insights into the physiology and pharmacology of vitamin C', *Cmaj*, 164(3), pp. 353–355.

- Palincaş, N. (2014) 'Body and Social Order in Middle Bronze Age Transylvania (Central Romania, c. 1900 – 1450 bc)', *European Journal of Archaeology*. Nona Palincaş, 17(2), pp. 301–328. doi: 10.1179/1461957114Y.0000000059.
- Panter-Brick, C. (1998) *Biosocial perspectives on children*. Cambridge University Press.
- Papahagi, A. (2015) 'Lost Libraries and Surviving Manuscripts: The Case of Medieval Transylvania', *Library & Information History*, 31(1), pp. 35–53. doi: 10.1179/1758348914Z.00000000073.
- Papp, J. (2013) 'Collecting antiquities and curiosities in eighteenth-century Transylvania: the Saxon Lutheran pastor Laurentius Weidenfelder and his network', *Journal of the History of Collections*, 25(3), pp. 373–389. doi: 10.1093/jhc/fht004.
- Pearce, S. H. and Cheetham, T. D. (2010) 'Diagnosis and management of vitamin D deficiency', *BMJ*, 340(jan11 1), pp. b5664–b5664. doi: 10.1136/bmj.b5664.
- Pearson, J. A. *et al.* (2010) 'Exploring the relationship between weaning and infant mortality: An isotope case study from Aşıklı Höyük and Çayönü Tepesi', *American Journal of Physical Anthropology*, 143(3), pp. 448–457. doi: 10.1002/ajpa.21335.
- Pearson, J. A. *et al.* (2015) 'Stable carbon and nitrogen isotope analysis and dietary reconstruction through the life course at Neolithic Çatalhöyük, Turkey', *J. Soc. Archaeol.*, 15(2), pp. 210–232.
- Pedersen, D. (2002) 'Political violence, ethnic conflict, and contemporary wars: Broad implications for health and social well-being', *Social Science and Medicine*, 55(2), pp. 175–190. doi: 10.1016/S0277-9536(01)00261-1.
- Pellegrini, M., Lee-Thorp, J. A. and Donahue, R. E. (2011) 'Exploring the variation of the $\delta^{18}O_p$ and $\delta^{18}O_c$ relationship in enamel increments', *Palaeogeography, Palaeoclimatology, Palaeoecology*, 310(1–2), pp. 71–83. doi: 10.1016/j.palaeo.2011.02.023.
- Pendery, S. and Koon, H. (2013) 'Scurvy's impact on European colonization in Northeastern North America', in Pope, P. and Lewis-Simpson, S. (eds) *Exploring Atlantic Transitions: Archaeologies of transience and permanence in new founds lands*. Woodbridge, UK: The Boydell Press, pp. 57–65.
- Pettifor, J. (2003) 'Nutritional rickets', in Glorieux, F., Pettifor, J., and Jüppner, H. (eds) *Pediatric bone biology and diseases*. San Diego: Academic Press, pp. 541–565.
- Pettifor, J. and Daniels, E. (1997) 'Vitamin D deficiency and nutritional rickets in children', in Feldman, D., Glorieux, F., and Pike, J. (eds) *Vitamin D*. San Diego: Academic Press, pp. 663–679.
- Phenice, T. (1967) 'A newly developed visual method of sexing the Os Pubis', *Am J Phys Anthropol*, 30, pp. 297–302.
- Pichot, P. and Hassan, J. (1973) 'Masked depression and depressive equivalents—Problems of definition and diagnosis', *Masked depression*. Huber Bern, Switzerland, pp. 61–76.

- Pimentel, L. (2003) 'Scurvy: historical review and current diagnostic approach.', *The American journal of emergency medicine*, 21(4), pp. 328–32. doi: 10.1016/S0735-6757(03)00083-4.
- Pollard, A. M., Heron, C. and Armitage, R. A. (2017) *Archaeological Chemistry*. 3rd Editio. Cambridge, UK: Royal Society of Chemistry. Available at: https://books.google.co.uk/books?id=G2_ZDQAAQBAJ.
- Pop, I.-A. (2013) 'Religiones and Nacione in Transylvania during the 16th Century: between acceptance and exclusion', *Journal for the Study of Religions and Ideologies*, 12(34), pp. 209–236.
- Pop, I. and Nagler, T. (2010) *The history of Transylvania: Vol I (until 1541)*. Cluj-Napoca: Romanian Academy: Center for Transylvanian Studies.
- Popa-Gorjanu, C. (2012) 'Transylvania Identities in the Middle Ages', pp. 175–190.
- Power, D. (2006) *Short Oxford History of Europe: Central Middle Ages (950-1320 AD)*. Oxford: Oxford University Press.
- Prader, A., Tanner, J. M. and von Harnack, G. A. (1963) 'Catch-up growth following illness or starvation: An example of developmental canalization in man', *The Journal of Pediatrics*. Elsevier, 62(5), pp. 646–659. doi: 10.1016/S0022-3476(63)80035-9.
- Previt e-Orton, C. W. (1975) *Cambridge Medieval History, Shorter: Volume 1, The Later Roman Empire to the Twelfth Century*. Cambridge University Press (Later Roman Empire to the Twelfth Century). Available at: <https://books.google.co.uk/books?id=RXU5AAAIAAJ>.
- Price, T. ., Grupe, G. and Schr oter, P. (1994) 'Reconstruction of migration patterns in the Bell Beaker period by stable strontium isotope analysis', *Applied Geochemistry*, 9(4), pp. 413–417. doi: 10.1016/0883-2927(94)90063-9.
- Price, T. D. *et al.* (2004) 'Strontium isotopes and prehistoric human migration: The Bell Beaker period in central Europe', *European Journal of Archaeology*, 7(1), pp. 9–40. doi: 10.1177/1461957104047992.
- Price, T. D., Burton, J. H. and Bentley, R. A. (2002) 'The characterisation of biologically-available strontium isotope ratios for investigation of prehistoric migration', *Archaeometry*, 44(1), pp. 117–135. Available at: <http://discovery.ucl.ac.uk/172338/>.
- Prinze, Z. (1999) *Scurvy and its prevention and control in major emergencies*. Dept. of N. World Health Organisation. doi: WHO/NHD/99.11.
- Quinn, C. P. and Ciugudean, H. (2018) 'Settlement placement and socio-economic priorities: Dynamic landscapes in Bronze Age Transylvania', *Journal of Archaeological Science: Reports*. Elsevier, 19(April 2017), pp. 936–948. doi: 10.1016/j.jasrep.2017.05.046.
- Radu, C. *et al.* (2015) 'Multiple Cases with Probable Treponemal Infection from 16th to 19th Centuries Romania', *International Journal of Osteoarchaeology*, 26(August 2014), pp. 563–573. doi: 10.1002/oa.2444.

- Radu, C. and Soficaru, A. D. (2016) 'Dental developmental defects in a subadult from 16th–19th centuries Bucharest, Romania', *International Journal of Paleopathology*. Elsevier Inc., 15, pp. 33–38. doi: 10.1016/j.ijpp.2016.08.001.
- Raisz, L. G. (2005) 'Pathogenesis of osteoporosis : concepts , conflicts , and prospects Find the latest version : Science in medicine Pathogenesis of osteoporosis : concepts , conflicts , and prospects', *The Journal of Clinical investigation*, 115(12), pp. 3318–3325. doi: 10.1172/JCI27071.3318.
- Raxter, M. H. *et al.* (2008) 'Stature estimation in ancient Egyptians: A new technique based on anatomical reconstruction of stature', *American Journal of Physical Anthropology*, 136(2), pp. 147–155. doi: 10.1002/ajpa.20790.
- Raxter, M. H., Ruff, C. B. and Auerbach, B. M. (2007) 'Technical note: Revised fully stature estimation technique', *American Journal of Physical Anthropology*, 133(2), pp. 817–818. doi: 10.1002/ajpa.20588.
- Redfern, R. C. *et al.* (2016) 'Going south of the river: A multidisciplinary analysis of ancestry, mobility and diet in a population from Roman Southwark, London', *Journal of Archaeological Science*, 74, pp. 11–22. doi: 10.1016/j.jas.2016.07.016.
- Reid, D. J. and Dean, M. C. (2000) 'Brief communication: The timing of linear hypoplasia on human anterior teeth', *Am. J. Phys. Anthropol.*, 113(November), pp. 135–139. doi: 10.1002/1096-8644(200009)113.
- Reid, D. J. and Dean, M. C. (2006) 'Variation in modern human enamel formation times', *Journal of Human Evolution*, 50(3), pp. 329–346. doi: 10.1016/j.jhevol.2005.09.003.
- Reitsema, L. J. and McIlvaine, B. K. (2014) 'Reconciling “stress” and “health” in physical anthropology: What can bioarchaeologists learn from the other subdisciplines?', *American Journal of Physical Anthropology*, 155(2), pp. 181–185. doi: 10.1002/ajpa.22596.
- Reitsema, L. J., Vercellotti, G. and Boano, R. (2016) 'Subadult dietary variation at Trino Vercellese, Italy, and its relationship to adult diet and mortality', *American Journal of Physical Anthropology*, 160(4), pp. 653–664. doi: 10.1002/ajpa.22995.
- Retzius, A. (1837) 'Bemerkungen über den inneren Bau der Zähne', *mit besonderer Rücksicht auf dem in Zahnknochen vorkommenden Röhrenbau.*(Müllers) *Arch Anat Physiol*, 1837, pp. 486–566.
- Reynard, L. M. and Tuross, N. (2015) 'The known, the unknown and the unknowable: Weaning times from archaeological bones using nitrogen isotope ratios', *Journal of Archaeological Science*. Elsevier Ltd, 53, pp. 618–625. doi: 10.1016/j.jas.2014.11.018.
- Ribot, I. and Roberts, C. A. (1996) 'A Study of Non-specific Stress Indicators and Skeletal Growth in Two Mediaeval Subadult Populations', *Journal of Archaeological Science*, 23(1), pp. 67–79. doi: 10.1006/jasc.1996.0006.
- Robb, J. *et al.* (2001) 'Social “status” and biological “status”: A comparison of grave goods and skeletal indicators from Pontecagnano', *American Journal of Physical Anthropology*, 115(3), pp. 213–222. doi: 10.1002/ajpa.1076.

Roberts, C. A. (2006) 'A View from Afar: Bioarchaeology in Britain', in Buikstra, J. E. and Beck, L. A. (eds) *Bioarchaeology: the contextual analysis of human remains*. London: Academic Press, pp. 417–440.

Roberts, C. A. *et al.* (2016) "'Til Poison Phosphorous Brought them Death": A potentially occupationally-related disease in a post-medieval skeleton from north-east England.', *International Journal of Paleopathology*. Elsevier Inc., 13, pp. 39–48. doi: 10.1016/j.ijpp.2015.12.001.

Roberts, C. A. (2018) *Human remains in archaeology : a handbook*. 2nd edn. York, UK: Council for British Archaeology.

Roberts, C. A. and Connell, B. (2004) 'Guidance on recording palaeopathology', in Brickley, M. and McKinley, J. I. (eds) *Guidelines to the standards for recording human remains*. Southampton: British Association for Biological Anthropology and Osteoarchaeology, pp. 34–40. Available at: <http://scholar.google.com/scholar?hl=en&btnG=Search&q=intitle:Guidelines+to+the+Standards+for+Recording+Human+Remains#0>.

Roberts, C. A. and Steckel, R. H. (2018) 'The Developmental Origins of Health and Disease: Early Life Health Conditions and Adult Age at Death in Europe', *The Backbone of Europe: Health, Diet, Work and Violence over Two Millennia*, pp. 325–351.

Roberts, C. and Manchester, K. (2005a) *The Archaeology of Disease*. 3rd edn. Stroud: The History Press.

Roberts, C. and Manchester, K. (2005b) 'The Study of Paleopathology', *The Archaeology of Disease*, 44(January), pp. 1–21.

Roberts, P. *et al.* (2017) 'Calling all archaeologists: guidelines for terminology, methodology, data handling, and reporting when undertaking and reviewing stable isotope applications in archaeology', *Rapid Communications in Mass Spectrometry*, (November 2017), pp. 361–372. doi: 10.1002/rcm.8044.

Ruff, C. B. (2008) 'Biomechanical analyses of archaeological human skeletons', *Biological anthropology of the human skeleton*. John Wiley & Sons, Ed, 2, pp. 183–206.

Ruffer, M. A. (1913) 'Studies in paleopathology in Egypt', *The Journal of Pathology and Bacteriology*, 18, pp. 149–162.

Sachan, A. *et al.* (2005) 'High prevalence of vitamin D deficiency among pregnant women and their newborns in northern India', *The American journal of clinical nutrition*. Oxford University Press, 81(5), pp. 1060–1064.

Said-Mohamed, R., Pettifor, J. M. and Norris, S. A. (2017) 'Life History theory hypotheses on child growth: Potential implications for short and long-term child growth, development and health', *American Journal of Physical Anthropology*, (October 2017), pp. 4–19. doi: 10.1002/ajpa.23340.

- Sandberg, P. A. *et al.* (2014) 'Intra-tooth stable isotope analysis of dentine: A step toward addressing selective mortality in the reconstruction of life history in the archaeological record', *American Journal of Physical Anthropology*, 155(2), pp. 281–293. doi: 10.1002/ajpa.22600.
- Sankar, M. J. *et al.* (2015) 'Optimal breastfeeding practices and infant and child mortality: A systematic review and meta-analysis', *Acta Paediatrica, International Journal of Paediatrics*, 104, pp. 3–13. doi: 10.1111/apa.13147.
- Saunders, S. R. *et al.* (1992) 'A test of several methods of skeletal age estimation using a documented archaeological sample', *Can. Soc. Forens. Sci.*, 25(2), pp. 97–118.
- Scheuer, J. and Black, S. (2000) *Developmental Juvenile Osteology*. London: Elsevier Academic Press.
- Scheuer, J. L. and Black, S. (2000) 'Development and ageing of the juvenile skeleton', in Cox, M. and Mays, S. (eds) *Human osteology in archaeology and forensic science*. London: Greenwich Medical Media Ltd, pp. 9–22.
- Schmidt, J., Kwok, C. and Keenleyside, A. (2016) 'Infant feeding practices and childhood diet at Apollonia Pontica: Isotopic and dental evidence', *American Journal of Physical Anthropology*, 159(2), pp. 284–299. doi: 10.1002/ajpa.22874.
- Schoenheimer, R. (1964) 'The Dynamic State of Body Constituents (1942)', *Schönheimer The Dynamic State of the Body Constituents 1942*.
- Schoeninger, M. J. and DeNiro, M. J. (1982) 'Carbon isotope ratios of apatite from fossil bone cannot be used to reconstruct diets of animals', *Nature*, 297(5867), pp. 577–578. doi: 10.1038/297577a0.
- Schoeninger, M. J. and DeNiro, M. J. (1984) 'Nitrogen and carbon isotopic composition of bone collagen from marine and terrestrial animals', *Geochimica et Cosmochimica Acta*, 48(4), pp. 625–639. doi: 10.1016/0016-7037(84)90091-7.
- Schoeninger, M. J., DeNiro, M. J. and Tauber, H. (1983) 'Stable Nitrogen Isotope Ratios of Bone Collagen Reflect Marine and Terrestrial Components of Prehistoric Human Diet', *Science*, 220(4604), pp. 1381–1383.
- Schoeninger, M. J., Moore, J. and Sept, J. M. (1999) 'Subsistence strategies of two "savanna" chimpanzee populations: the stable isotope evidence.', *American journal of primatology*, 49(4), pp. 297–314. doi: 10.1002/(SICI)1098-2345(199912)49:4<297::AID-AJP2>3.0.CO;2-N.
- Schour, I. and Poncher, H. G. (1937) 'Rate of apposition of enamel and dentin, measured by the effect of acute fluorosis', *American Journal of Diseases of Children*, 54, pp. 757–776.
- Schulting, R. J. (1998) 'Slighting the sea : stable isotope evidence for the transition to farming in northwestern Europe', *Documenta praehistorica / Porocilo o raziskovanju paleolitika, neolitika in eneolitika v Sloveniji*, 25(January 1998), pp. 203–218.

- Schwarcz, H. P. and Schoeninger, M. J. (1991) 'Stable isotope analyses in human nutritional ecology', *American Journal of Physical Anthropology*, 34(13 S), pp. 283–321. doi: 10.1002/ajpa.1330340613.
- Sealy, J. *et al.* (1987) 'Nitrogen isotopic ecology in southern Africa: Implications for environmental and dietary tracing', *Geochimica et Cosmochimica Acta*, 51, pp. 2707–2718.
- Sealy, J., Armstrong, R. and Schrire, C. (1995) 'Beyond lifetime averages: tracing life histories through isotopic analysis of different calcified tissues from archaeological human skeletons', *Antiquity* 69, pp. 290–300. Available at: [https://www-cambridge-org.ezphost.dur.ac.uk/core/services/aop-cambridge-core/content/view/31115D0436C3B7A12A160DBC97501BAD/S0003598X00064693a.pdf/beyond_lifetime_averages_tracing_life_histories_through_isotopic_analysis_of_different_calcified_tissues_from](https://www.cambridge-org.ezphost.dur.ac.uk/core/services/aop-cambridge-core/content/view/31115D0436C3B7A12A160DBC97501BAD/S0003598X00064693a.pdf/beyond_lifetime_averages_tracing_life_histories_through_isotopic_analysis_of_different_calcified_tissues_from) (Accessed: 25 November 2018).
- Sealy, J. C. *et al.* (1991) '⁸⁷Sr/⁸⁶Sr as a dietary indicator in modern and archaeological bone', *Journal of Archaeological Science*. Elsevier, 18(3), pp. 399–416.
- Seghedi, I. *et al.* (2004) 'Neogene-Quaternary magmatism and geodynamics in the Carpathian- Pannonian region: A synthesis', *Lithos*, 72(3–4), pp. 117–146. doi: 10.1016/j.lithos.2003.08.006.
- Selye, H. (1936) 'A syndrome produced by diverse nocuous agents', *Nature*. London, 138(3479), p. 32.
- Selye, H. (1956) *The stress of life*.
- Selye, H. (1974) *Stress without distress*. Philadelphia, USA: Lippincott.
- Serenius, F., Elidrissy, A. T. H. and Dandona, P. (1984) 'Vitamin D nutrition in pregnant women at term and in newly born babies in Saudi Arabia', *Journal of Clinical Pathology*, 37(4), pp. 444–447. doi: 10.1136/jcp.37.4.444.
- Shapland, F. and Lewis, M. E. (2013) 'Brief communication: A proposed osteological method for the estimation of pubertal stage in human skeletal remains', *American Journal of Physical Anthropology*, 151(2), pp. 302–310. doi: 10.1002/ajpa.22268.
- Sharp, Z. (2017) 'Principles of stable isotope geochemistry', *Delta*, p. 344. doi: 10.1016/S0037-0738(97)00056-0.
- Sherratt, A. (1993) 'What Would a Bronze-Age World System Look Like? Relations Between Temperate Europe and the Mediterranean in Later Prehistory', *Journal of European Archaeology*. Routledge, 1(2), pp. 1–58. doi: 10.1179/096576693800719293.
- Siebke, I. *et al.* (2019) 'Those who died very young—Inferences from $\delta^{15}\text{N}$ and $\delta^{13}\text{C}$ in bone collagen and the absence of a neonatal line in enamel related to the possible onset of breastfeeding', *American Journal of Physical Anthropology*, (November 2018), pp. 1–14. doi: 10.1002/ajpa.23847.

- Sisodia, S. and Singh, B. N. (2012) 'Experimental Evidence for Nutrition Regulated Stress Resistance in *Drosophila ananassae*', 7(10). doi: 10.1371/journal.pone.0046131.
- Skoglund, P. *et al.* (2013) 'Accurate sex identification of ancient human remains using DNA shotgun sequencing', *Journal of Archaeological Science*. Elsevier Ltd, 40(12), pp. 4477–4482. doi: 10.1016/j.jas.2013.07.004.
- Snoddy, A. M. E. *et al.* (2017) 'Scurvy at the agricultural transition in the Atacama desert (ca 3600–3200 BP): nutritional stress at the maternal-foetal interface?', *International Journal of Paleopathology*. Elsevier, 18(November 2016), pp. 108–120. doi: 10.1016/j.ijpp.2017.05.011.
- Snoddy, A. M. E., Buckley, H. R. and Halcrow, S. E. (2016) 'More than metabolic: Considering the broader paleoepidemiological impact of Vitamin D deficiency in bioarchaeology', *American Journal of Physical Anthropology*, 160(2), pp. 183–196. doi: 10.1002/ajpa.22968.
- Soddy, F. (1913) 'Intra-atomic Charge', *Nature*, 92(2301), pp. 399–400. doi: 10.1038/092399c0.
- Soficaru, A. *et al.* (2014) 'Evaluation of discriminant functions for sexing skulls from visually assessed traits applied in the Rainer Osteological Collection (Bucharest, Romania)', *Homo*, 65(6), pp. 464–475. doi: 10.1016/j.jchb.2014.08.004.
- Solheim, T. (1993) 'A new method for dental age estimation in adults', *Forensic Science International*, 59(2), pp. 137–147. doi: 10.1016/0379-0738(93)90152-Z.
- Sorocovschi, V. and Pandi, G. (2002) 'Characteristics of river flow in the Transylvanian Basin', in Brebbia, C. A. and Zannetti, P. (eds) *Development and Application of Computer Techniques to Environmental Studies*. Southampton: WIT Press, pp. 489–498. Available at: <https://www.witpress.com/elibrary/wit-transactions-on-ecology-and-the-environment/51/391>.
- Steckel, R. (2005) 'Young adult mortality following severe physiological stress in childhood: Skeletal evidence', *Economics and Human Biology* 2, 3, pp. 314–328. doi: 10.1016/j.ehb.2005.05.006.
- Steckel, R. H. and Kjellström, A. (2018) *Measuring Community Health Using Skeletal Remains: A Health Index for Europe, The Backbone of Europe: Health, Diet, Work and Violence over Two Millennia*. Edited by R. Steckel *et al.* Cambridge: Cambridge University Press. doi: 10.1017/9781108379830.005.
- Steckel, R. R. H. (2005) 'Young adult mortality following severe physiological stress in childhood: Skeletal evidence', *Economics and Human Biology*, 3(2 SPEC. ISS.), pp. 314–328. doi: 10.1016/j.ehb.2005.05.006.
- Stewart, N. A. *et al.* (2016) 'The identification of peptides by nanoLC-MS/MS from human surface tooth enamel following a simple acid etch extraction', *RSC Advances*, 6(66), pp. 61673–61679. doi: 10.1039/c6ra05120k.

- Stewart, N. A. *et al.* (2017) 'Sex determination of human remains from peptides in tooth enamel'. doi: 10.1073/pnas.1714926115.
- Stone, I. (1966) 'On the Genetic Etiology of Scurvy', *Acta geneticae medicae et gemellologiae*, 15(4), pp. 345–350. doi: 10.1017/s1120962300014931.
- Stuart-Macadam, P. (1991) 'Anemia in roman Britain: poundbury camp', in Bush, H. and Zvelebil, M. (eds) *Health in Past Societies: Biocultural Interpretations of Human Skeletal Remains in Archaeological Contexts*. Oxford, UK: British Archaeological Research International Series, pp. 101–113.
- Stuart-Macadam, P. L. and Dettwyler, Katherine A (1995) *Breastfeeding*. Edited by P. L. Stuart-Macadam and K.A. Dettwyler. London, UK: Routledge of Taylor and Francis Group.
- Suess, H. E. (1958) 'The radioactivity of the atmosphere and hydrosphere.', *Annual review of nuclear science*, 8(February), pp. 243–256. doi: 10.1146/annurev.ns.18.120168.002203.
- Taylor, T. (2011) 'Aspects of Settlement Diversity and its classification in Southeast Europe before the Roman Period', *World Archaeology*, 19(1), pp. 1–22.
- Tejral, J. (2012) 'Cultural or Ethnic Changes? Continuity and Discontinuity on the Middle Danube ca A.D. 500', in Ivanišević, V. and Kazanskii, M. (eds) *The Pontic-Danubian Realm in the Period of the Great Migration*. Paris-Beograd, pp. 115–188.
- Temple, D. H. and Goodman, A. H. (2014) 'Bioarcheology has a "health" problem: Conceptualizing "stress" and "health" in bioarcheological research', *American Journal of Physical Anthropology*, 155(2), pp. 186–191. doi: 10.1002/ajpa.22602.
- Thayer, Z. M. and Kuzawa, C. W. (2014) 'Early origins of health disparities: material deprivation predicts maternal evening cortisol in pregnancy and offspring cortisol reactivity in the first few weeks of life', *American journal of human biology : the official journal of the Human Biology Council*, 26(6), pp. 723–730. doi: 10.1002/ajhb.22532.
- Thermo Electron Corporation (2004) *Finnigan GasBench II™ Operating Manual*. Bremen: Thermo Electron Corporation.
- Thomas, S. L. and Thomas, S. D. M. (2004) 'Displacement and health', *British Medical Bulletin*, 69, pp. 115–127. doi: 10.1093/bmb/ldh009.
- Thompson, E. (1982) *Romans and Barbarians: The decline of the Western Empire*. 2nd edn. London: The University of Wisconsin Press, Ltd.
- Thomson, J. J. *et al.* (1921) 'Discussion on isotopes', *Proceedings of the Royal Society of London. Series A, Containing Papers of a Mathematical and Physical Character*. JSTOR, 99(697), pp. 87–104.
- Tickner, F. J. and Medvei, V. C. (1958) 'Scurvy and the health of European crews in the Indian ocean in the seventeenth century', *Medical History*. 2012/08/16. Cambridge University Press, 2(1), pp. 36–46. doi: DOI: 10.1017/S0025727300023255.

- Tiplic, I. M. and Tiplic, M. E. (2014) 'Between cremation and inhumation the re-birth of Christianity in Transylvania (7th-10th century A.D.)', *European Journal of Science and Theology*, 10(3), pp. 171–177.
- Todd, M. (1995) *The Early Germans*. 2nd edn. Oxford: Blackwell Publishing, Inc.
- Todd, T. W. (1920) 'Age changes in the pubic bone. I. The male white pubis', *American Journal of Physical Anthropology*. Wiley Online Library, 3(3), pp. 285–334.
- Tóth, A. *et al.* (2018) 'The environmental history of a former salt town in Transylvania (Sic, Northern Romania)', *Acta Archaeologica Academiae Scientiarum Hungaricae*, 69(1), pp. 185–206. doi: 10.1556/072.2018.69.1.8.
- Trotter, M. (1970) 'Estimation of Stature from Intact Long Limb Bones', *Personal Identification in Mass Disasters*, pp. 71–83.
- Trotter, M. and Gleser, G. (1944) *Estimation of stature from long bones of American whites and negroes*.
- Trotter, M. and Gleser, G. (1952) 'Estimation of stature from long bones of American Whites and Negroes', *American Journal of Physical Anthropology*, 10(4), pp. 463–514. doi: 10.1002/ajpa.1330100407.
- Turekian, K. K. and Kulp, J. L. (1956) 'Strontium content of human bones.', *Science (Washington)*. American Association for the Advancement of Science, 184, pp. 405–406.
- Tuross, N., Behrensmeyer, A. K. and Eanes, E. D. (1989) 'Strontium increases and crystallinity changes in taphonomic and archaeological bone', *Journal of Archaeological Science*. Elsevier, 16(6), pp. 661–672.
- Tykot, R. H. (2006) 'Isotope Analyses and the Histories of Maize', *Histories of Maize*, pp. 131–142. doi: 10.1016/B978-012369364-8/50262-X.
- Ubelaker, D. H. (2006) 'The Changing Role of Skeletal Biology at the Smithsonian', in Buikstra, J. E. and Beck, L. A. (eds) *Bioarchaeology: the contextual analysis of human remains*. Academic Press.
- Ubelaker, D. H. and De La Paz, J. S. (2012) 'Skeletal Indicators of Pregnancy and Parturition: A Historical Review', *Journal of Forensic Sciences*, 57(4), pp. 866–872. doi: 10.1111/j.1556-4029.2012.02102.x.
- Ubelaker, D. H. and Pap, I. (2008) 'Human Skeletal Biology from the Arpadian Age of Northeastern Hungary', *Anthropologie*, XLVI(1), pp. 25–36.
- Ubelaker, D. H. and Pap, I. (2009) 'Skeletal Evidence for Morbidity and Mortality in Copper Age Samples from Northeastern Hungary', *International Journal of Osteoarchaeology*, 19, pp. 23–35. doi: 10.1002/oa.

- Ubelaker, D. H., Pap, I. and Graver, S. (2006) 'Morbidity and Mortality in the Neolithic of Northeastern Hungary', *Anthropology*, 44(3), pp. 241–257. Available at: <https://media-proquest-com.virtual.anu.edu.au/media/pq/classic/doc/3228650921/fmt/pi/rep/NONE?cit%3Aauth=Ubelaker%2C+D+H%3BPap%2C+I%3BGraver%2C+S&cit%3Atitle=Morbidity+and+mortality+in+the+Neolithic+of+northeastern+Hungary&cit%3Apub=Anthropologie&cit%3Avo>.
- Urey, H. C. (1947) 'The thermodynamic properties of isotopic substances', *Journal of the Chemical Society (Resumed)*. Royal Society of Chemistry, pp. 562–581.
- Urey, H. C. and Greiff, L. J. (1935) 'Isotopic exchange equilibria', *Journal of the American Chemical Society*. ACS Publications, 57(2), pp. 321–327.
- Vadas, A. and Racz, L. (2011) 'Climatic Changes in the Carpathian Basin during the Middle Ages: The State of Research', *Research*, pp. 199–227.
- Vaiglova, P. *et al.* (2018) 'Of cattle and feasts: Multi-isotope investigation of animal husbandry and communal feasting at Neolithic Makryialos, northern Greece', *PLoS ONE*, 13(6), pp. 1–30. doi: 10.1371/journal.pone.0194474.
- Voas, M. *et al.* (2018) 'Milk and Honey: Isotopic Reconstruction of Infant Weaning in Medieval Transylvania', in *The 87th Annual Meeting of the American Association of Physical Anthropologists*. Austin, TX.
- Voerkelius, S. *et al.* (2010) 'Strontium isotopic signatures of natural mineral waters, the reference to a simple geological map and its potential for authentication of food', *Food Chemistry*. Elsevier Ltd, 118(4), pp. 933–940. doi: 10.1016/j.foodchem.2009.04.125.
- Wadhwa, P. D. *et al.* (2010) 'Developmental origins of health and disease: Brief history of the approach and current focus on epigenetic mechanisms', *Seminars in reproductive medicine*, 27(5), pp. 358–368. doi: 10.1055/s-0029-1237424.Developmental.
- Waldron, T. (1994) *Counting the Dead: The Epidemiology of Skeletal Populations*. Wiley. Available at: <https://books.google.co.uk/books?id=NElrAAAAMAAJ>.
- Waldron, T. (2009) *Palaeopathology*. New York: Cambridge University Press.
- Walker, P. L. *et al.* (2009) 'The causes of porotic hyperostosis and cribra orbitalia: A reappraisal of the iron-deficiency-anemia hypothesis', *American Journal of Physical Anthropology*, 139(2), pp. 109–125. doi: 10.1002/ajpa.21031.
- Waters-Rist, A. and Katzenberg, M. (2009) 'The effect of growth on stable nitrogen isotope ratios in subadult bone collagen', *International Journal of Osteoarchaeology*, 20(May 2008), pp. 172–191. doi: 10.1002/oa.
- Watts, R. (2011) 'Non-specific indicators of stress and their association with age at death in Medieval York: Using stature and vertebral neural canal size to examine the effects of stress occurring during different periods of development', *International Journal of Osteoarchaeology*, 21(5), pp. 568–576. doi: 10.1002/oa.1158.

- Webb, Emily C *et al.* (2015) 'Compound-specific amino acid isotopic proxies for detecting freshwater resource consumption', *Journal of Archaeological Science*, 63, pp. 104–114. doi: 10.1016/j.jas.2015.08.001.
- Webb, Emily C. *et al.* (2015) 'Integrating cortisol and isotopic analyses of archeological hair: Reconstructing individual experiences of health and stress', *American Journal of Physical Anthropology*, 156(4), pp. 577–594. doi: 10.1002/ajpa.22673.
- Webb, Y., Minson, D. J. and Dye, E. A. (1980) 'A dietary factor influencing ¹³C content of human hair'.
- Wells, C. (1975) 'Prehistoric and historical changes in nutritional diseases and associated conditions', *Progress in food & nutrition science*, 1(11–12), p. 729–779. Available at: <http://europepmc.org/abstract/MED/769083>.
- Wells, J. C. K. (2014) 'Adaptive variability in the duration of critical windows of plasticity: Implications for the programming of obesity', *Evolution, Medicine and Public Health*, 2014(1), pp. 109–121. doi: 10.1093/emph/eou019.
- Wheaton, B. (1994) 'Sampling the Stress Universe BT - Stress and Mental Health: Contemporary Issues and Prospects for the Future', in Avison, W. R. and Gotlib, I. H. (eds). Boston, MA: Springer US, pp. 77–114. doi: 10.1007/978-1-4899-1106-3_4.
- WHO (2009) *Infant and young child feeding*. Switzerland: World Health Organisation. Available at: https://www.who.int/maternal_child_adolescent/documents/9789241597494/en/.
- Whyte, M. P. and Thakker, R. V. (2009) 'Rickets and osteomalacia', *Medicine*. Elsevier Ltd, 37(9), pp. 483–488. doi: 10.1016/j.mpmed.2009.06.004.
- Wickman, F. E. (1941) 'On a new possibility of calculating the total amount of coal and bitumen', *Geologiska Föreningen i Stockholm Förhandlingar*. Taylor & Francis, 63(4), pp. 419–421.
- Wittwer-Backofen, U. *et al.* (2008) 'Basics in paleodemography: A comparison of age indicators applied to the early medieval skeletal sample of Lauchheim', *American Journal of Physical Anthropology*, 137(4), pp. 384–396. doi: 10.1002/ajpa.20881.
- Wood, J. W. *et al.* (1992) 'The Osteological Paradox', *Current Anthropology*, 33(4), pp. 343–370. doi: 10.1086/204084.
- Wright, L. E. and Yoder, C. J. (2003) 'Recent progress in bioarchaeology: approaches to the osteological paradox', *Journal of Archaeological Science*, 11(1), pp. 43–70.
- Yaussy, S. L., DeWitte, S. N. and Redfern, R. C. (2016) 'Frailty and famine: Patterns of mortality and physiological stress among victims of famine in medieval London', *American Journal of Physical Anthropology*, 160(2), pp. 272–283. doi: 10.1002/ajpa.22954.
- Yoder, C., Ubelaker, D. and Powell, J. (2001) 'Examination of variation in sternal rib end morphology relevant to age assessment', *Journal of Forensic Science*, 46(2), pp. 223–227.

- Zariņa, G. *et al.* (2016) 'Cribra orbitalia as a potential indicator of childhood stress: Evidence from paleopathology, stable C, N, and O isotopes, and trace element concentrations in children from a 17 th-18 th century cemetery in Jēkabpils, Latvia', *Journal of Trace Elements in Medicine and Biology*, 38, pp. 131–137. doi: 10.1016/j.jtemb.2016.05.008.
- Van Zeist, W., Wasylkova, K. and Behre, K.-E. (1991) 'Progress in old world palaeoethnobotany', *AA Balkema, Rotterdam*.
- Zsolt, N. (2013) 'Bögöz középkori temploma és temetője', in Petronella, K. (ed.) *Isis. Erdélyi Magyar Restaurátor Füzetek*. 13th edn. Székelyudvarhely, pp. 9–17.
- Zsolt, N. (2015) 'ARPADIAN AGE CHURCHES OF BÖGÖZ', in Dobos, A. *et al.* (eds) *Archaeologia Transylvanica Studia in honorem Stephani Bajusz*. Budapest: Martin Opitz Publishing House, pp. 359–422.
- Zsolt, N. and Gáll, E. (2015) 'The “ westernisation ” of the Transylvanian Basin : Migration and/or acculturation ? : Wearing hairpins in the 12th Century Transylvanian Basin', *VAMZ*, XLVIII(3), pp. 85–120.
- Zuckerman, M. K. *et al.* (2014) 'Anemia or scurvy: A pilot study on differential diagnosis of porous and hyperostotic lesions using differential cranial vault thickness in subadult humans', *International Journal of Paleopathology*, 5, pp. 27–33. doi: 10.1016/j.ijpp.2014.02.001.
- Zuckerman, M. K., Garofalo, E. M. and Ortner, D. J. (2007) 'Anemia or scurvy: distinguishing the etiology of porotic hyperostosis via differential cranial vault thickness in juvenile humans.', in *AMERICAN JOURNAL OF PHYSICAL ANTHROPOLOGY*. WILEY-LISS DIV JOHN WILEY & SONS INC, 111 RIVER ST, HOBOKEN, NJ 07030 USA, p. 256.

Period	Skeleton	Lab No.	Age Estimation	Sex Estimation	Element	Bulk C,N	Incremental C,N	Sr	O
Migration	<i>Modern</i>	ICL_river			Somesul Mic River				x
	<i>Modern</i>	ICL_plant			Corn husk	x		x	
	<i>Modern</i>	ICL_soil			Soil sample			x	
	<i>lcl128</i>	550			Cow molar	x		x	x
	<i>lcl148</i>	551			Pig molar	x		x	xx
	<i>lcl111</i>	552	young adult	⊖	L. Man. Perm. M1		x		
	<i>lcl111</i>	553			L. Max. M3		x	x	x
	<i>lcl120</i>	555	young adult	male?	R. Man. M3		x	x	x
	<i>lcl120</i>	556			L. Man. PM1		x		
	<i>lcl120</i>	557			rib fragment	x			
	<i>lcl123</i>	558	young adult	male?	R. Max. Perm. I2		x		
	<i>lcl123</i>	559			L. Man. Perm. M2		x		
	<i>lcl123</i>	560			rib fragment	x			
	<i>lcl127</i>	561	child	⊖	R. Man. Decid. m2		x		
	<i>lcl127</i>	562			L. Max. Perm. C		x		
	<i>lcl129</i>	563	child	⊖	R. Man. Decid. i2		x		
	<i>lcl129</i>	564			L. Max. Perm. M1		x		
	<i>lcl130</i>	565	middle adult	F?	R. Max. Perm. M2		x	x	x
	<i>lcl130</i>	566			R. Max. Perm. I1		x		
	<i>lcl130</i>	567			rib fragment	x			
	<i>lcl131</i>	568	child	⊖	L. Max. Decid. i1		x		
	<i>lcl131</i>	569			L. Man. Perm. M1		x		
	<i>lcl134</i>	575	adult	F	R. Max. Perm. C		x		
	<i>lcl134</i>	576			R. Max. Perm. M2		x	x	x
	<i>lcl134</i>	583			rib fragment	x			
	<i>lcl135</i>	577	young adult	F?	R. Man. Perm. C		x		
	<i>lcl135</i>	578			R. Man. M3		x	x	x
	<i>lcl135</i>	579			rib fragment	x			
	<i>lcl136</i>	580	middle adult	F?	L. Max. Perm. I1		x		
	<i>lcl136</i>	581			L. Max. M3		x	x	x

Key: ⊖ - unobservable; Max – maxillary; Man – mandibular; Perm – permanent; Decid – deciduous

*Tentative biological sex estimation for older adolescent individuals (assuming they were post-pubescent)

Period	Skeleton	Lab No.	Age Estimation	Sex Estimation	Element	Bulk C,N	Incremental C,N	Sr	O
Migration	<i>lcl136</i>	582			rib fragment	x			
	<i>lcl137</i>	584	young adult	F?	L. Max. Perm. I2		x		
	<i>lcl137</i>	585			L. Max. M3		x	x	x
	<i>lcl137</i>	586			rib fragment	x			
	<i>lcl138</i>	587	young adult	M?	L. Max. Perm. I1		x		
	<i>lcl138</i>	588			L. Man. M3		x	x	x
	<i>lcl138</i>	589			Rib Fragment	x			
	<i>lcl139</i>	590	middle adult	F?	L. Man. Perm. C		x		
	<i>lcl139</i>	591			L. Man. Perm. M2		x	x	x
	<i>lcl139</i>	592			rib fragment	x			
	<i>lcl140</i>	593	middle adult	M	L. Man. Perm. C		x		
	<i>lcl140</i>	594			L. Max. M3		x	x	x
	<i>lcl140</i>	595			rib fragment	x			
	<i>lcl141</i>	596	young adult	M	R. Max. Perm. M1		x		
	<i>lcl141</i>	597			L. Max. Perm. I1		x		
	<i>lcl141</i>	598			rib fragment	x			
	<i>lcl149</i>	601	middle adult	F	R. Max. Perm. C		x		
	<i>lcl149</i>	602			R. Man. Perm. M2		x	x	x
	<i>lcl149</i>	603			rib fragment	x			
	<i>lcl154</i>	606	young adult	F?	R. Max. M3		x	x	x
	<i>lcl154</i>	607			R. Max. Perm. I1		x		
	<i>lcl154</i>	608			rib fragment	x			
	<i>lcl155</i>	609	middle adult	F?	L. Man. M3		x	x	x
	<i>lcl155</i>	610			L. Max. Perm. M1		x		
	<i>lcl155</i>	611			rib fragment	x			
	<i>lcl156</i>	612	middle adult	F	L. Man. M3		x	x	x
	<i>lcl156</i>	613			L. Max. Perm. C		x		
	<i>lcl156</i>	614			rib fragment	x			

Key: Ø - unobservable; Max – maxillary; Man – mandibular; Perm – permanent; Decid – deciduous
 *Tentative biological sex estimation for older adolescent individuals (assuming they were post-pubescent)

Period	Skeleton	Lab No.	Age Estimation	Sex Estimation	Element	Bulk C,N	Incremental C,N	Sr	O
Middle Ages	<i>Modern</i>	BF_soil			Soil sample			x	
	<i>Modern</i>	BF_river			Tarnava Mare River				x
	<i>Modern</i>	BF_rain			Rain water				x
	<i>Modern</i>	BF_plant			Corn husk	x		x	
	<i>Fen6</i>	617	young adult	M	L. Max. Perm. M1			x	
	<i>Fen6</i>	618			R. Man. M3			x	x
	<i>Fen6</i>	619			rib fragment	x			
	<i>Fen9</i>	620	older adult	F?	R. Max. Perm. C			x	x
	<i>Fen9</i>	621			rib fragment	x			
	<i>Fen10</i>	622	adolescent	⊖	R. Man. Perm. M1			x	
	<i>Fen10</i>	623			R. Man. Perm. M2			x	x
	<i>Fen14</i>	624	middle adult	F?	L. Man. Perm. I2			x	x
	<i>Fen14</i>	625			rib fragment	x			
	<i>Fen15</i>	626	child	⊖	R. Man. Decid. m1			x	
	<i>Fen15</i>	627			R. Man. Perm. M1			x	
	<i>Fen17</i>	628	older adult	M	R. Man. Perm. I1			x	x
	<i>Fen17</i>	629			rib fragment	x			
	<i>Fen42</i>	630	infant	⊖	L. Man. Decid. i1			x	
	<i>Fen42</i>	631			L. Man. Perm. M1			x	
	<i>Fen43</i>	632	adolescent	⊖	L. Man. Perm. M1			x	
	<i>Fen43</i>	633			R. Max. M3			x	x
	<i>Fen50</i>	634	adolescent	⊖	L. Man. Perm. M1			x	
	<i>Fen50</i>	635			L. Max. M3			x	x
	<i>Fen52</i>	636	adolescent	⊖	L. Man. Perm. M1			x	
	<i>Fen52</i>	637			L. Man. M3			x	x
	<i>Bog10</i>	638	young adult	M?/?	L. Max. Perm. M1			x	x
	<i>Bog10</i>	639			R. Man. Perm. C			x	
	<i>Bog10</i>	640			rib fragment	x			
	<i>Bog59</i>	641	adolescent	?/M?*	L. Man. Perm. M1			x	

Key: ⊖ - unobservable; Max – maxillary; Man – mandibular; Perm – permanent; Decid – deciduous

*Tentative biological sex estimation for older adolescent individuals (assuming they were post-pubescent)

Period	Skeleton	Lab No.	Age Estimation	Sex Estimation	Element	Bulk C,N	Incremental C,N	Sr	O
Middle Ages	<i>Bog59</i>	642			L. Man. M3		x	x	x
	<i>Bog66</i>	643	middle adult	F?	R. Man. Perm. C		x	x	
	<i>Bog66</i>	644			rib fragment	x			
	<i>Bog109</i>	645	child	⊖	R. Man. Decid. m1	x	x	x	x
	<i>Bog109</i>	646			L. Max. Perm. I1		x		
	<i>Bog161</i>	647	young adult	M?	L. Max. Perm. I2		x		
	<i>Bog161</i>	648			L. Max. M3		x	x	x
	<i>Bog240</i>	649	adolescent	?/M?*	L. Man. Perm. M1		x		
	<i>Bog240</i>	650			L. Man. M3		x	x	x
	<i>Bog250</i>	651	child	⊖	L. Man. Decid. m1		x		
	<i>Bog250</i>	652			R. Man. Perm. M1		x		
	<i>Bog252</i>	653	middle adult	M?	R. Man. Perm. I1		x		
	<i>Bog252</i>	654			L. Man. Perm. C		x	x	x
	<i>Bog252</i>	655			rib fragment	x			
	<i>Bog255</i>	656	young adult	F	L. Max. Perm. I1		x		
	<i>Bog255</i>	657			L. Max. M3		x	x	x
	<i>Bog255</i>	658			rib fragment	x			
	<i>Bog265</i>	659	infant	⊖	L. Max. Decid. i1			x	
<i>Bog265</i>	660			L. Max. Decid. m1			x		

Key: ⊖ - unobservable; Max – maxillary; Man – mandibular; Perm – permanent; Decid – deciduous

*Tentative biological sex estimation for older adolescent individuals (assuming they were post-pubescent)

Burial Information

<i>Orientation</i>	<i>Position</i>	<i>Period</i>	<i>Cemetery Location</i>	<i>Assoc. Burials</i>

Anomalies: _____

Finds

<i>Artefacts</i>		<i>Animal Bone</i>	
<i>In Grave</i>	<i>With Skeleton</i>	<i>In Grave</i>	<i>With Skeleton</i>

Anomalies: _____

Excavation Notes:

<i>Completeness</i>	<i>Fragmentation</i>	<i>Preservation</i>

<i>Age Estimation</i>	<i>Sex Estimation</i>	<i>Stature Estimation</i>

<i>Pathology Notes:</i>

Isotope Samples Taken

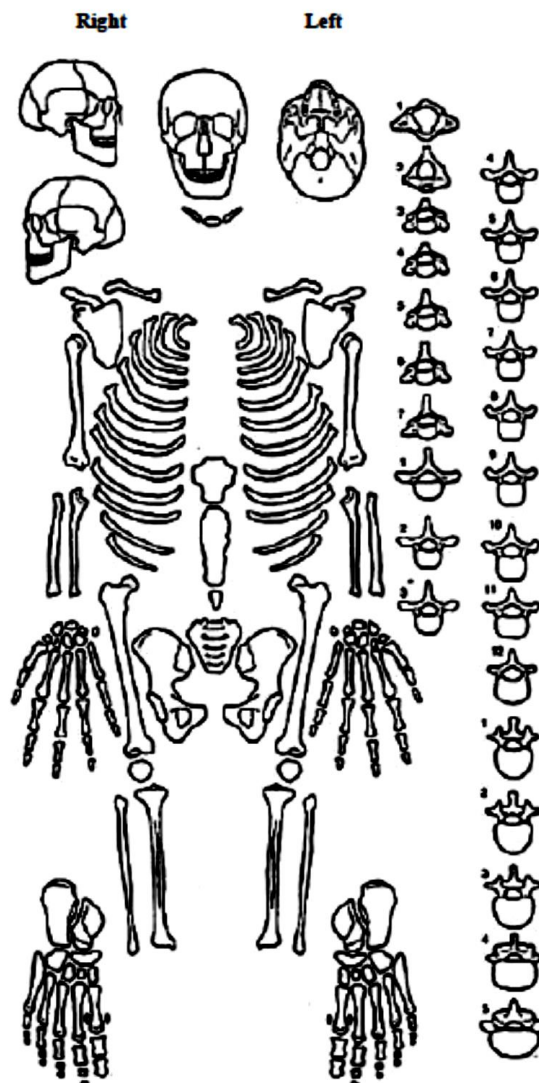
<i>Dentition 1</i>	<i>Dentition 2</i>	<i>Bone</i>

Dental Inventory

	R								L							
Maxillary	M3	M2	M1	PM2	PM1	C	I2	I1	I1	I2	C	PM1	PM2	M1	M2	M3
Mandibular	M3	M2	M1	PM2	PM1	C	I2	I1	I1	I2	C	PM1	PM2	M1	M2	M3

Key: absent - \emptyset , ci – initial cusp, Cco – coalescence cusp, Coc- cusp outline complete, Cr $\frac{1}{2}$ - crown $\frac{1}{2}$ complete, Cr $\frac{3}{4}$ - crown $\frac{3}{4}$ complete, Crc – crown, Ri – initial root, R $\frac{1}{4}$ - root $\frac{1}{4}$ complete, R $\frac{1}{2}$ - root $\frac{1}{2}$ complete, R $\frac{3}{4}$ - root $\frac{3}{4}$ complete, Rc – root complete, A $\frac{1}{2}$ - apex closed with wide PDL, Ac – apex closed, normal PDL

(AlQahtani, et al., 2010)



(After Arizona State Museum Human Remains Documentation Packet)

Age Estimation

Skeletal Fusion

Element	Stage	Age Range	Standard
<i>Clavicle</i>			
<i>Sternal Segments</i>			
<i>Acromion</i>			
<i>Proximal Humerus</i>			
<i>Medial Epicondyle Humerus</i>			
<i>Proximal Radius</i>			
<i>Proximal Ulna</i>			
<i>Distal Radius</i>			
<i>Distal Ulna</i>			
<i>Femoral Head</i>			
<i>Distal Femur</i>			
<i>Greater Trochanter</i>			
<i>Proximal Tibia</i>			
<i>Distal Tibia</i>			
<i>Distal Fibula</i>			
<i>Hamate</i>			
<i>Iliac Crest</i>			
<i>Ischial Tuberosity</i>			
<i>Sacral Segments</i>			
<i>Vertebral Endplate</i>			
<i>(Brothwell, 1981; Thompson & Black, 2007; Scheuer & Black, 2000)</i>			
<i>Skeletal Fusion Age</i>			

Method	Stage	Age Range	Standard
<i>Cervical Development</i>			<i>(Shapland and Lewis 2013)</i>
<i>Dental Wear</i>			<i>(Brothwell, 1981)</i>
<i>Pubic Symphysis</i>			<i>(Brooks & Suchey, 1990)</i>
<i>Auricular Surface</i>			<i>(Lovejoy, et al., 1985)</i>
<i>Rib Ossification</i>			<i>(Iscan et al., 1985)</i>
<i>Cranial Suture Fusion</i>			<i>(Buikstra & Ubelaker, 1994)</i>

Age Estimation	
Comments	

Sex Determination (Buikstra & Ubelaker, 1994; Phenice, 1969)

Element	Category	Element	Category
<i>Nuchal Crest</i>		<i>Sciatic Notch</i>	
<i>Mastoid Process</i>		<i>Ventral Arc</i>	
<i>Postzygomatic Arch</i>		<i>Preauricular Sulcus</i>	
<i>Frontal Bossing</i>		<i>Pelvic Arc</i>	
<i>Forehead Slope</i>		<i>Subpubic Concavity</i>	
<i>Orbital Rims</i>		<i>Subpubic Angle</i>	
<i>Supra-orbital Ridge</i>		<i>Ischiopubic Ramus</i>	
<i>Parietal Bossing</i>		<i>Obturator Foramen</i>	
<i>Ramus Flexure</i>			
<i>Gonial Flare</i>			
<i>Gonial Angle</i>			
<i>Anterior Mandible</i>			

*Male = M, Query Male = M?, Ambiguous = ?, Query Female = F?, Female = F

Post – Cranial Measurements (Bass, 1995)

Element	Right	Left	Ranges
<i>Clavicle Length</i>			<i>F – 138mm, M – 150mm</i>
<i>Scapula Glenoid Width</i>			<i>F – 26mm, M – 29mm</i>
<i>Humeral Head Width</i>			<i>F – 43mm, M – 47mm</i>
<i>Radial Head Width</i>			<i>F – 21mm, M – 23mm</i>
<i>Femoral Head Width</i>			<i>F – 43mm, M – 48mm</i>
<i>Femoral Dis. Epi. Width</i>			<i>F – 74mm, M – 76mm</i>

Sex Estimation	
Comments	

Post – Cranial Measurements

Element	Right (mm)	Left (mm)
<i>Scapula Glenoid Length</i>		
<i>Humerus Length</i>		
<i>Humerus Midshaft Width (M/L)</i>		
<i>Humeral Distal Epiphysis Width</i>		
<i>Radius Length</i>		
<i>Ulna Length</i>		
<i>Femoral Length (Straight)</i>		
<i>Femoral Length (Diagonal)</i>		

<i>Femoral Diaphysis Width (A/P)</i>		
<i>Femoral Diaphysis Width (M/L)</i>		
<i>Tibia Proximal Epiphysis Width</i>		
<i>Tibia Length (with condyle)</i>		
<i>Tibia Length (without condyle)</i>		
<i>Fibula Length</i>		

Stature Estimation

<i>Element</i>	<i>Length (cm)</i>	<i>Standard</i>	<i>Standard Error</i>
<i>Stature</i>			

*make sure to convert bone length from mm to cm (Trotter & Gleser, 1977)

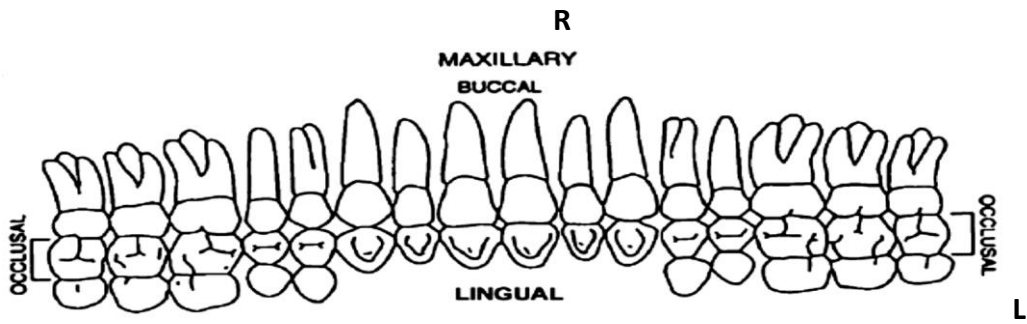
PATHOLOGY

<i>Pathology</i>	<i>Right</i>	<i>Area (mm)</i>	<i>Left</i>	<i>Area (mm)</i>
<i>Cribra Orbitalia</i>				
<i>Porotic Hyperostosis</i>				

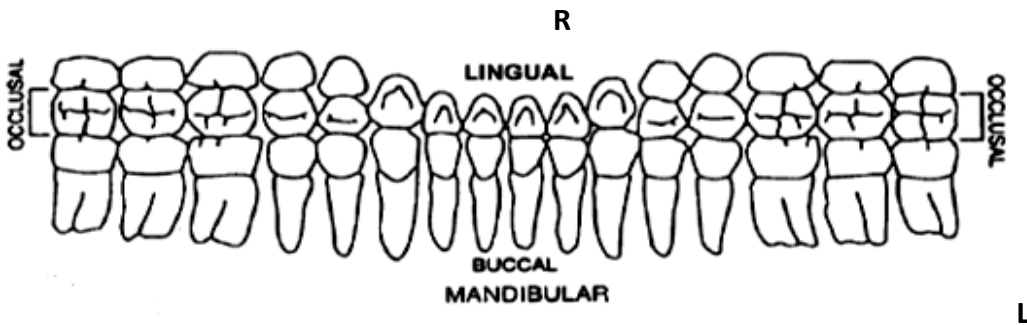
Present = √, Absent = ∅

- CO: (Stuart-Macadam, 1991)
- PH: (Stuart-Macadem, 1989)

Dental Pathology (after Arizona State Museum)



	M3	M2	M1	PM2	PM1	C	I2	I1	I1	I2	C	PM1	PM2	M1	M2	M3
Present																
Calculus																
DEH																
Caries																
Wear																



	M3	M2	M1	PM2	PM1	C	I2	I1	I1	I2	C	PM1	PM2	M1	M2	M3
Present																
Calculus																
DEH																
Caries																
Wear																

Key

Present	<i>P: present, AM: Ante-mortem, PM: post-mortem, B: broken, /: jaw bone absent, PL: present but loose</i>
Calculus	<i>o: occlusal, d: distal, l: lingual, la: labial, m: mesial, b: buccal, a: all</i>
DEH	<i>Pt: pit, L: line, G: groove</i>
Caries	<i>o: occlusal, d: distal, l: lingual, la: labial, m: mesial, b: buccal, a: all</i>

(Buikstra & Ubelaker, 1994; Hillson, 1996; Reid & Dean, 2000)

Periodontal Disease

<i>Upper Right</i>	<i>Upper Left</i>
<i>Lower Right</i>	<i>Lower Left</i>

Present = v, Absent = ∅

(Brothwell, 1981)

Burial Information

Orientation	Position	Period	Cemetery Location	Assoc. Burials

Anomalies: _____

Finds

Artefacts		Animal Bone	
In Grave	With Skeleton	In Grave	With Skeleton

Anomalies: _____

Excavation Notes:

Completeness	Fragmentation	Preservation

Age Estimation	Sex Estimation	Stature Estimation

Pathology Notes:

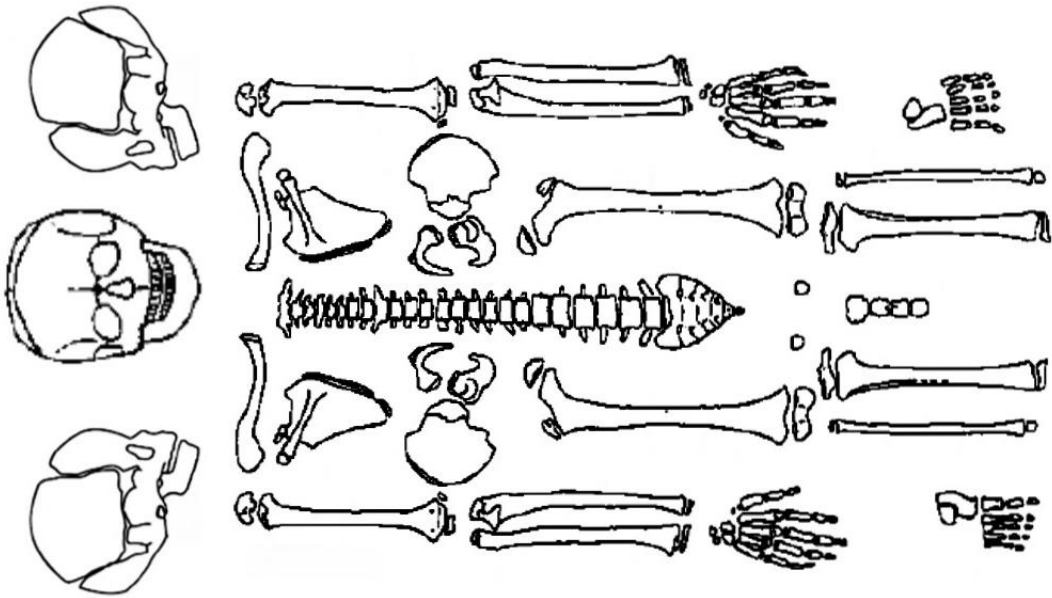
Isotope Sample Inventory

Dentition 1	Dentition 2

Dental Inventory

		R									L								
Maxillary	Permanent	M3	M2	M1	PM2	PM1	C	I2	I1	I1	I2	C	PM1	PM2	M1	M2	M3		
	Deciduous		M2	M1			C	I2	I1	I1	I2	C			M1	M2			
Mandibular	Deciduous		M2	M1			C	I2	I1	I1	I2	C			M1	M2			
	Permanent	M3	M2	M1	PM2	PM1	C	I2	I1	I1	I2	C	PM1	PM2	M1	M2	M3		

Key: absent - \emptyset , ci – initial cusp, Cco – coalescence cusp, Coc- cusp outline complete, Cr $\frac{1}{2}$ - crown $\frac{1}{2}$ complete, Cr $\frac{3}{4}$ - crown $\frac{3}{4}$ complete, Crc – crown, Ri – initial root, R $\frac{1}{4}$ - root $\frac{1}{4}$ complete, R $\frac{1}{2}$ - root $\frac{1}{2}$ complete, R $\frac{3}{4}$ - root $\frac{3}{4}$ complete, Rc – root complete, A $\frac{1}{2}$ - apex closed with wide PDL, Ac – apex closed, normal PDL (AlQahtani, et al., 2010)



Age Estimation

Skeletal Fusion

Element	Stage	Age Range	Source
Clavicle			
Sternal Segments			
Acromion			
Proximal Humerus			
Medial Epicondyle Humerus			
Proximal Radius			
Proximal Ulna			
Distal Radius			
Distal Ulna			
Femoral Head			
Distal Femur			
Greater Trochanter			
Proximal Tibia			
Distal Tibia			
Distal Fibula			
Hamate			
Iliac Crest			
Ischial Tuberosity			
Sacral Segments			
Vertebral Endplate			
(Scheuer & Black, 2000; Thompson & Black, 2007; Brothwell, 1981)			
Skeletal Fusion Age			

Method	Stage	Age Range	Source
Cervical Development			(Shapland and Lewis 2013)
Dental Wear			(Brothwell, 1981)
Pubic Symphysis			(Brooks & Suchey, 1990)
Auricular Surface			(Lovejoy, et al., 1985)
Rib Ossification			(Iskan et al., 1985)
Cranial Suture Fusion			(Buikstra & Ubelaker, 1994)
Dental Formation			(AlQahtani, et al., 2010)

Age Estimation	
Comments	

Post Cranial Measurements

Element	Right (mm)	Left (mm)
Scapula Glenoid Length		
Humerus Length		
Humerus Midshaft Width (M/L)		
Humeral Distal Epiphysis Width		
Radius Length		
Ulna Length		
Femoral Length (Straight)		
Femoral Length (Diagonal)		
Femoral Diaphysis Width (A/P)		
Femoral Diaphysis Width (M/L)		
Tibia Proximal Epiphysis Width		
Tibia Length (with condyle)		
Tibia Length (without condyle)		
Fibula Length		

Stature Estimation

Element	Length (cm)	Standard	Standard Error
Stature			

*make sure to convert bone length from mm to cm (Trotter & Gleser, 1977)

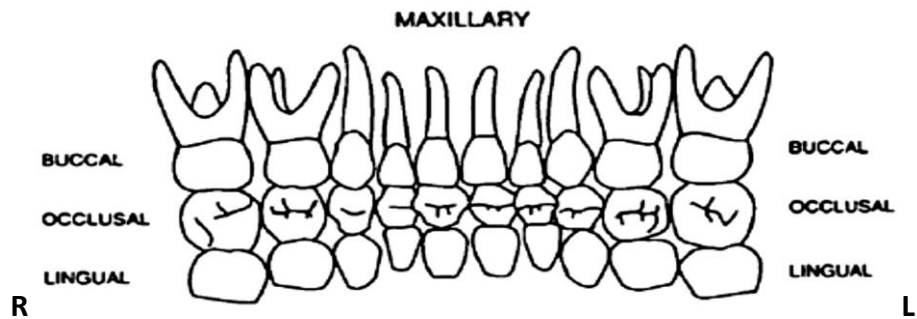
PATHOLOGY

Pathology	Right	Area (mm)	Left	Area (mm)
Cribra Orbitalia				
Porotic Hyperostosis				

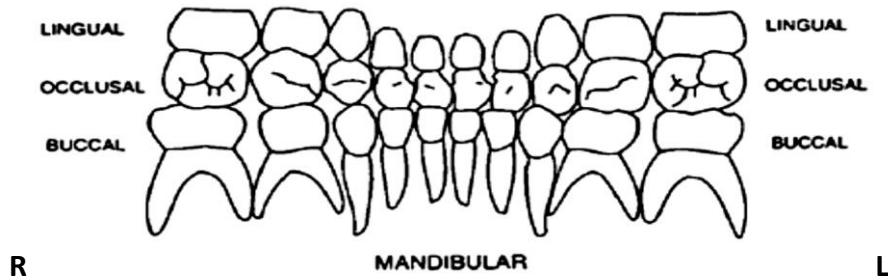
Present = √, Absent = ∅

CO: Stuart-Macadam, 1991; PH: (Stuart-Macadem, 1989)

Dental Pathology (after Arizona State Museum)



	m2	m1	c	i2	i1	i1	i2	c	m1	m2
Present										
Calculus										
DEH										
Caries										
Wear										



	m2	m1	c	i2	i1	i1	i2	c	m1	m2
Present										
Calculus										
DEH										
Caries										
Wear										

Key

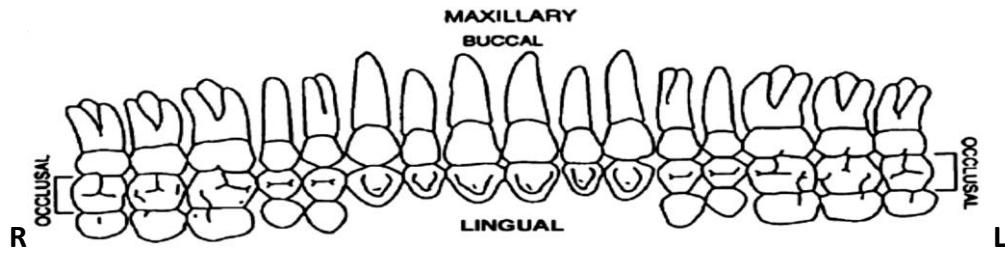
Present	P: present, AM: Ante-mortem, PM: post-mortem, B: broken, /: jaw bone absent, PL: present but loose
Calculus	o: occlusal, d: distal, l: lingual, la: labial, m: mesial, b: buccal, a: all
DEH	Pt: pit, L: line, G: groove
Caries	o: occlusal, d: distal, l: lingual, la: labial, m: mesial, b: buccal, a: all

(Buikstra & Ubelaker, 1994; Hillson, 1996; Reid & Dean, 2000)

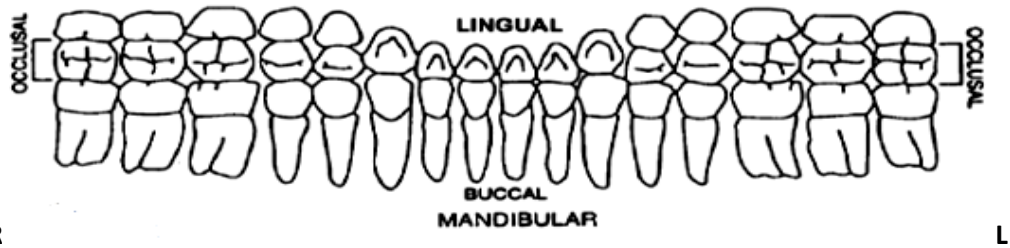
Periodontal Disease

Upper Right	Upper Left
Lower Right	Lower Left

Present = √, Absent = ∅ Source: Brothwell, 1981



	M3	M2	M1	PM2	PM1	C	I2	I1	I1	I2	C	PM1	PM2	M1	M2	M3
Present																
Calculus																
DEH																
Caries																
Wear																



	M3	M2	M1	PM2	PM1	C	I2	I1	I1	I2	C	PM1	PM2	M1	M2	M3
Present																
Calculus																
DEH																
Caries																
Wear																

Key

Present	P: present, AM: Ante-mortem, PM: post-mortem, B: broken, /: jaw bone absent, PL: present but loose
Calculus	o: occlusal, d: distal, l: lingual, la: labial, m: mesial, b: buccal, a: all
DEH	Pt: pit, L: line, G: groove
Caries	o: occlusal, d: distal, l: lingual, la: labial, m: mesial, b: buccal, a: all

Metabolic Disease

Skeletal Lesion	Location
Woven Bone: sphenoid	
Woven Bone: mandible	
Woven Bone: Orbits	
Friable Surface	
Flared Metaphyses	
Long Bone: Bowing	
Haemorrhagic Staining	

Prepared for: Durham University

Contact(s): Dr Janet Montgomery

Iso-Analytical Reference: 170823-2

Cust. Ref No.: A186794

Material: Tooth enamel

Analysis: Carbonate isotopes

Date Arrived: 23 August, 2017

Report Date: 26 September, 2017

Prepared by: Steve Brookes

Results File: 170823-2-results.xls

We have completed $\delta^{13}\text{C}$ and $\delta^{18}\text{O}$ of the carbonate in the tooth enamel samples that we received from you on August 23rd 2017. The results of analysis can be found attached as an MS Excel worksheet with the above file name.

Carbon-13 and Oxygen-18 Analysis of Carbonate in Apatite

Samples were weighed into clean ExetainerTM tubes and then flushed with 99.995 % helium. After flushing, phosphoric acid was added to the samples and they were allowed to react in the acid overnight to allow complete conversion of carbonate to CO₂. Reference and control materials were prepared the same way.

The CO₂ gas liberated from samples was then analysed by Continuous Flow-Isotope Ratio Mass Spectrometry (CF-IRMS). Carbon dioxide was sampled from the ExetainerTM tubes into a continuously flowing He stream using a double holed needle. The CO₂ was resolved on a packed column gas chromatograph and the resultant chromatographic peak carried forward into the ion source of a Europa Scientific 20-20 IRMS where it is ionized and accelerated. Gas species of different mass are separated in a magnetic field then simultaneously measured using a Faraday cup collector array to measure the isotopomers of CO₂ at m/z 44, 45, and 46.

The phosphoric acid used for digestion had been prepared for isotopic analysis in accordance with Coplen *et al.* (1983) *Nature*, **302**, 236-238, was injected through the septum into the vials.

The reference material used during analysis of your samples was IA-R022 (Iso-Analytical working standard calcium carbonate, $\delta^{13}\text{C}_{\text{V-PDB}} = -28.63 \text{ ‰}$ and $\delta^{18}\text{O}_{\text{V-PDB}} = -22.69 \text{ ‰}$). IA-R022, NBS-18 (carbonatite, $\delta^{13}\text{C}_{\text{V-PDB}} = -5.01 \text{ ‰}$ and $\delta^{18}\text{O}_{\text{V-PDB}} = -2.46 \text{ ‰}$).

PDB = -23.20
and IA-R066
(chalk, $\delta^{13}\text{C}_\text{V}$ -



‰)

+2.33 ‰ and $\delta^{18}\text{O}_\text{V-PDB} = -1.52$ ‰) were run as quality control check samples during analysis of your samples. PDB =

Acid preparations of samples and controls are measured directly against acid preparations of our working calcium carbonate standard. This procedure removes the need to apply separate corrections for temperature dependent isotope fractionation. The results obtained for the NBS18 and IA-R066 controls are used to check and correct the data as required. Results for these are included in the tabulated results.

IA-R022 has been calibrated against and is traceable to NBS-18 and NBS-19 (limestone, $\delta^{13}\text{C}_\text{V-PDB} = +1.95$ ‰ and $\delta^{18}\text{O}_\text{V-PDB} = -2.2$ ‰). IA-R066 has been calibrated against and is traceable to NBS-18 and IAEA-CO-1 (carrara marble, $\delta^{13}\text{C}_\text{V-PDB} = +2.5$ ‰ and $\delta^{18}\text{O}_\text{V-PDB} = -2.4$ ‰).

NBS-18, NBS-19 and IAEA-CO-1 are inter-laboratory comparison standard materials distributed by the International Atomic Energy Agency (IAEA).

The equivalent calcium carbonate content values (%) were derived by comparing the total ion beam data for the samples against the pure calcium carbonate references.

Sample Storage

Any un-used sample material will be returned to you. If you require any further information regarding the analysis or wish to discuss any related issues, please do not hesitate to contact us.

Analysed & Reported by:

Steve Brookes, PhD

Checked by:

Charles Belanger, BSc

For and on behalf of:

Iso-Analytical Limited
The Quantum
Phase 3
Marshfield Bank
Crewe Cheshire CW2 8UY

Tel.: +44 (0)1270 509533

Fax.: +44 (0)1270 509511

Email: info@iso-analytical.com

Test Variable	Grouping Variable	Statistical Test	F	P (0.05)	Significantly different relationships	
Stature	Combined					
	Period	Ind. T-test (unequal variance)		0.901		
	Site	One-way Anova	0.756	0.475		
	Age Category	One-way Anova	0.678	0.611		
	Sex Estimation	One-way Anova	17.405	0.000	male/M? - female/F?	
	Lesions	Ind. T-test (unequal variance)				
	Assemblage Comparison					
	Period/Sex Estimation	Ind. T-test (unequal variance)	0.014	0.000	Migration Period male/M? - Migration Period female/F?	
			0.280	0.000	Middle Age male/M? - Middle Age female/F?	
	Priod/Age Category	One-way Anova	0.693	0.518	Migration Period	
		0.385	0.818	Middle Ages		
Enamel defects	Combined					
	Period	Pearson Chi-Square Test		0.011	Migration Period - Middle Ages [$\chi^2(1)=6.48$]	
	Site	Pearson Chi-Square Test		0.030	Bogoz-Fenyed-Iclod [$\chi^2(2)=7.01$]	
	Age Category	Pearson Chi-Square Test		0.638		
	Sex Estimation	Pearson Chi-Square Test		0.313		
	Assemblage Comparison					
	Period/Sex Estimation	Pearson Chi-Square Test		0.066	Migration Period male/M? - female/F? [$\chi^2(2)=5.45$]	
				0.642	Middle Ages	
	Priod/Age Category	Pearson Chi-Square Test		0.493	Migration Period	
				0.328	Middle Ages	
Cribra orbitalia	Combined					
	Period	Pearson Chi-Square Test		0.549		
	Site	Pearson Chi-Square Test		0.409		
	Age Category	Pearson Chi-Square Test		0.061		
	Sex Estimation	Pearson Chi-Square Test		0.313		
	Assemblage Comparison					
	Period/Sex Estimation	Pearson Chi-Square Test		0.024	Migration Period male/M? - female/F? [$\chi^2(4)=11.27$]	
				0.105	Middle Ages	
	Priod/Age Category	Pearson Chi-Square Test		0.086	Migration Period	
				0.247	Middle Ages	

Test Variable	Grouping Variable	Statistical Test	P (0.05)	Significantly different relationships	
$\delta^{13}\text{C}_{\text{INCR}}$ (mean)	Combined				
	Period	Independent-sample Kolmogorov-Smirnov	0.000	Migration Period - Middle Ages	
	Site	Independent-sample Kruskal-Wallis	0.015	Fenyed - Iclod (Adj. Sig. 0.028)	
	Age Category	Independent-sample Kruskal-Wallis	0.152		
	Sex Estimation	Independent-sample Kolmogorov-Smirnov	0.028	male/M? - female/F?	
	Lesions	Independent-sample Kolmogorov-Smirnov	0.154		
	Assemblage Comparison				
	Period/Sex	Independent-sample Kruskal-Wallis	0.003	MP female - MA males (Adj Sig. 0.003) MP female - MA female (Sig. 0.020) MP male - MP female (Sig. 0.009)	
	Period/Age	Independent-sample Kruskal-Wallis	0.013	MP adults - MA non-adults (Adj, Sig. 0.048) MP adults - MA adults (Adj Sig. 0.002)	
	Lesions/Sex	Independent-sample Kruskal-Wallis	0.018	MA Male without lesions - MP female without lesions (Sig. 0.040) MA male without lesions - MP female with lesions (Sig. 0.012) MP male without lesions - MP female without lesions (Sig. 0.032) MP male without lesions - MP female with lesions (Sig. 0.004) MA male with lesions - MP female without lesions (Sig. 0.037) MA male with lesions - MP female with lesions (Sig. 0.005)	
	Lesions/Age	Independent-sample Kruskal-Wallis	0.015	MA non-adults with lesions - MP adults with lesions (Adj. Sig. 0.022) MP non-adults without lesions - MP adults with lesions (Sig. 0.026) MA adults with lesions - MP adults with lesions (Sig 0.015) MP adults without lesions - MP adults with lesions (Sig. 0.043)	
	$\delta^{15}\text{N}_{\text{INCR}}$ (mean)	Combined			
		Period	Independent-sample Kolmogorov-Smirnov	0.560	
Site		Independent-sample Kruskal-Wallis	0.152		
Age Category		Independent-sample Kruskal-Wallis	0.001	middle adult - child (Adj. Sig. 0.001) middle adult - infant (Sig. 0.004) young adult - child (Adj. Sig. 0.025) young adult - infant (Sig. 0.018) adolescent - child (Sig. 0.009) adolescent - infant (Sig. 0.044)	
Combined					
Lesions		Independent-sample Kolmogorov-Smirnov	0.460		
Assemblage Comparison					
Period/Sex Estimation		Independent-sample Kruskal-Wallis	0.680		

Test Variable	Grouping Variable	Statistical Test	P (0.05)	Significantly different relationships
$\delta^{15}\text{N}_{\text{INCR}}$ (mean)	Priod/Age Category	Independent-sample Kruskal-Wallis	0.004	MP adults - MP non-adult (Sig. 0.036) MP adults - MA non-adults (Adj. Sig. 0.008) MA adults - MA non-adults (Sig. 0.016)
	Lesions/Sex Estimation	Independent-sample Kruskal-Wallis	0.846	
	Lesions/Age Category	Independent-sample Kruskal-Wallis	0.002	MP non-adults without lesions - MA non-adults with lesions (Sig. 0.016) MP non-adults without lesions - MP non-adults with lesions (Sig. 0.011) MA adults with lesions - MA non-adults with lesions (Sig. 0.004) MA adults with lesions - MP non-adults with lesions (Sig. 0.005) MP adults with lesions - MA non-adults with lesions (Adj. Sig. 0.048) MP adults with lesions - MP non-adults with lesions (Sig. 0.003) MP adult without lesions - MA non-adults with lesions (Sig. 0.015) MP adults without lesions - MP non-adults with lesions (Sig. 0.015)
$\delta^{13}\text{C}_{\text{BONE}}$	Combined			
	Period	Independent-sample Kolmogorov-Smirnov	0.006	Migration Period - Middle Ages
	Site	Independent-sample Kruskal-Wallis	0.020	
	Age Category	Independent-sample Kruskal-Wallis	0.133	
	Sex Estimation	Independent-sample Kolmogorov-Smirnov	0.667	
	Lesions	Independent-sample Kolmogorov-Smirnov	0.135	
	Assemblage Comparison			
	Period/Sex Estimation	Independent-sample Kruskal-Wallis	0.171	
	Priod/Age Category	Independent-sample Kruskal-Wallis	0.085	
	Lesions/Sex Estimation	Independent-sample Kruskal-Wallis	0.257	
Lesions/Age Category	Independent-sample Kruskal-Wallis	0.092		
$\delta^{15}\text{N}_{\text{BONE}}$	Combined			
	Period	Independent-sample Kolmogorov-Smirnov	0.484	
	Site	Independent-sample Kruskal-Wallis	0.814	
	Age Category	Independent-sample Kruskal-Wallis	0.413	
	Sex Estimation	Independent-sample Kolmogorov-Smirnov	0.049	male/M? - female/F?
	Lesions	Independent-sample Kolmogorov-Smirnov	0.295	
	Assemblage Comparison			
	Period/Sex Estimation	Independent-sample Kruskal-Wallis	0.399	
	Priod/Age Category	Independent-sample Kruskal-Wallis	0.579	
	Lesions/Sex Estimation	Independent-sample Kruskal-Wallis	0.210	
Lesions/Age Category	Independent-sample Kruskal-Wallis	0.357		

Test Variable	Grouping Variable	Statistical Test	P (0.05)	Significantly different relationships
$\delta^{18}\text{O}$	Combined			
	Period	Independent T-test	0.785	
	Site (Iclod, Bogoz, Fenyed)	One-way Anova	0.876	
	Age Category	One-way Anova	0.340	
	Sex Estimation	One-way Anova	0.973	
	Lesions	Independent T-test	0.673	
	Assemblage Comparison			
	Period/Sex Estimation	One-way Anova	0.731	
	Period/Age Category	One-way Anova	0.782	
	Lesions/Sex Estimation	One-way Anova	0.445	
	Lesions/Age Category	One-way Anova	0.374	
$^{87}\text{Sr}/^{86}\text{Sr}$	Combined			
	Period	Independent-sample Kolmogorov-Smirnov	0.006	Migration Period - Middle Ages
	Site	Independent-sample Kruskal-Wallis	0.027	Fenyed - Iclod (Adj. Sig. 0.021)
	Age Category	Independent-sample Kruskal-Wallis	0.050	Adult-Young Adult (Sig. 0.033) Adult-Middle Adult (Sig. 0.015) Adolescent-Young Adult (Sig. 0.050) Adolescent-Middle Adult (Sig. 0.013)
	Sex Estimation	Independent-sample Kolmogorov-Smirnov	0.332	
	Lesions	Independent-sample Kolmogorov-Smirnov	0.837	
	Assemblage Comparison			
	Period/Sex Estimation	Independent-sample Kruskal-Wallis	0.639	
	Period/Age Category	Independent-sample Kruskal-Wallis	0.082	
	Lesions/Sex Estimation	Independent-sample Kruskal-Wallis	0.721	
	Lesions/Age Category	Independent-sample Kruskal-Wallis	0.325	

ID	EH		PO	CO		AG	SKELETAL LESION(S)
	# of defects	# of teeth present		R	L		
Migration Period							
<i>ICL111</i>	3	19	U	U	U	U	
<i>ICL120</i>	0	16	A	P	P	U	Tibial plateau turned medially (bilateral), possible anterior bowing of bilateral femoral shaft (broken)
<i>ICL122</i>	0	1	U	U	U	U	
<i>ICL123</i>	0	24	A	U	U	U	Mixed woven and lamellar bone present on the mid-shaft of the anterior crest on the left tibia (6x2 cm), tibial plateau slightly turned medially (left)
<i>ICL124</i>	0	0	U	U	U	U	
<i>ICL125</i>	0	0	U	U	U	U	
<i>ICL127</i>	1	27	U	U	U	P	
<i>ICL129</i>	0	17	A	P	P	P	Flared appearance to the metaphyses of the distal femora and proximal tibiae Porous new bone formation to the right of the frontal crest on the endocranial surface of the frontal bone (1x0.5cm) Porosity present on the anterior surface of the mandible and on the superior marginal of the external auditory meatus (bilaterally)
<i>ICL130</i>	4	21	A	P	P	U	AMTL Porous woven bone present on the anterior surface of the left zygomatic bone and on the anterior surface of the right greater wing of the sphenoid
<i>ICL131</i>	0	11	U	U	P	P	Porosity present on the anterior margin of the external auditory meatus (bilateral), on the superior aspect of the internal occipital protuberance, the right palatine process (maxillae) and the body and right greater wing of the sphenoid
<i>ICL134</i>	8	26	A	A	A	U	
<i>ICL135</i>	0	11	U	U	U	U	AMTL, caries
<i>ICL136</i>	0	16	U	A	A	U	
<i>ICL137</i>	7	27	A	P	P	U	Porosity present on the internal occipital protuberance (2x2cm), caries, distal femoral epiphysis (right) turned antero-lateral
<i>ICL138</i>	1	19	A	U	U	U	
<i>ICL139</i>	3	13	A	A	A	U	

Key: EH – enamel hypoplasia; PO – porotic hyperostosis; CO – cribra orbitalia; AG – arrested growth; A – lesion was absent; P – lesion was present; U – skeletal element was absent or unobservable; AMTL – antemortem tooth loss

ID	EH		PO	CO		AG	SKELETAL LESION(S)
	# of defects	# of teeth present		R	L		
ICL140	5	28	A	P	P	U	Possible slight anterior bowing of bilateral femoral shaft (broken)
ICL141	3	22	A	P	A	U	Porosity present on the palatine processes of the maxillae, anterior surface of the mandible, along the sagittal sulcus (occipital bone) Porous new bone present on the superior margin of the external auditory meatus (bilateral)
ICL142	0	0	U	U	U	U	
ICL149	2	13	A	P	P	U	Two patches of porous woven bone on the endocranial surface of the frontal bone above the left orbit, 2cm left of the frontal crest (1x1cm, 2x2cm), AMTL
ICL151	0	0	U	U	U	U	
ICL153	0	4	U	U	U	U	
ICL154	0	28	A	A	A	U	Caries
ICL155	3	24	A	A	A	U	AMTL, caries
ICL156	3	28	A	A	A	U	Porosity present on the palatine processes of the maxillae
Middle Ages							
FEN1	0	20	U	P	P	P	<i>Porosity present around the margin of the right external auditory meatus, lateral surfaces of the great wings of the sphenoid (bilateral) and on the inferior aspect of the pars basilaris</i>
FEN2	0	23	U	A	P	U	
FEN3	0	2	U	P	A	U	<i>Antemortem tooth loss (AMTL)</i>
FEN5	0	12	A	P	U	U	<i>AMTL</i>
FEN6	2	24	A	A	A	U	<i>Porosity present across superior body of the sphenoid</i>
FEN7	0	1	A	A	P	U	
FEN9	1	13	U	U	U	U	
FEN10	2	20	A	A	U	U	<i>Porosity present on the anterior surface of the left greater wing of the sphenoid, inferior surface of the pars basilaris (1x2cm), and along the medial surface of the left frontal process (maxilla, 0.5x1cm)</i>
FEN11		0	U	U	U	U	
FEN12		0	U	U	U	U	

Key: EH – enamel hypoplasia; PO – porotic hyperostosis; CO – cribra orbitalia; AG – arrested growth; A – lesion was absent; P – lesion was present; U – skeletal element was absent or unobservable; AMTL – antemortem tooth loss

ID	EH		PO	CO		AG	SKELETAL LESION(S)
	# of defects	# of teeth present		R	L		
FEN13		0	U	U	U	U	
FEN14	3	25	A	A	U	U	
FEN15	0	19	A	A	P	U	<i>Porous woven bone present on the posterior surface of the right greater wing of the sphenoid (1x1cm)</i>
FEN16	0	2	A	A	A	U	
FEN17	0	4	A	A	A	U	<i>Tibial plateau turned medially (bilateral), possible anterior bowing of femoral shaft (bilateral), lytic lesions on both sides of the frontal crest (endocranial frontal bone, 5mm circles)</i>
FEN17A	0	1	U	P	P	U	<i>Porosity present on the inferior surface of the pars basilaris of the occipital bone, AMTL</i>
FEN18	0	6	U	P	U	U	AMTL
FEN19	0	6	U	A	A	U	
FEN20	0	7	U	U	U	U	AMTL
FEN21	0	28	A	U	A	U	<i>Porosity present on the anterior mandible (1x1cm) and on the inferior surface of the pars basilaris.</i>
FEN22	0	3	U	U	U	U	
FEN23		0	U	U	U	U	
FEN24		0	U	U	U	U	
FEN25	0	3	A	A	U	U	<i>Porosity present on the internal occipital protuberance (1x1cm)</i>
FEN26		0	U	U	U	U	
FEN27	0	19	U	U	U	U	
FEN28	5	26	A	U	P	U	<i>Porosity present on the inferior surface of the pars basilaris of the occipital bone (1x1cm) and around the superior margin of the left external auditory meatus</i>
FEN29	0	18	U	U	U	U	
FEN30	0	6	U	U	U	U	<i>Porosity present on the inferior surface of the pars basilaris of the occipital bone (0.5x0.5cm)</i>
FEN32	0	27	U	U	U	U	AMTL

Key: EH – enamel hypoplasia; PO – porotic hyperostosis; CO – cribra orbitalia; AG – arrested growth; A – lesion was absent; P – lesion was present; U – skeletal element was absent or unobservable; AMTL – antemortem tooth loss

ID	EH		PO	CO		AG	SKELETAL LESION(S)
	# of defects	# of teeth present		R	L		
FEN34	1	6	A	U	U	U	<i>Lytic lesion present on the endocranial surface of the front bone just to the right of the frontal crest (2x1cm), AMTL</i>
FEN35	0	26	U	U	U	U	
FEN36	0	5	A	U	U	U	<i>Porosity present along the inferior margin of the external auditory meatus (bilateral) and on the on superior body and posterior surface on the left greater wing of the sphenoid</i>
FEN37	0	28	U	A	P	U	
FEN38	0	33	U	U	U	U	
FEN39		0	U	U	U	U	
FEN40	1	24	A	U	U	U	
FEN41	0	26	A	U	U	U	
FEN42	0	27	A	U	U	U	
FEN43	1	21	A	A	A	U	<i>Striated lamellar bone present on the midshaft of the anterior crest of the right tibia (3x6cm)</i>
FEN44	0	26	A	A	A	U	
FEN45	0	20	A	P	P	P	
FEN46	0	7	U	U	U	U	
FEN48	0	29	U	P	P	U	<i>Tibial plateau turned medially (left), caries</i>
FEN49	1	25	A	U	U	A	
FEN50	8	27	A	U	U	U	<i>Lytic lesion present on the endocranial surface of the frontal bone approximately 2cm from the frontal crest bilaterally (2x1cm, 1x1cm), porosity on superior margin of the left external auditory meatus and the superior body of the sphenoid</i>
FEN52	1	18	A	U	U	U	
BOG1	0	0	U	U	U	U	
BOG3	2	3	U	U	U	P	<i>Friable surface on the anterior metaphyses of the proximal humeri</i>
BOG6		0	U	U	U	U	

Key: EH – enamel hypoplasia; PO – porotic hyperostosis; CO – cribra orbitalia; AG – arrested growth; A – lesion was absent; P – lesion was present; U – skeletal element was absent or unobservable; AMTL – antemortem tooth loss

ID	EH		PO	CO		AG	SKELETAL LESION(S)
	# of defects	# of teeth present		R	L		
BOG10	2	9	A	A	A	U	Porosity present on the superior aspect of the internal occipital protuberance of the occipital bone, on the superior body of the sphenoid, and the superior margin of the external auditory meatus (left). Caries
BOG13	0	14	A	A	A	U	Lytic lesion present on the posterior surface of the right greater wing of the sphenoid lateral to the body (1.5x1cm) Porous woven bone present on the superior margin of the external auditory meatus (bilateral), AMTL
BOG14	0	8	A	A	A	U	AMTL
BOG16		0	U	U	U	U	
BOG18	0	25	A	P	P	U	Porosity present on the superior margin of the external auditory meatus (bilateral) and on the postero-lateral aspect of the greater wings of the sphenoid, AMTL, caries
BOG19		0	U	U	U	U	
BOG33		0	U	U	U	U	
BOG35	0	15	A	A	A	U	
BOG40		0	U	U	U	U	
BOG52		0	U	U	U	U	
BOG54	0	7	A	A	A	U	Porosity present on the right palatine process and in the right maxillary sinus. Porous woven bone present in the right maxillary sinus. AMTL, tibial plateau turns medially (bilateral) and the distal femoral epiphysis (L) extends postero-medially with possible soft tissue damage
BOG55		0	U	U	U	U	
BOG57		0	U	U	U	U	
BOG59	3	17	U	U	U	A	Friable surface along the posterior proximal metaphysis of the right tibia and along the posterior distal metaphysis of the right femur

Key: EH – enamel hypoplasia; PO – porotic hyperostosis; CO – cribra orbitalia; AG – arrested growth; A – lesion was absent; P – lesion was present; U – skeletal element was absent or unobservable; AMTL – antemortem tooth loss

ID	EH		PO	CO		AG	SKELETAL LESION(S)
	# of defects	# of teeth present		R	L		
BOG63		0	U	U	U	U	
BOG66	0	15	P	A	A	U	Pinpoint porosity present across the 80% of the ectocranial surface of the right parietal bone Porosity and new bone formation above the superior margin of the external auditory meatus (bilateral)
BOG67		0	U	U	U	U	
BOG77		0	U	U	U	U	
BOG78		0	U	U	U	U	
BOG79A		0	A	A	A	U	
BOG79B		0	U	U	U	U	
BOG85	0	5	A	P	P	U	Porosity present on the superior body of the sphenoid
BOG89		0	U	U	U	U	
BOG93		0	U	U	U	U	
BOG95		0	U	U	U	U	
BOG102	0	11	U	U	U	U	Porosity present on the superior body of the sphenoid and on the inferior surface of the pars basilaris of the occipital bone
BOG103		0	U	U	U	U	
BOG107	0	23	A	U	P	U	
BOG108	0	9	A	A	A	U	
BOG109	0	4	A	A	P	P	Porosity present on the mental eminence of the mandible and the anterior surface of the maxillae lateral to the frontal process. Friable surface and new woven bone on the inferior neck of femora
BOG112		0	U	U	U	U	
BOG123		0	U	U	U	U	
BOG125		0	U	U	U	U	
BOG127		0	U	U	U	U	Friable surfaces around the distal metaphyses of the femora and the posterior proximal tibiae metaphyses
BOG128		0	A	A	A	U	Friable surfaces around the distal femora metaphyses

Key: EH – enamel hypoplasia; PO – porotic hyperostosis; CO – cribra orbitalia; AG – arrested growth; A – lesion was absent; P – lesion was present; U – skeletal element was absent or unobservable; AMTL – antemortem tooth loss

ID	EH		PO	CO		AG	SKELETAL LESION(S)
	# of defects	# of teeth present		R	L		
BOG129		0	U	U	U	U	
BOG130		0	U	U	U	U	
BOG131		0	U	U	U	U	
BOG132		0	U	U	U	U	
BOG134		0	U	U	U	U	
BOG135		0	U	U	U	U	Mixed woven and lamellar bone present on the lateral midshaft of the left tibia (6x3cm) and the proximal metaphysis lateral to the tibial tuberosity (3x2cm). Large "button" of mixed bone present on the lateral midshaft of the right tibia (1x2.5cm)
BOG137	3	25	U	A	P	U	
BOG138	2	11	U	U	U	U	caries
BOG144	0	23	A	P	A	P	Caries
BOG146		0	U	U	U	U	
BOG149	2	15	P	U	U	U	AMTL, possible slight anterior bowing of bilateral forma (broken)
BOG152		0	A	A	A	U	
BOG153		0	U	U	U	U	Porous woven bone present on the medial surface on the right calcaneus (1x1cm) and bilateral distal tibia just superior to the medial malleolus (2x1cm)
BOG161	5	22	A	A	A	U	
BOG169		0	U	U	U	U	
BOG172		0	U	U	U	U	
BOG174		0	U	U	U	U	
BOG176	0	1	A	A	A	U	Porous new bone formation present on the anterior maxillae and zygomatic bones, Porosity and new woven bone (spider web appearance) present in both maxillary sinuses, AMTL
BOG177		0	U	U	U	U	
BOG179		0	U	U	U	U	

Key: EH – enamel hypoplasia; PO – porotic hyperostosis; CO – cribra orbitalia; AG – arrested growth; A – lesion was absent; P – lesion was present; U – skeletal element was absent or unobservable; AMTL – antemortem tooth loss

ID	EH		PO	CO		AG	SKELETAL LESION(S)
	# of defects	# of teeth present		R	L		
BOG182		0	U	U	U	U	
BOG194	9	24	A	A	A	P	Porosity present on the superior margin of the left external auditory meatus and the posterior surface of the left greater wing of the sphenoid
BOG196	0	20	A	A	A	U	Porosity and new woven bone (spider web appearance) present in both maxillary sinuses, AMTL, caries
BOG197	0	1	A	A	A	U	AMTL
BOG200		0	U	U	U	U	
BOG210		0	U	U	U	U	
BOG211		0	U	U	U	U	
BOG212		0	U	U	U	U	
BOG231		0	U	U	U	U	
BOG240	0	24	U	U	U	P	Dark subperiosteal staining on the os coxa and femur (L femoral head and distal shaft/epiphysis), possible lateral bowing of femora shafts
BOG243		0	U	U	U	U	
BOG246A		0	U	U	U	U	
BOG246B		0	U	U	U	U	
BOG247		0	A	A	A	P	Porosity present on the anterior surface of the greater wings of the sphenoid and the inferior surface of the pars basilaris. Porous woven bone present on the squama of the temporal bones (bilateral) and along the anterior body of the mandible.
BOG248		0	U	U	U	U	
BOG249	0	3	A	A	A	U	AMTL
BOG250	0	4	A	P	U	P	Porosity present on the superior margin on the external auditory meatus (bilateral), the anterior surface of the right greater wing of the sphenoid, and on the mental eminence of the mandible. Friable surfaces on the anterior proximal humeri, right posterior distal femur, and the proximal posterior tibiae

Key: EH – enamel hypoplasia; PO – porotic hyperostosis; CO – cribra orbitalia; AG – arrested growth; A – lesion was absent; P – lesion was present; U – skeletal element was absent or unobservable; AMTL – antemortem tooth loss

ID	EH		PO	CO		AG	SKELETAL LESION(S)
	# of defects	# of teeth present		R	L		
BOG251	3	11	A	A	A	U	Porosity present on the superior margin of the external auditory meatus (bilateral)
BOG252	0	7	A	A	A	U	Porosity present on the superior aspect of the internal occipital protuberance of the occipital bone and the superior margin of the right external auditory meatus, AMTL, caries
BOG253		0	U	U	U	U	
BOG254	0	1	U	U	U	U	Porosity present on the inferior pars basilaris, along the superior margin of external auditory meatus (bilateral), and the internal occipital protuberance
BOG255	8	27	A	P	A	U	Porous woven bone present on the visceral surface of two rib fragments (1x4cm, 1x2cm), periodontal disease (lower right quadrant), deep depression of internal occipital protuberance and deep transverse sulcus on the occipital bone
BOG260		0	U	U	U	U	
BOG262		0	U	U	U	U	
BOG264	0	3	U	U	U	U	Porosity and woven bone on the anterior mandible. Friable surfaces on the right anterior proximal femur metaphysis, right later proximal ulna, and right anterior proximal radius
BOG265	0	15	A	P		A	New woven bone and porosity present on the anterior body of the mandible, on the right temporal bone around the external auditory meatus and squama, on the condyles of the occipital bone, Lytic lesion present on the inferior body of the pars basilaris (1x1cm) Porosity on the superior body of the sphenoid Friable surfaces and flared metaphyses on the left and right proximal humeri, the right posterior proximal femur, and the left posterior proximal femur
BOG270		0	U	U	U	U	

Key: EH – enamel hypoplasia; PO – porotic hyperostosis; CO – cribra orbitalia; AG – arrested growth; A – lesion was absent; P – lesion was present; U – skeletal element was absent or unobservable; AMTL – antemortem tooth loss

ID	EH		PO	CO		AG	SKELETAL LESION(S)
	# of defects	# of teeth present		R	L		
BOG272	0	1	A	U	P	U	Porosity present on the superior aspect of the internal occipital protuberance and the superior margin of the external auditory meatus (bilateral) Circular lytic lesions present on the endocranial occipital bone inferior to the right transverse sulcus (1x2cm), AMTL
BOG273		0	U	U	U	U	
BOG275		0	U	P	P	U	
BOG276		0	U	U	U	U	
BOG281	0	4	A	A	P	P	Porous woven bone across the palate (bilateral)
BOG282		0	U	U	U	U	
BOG283		0	U	U	U	U	
BOG284		0	U	U	U	U	
BOG286		0	U	U	U	U	
BOG287		0	U	U	U	U	
BOG289	0	15	A	A	A	U	Porosity present on the superior margin of the external auditor meatus (bilateral) and the superior body of the sphenoid, AMTL, caries, periodontal disease (upper right quadrant)
BOG290	0	4	A	P	P	U	Porosity and lytic lesion on the left temporal bone antero-inferior to the zygomatic process (1x1cm) Porosity and new woven bone formation on the superior and inferior body of the pars basilaris, AMTL

Key: EH – enamel hypoplasia; PO – porotic hyperostosis; CO – cribra orbitalia; AG – arrested growth; A – lesion was absent; P – lesion was present; U – skeletal element was absent or unobservable; AMTL – antemortem tooth loss

ICL 111											
left mandibular permanent M1						left maxillary M3					
Section	%N	$\delta^{15}\text{N}$	%C	$\delta^{13}\text{C}$	C:N	Section	%N	$\delta^{15}\text{N}$	%C	$\delta^{13}\text{C}$	C:N
1	15.8	10.4	42.3	-18.0	3.1	1	16.3	10.2	43.4	-17.7	3.1
2	15.9	10.1	42.9	-18.5	3.1	2	16.3	10.2	42.9	-18.3	3.1
3	15.8	10.5	42.9	-18.2	3.2	3	16.4	9.9	44.0	-18.9	3.1
4	15.8	10.5	42.3	-18.3	3.1	4	16.2	9.8	41.5	-19.1	3.0
5	15.8	9.9	42.4	-19.2	3.1	5	15.8	9.7	42.7	-19.1	3.2
6	15.7	10.0	42.5	-18.7	3.2	6	15.9	9.6	41.8	-18.5	3.1
7	15.8	9.8	42.4	-18.9	3.1	7	15.9	9.9	44.1	-17.6	3.2
8	15.6	9.9	43.1	-18.4	3.2	8	15.8	9.6	43.0	-18.2	3.2
9	15.6	10.0	41.5	-16.1	3.1	9	15.7	10.4	41.9	-16.3	3.1
10	15.6	10.2	42.5	-16.2	3.2	10	15.7	10.0	42.5	-16.9	3.2
11	15.7	10.5	43.2	-16.1	3.2	11	15.5	10.2	41.2	-16.4	3.1
12	15.6	10.5	44.4	-16.3	3.3	12	15.4	10.0	41.5	-16.5	3.1
13	15.7	10.7	43.0	-16.4	3.2	13	15.3	9.8	42.0	-17.1	3.2
14	15.6	10.7	42.8	-16.3	3.2	14	15.3	10.2	41.1	-17.2	3.1
15	15.6	10.9	42.4	-16.8	3.2						
16	15.5	10.7	42.3	-17.4	3.2						
17	15.6	10.6	42.9	-17.4	3.2						
ICL 120											
left mandibular PM1						right mandibular M3					
Section	%N	$\delta^{15}\text{N}$	%C	$\delta^{13}\text{C}$	C:N	Section	%N	$\delta^{15}\text{N}$	%C	$\delta^{13}\text{C}$	C:N
1	15.6	10.6	42.6	-18.1	3.2	1	15.1	10.7	41.5	-18.4	3.2
2	15.6	10.4	42.8	-17.7	3.2	2	15.2	10.1	41.7	-18.1	3.2
3	15.5	10.4	42.1	-17.3	3.2	3	15.2	10.0	42.2	-18.0	3.2
4	15.6	10.7	43.2	-17.5	3.2	4	15.2	9.5	42.7	-17.9	3.3
5	15.5	10.5	43.0	-17.1	3.2	5	15.3	9.3	43.6	-18.3	3.3
6	15.6	10.5	43.6	-17.2	3.3	6	15.2	9.5	41.8	-18.8	3.2
7	15.5	10.3	42.7	-17.6	3.2	7	15.2	10.1	42.5	-18.0	3.3
8	15.7	10.1	43.5	-18.2	3.2	8	15.2	10.4	42.4	-17.4	3.3
9	15.7	9.9	43.1	-18.5	3.2	9	15.0	10.5	41.5	-17.5	3.2
10	15.6	9.9	42.5	-18.6	3.2	10	15.1	10.5	42.5	-17.5	3.3
11	15.6	10.0	42.3	-19.1	3.2	11	15.3	10.4	42.2	-17.8	3.2
12	15.5	10.3	42.5	-18.9	3.2	12	15.0	10.4	40.9	-17.6	3.2
13	15.5	10.2	42.2	-19.4	3.2	13	15.1	11.0	41.3	-17.3	3.2
14	15.4	10.0	42.3	-18.7	3.2	14	14.8	11.5	40.4	-17.0	3.2
15	15.2	10.1	42.6	-17.9	3.3	15	14.8	11.3	42.4	-17.4	3.3
16	15.3	9.7	42.7	-17.1	3.3	16	14.9	10.8	41.4	-17.8	3.2
17	15.5	9.8	43.9	-18.8	3.3	17	14.8	10.7	41.5	-17.8	3.3
18	15.5	10.0	44.0	-20.3	3.3	18	14.9	11.2	41.7	-17.0	3.3
19	15.6	10.5	43.3	-20.8	3.2						
20	15.6	10.4	41.9	-20.9	3.1						

ICL 123						ICL 127					
right maxillary permanent I2						left mandibular permanent M2					
Section	%N	$\delta^{15}\text{N}$	%C	$\delta^{13}\text{C}$	C:N	Section	%N	$\delta^{15}\text{N}$	%C	$\delta^{13}\text{C}$	C:N
1	16.0	13.0	42.8	-17.8	3.1	1	15.8	11.9	42.1	-19.6	3.1
2	16.2	12.6	42.5	-17.5	3.1	2	16.0	11.3	41.8	-18.6	3.0
3	16.2	11.7	42.7	-17.8	3.1	3	15.7	10.9	42.4	-17.5	3.1
4	16.3	11.2	42.6	-18.1	3.1	4	15.7	11.3	42.8	-18.2	3.2
5	16.2	11.7	42.2	-18.1	3.0	5	16.1	10.9	43.6	-18.5	3.2
6	16.2	12.2	42.5	-17.4	3.1	6	15.9	11.0	42.1	-18.4	3.1
7	16.0	12.0	42.1	-17.0	3.1	7	15.8	11.2	41.6	-17.9	3.1
8	17.8	10.5	47.6	-18.0	3.1	8	16.0	11.4	43.0	-17.6	3.1
9	18.0	10.0	46.0	-19.0	3.0	9	15.8	11.1	42.0	-17.5	3.1
10	17.5	10.5	45.0	-19.1	3.0	10	15.9	11.4	42.1	-17.6	3.1
11	17.6	9.9	45.6	-17.9	3.0	11	15.8	11.3	44.4	-17.6	3.3
12	18.2	9.0	47.9	-17.3	3.1	12	15.9	11.5	43.4	-17.5	3.2
13	17.7	9.4	46.8	-17.1	3.1	13	15.7	11.2	41.3	-17.1	3.1
14	17.7	9.3	45.8	-17.4	3.0	14	15.8	11.6	42.6	-16.4	3.1
15	17.3	10.4	45.6	-17.6	3.1	15	15.8	11.8	41.4	-17.7	3.1
16	17.7	9.7	47.5	-17.8	3.1	16	15.7	12.0	41.8	-18.7	3.1
17	17.3	10.0	45.5	-18.1	3.1	17	15.8	12.1	41.5	-18.6	3.1
18	17.2	10.2	45.0	-18.6	3.1	18	15.6	12.2	41.6	-18.5	3.1
19	17.0	10.2	45.7	-19.2	3.1						
20	17.0	10.2	45.3	-19.2	3.1						
left mandibular deciduous m2						left maxillary permanent C					
Section	%N	$\delta^{15}\text{N}$	%C	$\delta^{13}\text{C}$	C:N	Section	%N	$\delta^{15}\text{N}$	%C	$\delta^{13}\text{C}$	C:N
1	15.4	13.5	42.5	-17.0	3.2	1	14.4	14.7	41.4	-17.8	3.4
2	15.5	14.1	43.2	-16.7	3.2	2	15.9	13.8	44.8	-18.0	3.3
3	15.5	14.5	43.5	-16.3	3.3	3	15.8	13.4	44.4	-18.5	3.3
4	15.5	14.2	42.5	-16.3	3.2	4	15.9	12.6	44.5	-19.4	3.3
5	15.5	14.5	42.7	-16.1	3.2	5	16.0	12.4	44.8	-19.2	3.3
6	15.6	14.2	43.1	-16.4	3.2	6	16.0	11.3	44.6	-19.6	3.3
7	15.5	14.3	42.4	-16.6	3.2	7	16.0	11.5	44.6	-19.9	3.2
8	15.4	13.4	43.0	-17.1	3.3	8	15.8	11.7	43.8	-19.7	3.2
9	15.6	13.8	42.4	-17.0	3.2	9	15.7	11.2	43.4	-19.7	3.2
10	15.7	12.8	42.8	-17.6	3.2	10	15.7	10.6	43.7	-19.3	3.3
11	15.5	13.4	42.8	-16.8	3.2	11	15.8	10.4	43.0	-18.6	3.2
12	15.5	12.7	42.6	-17.3	3.2	12	15.6	10.6	43.9	-18.9	3.3
13	15.4	12.8	42.4	-17.7	3.2	13	15.7	10.3	44.8	-19.0	3.3
14	15.2	12.5	42.6	-18.2	3.3	14	15.5	10.4	43.2	-18.8	3.2
15	15.1	12.5	42.8	-18.8	3.3	15	15.4	10.5	44.4	-18.7	3.4
						16	15.5	10.5	44.9	-19.5	3.4

ICL 129						ICL 130					
right mandibular deciduous i2						left maxillary permanent M1					
Section	%N	$\delta^{15}\text{N}$	%C	$\delta^{13}\text{C}$	C:N	Section	%N	$\delta^{15}\text{N}$	%C	$\delta^{13}\text{C}$	C:N
1	14.9	13.1	42.3	-16.0	3.3	1	15.4	13.2	44.0	-16.4	3.3
2	15.1	13.4	42.4	-15.9	3.3	2	15.4	11.6	43.8	-17.3	3.3
3	15.0	13.7	41.3	-15.7	3.2	3	15.3	11.1	45.1	-20.3	3.4
4	15.7	13.8	41.9	-15.6	3.1	4	15.4	12.8	42.6	-19.1	3.2
5	15.1	13.9	43.1	-16.0	3.3	5	15.2	12.0	45.2	-18.9	3.5
6	14.2	13.1	41.6	-17.4	3.4	6	15.4	9.8	43.9	-19.1	3.3
7	14.8	12.9	42.1	-17.5	3.3	7	15.3	10.8	44.1	-19.3	3.4
8	14.1	12.5	40.8	-17.8	3.4						
9	13.0	10.9	39.6	-18.0	3.6						
left maxillary permanent i1						right maxillary permanent M2					
Section	%N	$\delta^{15}\text{N}$	%C	$\delta^{13}\text{C}$	C:N	Section	%N	$\delta^{15}\text{N}$	%C	$\delta^{13}\text{C}$	C:N
1	15.0	12.3	41.9	-17.9	3.3	1	15.4	10.1	42.8	-17.1	3.2
2	15.2	11.3	42.2	-17.1	3.2	2	16.0	9.5	44.7	-18.1	3.3
3	15.1	10.3	40.9	-16.5	3.2	3	15.7	9.2	43.0	-17.2	3.2
4	15.2	10.8	41.9	-16.6	3.2	4	15.6	9.7	42.9	-16.6	3.2
5	15.1	10.7	41.3	-16.4	3.2	5	15.7	9.6	42.8	-16.4	3.2
6	15.1	10.8	41.1	-16.3	3.2	6	15.7	9.7	44.5	-16.0	3.3
7	15.3	10.6	41.7	-16.5	3.2	7	16.0	10.0	43.3	-16.0	3.2
8	15.3	10.0	42.8	-17.0	3.3	8	15.7	10.0	44.1	-15.4	3.3
9	15.2	9.9	41.4	-17.3	3.2	9	15.6	9.8	44.4	-15.3	3.3
10	15.3	9.8	41.9	-17.8	3.2	10	15.8	9.5	43.1	-15.7	3.2
11	15.1	9.9	41.3	-18.2	3.2	11	15.8	9.4	43.2	-16.2	3.2
12	15.1	9.5	41.2	-18.0	3.2	12	15.6	9.4	43.2	-16.3	3.2
13	15.4	9.5	42.0	-17.7	3.2	13	15.9	8.9	44.2	-16.5	3.2
14	15.3	9.6	42.4	-17.1	3.2	14	15.8	9.2	43.2	-16.3	3.2
15	15.1	9.5	41.4	-16.6	3.2	15	15.8	9.3	43.8	-15.4	3.2
16	15.1	9.6	41.0	-16.5	3.2	16	15.6	9.3	43.7	-14.7	3.3
17	15.0	9.6	41.1	-16.3	3.2	17	15.5	9.3	43.0	-14.0	3.2
18	15.3	9.4	41.4	-16.1	3.2	18	15.5	9.4	43.5	-14.8	3.3
19	15.2	9.6	41.4	-16.1	3.2	19	15.6	9.4	43.7	-15.3	3.3
20	15.3	9.6	42.3	-15.9	3.2	20	15.6	9.3	43.9	-15.3	3.3
21	15.1	9.7	41.5	-15.7	3.2	21	15.5	9.5	44.8	-15.3	3.4
22	15.3	9.9	42.1	-15.6	3.2						
23	15.2	10.3	42.7	-16.0	3.3						
ICL 131						ICL 130					
left maxillary deciduous i1						left mandibular permanent M1					
Section	%N	$\delta^{15}\text{N}$	%C	$\delta^{13}\text{C}$	C:N	Section	%N	$\delta^{15}\text{N}$	%C	$\delta^{13}\text{C}$	C:N
1	15.1	13.2	42.2	-16.9	3.3	1	15.9	14.8	45.1	-17.5	3.3
2	14.5	13.9	41.7	-17.3	3.4	2	15.9	13.9	43.4	-18.7	3.2
3	14.9	14.1	41.2	-17.3	3.2	3	16.1	13.4	43.2	-18.6	3.1
4	15.0	14.3	42.0	-17.4	3.3	4	16.2	12.8	44.4	-18.5	3.2
5	14.9	14.0	41.5	-18.3	3.2	5	16.1	11.5	44.7	-18.5	3.2

6	14.4	14.0	41.5	-18.5	3.4	6	16.1	11.5	44.7	-18.2	3.2
7	15.0	13.4	41.8	-18.7	3.3	7	16.3	10.8	44.8	-18.3	3.2
8	14.9	13.2	41.8	-18.8	3.3	8					
9	15.5	13.1	42.9	-18.4	3.2	9					
10	14.6	12.4	41.9	-18.5	3.3	10					
11	12.9	12.5	37.3	-18.3	3.4	11					
12	12.9	12.5	37.3	-18.3	3.4	12					
13	14.5	12.1	42.1	-18.0	3.4	13					
14	15.1	11.9	41.8	-17.7	3.2	14					
15	15.0	11.5	42.4	-18.3	3.3	15					
ICL 134											
right maxillary permanent C						right maxillary permanent M2					
Section	%N	$\delta^{15}\text{N}$	%C	$\delta^{13}\text{C}$	C:N	Section	%N	$\delta^{15}\text{N}$	%C	$\delta^{13}\text{C}$	C:N
1	15.2	13.4	42.1	-17.4	3.2	1	16.5	14.0	45.9	-17.1	3.3
2	15.4	11.5	42.8	-17.6	3.2	2	16.7	12.4	47.1	-17.7	3.3
3	15.5	10.8	43.3	-17.5	3.3	3	16.4	11.7	45.2	-17.5	3.2
4	15.6	11.0	42.8	-16.6	3.2	4	16.3	11.2	45.7	-17.6	3.3
5	15.5	11.4	42.5	-16.5	3.2	5	16.6	10.3	46.5	-18.1	3.3
6	15.4	11.2	43.2	-16.6	3.3	6	16.2	10.2	45.9	-17.6	3.3
7	15.6	10.9	43.7	-16.5	3.3	7	16.4	10.2	46.5	-17.0	3.3
8	15.4	10.5	43.2	-16.9	3.3	8	16.5	10.6	45.8	-16.7	3.2
9	15.5	10.1	42.7	-17.5	3.2	9	16.5	10.6	45.3	-16.8	3.2
10	15.5	10.1	42.9	-17.8	3.2	10	16.4	10.5	44.8	-16.8	3.2
11	15.5	10.2	42.8	-18.2	3.2	11	16.4	10.7	44.5	-16.2	3.2
12	15.3	10.5	42.4	-18.2	3.2	12	16.4	10.8	45.4	-16.2	3.2
13	15.5	10.4	42.6	-17.6	3.2	13	16.1	11.0	45.7	-16.4	3.3
14	15.4	10.6	42.5	-16.9	3.2	14	16.0	11.0	44.0	-16.5	3.2
15	15.5	10.2	42.1	-16.5	3.2	15	15.9	10.5	45.7	-17.3	3.4
16	15.5	10.2	42.8	-16.4	3.2	16	15.9	10.6	45.2	-18.1	3.3
17	15.4	10.4	42.4	-16.2	3.2						
18	15.3	10.5	42.0	-16.4	3.2						
19	15.3	10.8	42.1	-16.4	3.2						
20	15.3	10.9	42.7	-16.3	3.2						
21	15.3	10.9	43.3	-16.7	3.3						
22	15.5	11.0	42.9	-16.6	3.2						
23	15.5	10.9	43.5	-16.1	3.3						
24	15.3	10.8	42.6	-16.4	3.2						
25	15.3	11.3	43.1	-15.8	3.3						
ICL 135											
right mandibular permanent C						right mandibular M3					
Section	%N	$\delta^{15}\text{N}$	%C	$\delta^{13}\text{C}$	C:N	Section	%N	$\delta^{15}\text{N}$	%C	$\delta^{13}\text{C}$	C:N
1	14.8	11.6	40.8	-18.0	3.2	1	15.0	10.9	40.9	-17.7	3.2
2	15.3	11.6	41.1	-18.2	3.1	2	15.4	10.7	42.5	-18.2	3.2
3	15.3	11.1	41.9	-18.4	3.2	3	15.1	11.1	40.9	-17.1	3.2
4	15.3	10.9	42.0	-18.3	3.2	4	15.3	11.1	43.0	-16.5	3.3
5	15.4	10.7	42.0	-18.0	3.2	5	15.5	11.5	43.2	-16.7	3.3
6	15.3	10.5	42.3	-17.9	3.2	6	15.1	11.1	41.1	-17.1	3.2
7	15.4	10.5	41.9	-17.3	3.2	7	14.9	10.9	40.7	-17.3	3.2

8	15.5	10.4	42.1	-16.7	3.2	8	15.1	11.1	44.5	-17.6	3.4
9	15.4	9.8	42.1	-17.2	3.2	9	15.3	10.8	43.0	-17.9	3.3
10	15.3	9.4	41.9	-17.6	3.2	10	14.8	11.3	42.8	-17.7	3.4
11	15.3	9.5	41.8	-17.9	3.2	11	15.0	11.1	40.8	-17.7	3.2
12	21.4	9.5	58.6	-18.1	3.2	12	14.9	11.0	41.9	-17.4	3.3
13	15.3	9.8	41.6	-18.3	3.2	13	15.0	11.0	41.6	-17.5	3.2
14	15.4	9.8	41.7	-17.9	3.2	14	15.1	11.3	42.6	-17.8	3.3
15	15.3	9.7	41.2	-17.6	3.1	15	15.0	11.6	42.8	-17.4	3.3
16	15.3	9.8	42.1	-17.5	3.2	16	14.9	11.6	42.6	-17.7	3.3
17	15.4	9.9	41.7	-17.4	3.2	17	14.8	11.8	42.0	-17.9	3.3
18	15.4	10.0	42.5	-17.5	3.2						
19	15.3	10.1	42.1	-17.6	3.2						
20	15.3	10.3	42.3	-17.5	3.2						
21	15.3	11.0	42.2	-17.7	3.2						
ICL 136											
left maxillary permanent I1						left maxillary M3					
Section	%N	$\delta^{15}\text{N}$	%C	$\delta^{13}\text{C}$	C:N	Section	%N	$\delta^{15}\text{N}$	%C	$\delta^{13}\text{C}$	C:N
1	15.7	13.1	45.4	-15.8	3.4	1	15.7	11.5	45.0	-17.0	3.3
2	15.5	12.9	45.1	-16.8	3.4	2	15.8	10.8	44.5	-18.4	3.3
3	15.7	12.8	43.5	-14.8	3.2	3	15.7	10.8	45.1	-18.1	3.3
4	15.5	12.6	45.2	-17.7	3.4	4	16.0	11.0	44.7	-17.4	3.3
5	15.4	11.8	43.1	-18.0	3.3	5	15.9	11.1	45.1	-17.6	3.3
6	15.6	11.1	43.1	-15.8	3.2	6	15.9	11.5	45.5	-17.2	3.3
7	15.7	10.7	43.8	-15.6	3.3	7	16.0	11.7	46.8	-16.6	3.4
8	15.5	10.6	42.3	-15.4	3.2	8	16.1	11.9	44.6	-16.5	3.2
9	15.7	10.7	44.6	-17.1	3.3	9	16.0	11.9	45.3	-17.2	3.3
10	15.7	10.5	44.3	-17.1	3.3	10	15.9	12.0	45.0	-17.4	3.3
11	15.6	10.7	43.5	-17.6	3.2	11	16.0	12.1	44.1	-17.5	3.2
12	15.6	10.9	42.2	-16.0	3.2	12	16.0	12.0	44.6	-17.1	3.2
13	15.1	11.2	42.0	-17.0	3.2	13	15.9	12.0	44.0	-16.7	3.2
14	15.5	11.4	43.7	-15.7	3.3	14	15.8	11.8	44.8	-17.4	3.3
15	15.2	11.7	43.6	-15.7	3.3	15	15.6	12.0	43.6	-17.2	3.3
						16	15.6	12.1	44.1	-17.6	3.3
						17	15.8	12.0	44.6	-17.6	3.3
ICL 137											
left maxillary permanent I2						left maxillary M3					
Section	%N	$\delta^{15}\text{N}$	%C	$\delta^{13}\text{C}$	C:N	Section	%N	$\delta^{15}\text{N}$	%C	$\delta^{13}\text{C}$	C:N
1	16.7	9.3	45.9	-18.0	3.2	1	15.6	12.6	41.4	-18.6	3.1
2	17.0	9.7	47.2	-17.2	3.2	2	15.9	12.0	45.0	-17.4	3.3
3	16.8	10.4	46.2	-17.9	3.2	3	16.1	12.4	44.7	-17.1	3.2
4	16.9	10.4	44.0	-18.8	3.0	4	15.9	11.7	44.9	-19.0	3.3
5	16.7	10.7	44.5	-18.0	3.1	5	16.1	11.3	44.7	-18.8	3.2
6	16.4	10.7	46.0	-16.7	3.3	6	16.0	11.5	43.4	-18.1	3.2
7	16.3	9.9	45.4	-16.4	3.2	7	15.8	11.4	44.2	-18.2	3.3
8	16.2	10.4	45.4	-15.9	3.3	8	15.9	11.6	44.3	-17.3	3.2
9	15.9	11.0	42.3	-15.9	3.1	9	15.8	11.4	43.4	-17.7	3.2
10	15.2	11.2	41.9	-17.4	3.2	10	16.0	11.4	44.3	-17.7	3.2
11	15.9	11.0	46.4	-19.2	3.4	11	15.7	11.4	43.4	-18.2	3.2

12	15.9	11.0	44.1	-18.2	3.2	12	15.7	11.5	42.5	-18.6	3.2
13	15.7	10.9	44.9	-18.5	3.3	13	15.4	11.6	43.7	-18.7	3.3
14	15.8	11.3	44.9	-18.5	3.3	14	15.2	11.7	43.0	-18.5	3.3
15	15.8	11.7	45.3	-18.6	3.3	15	15.1	12.2	43.0	-18.2	3.3
16	15.7	12.2	45.1	-18.7	3.4						
17	15.8	12.6	45.0	-18.6	3.3						
18	15.7	12.2	44.9	-18.0	3.3						
ICL 138											
left maxillary permanent I1						left mandibular M3					
Section	%N	$\delta^{15}\text{N}$	%C	$\delta^{13}\text{C}$	C:N	Section	%N	$\delta^{15}\text{N}$	%C	$\delta^{13}\text{C}$	C:N
1	15.3	14.9	42.2	-17.1	3.2	1	15.9	10.2	43.9	-15.9	3.2
2	15.6	13.1	42.8	-17.8	3.2	2	15.8	10.0	44.8	-16.7	3.3
3	15.5	11.3	43.0	-18.3	3.2	3	15.7	9.9	44.6	-17.4	3.3
4	15.5	10.1	42.3	-18.5	3.2	4	15.9	10.0	44.7	-17.8	3.3
5	15.5	9.9	42.7	-18.6	3.2	5	15.8	10.0	44.4	-19.4	3.3
6	15.7	9.7	42.7	-18.9	3.2	6	15.5	10.2	44.1	-19.0	3.3
7	15.7	10.0	42.9	-18.9	3.2	7	15.6	10.4	44.0	-19.0	3.3
8	15.8	9.9	43.0	-18.4	3.2	8	16.0	10.5	45.6	-15.9	3.3
9	15.6	10.0	43.2	-17.6	3.2	9	15.5	10.6	43.7	-15.9	3.3
10	15.6	10.2	42.6	-16.6	3.2	10	15.5	10.7	43.9	-16.5	3.3
11	15.6	10.3	43.1	-16.4	3.2	11	16.1	11.2	45.1	-16.5	3.3
12	15.5	10.2	42.3	-16.4	3.2	12	15.6	11.1	45.0	-17.3	3.4
13	15.6	10.4	43.7	-16.6	3.3	13	15.8	11.3	43.4	-17.1	3.2
14	15.7	10.2	42.7	-16.9	3.2	14	15.6	11.3	43.5	-17.4	3.2
15	15.2	10.3	42.0	-16.8	3.2						
16	15.5	10.1	42.6	-17.1	3.2						
17	15.6	10.2	43.2	-17.1	3.2						
18	15.6	10.2	42.8	-17.0	3.2						
19	15.6	10.6	43.1	-16.4	3.2						
20	15.5	10.6	43.2	-15.5	3.3						
21	15.5	10.4	43.2	-16.4	3.3						
ICL 139											
left mandibular permanent C						left mandibular permanent M2					
Section	%N	$\delta^{15}\text{N}$	%C	$\delta^{13}\text{C}$	C:N	Section	%N	$\delta^{15}\text{N}$	%C	$\delta^{13}\text{C}$	C:N
1	15.2	13.3	41.7	-17.2	3.2	1	15.7	10.7	44.6	-16.6	3.3
2	15.3	11.4	42.2	-16.6	3.2	2	15.5	10.6	44.0	-16.7	3.3
3	15.3	10.3	41.7	-17.3	3.2	3	15.5	11.3	45.0	-15.1	3.4
4	15.9	10.3	43.7	-17.6	3.2	4	15.5	10.9	43.7	-13.8	3.3
5	15.3	10.5	41.9	-17.1	3.2	5	15.6	10.1	45.7	-15.0	3.4
6	15.4	11.0	41.6	-16.4	3.2	6	15.5	9.7	44.0	-16.4	3.3
7	15.5	11.0	42.3	-15.2	3.2	7	15.6	9.7	44.6	-17.5	3.3
8	15.3	11.0	42.1	-14.1	3.2	8	15.5	9.5	44.2	-18.4	3.3
9	15.4	10.7	42.3	-14.3	3.2	9	15.5	9.3	42.6	-18.4	3.2
10	15.5	10.0	41.9	-15.3	3.2	10	15.8	9.3	45.2	-18.2	3.3
11	15.3	9.8	42.5	-16.1	3.2	11	15.8	9.4	45.5	-18.0	3.4
12	15.4	9.7	42.0	-16.8	3.2	12	16.0	9.5	44.0	-16.4	3.2
13	15.3	9.6	42.1	-17.7	3.2	13	15.8	9.6	45.1	-16.0	3.3
14	15.3	9.6	42.3	-18.3	3.2	14	15.5	9.7	43.6	-15.9	3.3

15	15.3	9.4	41.9	-18.3	3.2	15	15.5	9.4	44.2	-15.7	3.3
16	15.5	9.3	42.5	-18.4	3.2	16	15.6	9.7	44.2	-16.1	3.3
17	15.4	9.2	41.7	-17.7	3.2						
18	15.2	9.4	41.7	-16.6	3.2						
19	15.3	9.3	42.4	-16.4	3.2						
20	15.2	9.2	41.3	-16.2	3.2						
21	15.3	9.4	41.8	-16.2	3.2						
ICL 140											
left mandibular permanent C						left maxillary M3					
Section	%N	$\delta^{15}\text{N}$	%C	$\delta^{13}\text{C}$	C:N	Section	%N	$\delta^{15}\text{N}$	%C	$\delta^{13}\text{C}$	C:N
1	15.4	12.0	43.9	-16.7	3.3	1	15.8	9.4	42.9	-15.0	3.2
2	15.5	10.4	44.0	-19.1	3.3	2	15.5	9.4	41.5	-14.0	3.1
3	15.4	9.8	44.7	-19.2	3.4	3	15.4	8.8	42.4	-15.2	3.2
4	15.5	9.8	43.3	-16.9	3.3	4	15.5	8.7	42.7	-17.4	3.2
5	15.4	10.0	45.5	-17.0	3.4	5	15.6	8.8	41.8	-17.6	3.1
6	15.5	9.3	44.0	-13.7	3.3	6	15.6	8.9	43.1	-16.6	3.2
7	15.5	9.5	45.0	-18.3	3.4	7	15.8	9.2	43.0	-16.8	3.2
8	15.5	9.7	44.7	-19.1	3.4	8	15.8	9.3	44.3	-16.4	3.3
9	15.6	9.4	45.2	-19.2	3.4	9	15.4	9.4	43.1	-17.3	3.3
10	15.5	9.3	44.4	-19.1	3.3	10	15.4	9.2	43.6	-17.5	3.3
11	15.5	9.4	42.8	-16.3	3.2	11	15.4	9.3	41.3	-17.8	3.1
12	15.3	9.1	44.0	-16.1	3.4	12	15.5	9.5	43.8	-17.3	3.3
13	15.3	9.3	43.7	-16.5	3.3	13	15.6	9.6	43.0	-16.9	3.2
14	15.4	9.5	43.5	-17.1	3.3	14	15.3	9.7	43.1	-17.1	3.3
15	15.3	9.2	43.5	-17.6	3.3	15	15.5	9.7	41.6	-17.6	3.1
16	15.5	9.3	44.0	-17.5	3.3	16	15.6	9.7	42.3	-18.2	3.2
17	15.5	9.4	44.0	-17.7	3.3	17	15.8	10.1	43.7	-16.7	3.2
18	15.4	9.4	44.0	-17.3	3.3	18	15.5	10.7	43.5	-16.3	3.3
19	15.0	9.2	43.4	-17.1	3.4	19	15.6	10.4	43.3	-17.1	3.2
20	15.4	9.4	43.8	-16.6	3.3						
21	15.3	9.2	44.0	-18.8	3.4						
22	15.5	9.5	45.1	-19.1	3.4						
23	15.6	9.5	43.7	-18.3	3.3						
24	15.3	10.3	43.4	-16.8	3.3						
ICL 141											
right maxillary permanent M1						left maxillary permanent I1					
Section	%N	$\delta^{15}\text{N}$	%C	$\delta^{13}\text{C}$	C:N	Section	%N	$\delta^{15}\text{N}$	%C	$\delta^{13}\text{C}$	C:N
1	15.0	15.8	43.1	-17.9	3.4	1	15.3	16.0	43.8	-17.7	3.4
2	15.2	15.3	43.5	-17.3	3.3	2	15.2	15.1	43.9	-17.6	3.4
3	15.3	15.5	41.8	-17.3	3.2	3	15.5	13.3	44.4	-17.9	3.3
4	15.3	12.1	43.0	-17.5	3.3	4	15.4	12.1	43.8	-18.2	3.3
5	16.1	11.6	41.7	-17.5	3.0	5	15.4	11.6	44.2	-18.5	3.3
6	15.3	11.3	41.5	-18.2	3.2	6	15.5	11.6	42.8	-18.5	3.2
7	15.8	11.1	40.7	-17.9	3.0	7	15.8	11.4	43.4	-18.5	3.2
8	15.2	11.2	41.6	-18.2	3.2	8	15.6	11.2	44.2	-18.1	3.3
9	15.3	11.1	42.1	-18.0	3.2	9	15.7	11.1	43.3	-17.9	3.2
10	15.1	11.1	42.0	-17.9	3.2	10	15.6	10.6	43.8	-18.1	3.3
11	15.7	11.0	40.5	-17.5	3.0	11	15.8	10.8	43.6	-18.0	3.2

12	15.2	10.5	41.1	-17.6	3.1	12	15.8	10.7	44.9	-18.2	3.3
13	15.1	10.7	42.2	-17.5	3.3	13	16.0	10.7	45.5	-18.0	3.3
14	15.9	10.7	40.4	-16.9	3.0	14	15.6	10.8	44.7	-18.0	3.3
15	15.1	10.9	41.7	-17.0	3.2	15	15.6	11.0	43.9	-18.0	3.3
16	15.2	10.9	42.2	-17.4	3.2	16	15.4	11.0	44.0	-18.0	3.3
17	15.1	10.8	41.7	-17.6	3.2	17	15.6	11.0	44.0	-17.7	3.3
18	15.2	11.0	42.2	-17.7	3.2	18	15.7	11.1	43.3	-17.7	3.2
19	15.8	11.0	40.9	-17.1	3.0	19	15.6	11.2	43.5	-17.9	3.3
						20	15.7	10.9	43.6	-17.8	3.2
						21	15.7	10.7	44.6	-17.8	3.3
						22	15.6	11.4	42.7	-18.0	3.2
ICL 149											
right maxillary permanent C						right mandibular permanent M2					
Section	%N	$\delta^{15}\text{N}$	%C	$\delta^{13}\text{C}$	C:N	Section	%N	$\delta^{15}\text{N}$	%C	$\delta^{13}\text{C}$	C:N
1	14.7	13.3	41.4	-17.3	3.3	1	16.6	9.8	46.2	-16.1	3.3
2	14.9	11.3	41.8	-18.3	3.3	2	16.8	9.4	46.9	-15.6	3.2
3	14.9	10.4	40.7	-17.9	3.2	3	16.8	8.7	46.8	-16.1	3.3
4	14.7	10.1	38.5	-16.6	3.0	4	16.8	8.8	46.4	-17.4	3.2
5	14.9	10.3	39.2	-15.8	3.1	5	16.4	9.2	45.1	-17.6	3.2
6	14.9	10.2	39.2	-15.7	3.1	6	16.7	9.4	45.0	-17.4	3.1
7	15.7	10.0	40.0	-15.7	3.0	7	16.7	9.5	46.6	-16.9	3.3
8	15.0	9.5	38.3	-15.9	3.0	8	16.4	9.2	44.8	-17.1	3.2
9	15.0	9.4	38.4	-16.1	3.0	9	15.5	9.8	43.8	-17.1	3.3
10	14.9	9.2	38.3	-17.0	3.0	10	16.3	9.8	44.0	-17.1	3.2
11	15.0	9.1	39.8	-17.5	3.1	11	16.5	10.2	45.8	-17.1	3.2
12	15.0	9.3	38.2	-17.2	3.0	12	16.4	10.4	46.5	-16.8	3.3
13	14.7	9.5	40.7	-17.1	3.2	13	16.4	11.4	46.3	-16.7	3.3
14	14.8	9.5	40.6	-17.1	3.2	14	16.2	11.4	44.9	-16.7	3.2
15	15.0	9.7	40.7	-16.7	3.2	15	16.2	11.6	45.6	-15.0	3.3
16	14.7	9.7	41.1	-16.6	3.3	16	16.0	11.6	45.6	-14.5	3.3
17	15.0	9.6	41.8	-16.5	3.3						
18	14.9	9.7	41.3	-16.7	3.2						
19	14.8	9.9	41.1	-16.9	3.2						
20	14.9	10.2	41.1	-17.1	3.2						
21	14.8	11.1	41.6	-17.0	3.3						
22	14.8	11.4	42.4	-16.6	3.3						
23	14.8	11.6	40.9	-15.4	3.2						
ICL 154											
right maxillary permanent I1						right maxillary M3					
Section	%N	$\delta^{15}\text{N}$	%C	$\delta^{13}\text{C}$	C:N	Section	%N	$\delta^{15}\text{N}$	%C	$\delta^{13}\text{C}$	C:N
1	15.4	15.2	43.1	-16.7	3.3	1	17.3	9.8	47.7	-17.3	3.2
2	15.5	13.6	44.5	-18.7	3.3	2	16.0	9.3	43.9	-17.1	3.2
3	15.3	11.6	43.4	-17.0	3.3	3	15.9	9.5	44.3	-16.8	3.3
4	15.6	11.0	43.6	-16.2	3.3	4	15.9	9.2	43.6	-18.6	3.2
5	15.4	10.8	42.9	-15.9	3.3	5	16.2	9.2	45.6	-18.6	3.3
6	15.4	10.5	42.8	-16.2	3.2	6	16.2	9.6	45.4	-18.2	3.3
7	15.4	10.1	43.6	-19.7	3.3	7	16.2	9.9	45.5	-17.2	3.3
8	15.3	10.1	43.5	-19.3	3.3	8	16.0	10.2	44.6	-17.0	3.3

9	15.7	10.7	42.6	-16.9	3.2	9	16.1	10.5	43.6	-17.2	3.2
10	15.3	9.8	44.3	-18.7	3.4	10	15.5	11.5	42.7	-17.1	3.2
11	15.3	9.8	44.4	-17.4	3.4	11	15.3	12.0	41.8	-16.3	3.2
12	15.4	9.7	44.3	-19.2	3.4	12	15.4	12.4	42.2	-15.0	3.2
13	15.4	10.0	44.4	-19.4	3.4	13	15.5	11.6	43.2	-15.9	3.3
14	15.3	10.1	44.4	-17.7	3.4	14	15.8	11.5	43.6	-15.9	3.2
15	15.4	10.3	42.8	-17.2	3.2	15	15.3	11.8	43.2	-15.6	3.3
16	15.6	10.2	43.4	-17.9	3.3	16	15.6	11.7	43.2	-15.1	3.2
17	15.4	10.4	42.6	-17.1	3.2	17	15.2	11.2	41.9	-18.1	3.2
18	15.4	10.1	43.9	-16.6	3.3	18	15.4	11.1	41.4	-17.2	3.1
19	15.4	10.1	44.1	-18.4	3.3	19	15.2	11.3	43.4	-18.0	3.3
20	15.4	9.9	42.9	-15.9	3.2	20	15.1	11.6	43.5	-18.3	3.4
21	15.4	9.9	43.0	-15.8	3.3						
22	15.5	10.0	42.9	-16.7	3.2						
23	15.2	10.4	45.8	-18.8	3.5						
24	15.2	10.9	43.4	-17.3	3.3						
ICL 155											
left maxillary permanent M1						left mandibular M3					
Section	%N	$\delta^{15}\text{N}$	%C	$\delta^{13}\text{C}$	C:N	Section	%N	$\delta^{15}\text{N}$	%C	$\delta^{13}\text{C}$	C:N
1	15.5	15.5	43.2	-18.6	3.3	1	15.9	10.9	45.2	-18.2	3.3
2	15.8	14.5	44.3	-18.3	3.3	2	15.4	10.5	43.6	-18.2	3.3
3	15.5	14.2	41.2	-18.0	3.1	3	16.2	10.8	45.1	-18.1	3.3
4	15.9	13.1	43.3	-18.7	3.2	4	16.4	10.4	45.5	-18.5	3.2
5	15.5	12.6	42.4	-18.1	3.2	5	15.4	10.2	43.9	-18.3	3.3
6	15.9	12.3	44.3	-18.7	3.3	6	16.1	10.7	44.5	-18.4	3.2
7	15.5	12.5	44.1	-18.9	3.3	7	16.2	11.0	45.0	-18.1	3.2
8	15.4	12.2	40.7	-18.4	3.1	8	16.6	11.0	45.6	-17.4	3.2
9	15.4	12.4	43.9	-18.8	3.3	9	16.2	11.2	45.7	-17.6	3.3
10	15.5	12.0	43.2	-19.3	3.3	10	16.2	11.4	45.0	-17.7	3.2
11	15.5	11.8	44.5	-19.4	3.3	11	16.1	11.8	44.8	-17.8	3.2
12	15.7	11.4	44.7	-19.3	3.3	12	15.9	12.0	46.0	-17.8	3.4
13	15.9	11.4	41.8	-19.0	3.1	13	15.4	12.1	44.9	-17.5	3.4
14	15.9	11.1	44.1	-19.1	3.2	14	15.1	12.1	43.0	-17.2	3.3
15	15.6	11.3	45.1	-19.4	3.4	15	15.3	11.3	44.9	-17.1	3.4
16	15.2	11.2	43.3	-19.6	3.3	16	15.4	11.2	46.2	-18.1	3.5
17	15.2	11.2	44.3	-19.8	3.4	17	14.8	11.3	45.7	-19.0	3.6
18	15.3	10.9	38.3	-18.9	2.9						
19	15.3	10.5	44.6	-19.5	3.4						
ICL 156											
left maxillary permanent C						left mandibular M3					
Section	%N	$\delta^{15}\text{N}$	%C	$\delta^{13}\text{C}$	C:N	Section	%N	$\delta^{15}\text{N}$	%C	$\delta^{13}\text{C}$	C:N
1	15.3	15.2	43.5	-11.7	3.3	1	16.2	9.7	44.7	-16.3	3.2
2	15.5	13.4	43.5	-11.6	3.3	2	16.1	9.5	45.1	-16.4	3.3
3	15.5	11.8	43.1	-13.6	3.2	3	15.7	9.8	43.8	-18.1	3.3
4	15.7	10.7	43.4	-15.6	3.2	4	16.0	9.5	45.3	-17.6	3.3
5	15.5	10.1	42.9	-18.1	3.2	5	16.0	9.6	44.6	-16.7	3.2
6	15.5	9.7	42.7	-18.9	3.2	6	16.3	9.2	43.7	-17.2	3.1
7	15.4	9.3	43.6	-18.1	3.3	7	15.9	9.3	43.9	-17.8	3.2

8	15.5	8.9	42.9	-17.6	3.2	8	15.8	9.3	42.8	-18.0	3.2
9	15.6	9.2	43.4	-17.2	3.2	9	16.0	9.2	44.2	-18.1	3.2
10	15.6	8.9	43.3	-16.3	3.2	10	16.0	9.7	45.2	-18.1	3.3
11	15.6	8.4	45.1	-15.6	3.4	11	15.7	9.8	44.8	-18.1	3.3
12	15.5	8.4	45.9	-16.0	3.4	12	15.6	10.3	44.1	-17.9	3.3
13	15.4	8.8	43.8	-16.6	3.3	13	15.7	11.0	45.0	-17.2	3.3
14	15.6	8.9	44.3	-16.2	3.3	14	15.7	11.5	44.5	-17.5	3.3
15	15.5	9.6	45.4	-16.5	3.4	15	15.7	12.0	44.7	-18.2	3.3
16	15.5	10.0	43.9	-16.3	3.3	16	15.6	12.1	44.4	-17.3	3.3
17	15.4	9.8	46.2	-15.6	3.5						
18	15.4	10.1	43.7	-15.4	3.3						
19	15.6	10.3	42.8	-16.2	3.2						

FEN 6						FEN 6					
left maxillary permanent M1						right mandibular M3					
Section	%N	$\delta^{15}\text{N}$	%C	$\delta^{13}\text{C}$	C:N	Section	%N	$\delta^{15}\text{N}$	%C	$\delta^{13}\text{C}$	C:N
1	15.6	14.0	40.5	-16.9	3.0	1	16.1	9.7	45.0	-19.5	3.3
2	15.5	13.0	40.0	-16.9	3.0	2	16.2	9.4	43.8	-19.4	3.2
3	15.5	11.7	40.4	-17.5	3.0	3	16.3	9.8	45.0	-19.2	3.2
4	15.4	12.3	41.2	-17.3	3.1	4	16.5	10.0	46.5	-18.3	3.3
5	15.6	10.9	41.3	-17.8	3.1	5	16.5	9.7	46.6	-18.6	3.3
6	15.6	10.2	41.7	-18.5	3.1	6	16.3	9.8	45.4	-18.5	3.2
7	15.5	10.2	40.6	-18.9	3.1	7	15.9	9.7	42.6	-18.7	3.1
8	15.5	9.2	40.8	-19.1	3.1	8	16.2	9.4	43.8	-18.7	3.2
9	15.5	8.8	40.8	-19.2	3.1	9	16.4	9.1	44.1	-18.6	3.1
10	15.4	8.9	43.1	-19.1	3.3	10	16.8	8.8	46.0	-18.5	3.2
11	15.4	9.0	40.9	-19.1	3.1	11	16.3	9.0	45.6	-18.2	3.3
12	15.5	9.1	42.2	-19.0	3.2	12	16.6	9.5	45.8	-18.0	3.2
13	15.5	9.1	42.9	-18.8	3.2	13	16.3	9.5	45.7	-18.3	3.3
14	15.5	9.0	41.0	-18.8	3.1	14					
15	15.6	9.2	39.9	-18.5	3.0						
16	15.6	9.1	40.3	-18.5	3.0						
17	15.6	9.3	41.0	-18.3	3.1						
18	15.6	9.1	40.7	-18.4	3.0						
19	15.4	9.1	40.5	-19.5	3.1						

FEN 9					
right maxillary permanent C					
Section	%N	$\delta^{15}\text{N}$	%C	$\delta^{13}\text{C}$	C:N
1	15.1	14.6	39.8	-16.8	3.1
2	15.7	13.3	42.3	-17.6	3.1
3	15.7	12.0	42.1	-18.9	3.1
4	15.6	11.8	42.6	-19.2	3.2
5	15.7	11.0	42.1	-19.6	3.1
6	15.7	10.6	40.2	-19.4	3.0
7	16.0	10.1	40.8	-19.0	3.0
8	15.6	10.1	40.3	-18.7	3.0
9	15.8	9.9	42.0	-17.6	3.1
10	15.6	9.8	42.0	-17.5	3.1
11	15.7	9.8	41.1	-17.3	3.1

12	15.6	9.8	41.7	-17.1	3.1						
13	15.6	9.9	42.0	-17.2	3.1						
14	15.8	10.1	42.6	-16.9	3.1						
15	15.6	10.0	42.1	-16.8	3.1						
16	14.9	10.3	43.5	-16.1	3.4						
17	15.0	10.2	41.8	-16.6	3.2						
18	15.2	10.3	42.4	-16.9	3.3						
19	15.2	10.1	43.3	-17.3	3.3						
20	15.2	9.6	42.8	-18.4	3.3						
21	15.2	9.6	42.6	-18.9	3.3						
22	15.2	9.9	42.4	-19.2	3.3						
23	15.2	10.0	41.9	-19.0	3.2						
FEN 10											
right mandibular permanent M1						right mandibular permanent M2					
Section	%N	$\delta^{15}\text{N}$	%C	$\delta^{13}\text{C}$	C:N	Section	%N	$\delta^{15}\text{N}$	%C	$\delta^{13}\text{C}$	C:N
1	15.5	14.2	41.0	-19.5	3.1	1	16.0	10.8	45.1	-19.9	3.3
2	15.5	13.6	40.0	-19.9	3.0	2	16.3	10.4	45.2	-19.8	3.2
3	15.4	12.5	42.4	-19.6	3.2	3	16.3	10.4	43.5	-19.8	3.1
4	15.5	11.5	40.7	-19.8	3.1	4	16.3	10.8	45.6	-19.4	3.3
5	15.5	10.8	39.8	-20.2	3.0	5	16.7	10.5	47.7	-19.3	3.3
6	15.4	10.9	42.7	-20.1	3.2	6	16.2	10.8	44.4	-18.9	3.2
7	15.4	10.2	41.0	-20.4	3.1	7	16.7	10.7	44.8	-19.2	3.1
8	15.7	10.4	40.8	-20.2	3.0	8	16.2	10.2	45.0	-19.7	3.2
9	15.4	10.6	40.5	-20.0	3.1	9	16.0	10.3	44.8	-19.7	3.3
10	15.4	10.4	39.9	-20.1	3.0	10	15.8	10.6	44.7	-19.8	3.3
11	15.5	10.5	40.7	-20.0	3.1	11	15.7	10.7	44.0	-20.2	3.3
12	15.6	10.3	40.9	-19.9	3.1	12	15.4	10.5	44.5	-20.1	3.4
13	15.6	10.4	39.9	-19.9	3.0	13	15.4	10.5	42.5	-20.1	3.2
14	15.4	10.1	40.6	-19.9	3.1	14	15.2	10.6	44.8	-20.1	3.4
15	15.6	10.4	41.3	-19.5	3.1						
16	15.6	10.3	40.7	-19.7	3.0						
17	15.7	10.3	42.3	-19.6	3.2						
18	15.7	10.3	41.1	-19.4	3.1						
19	15.7	10.7	41.1	-19.2	3.1						
20	15.6	11.1	40.8	-18.8	3.1						
21	15.4	10.8	40.7	-19.3	3.1						
FEN 14											
left mandibular permanent I2											
Section	%N	$\delta^{15}\text{N}$	%C	$\delta^{13}\text{C}$	C:N						
1	15.4	10.9	43.7	-18.4	3.3						
2	15.4	10.0	43.8	-18.0	3.3						
3	15.7	10.1	42.5	-17.8	3.2						
4	15.6	10.0	41.3	-17.4	3.1						
5	15.5	9.9	39.9	-17.4	3.0						
6	15.6	10.0	42.1	-17.3	3.1						
7	15.6	9.7	43.2	-17.3	3.2						
8	15.6	9.5	43.1	-17.3	3.2						
9	15.6	9.5	43.3	-17.2	3.2						
10	15.5	9.4	43.5	-17.5	3.3						
11	15.5	9.4	45.0	-17.8	3.4						
12	15.6	9.5	45.0	-18.4	3.4						

13	15.4	9.6	42.5	-18.6	3.2								
14	15.4	9.6	41.9	-18.7	3.2								
15	15.6	9.7	42.0	-18.6	3.2								
16	16.6	9.5	44.6	-18.7	3.1								
17	15.5	9.3	45.2	-18.9	3.4								
18	15.4	9.7	45.1	-18.8	3.4								
19	15.5	10.0	44.5	-18.4	3.4								
20	15.6	9.9	44.7	-18.0	3.3								
FEN 15													
right mandibular deciduous m1						right mandibular permanent M1							
Section	%N	$\delta^{15}\text{N}$	%C	$\delta^{13}\text{C}$	C:N	Section	%N	$\delta^{15}\text{N}$	%C	$\delta^{13}\text{C}$	C:N		
1	14.9	13.6	41.7	-18.8	3.3	1	15.1	13.9	42.2	-19.3	3.2		
2	15.0	14.2	42.2	-18.9	3.3	2	15.7	13.6	43.8	-19.2	3.3		
3	14.8	13.9	41.3	-19.1	3.3	3	15.5	12.8	42.9	-19.4	3.2		
4	14.9	14.3	41.6	-18.9	3.2	4	15.2	13.0	42.6	-19.2	3.3		
5	15.2	14.4	41.9	-19.3	3.2	5	15.8	12.6	44.7	-19.2	3.3		
6	15.0	14.3	43.3	-19.3	3.4	6	15.5	12.0	42.5	-19.5	3.2		
7	15.2	13.8	42.8	-19.1	3.3	7	15.6	11.9	43.0	-19.5	3.2		
8	15.1	13.7	42.2	-19.0	3.3	8	15.4	11.5	40.9	-19.5	3.1		
9	15.0	13.8	42.2	-19.1	3.3	9	15.4	11.4	43.0	-19.4	3.3		
10	15.0	13.7	44.0	-19.1	3.4	10	15.5	11.2	43.1	-19.5	3.3		
11	15.0	13.4	42.7	-18.8	3.3	11	15.7	11.1	43.6	-19.4	3.2		
12	15.1	12.9	42.3	-19.1	3.3								
13	14.9	13.0	43.1	-19.2	3.4								
14	14.6	12.6	43.1	-19.4	3.4								
15	14.6	12.2	42.9	-19.5	3.4								
FEN 17													
left maxillary permanent M1													
Section	%N	$\delta^{15}\text{N}$	%C	$\delta^{13}\text{C}$	C:N								
1	15.3	14.3	44.5	-20.3	3.4								
2	15.4	14.1	45.0	-20.2	3.4								
3	15.3	13.5	43.8	-20.1	3.3								
4	15.4	13.6	44.6	-20.1	3.4								
5	15.4	13.3	42.4	-19.4	3.2								
6	15.7	12.8	44.7	-19.8	3.3								
7	15.7	12.5	45.0	-19.5	3.3								
8	15.6	12.2	44.4	-20.0	3.3								
9	15.6	12.3	44.1	-19.9	3.3								
10	15.6	12.3	44.4	-20.1	3.3								
11	15.3	12.2	43.7	-19.9	3.3								
12	15.6	12.0	43.5	-19.8	3.3								
13	15.4	11.9	42.3	-20.0	3.2								
14	15.7	11.8	44.9	-19.5	3.3								
15	15.7	11.6	44.2	-19.6	3.3								
16	15.7	11.9	43.3	-19.1	3.2								
17	15.6	11.9	43.4	-19.5	3.2								
18	15.2	12.2	42.4	-19.7	3.2								
19	15.5	12.3	43.6	-19.7	3.3								
20	15.6	12.5	44.3	-19.9	3.3								
21	15.1	12.2	43.8	-20.2	3.4								

FEN 42						left mandibular permanent M1					
Section	%N	$\delta^{15}\text{N}$	%C	$\delta^{13}\text{C}$	C:N	Section	%N	$\delta^{15}\text{N}$	%C	$\delta^{13}\text{C}$	C:N
1	14.1	12.6	40.1	-19.5	3.3	1	15.3	12.8	44.6	-20.1	3.4
2	13.9	13.0	40.3	-19.4	3.4	2	15.6	12.9	44.2	-20.0	3.3
3	14.1	12.9	40.4	-19.5	3.3	3	15.9	12.9	43.6	-20.1	3.2
4	14.6	12.6	42.7	-19.7	3.4	4	15.9	13.3	45.3	-19.8	3.3
5	14.2	12.6	39.1	-19.7	3.2						
6	14.4	12.9	40.4	-19.5	3.3						
7	14.6	13.4	37.3	-19.4	3.0						
8	14.6	13.7	38.0	-19.4	3.0						
9	14.3	13.6	38.9	-19.3	3.2						
FEN 43						left mandibular permanent M1					
Section	%N	$\delta^{15}\text{N}$	%C	$\delta^{13}\text{C}$	C:N	Section	%N	$\delta^{15}\text{N}$	%C	$\delta^{13}\text{C}$	C:N
1	15.7	11.5	45.2	-22.7	3.4	1	15.1	11.4	39.6	-19.6	3.0
2	15.9	11.4	45.1	-23.1	3.3	2	15.4	11.6	40.7	-19.4	3.1
3	15.7	11.0	44.9	-23.3	3.3	3	15.2	11.8	39.2	-19.7	3.0
4	15.7	11.1	44.6	-23.5	3.3	4	15.2	11.4	39.4	-19.6	3.0
5	15.8	11.3	45.8	-23.3	3.4	5	15.1	11.8	40.4	-19.6	3.1
6	15.8	11.1	44.8	-21.6	3.3	6	15.2	11.7	40.1	-19.8	3.1
7	15.9	11.1	44.7	-22.1	3.3	7	15.1	11.4	43.1	-19.5	3.3
8	15.9	11.0	44.8	-22.4	3.3						
9	15.7	11.3	44.4	-21.9	3.3						
10	15.7	11.2	44.0	-21.9	3.3						
11	15.7	11.2	44.7	-21.7	3.3						
12	15.8	11.2	45.0	-20.8	3.3						
13	15.8	11.3	44.5	-22.0	3.3						
14	15.7	11.4	42.6	-18.9	3.2						
15	15.8	11.3	41.9	-20.0	3.1						
16	15.6	11.2	44.0	-20.6	3.3						
17	15.8	11.4	41.9	-19.8	3.1						
18	15.7	11.3	42.6	-20.6	3.2						
19	15.7	11.6	41.8	-21.0	3.1						
20	15.8	11.2	41.6	-20.4	3.1						
21	15.6	11.3	41.2	-20.5	3.1						
22	15.5	11.6	41.4	-20.1	3.1						
FEN 50						left mandibular permanent M1					
Section	%N	$\delta^{15}\text{N}$	%C	$\delta^{13}\text{C}$	C:N	Section	%N	$\delta^{15}\text{N}$	%C	$\delta^{13}\text{C}$	C:N
1	15.5	14.4	40.6	-20.2	3.1	1	16.1	11.9	45.5	-20.6	3.3
2	15.7	13.5	42.4	-20.1	3.2	2	16.3	11.9	45.7	-20.2	3.3
3	15.7	12.7	42.3	-20.2	3.1	3	16.4	11.7	46.4	-19.9	3.3
4	15.8	11.3	42.4	-20.5	3.1	4	16.4	11.6	44.6	-19.7	3.2
5	15.7	10.7	40.2	-20.6	3.0	5	16.0	11.9	45.1	-19.6	3.3
6	15.7	10.4	44.2	-21.0	3.3						
7	15.6	10.5	43.1	-20.4	3.2						
8	15.8	10.5	43.3	-21.4	3.2						
9	15.8	10.4	43.6	-20.5	3.2						
10	15.7	10.4	40.7	-20.5	3.0						
11	15.7	10.1	43.3	-21.4	3.2						

12	15.6	10.1	44.4	-20.3	3.3						
13	15.8	10.3	46.4	-20.6	3.4						
14	15.8	10.2	44.7	-20.6	3.3						
15	15.6	10.3	44.0	-20.7	3.3						
16	15.7	10.2	45.1	-20.7	3.4						
17	16.0	10.4	44.6	-21.1	3.3						
18	15.6	10.7	43.8	-20.6	3.3						
19	15.7	10.7	45.1	-19.8	3.3						
20	15.6	11.2	45.9	-20.7	3.4						
FEN 52											
left mandibular permanent M1						left mandibular M3					
Section	%N	$\delta^{15}\text{N}$	%C	$\delta^{13}\text{C}$	C:N	Section	%N	$\delta^{15}\text{N}$	%C	$\delta^{13}\text{C}$	C:N
1	15.7	13.4	45.6	-16.8	3.4	1	15.6	10.7	43.1	-18.2	3.2
2	15.9	12.2	46.3	-17.2	3.4	2	15.5	10.8	40.0	-17.8	3.0
3	15.9	11.0	46.3	-17.2	3.4	3	15.4	10.8	40.3	-18.0	3.1
4	15.8	10.2	45.2	-17.2	3.3	4	15.3	10.7	40.3	-18.7	3.1
5	15.8	9.7	44.6	-17.3	3.3	5	15.3	10.8	40.4	-19.1	3.1
6	15.7	9.7	44.6	-17.8	3.3	6	15.2	10.4	41.3	-18.8	3.2
7	15.8	9.8	45.9	-18.1	3.4	7	14.9	10.4	39.9	-18.6	3.1
8	15.7	9.5	44.6	-17.6	3.3	8	14.6	10.4	40.6	-19.2	3.2
9	15.8	9.6	45.1	-17.5	3.3						
10	15.7	9.4	45.4	-17.8	3.4						
11	15.7	9.4	46.0	-17.2	3.4						
12	15.6	9.4	45.3	-17.1	3.4						
13	15.7	9.3	45.8	-16.8	3.4						
14	15.7	9.6	46.2	-16.6	3.4						
15	15.6	10.2	47.3	-16.9	3.5						
16	15.7	11.1	45.9	-17.8	3.4						
BOG 10											
left maxillary permanent M1						right mandibular permanent C					
Section	%N	$\delta^{15}\text{N}$	%C	$\delta^{13}\text{C}$	C:N	Section	%N	$\delta^{15}\text{N}$	%C	$\delta^{13}\text{C}$	C:N
1	15.6	13.3	45.3	-16.6	3.4	1	14.8	13.1	43.0	-16.9	3.4
2	15.8	12.7	44.9	-17.6	3.3	2	14.9	12.1	42.8	-18.6	3.3
3	15.9	12.2	45.3	-18.7	3.3	3	15.1	11.5	42.3	-19.1	3.3
4	15.8	12.1	42.7	-17.7	3.2	4	15.2	11.6	42.1	-18.9	3.2
5	15.7	11.1	43.8	-19.7	3.3	5	15.1	11.0	41.7	-18.4	3.2
6	15.8	10.9	45.0	-19.9	3.3	6	15.2	10.7	42.9	-18.4	3.3
7	15.8	10.6	44.7	-19.5	3.3	7	15.3	10.7	42.6	-18.2	3.2
8	15.9	10.5	46.5	-19.3	3.4	8	15.3	10.8	42.0	-18.1	3.2
9	15.6	9.9	44.5	-19.6	3.3	9	15.2	11.0	42.4	-18.1	3.3
10	15.8	10.0	45.0	-19.4	3.3	10	15.4	10.5	41.7	-18.1	3.2
11	15.6	10.0	45.8	-19.3	3.4	11	15.1	10.1	43.2	-17.7	3.3
12	15.5	10.2	46.1	-19.4	3.5	12	15.3	9.7	43.5	-17.8	3.3
13	15.8	10.1	45.8	-19.0	3.4	13	15.1	9.2	42.8	-18.1	3.3
14	15.3	10.5	44.0	-17.6	3.4	14	15.1	9.1	42.4	-17.8	3.3
15	15.3	10.8	45.6	-17.8	3.5	15	14.8	9.3	40.8	-17.9	3.2
16	15.4	10.3	45.8	-17.6	3.5	16	14.6	9.7	42.6	-17.6	3.4
						17	14.5	10.1	41.8	-17.9	3.4
						18	14.3	9.8	43.4	-18.6	3.5
						19	14.4	9.4	43.3	-18.8	3.5
						20	14.3	9.5	43.2	-19.1	3.5

						21	14.3	9.9	42.2	-18.9	3.4
						22	14.5	10.1	41.3	-18.8	3.3
BOG 59											
left mandibular permanent M1						left mandibular M3					
Section	%N	$\delta^{15}\text{N}$	%C	$\delta^{13}\text{C}$	C:N	Section	%N	$\delta^{15}\text{N}$	%C	$\delta^{13}\text{C}$	C:N
1	14.9	13.8	40.4	-19.4	3.2	1	15.0	10.6	40.8	-19.4	3.2
2	15.3	13.4	39.6	-19.3	3.0	2	15.1	10.3	41.4	-19.4	3.2
3	15.3	13.2	39.3	-19.3	3.0	3	15.3	10.3	41.9	-19.1	3.2
4	15.2	12.3	40.3	-19.5	3.1	4	15.2	10.4	41.9	-19.2	3.2
5	15.3	12.6	39.5	-19.5	3.0	5	15.4	10.8	41.2	-19.3	3.1
6	15.1	11.5	39.9	-19.6	3.1	6	15.5	11.4	41.7	-19.4	3.1
7	15.2	11.1	40.6	-19.6	3.1	7	14.9	11.5	40.3	-19.4	3.2
8	15.5	10.5	41.2	-19.5	3.1	8	14.8	11.4	40.9	-19.5	3.2
9	15.5	10.4	41.5	-19.6	3.1	9	15.2	11.8	42.0	-19.6	3.2
10	15.3	10.5	39.9	-19.4	3.0	10	14.8	11.1	40.3	-19.9	3.2
11	15.3	10.6	40.2	-19.5	3.1	11	15.0	11.0	39.8	-19.7	3.1
12	15.3	10.5	41.4	-19.7	3.2	12	14.8	10.5	41.4	-19.8	3.3
13	15.4	10.6	40.9	-19.5	3.1	13	14.5	10.4	40.1	-19.9	3.2
14	15.4	10.6	42.3	-19.4	3.2						
15	15.2	10.4	41.5	-19.4	3.2						
16	15.4	10.5	41.0	-19.3	3.1						
17	15.5	10.7	41.4	-19.2	3.1						
18	15.5	10.8	41.4	-19.1	3.1						
19	15.3	10.5	41.3	-19.0	3.2						
20	15.2	10.0	40.7	-19.2	3.1						
21	15.1	9.9	40.7	-19.2	3.2						
22	15.0	10.1	42.4	-19.2	3.3						
23	15.0	10.5	42.5	-19.6	3.3						
BOG 66											
right mandibular permanent C											
Section	%N	$\delta^{15}\text{N}$	%C	$\delta^{13}\text{C}$	C:N						
1	15.8	11.6	41.3	-19.3	3.0						
2	15.8	11.5	41.1	-19.4	3.0						
3	15.7	11.7	41.6	-19.7	3.1						
4	15.9	12.2	41.5	-19.7	3.1						
5	16.0	12.2	40.9	-19.9	3.0						
6	16.3	11.9	42.4	-19.8	3.0						
7	16.0	11.6	42.6	-19.7	3.1						
8	16.0	11.4	43.0	-19.6	3.1						
9	16.4	11.0	43.3	-19.6	3.1						
10	16.3	10.8	43.4	-19.4	3.1						
11	16.1	11.1	42.5	-19.2	3.1						
12	16.0	11.1	42.2	-19.4	3.1						
13	15.7	11.0	41.7	-19.5	3.1						
14	15.9	11.3	42.6	-19.3	3.1						
15	15.9	10.9	43.3	-19.3	3.2						
16	16.0	11.1	41.0	-19.1	3.0						
17	16.2	11.2	40.1	-19.2	2.9						
18	16.2	11.6	40.9	-19.1	2.9						
19	16.1	11.5	41.7	-19.1	3.0						
20	15.8	11.5	40.3	-19.3	3.0						

BOG 109											
right mandibular deciduous m1						left maxillary permanent I1					
Section	%N	$\delta^{15}\text{N}$	%C	$\delta^{13}\text{C}$	C:N	Section	%N	$\delta^{15}\text{N}$	%C	$\delta^{13}\text{C}$	C:N
1	14.8	14.2	40.0	-18.4	3.2	1	14.6	15.4	41.4	-18.4	3.3
2	15.0	14.4	38.2	-18.2	3.0	2	14.9	15.1	41.1	-18.2	3.2
3	15.3	14.4	41.0	-18.3	3.1	3	14.8	14.7	41.5	-18.3	3.3
4	15.2	14.4	40.1	-18.3	3.1	4	15.3	13.8	41.0	-18.6	3.1
5	15.5	14.0	40.7	-18.4	3.1	5	15.1	12.7	40.8	-19.2	3.2
6	15.1	13.8	40.1	-18.5	3.1	6	15.0	13.2	40.1	-18.9	3.1
7	15.3	13.7	41.7	-18.4	3.2	7	14.8	12.9	38.9	-19.1	3.1
8	15.5	13.3	40.3	-18.6	3.0	8	14.9	12.5	39.3	-19.2	3.1
9	15.0	12.8	38.7	-18.9	3.0						
10	15.1	12.4	39.5	-19.2	3.0						
11	14.8	11.9	39.8	-19.5	3.1						
12	15.0	11.8	39.9	-19.5	3.1						
13	14.7	12.1	40.3	-19.9	3.2						
BOG 161											
left maxillary permanent I2						left maxillary M3					
Section	%N	$\delta^{15}\text{N}$	%C	$\delta^{13}\text{C}$	C:N	Section	%N	$\delta^{15}\text{N}$	%C	$\delta^{13}\text{C}$	C:N
1	14.9	12.7	43.9	-18.1	3.4	1	15.2	11.5	42.9	-18.8	3.3
2	15.0	11.8	43.3	-18.5	3.4	2	15.2	11.0	40.5	-18.3	3.1
3	14.8	11.5	41.1	-18.9	3.2	3	15.6	10.9	41.0	-16.1	3.1
4	15.0	11.2	42.8	-19.2	3.3	4	15.6	10.7	40.7	-16.5	3.0
5	15.2	11.5	43.4	-18.9	3.3	5	15.5	11.1	41.5	-18.0	3.1
6	15.1	11.2	42.4	-18.7	3.3	6	15.4	11.3	42.1	-19.0	3.2
7	15.0	11.0	41.7	-18.5	3.2	7	15.2	11.2	41.6	-19.3	3.2
8	15.0	11.0	44.7	-18.7	3.5	8	15.1	11.1	40.6	-19.2	3.1
9	16.7	9.9	44.5	-18.1	3.1	9	15.3	10.9	41.1	-19.0	3.1
10	16.5	10.0	45.7	-17.9	3.2	10	15.3	11.2	40.8	-18.7	3.1
11	16.2	10.0	45.1	-17.7	3.2	11	15.2	11.1	41.9	-18.6	3.2
12	16.2	10.3	46.0	-17.7	3.3	12	15.2	11.0	42.1	-18.4	3.2
13	16.3	10.5	44.6	-17.5	3.2	13	15.1	11.2	41.1	-18.9	3.2
14	16.1	11.0	45.8	-18.1	3.3	14					
15	16.0	11.2	44.8	-18.2	3.3	15	15.1	11.2	42.0	-19.0	3.2
16	15.9	11.2	44.8	-18.5	3.3						
17	15.5	11.4	43.1	-18.4	3.2						
18	15.5	11.5	44.2	-18.5	3.3						
19	15.4	11.4	44.6	-18.5	3.4						
20	15.6	11.4	44.5	-19.3	3.3						
21	15.5	11.3	42.1	-17.2	3.2						
22	15.3	11.1	44.2	-18.1	3.4						
BOG 240											
left mandibular permanent M1						left mandibular M3					
Section	%N	$\delta^{15}\text{N}$	%C	$\delta^{13}\text{C}$	C:N	Section	%N	$\delta^{15}\text{N}$	%C	$\delta^{13}\text{C}$	C:N
1	15.2	11.9	41.9	-19.3	3.2	1	15.7	11.7	42.6	-19.8	3.2
2	15.2	11.2	41.8	-19.0	3.2	2	15.4	11.7	44.1	-20.1	3.3
3	15.4	11.2	40.2	-19.1	3.0	3	15.7	11.3	44.3	-20.1	3.3
4	15.4	10.7	41.8	-19.2	3.2	4	15.6	11.5	45.9	-20.1	3.4
5	15.4	10.9	40.7	-19.2	3.1	5	15.7	11.7	44.0	-19.7	3.3
6	15.4	10.9	42.5	-19.0	3.2	6	15.7	11.9	44.5	-19.9	3.3
7	15.3	11.0	41.4	-19.0	3.2	7	15.9	12.0	44.8	-19.0	3.3

Appendix 5.4. Results: incremental dentine (C, N)

8	15.4	11.3	40.9	-18.9	3.1	8	16.0	12.4	44.0	-18.9	3.2
9	15.3	11.2	41.6	-18.7	3.2	9	15.6	12.5	43.9	-18.9	3.3
10	15.4	11.1	42.0	-19.0	3.2	10	15.8	12.7	45.3	-18.7	3.3
11	15.4	11.2	40.0	-18.9	3.0						
12	15.5	11.3	40.1	-18.8	3.0						
13	15.3	11.2	40.6	-18.9	3.1						
14	15.4	11.3	40.3	-18.9	3.0						
15	15.4	11.2	39.3	-19.0	3.0						
16	15.4	11.4	40.0	-19.0	3.0						
17	15.4	11.7	41.8	-18.9	3.2						
18	15.4	11.6	40.0	-18.9	3.0						
19	15.6	11.9	40.9	-18.9	3.1						
20	15.4	12.3	42.5	-19.0	3.2						
BOG 250											
left mandibular deciduous m1						right mandibular permanent M1					
Section	%N	$\delta^{15}\text{N}$	%C	$\delta^{13}\text{C}$	C:N	Section	%N	$\delta^{15}\text{N}$	%C	$\delta^{13}\text{C}$	C:N
1	15.0	12.9	39.1	-18.7	3.0	1	15.4	14.0	43.8	-19.4	3.3
2	15.2	13.5	41.2	-18.8	3.2	2	15.4	13.8	44.3	-19.4	3.4
3	15.2	13.6	40.1	-19.2	3.1	3	15.9	12.1	44.2	-19.5	3.2
4	15.2	14.1	40.9	-19.1	3.1	4	15.7	13.0	43.7	-19.5	3.2
5	15.1	14.0	39.8	-19.0	3.1	5	15.9	11.0	45.7	-19.7	3.3
6	15.3	13.4	40.6	-19.2	3.1	6	15.3	10.5	43.0	-19.9	3.3
7	15.4	12.8	40.7	-19.3	3.1						
8	15.3	12.2	39.8	-19.3	3.0						
9	15.3	11.6	40.6	-19.3	3.1						
10	15.3	11.2	38.8	-19.4	3.0						
11	15.3	10.5	40.9	-19.1	3.1						
12	15.1	10.6	39.8	-19.1	3.1						
13	14.8	10.6	40.1	-19.3	3.2						
14	14.7	10.7	39.6	-19.6	3.1						
BOG 252											
right mandibular permanent I1						left mandibular permanent C					
Section	%N	$\delta^{15}\text{N}$	%C	$\delta^{13}\text{C}$	C:N	Section	%N	$\delta^{15}\text{N}$	%C	$\delta^{13}\text{C}$	C:N
1	15.8	11.4	40.1	-19.6	3.0	1	15.5	10.8	40.6	-19.6	3.0
2	15.3	10.8	43.8	-19.7	3.3	2	15.8	10.6	41.4	-19.4	3.1
3	15.5	10.9	44.4	-19.7	3.3	3	15.7	10.2	40.4	-19.0	3.0
4	15.7	10.8	43.7	-19.3	3.2	4	15.8	10.6	40.3	-19.1	3.0
5	15.8	10.4	44.2	-18.8	3.3	5	15.7	11.2	40.3	-19.2	3.0
6	15.6	10.7	43.9	-19.0	3.3	6	15.7	11.5	41.3	-19.3	3.1
7	15.8	11.0	45.1	-18.8	3.3	7	15.7	10.6	41.7	-19.1	3.1
8	15.7	11.3	44.1	-19.0	3.3	8	15.6	10.4	42.0	-19.0	3.1
9	15.6	11.5	44.0	-19.3	3.3	9	15.7	10.5	41.4	-19.1	3.1
10	15.7	10.7	44.3	-19.0	3.3	10	15.8	10.7	41.1	-19.2	3.0
11	15.6	10.2	44.6	-18.8	3.3	11	15.8	10.6	41.5	-19.2	3.1
12	15.7	10.4	45.7	-18.8	3.4	12	15.6	10.5	40.6	-19.0	3.0
13	15.7	10.4	44.9	-19.0	3.3	13	16.0	10.4	42.5	-18.2	3.1
14	15.9	10.4	44.7	-18.8	3.3	14	15.8	10.3	40.1	-18.4	3.0
15	15.7	10.3	44.3	-19.1	3.3	15	15.8	10.5	41.2	-18.4	3.0
16	15.8	10.3	43.8	-19.3	3.2	16	15.6	10.4	41.4	-18.5	3.1
17	15.7	10.3	43.7	-19.5	3.2	17	15.7	10.0	41.4	-18.6	3.1
18	15.7	10.2	41.2	-19.2	3.1	18	15.7	9.7	41.8	-18.2	3.1

19	15.5	10.3	43.4	-18.5	3.3	19	15.7	9.5	41.5	-18.2	3.1
20	15.7	10.6	44.8	-18.6	3.3	20	15.7	9.4	41.5	-18.4	3.1
						21	15.8	9.4	41.1	-18.4	3.0
						22	15.9	9.5	40.9	-18.3	3.0
						23	15.7	9.4	41.5	-18.1	3.1
						24	15.5	9.9	40.8	-17.6	3.1
BOG 255											
left maxillary permanent I1						left maxillary M3					
Section	%N	$\delta^{15}\text{N}$	%C	$\delta^{13}\text{C}$	C:N	Section	%N	$\delta^{15}\text{N}$	%C	$\delta^{13}\text{C}$	C:N
1	15.6	13.3	42.6	-18.7	3.2	1	15.4	11.2	40.3	-19.2	3.0
2	15.5	13.1	41.6	-18.9	3.1	2	15.4	11.3	39.6	-19.3	3.0
3	15.5	12.4	42.3	-19.2	3.2	3	15.5	10.9	40.3	-19.2	3.0
4	15.6	11.7	43.4	-19.5	3.2	4	15.5	10.8	39.5	-19.1	3.0
5	15.7	11.3	41.2	-19.3	3.1	5	15.4	10.9	40.7	-19.2	3.1
6	15.8	11.0	41.3	-19.0	3.1	6	15.3	10.8	39.4	-19.3	3.0
7	15.7	11.1	41.3	-19.0	3.1	7	15.5	11.0	40.5	-19.6	3.1
8	15.7	11.0	41.3	-19.1	3.1	8	15.4	11.5	40.8	-19.7	3.1
9	15.7	10.9	41.4	-19.2	3.1	9	15.5	11.4	41.4	-19.7	3.1
10	15.7	10.8	41.5	-19.4	3.1	10	15.5	11.1	40.1	-19.7	3.0
11	15.9	10.4	41.7	-19.6	3.1	11	15.4	11.2	39.5	-19.5	3.0
12	15.8	10.1	41.4	-19.5	3.1	12	15.3	10.8	40.4	-19.4	3.1
13	15.7	10.0	43.1	-19.4	3.2	13	15.4	10.7	40.7	-19.2	3.1
14	15.8	9.9	42.3	-19.4	3.1	14	15.4	10.7	41.2	-19.4	3.1
15	15.7	9.9	40.7	-19.3	3.0	15	15.4	10.3	41.0	-19.2	3.1
16	15.9	9.9	44.9	-19.2	3.3	16	15.2	10.2	40.7	-19.1	3.1
17	15.8	9.9	42.6	-19.5	3.1	17	15.3	10.8	41.5	-18.9	3.2
18	15.8	10.2	43.6	-19.4	3.2	18	15.6	11.1	43.3	-19.4	3.2
19	15.7	10.3	41.9	-19.5	3.1						
20	15.6	10.1	42.1	-19.6	3.1						
21	15.5	10.9	44.6	-19.6	3.4						
BOG 265											
left maxillary deciduous i1						left maxillary deciduous m1					
Section	%N	$\delta^{15}\text{N}$	%C	$\delta^{13}\text{C}$	C:N	Section	%N	$\delta^{15}\text{N}$	%C	$\delta^{13}\text{C}$	C:N
1	15.0	13.1	41.5	-16.6	3.2	1	15.7	13.0	40.9	-17.4	3.0
2	15.0	13.1	41.5	-16.9	3.2	2	15.6	13.2	41.6	-17.3	3.1
3	15.1	13.4	40.5	-17.1	3.1	3	15.9	13.3	41.5	-17.4	3.0
4	15.1	13.5	41.4	-17.2	3.2	4	15.7	13.9	43.4	-17.6	3.2
5	14.6	13.9	42.4	-17.7	3.4						
6	14.5	14.5	40.2	-17.5	3.2						

ID	EH	PO	CO	AG	OTHER SKELETAL LESION(S)	DIFFERENTIAL DIAGNOSIS
ICL111	P	U	U	U		nutritional deficiencies, metabolic disorders, physiological stress, infection
ICL120	A	A	P	U	Tibial plateau turned medially (bilateral), possible anterior bowing of bilateral femoral shaft (PMD)	<u>Likely</u> : metabolic disorder (rickets) <u>Other</u> : anaemia(s), nutritional deficiencies, trauma, physiological stress, infection
ICL123	A	A	U	U	Mixed woven and lamellar bone present on the mid-shaft of the anterior crest on the left tibia (6x2 cm), tibial plateau slightly turned medially (left)	<u>Likely</u> : metabolic disorder (rickets) <u>Other</u> : trauma, infection
ICL127	P	U	U	P		anaemia, nutritional deficiencies, metabolic disorders, physiological stress, infection
ICL129	A	A	P	P	Flared appearance to the metaphyses of the distal femora and proximal tibiae, porous new bone formation to the right of the frontal crest on the endocranial surface of the frontal bone (1x0.5cm), porosity present on the anterior surface of the mandible and on the superior marginal of the external auditory meatus (bilaterally)	<u>Likely</u> : metabolic disorder (scurvy) <u>Other</u> : infection, normal growth
ICL130	P	A	P	U	AMTL	anaemia, nutritional deficiencies, metabolic disorders, physiological stress, infection
ICL131	A	U	P	P	Porous woven bone present on the anterior surface of the left zygomatic bone and on the anterior surface of the right greater wing of the sphenoid, porosity present on the anterior margin of the external auditory meatus (bilateral), on the superior aspect of the internal occipital protuberance, the right palatine process (maxillae) and the body and right greater wing of the sphenoid	<u>Likely</u> : metabolic disorder (scurvy) <u>Other</u> : rickets, anaemia, normal growth
ICL134	P	A	A	U		anaemia, nutritional deficiencies, metabolic disorders, physiological stress, infection

ID	EH	PO	CO	AG	OTHER SKELETAL LESION(S)	DIFFERENTIAL DIAGNOSIS
ICL136	A	U	A	U		anaemia, nutritional deficiencies, metabolic disorders, physiological stress, infection
ICL137	P	A	P	U	Porosity present on the internal occipital protuberance (2x2cm), caries, distal femoral epiphysis (right) turned antero-lateral	<u>Likely</u> : nutritional deficiency, metabolic disorder <u>Other</u> : trauma, anaemia
ICL138	P	A	U	U		nutritional deficiencies, metabolic disorders, physiological stress, infection
ICL139	P	A	A	U		nutritional deficiencies, metabolic disorders, physiological stress, infection
ICL140	P	A	P	U	Possible slight anterior bowing of bilateral femoral shaft (broken)	anaemia, nutritional deficiencies, metabolic disorders, physiological stress, infection
ICL141	P	A	P	U	Porosity present on the palatine processes of the maxillae, anterior surface of the mandible, along the sagittal sulcus (occipital bone), porous new bone present on the superior margin of the external auditory meatus (bilateral)	<u>Likely</u> : metabolic disorder (scurvy) <u>Other</u> : infection, anaemia, physiological stress, nutritional deficiency
ICL149	P	A	P	U	Two patches of porous woven bone on the endocranial surface of the frontal bone above the left orbit, 2cm left of the frontal crest (1x1cm, 2x2cm), AMTL	nutritional deficiency, metabolic disorder, infection, anaemia, physiological stress
ICL155	P	A	A	U	AMTL, caries	nutritional deficiencies, metabolic disorders, physiological stress, infection
ICL156	P	A	A	U	Porosity present on the palatine processes of the maxillae	<u>Likely</u> : nutritional deficiency <u>Other</u> : metabolic disorder, infection, anaemia, physiological stress
FEN1	A	U	P	P	Porosity present around the margin of the right external auditory meatus, lateral surfaces of the great wings of the sphenoid (bilateral) and on the inferior aspect of the pars basilaris	<u>Likely</u> : metabolic disorder (scurvy) <u>Other</u> : nutritional deficiency, infection, anaemia, physiological stress

ID	EH	PO	CO	AG	OTHER SKELETAL LESION(S)	DIFFERENTIAL DIAGNOSIS
FEN2	A	U	P	U		anaemia, nutritional deficiencies, metabolic disorders, physiological stress, infection
FEN3	A	U	P	U	AMTL	anaemia, nutritional deficiencies, metabolic disorders, physiological stress, infection
FEN5	A	A	P	U	AMTL	anaemia, nutritional deficiencies, metabolic disorders, physiological stress, infection
FEN6	P	A	A	U	Porosity present across superior body of the sphenoid	nutritional deficiencies, metabolic disorders, physiological stress
FEN7	A	A	P	U		anaemia, nutritional deficiencies, metabolic disorders, physiological stress, infection
FEN9	P	U	U	U		nutritional deficiencies, metabolic disorders, physiological stress, infection
FEN10	P	A	A	U	Porosity present on the anterior surface of the left greater wing of the sphenoid, inferior surface of the pars basilaris (1x2cm), and along the medial surface of the left frontal process (maxilla, 0.5x1cm)	<u>Likely</u> : metabolic disorder (scurvy) <u>Other</u> : nutritional deficiency, anaemia, physiological stress, normal growth
FEN14	P	A	A	U		nutritional deficiencies, metabolic disorders, physiological stress, infection
FEN15	A	A	P	U	Porous woven bone present on the posterior surface of the right greater wing of the sphenoid (1x1cm)	metabolic disorder, nutritional deficiency, physiological stress, normal growth
FEN17	A	A	A	U	Tibial plateau turned medially (bilateral/ PMD), possible anterior bowing of femoral shaft (bilateral), lytic lesions on both sides of the frontal crest (endocranial frontal bone, 5mm circles)	metabolic disorder, nutritional deficiency, physiological stress, trauma
FEN17A	A	U	P	U	Porosity present on the inferior surface of the pars basilaris of the occipital bone, AMTL	nutritional deficiencies, metabolic disorders, physiological stress, infection, anaemia
FEN18	A	U	P	U	AMTL	nutritional deficiencies, metabolic disorders, physiological stress, infection, anaemia

ID	EH	PO	CO	AG	OTHER SKELETAL LESION(S)	DIFFERENTIAL DIAGNOSIS
FEN21	A	A	A	U	Porosity present on the anterior mandible (1x1cm) and on the inferior surface of the pars basilaris	normal growth, nutritional deficiencies, metabolic disorders, physiological stress, infection, anaemia
FEN28	P	A	P	U	Porosity present on the inferior surface of the pars basilaris (1x1cm) and around the superior margin of the left external auditory meatus	metabolic disorder, nutritional deficiency, physiological stress, normal growth, anaemia
FEN30	A	U	U	U	Porosity present on the inferior surface of the pars basilaris of the occipital bone (0.5x0.5cm)	normal growth, nutritional deficiencies, metabolic disorders, physiological stress, infection, anaemia
FEN34	P	A	U	U	Lytic lesion present on the endocranial surface of the front bone just to the right of the frontal crest (2x1cm), AMTL	physiological stress, nutritional deficiency
FEN36	A	A	U	U	Porosity present along the inferior margin of the external auditory meatus (bilateral) and on the superior body and posterior surface on the left greater wing of the sphenoid	metabolic disorder, nutritional deficiency, physiological stress, normal growth
FEN37	A	U	P	U		anaemia, nutritional deficiencies, metabolic disorders, physiological stress, infection
FEN40	P	A	U	U		nutritional deficiencies, metabolic disorders, physiological stress, infection
FEN43	P	A	A	U	Striated lamellar bone present on the midshaft of the anterior crest of the right tibia (3x6cm)	physiological stress, nutritional deficiency, metabolic disorder, infection, normal growth
FEN45	A	A	P	P		anaemia, nutritional deficiencies, metabolic disorders, physiological stress, infection
FEN48	A	U	P	U	Tibial plateau turned medially (left), caries	anaemia, nutritional deficiencies, metabolic disorders, physiological stress, infection
FEN49	P	A	U	A		nutritional deficiencies, metabolic disorders, physiological stress, infection

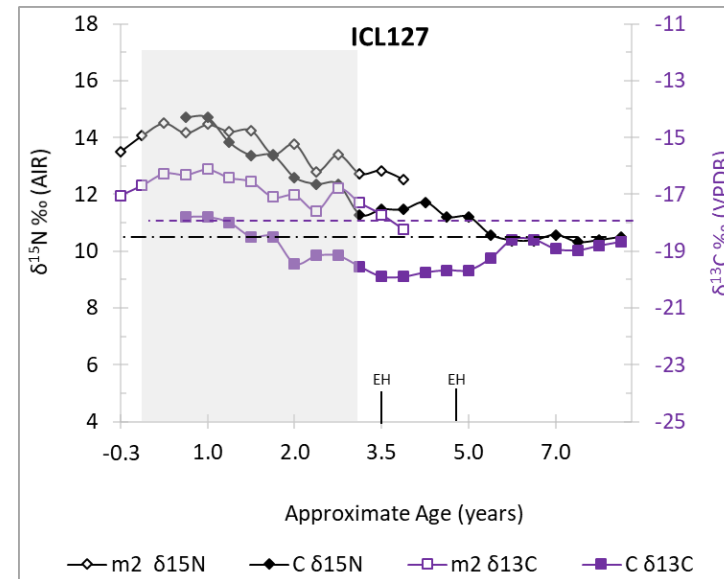
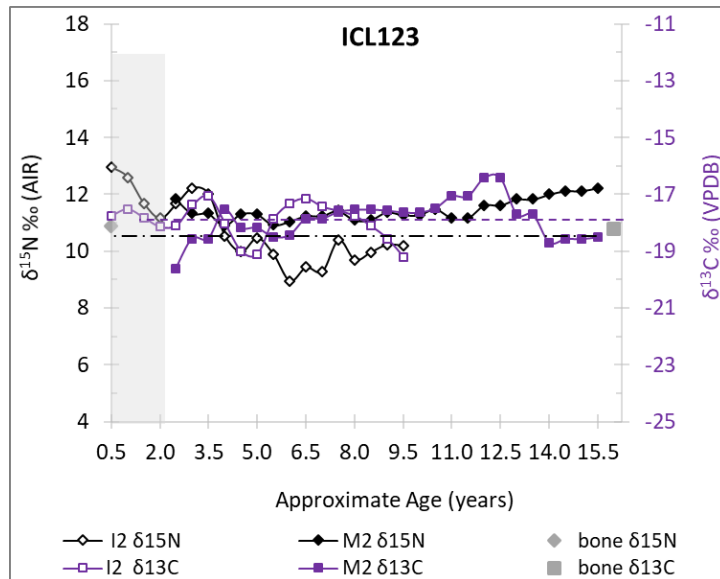
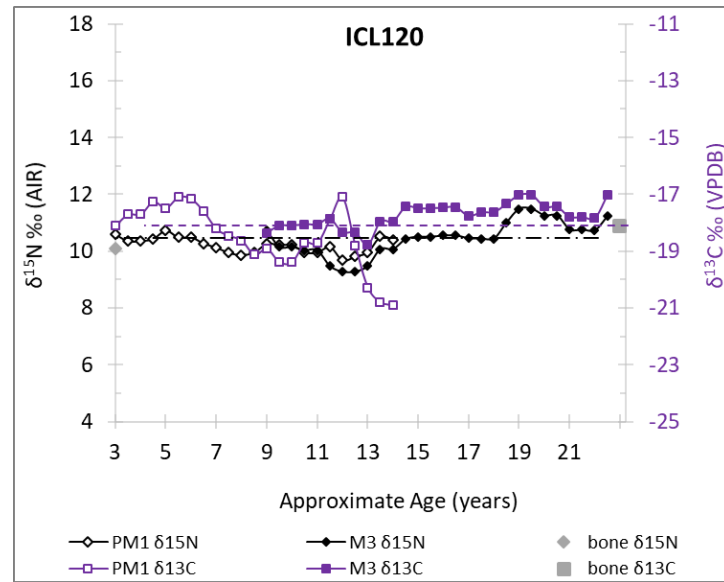
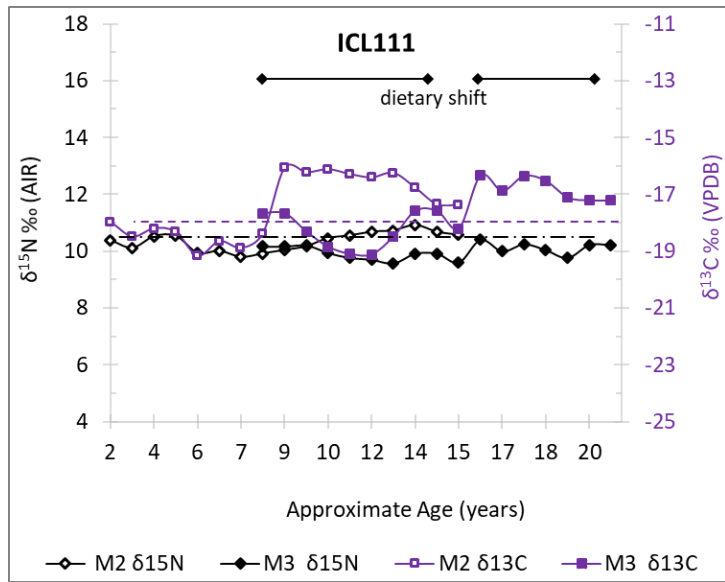
ID	EH	PO	CO	AG	OTHER SKELETAL LESION(S)	DIFFERENTIAL DIAGNOSIS
FEN50	P	A	U	U	Lytic lesion present on the endocranial surface of the frontal bone approximately 2cm from the frontal crest bilaterally (2x1cm, 1x1cm), porosity on superior margin of the left external auditory meatus and the superior body of the sphenoid	nutritional deficiencies, metabolic disorders, physiological stress, infection
FEN52	P	A	U	U		nutritional deficiencies, metabolic disorders, physiological stress, infection
BOG3	P	U	U	P	Friable surface on the anterior metaphyses of the proximal humeri	<u>Likely:</u> metabolic disorder (scurvy) <u>Other:</u> nutritional deficiency, anaemia, physiological stress, normal growth
BOG10	P	A	A	U	Porosity present on the superior aspect of the internal occipital protuberance, on the superior body of the sphenoid, and the superior margin of the external auditory meatus (left). Lytic lesion present on the posterior surface of the right greater wing of the sphenoid lateral to the body (1.5x1cm), caries	<u>Likely:</u> metabolic disorder (scurvy) <u>Other:</u> nutritional deficiency, anaemia, physiological stress, infection
BOG13	A	A	A	U	Porous woven bone present on the superior margin of the external auditory meatus (bilateral), AMTL	infection, trauma
BOG18	A	A	P	U	Porosity present on the superior margin of the external auditory meatus (bilateral) and on the postero-lateral aspect of the greater wings of the sphenoid, AMTL, caries	anaemia, nutritional deficiencies, metabolic disorders, physiological stress, infection
BOG54	A	A	A	U	Porosity present on the right palatine process and in the right maxillary sinus, porous woven bone present in the right maxillary sinus, AMTL, tibial plateau turns medially (bilateral) and the distal femoral epiphysis (L) extends postero-medially with possible soft tissue damage	<u>Likely:</u> metabolic disorder (rickets) <u>Other:</u> nutritional deficiency, anaemia, physiological stress, infection

ID	EH	PO	CO	AG	OTHER SKELETAL LESION(S)	DIFFERENTIAL DIAGNOSIS
BOG59	P	U	U	A	Friable surface along the posterior proximal metaphysis of the right tibia and along the posterior distal metaphysis of the right femur	nutritional deficiencies, metabolic disorders, physiological stress, normal growth
BOG66	A	P?	A	U	Pinpoint porosity present across the 80% of the ectocranial surface of the right parietal bone, porosity and new bone formation above the superior margin of the external auditory meatus (bilateral)	anaemia, nutritional deficiencies, metabolic disorders, physiological stress, infection
BOG85	A	A	P	U	Porosity present on the superior body of the sphenoid	anaemia, nutritional deficiencies, metabolic disorders, physiological stress, infection
BOG102	A	U	U	U	Porosity present on the superior body of the sphenoid and on the inferior surface of the pars basilaris of the occipital bone	metabolic disorder, nutritional deficiency, normal growth
BOG107	A	A	P	U		anaemia, nutritional deficiencies, metabolic disorders, physiological stress, infection
BOG109	A	A	P	P	Porosity present on the mental eminence of the mandible and the anterior surface of the maxillae lateral to the frontal process, friable surface and new woven bone on the inferior neck of femora	<u>Likely</u> : metabolic disorder (scurvy) <u>Other</u> : nutritional deficiency, anaemia, physiological stress, normal growth
BOG127	U	U	U	U	Friable surfaces around the distal metaphyses of the femora and the posterior proximal tibiae metaphyses	metabolic disorder, nutritional deficiency, physiological stress, normal growth
BOG135	U	U	U	U	Mixed woven and lamellar bone present on the lateral midshaft of the left tibia (6x3cm) and the proximal metaphysis lateral to the tibial tuberosity (3x2cm), "button" of mixed bone present on the lateral midshaft of the right tibia (1x2.5cm)	infection, trauma
BOG137	P	U	P	U		anaemia, nutritional deficiencies, metabolic disorders, physiological stress, infection
BOG138	p	U	U	U	caries	nutritional deficiencies, metabolic disorders, physiological stress, infection

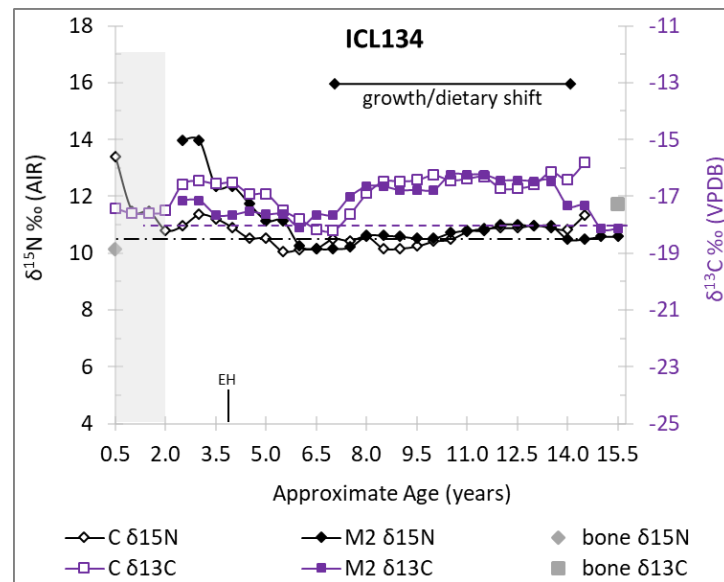
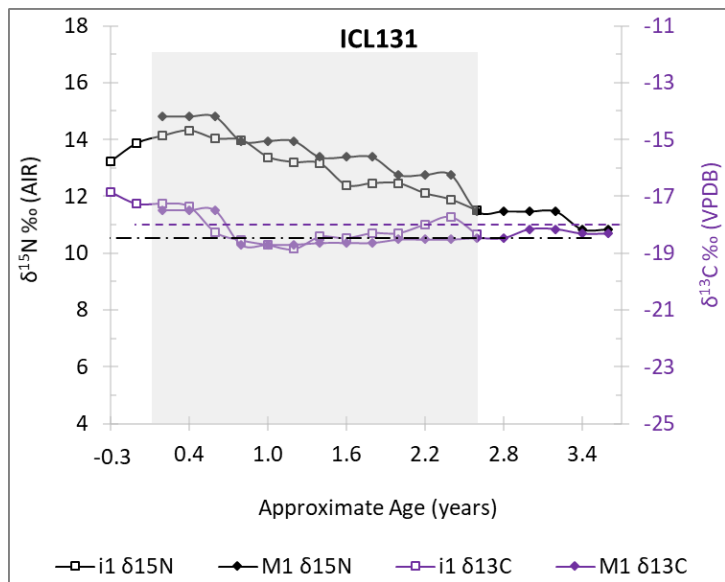
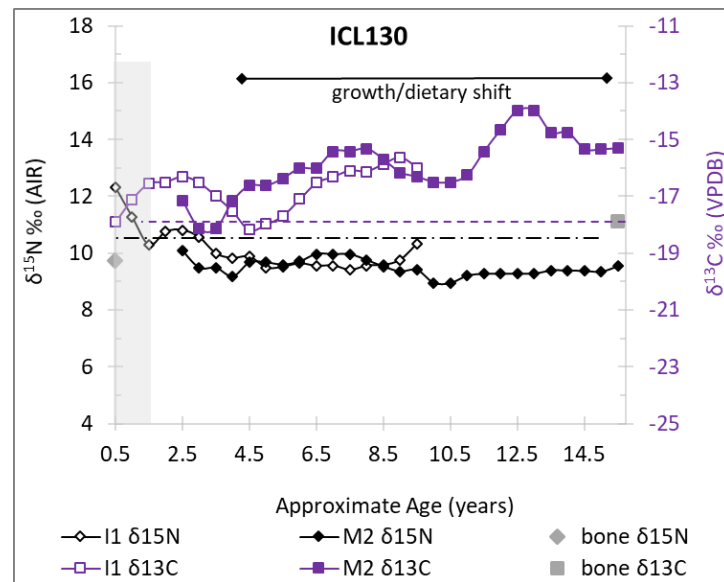
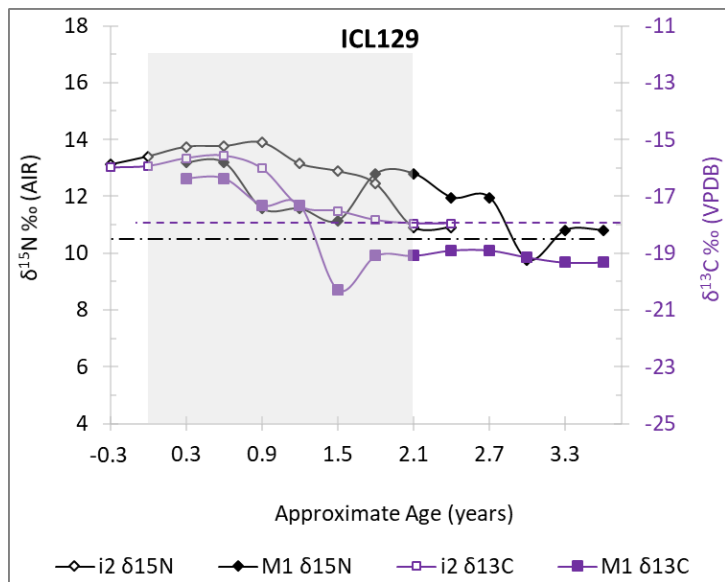
ID	EH	PO	CO	AG	OTHER SKELETAL LESION(S)	DIFFERENTIAL DIAGNOSIS
BOG144	A	A	P	P	Caries	anaemia, nutritional deficiencies, metabolic disorders, physiological stress, infection
BOG149	P	P	U	U	AMTL, possible slight anterior bowing of bilateral formulae (broken)	anaemia, nutritional deficiencies, metabolic disorders, physiological stress, infection
BOG153	U	U	U	U	Porous woven bone present on the medial surface on the right calcaneus (1x1cm) and bilateral distal tibiae just superior to the medial malleolus (2x1cm)	trauma, infection, normal growth
BOG161	P	A	A	U		nutritional deficiencies, metabolic disorders, physiological stress, infection
BOG176	A	A	A	U	Porous new bone formation present on the anterior maxillae and zygomatic bones, new woven bone (spider web appearance) present in both maxillary sinuses, AMTL	metabolic disorder, nutritional deficiency, infection, trauma
BOG194	P	A	A	P	Porosity present on the superior margin of the left external auditory meatus and the posterior surface of the left greater wing of the sphenoid	<u>Likely:</u> metabolic disorder (scurvy) <u>Other:</u> nutritional deficiency, anaemia, physiological stress, normal growth, infection
BOG196	A	A	A	U	Porosity and new woven bone (spider web appearance) present in both maxillary sinuses, AMTL, caries	infection, trauma, nutritional deficiency
BOG240	A	U	U	P	Dark subperiosteal staining on the os coxa and femur (L femoral head and distal shaft/epiphysis), possible lateral bowing of femora shafts	<u>Likely:</u> metabolic disorder (rickets, scurvy) <u>Other:</u> nutritional deficiency, anaemia, physiological stress, normal growth
BOG247	U	A	A	P	Porosity present on the anterior surface of the greater wings of the sphenoid and the inferior surface of the pars basilaris, porous woven bone present on the squama of the temporal bones (bilateral) and along the anterior body of the mandible	<u>Likely:</u> metabolic disorder (scurvy) <u>Other:</u> nutritional deficiency, anaemia, physiological stress, normal growth

ID	EH	PO	CO	AG	OTHER SKELETAL LESION(S)	DIFFERENTIAL DIAGNOSIS
BOG250	A	A	P	P	Porosity present on the superior margin on the external auditory meatus (bilateral), the anterior surface of the right greater wing of the sphenoid, and on the mental eminence of the mandible, friable surfaces on the anterior proximal humeri, right posterior distal femur, and the proximal posterior tibiae	<u>Likely</u> : metabolic disorder (scurvy) <u>Other</u> : nutritional deficiency, anaemia, physiological stress, normal growth
BOG251	P	A	A	U	Porosity present on the superior margin of the external auditory meatus (bilateral)	nutritional deficiencies, metabolic disorders, physiological stress, infection
BOG252	A	A	A	U	Porosity present on the superior aspect of the internal occipital protuberance and the superior margin of the right external auditory meatus, AMTL, caries	trauma, infection, nutritional deficiency
BOG254	A	U	U	U	Porosity present on the inferior pars basilaris, along the superior margin of external auditory meatus (bilateral), and the internal occipital protuberance	trauma, infection, nutritional deficiency
BOG255	P	A	P	U	Porous woven bone present on the visceral surface of two rib fragments (1x4cm, 1x2cm), periodontal disease (lower right quadrant), deep depression of internal occipital protuberance and deep transverse sulcus on the occipital bone	infection, nutritional deficiencies, physiological stress
BOG264	A	U	U	U	Porosity and woven bone on the anterior mandible, friable surfaces on the right anterior proximal femur metaphysis, right later proximal ulna, and right anterior proximal radius	<u>Likely</u> : metabolic disorder <u>Other</u> : nutritional deficiency, physiological stress, normal growth

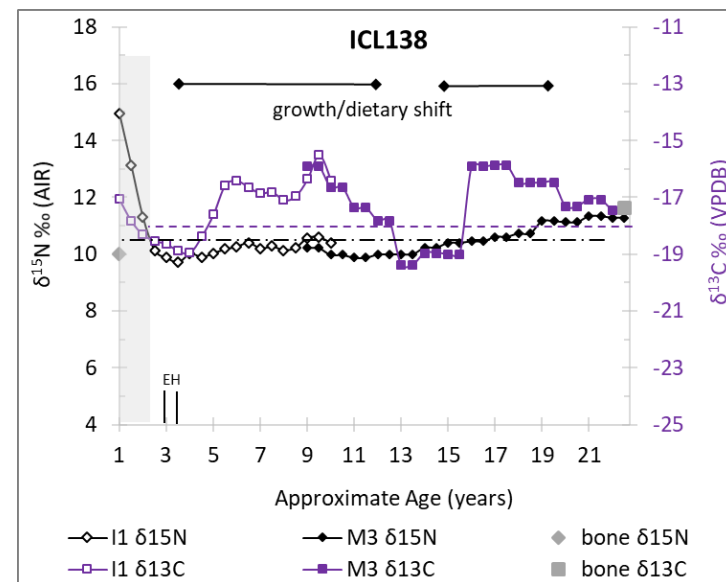
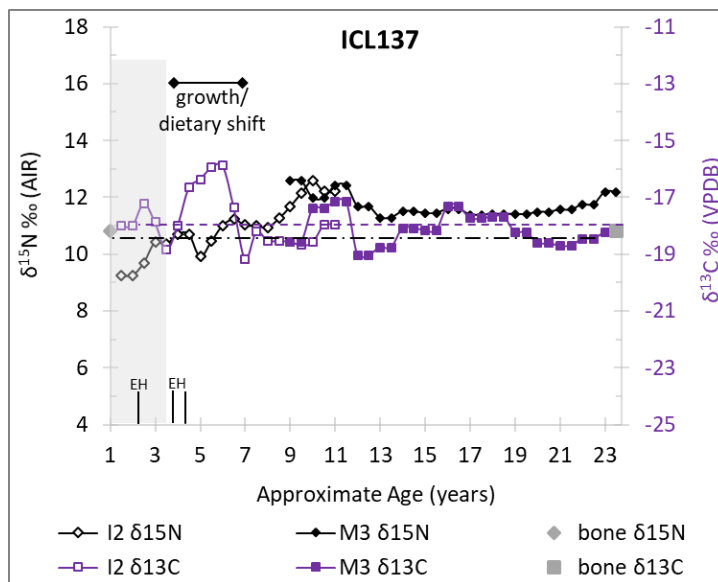
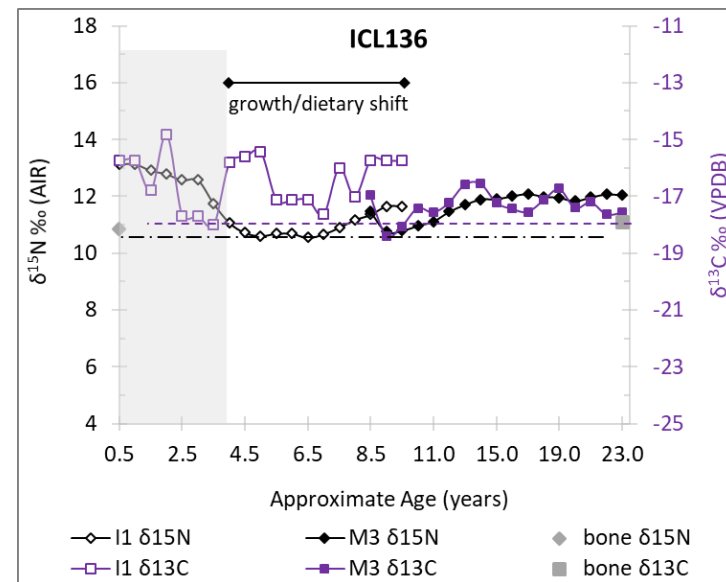
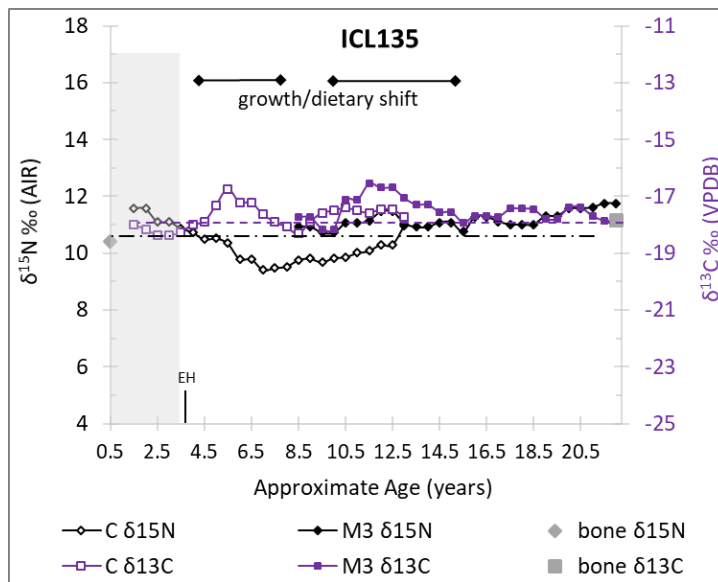
ID	EH	PO	CO	AG	OTHER SKELETAL LESION(S)	DIFFERENTIAL DIAGNOSIS
BOG265	A	A	P	A	New woven bone and porosity present on the anterior body of the mandible, on the right temporal bone around the external auditory meatus and squama, on the condyles of the occipital bone, lytic lesion present on the inferior body of the pars basilaris (1x1cm), porosity on the superior body of the sphenoid, friable surfaces and flared metaphyses on the left and right proximal humeri, the right posterior proximal femur, and the left posterior proximal femur	<u>Likely</u> : metabolic disorder (scurvy) <u>Other</u> : nutritional deficiency, anaemia, physiological stress, normal growth
BOG272	A	A	P	U	Porosity present on the superior aspect of the internal occipital protuberance and the superior margin of the external auditory meatus (bilateral), circular lytic lesions present on the endocranial occipital bone inferior to the right transverse sulcus (1x2cm), AMTL	infection, anaemia, nutritional deficiencies, physiological stress
BOG275	U	U	P	U		anaemia, nutritional deficiencies, metabolic disorders, physiological stress, infection
BOG281	A	A	P	P	Porous woven bone across the palate (bilateral)	nutritional deficiencies, metabolic disorders, physiological stress, infection
BOG289	A	A	A	U	Porosity present on the superior margin of the external auditor meatus (bilateral) and the superior body of the sphenoid, AMTL, caries, periodontal disease (upper right quadrant)	infection, nutritional deficiencies, physiological stress, trauma
BOG290	A	A	P	U	Porosity and lytic lesion on the left temporal bone antero-inferior to the zygomatic process (1x1cm), porosity and new woven bone formation on the superior and inferior body of the pars basilaris, AMTL	infection, nutritional deficiencies, physiological stress, trauma



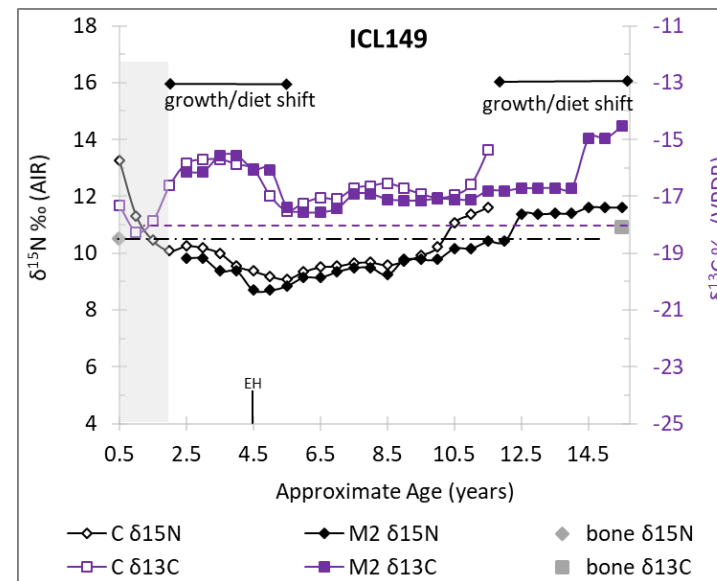
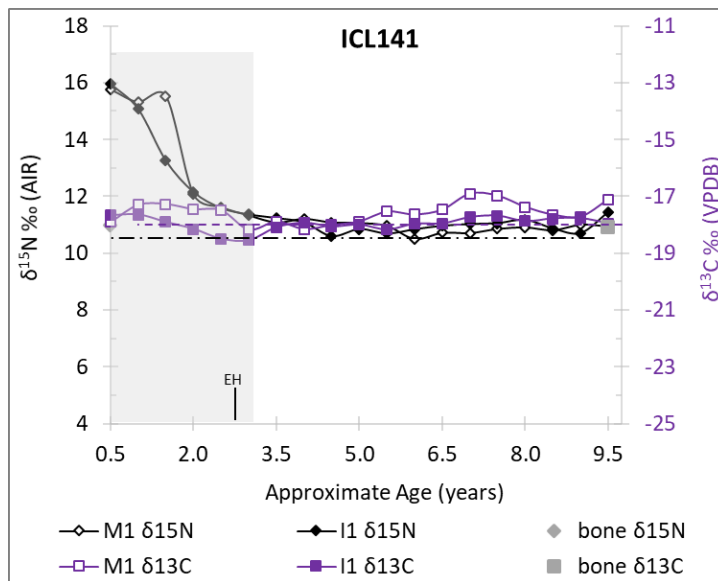
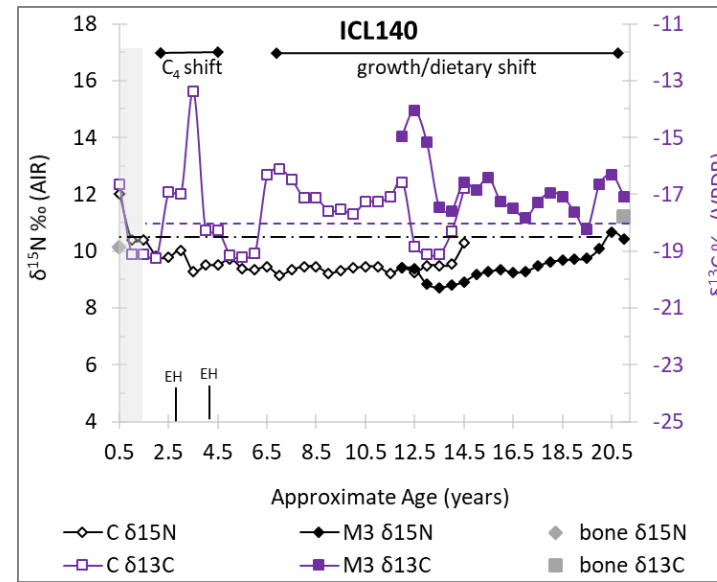
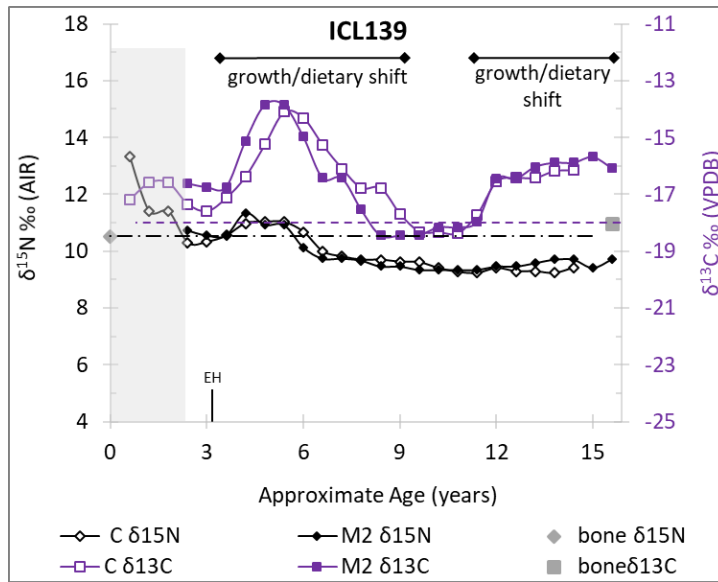
Key: The vertical shaded boxes indicate the probable breastfeeding/weaning period. AFM: $\delta^{13}\text{C}$ – dashed purple line; $\delta^{15}\text{N}$ – dot-dash black line. EH signifies the approximate age at which hypoplastic event occurred.



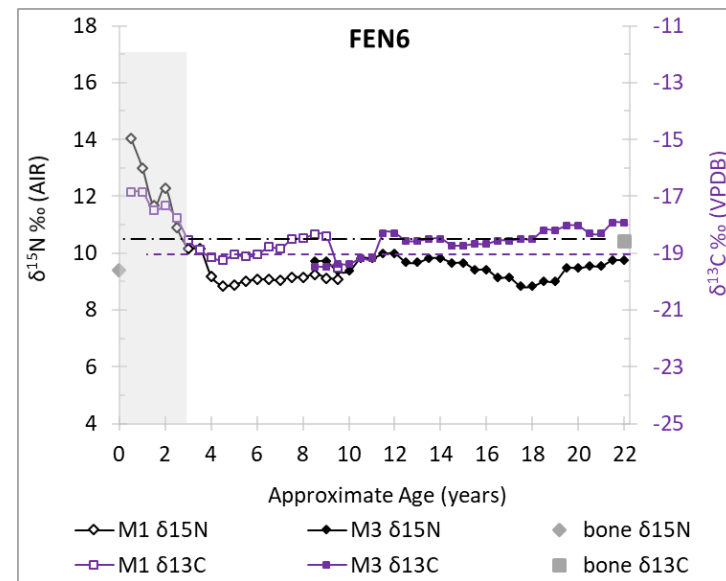
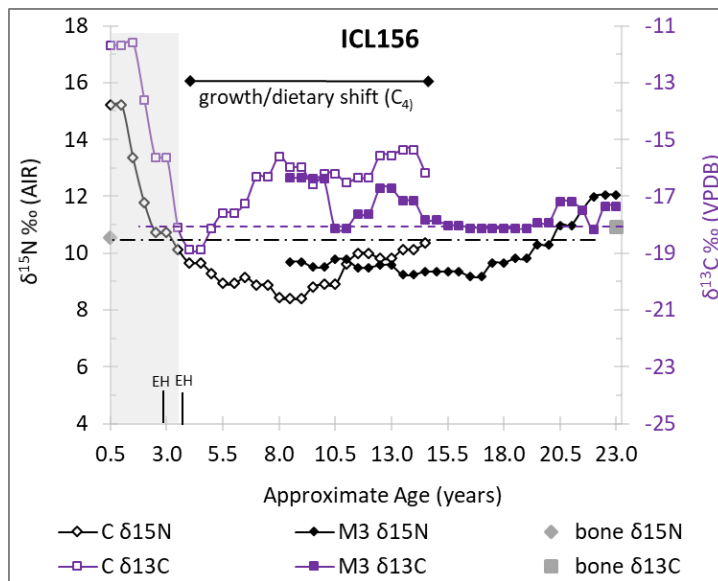
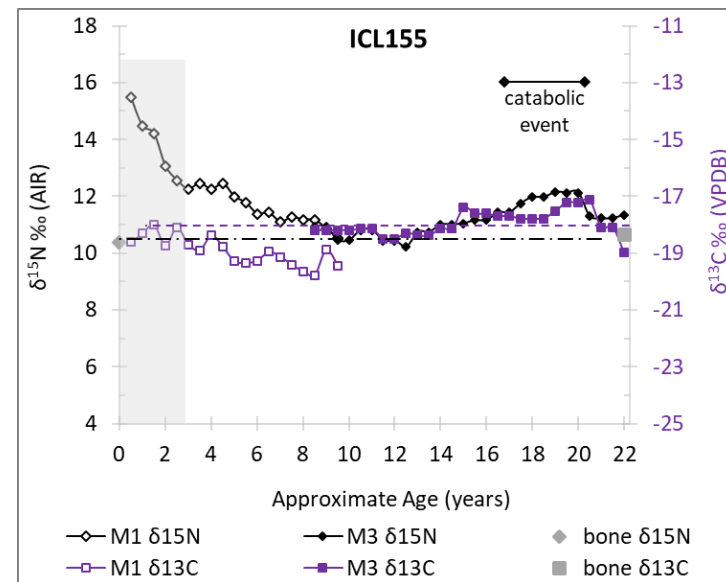
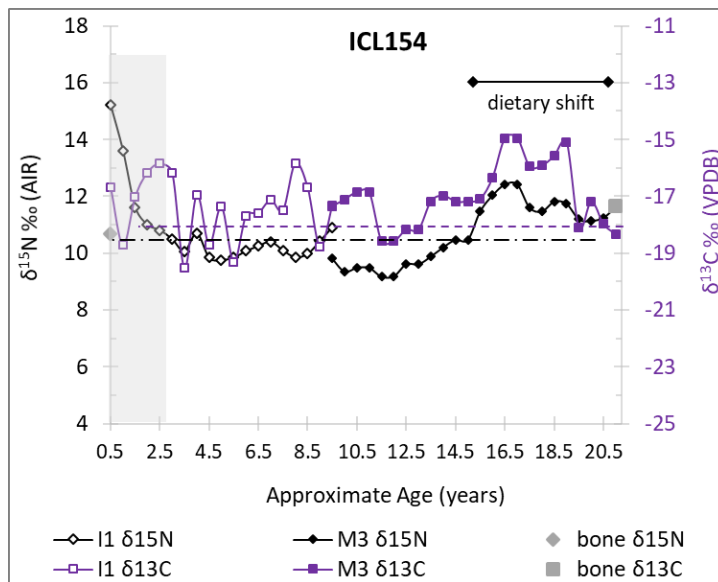
Key: The vertical shaded boxes indicate the probable breastfeeding/weaning period. AFM: $\delta^{13}\text{C}$ – dashed purple line; $\delta^{15}\text{N}$ – dot-dash black line. EH signifies the approximate age at which hypoplastic event occurred.



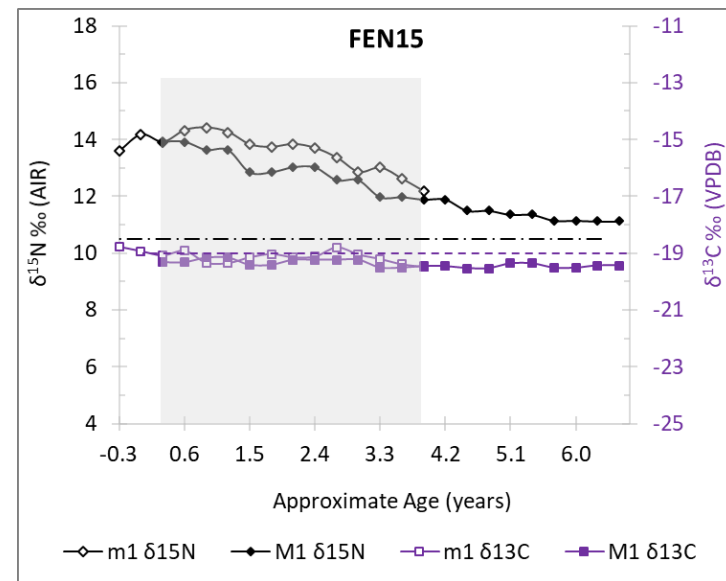
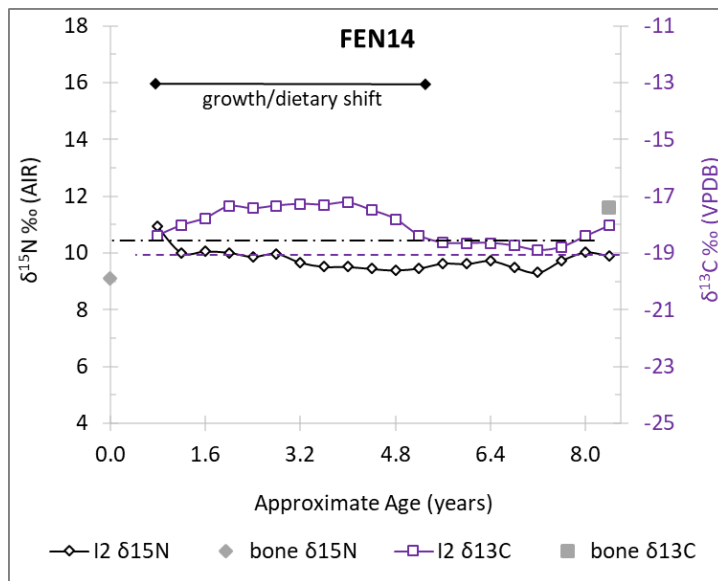
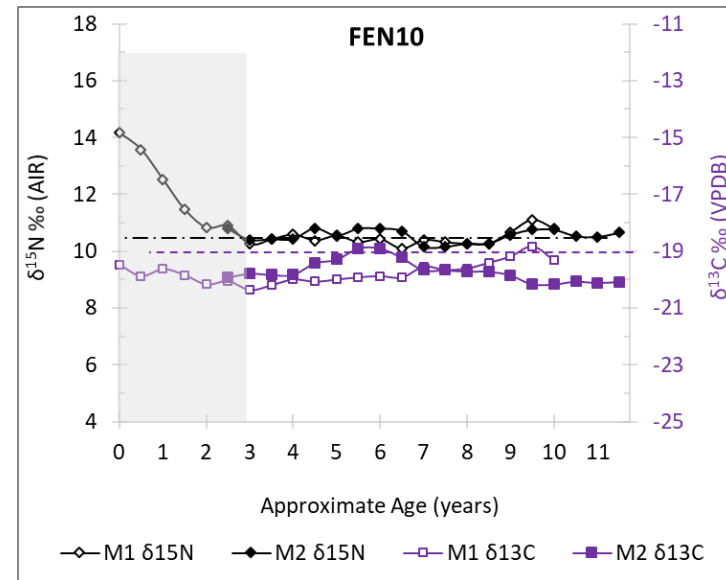
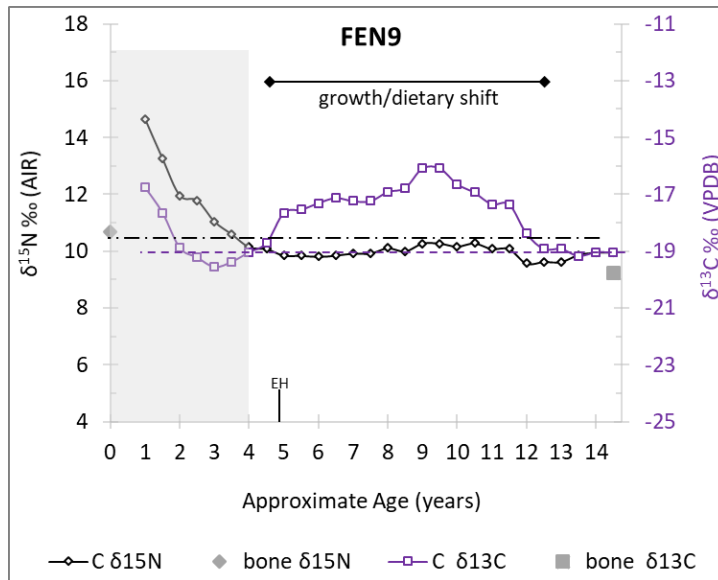
Key: The vertical shaded boxes indicate the probable breastfeeding/weaning period. AFM: $\delta^{13}\text{C}$ – dashed purple line; $\delta^{15}\text{N}$ – dot-dash black line. EH signifies the approximate age at which hypoplastic event occurred.



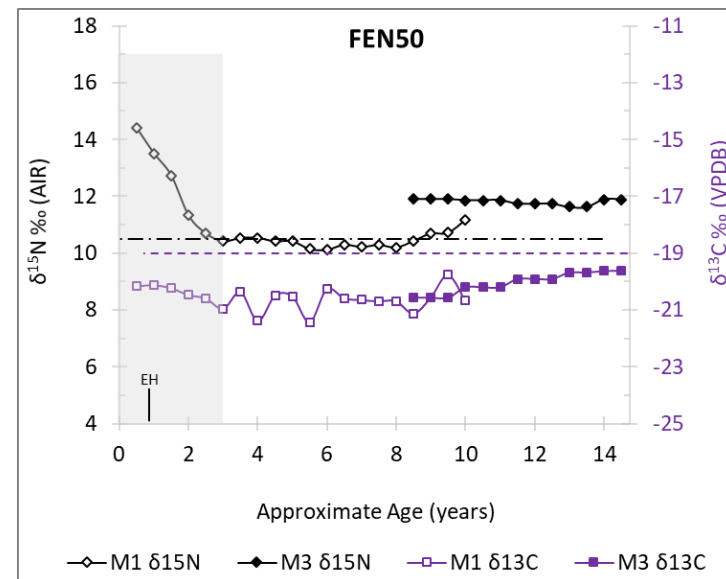
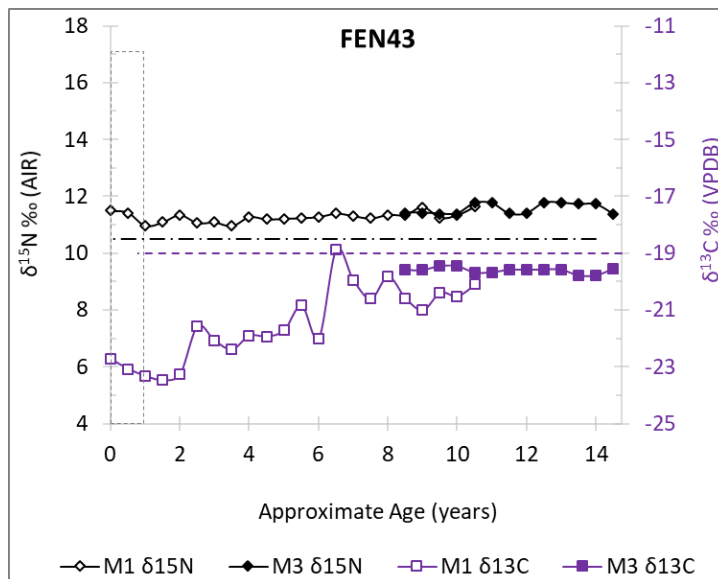
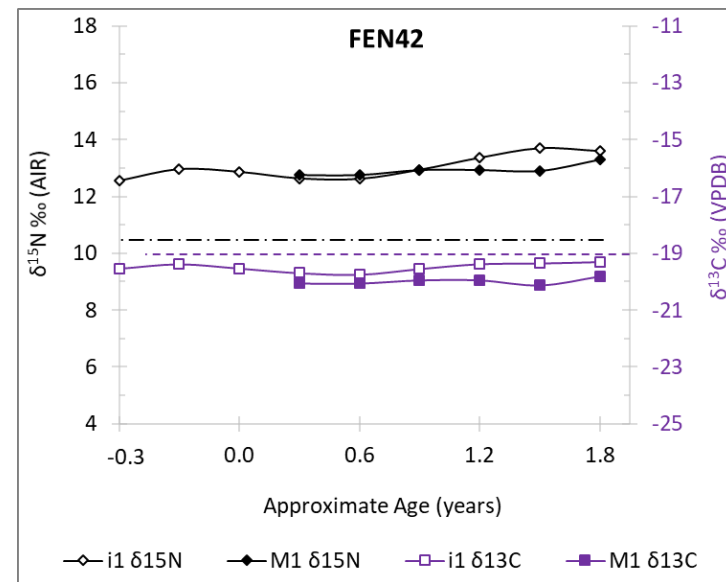
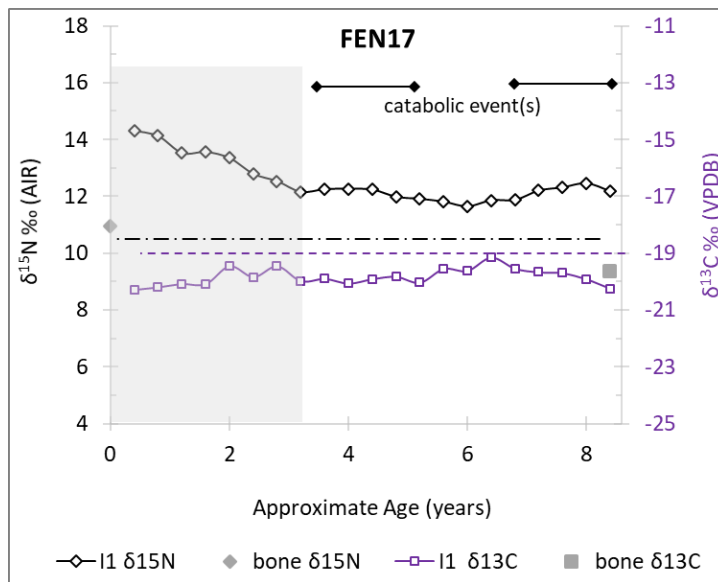
Key: The vertical shaded boxes indicate the probable breastfeeding/weaning period. AFM: $\delta^{13}\text{C}$ – dashed purple line; $\delta^{15}\text{N}$ – dot-dash black line. EH signifies the approximate age at which hypoplastic event occurred.



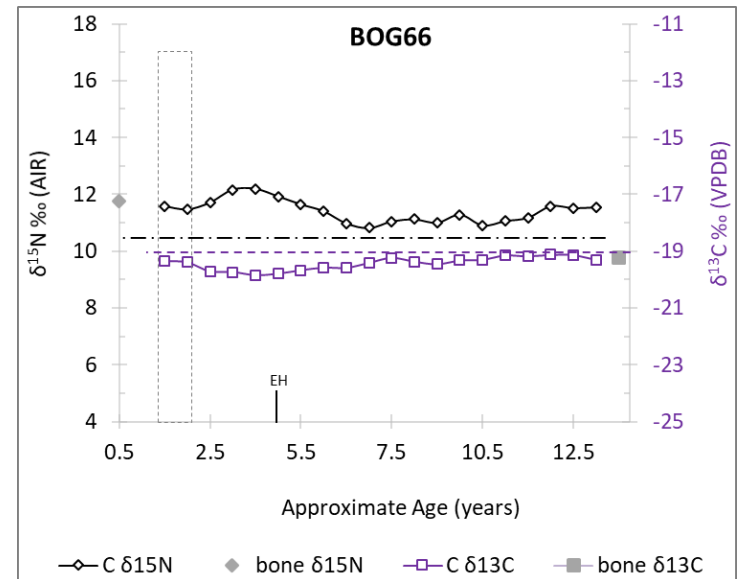
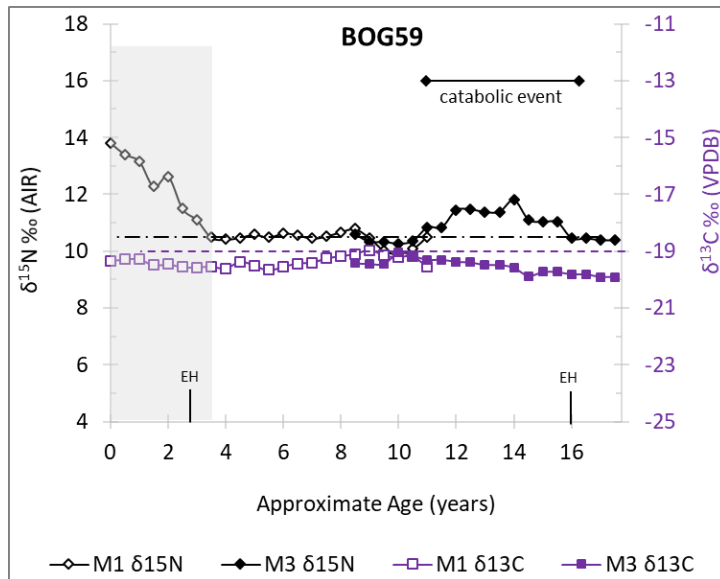
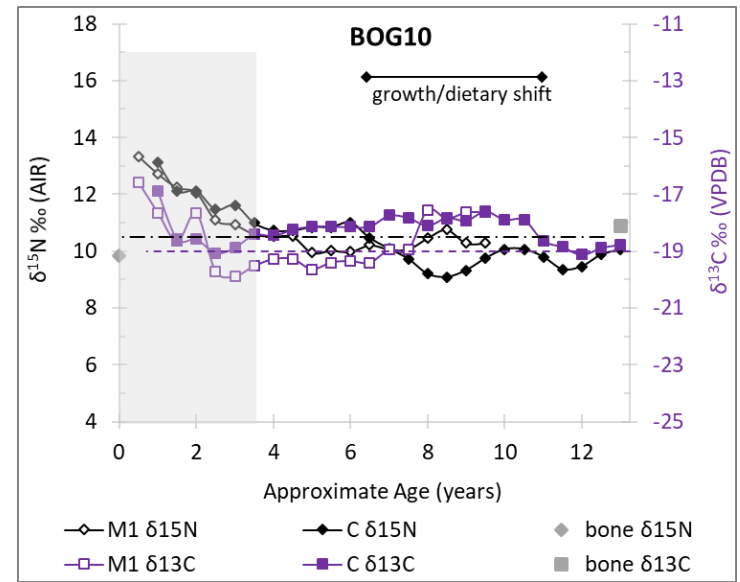
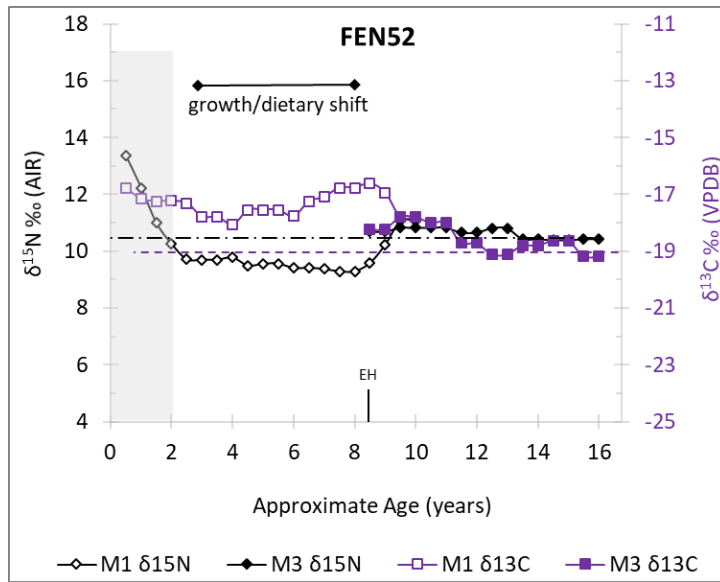
Key: The vertical shaded boxes indicate the probable breastfeeding/weaning period. AFM: $\delta^{13}\text{C}$ – dashed purple line; $\delta^{15}\text{N}$ – dot-dash black line. EH signifies the approximate age at which hypoplastic event occurred.



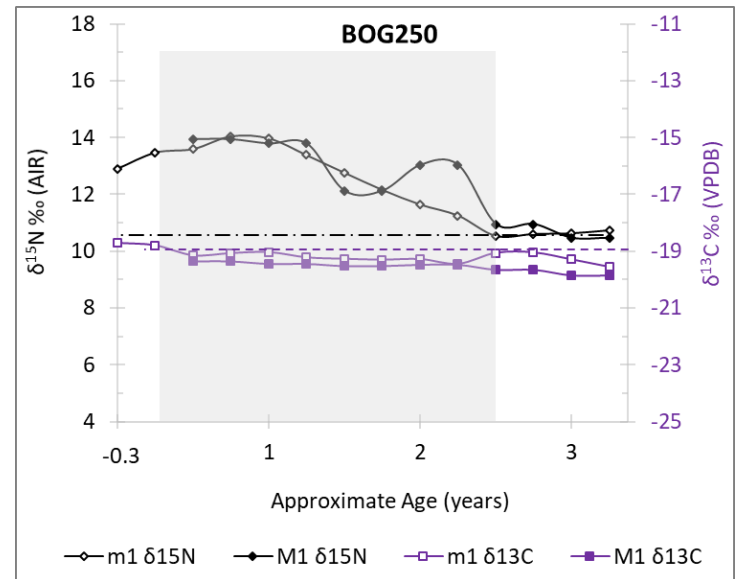
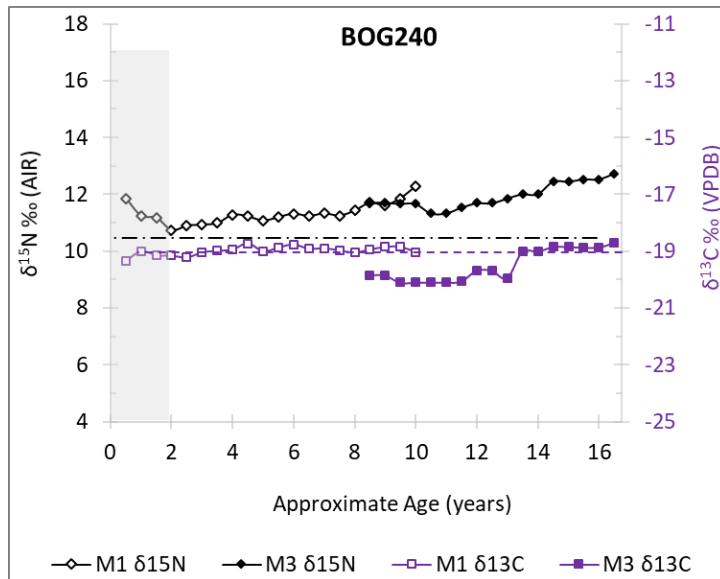
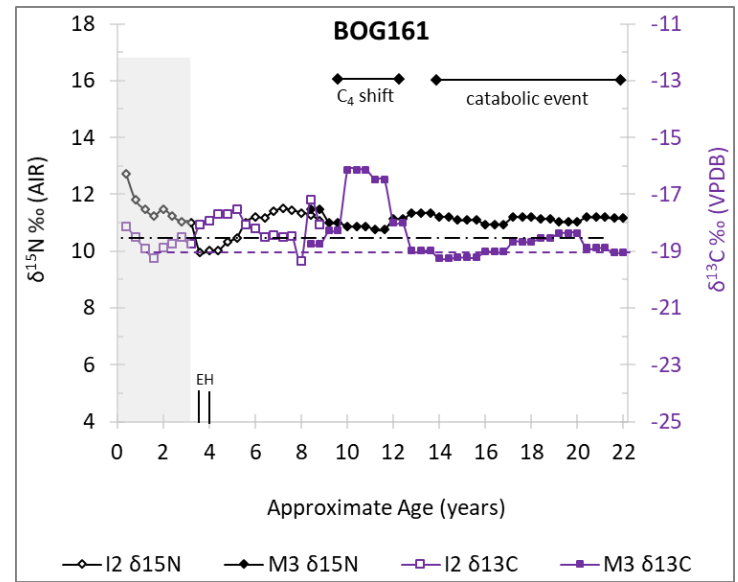
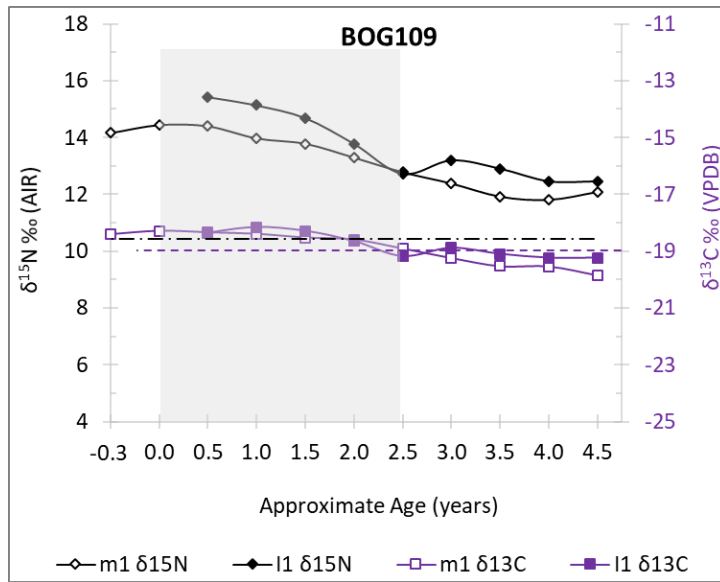
Key: The vertical shaded boxes indicate the probable breastfeeding/weaning period. AFM: $\delta^{13}\text{C}$ – dashed purple line; $\delta^{15}\text{N}$ – dot-dash black line. EH signifies the approximate age at which hypoplastic event occurred.



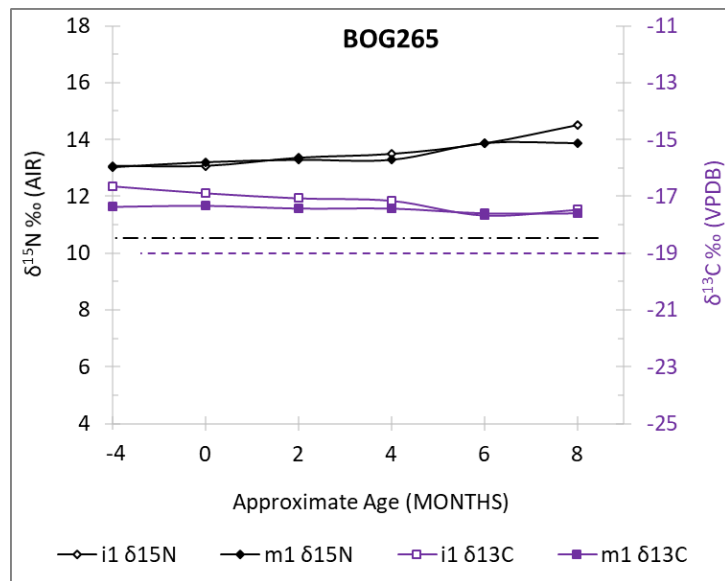
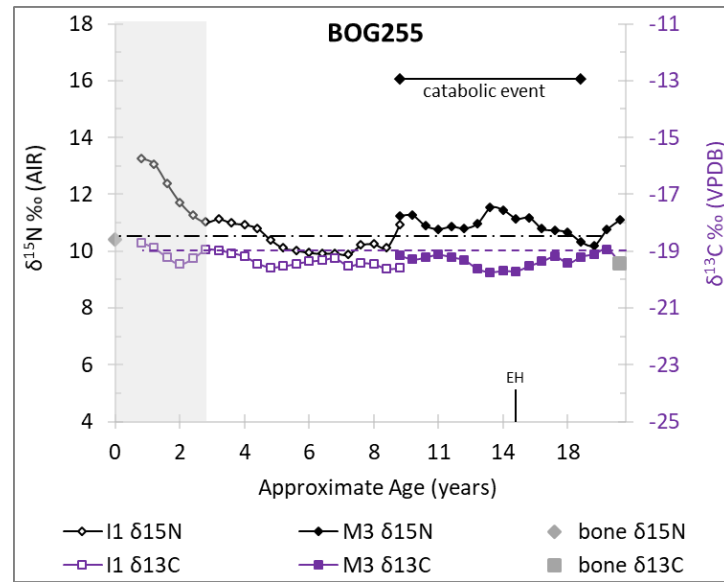
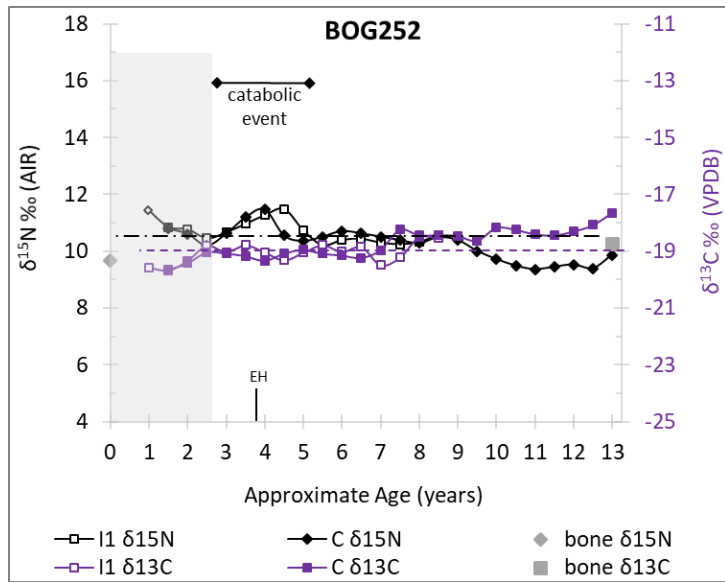
Key: The vertical shaded boxes indicate the probable breastfeeding/weaning period. AFM: $\delta^{13}\text{C}$ – dashed purple line; $\delta^{15}\text{N}$ – dot-dash black line. EH signifies the approximate age at which hypoplastic event occurred.



Key: The vertical shaded boxes indicate the probable breastfeeding/weaning period. AFM: $\delta^{13}\text{C}$ – dashed purple line; $\delta^{15}\text{N}$ – dot-dash black line. EH signifies the approximate age at which hypoplastic event occurred.



Key: The vertical shaded boxes indicate the probable breastfeeding/weaning period. AFM: $\delta^{13}\text{C}$ – dashed purple line; $\delta^{15}\text{N}$ – dot-dash black line. EH signifies the approximate age at which hypoplastic event occurred.



Key: The vertical shaded boxes indicate the probable breastfeeding/weaning period. AFM: $\delta^{13}\text{C}$ – dashed purple line; $\delta^{15}\text{N}$ – dot-dash black line. EH signifies the approximate age at which hypoplastic event occurred.